THERAPEUTIC AGENTS AND TARGETS TO MINIMIZE ISCHEMIC BRAIN INJURY

EDITED BY: Bruno Meloni, Thiruma Valavan Arumugam, Rajiv Ram Ratan, Geoffrey Alan Donnan and Emmanuel Pinteaux

PUBLISHED IN: Frontiers in Neurology

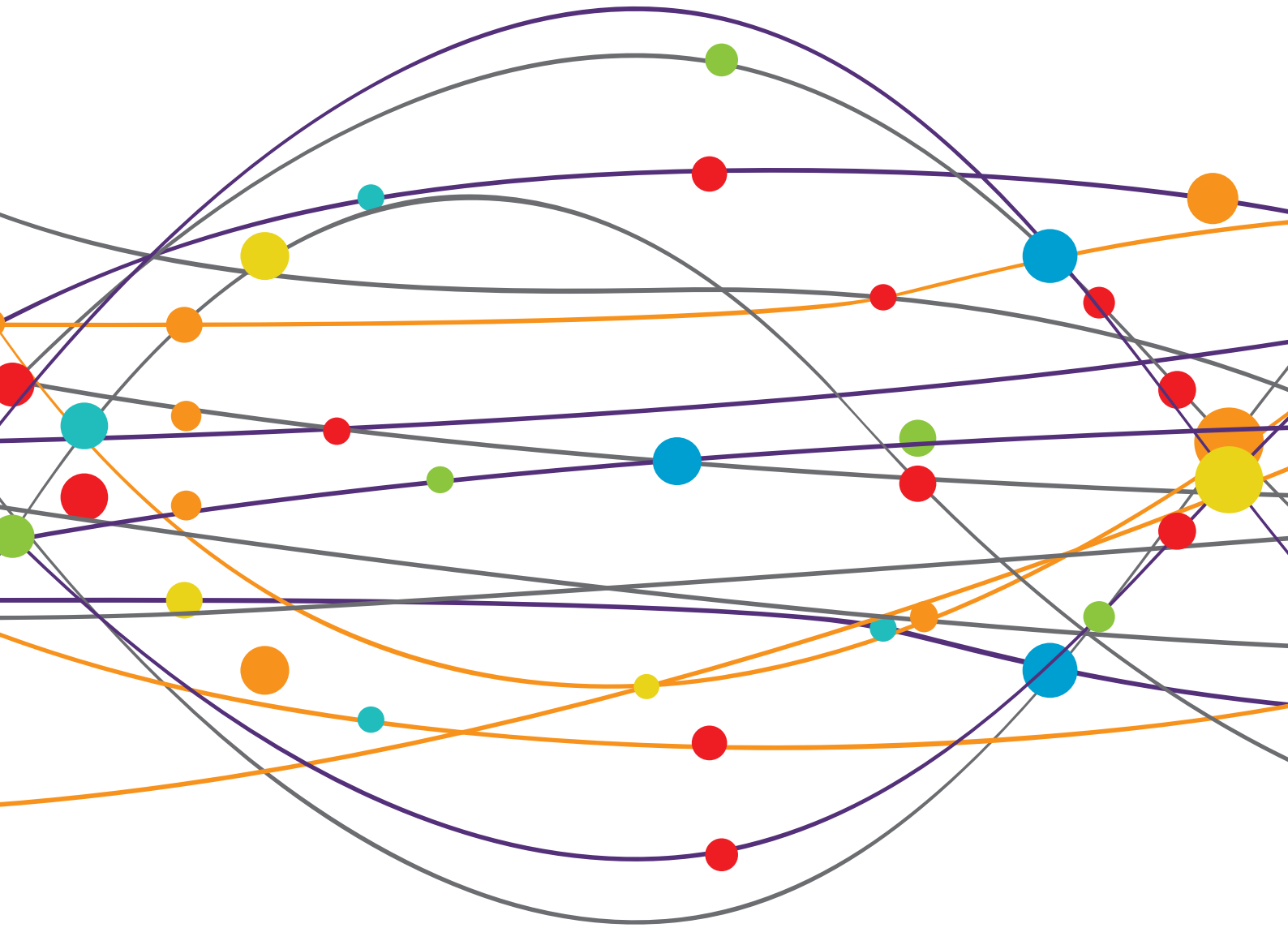

frontiers Research Topics

ISSN 1664-8714
ISBN 978-2-88971-727-9
DOI 10.3389/978-2-88971-727-9

About Frontiers

Frontiers is more than just an open-access publisher of scholarly articles: it is a pioneering approach to the world of academia, radically improving the way scholarly research is managed. The grand vision of Frontiers is a world where all people have an equal opportunity to seek, share and generate knowledge. Frontiers provides immediate and permanent online open access to all its publications, but this alone is not enough to realize our grand goals.

Frontiers Journal Series

The Frontiers Journal Series is a multi-tier and interdisciplinary set of open-access, online journals, promising a paradigm shift from the current review, selection and dissemination processes in academic publishing. All Frontiers journals are driven by researchers for researchers; therefore, they constitute a service to the scholarly community. At the same time, the Frontiers Journal Series operates on a revolutionary invention, the tiered publishing system, initially addressing specific communities of scholars, and gradually climbing up to broader public understanding, thus serving the interests of the lay society, too.

Dedication to Quality

Each Frontiers article is a landmark of the highest quality, thanks to genuinely collaborative interactions between authors and review editors, who include some of the world's best academicians. Research must be certified by peers before entering a stream of knowledge that may eventually reach the public - and shape society; therefore, Frontiers only applies the most rigorous and unbiased reviews.
Frontiers revolutionizes research publishing by freely delivering the most outstanding research, evaluated with no bias from both the academic and social point of view. By applying the most advanced information technologies, Frontiers is catapulting scholarly publishing into a new generation.

What are Frontiers Research Topics?

Frontiers Research Topics are very popular trademarks of the Frontiers Journals Series: they are collections of at least ten articles, all centered on a particular subject. With their unique mix of varied contributions from Original Research to Review Articles, Frontiers Research Topics unify the most influential researchers, the latest key findings and historical advances in a hot research area! Find out more on how to host your own Frontiers Research Topic or contribute to one as an author by contacting the Frontiers Editorial Office: frontiersin.org/about/contact

THERAPEUTIC AGENTS AND TARGETS TO MINIMIZE ISCHEMIC BRAIN INJURY

Topic Editors:
Bruno Meloni, University of Western Australia, Australia
Thiruma Valavan Arumugam, La Trobe University, Australia
Rajiv Ram Ratan, Burke Neurological Institute (BNI), United States
Geoffrey Alan Donnan, University of Melbourne, Australia
Emmanuel Pinteaux, The University of Manchester, United Kingdom

BM would like to declare that he has filed patents for the application of arginine-rich peptide as neuroprotective agents for stroke and other neurological disorders. RRR patents licensed by Neuronasal Inc., a company that he also consults for and has equity interest in. All other Topic Editors declare no competing interests with regards to the Research Topic subject.

Citation: Meloni, B., Arumugam, T. V., Ratan, R. R., Donnan, G. A., Pinteaux, E., eds. (2021). Therapeutic Agents and Targets to Minimize Ischemic Brain Injury. Lausanne: Frontiers Media SA. doi: 10.3389/978-2-88971-727-9

Table of Contents

frontiers in Neurology

SYSTEMATIC REVIEW
published: 25 February 2020
doi: 10.3389/fneur.2020.00108

Cationic Arginine-Rich Peptides (CARPs): A Novel Class of Neuroprotective Agents With a Multimodal Mechanism of Action

Bruno P. Meloni[1,2,3]*, *Frank L. Mastaglia*[2,3] *and Neville W. Knuckey*[1,2,3]

[1] *Department of Neurosurgery, QEII Medical Centre, Sir Charles Gairdner Hospital, Nedlands, WA, Australia,* [2] *Perron Institute for Neurological and Translational Science, Nedlands, WA, Australia,* [3] *Centre for Neuromuscular and Neurological Disorders, The University of Western Australia, Nedlands, WA, Australia*

There are virtually no clinically available neuroprotective drugs for the treatment of acute and chronic neurological disorders, hence there is an urgent need for the development of new neuroprotective molecules. Cationic arginine-rich peptides (CARPs) are an expanding and relatively novel class of compounds, which possess intrinsic neuroprotective properties. Intriguingly, CARPs possess a combination of biological properties unprecedented for a neuroprotective agent including the ability to traverse cell membranes and enter the CNS, antagonize calcium influx, target mitochondria, stabilize proteins, inhibit proteolytic enzymes, induce pro-survival signaling, scavenge toxic molecules, and reduce oxidative stress as well as, having a range of anti-inflammatory, analgesic, anti-microbial, and anti-cancer actions. CARPs have also been used as carrier molecules for the delivery of other putative neuroprotective agents across the blood-brain barrier and blood-spinal cord barrier. However, there is increasing evidence that the neuroprotective efficacy of many, if not all these other agents delivered using a cationic arginine-rich cell-penetrating peptide (CCPPs) carrier (e.g., TAT) may actually be mediated largely by the properties of the carrier molecule, with overall efficacy further enhanced according to the amino acid composition of the cargo peptide, in particular its arginine content. Therefore, in reviewing the neuroprotective mechanisms of action of CARPs we also consider studies using CCPPs fused to a putative neuroprotective peptide. We review the history of CARPs in neuroprotection and discuss in detail the intrinsic biological properties that may contribute to their cytoprotective effects and their usefulness as a broad-acting class of neuroprotective drugs.

Keywords: cationic arginine-rich peptides, neuroprotection, cell-penetrating peptides, arginine, guanidinium head group, TAT

OPEN ACCESS

Edited by:
Heike Wulff,
University of California, Davis, United States

Reviewed by:
Rajesh Khanna,
University of Arizona, United States
Maria Calvo-Rodriguez,
Massachusetts General Hospital, Harvard Medical School, United States

***Correspondence:**
Bruno P. Meloni
bruno.meloni@perron.uwa.edu.au

Specialty section:
This article was submitted to Stroke, a section of the journal Frontiers in Neurology

Received: *10 December 2019*
Accepted: *30 January 2020*
Published: *25 February 2020*

Citation:
Meloni BP, Mastaglia FL and Knuckey NW (2020) Cationic Arginine-Rich Peptides (CARPs): A Novel Class of Neuroprotective Agents With a Multimodal Mechanism of Action. Front. Neurol. 11:108. doi: 10.3389/fneur.2020.00108

INTRODUCTION

Despite the enormous global impact of neurological disorders and the extensive research over many decades, there is still a lack of proven clinically effective pharmacological neuroprotective therapies capable of reducing the severity of brain or spinal cord tissue injury in acute (e.g., stroke, traumatic brain injury and spinal cord injury, and hypoxic-ischemic encephalopathy) or chronic (Alzheimer's

disease, Parkinson's disease, and amyotrophic lateral sclerosis) neurological disorders. The few neuroprotective treatments that are available, such as riluzole for amyotrophic lateral sclerosis and memantine for Alzheimer's disease provide only modest benefits. While hypothermia is used as a neuroprotective therapy for neonatal encephalopathy and for comatose survivors of cardiac arrest, it is difficult to implement due to the need for specialized equipment and intensive patient monitoring, and its efficacy is also limited.

Hence, the development of effective neuroprotective drugs for the treatment of a variety of neurological disorders remains an urgent priority. To make matters worse, due to past clinical failures, some researchers, physicians, and pharmaceutical companies are reluctant to continue research focused on the development of neuroprotective agents. However, most impartial observers would agree that the benefits of continuing to pursue the discovery of neuroprotective therapies far outweigh the risks. With this in mind, it is also intuitive that in order to increase the chances of achieving translational success at the clinical level, it is preferable that any new neuroprotective drug should have a multimodal mechanism of action. To this end, cationic arginine-rich peptides (CARPs) represent a relatively novel and expanding class of compounds, which possess an array of intrinsic neuroprotective properties, and are thus ideal molecules for development as therapies for a broad range of neurological disorders.

GENERAL ASPECTS OF CARPS

As the name suggests, critical factors for CARP neuroprotection are their positive charge and arginine content as well as, the ability to traverse membrane lipid bilayers. Whereas, cationic charge can be imparted by the presence of the positively charged amino acids arginine and lysine (**Figure 1A**), which have a net charge of +1 at pH 7, arginine is the amino acid essential for neuroprotection. Histidine, the other positively charged amino acid only provides a modest contribution to peptide charge with a net charge of +0.1 at pH 7. Furthermore, CARPs represent a broader class of bioactive peptides with a number of other properties that may contribute to their neuroprotective actions, including the ability to reduce intracellular calcium influx, antagonize cell surface receptor function, target mitochondria, scavenge reactive molecules, induce cell signaling, stabilize proteins, inhibit proteolytic enzymes, and reduce inflammation, and in addition to being neuroprotective also have anti-nociceptive, cardioprotective, anti-microbial and anti-cancer properties.

CARPs have demonstrated neuroprotection in *in vitro* neuronal injury models (e.g., excitotoxicity, oxygen-glucose deprivation), in *in vivo* models of acute central nervous system (CNS) injury (e.g., stroke, traumatic brain injury, perinatal hypoxia-ischemia, traumatic brain injury, spinal cord injury, and epilepsy) and in models of chronic neurodegenerative disorders

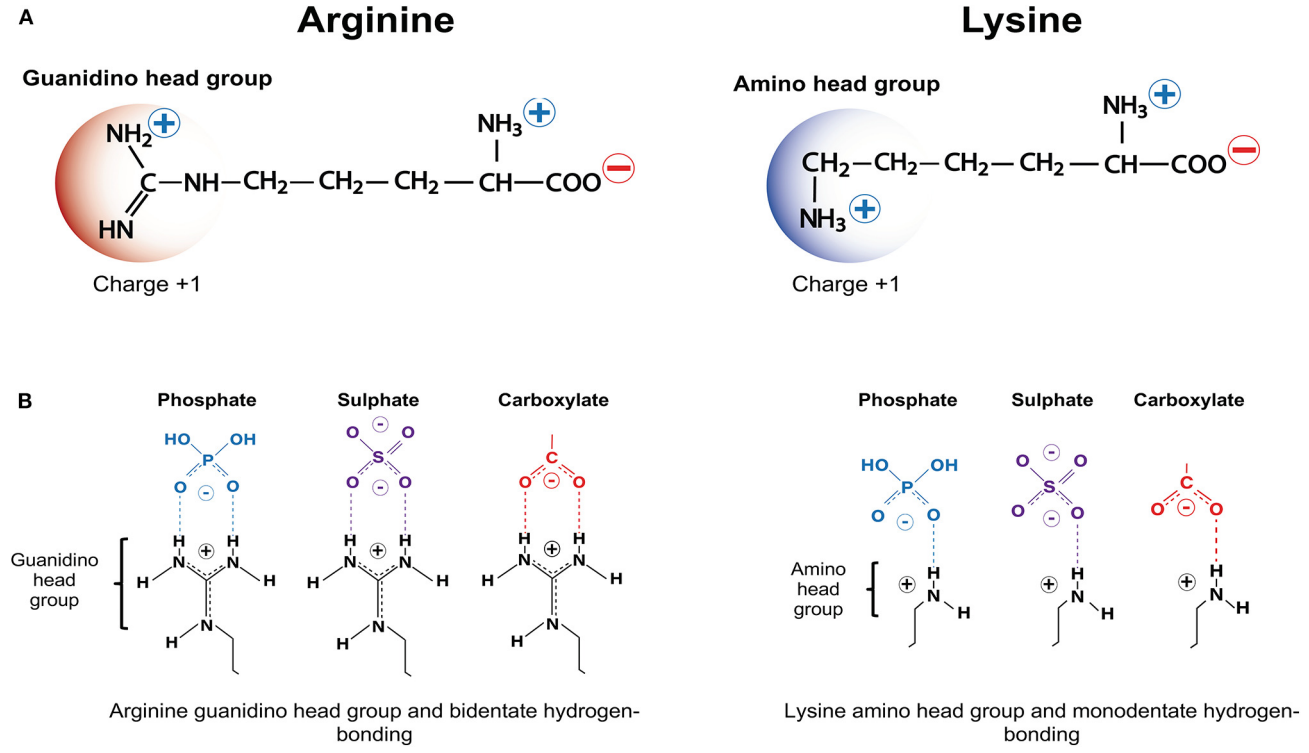

FIGURE 1 | Positively charged amino acids arginine and lysine, and hydrogen bonding. **(A)** Arginine and lysine depicting positively charged guanindino head group and amino head group, respectively. **(B)** Arginine guanindino head groups and lysine amino head groups forming bidentate hydrogen-bonding and monodentate hydrogen-bonding, respectively, with phosphate, sulfate and carboxylate anionic moieties.

(e.g., Parkinson's and Alzheimer's disease) and neuropathic pain (**Tables 1**–**3**). Furthermore, it is important to acknowledge that neuroprotective CARPs can be categorized into three main groups; (i) poly-arginine peptides, cationic arginine-rich cell-penetrating peptides (CCPPs) or peptides derived from proteins (**Table 1**); (ii) putative neuroprotective peptides fused to CCPPs (**Table 2**); and (iii) endogenous peptides (**Table 3**).

The aim of this review is to highlight the recognition of CARPs as a novel class of peptide with great promise for the treatment of acute and chronic neurological disorders, and in so doing summarize their known neuroprotective mechanisms of action, as well as other potential actions whereby they may exert beneficial effects in injured or affected cells. Within this group of compounds are included many putative neuroprotective peptides fused to CCPPs (e.g., TAT, R9, penetratin) that have been developed (**Table 2**). In this review, such peptides are also classified as CARPs, and we propose that in many, if not all instances their putative neuroprotective effects may actually be mediated by the arginine content and positive charge of the carrier and/or cargo peptide, rather than the cargo peptide itself.

GENERIC FEATURES OF NEUROPROTECTIVE CARPs

In general terms, neuroprotective CARPs typically possess the following properties: (i) range in size from 4 to 40 amino acids; (ii) positive net charge $\geq +2$ to $+20$; (iii) one or more positively

TABLE 1 | CARPs with neuroprotective and other neuroactive properties.

Peptide name	Peptide sequence	% Arginine	Net charge at pH 7	Neuronal injury model	References
R6 and CARP 6-mers	RRRRRR-NH_2, RRRRWW-NH_2, rrrrrw-NH_2, rrrrww-NH_2, Ac-MCRRKR-NH_2, Ac-LCRRKF-NH_2, Ac-RRWWIR-NH_2	33–100%	+4 to +6	Excitotoxicity, pain	(1, 2)
SS-31, SS-20	rDmtKF-NH_2, FrFK-NH_2	25%	+3	Stroke, MPTP, SCI, AD, pain	(3–7)
TAT, TAT-D	YGRKKRRQRRRG, ygrkkrrqrrrg	50%	+8	Excitotoxicity, stroke	(8–13)
Penetratin	RQIKIWFQNRRMKWKK	19%	+7	Excitotoxicity	(12)
R7, C-R5, C-R7, C-r7	RRRRRRR-NH_2, C-s-s-CRRRRR-NH_2, C-s-s-CRRRRRRR-NH_2, C-s-s-crrrrr-NH_2	71–100%	+6 to +8	Excitotoxicity	(14)
R8 to R15, R9D, R18, R18D, R22	RRRRRRRR to RRRRRRRRRRRRRRR, rrrrrrrrr-NH_2, RRRRRRRRRRRRRRRRR, rrrrrrrrrrrrrrrr, RRRRRRRRRRRRRRRRRRRRR	100%	+6 to +22	Excitotoxicity, stroke, HIE, TBI, AD	(12, 15–27)
BEN2540, BEN0540, BEN1079	Ac-WGCCGRSSRRRRTR-NH_2, Ac-PFLKRVPACLRLRR-NH_2, Ac-RCGRASRCRVRWMRRRRI-NH_2	29–44%	+4.9 to +8.9	Excitotoxicity	(15)
XIP, R9/X7/R9, NCXBP3	RRLLFYKYVYKRYRAGKQRG, RRRRRRRRRPGRVVGGRRRRRRRRR, RRERRRRSCAGCSRARGSCRSCRR-NH_2	25–80%	+8 to +19	Excitotoxicity	(15)
LMWP	VSRRRRRRGGRRRR	71%	+10	Excitotoxicity	(16)
R10W4D, R10W8, R12W8a, R12F8, R12Y8	wwrrrrrwwrrrrr-NH_2, WWRRRWWRRRRWWRRRWW, WWRRRRWWRRRRWWRRRRWW, FFRRRRFFRRRRFFRRRRFF, YYRRRRYYRRRRYYRRRRYY	55–71%	+11 to +12	Excitotoxicity	(16)
D3, D3D3, RD2	rprtrlhthrnr-NH_2, rprtrlhthrnrrprtrlhthrnr-NH_2, ptlhthnrrrrr-NH_2	42%	+6.2 to +11.4	AD	(28–30)
IDR-1018	VRLIVAVRIWRR-NH_2	33%	+5	HIE	(31)
Hi1a	NECIRKWLSCVDRKNDCCEGLECYKRRHSFEVCVPIPGFCLVKWKQC DGRERDCCAGLECWKRSGNKSSVCAPIT	9%	+3.3	Stroke	(32)
APP96-110	Ac-NWCKRGRQCKTHPH-NH_2	14%	+4	TBI	(33–35)
COG133	Ac-LRVRLASHLRKLRKRLL-NH_2	29%	+7.1	Excitotoxicity, HIE, TBI, EAE, LPS, AD	(36–41)
COG1410	Ac-ASAibLRKLAibKRLL-NH_2	17%	+4	Stroke, SAH, TBI, ICH, SCI	(24, 42–52)
CN-105	Ac-VSRRR-NH_2	60%	+3	Stroke, TBI, ICH	(53–55)
PRARIY	PRARIY	33%	+2	Stroke, SCI	(56, 57)
Syn 1020	Ac-RY(3-Cl)YRWR-NH_2	50%	+3	Pain	(58)

At the N-terminus, Ac indicates acetyl and at the C-terminus NH_2 indicates amide. Lower case single letter code indicates D-isoform of the amino acid. Aib, 2-Aminoisobutyric acid or 2-methylalanine; s-s, disulfide bond; Y(3-Cl), 3-chloro-L-tyrosine. AD, Alzheimer's disease; CARPs, cationic arginine-rich peptides; Dmt, 2′,6′-dimethyl-L-tyrosine; EAE, Experimental autoimmune encephalomyelitis; HIE, hypoxia-ischaemia encephalopathy; ICH, intracerebral hemorrhage; LMWP, Low molecular weight protamine; LPS, Lipopolysaccharide; MPTP, 1-methyl-4-phenyl-1,2,3,6-tetrahydropyridine; MS, multiple sclerosis; PNI, peripheral nerve injury; SAH, subarachnoid hemorrhage; SCI, spinal cord injury; stroke, ischaemic stroke; TBI, traumatic brain injury.

TABLE 2 | Studies demonstrating neuroprotective and other neuroactive properties of peptides fused to TAT and other cell penetrating peptides.

Peptide name	Peptide sequence	% Arginine	Net charge at pH 7	Neuronal injury model	References
TAT-NR2B9c (NA-1)	YGRKKRRQRRR-KLSSIESDV	30%	+7	Excitotoxicity, stroke, HIE, ICH, AD, epilepsy, pain	(59–68)
JNKI-1D-TAT, JNKI-1-TAT	dqsrpvqpflnlttprkprpp-rrrqrrkkrg-NH_2, GRKKRRQRRR-PP-RPKRPTTLNLFPQVPRSQD-NH_2	29%	+12	Excitotoxicity, stroke, HIE, ICH, TBI, AD, SCI, SMA, epilepsy, pain	(60, 69–83)
TAT-JIP-1	GRKKRRQRRR-RPKRPTTLNLF	38%	+11	Excitotoxicity, stroke, GCI, PD	(84–86)
δSV1-1-TAT	YGRKKRRQRRR-SFNSYELGSL	28%	+7	Stroke	(87, 88)
TAT-JBD	GRKKRRQRRR-PP-RPKRPTTLNLFPQVPRSQDT	28%	+11	HIE, GCI	(89, 90)
TAT-NPEG4-(IETDV)2	YGRKKRRQRRR-(Peg)4-(IESDV)2	28%	+9	Stroke, pain, epilepsy, cortical spreading depression	(91–95)
JNK3-N-TAT	YGRKKRRQRR-RCSEPTLDVKI	29%	+6.9	PD	(96, 97)
Src40–49Tat	KPASADGHRGY-GRKKRRQRRR	33%	+9.1	Pain	(98)
TAT-Sab_{KIM1}	GFESLSVPSPLDLSGPRVVAPP-RRRQRRKKRG-NH_2	22%	+8	PD	(99)
TAT-CBD3	YGRKKRRQRRR-ARSRLAELRGVPRGL	38%	+11	Excitotoxicity, stroke, TBI, pain	(100–105)
R9-CBD3	RRRRRRRRR-ARSRLAELRGVPRGL	54%	+12		
TAT-CBD3A6K	YGRKKRRQRRR-ARSRLKELRGVPRGL	38%	+12		
TAT-CRMP-2	YGRKKRRQRR-GVPRGLYDGVCEV	26%	+6.9	Excitotoxicity, stroke, OGD	(106–108)
TAT-$NR2B_{ct}$	YGRKKRRQRRR-KKNRNKLRRQHSY	37%	+14.1	Excitotoxicity, stroke	(109–111)
TAT-$NR2B_{ct}$s	YGRKKRRQRRR-NRRRNSKLQHKKY	35%	+14.1	Excitotoxicity	(109, 110)
Tat-$D2_{LIL3-29-2}$	YGRKKRRQRRR-MKSNGSFPVNRRRMD	34%	+11	Depression	(112)
Penetratin-COG133 (COG112)	Ac-RQIKIWFQNRRMKWKK-LRVRLASHLRKLRKRLL-NH_2	24%	+14.1	TBI, EAE, AD, axonal regeneration, spinal cord demyelination	(40, 41, 47, 113–115)
TAT-NR2Bct-CTM	YGRKKRRQRRR-KKNRNKLRRQHSY-KFERQKILDQRFFE	35%	+15.1	Stroke	(116)
CN2097	RRRRRRRC-s-s-CKNYKKTEV (cyclic or linear)	41%	+9	Excitotoxicity, pain	(14, 117)
P42-TAT	AASSGVSTPGSAGHDIITEQPRS-GG-YGRKKRRQRRR	19%	+7.1	Huntington's disease	(118)
TAT-p53DM	YGRKKRRQRRR-RVCACPGRDRRT	43%	+11	288,289	(14, 109, 119, 120)
TAT-p53DMs	YGRKKRRQRRR-CCPGECVRTRRR	43%	+11	Excitotoxicity	(109)
TAT-CN21	YGRKKRRQRR-KRPPKLGQIGRSKRVVIEDDR	29%	+11	Excitotoxicity, stroke, GCI	(121–123)
PYC36-TAT, PYC36D-TAT	GRKKRRQRRRGG-LQGRRRQGYQSIKP, pkisqygqrrrgqlgg-rrrqrrkkrg	35%	+12	Excitotoxicity	(10)
TAT-GluR6-9c	YGRKKRRQRR-RLPGKETMA	32%	+8	Excitotoxicity, GCI, stroke, OGD	(124–126)
TAT-mGluR1	YGRKKRRQRRR-VIKPLTKSYQGSGK	24%	+11	Excitotoxicity, HIE, SAH	(127–129)
TAT-K13	YGRKKRRQRR-KEIVSRNKRRYQED	33%	+9	Stroke	(130)
TAT-Indip	YGRKKRRQRRR-GEPHKFKREW	33%	+9.1	Excitotoxicity, ALS	(109, 131)
TAT-Indip-K/R	YGRKKRRQRRR-GEPHRFRREW	43%	+9.1	Excitotoxicity	(109)
TAT-GESV, D-TAT-GESV	RRRQRRKKRG-YAGQWGESV, rrrqrrkkrg-yagqwgesv	32%	+7	Excitotoxicity, HIE, pain	(132–134)
TAT-NEP1-40	YGRKKRRQRRR-RIYKGVIQAIQKSDEGHPFRAYLESEVAISEELVQK YSNS	16%	+7.1	Stroke, OGD	(135, 136)
TAT-NBD	YGRKKRRQRRR-TALDWSLWQTE	27%	+6	HIE	(137)
TAT-ψεHSP90	YGRKKRRQRRR-PKDNEER	39%	+8	Stroke, OGD	(138)
TAT-Bec	YGRKKRRQRRR-GG-TNVFNATFEIWHDGEFGT	19%	+6.1	SCI	(139)
TAT-gp91ds	GRKKRRQRRR-CSTRIRRQL-NH_2	47%	+12	SCI, TBI, SAH	(140–142)
TAT-ISP	GRKKRRQRRR-CDMAEHMERLKANDSLKLSQEYESI-NH_2	20%	+6	SCI	(143)
Tat-Cav3.2-III-IV	YGRKKRRQRRR-EARRREEKRLRRLERRRRKAQ	50%	+16	Pain	(144)

(Continued)

TABLE 2 | Continued

Peptide name	Peptide sequence	% Arginine	Net charge at pH 7	Neuronal injury model	References
TAT-μCL	YGRKKRRQRRR-PPQPDALKSRTLR	33%	+10	Retinal degeneration	(145)
ST2-104	RRRRRRRRR-ARSRLAELRGVPRGL	54%	+12	Pain	(146)
TAT-STEP	YGRKKRRQRRR -GLQERRGSNVSLTLDM	30%	+8	Excitotoxicity, stroke, OGD	(147)
TAT-K	YGRKKRRQRRR-PP-LNRTPSTVTLNNNT	26%	+9	Excitotoxicity	(148)
TAT-P110	YGRKKRRQRRR-GG-DLLPRGT	35%	+9	Stroke, Huntington's disease	(149, 150)
TAT-C6	GRKKRRQRRR-CRRGGSLKAAPGAGTRR	37%	+14	Stroke	(151)
Analog 4 and 5	Y-βP-WFGG-RRRRR, YaWFGG-RRRRR	45%	+5	Pain	(152)
Aβ1-6_{A2V}TAT(D)	grkkrrqrrr-gggg-dvefrh	35%	+8.1	AD	(153)
DEETGE-CAL-TAT	RKKRRQRRR-PLFAER-LDEETGEFLP-NH_2	28%	+5	GCI	(154)
TAT-T406	RKKRRQRR-IAYSSSETPNRHDML	29%	+7.1	Pain	(155)
TAT-21-40	RKKRRQRRR-RIPLSKREGIKWQRPRFTRQ	38%	+14	Excitotoxicity, stroke, OGD	(156)
TAT-C1aB	YGRKKRRQRRR-HLSPNKWKW	30%	+10.1	Excitotoxicity, stroke	(157)
TAT-2ASCV	YGRKKRRQRRR-TVNEKVSC	31%	+8	Pain	(158)
TAT-NTS	YGRKKRRQRRR-RSFPHLRRVF-NH_2	43%	+12.1	Stroke, OGD	(159)
TAT-CBD3M5L	YGRKKRRQRR-ARSRMA	44%	+9	Pain	(160)
TDP-r8	YrFG-rrrrrrrr-G	69%	+9	Pain	(161)
TAT-Pro-ADAM10	YGRKKRRQRR-PKLPPPKPLPGTLKRRRPPQP	27%	+14	Huntington's disease	(162)

At the N-terminus, Ac indicates acetyl and at the C-terminus NH_2 indicates amide. Lower case single letter code indicates D-isoform of the amino acid. Aib, 2-Aminoisobutyric acid or 2-methylalanine; s-s, disulfide bond; AD, Alzheimer's disease; ALS, amyotrophic lateral sclerosis; EAE, Experimental autoimmune encephalomyelitis; GCI, global cerebral ischaemia; HIE, hypoxia-ischaemia encephalopathy; ICH, intracerebral hemorrhage; OGD, oxygen glucose deprivation; PD, Parkinson's disease; SAH, subarachnoid hemorrhage; SCI, spinal cord injury; SMA, spinal muscular atrophy; stroke, ischaemic stroke; TBI, traumatic brain injury.

TABLE 3 | Endogenous CARPs with neuroprotective and cytoprotective properties.

Peptide name	Peptide sequence	% Arginine	Net charge at pH 7	Neural/cell injury model	References
Apelin-13	QRPRLSHKGPMPF	15%	+3.1	Excitotoxicity, stroke, TBI, ICH, SCI, pain	(163–176)
Apelin-17	KFRRQRPRLSHKGPMPF	23%	+6.1		
Apelin-36	LVQPRGSRNGPGPWQGGRRKFRRQRPRLSHKGPMPF	20%	+10.1		
Dynorphin A 1-13, Dynorphin A 1-17	YGGFLRRIRPKLK, YGGFLRRIRPKLKWDNQ	23%	+5	Pain, stroke, LPS	(177–179)
PACAP38	HSDGIFTDSYSRYRKQMAVKKYLAAVLGKRYKQRVKNK	11%	+9.1	Excitotoxicity, stroke, GCI, TBI, PD, pain	(180–185)
Ghrelin	GSSFLSPEHQRVQQRKESKKPPAKLQPR	11%	+5.1	Stroke, PD, AD, SAH, epilepsy, TBI, pain	(186–192)
Humanin	MAPRGFSCLLLLTSEIDLPVKRRA	12%	+2	Excitotoxicity, stroke, AD, SAH, HIE	(193–197)
PR-39	RRRPRPPYLPRPRPPPFFPPRLPPRIPPGFPPRFPPRFP	25%	+10	Hypoxia, ischaemia/reperfusion, oxidative stress: endothelial cells, HeLa cells, myocardial infarction	(198–200)
PR-11	RRRPRPPYLPR	45+	+5		
Protamine	PRRRRSSSRPVRRRRRPRVSRRRRRRGGRRR	66%	+21	Excitotoxicity, stroke	(16)

AD, Alzheimer's disease; GCI, global cerebral ischaemia; HIE, hypoxia-ischaemia encephalopathy; ICH, intracerebral hemorrhage; LPS, Lipopolysaccharide; SAH, subarachnoid hemorrhage; SCI, spinal cord injury; PD, Parkinson's disease; stroke, ischaemic stroke; TBI, traumatic brain injury.

charged arginine residues that comprise between 20 and 100% of the peptide; (iv) other positively charged amino acids namely lysine and histidine; (v) amphiphilicity due to the presence of both hydrophilic (e.g., arginine, lysine) and hydrophobic (e.g., tryptophan, phenylalanine, tyrosine) amino acids; and (vi) endocytic and/or non-endocytic cell membrane traversing properties, including the ability to cross the blood-brain and blood-spinal cord barriers (BBB/BSCB). Invariably, CARPs are commercially or chemically synthesized using solid-phase peptide synthesis. One exception is the CARP, protamine (**Table 3**), which is purified from salmon milt or generated recombinantly. Due to the capacity of CARPs to traverse cellular membranes and localize to different organs within the body, they have been the subject of several experimental and review articles examining their bioavailability (201–203) and therefore this subject is not covered in this review.

HISTORICAL OVERVIEW OF CARPS AND NEUROPROTECTION STUDIES

Key historical events in the recognition and application of CARPs as neuroprotective agents are summarized in **Figure 2**. The first study to identify the neuroprotective properties of CARPs was in 1998 when Ferrer-Montiel et al. (1) screened a 6-mer peptide library containing over 49,000 different peptides for their ability to block glutamate-evoked ionic currents in *Xenopus* oocytes expressing the NR1 and NR2A NMDA receptor subunits. Hexapeptides containing at least two arginine (R) residues at any position as well as one or more lysine (K), tryptophan (W), and cysteine (C) residues displayed ionic current blocking activity. Further analysis revealed that C-carboxyl amidated (-NH_2; note C-carboxyl amidation removes the negatively charged COO^- C-terminus thereby increasing peptide net charge by +1) dipeptides RR-NH_2 (net charge +3) and RW-NH_2 (net charge +2) were also capable of blocking NMDA receptor activity. Similarly, certain amino acid residues within arginine-rich hexapeptides inhibited the NMDA receptor blocking ability of the peptide (e.g., RFMRNR-NH_2; net charge +4, was ineffective; M, methionine; N, asparagine). In addition, increasing oligo-arginine peptide length from 2 to 6 resides (e.g., R2-NH_2 vs. R3-NH_2 vs. R6-NH_2) increased blocking activity. In a NMDA excitotoxicity model (NMDA: 200 μM/20 min) using cultured hippocampal neurons, arginine-rich hexapeptides (**Table 1**), especially those also containing one or two tryptophan residues displayed high-levels of neuroprotection, and the neuroprotective action of the peptides was not stereo-selective with L- and D-isoform peptides showing similar efficacy. The ability of tryptophan to improve peptide neuroprotective efficacy is of particular interest as tryptophan residues also increase the uptake efficacy of CCPPs (204–208).

Other observations concluded that: (i) whereas cationic arginine-rich hexapeptides were highly efficient at blocking NMDA receptor evoked ionic currents (80–100%), some peptides (e.g., RRRCWW-NH_2 and RYYRRW-NH_2) also blocked AMPA receptor currents by over 60%. In subsequent studies, the peptide RRRRWW-NH_2 was demonstrated to antagonize the vanilloid receptor 1 (VR1; also known as the transient receptor potential cation channel subfamily V member 1; TRPV1) mediated currents in a *Xenopus* expression system and reduce calcium influx in rat dorsal root ganglion neurons following capsaicin or resiniferatoxin VR1 receptor stimulation (2, 209).

Neuroprotective Properties of Cationic Arginine-Rich Cell-Penetrating Peptides TAT, R9, and Penetratin

Shortly after the work of Ferrer-Montiel et al. (1), the CCPP TAT (see **Table 1** for sequence and net charge) was demonstrated to have the capacity to transport large protein cargos across the BBB (210). Subsequently, the TAT peptide became increasingly utilized as a carrier molecule to deliver various cargos into the brain, including putative neuroprotective peptides and proteins (**Figure 2**). To date over fifty different TAT-fused neuroprotective peptides have been shown to have positive effects in different *in vitro* and/or animal CNS injury models (**Table 2**). However, not surprisingly in light of the Ferrer-Montiel et al. (1) findings, experiments in other laboratories demonstrated that the TAT peptide itself possesses modest neuroprotective actions in *in vitro* excitotoxicity and *in vivo* ischemic injury models (8–11). Subsequently, it was reported that the CCPPs, R9 (**Table 1**), and penetratin (**Table 1**) were 17- and 4.6-fold, respectively more neuroprotective than TAT in a severe cortical neuronal glutamic acid excitotoxicity cell death model (glutamic acid: 100

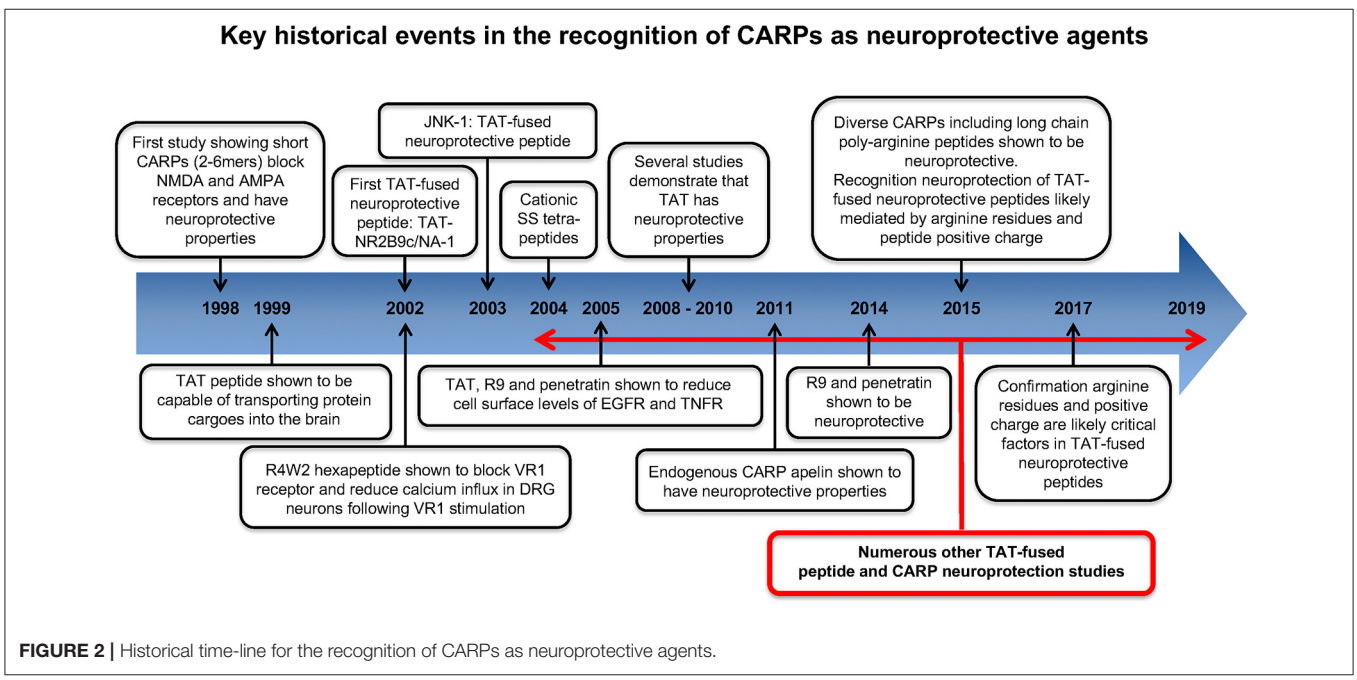

FIGURE 2 | Historical time-line for the recognition of CARPs as neuroprotective agents.

μM/5 min; **Figure 3**) (12). These findings also raised the first clues that the neuroprotective actions of putative neuroprotective peptides fused to CCPPs may in fact be mediated by the carrier peptide.

Further Validation and Characterization of CARPs as Neuroprotective Agents

Later, *in vitro* studies confirmed that other CARPs (e.g., protamine, LMWP, XIP; **Tables 1**, **3**) and long-chain poly-arginine peptides (**Table 1**) were also highly neuroprotective, with efficacy increasing with increasing arginine content and peptide positive charge, plateauing at around 15–18 arginine residues for arginine polymers (15, 16). Furthermore, the requirement for arginine residues, rather than lysine residues, was demonstrated to be critical for neuroprotection, with the K10 peptide (10-mer of lysine; net charge +10) displaying limited efficacy in a neuronal glutamic acid excitotoxic model (15). In addition, the importance of peptide charge was confirmed by the finding that the glutamic acid containing neutrally charged R9/E9 peptide (RRRRRRRRREEEEEEEEE; net charge 0; E = glutamic acid) displayed no neuroprotection in the excitotoxic model (15).

Based on the above findings, it was hypothesized that CARP neuroprotection is largely mediated by the positively charged guanidinium head-group, which is unique to arginine (**Figure 1A**) (note: lysine possesses a positively charged amide group; **Figure 1A**) (15, 109). These findings also support the notion that peptide neuroprotective efficacy appears to be correlated with the same features that are critical for the endocytic and/or non-endocytic membrane traversing properties of CCPPs (14, 15, 109, 211). It was also demonstrated in an *in vitro* glutamic acid excitotoxicity model that the hydrophobic aromatic amino acids tryptophan, and to a lesser extent phenylalanine and tyrosine can significantly improve CARP neuroprotective efficacy. In contrast, alanine and glycine resides reduce peptide neuroprotective efficacy (15, 16). Importantly, tryptophan residues are also known to increase the cell-penetrating properties of CCPPs, providing further evidence that neuroprotection is closely linked to the peptide membrane traversing capacity of the peptides.

Studies have also demonstrated that a 10-min pre-treatment of neuronal cultures with CARPs induces a pre-conditioning neuroprotective response lasting up to 2–5 h post-treatment (15–17). Similar to the findings of Ferrer-Montiel et al. (1), it was also observed that there was no stereo-selectivity in terms of neuroprotective efficacy of L- and D-enantiomer CARPs, which suggests that with respect to neuroprotection, peptide electrostatic interactions are more important than peptide structural interactions of the peptide with specific biological targets. Importantly, CARPs have the capacity to significantly inhibit neuronal intracellular calcium influx in the glutamic acid excitotoxicity model (15–17, 109).

Consistent with *in vitro* findings, CARPs (e.g., R9D, R12, R18, R18D, protamine; **Tables 1**, **3**) were also demonstrated to provide significant neuroprotection and improve functional outcomes in rat models of permanent and/or transient middle cerebral artery occlusion (MCAO), perinatal hypoxia-ischemia and traumatic brain injury (15, 16, 18–24, 212) and a non-human primate MCAO stroke model (26). Positive neuroprotective effects with R9D and R18D, which are the D-enantiomers of R9 and R18, also confirmed the lack of stereo-specificity for CARP efficacy *in vivo*.

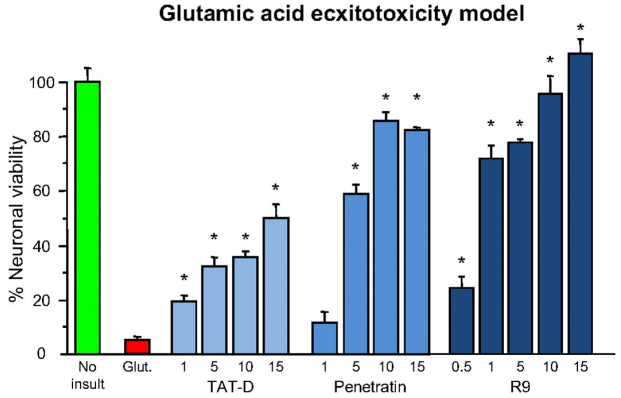

FIGURE 3 | Neuroprotective efficacy of cationic arginine-rich cell-penetrating peptides in glutamic acid excitotoxicity model. Peptides present in neuronal cultures for 10 min before and during (half concentration) 5-min glutamic acid exposure. Neuronal viability measured 24 h following glutamic acid exposure. Concentration of peptide in μM. MTS assay data were expressed as percentage neuronal viability with no insult control taken as 100% viability and glutamic acid control (Glut.) taken as 5% (mean ± SE; $n = 4$; $^{*}P < 0.05$). Adapted from Meloni et al. (12).

In 2015, Marshall et al. (14) also confirmed the *in vivo* neuroprotective properties of CARPs including poly-arginine R7 (**Table 1**), as well as the TAT and TAT-NR2B9c (also known as NA-1; **Table 2**) peptides in rat retinal ganglion cells exposed to NMDA (20 nmol; 3 μL intravitreal injection). The study also demonstrated that CARPs containing a terminal cysteine residue improved neuroprotective efficacy; this could be due to the cysteine residue improving peptide stability and/or enhancing anti-oxidant properties. Marshall et al. (14) also considered that it was likely that the cell-penetrating properties of the CARPs along with the guanidinium head group of arginine and peptide positive charge were the "driving force" for neuroprotection. Furthermore, and as proposed by Meloni et al. (211), Marshall et al. (14) also suggested that cargo peptides designed to inhibit cell death following NMDA excitotoxicity (e.g., peptides CN2097; CKNYKKTEV and NR2B9c; KLSSIESDV) and fused to a CCPP (e.g., R7 for CN2097 and TAT for NR2B9c) were unlikely to be the active component mediating neuroprotection in the retinal ganglion cell NMDA excitotoxic injury model.

In 2017, McQueen et al. (110) re-evaluated the neuroprotective mechanism of action of the death-associated protein kinase 1 protein (DAPK1) blocking peptide TAT-NR2Bct (**Table 2**) and its scrambled control TAT-NR2Bcts (**Table 2**). DAPK1 is a calcium-calmodulin regulated protein activated in neurons following NMDA receptor over-stimulation as occurs in ischemia mediated excitotoxicity. TAT-NR2Bct was designed to competitively inhibit activated DAPK1 binding to the NR2B subunit protein, and thereby block subsequent downstream damaging cellular events caused by NMDA receptor over-activation. Interestingly, Meloni et al. (109) had earlier examined

the TAT-NR2Bct and TAT-NR2Bcts peptides and demonstrated high neuroprotective efficacy for both peptides in the glutamic acid excitotoxicity model. Therefore, it was not surprising that McQueen et al. (110) also found that both TAT-NR2Bct and TAT-NR2Bcts, along with a randomly designed CARP (RRRTQNRRNRRTSRQNRRRSRRRR; net charge +15) were neuroprotective in a neuronal NMDA excitotoxicity model. On the basis of their findings they concluded that neuroprotection was dependent on peptide positive charge and independent of peptide sequence and DAPK1 signaling.

Taken together, the above studies provide irrefutable evidence of the neuroprotective properties of CARPs in various experimental situations and in doing so, raise two important issues in regard their application in neuroprotection: (i) what are the precise neuroprotective mechanisms operating; and (ii) the need to re-evaluate studies using CARPs and CCPPs for the delivery of neuroactive cargos into the CNS, particularly putative neuroprotective peptides. Both these topics are discussed below. Also, because it is likely that CARPs interact with negatively charged cell membrane structures, an interaction that appears to be critical for neuroprotection, the mechanisms associated with the affinity of CARPs to cell membranes will also be discussed. Interestingly, it is the interaction of CARPs with negatively charged bacterial and cancer cell cytoplasmic membrane structures that is considered to be one of the mechanisms responsible for their anti-bacterial and anti-cancer properties (213, 214).

PUTATIVE NEUROACTIVE PEPTIDES FUSED TO CATIONIC ARGININE-RICH CELL-PENETRATING PEPTIDES AND NEUROPROTECTION

Given that CARPs possess intrinsic neuroprotective properties raises questions regarding the mode of action of other putative neuroprotective peptides when they are fused to a carrier CCPP (**Table 2**). As alluded to above, it is likely that the neuroprotection provided by such putative neuroprotective peptides fused to CCPPs, is mediated not by the actions of the cargo molecule *per se*, but by the carrier itself with potency being further enhanced by the amino acid content (e.g., arginine, lysine, cysteine, and tryptophan resides) and/or stability provided by the cargo peptide. In essence, a putative neuroprotective peptide fused to an arginine-rich cell-penetrating carrier peptide will possess the properties of a CARP; the only exception being if a negatively charged cargo peptide neutralizes the positive charge of the carrier peptide.

In 2015 we published a review article (109) highlighting the likelihood of the neuroprotective mechanism of action of putative neuroprotective peptide fused to cell-penetrating carrier peptides being mediated by the carrier molecule. Three of the most commonly used TAT-fused neuroprotective peptides TAT-NR2B9c, TAT-JNKI-1 and TAT-CBD3, as well as several other less characterized TAT-fused peptides (e.g., TAT-p53DM, TAT-s-p53DM, TAT-NR2Bct, TAT-NR2Bcts, Indip/IndipK-R) were analyzed based on theoretical grounds, and on our own and other previous experimental studies in relation to neuroprotective mechanism of action. Following this analysis, we provided several lines of evidence to support the view that TAT-fused neuroprotective peptides are behaving as neuroprotective CARPs, and not by the proposed intended mechanism of action of the cargo peptide. This evidence included: (1) the ability of the peptides to reduce intracellular calcium influx, even though this was never an intended mechanism of action of the cargo peptide; (2) despite targeting intracellular proteins, the peptides often reduced surface expression or interfered with plasma membrane ion channel receptors; (3) lack of efficacy and inability of the peptide to reduce neuronal calcium influx when introduced directly into the cell; (4) improved peptide efficacy when TAT was replaced with R9 (increasing peptide positive charge and arginine content) or replacing neutral or negatively charged amino acids with positively charged arginine or lysine; (5) decreased peptide efficacy when replacing amino acids with alanine, which is known to reduce membrane traversing properties of cell-penetrating peptides; (6) demonstrating neuroprotective properties of CCPP-fused scrambled cargo control peptides; and (7) due to endosomal entrapment and/or peptide degradation it is possible cargo peptides have a limited capacity to interact with their intended intracellular target. Importantly, the subsequent studies of Marshall et al. (14) and McQueen et al. (110) (described above) further validate the view that the mechanism of action of TAT-fused neuroprotective peptides is likely to be mediated by the carrier peptide, and by extension the arginine content and positive charge of the peptide.

In order to confirm the specific action of a neuroactive peptide cargo fused to a carrier CCPP, we recommend that the neuroprotective or other intended neuroactive actions of the peptide should be reassessed after the introduction of arginine substitutions into the cargo peptide. The introduction of arginine residues into the cargo peptide should abolish the proposed/intended neuroprotective action of the cargo peptide. However, if the action of the carrier-cargo peptide is maintained or enhanced it is likely that the neuroprotective action of the peptide was mediated by the cationic and arginine-rich properties of the peptide. Alternatively, the peptide could be synthesized in the same amino acid sequence (as opposed to retro-inversely) with D-isoform amino acids, which would drastically alter the peptide's steric structure and binding specificity/affinity to its intended target, whereas its electro-physiochemical properties would be similar. Finally, the CCPP carrier molecule could be replaced with a non-arginine containing cell-penetrating peptide (e.g., TP10 or MAP).

CARPS AND THEIR INTERACTION WITH CELLULAR MEMBRANES

CARPs have the capacity to form electrostatic interactions with anionic phosphate, sulfate and carboxylate moieties (**Figure 1B**) present on structures found in the plasma membrane and in membranes of cellular organelles (e.g., mitochondria, nucleus, endoplasmic reticulum, golgi, endosomes). These anionic

chemical moieties are located within membrane proteoglycans (heparin sulfate proteoglycans: HSPGs; chondroitin sulfate proteoglycans: CSPGs; dermatan sulfate proteoglycans: DSPGs; keratin sulfate proteoglycans: KSPGs), glycoproteins, glycosphingolipids, and phospholipids as well as negatively charged aspartate and glutamate residues within protein receptors and other protein structures embedded in cellular membranes (**Supplementary Table 1**).

Negatively charged phosphate groups are a component of phospholipids that make-up cellular membrane bilayers (e.g., plasma membrane, inner and outer mitochondrial membrane, nuclear membrane, and endoplasmic reticulum membrane). There are at least five negatively charged membrane phospholipids including the mitochondrial membrane specific phospholipid cardiolipin, which possess a net charge of between −1 to −4 at pH 7 (**Supplementary Table 1**).

Proteoglycans a type of glycoprotein found on the surface of most cells and consist of a protein core and glycosaminoglycans (GAGs), which are long un-branched polysaccharides consisting of a repeating disaccharide subunit. Negatively charged sulfate groups are located on the polysaccharide repeating disaccharide subunits. In addition, the monosaccharide sialic acid is located at the end of the sugar chains attached to glycoproteins and has a negatively charged carboxyl group. Glycoproteins have important cellular functions, such as cell surface ligand receptor binding, cell signaling, cell adhesion, endocytosis, and binding extracellular matrix molecules (e.g., growth factors, enzymes, protease inhibitors, chemokines).

Glycolipids consist of a membrane lipid moiety covalently attached to a monosaccharide or polysaccharide. Glycolipids, namely glycosphingolipids, are negatively charged due to the presence of sialic acid. A glycosphingolipid containing one or more sialic acid residues is also known as a ganglioside. Gangliosides are expressed on most cells, but are more abundantly expressed on the cell surface of neurons, and are found ubiquitously throughout the CNS (215). They play a key role in modulating ion channel function, receptor signaling, cell-to-cell recognition and adhesion and regulation of neuronal excitability (216, 217). Membrane protein receptors rich in the acidic amino acids aspartate and glutamate also possess a negatively charged carboxylic moiety on their side chain.

With respect to the interaction of CARPs with anionic moieties, the positively charged arginine guanidinium head group forms bidentate hydrogen bonds with sulfates, carboxylates and phosphates, whereas the positively charged lysine amide head group forms weaker monodentate hydrogen bonds (**Figure 1B**). In addition, arginine and lysine cationic side chains can form salt bridges with the negatively charged aspartate and glutamate carboxylate C-termini, and cation-π interactions with the aromatic amino acids tryptophan, phenylalanine and tyrosine in proteins (218, 219). Interestingly, many neurotransmitters and drug-receptor interactions involve cation-π interactions (219). Together, the different electrostatic interaction between CARPs and plasma membrane structures can induce cellular uptake of the peptide by endocytic and non-endocytic pathways (220–224). Furthermore, peptide charge, arginine content and arginine distribution within the peptide, and the extent and density of the negatively charged moieties present on the cell surface play a significant role in terms of uptake efficacy (225–227). Peptide positive charge and arginine guanidinium head groups are also critical elements responsible for the ability of CARPs to target organelle membranes, such as the outer and inner mitochondrial membranes, which contain the negatively charged phospholipids cardiolipin (charge −2) and phosphatidylinositol 4, 5-bisphosphate (PIP2; charge −4) (**Supplementary Table 1**).

Importantly, studies have demonstrated that peptide characteristics that are known to increase the cell membrane traversing properties of CARPs, such as arginine content, peptide charge and presence of the aromatic amino acid tryptophan are also linked to increased peptide neuroprotective potency (1, 15, 16, 211).

CARPS HAVE MULTIMODAL NEUROPROTECTIVE MECHANISMS OF ACTION

Data obtained in our laboratory and others using neuronal and non-neuronal cells indicate that CARPs have multimodal mechanisms of action targeting cell surface ion channel receptors and other receptors, mitochondria, proteolytic enzymes, oxidative stress/free radical molecules, protein stability, and pro-survival signaling, as well as having anti-inflammatory and immune regulatory actions (**Figure 4**). Evidence supporting these different neuroprotective mechanisms is provided below.

Inhibition of Excitotoxic Neuronal Death and Excitotoxic Neuronal Calcium Influx

Our laboratory has established that CARPs are highly effective at reducing excitotoxic neuronal death and that they have the capacity to reduce glutamic acid induced neuronal calcium influx (9, 10, 15, 19, 109). These findings provide a mechanism in which CARPs inhibit glutamate-evoked ionic currents in *Xenopus* oocytes expressing NMDA receptors (1), and NMDA excitotoxic neuronal death in neuronal cultures *in vitro* and retinal ganglion cells *in vivo* (14, 59, 69, 110). In addition, other CARPs reduce potassium depolarization-induced calcium-influx (e.g., R9-CBD3-A6K, TAT-L1, TAT-ct-dis) and sodium currents and sodium influx (e.g., t-CSM) in cultured dorsal root ganglion neurons (see **Supplementary Table 2** for details).

The ability of CARPs to reduce glutamate receptor and other receptor mediated intracellular neuronal calcium influx is likely to be a primary mechanism accounting for their neuroprotective efficacy in protecting neurons in injury models associated with excitotoxicity and excessive neuronal intracellular calcium influx. As a mechanism whereby CARPs act to reduce the intracellular influx of calcium and potentially other ions, we hypothesized (109) that CARPs have the capacity to induce the endocytic internalization of cell surface ion channel receptors (**Figure 4**). In support of this hypothesis we subsequently showed that R12, as well as the TAT-fused neuroprotective peptide TAT-NR2B9c, reduces neuronal cell surface expression of the glutamate receptor subunit protein, NR2B (228). Importantly, several

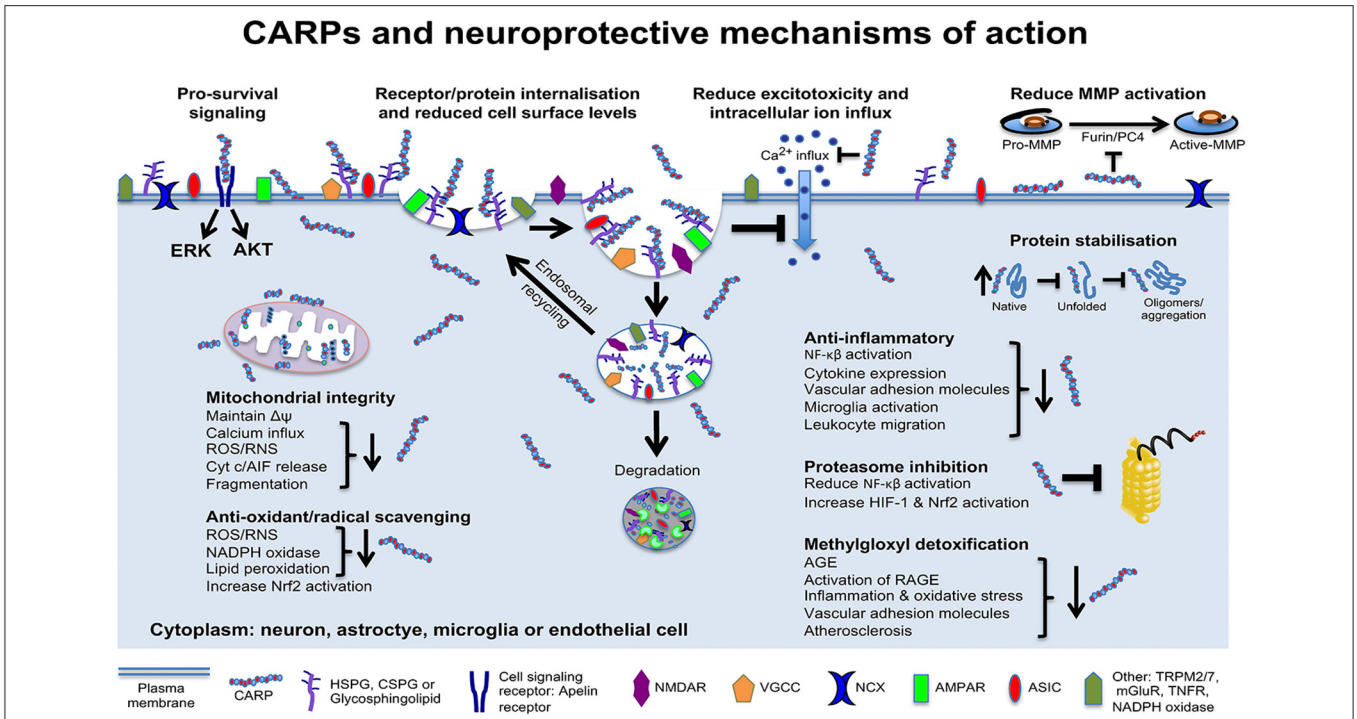

FIGURE 4 | Schematic representation of CARP neuroprotective mechanisms of action. Model applies to neurons and potentially astrocytes, brain endothelial cells, oligodendrocytes, pericytes, and microglia. AGE, advanced glycation end products; RAGE, AGE receptors; AIF, apoptosis inducing factor; AKT, protein kinase B; Cyt c, cytochrome c; ERK, extracellular signal–regulated kinase; HIF-1, hypoxia-inducible factor-1; MMPs, matrix metalloproteinases; $\Delta\psi$, mitochondrial transmembrane potential; NF-κB, nuclear factor kappa-light-chain-enhancer of activated B cells; Nrf2, nuclear factor erythroid 2-related factor 2; RNS, reactive nitrogen species; ROS, reactive oxygen species. NMDAR, N-methyl-D-aspartate receptor; AMPAR, α-amino-3-hydroxy-5-methyl-4-isoxazolepropionic acid receptor; NCX, sodium calcium exchanger; VGCC, voltage-gated calcium channels; ASIC, acid-sensing ion channels; TRPM2/7, transient receptor potential cation channels 2 and 7; mGluR, metabotropic glutamate receptor; TNFR, tumor necrosis factor receptor.

CCPPs (e.g., TAT, penetratin, R9) have also been demonstrated to reduce TNF (tumor necrosis factor) and EGF (epidermal growth factor) receptors in non-neuronal cells via an endocytic internalization mechanism (**Supplementary Table 2**) (229).

Interaction With Membrane Ion Receptors/Channels/Transporters

Many other studies have described the ability of CARPs to reduce neuronal and non-neuronal cell surface levels and/or activity of NMDA receptors, and other ion and non-ion channel receptors (see **Supplementary Table 2**). While these studies provide ample evidence for the ability of CARPs to perturb cell surface receptors it raises the question how different peptides with diverse amino acid sequences possess the ability to reduce cell surface levels and/or antagonize receptor function. As mentioned above, one mechanism involves CARP induced internalization of cell surface receptors. However, it is also possible CARPs antagonize ion channel receptor function by electrostatic interactions. For example, CARP electrostatic interactions with receptor anionic moieties may alter receptor function or interfere with ion transport within the receptor pore. In support of this, the guanidine moiety in arginine residues and in other molecules play a critical role in voltage-gated and ligand-gated ion channel function (see section Compounds Containing the Guanidinium Moiety and Neuroprotection) (230–237). For example, the guanidino moiety in agmatine, a molecule with neuroprotective properties (**Supplementary Table 3**), has been identified as being capable of interacting with a site within the NMDA receptor channel and calcium voltage channels and blocking their function (238). Interestingly, polyamines (e.g., putrescine and spermine) a class of compounds that also contain positively charged amino groups also have the capacity to block ion channels, including glutamate receptor and potassium channels (239). Given that positive charge is a critical factor for CARP neuroprotection and charge is independent of peptide amino acid sequence, provides additional support for a mechanism involving an electrostatic interaction perturbing ion channel function. Hence, there is good evidence to indicate that the structure and charge of the guanidine moieties in CARPs have the capacity to block ion channel receptor function, providing an additional mechanism whereby the peptides can reduce the toxic effects of intracellular ion influx associated with excitotoxicity and ion channel over-stimulation.

Mitochondrial Targeting and Maintenance of Mitochondrial Integrity

CARPs have the capacity to target mitochondria and exert positive effects on the organelle, with potential neuroprotective

outcomes. This topic has been the subject of several reviews by the developers of the mitochondrial targeting SS cationic arginine-containing tetrapeptides (240), and more recently by our own laboratory (241), and therefore will be discussed only briefly here.

After entering cells, CARPs target and enter mitochondria due to the presence in the outer and inner mitochondrial membranes of negatively charged phospholipids (e.g., cardiolipin, PIP2), and because of the mitochondrial transmembrane potential ($\Delta\Psi m$). It is also possible that electrostatic interactions of CARPs with negatively charged free mitochondrial DNA contributes to the retention of the peptides in the organelle. At the site of the outer mitochondrial membrane, CARPs can inhibit the toxic influx of calcium into mitochondria, possibly by perturbing ion channel receptors (e.g., MCU, VDAC, NCX) and other membrane proteins (e.g., mitochondrial permeability transition pore proteins) responsible for the movement of calcium ions into mitochondria.

CARPs can also perturb other outer membrane proteins that are detrimental to mitochondrial function and cell survival. For example, CARPs interfere with BAX, the mitochondrial permeability transition pore and other pro-apoptotic proteins that localize to the outer mitochondrial membrane during cell death or interfere with proteins that promote mitochondrial fission and mitophagy. Inhibition of mitochondrial fission enables maintenance of mitochondria as filamentous structures, which enables toxic products generated by dysfunctional mitochondria to be distributed over a large organelle volume and thereby minimizing any detrimental effects. Furthermore, due to their interactions with cardiolipin, CARPs assist in stabilizing and preserving cristae architecture and the electron transport chain with positive effects on ATP maintenance, reduced reactive nitrogen species/reactive oxygen species (ROS/RNS) generation, as well as maintenance of cytochrome c native tertiary structure, function, oxidation state and location within the inner mitochondrial membrane. In addition, the anti-oxidant and free radical scavenging properties of CARPs (discussed below) would also have positive influences in reducing the toxic effects of excessive ROS/RNS generation by mitochondria during cellular stress.

Anti-oxidant and Free Radical Scavenging Properties

Due to the amino acid arginine, CARPs are likely to act as anti-oxidant and/or free radical scavenging molecules in their own right. Although L-arginine is utilized by nitric oxide synthase as a substrate for nitric oxide generation, which is a key regulator of endothelial cell function and blood flow, the amino acid has other properties. Arginine is unique in possessing a N-terminal guanidinium head group (**Figure 1A**) and guanidinium containing small molecules are known to possess properties that mitigate the effects of oxidative stress. For example, L- and D-arginine, along with aminoguanidine, methylguanidine, guanidine, and creatine, which are all structurally related to arginine have the ability to scavenge one or more of the following reactive molecules: superoxide, peroxynitrate, hydroxyl radicals, hydrogen peroxide, hypochlorous acid, and breakdown products of lipid peroxidation (e.g., reactive aldehydes: malondialdehyde and 4-hydroxynonenal) (242–249).

The anti-oxidant properties of aminoguanidine, which also possesses neuroprotective actions (**Supplementary Table 3**), were demonstrated *in vitro* with the agent reducing rat retinal Muller cell hydrogen peroxide oxidant induced apoptosis, ROS production and lipid peroxidation, and *in vivo* by reducing the level of lipid peroxides in the vitreous of diabetic rats (246). Furthermore, both L- and D-arginine reduced oxidative impairment to myocardial contractility of perfused rat hearts subjected to oxygen radical generation (249). L- and D-arginine and L- and D-arginine polymers (e.g., poly-arginine R9) have beneficial effects on vascular endothelial cell and cardiovascular function and have anti-atherosclerotic properties (242, 250–252). These positive effects have also been observed with D-arginine containing peptides and therefore are likely to be independent of the nitric oxide pathway, as D-arginine is not readily metabolized by nitric oxide synthase. In support of this, in *Caenorhabditis elegans,* which lacks nitric oxide synthase (NOS), exposure to exogenous L-arginine prolongs worm lifespan under oxidative stress growth conditions (253).

Szeto-Schiller (SS) peptides are short tetrapeptides with alternating basic (e.g., arginine, lysine, or ornithine) and aromatic (e.g., tyrosine, dimethyltyrosine, tryptophan, or phenylalanine) amino acids, but usually containing at least one arginine and one tyrosine or dimethyltyrosine residue (240). Several SS peptides (e.g., SS-31, SS-20, mCPP-1; **Table 1**) have demonstrated anti-oxidant properties by way of reducing ROS levels in cells grown under normal or oxidative stress conditions. Whereas, the anti-oxidant action of SS peptides has been attributable to the tyrosine and dimethyltyrosine residues, based on the free radial scavenging properties of guanidinium containing molecules it is likely that the arginine residue also contributes to the anti-oxidant property of SS peptides.

Larger CARP's also have anti-oxidant and lipid peroxidation reducing properties. A lactoferrin derived peptide f8 (GRRRR SVQWCAVSQPEATKCFQWQRNMRKVRGPPVSCIKRDSP IQCIQ; net charge +8.7) and a casein derived peptide f12 YP YYGTNLYQRRPAIAINNPYVPRTYYANPAVVRPHAQIPQ RQYLPNSHPPTVVRRP; net charge +7.2) have demonstrated anti-oxidant activity in an *in vitro* free radical scavenging assay (254). While both f8 and f12 are large peptides with interspersed arginine residues, molecular modeling revealed the peptides display a configuration with a highly cationic electrostatic surface, with arginine residues facing on the outside of the peptide. In addition, the human cathelicidin anti-microbial peptide LL-27 (LGDFFRKSKEKIGKEFKRIVQ RIKDFL; net charge +5) inhibits the oxidation of low density (LDL) and high density (HDL) lipoproteins and can reduce fatty acid hydroperoxides in *in vitro* oxidation models (255). As demonstrated with protamine, CARPs also bind negatively charged oxidized-LDLs, inhibit their engagement to the lectin-like oxidized low-density lipoprotein receptor-1 (LOX-1), which can stimulate intracellular signaling cascades detrimental in ischemia-reperfusion cerebral injury (256, 257). Similarly, the cathelicidin PR-39 (RRRPRPPYLPRPRPPPFFPPRLPPRIPP GFPPRFPPRFP; net charge +10) protects HeLa cells from

apoptotic cell death induced by the oxidizing agent tert-butyl hydroperoxide (198), and inhibits hypoxia induced cell death of endothelial cells (199).

Another mechanism how CARPs can reduce oxidative stress is by inhibiting the activity of the plasma membrane superoxide generating enzyme complex nicotinamide adenine dinucleotide phosphate oxidase (NADPH oxidase), with one study indicating inhibition is associated with the presence of poly basic amino acid consisting of arginine, lysine or histidine motifs (258). The CARPs PR-39, PR-26 (amino acids 1–26 of PR-39; net charge +8), gp91ds-tat (**Table 2**), and TAT-NR2B9c all inhibit NADPH oxidase function or superoxide generation in cell free systems and/or in different cells both *in vitro* and *in vivo* (259–261). The NADPH oxidase complex consists of 5 subunits with PR-39 and PR-26 binding to the SH3 (SRC homology 3) domain within the $p47^{phox}$ subunit, which disrupts binding to the $p22^{phox}$ subunit (261). The gp91ds-tat is derived from the NADPH oxidase Nox2 cytosolic B loop (mouse Nox2; amino acids 86–94) subunit and was designed to inhibit Nox2 interacting with $p47^{phox}$ (260). TAT-NR2B9c inhibits the generation of superoxide and phosphorylation of $p47^{phox}$ in cultured neurons exposed to NMDA (259). It was concluded that inhibition of NMDA receptor-PDS-95 mediated signaling by TAT-NR2B9c prevented phosphorylation of $p47^{phox}$ and activation of NADPH oxidase. However, for both the gp91ds-tat and TAT-NR2B9c peptides a direct inhibitory action on NADPH oxidase associated with the arginine content and positive charge of the peptides cannot be ruled out. In addition, given all four peptides have cell-penetrating properties, it is possible that these and other CARPs disrupt the membrane assembly of NADPH oxidase units within the plasma membrane. Since superoxide generation is also associated with inflammatory responses, inhibition of NADPH oxidase activity would also contribute to the anti-inflammatory properties of CARPs.

While the anti-oxidant properties of CARPs need to be further investigated, available evidence suggests that arginine residues within the peptide have the potential to exert anti-oxidant and/or free radical scavenging actions. Furthermore, it could be hypothesized that the multiple arginine resides within CARPs will act as a multivalent anti-oxidant compound, which depending on the number and arrangement of the guanidinium moieties would provide considerably more potency per molecule than arginine alone or a molecule containing a single guanidine moiety.

Methylglyoxal Scavenging and Glycation End-Products

Glyoxal compounds are highly reactive cell permeable dicarbonyls produced predominantly as a by-product of glycolysis, and are precursors in the formation of advanced glycation end-products (AGEs). An important dicarbonyl with respect to cellular toxicity is methylglyoxal, which reacts irreversibly with arginine and lysine residues and reversibly with cysteine resides on proteins causing functional impairment (262). Methylgyloxal also reacts with nucleic acids and lipids, and its production is associated with oxidative stress and ROS generation. The glycation of arginine and lysine by methylglyoxal forms the AGEs hydro-imidazolone, methylglyoxal-hydroimdazolone 1 (MG-H1), argpyrimidine, and MG-derived lysine dimer. In addition, to altering protein function, AGE-modified proteins interact with AGE receptors (RAGE), which stimulate the expression of inflammatory genes and ROS generation. AGEs are increased in diabetes, vascular disease, cerebral ischemia, renal failure, aging and chronic disorders, such as Alzheimer's disease, Parkinson's disease and liver cirrhosis. Methylgyloxal can affect mitochondrial function, up-regulate vascular adhesion molecules (e.g., P-selectin and E-selectin) that contribute to leucocyte adhesion (263), and cause glycation of the BBB vascular tight junction protein occluding (264) and the basement membrane extracellular protein fibronectin (265) resulting in altered endothelial function.

Given that methylglyoxal readily targets basic amino acids, it is likely that arginine (and lysine/cysteine) residues within CARPs react with and act as methylglyoxal scavengers, thereby reducing their toxic effects on intra- and extra-cellular proteins, and RAGE activation. Methylgloxal is normally detoxified by the glyoxalase system (glyoxalase-1 and glyoxalase-2), which utilizes glutathione as a co-factor, however neurons are particularly susceptible to methylgloxal due to the high glycolytic activity of the brain and the reduced capacity of the glyoxalase system in neurons. The capacity of the glyoxalase system in the brain deceases with age, especially after the fifth decade of life, and an increase in MG-H1 modified mitochondrial proteins is linked to aging and increased ROS production (266); increasing glyoxalase capacity in *C. elegan* increases life span in this organism (267). Furthermore, any additional stress within the brain as occurs in cerebral ischemia/reperfusion, as well as in chronic neurological disorders is likely to lead to an excessive production of methylgloxal and/or reduced capacity to detoxify methylgloxal.

Importantly, arginine and other guanidinium containing molecules (e.g., aminoguanidine, metformin) have the capacity to scavenge methylglyoxal and prevent AGEs (268, 269). For example, at one stage aminoguanidine was being developed as a therapeutic agent for the prevention of AGEs in diabetes, and both L- and D-arginine can effectively scavenge and attenuate the harmful effects of methylgloxal on cultured endothelial cells (270). However, it is considered that small molecule methylglyoxal scavengers are not sufficiently potent and/or suffer from short half-lives to be effective *in vivo*. In contrast, arginine-containing penta-peptides peptides (CycK[Myr]RRRRE; Cyc, cyclic peptide; Myr, myristic acid; and myr-KRRRRE; net charge +4) also possess methylglyoxal scavenging activity (271), and CycK(Myr)RRRRE prevents methylglyoxal induced pain in mice, and is being considered as a therapy for pain and other diabetic complications associated with methylglyoxal toxicity (271).

Inhibition of Matrix Metalloproteinase Activation and the Proteasome

Another mechanism whereby CARPs may exert a neuroprotective effect is by their ability to indirectly prevent the

activation of matrix metalloproteinases (MMPs) by inhibiting proprotein convertase (PC) activation. Proprotein convertase consists of a family of proteolytic enzymes that cleave inactive proteins, including MMPs into an active state. Poly-arginine peptides and other CARPs are potent inhibitors of convertases, such as furin, PC1, PC4, PC5/6, and PC7 (272–276).

Furin is a ubiquitously expressed convertase that is regulated by hypoxia-inducible factor-1 (HIF-1) (277) and up-regulated in the ischemic brain (278, 279), and can activate MMP2, MMP3, and MMP14 (280). Furthermore, MMP3 can activate MMP1, MMP7 and MMP9, and MMP14 can activate MMP2 and MMP2 can activate MMP9 (281, 282). Significantly, following ischemic stroke MMP2, MMP3, MMP7, MMP9, and MMP14 are either up-regulated or activated in the brain. Moreover, MMP activation is associated with degradation of the neurovascular unit and BBB disruption, which in turn can result in cerebral edema, leukocyte infiltration and secondary hemorrhage after ischemia (279, 281, 282). It is also possible that proprotein convertases have other protein substrates, which when activated are potentially neuro-damaging, however this is an area that has as yet not been explored.

The ability of poly-arginine peptides to inhibit proprotein convertases, similar to peptide neuroprotection (15), increases with increasing polymer length (e.g., R9 > R8 > R7 > R6) (272). In addition, convertase inhibition is not stereospecific with both to L- and D-isoform peptides having the capacity to inhibit enzyme activity. The electrostatic interaction between CARPs and the negatively charged surface of convertases is believed to be the mechanism responsible for the inhibitory actions of the peptides. Interestingly, a penetratin-fused peptide (P-IQACRH: RQIKIWFQNRRMKWKK-IQACRG; net charge +7.9) that mimics the active site of caspases 1, 2, 3, 6, 7 and 14 and acts as a competitive inhibitor for these enzymes, inhibited caspase and MMP9 activation following NMDA-induced excitotoxicity in an *in vivo* retinal ganglion cell injury model (283). However, the peptide also reduced NMDA-induced retinal ganglion cell death in culture and *in vivo*, and hence it is possible that the anti-excitotoxic properties of P-IQACRH, rather than a direct down-stream inhibition of caspases and MMP9 was responsible for blocking the activation of the enzymes. The P-IQACRH study highlights the caution that is needed when analyzing the neuroprotective actions of CARPs.

CARPs can also inhibit other proteolytic enzymes, such as cathepsin C (284) as well as, the activity of the proteasome (285–289). Importantly, treatments known to inhibit the proteasome, which is responsible for the degradation of short-lived cytosolic proteins, is known to reduce the severity of brain injury after stroke (290–293).

With respect to proteasomal inhibition, the CARP PR-39 (see above) can reversibly bind to the α7 subunit of the 26S proteasome and block degradation of the nuclear factor-κB (NF-κB) inhibitor protein IκBα. Interestingly, studies utilizing PR-39 indicate that proteasomal inhibition occurs via a unique allosteric, reversible and substrate selective mechanism without inhibiting overall-proteasome proteolytic activity, which in itself could be deleterious by interfering with normal cellular processes. In contrast, mild levels of proteasome inhibition can induce a protective pre-conditioning response that can protect cells from oxidative stress (294). Similarly, ischemic pre-conditioning, which can reduce brain injury following stroke is associated with proteasomal inhibition (293). PR-39 abolished NF-κB-dependent gene expression in cultured endothelial cells exposed to TNF-α, and in the pancreases and hearts of mice following induction of acute pancreatitis and myocardial infarction, including the up-regulation of vascular cell adhesion molecule-1 (VCAM-1) and intercellular adhesion molecule-1 (ICAM-1) (285). Other studies have also demonstrated that PR-39 can reduce infarct size and have beneficial effects on microvascular cells in myocardial reperfusion injury models by blocking proteasome-mediated degradation of IκBα (200).

In contrast to blocking activation of the NF-κB, inhibition of the proteasome is likely to enhance activation of the transcription factor HIF-1, which is considered one of the most critical adaptive gene expression responses to low oxygen concentrations. Hypoxia-inducible factor-1 consists of the HIF-α and HIF-β subunits, the former undergoing proteasomal degradation during normoxia, and the latter being constitutively expressed. Therefore, inhibition of the proteasome will enhance and/or prolong HIF-1 activation in the brain during and following cerebral ischemia, thereby enhancing any neuroprotective actions of the transcription factor. For example, PR-39 was demonstrated to inhibit the proteasome-dependent degradation of HIF-α and stimulate angiogenesis by accelerating the formation of vascular structures in cultured endothelial cells and *in vivo* in the myocardium (295). A similar effect was demonstrated in the brain after stroke with a small molecule proteasome inhibitor resulting in accumulation of HIF-α and enhanced angio-neurogenesis (291).

Inhibition of the proteasome can also enhance the activity of the transcription factor nuclear factor E2-related factor 2 (Nrf2), which regulates the expression of multiple cytoprotective genes, particularly those involved in mitigating oxidative stress (e.g., HO-1, SOD1, NAD[P]H dehydrogenase, glutathione S-transferase) (296). Under normal conditions, cytoplasmic Nrf2 is bound to kelch-like ECH-associated protein 1 (Keap1), in which it is subject to proteasomal degradation, however oxidative stress disables keap1, allowing Nrf2 to accumulate, translocate to the nucleus and activate gene expression. Interestingly, a Nrf2 amino acid derived sequence (LQLDEETGEFLPIQ) has been developed that disrupts the Nrf2-Keap1 interaction, and when fused to TAT (TAT-14: YGRKKRRQRRR-LQLDEETGEFLPIQ; charge +4) or R7 (7R-ETGE: RRRRRRRR-LQLDEETGEFLPIQ; net charge +4) has been demonstrated to activate Nrf2 and cytoprotective gene expression in THP-1 monocyte and RAW 264.7 macrophage cell lines (297, 298). Furthermore, the TAT-14 peptide modified to contain a calpain cleavage sequence (TAT-CAL-DEETGE: **Table 2**) increased Nrf2-regulated gene expression in the brain (299) and is beneficial when administered to rodents after global cerebral ischemia and TBI (154, 299). It remains to be determined if the Nrf2 peptides are activating Nrf2 by directly disrupting the Nrf2-Keap1 interaction or by inhibiting the proteasome. Also of interest is the demonstration that in rats, oral treatment with arginine, resulted in the up-regulation of proteins associated with the Nrf2 pathway in liver and plasma (300).

Reducing the Inflammatory Response

Whereas, few studies have specifically examined neuroprotective CARPs in the setting of neuro-inflammation, this class of peptide has well-established anti-inflammatory properties that are potentially beneficial in neurodegenerative disorders. It is likely CARPs exert differential effects on the immune response by targeting both the CNS and peripheral immune responses by several mechanisms. As explained above, the ability of CARPs to inhibit the proteasome will reduce NF-κB activation and the expression of genes involved in pro-inflammatory pathways. Interestingly, the CARP AIP6 (RLRWR; net charge +3) can inhibit NF-κB activity by an alternative mechanism, by binding to and blocking NF-κβ p65 sub-unit binding to DNA and inhibiting its transcriptional activity (301). The p65 subunit is a negatively charged protein, and hence it is possible that CARPs have the capacity to interfere with this NF-κβ sub-unit through an electrostatic interaction. Similarly, because CARPs can interfere with cell surface receptors levels and/or function, it is also possible they reduce the inflammatory response associated with ligands (e.g., cytokines, chemokines, intracellular molecules) binding to receptors on immune cells.

Proteins regulated by NF-κB and involved in the inflammatory response include cytokines (e.g., IL-1, TNF-α), chemokines (e.g., MCP-1, CXCL1) and vascular adhesion molecules (e.g., ICAM-1, VAM-1) (302). To this end, NF-κB is responsible for up-regulating cerebral vascular adhesion molecules VCAM-1 and ICAM-1, which during cerebral reperfusion promotes macrophage and neutrophil infiltration into the brain. Although the ability of CARPs to reduce vascular adhesion molecule expression in the cerebral vasculature has not been examined, PR-39 can reduce VCAM-1 and ICAM-1 protein levels in heart tissue following myocardial infarction in mice and in cultured vascular endothelial cells following exposure to TNF-α (285), and leukocyte adhesion to rat mesenteric venules after ischemia and reperfusion (303). In addition, the TAT peptide reduces the production of multiple cytokines (e.g., G-CSF, IL-6, MIP1α, TNF-α, and IFN-γ) in cultured human lung epithelial cells following protein kinase C stimulation by phorbol 12, 13-dibutyrate, a stimulus associated with NF-κβ activation (304). In line with the ability of CARPs to inhibit the proteasome, TAT reduced degradation of the NF-κβ inhibitory subunit IK-κβ in lung epithelial cells following protein kinase C activation. Similarly, AIP6 demonstrated anti-inflammatory effects in cultured activated macrophages by decreasing TNF-α and prostaglandin-E secretion and in a mouse model of paw inflammation reduced levels of TNF-α, IL-1β, and IL-6 protein in affected tissue (301).

CARPs can also bind to oxidized phospholipids (e.g., ox-LDLs) which are known pro-inflammatory molecules and play an important role in atherosclerosis and other inflammatory disorders. Due to the high lipid content of the brain, any conditions that increase oxidative stress will generate oxidized phospholipids. Binding of CARPs to oxidized phospholipids is believed to enhance their clearance, as well as reduce their inflammatory potential and inhibitory effects on anti-oxidant enzymes associated with lipoproteins and the cell membrane (255, 305). The CARP E5 (Ac-SHLRKLRKRLLRDADDKRLA-NH_2; net charge +6) was demonstrated to bind oxidized phospholipids and inhibit their pro-inflammatory function in human blood (305). In addition, pre-treatment of macrophage (RAW264.7) and endothelial (HUVEC) cell lines with the LL-27 reduces pro-inflammatory gene expression, whereas pre-incubation of oxidized phospholipid with the peptide prior to administration to mice reduces serum IL-6 and TNF-α levels (255). Similarly, the Apolipoprotein E (ApoE) protein derived CARP Ac-hE18A-NH_2 (Ac-RKLRKRLLRDWLKAFYDKVAEKLKEAF-NH_2; net charge +6) can bind bacterial lipopolysaccharides (LPS) and reduce its inflammatory (e.g., TNF-α, IL-6 production) inducing properties in human blood and primary leukocytes and a monocyte cell line (306). Ac-hE18A-NH_2 can also inhibit LPS-induced VCAM-1 expression, and reduce monocyte adhesion in HUVECs, as well as the secretion of IL-6 and monocyte chemoattractant protein-1 (MCP-1) from THP-1 monocyte cells exposed to LPS (307). Also, the CARP TAT-14 (see above), which while developed to activate Nrf-2, reduces TNF-α production in THP-1 monocyte cells following LPS stimulation (297).

Other ApoE derived peptides have also demonstrated anti-inflammatory properties. The two almost identical ApoE derived peptides, ApoE-133–150 (ApoE-133–150: Ac-LRVRLASHLRKLRKRLLR-NH_2; net charge +8.1) and COG-133 (**Table 1**) suppress cytokine expression (IL-8 or TNF-α) and other inflammatory mediators (e.g., COX or NO) in THP-1 monocytes or BV-2 microglia cells stimulated with LPS (308, 309). COG-133 treatment can suppress systemic and brain levels of TNF-α and IL-6 in mice after LPS administration (36). The COG112 peptide, which comprises COG133 fused to the CCPP penetratin (**Table 2**) inhibits the inflammatory response in mouse models of pathogen or injury induced colitis by reducing several pro-inflammatory mediators. For example, COG112 attenuated cytokine and chemokine expression, iNOS expression and nitric oxide production in mouse colon epithelial cell cultures and in colon tissue in mice following exposure to *Citrobacter rodentium* (310, 311). It was also demonstrated that COG112 inhibited NF-κB activation in colon cells and tissue following bacterial stimulation (310, 311).

The CARP PACAP38 (**Table 3**), which is derived from the neuropeptide pituitary adenylate cyclase-activating polypeptide (PACAP) binds the adenylate-cyclase-activating receptor stimulating adenylate cyclase and subsequently increases intracellular cAMP, which is a signaling molecule important in many biological processes. PACAP38 is a predominant cleavage product of PACAP, which exerts several functions within the CNS, including acting as a neurotransmitter and neuromodulator and modulating inflammatory responses. The peptide has cell-penetrating properties (312), is widely distributed within the CNS and has neuroprotective actions in excitotoxicity, retinal ischemia, stroke and traumatic brain injury models (313–318). With respect to its anti-inflammatory actions, PACAP38 can reduce the activation of cultured primary microglia to hypoxia by inhibiting induction of nitric oxide, iNOS, and p38 as well as reducing TNF-α secretion (315).

Furthermore, following traumatic brain injury, PACAP38 treatment reduces cerebral inflammation by reducing toll-like receptor-4 (TLR-4) up-regulation, and its downstream mediators. For example, treatment reduced TNF-α and IL-1β levels, reduced NF-κβ p65 sub-unit levels in nuclei, and increased levels of the NF-κβ inhibitory subunit IκB-α in the brain (318). Additionally, PACAP38 ablated TLR-4 up-regulation in the brain and in BV-2 microglia following exposure to the TLR-4 agonist LPS (319). Similarly, the LL-37 anti-microbial CARP (LLGDFFRKSKEKIGKEFKRIVQRIKDFLRNLVPRTES; net charge +6) attenuates activation of cultured dendritic cells to different TLR ligands (320).

The CARP dRK (rrkrrr; net charge +6; lower case indicates D-isoform amino acids) was identified based on its ability to block the interaction between VEGF and the VEGF receptor. The dRK peptide can reduce TNF-α and IL-6 production in normal peripheral blood monocytes and synovial fluid mononuclear cells of rheumatoid arthritis patients following VEGF stimulation (321). In a mouse model of collagen-induced arthritis, dKR reduced paw inflammation and serum levels of IL-6 (321). While it was believed that dKR was directly inhibiting the pro-inflammatory effects of VEGF and its receptor, it is possible the peptide was inhibiting VEGF induced activation of NF-κβ. In a different collagen-induced arthritis mouse model, the CARPs IG-19 (IGKEFKRIVQRIKDFLRNL-NH_2; net charge +5) and IDR-1018 (**Table 1**) both reduced the number of limbs affected, and IG-19 reduced overall disease severity (322). Subsequent examination of IG-19 treated mice revealed reduced serum levels of the pro-inflammatory cytokines TNF-α and IFN-γ and reduced cellular infiltration and cartilage degradation in arthritic joints. Interestingly, in a more recent study, IDR-108 prolonged anti-inflammatory TGFβ gene expression and suppressed early pro-inflammatory IL-1β gene expression levels in a human endothelial cell line (EA.hy926) cultivated in a high glucose environment to induce cell stress (323). In another study, treatment of arthritic mice with a peptide developed to mimic the action of Bcl-2 homology 3 (BH3) domain-only proteins (TAT-BH3: Ac-RKKRR-O-RRR-EIWIAQELRRIGDEFNAYYAR; net charge +6) ameliorated arthritis development and reduced the number of myeloid cells in the affected joint (324).

The CARP R9-SOCS1-KIR (RRRRRRRRR-DTHFRTFRSHSDYRRI; net charge +11.2) was developed to inhibit suppressor of cytokine signaling 1 (SOCS1) signaling, which can result in JAK/STAT or NF-κβ activation. This peptide blocked the activation and nuclear translocation of STAT1α, STAT3, and NF-κB p65 and inflammatory effects induced by IFN-γ, TNF-α, and IL-17A in the ARPE-19 human retinal pigment epithelial cell line (325). Topical delivery of R9-SOCS1-KIR also reduced inflammatory cell infiltration into the eye in a mouse model of experimental autoimmune uveitis. Furthermore, in a mouse model of *Pseudomonas aeruginosa* induced keratitis, R9D (**Table 1**) treatment reduced disease severity and concentrations of corneal TNF-α, IFN-γ, IL-10, and GM-CSF (326).

The cationic arginine-rich human beta-defensin derived peptide hBD3-3 (GKCSTRGRKCCRRKK; net charge +8) has demonstrated *in vitro* and *in vivo* anti-inflammatory actions. In a macrophage cell line (RAW264.7) pre-treatment with hBD3-3 reduced iNOS, TNF-α, and IL-6 protein expression (327). In addition, mice treated with hBD3-3 and injected with LPS had reduced plasma levels of TNF-α and IL-1β and reduced neutrophil infiltration into lung regions affected by LPS induced inflammation. Finally, as NF-κβ activation is involved in iNOS, TNF-α and IL-6 expression, studies in RAW264.7 cells revealed that hBD3-3 significantly inhibited degradation of the NF-κβ inhibitory subunit IκB-α, as well as the translocation of the NF-κβ p65 subunit to the nucleus.

CARPs may also inhibit inflammation by reducing activation of components of the complement system. Protamine (**Table 1**) and large poly-L-arginine peptides antagonize complement protein C5a binding to its receptor C5aR1 (or CD88) in leukocytes (328). C5aR is a transmembrane G-protein-coupled receptor expressed on neutrophils, monocytes, eosinophils, and non-myeloid cells, including liver cells and alveolar and kidney tubular epithelial cells, some classes of neurons and microglia and astrocytes. Importantly activation of the complement system following stroke/cerebral ischemia and other neurological conditions is associated with unfavorable outcomes and inhibition of C5a improves outcomes (329). Antagonism of the C5aR is thought to be due to an electrostatic interaction between the CARP and anionic sites within the receptor (328).

In some situations, CARPs may induce pro-inflammatory responses. For example, a large poly-arginine peptide (R100; 100-mer, 12.5–13.5 kDa) can bind to TLR-4 and induce cytokine and interferon gene expression in mouse splenocytes comprising mostly of B-cells, but also T-cells and monocytes (330). The peptides ApoE-133–150 and IDR-1018 increase secretion of the cytokine MCP-1 in human blood mononuclear cells (309). In one study, IDR-1018 also increased neutrophil adherence to EA.hy926 endothelial cells and promoted neutrophil migration and cytokine production (e.g., IL-8, MCP-1, MCP-3) (331).

Pro-survival Signaling

Due to the ability of CARPs to interact with cell surface receptors it appears they also have the capacity to stimulate receptor mediated pro-survival signaling pathways. The best example of CARP pro-survival signaling has been demonstrated with apelin peptides.

Apelin is a highly conserved arginine-rich peptide first identified in 1998 following its isolation in bovine stomach extracts. The peptide is expressed as a 77 amino acid preprotein, which can be processed into at least three bioactive carboxy-terminal fragments including apelin-36, apelin-17, and apelin-13 (**Table 3**). All apelin peptides can bind the G-protein coupled apelin receptor (originally named APJ) and induce cell signaling (332), with positively charged arginine and lysine resides in apelin, and negatively charged aspartate and glutamate resides in the extracellular N-terminal region of the apelin receptor important for receptor binding and internalization (333, 334). Apelin peptides and the apelin receptor are widely expressed throughout the body including brain, heart, adipose, skeletal muscle, kidney, and lung. The apelin/apelin receptor system regulates cardiac and vascular function, glucose metabolism, fluid homeostasis, cell survival, and angiogenesis. Other CARPs

including poly-arginine peptide R9D and protamine can bind to the apelin receptor (333, 335). Interestingly, pre-treatment of cells with R9D and protamine appears to inhibit subsequent apelin receptor signaling. However, this is likely due to the R9D and protamine peptides desensitizing the receptor or inducing receptor internalization because pre-treatment of cells with apelin peptides also decreases apelin receptor cell signaling (336). The apelin receptor can dimerise with the κ-opioid G-protein-coupled receptor (KOR) and bind both apelin and dynorphin A peptides (**Table 3**) and activate extracellular signal–regulated kinase 1/2 (ERK1/2) signaling (337).

Established signaling events activated by the apelin receptor are the AMP-activated protein kinase (AMPK), ERK1/2 and phosphatidyl inositol 3-kinase/protein kinase B (PI3K/AKT) pathways (338–340). The AMPK pathway is a major energy sensing system that monitors for low levels of energy molecules, such as ATP and AMP to induce cellular adaptive metabolic changes to preserve and better utilize remaining energy substrates and maintain mitochondrial function. In addition, AMPK can activate the transcription factor Nrf2, resulting in the expression of anti-oxidant proteins. The ERK pathway has diverse actions including cell survival mediated by the expression of pro-survival proteins (e.g., BCL2) and inhibition of pro-apoptotic proteins (e.g., BAD). Similarly, the PI3K/AKT pathway promotes cell survival by targeting and phosphorylating proteins that regulate cell death and survival, cell migration and metabolism and angiogenesis.

With respect to neuroprotection, apelin peptides reduce intracellular calcium influx and neuronal death following NMDA receptor mediated excitotoxicity (163–166, 341), and improve outcomes in animal stroke, perinatal hypoxia-ischemia, traumatic brain injury, intracerebral hemorrhage and Alzheimer's disease models (see **Table 3**). The neuroprotective mechanism of action of apelin peptides have been attributed to AMPK, ERK, and/or AKT mediated signaling by inhibiting apoptosis, suppressing inflammation, reducing ER stress, preserving BBB integrity and stimulating angiogenesis (163, 166–170, 340–342), as well as mechanisms independent of apelin receptor signaling (164, 165).

The endogenous CARP toddler (also known as elabela/apela; QRPVNLTMRRKLRKHNCLQRRCMPLHSRVPFP; net charge +9.1) can also bind the apelin receptor and induce ERK signaling (343). Whereas, an anti-microbial CARP SR-0379 (MLKLIFLHRLKRMRKRLKRK; net charge +11) can stimulate ERK and AKT phosphorylation in dermal fibroblasts via a cell surface integrin receptor (344). In addition, the anti-microbial LL-37 peptide can bind to cell surface receptors in different cells, and activate downstream ERK, AKT, or P38 signaling (345, 346). Finally, protamine and polycationic arginine and lysine peptides interact with and enhance the EGF receptor tyrosine kinase activity and thereby enhance cell signaling activated by the receptor (347, 348).

Inhibiting Protein Aggregation in Neurodegenerative Disorders

Protein misfolding can lead to protein aggregation, and the accumulation of specific protein oligomers, aggregates and fibrils is the hallmark of several chronic neurodegenerative disorders, such as Alzheimer's disease (e.g., Aβ peptide, tau), Parkinson's disease (e.g., α-synuclein), Huntington's disease (e.g., Huntingtin), and amyotrophic lateral sclerosis (e.g., SOD1). Arginine is a common additive to protein solutions to facilitate protein folding, and to help maintain protein stability and inhibit protein aggregation (349, 350). Since arginine can stabilize proteins and inhibit self-aggregation, it is possible CARPs can also reduce protein misfolding and aggregation, and is a mechanism through which CARPs may be beneficial in animal models of human neurodegenerative disorders associated with proteinopathies.

The guanidinium head group of arginine and the ability of arginine to self-associate to form clusters (n-mers; $n > 2$) is considered a critical mechanism responsible for suppressing protein aggregation (349). Arginine clusters associate with the surface of proteins, namely aromatic (e.g., tryptophan) and negatively charged (e.g., glutamate) amino acid residues via cation-π interactions and hydrogen bonding, respectively. The interaction of arginine clusters with hydrophobic residues not normally exposed in the native state stabilizes partially unfolded proteins and act to "crowd around" proteins to prevent aggregation (350). Hence, it is conceivable that CARPs, such as poly-arginine molecules due to their multivalent arginine arrangement behave in a similar fashion to arginine clusters to prevent protein aggregation. For example, CARPs that inhibit Aβ oligomer formation, which is considered neurotoxic include KLVFFRRRRRR (net charge +7) and R5 (RRRRRR: net charge +5) (351), 15M (Ac-VITNPNRRNRTPQMLKR-NH_2: net charge +5) (352) SRPGLRR (net charge +3) (353), RR-7-animo-4-trifluromethylcoumarin (net charge +3) (354) RI-OR2-TAT (Ac-rGffvlkGrrrrkkrGy-NH_2: charge +9) (355) R8-Aβ (25–35) (rrrrrrrr-gsnkgaiiglm: net charge +10) (356), and the related D3 and RD2 peptides (**Table 1**) (28, 29). In a mouse model of Alzheimer's disease, R9 administered subcutaneously over 4 weeks, decreased brain Aβ deposits by 15%, albeit the reduction was not statistically significant (357). In addition, poly-arginine (5–15 kDa; 32–96-mers) can inhibit the aggregation of a tau mutant protein (P301L) commonly associated with tauopathy (358), and the CARPs P42-TAT (**Table 2**) (118) and TAT-P110 (**Table 2**) (149) inhibit aggregation of mutant Huntingtin protein. Interestingly, several of the key proteins that accumulate in the CNS in chronic neurodegenerative disorders are negatively-charged (e.g., Aβ 1–42: −2.7; tau: −6.2; α-synuclein: −8.9; Huntington: −59.7; SOD1: −5.5), which would increase their electrostatic affinity to positively-charged molecules, and make them ideal therapeutic targets for CARPs.

ENDOGENOUS CARPS AND NEUROPROTECTION

The endogenous PACAP38 peptide is a member of the secretin/glucagon/growth hormone-releasing hormone superfamily, and its neuroprotective properties have been discussed above. Dynorphins are widely distributed in the CNS and consist of two main peptides dynorphin A (**Table 3**) and dynorphin B (**Table 3**) that bind the κ-opioid receptor to induce

analgesia (359). Interestingly, many other synthetic CARPs also have analgesic properties (see **Tables 1**, **2**). Dynorphin A and dynorphin B are synthesized as the precursor protein predynorphin, which is then proteolytically cleaved to the smaller peptides. The dynorphin A peptide has also been shown to be neuroprotective in a rat stroke model (177).

Similarly, different classes of endogenous anti-microbial peptides (e.g., defensins, cathelicidins, bactenecin) have been derived from mammals, many of which are cationic and arginine-rich. Anti-microbial peptides are mainly produced by leukocytes and act as a defense against bacteria, fungi and viruses, and act either directly or by modulating inflammatory responses. Interestingly, several cationic arginine-rich anti-microbial peptides have also been shown to have neuroprotective properties in stroke, perinatal hypoxia-ischemia and traumatic brain injury animal models (**Table 2**).

COMPOUNDS CONTAINING THE GUANIDINIUM MOIETY AND NEUROPROTECTION

As mentioned above, arginine is unique in possessing a guanidinium head group, and most likely the critical element imparting the neuroprotective properties of CARPs. It is therefore not surprising that compounds containing the guanidinium moiety including arginine, arginine-based NOS inhibitors (e.g., L-NNA, L-NAME), the drugs metformin, phenformin, amiloride, and aminoguanidine, the toxin tetrodotoxin and the endogenous neuroactive molecule agmatine have neuroprotective properties in *in vitro* neuronal injury models (e.g., excitotoxicity, oxygen-glucose deprivation) and in animal models of stroke, perinatal hypoxia-ischemia, spinal cord injury, traumatic brain injury Parkinson's disease and Alzheimer's disease (**Supplementary Table 3**). It is thus conceivable that CARPs and other guanidinium moiety containing small molecules, at least in part, share the same neuroprotective mechanism of actions including anti-excitotoxic properties. In support of their anti-excitotoxic properties different guanidinium moiety containing molecules have been demonstrated to inhibit voltage gated and ligand-gated ion channels (230–237). However, because CARPs are multivalent guanidinium-agents they are likely to possess greater potency at the molar level than molecules that contain only one or several guanidine moieties, and have a greater capacity to traverse cell membranes.

Metformin and phenformin are biguanindine anti-hyperglycemic agents, which have been used for the treatment of diabetes for over 50 years. Like CARPs, metformin can activate AMPK signaling, target and suppress mitochondrial ROS production, limit calcium induced intracellular toxicity, scavenge methylglyoxal and reduce neuroinflammation (269). Aminoguanidine can also scavenge methylglyoxal and other dicarbynols (25). Agmatine is an endogenous divalent cationic guanidine. In the brain it is considered a putative neurotransmitter, in which it can be released from synaptic vesicles following membrane depolarization. It binds to various receptors (e.g., α2 adrenergic receptor) and can block NMDA receptors and other cation ligand-gated channels, with studies indicating that agmatine binds to the receptor near the channel pore and that the guanidinium group is critical for binding (360).

Arginine-based nitric oxide inhibitors, such as L-NNA and L-NAME are commonly used in *in vitro* excitotoxic and animal stroke studies to determine the neurodamaging role of nitric oxide over-production in neuronal death and ischemic brain tissue injury. However, given the potential anti-excitotoxic action of the guanidine moiety, it is possible that arginine-based NOS inhibitors in the setting of excitotoxicity are actually suppressing the activation of NMDA receptors and ion voltage gated channels, thereby indirectly rather than directly inhibiting NOS activation. There are several lines of evidence that support this hypothesis. Following excitotoxicity, it is difficult to imagine that by blocking neuronal nitric oxide production, but not the toxic intracellular influx of calcium is able to provide high level neuroprotection (361). In addition, arginine-based NOS inhibitors are not readily taken up by cells and possess slow NOS binding kinetics (362), but are neuroprotective when added at the same time as the excitotoxic agent, which favors an extracellular (i.e., cell surface) rather than an intracellular (i.e., NOS) mechanism of action. In addition, L-NAME is a weak NOS inhibitor, which is hydrolyzed by ubiquitous esterases to the more potent L-NNA, thus requiring additional time for the inhibitor to exert its NOS inhibitory effects.

CONCLUDING REMARKS

There is now overwhelming evidence from experimental studies that CARPs represent a novel class of neuroprotective agent with great potential for the treatment of neurological disorders. However, only two CARPs with neuroprotective properties (TAT-NR2B9c/NA-1 and CN-105) have so far progressed to clinical trials for a neurological condition (363–365). Further studies are required to obtain a more complete understanding of the neuroprotective mechanisms of action of CARPs in acute CNS injury and chronic neurodegenerative disease models. Despite this, based on experimental studies to date it appears that CARPs have the potential to be developed as therapeutics for the treatment of a diverse range of neurological disorders including stroke, perinatal hypoxia-ischemia, traumatic brain injury and spinal cord injury as well as, epilepsy and pain, and potentially even chronic degenerative neurological disorders, such as Alzheimer's disease, Parkinson's disease, amyotrophic lateral sclerosis, and Huntington's disease. Importantly, CARPs have properties that greatly enhance the likelihood of translational success at the clinical level including possessing a pluripotent mechanism of action, the capacity to enter the CNS, and the ability to exert a broad range of beneficial extracellular, intracellular and intra-organelle effects. Based on human studies with TAT-fused peptides, such as TAT-NR2B9c/NA-1 (366), the poly-arginine peptide R9/ALX40-4C (367), and arginine-rich peptides CN-105 (365), protamine (368) and RD2 (369), it appears this class of peptide has a favorable safety profile. Moreover, our recent experimental neuroprotection study with the poly-arginine peptide R18 in a non-human primate stroke

model (26), has not disclosed any neurological or other toxic effects, which also augurs well for the translational potential of other CARPs to the clinical arena.

With respect to previous studies using cationic and arginine-rich peptides including those fused to a CCPP in neuroprotective, neuroactive or cytoprotective studies we believe that due to the cofounding effects of peptide positive charge and arginine residues, the mechanisms of action of theses peptides need to be critically re-evaluated.

Finally, given that CARPs with different amino acid sequences or modifications will have different physio-chemical and biological properties, future studies should focus on examining if new CARPs with more targeted molecular mechanisms of actions can be designed to improve therapeutic efficacy for specific neurological disorders.

DATA AVAILABILITY STATEMENT

All datasets generated for this study are included in the article/**Supplementary Material**.

AUTHOR CONTRIBUTIONS

BM conceptualized and wrote the review. FM and NK provided the additional input into the content of the review and in drafting the manuscript. BM, FM, and NK contributed to the writing of the manuscript. BM prepared the figures and tables provided in the manuscript.

ACKNOWLEDGMENTS

This study has been supported by the Perron Institute and the Department of Neurosurgery, Sir Charles Gairdner Hospital. We thank Raphe Patmore for assistance with illustrations.

SUPPLEMENTARY MATERIAL

The Supplementary Material for this article can be found online at: https://www.frontiersin.org/articles/10.3389/fneur.2020.00108/full#supplementary-material

REFERENCES

1. Ferrer-Montiel AV, Merino JM, Blondelle SE, Perez-Payà E, Houghten RA, Montal M. Selected peptides targeted to the NMDA receptor channel protect neurons from excitotoxic death. *Nat Biotechnol.* (1998) 16:286–91. doi: 10.1038/nbt0398-286
2. Planells-Cases R, Aracil A, Merino JM, Gallar J, Pérez-Payá E, Belmonte C, et al. Arginine-rich peptides are blockers of VR-1 channels with analgesic activity. *FEBS Lett.* (2000) 481:131–36. doi: 10.1016/S0014-5793(00)01982-7
3. Yang L, Zhao K, Calingasan NY, Luo G, Szeto HH, Beal MF. Mitochondria targeted peptides protect against 1-methyl-4-phenyl-1,2,3,6-tetrahydropyridine neurotoxicity. *Antioxid Redox Signal.* (2009) 11:2095–104. doi: 10.1089/ars.2009.2445
4. Manczak M, Mao P, Calkins MJ, Cornea A, Reddy AP, Murphy MP, et al. Mitochondria-targeted antioxidants protect against amyloid-beta toxicity in Alzheimer's disease neurons. *J Alzheimers Dis.* (2010) 20:609–31. doi: 10.3233/JAD-2010-100564
5. Kim EH, Tolhurst AT, Szeto HH, Cho SH. Targeting CD36-mediated inflammation reduces acute brain injury in transient but not permanent ischemic stroke. *CNS Neurosci Ther.* (2015) 21:385–91. doi: 10.1111/cns.12326
6. Zhu LL, Li MQ, He F, Zhou SB, Jiang W. Mitochondria targeted peptide attenuates mitochondrial dysfunction controls inflammation and protects against spinal cord injury-induced lung injury. *Cell Physiol Biochem.* (2017) 44:388–400. doi: 10.1159/000484919
7. Toyama S, Shimoyama N, Szeto HH, Schiller PW, Shimoyama M. Protective effect of a mitochondria-targeted peptide against the development of chemotherapy-induced peripheral neuropathy in mice. *ACS Chem Neurosci.* (2018) 9:1566–71. doi: 10.1021/acschemneuro.8b00013
8. Xu W, Zhou M, Baudry M. Neuroprotection by cell permeable TAT-mGluR1 peptide in ischemia: synergy between carrier and cargo sequences. *Neuroscientist.* (2008) 14:409–14. doi: 10.1177/1073858407309762
9. Vaslin A, Rummel C, Clarke PG. Unconjugated TAT carrier peptide protects against excitotoxicity. *Neurotox Res.* (2009) 15:123–6. doi: 10.1007/s12640-009-9012-6
10. Meade AJ, Meloni BP, Mastaglia FL, Watt PM, Knuckey NW. AP-1 inhibitory peptides attenuate *in vitro* cortical neuronal cell death induced by kainic acid. *Brain Res.* (2010) 1360:8–16. doi: 10.1016/j.brainres.2010.09.007
11. Meade AJ, Meloni BP, Cross JL, Bakker AJ, Fear MW, Mastaglia FL, et al. AP-1 inhibitory peptides are neuroprotective following acute glutamate excitotoxicity in primary cortical neuronal cultures. *J Neurochem.* (2010) 112:258–70. doi: 10.1111/j.1471-4159.2009.06459.x
12. Meloni BP, Craig AJ, Milech N, Hopkins RM, Watt PM, Knuckey NW. The neuroprotective efficacy of cell-penetrating peptides TAT penetratin Arg-9 and Pep-1 in glutamic acid kainic acid and *in vitro* ischemia injury models using primary cortical neuronal cultures. *Cell Mol Neurobiol.* (2014) 34:173–81. doi: 10.1007/s10571-013-9999-3
13. Craig AJ, Meloni BP, Watt PM, Knuckey NW. Attenuation of neuronal death by peptide inhibitors of AP-1 activation in acute and delayed *in vitro* ischaemia (oxygen/glucose deprivation) models. *Int J Pept Res Ther.* (2011) 17:1–6. doi: 10.1007/s10989-010-9234-8
14. Marshall J, Wong KY, Rupasinghe CN, Tiwari R, Zhao X, Berberoglu ED, Sinkler C, et al. Inhibition of N-methyl-D-aspartate-induced retinal neuronal death by polyarginine peptides is linked to the attenuation of stress-induced hyperpolarization of the inner mitochondrial membrane potential. *J Biol Chem.* (2015) 290:22030–48. doi: 10.1074/jbc.M115.662791
15. Meloni BP, Brookes LM, Clark VW, Cross JL, Edwards AB, Anderton RS, et al. Poly-arginine and arginine-rich peptides are neuroprotective in stroke models. *J Cereb Blood Flow Metab.* (2015) 35:993–1004. doi: 10.1038/jcbfm.2015.11
16. Meloni BP, Milani D, Cross JL, Clark VW, Edwards AB, Anderton RS, et al. Assessment of the neuroprotective effects of arginine-rich protamine peptides poly-arginine peptides (R12-cylic R22) and arginine-tryptophan containing peptides following *in vitro* excitotoxicity and/or permanent middle cerebral artery occlusion in rats. *Neuromol Med.* (2017) 19:271–85. doi: 10.1007/s12017-017-8441-2
17. Edwards AB, Cross JL, Anderton RS, Knuckey NW, Meloni BP. Characterisation of neuroprotective efficacy of modified poly-arginine-9 (R9) peptides in neuronal glutamic acid excitotoxicity model. *Mol Cell Biochem.* (2017) 426:75–85. doi: 10.1007/s11010-016-2882-z
18. Milani D, Clark VW, Cross JL, Anderton RS, Knuckey NW, Meloni BP. Poly-arginine peptides reduce infarct volume in a permanent middle cerebral artery rat stroke model. *BMC Neurosci.* (2016) 17:19. doi: 10.1186/s12868-016-0253-z

19. Milani D, Knuckey NW, Cross JL, Anderton RS, Meloni BP. The R18 polyarginine peptide is more effective than the TAT-NR2B9c (NA-1) peptide when administered 60 minutes after permanent middle cerebral artery occlusion in the rat. *Stroke Res Treat.* (2016) 2016:2372710. doi: 10.1155/2016/2372710
20. Milani D, Cross JL, Anderton RS, Blacker DJ, Knuckey NW, Meloni BP. Neuroprotective efficacy of R18 poly-arginine and NA-1 (TAT-NR2B9c) peptides following transient middle cerebral artery occlusion in the rat. *Neurosci Res.* (2017) 114:9–15. doi: 10.1016/j.neures.2016.09.002
21. Milani D, Bakeberg MC, Cross JL, Clark VW, Anderton RS, Blacker DJ, et al. Comparison of neuroprotective efficacy of poly-arginine R18 and R18D (D-enantiomer) peptides following permanent middle cerebral artery occlusion in the Wistar rat and *in vitro* toxicity studies. *PLoS ONE.* (2018) 13:e0193884. doi: 10.1371/journal.pone.0193884
22. Edwards AB, Cross JL, Anderton RS, Knuckey NW, Meloni BP. Poly-arginine R18 and R18D (D-enantiomer) peptides reduce infarct volume and improves behavioural outcomes following perinatal hypoxic-ischaemic encephalopathy in the P7 rat. *Mol Brain.* (2018) 11:1–12. doi: 10.1186/s13041-018-0352-0
23. Edwards AB, Anderton RS, Knuckey NW, Meloni BP. Assessment of therapeutic window for poly-arginine-18D (R18D) in a P7 rat model of perinatal hypoxic-ischaemic encephalopathy. *J Neurosci Res.* (2018) 96:1816–26. doi: 10.1002/jnr.24315
24. Chiu LS, Anderton RS, Cross JL, Clark VW, Edwards AB, Knuckey NW, et al. Assessment of neuroprotective peptides poly-arginine R18 COG1410 and APP96–110 experimental traumatic brain injury and *in vitro* neuronal excitotoxicity. *Transl Neurosci.* (2017) 15:147–57. doi: 10.1515/tnsci-2017-0021
25. Kikuchi S, Shinpo K, Moriwaka F, Makita Z, Miyata T, Tashiro K. Neurotoxicity of methylglyoxal and 3-deoxyglucosone on cultured cortical neurons: synergism between glycation and oxidative stress possibly involved in neurodegenerative diseases. *J Neurosci Res.* (1999) 57:280–9. doi: 10.1002/(SICI)1097-4547(19990715)57:2<280::AID-JNR14>3.0.CO;2-U
26. Meloni BP, Chen Y, Harrison KA, Nashed JY, Blacker DJ, South SM, et al. Poly-arginine peptide-18 (R18) reduces brain injury and improves functional outcomes in a nonhuman primate stroke model. *Neurotherapeutics*. (2019). doi: 10.1007/s13311-019-00809-1. [Epub ahead of print].
27. Batulu H, Du G-J, Li D-Z, Sailike D, Fan Y-H, Geng D. Effect of poly-arginine R18 on neurocyte cell growth via autophagy in traumatic brain injury. *Exp Ther Med.* (2019) 17:4109–15. doi: 10.3892/etm.2019.7423
28. van Groen T, Wiesehan K, Funke SA, Kadish I, Nagel-Steger L, Willbold D. Reduction of Alzheimer's disease amyloid plaque load in transgenic mice by D3, a D-enantiomeric peptide identified by mirror image phage display. *ChemMedChem*. (2008) 3:1848–52. doi: 10.1002/cmdc.200800273
29. van Groen T, Schemmert S, Brener O, Gremer L, Ziehm T, Tusche M, et al. The Aβ oligomer eliminating D-enantiomeric peptide RD2 improves cognition without changing plaque pathology. *Sci Rep*. (2017) 7:16275. doi: 10.1038/s41598-017-16565-1
30. Dunkelmann T, Teichmann K, Ziehm T, Schemmert S, Frenzel D, Tusche M, et al. Aβ oligomer eliminating compounds interfere successfully with pEAβ(3–42) induced motor neurodegenerative phenotype in transgenic mice. *Neuropeptides*. (2018) 67:27–35. doi: 10.1016/j.npep.2017.11.011
31. Bolouri H, Sävman K, Wang W, Thomas A, Maurer N, Dullaghan E, et al. Innate defense regulator peptide 1018 protects against perinatal brain injury. *Ann Neurol.* (2014) 75:395–41. doi: 10.1002/ana.24087
32. Chassagnon IR, McCarthy CA, Chin YK, Pineda SS, Keramidas A, Mobli M, et al. Potent neuroprotection after stroke afforded by a double-knot spider-venom peptide that inhibits acid-sensing ion channel 1a. *Proc Natl Acad Sci USA*. (2017) 114:3750–5. doi: 10.1073/pnas.1614728114
33. Corrigan F, Pham CL, Vink R, Blumbergs PC, Masters CL, van den Heuvel C, et al. The neuroprotective domains of the amyloid precursor protein in traumatic brain injury are located in the two growth factor domains. *Brain Res.* (2011) 1378:137–43. doi: 10.1016/j.brainres.2010.12.077
34. Corrigan F, Thornton E, Roisman LC, Leonard AV, Vink R, Blumbergs PC, et al. The neuroprotective activity of the amyloid precursor protein against traumatic brain injury is mediated via the heparin binding site in residues 96–110. *J Neurochem.* (2014) 128:196–204. doi: 10.1111/jnc.12391
35. Plummer SL, Corrigan F, Thornton E, Woenig JA, Vink R, Cappai R, et al. The amyloid precursor protein derivative APP96–110 is efficacious following intravenous administration after traumatic brain injury. *PLoS ONE.* (2018) 13:e0190449. doi: 10.1371/journal.pone.0190449
36. Lynch JR, Tang W, Wang H, Vitek MP, Bennett ER, Sullivan PM, et al. APOE genotype and an ApoE-mimetic peptide modify the systemic and central nervous system inflammatory response. *J Biol Chem*. (2003) 278:48529–33. doi: 10.1074/jbc.M306923200
37. Aono M, Bennett ER, Kim KS, Lynch JR, Myers J, Pearlstein RD, et al. Protective effect of apolipoprotein E-mimetic peptides on N-methyl-D-aspartate excitotoxicity in primary rat neuronal-glial cell cultures. *Neuroscience.* (2003) 116:437–45. doi: 10.1016/S0306-4522(02)00709-1
38. Lynch JR, Wang H, Mace B, Leinenweber S, Warner DS, Bennett ER, et al. A novel therapeutic derived from apolipoprotein E reduces brain inflammation and improves outcome after closed head injury. *Exp Neurol.* (2005) 192:109–16. doi: 10.1016/j.expneurol.2004.11.014
39. McAdoo JD, Warner DS, Goldberg RN, Vitek MP, Pearlstein R, Laskowitz DT. Intrathecal administration of a novel apoE-derived therapeutic peptide improves outcome following perinatal hypoxic-ischemic injury. *Neurosci Lett.* (2005) 381:305–8. doi: 10.1016/j.neulet.2005.02.036
40. Li FQ, Sempowski GD, McKenna SE, Laskowitz DT, Colton CA, Vitek MP. Apolipoprotein E-derived peptides ameliorate clinical disability and inflammatory infiltrates into the spinal cord in a murine model of multiple sclerosis. *J Pharmacol Exp Ther.* (2006) 318:956–65. doi: 10.1124/jpet.106.103671
41. Sarantseva S, Timoshenko S, Bolshakova O, Karaseva E, Rodin D, Schwarzman AL, et al. Apolipoprotein E-mimetics inhibit neurodegeneration and restore cognitive functions in a transgenic *Drosophila* model of Alzheimer's disease. *PLoS ONE.* (2009) 4:e8191. doi: 10.1371/journal.pone.0008191
42. Gao J, Wang H, Sheng H, Lynch JR, Warner DS, Durham L, Vitek MP, et al. A novel apoE-derived therapeutic reduces vasospasm and improves outcome in a murine model of subarachnoid haemorrhage. *Neurocrit Care.* (2006) 4:25–31. doi: 10.1385/NCC:4:1:025
43. Hoane MR, Pierce JL, Holland MA, Birky ND, Dang T, Vitek MP, et al. The novel apolipoprotein E-based peptide COG1410 improves sensorimotor performance and reduces injury magnitude following cortical contusion injury. *J Neurotrauma.* (2007) 24:1108–18. doi: 10.1089/neu.2006.0254
44. Hoane MR, Kaufman N, Vitek MP, McKenna SE. COG1410 improves cognitive performance and reduces cortical neuronal loss in the traumatically injured brain. *J Neurotrauma.* (2009) 26:121–9. doi: 10.1089/neu.2008.0565
45. Jiang Y, Brody DL. Administration of COG1410 reduces axonal amyloid precursor protein immunoreactivity and microglial activation after controlled cortical impact in mice. *J Neurotrauma.* (2012) 29:2332–41. doi: 10.1089/neu.2012.2362
46. Kaufman NA, Beare JE, Tan AA, Vitek M P, McKenna SE, Hoane MR. COG1410 an apolipoprotein E-based peptide improves cognitive performance and reduces cortical loss following moderate fluid percussion injury in the rat. *Behav Brain Res.* (2010) 214:395–401. doi: 10.1016/j.bbr.2010.06.017
47. Laskowitz DT, McKenna SE, Song P, Wang H, Durham L, Yeung N, et al. COG1410 a novel apolipoprotein E-based peptide improves functional recovery in a murine model of traumatic brain injury. *J Neurotrauma.* (2007) 24:1093–97. doi: 10.1089/neu.2006.0192
48. Laskowitz DT, Lei B, Dawson HN, Wang H, Bellows ST, Christensen DJ, et al. The apoE-mimetic peptide COG1410 improves functional recovery in a murine model of intracerebral haemorrhage. *Neurocrit Care.* (2012) 16:316–26. doi: 10.1007/s12028-011-9641-5
49. James ML, Sullivan PM, Lascola CD, Vitek MP, Laskowitz DT. Pharmacogenomic effects of apolipoprotein E on intracerebral haemorrhage. *Stroke.* (2009) 40:632–9. doi: 10.1161/STROKEAHA.108.530402
50. Tukhovskaya EA, Yukin AY, Khokhlova ON, Murashev AN, Vitek MP. COG1410 a novel apolipoprotein-E mimetic improves functional and morphological recovery in a rat model of focal brain ischemia. *J Neurosci Res.* (2009) 87:677–82. doi: 10.1002/jnr.21874
51. Wang R, Hong J, Lu M, Neil JE, Vitek MP, Liu X, et al. ApoE mimetic ameliorates motor deficit and tissue damage in rat spinal cord injury. *J Neurosci Res.* (2014) 92:884–92. doi: 10.1002/jnr.23371

52. Wu Y, Pang J, Peng J, Cao F, Vitek MP, Li F, Jiang Y, et al. An apoE-derived mimic peptide COG1410 alleviates early brain injury via reducing apoptosis and neuroinflammation in a mouse model of subarachnoid haemorrhage. *Neurosci Lett.* (2016) 627:92–9. doi: 10.1016/j.neulet.2016.05.058
53. Lei B, James ML, Liu J, Zhou G, Venkatraman TN, Lascola CD, et al. Neuroprotective pentapeptide CN-105 improves functional and histological outcomes in a murine model of intracerebral haemorrhage. *Sci Rep.* (2016) 6:34834. doi: 10.1038/srep34834
54. Laskowitz DT, Wang H, Chen T, Lubkin DT, Cantillana V, Tu TM, et al. Neuroprotective pentapeptide CN-105 is associated with reduced sterile inflammation and improved functional outcomes in a traumatic brain injury murine model. *Sci Rep.* (2017) 7:46461. doi: 10.1038/srep46461
55. Tu TM, Kolls BJ, Soderblom EJ, Cantillana V, Ferrell PD, Moseley MA, et al. Apolipoprotein E mimetic peptide CN-105 improves outcomes in ischemic stroke. *Ann Clin Transl Neurol.* (2017) 4:246–65. doi: 10.1002/acn3.399
56. Zhao LR, Spellman S, Kim J, Duan WM, McCarthy JB, Low WC. Synthetic fibronectin peptide exerts neuroprotective effects on transient focal brain ischemia in rats. *Brain Res.* (2005) 1054:1–8. doi: 10.1016/j.brainres.2005.04.056
57. King VR, Hewazy D, Alovskaya A, Phillips JB, Brown RA, Priestley JV. The neuroprotective effects of fibronectin mats and fibronectin peptides following spinal cord injury in the rat. *Neuroscience.* (2010) 168:523–30. doi: 10.1016/j.neuroscience.2010.03.040
58. Khroyan TV, Polgar WE, Orduna J, Zaveri NT, Judd AK, Tuttle DJ, et al. Anti-nociceptive and anti-allodynic effects of a high affinity NOP hexapeptide [Ac-RY(3-Cl)YRWR-NH_2] (Syn 1020) in rodents. *Eur J Pharmacol.* (2007) 560:29–35. doi: 10.1016/j.ejphar.2006.12.015
59. Aarts M, Liu Y, Liu L, Besshoh S, Arundine M, Gurd JW, et al. Treatment of ischemic brain damage by perturbing NMDA receptor-PSD-95 protein interactions. *Science.* (2002) 298:846–50. doi: 10.1126/science.1072873
60. Soriano FX, Martel MA, Papadia S, Vaslin A, Baxter P, Rickman C, et al. Specific targeting of pro-death NMDA receptor signals with differing reliance on the NR2B PDZ ligand. *J Neurosci.* (2008) 28:10696–710. doi: 10.1523/JNEUROSCI.1207-08.2008
61. Sun HS, Doucette TA, Liu Y, Fang Y, Teves L, Aarts M, et al. Effectiveness of PSD95 inhibitors in permanent and transient focal ischemia in the rat. *Stroke.* (2008) 39:2544–53. doi: 10.1161/STROKEAHA.107.506048
62. Ittner LM, Ke YD, Delerue F, Bi M, Gladbach A, van Eersel J, et al. Dendritic function of tau mediates amyloid-beta toxicity in Alzheimer's disease mouse models. *Cell.* (2010) 142:387–97. doi: 10.1016/j.cell.2010.06.036
63. Bråtane BT, Cui H, Cook DJ, Bouley J, Tymianski M, Fisher M. Neuroprotection by freezing ischemic penumbra evolution without cerebral blood flow augmentation with a postsynaptic density-95 protein inhibitor. *Stroke.* (2011) 42:3265–70. doi: 10.1161/STROKEAHA.111.618801
64. D'Mello R, Marchand F, Pezet S, McMahon SB, Dickenson AH. Perturbing PSD-95 interactions with NR2B-subtype receptors attenuates spinal nociceptive plasticity and neuropathic pain. *Mol Ther.* (2012) 19:1780–92. doi: 10.1038/mt.2011.42
65. Cook DJ, Teves L, Tymianski M. Treatment of stroke with a PSD-95 inhibitor in the gyrencephalic primate brain. *Nature.* (2012) 483:213–7. doi: 10.1038/nature10841
66. Srejic LR, Hutchison WD, Aarts MM. Uncoupling PSD-95 interactions leads to rapid recovery of cortical function after focal stroke. *J Cereb Blood Flow Metab.* (2013) 33:1937–43. doi: 10.1038/jcbfm.2013.153
67. Xu B, Xiao AJ, Chen W, Turlova E, Liu R, Barszczyk A, et al. Neuroprotective effects of a PSD-95 inhibitor in neonatal hypoxic-ischemic brain injury. *Mol Neurobiol.* (2016) 53:5962–70. doi: 10.1007/s12035-015-9488-4
68. Wang Z, Chen Z, Yang J, Yang Z, Yin J, Duan X, et al. Treatment of secondary brain injury by perturbing postsynaptic density protein-95-NMDA receptor interaction after intracerebral hemorrhage in rats. *J Cereb Blood Flow Metab.* (2019) 39:1588–601. doi: 10.1177/0271678X18762637
69. Borsello T, Clarke PG, Hirt L, Vercelli A, Repici M, Schorderet DF, et al. A peptide inhibitor of c-Jun N-terminal kinase protects against excitotoxicity and cerebral ischemia. *Nat Med.* (2003) 9:1180–86. doi: 10.1038/nm911
70. Hirt L, Badaut J, Thevenet J, Granziera C, Regli L, Maurer F, et al. D-JNKI1 a cell-penetrating c-Jun-N-terminal kinase inhibitor protects against cell death in severe cerebral ischemia. *Stroke.* (2004) 35:1738–43. doi: 10.1161/01.STR.0000131480.03994.b1
71. Zhuang ZY, Wen YR, Zhang DR, Borsello T, Bonny C, Strichartz GR, et al. A peptide c-Jun N-terminal kinase (JNK) inhibitor blocks mechanical allodynia after spinal nerve ligation: respective roles of JNK activation in primary sensory neurons and spinal astrocytes for neuropathic pain development and maintenance. *J Neurosci.* (2006) 26:3551–60. doi: 10.1523/JNEUROSCI.5290-05.2006
72. Centeno C, Repici M, Chatton JY, Riederer BM, Bonny C, Nicod P, et al. Role of the JNK pathway in NMDA-mediated excitotoxicity of cortical neurons. *Cell Death Differ.* (2007) 14:240–53. doi: 10.1038/sj.cdd.4401988
73. Esneault E, Castagne V, Moser P, Bonny C, Bernaudin M. D-JNKi a peptide inhibitor of c-Jun N-terminal kinase promotes functional recovery after transient focal cerebral ischemia in rats. *Neuroscience.* (2008) 152:308–20. doi: 10.1016/j.neuroscience.2007.12.036
74. Wiegler K, Bonny C, Coquoz D, Hirt L. The JNK inhibitor XG-102 protects from ischemic damage with delayed intravenous administration also in the presence of recombinant tissue plasminogen activator. *Cerebrovasc Dis.* (2008) 26:360–6. doi: 10.1159/000151639
75. Dykstra CM, Ratnam M, Gurd JW. Neuroprotection after status epilepticus by targeting protein interactions with postsynaptic density protein 95. *J Neuropathol Exp Neurol.* (2009) 68:823–31. doi: 10.1097/NEN.0b013e3181ac6b70
76. Ginet V, Puyal J, Magnin G, Clarke PG, Truttmann AC. Limited role of the c-Jun N-terminal kinase pathway in a neonatal rat model of cerebral hypoxia-ischemia. *J Neurochem.* (2009) 108:552–62. doi: 10.1111/j.1471-4159.2008.05797.x
77. Ortolano F, Colombo A, Zanier ER, Sclip A, Longhi L, Perego C, et al. c-Jun N-terminal kinase pathway activation in human and experimental cerebral contusion. *J Neuropathol Exp Neurol.* (2009) 68:964–71. doi: 10.1097/NEN.0b013e3181b20670
78. Bessero AC, Chiodini F, Rungger-Brändle E, Bonny C, Clarke PG. Role of the c-Jun N-terminal kinase pathway in retinal excitotoxicity and neuroprotection by its inhibition. *J Neurochem.* (2010) 113:1307–18. doi: 10.1111/j.1471-4159.2010.06705.x
79. Michel-Monigadon D, Bonny C, Hirt L. c-Jun N-terminal kinase pathway inhibition in intracerebral haemorrhage. *Cerebrovasc Dis.* (2010) 29:564–70. doi: 10.1159/000306643
80. Spigolon G, Veronesi C, Bonny C, Vercelli A. c-Jun N-terminal kinase signaling pathway in excitotoxic cell death following kainic acid-induced status epilepticus. *Eur J Neurosci.* (2010) 31:1261–72. doi: 10.1111/j.1460-9568.2010.07158.x
81. Sclip A, Antoniou X, Colombo A, Camici GG, Pozzi L, Cardinetti D, et al. c-Jun N-terminal kinase regulates soluble Aβ oligomers and cognitive impairment in AD mouse model. *J Biol Chem.* (2011) 286:43871–80. doi: 10.1074/jbc.M111.297515
82. Repici M, Chen X, Morel MP, Doulazmi M, Sclip A, Cannaya V, et al. Specific inhibition of the JNK pathway promotes locomotor recovery and neuroprotection after mouse spinal cord injury. *Neurobiol Dis.* (2012) 46:710–21. doi: 10.1016/j.nbd.2012.03.014
83. Schellino R, Boido M, Borsello T, Vercelli A. Pharmacological c-Jun NH_2-terminal kinase (JNK) pathway inhibition reduces severity of spinal muscular atrophy disease in mice. *Front Mol Neurosci.* (2018) 11:308. doi: 10.3389/fnmol.2018.00308
84. Gao Y, Signore AP, Yin W, Cao G, Yin XM, Sun F, et al. Neuroprotection against focal ischemic brain injury by inhibition of c-Jun N-terminal kinase and attenuation of the mitochondrial apoptosis-signaling pathway. *J Cereb Blood Flow Metab.* (2005) 25:694–712. doi: 10.1038/sj.jcbfm.9600062
85. Guan QH, Pei DS, Zong YY, Xu TL, Zhang GY. Neuroprotection against ischemic brain injury by a small peptide inhibitor of c-Jun N-terminal kinase (JNK) via nuclear and non-nuclear pathways. *Neuroscience.* (2006) 139:609–27. doi: 10.1016/j.neuroscience.2005.11.067
86. Arthur PG, Matich GP, Pang WW, Yu DY, Bogoyevitch MA. Necrotic death of neurons following an excitotoxic insult is prevented by a peptide inhibitor of c-jun N-terminal kinase. *J Neurochem.* (2007) 102:65–76. doi: 10.1111/j.1471-4159.2007.04618.x

87. Bright R, Raval AP, Dembner JM, Pérez-Pinzón MA, Steinberg GK, Yenari MA, et al. Protein kinase C delta mediates cerebral reperfusion injury *in vivo*. *J Neurosci.* (2004) 24:6880–8. doi: 10.1523/JNEUROSCI.4474-03.2004
88. Bright R, Steinberg GK, Mochly-Rosen D. DeltaPKC mediates microcerebrovascular dysfunction in acute ischemia and in chronic hypertensive stress *in vivo*. *Brain Res.* (2007) 1144:146–55. doi: 10.1016/j.brainres.2007.01.113
89. Nijboer CH, van der Kooij MA, Van Bel F, Ohl F, Heijnen CJ, Kavelaars A. Inhibition of the JNK/AP-1 pathway reduces neuronal death and improves behavioral outcome after neonatal hypoxic-ischemic brain injury. *Brain Behav Immun.* (2010) 24:812–21. doi: 10.1016/j.bbi.2009.09.008
90. Nijboer CH, Bonestroo HJ, Zijlstra J, Kavelaars A Heijnen CJ. Mitochondrial JNK phosphorylation as a novel therapeutic target to inhibit neuroinflammation and apoptosis after neonatal ischemic brain damage. *Neurobiol Dis.* (2013) 54:432–44. doi: 10.1016/j.nbd.2013.01.017
91. Bach A, Clausen BH, Kristensen LK, Andersen MG, Ellman DG, Hansen PBL, et al. Selectivity efficacy and toxicity studies of UCCB01–144 a dimeric neuroprotective PSD-95 inhibitor. *Neuropharmacology.* (2019) 150:100–11. doi: 10.1016/j.neuropharm.2019.02.035
92. Bach A, Clausen BH, Møller M, Vestergaard B, Chi CN, Round A, et al. A high-affinity dimeric inhibitor of PSD-95 bivalently interacts with PDZ1–2 and protects against ischemic brain damage. *Proc Natl Acad Sci USA.* (2012) 109:3317–22. doi: 10.1073/pnas.1113761109
93. Andreasen JT, Nasser A, Caballero-Puntiverio M, Sahlholt M, Bach A, Gynther M, et al. Effects of the dimeric PSD-95 inhibitor UCCB01–144 in mouse models of pain cognition and motor function. *Eur J Pharmacol.* (2016) 780:166–73. doi: 10.1016/j.ejphar.2016.03.045
94. Kucharz K, Søndergaard Rasmussen I, Bach A, Strømgaard K, Lauritzen M. PSD-95 uncoupling from NMDA receptors by Tat-N-dimer ameliorates neuronal depolarization in cortical spreading depression. *J Cereb Blood Flow Metab.* (2017) 37:1820–8. doi: 10.1177/0271678X16645595
95. Colciaghi F, Nobili P, Cipelletti B, Cagnoli C, Zambon S, Locatelli D, et al. Targeting PSD95-nNOS interaction by Tat-N-dimer peptide during status epilepticus is neuroprotective in MAM-pilocarpine rat model. *Neuropharmacology.* (2019) 153:82–97. doi: 10.1016/j.neuropharm.2019.04.028
96. Pan J, Qian J, Zhang Y, Ma J, Wang G, Xiao Q, et al. Small peptide inhibitor of JNKs protects against MPTP-induced nigral dopaminergic injury via inhibiting the JNK-signaling pathway. *Lab Invest.* (2010) 90:156–67. doi: 10.1038/labinvest.2009.124
97. Pan J, Li H, Zhang B, Xiong R, Zhang Y, Kang WY, et al. Small peptide inhibitor of JNK3 protects dopaminergic neurons from MPTP induced injury via inhibiting the ASK1-JNK3 signaling pathway. *PLoS ONE.* (2015) 10:e0119204. doi: 10.1371/journal.pone.0119204
98. Liu XJ, Gingrich JR, Vargas-Caballero M, Dong YN, Sengar A, Beggs S, et al. Treatment of inflammatory and neuropathic pain by uncoupling Src from the NMDA receptor complex. *Nat Med.* (2008) 14:1325–32. doi: 10.1038/nm.1883
99. Chambers JW, Howard S, LoGrasso PV. Blocking c-Jun N-terminal kinase (JNK) translocation to the mitochondria prevents 6-hydroxydopamine-induced toxicity *in vitro* and *in vivo*. *J Biol Chem.* (2013) 288:1079–87. doi: 10.1074/jbc.M112.421354
100. Brittain JM, Chen L, Wilson SM Brustovetsky T, Gao X, Ashpole NM, et al. Neuroprotection against traumatic brain injury by a peptide derived from the collapsin response mediator protein 2 (CRMP2). *J Biol Chem.* (2011) 286:37778–92. doi: 10.1074/jbc.M111.255455
101. Brittain JM, Duarte DB, Wilson SM, Zhu W, Ballard C, Johnson PL, et al. Suppression of inflammatory and neuropathic pain by uncoupling CRMP-2 from the presynaptic Ca^{2+} channel complex. *Nat Med.* (2011) 17:822–9. doi: 10.1038/nm.2345
102. Brittain JM, Pan R, You H, Brustovetsky T, Brustovetsky N, Zamponi GW, et al. Disruption of NMDAR-CRMP-2 signaling protects against focal cerebral ischemic damage in the rat middle cerebral artery occlusion model. *Channels.* (2012) 6:52–9. doi: 10.4161/chan.18919
103. Piekarz AD, Due MR, Khanna M, Wang B, Ripsch MS, Wang R, et al. CRMP-2 peptide mediated decrease of high and low voltage-activated calcium channels attenuation of nociceptor excitability and anti-nociception in a model of AIDS therapy-induced painful peripheral neuropathy. *Mol Pain.* (2012) 8:2–19. doi: 10.1186/1744-8069-8-54
104. Ripsch MS, Ballard CJ, Khanna M, Hurley JH, White FA, Khanna R. A peptide uncoupling CRMP-2 from the presynaptic Ca^{2+} channel complex demonstrates efficacy in animal models of migraine and aids therapy-induced neuropathy. *Transl Neurosci.* (2012) 3:1–8. doi: 10.2478/s13380-012-0002-4
105. Moutal A, François-Moutal L Brittain JM, Khanna M, Khanna R. Differential neuroprotective potential of CRMP2 peptide aptamers conjugated to cationic hydrophobic and amphipathic cell penetrating peptides. *Front Cell Neurosci.* (2015) 8:471. doi: 10.3389/fncel.2014.00471
106. Bu X, Nan Zhang N, Yang X, Liu Y, Du J, Liang J, et al. Proteomic analysis of cPKCβII-interacting proteins involved in HPC-induced neuroprotection against cerebral ischemia of mice. *J Neurochem.* (2011) 117:346–56. doi: 10.1111/j.1471-4159.2011.07209.x
107. Yin Y, Wang Y, Chen L, Han S, Zhao L, Luo Y, et al. Tat-collapsin response mediator protein 2 (CRMP2) increases the survival of neurons after NMDA excitotoxity by reducing the cleavage of CRMP2. *Neurochem Res.* (2013) 38:2095–104. doi: 10.1007/s11064-013-1118-9
108. Yang X, Zhang X, Li Y, Han S, Howells DW, Li S, et al. Conventional protein kinase Cβ-mediated phosphorylation inhibits collapsin response-mediated protein 2 proteolysis and alleviates ischemic injury in cultured cortical neurons and ischemic stroke-induced mice. *J Neurochem.* (2016) 137:446–59. doi: 10.1111/jnc.13538
109. Meloni BP, Milani D, Edwards AB, Anderton RS, O'Hare Doig RL, Fitzgerald M, et al. Neuroprotective peptides fused to arginine-rich cell penetrating peptides: neuroprotective mechanism likely mediated by peptide endocytic properties. *Pharmacol Ther.* (2015) 153:36–54. doi: 10.1016/j.pharmthera.2015.06.002
110. McQueen J, Ryan TJ, McKay S, Marwick K, Baxter P, Carpanini SM, et al. Pro-death NMDA receptor signaling is promoted by the GluN2B C-terminus independently of Dapk1. *Elife.* (2017) 6:e17161. doi: 10.7554/eLife.17161.024
111. Tu W, Xu X, Peng L, Zhong X, Zhang W, Soundarapandian MM, et al. DAPK1 interaction with NMDA receptor NR2B subunits mediates brain damage in stroke. *Cell.* (2010) 140:222–34. doi: 10.1016/j.cell.2009.12.055
112. Pei L, Li S, Wang M, Diwan M, Anisman H, Fletcher PJ, et al. Uncoupling the dopamine D1-D2 receptor complex exerts antidepressant-like effects. *Nat Med.* (2010) 16:1393–5. doi: 10.1038/nm.2263
113. Li FQ, Fowler KA, Neil JE, Colton CA, Vitek MP. An apolipoprotein E-mimetic stimulates axonal regeneration and remyelination after peripheral nerve injury. *J Pharmacol Exp Ther.* (2010) 334:106–15. doi: 10.1124/jpet.110.167882
114. Ghosal K, Stathopoulos A, Thomas D, Phenis D, Vitek MP, Pimplikar SW. The apolipoprotein-E-mimetic COG112 protects amyloid precursor protein intracellular domain-overexpressing animals from Alzheimer's disease-like pathological features. *Neurodegener Dis.* (2013) 12:51–8. doi: 10.1159/000341299
115. Gu Z, Li F, Zhang YP, Shields LB, Hu X, Zheng Y, et al. Apolipoprotein E mimetic promotes functional and histological recovery in lysolecithin-induced spinal cord demyelination in mice. *J Neurol Neurophysiol.* (2013) 2014:10. doi: 10.4172/2155-9562.S12-010
116. Fan X, Jin W Y, Lu J, Wang J, Wang YT. Rapid and reversible knockdown of endogenous proteins by peptide-directed lysosomal degradation. *Nat Neurosci.* (2014) 17:471–80. doi: 10.1038/nn.3637
117. LeBlanc BW, Iwata M, Mallon AP, Rupasinghe CN, Goebel DJ, Marshall J, et al. A cyclic peptide targeted against PSD-95 blocks central sensitization and attenuates thermal hyperalgesia. *Neuroscience.* (2010) 167:490–500. doi: 10.1016/j.neuroscience.2010.02.031
118. Arribat Y, Talmat-Amar Y, Paucard A, Lesport P, Bonneaud N, Bauer C, et al. Systemic delivery of P42 peptide: a new weapon to fight Huntington's disease. *Acta Neuropathol Commun.* (2014) 2:86. doi: 10.1186/s40478-014-0086-x
119. Pei L, Shang Y, Jin H, Wang S, Wei N, Yan H, et al. DAPK1-p53 interaction converges necrotic and apoptotic pathways of ischemic neuronal death. *J Neurosci.* (2014) 34:6546–56. doi: 10.1523/JNEUROSCI.5119-13.2014
120. Wang X, Pei L, Yan H, Wang Z, Wei N, Wang S, et al. Intervention of death-associated protein kinase 1-p53 interaction exerts the therapeutic effects against stroke. *Stroke.* (2014) 45:3089–91. doi: 10.1161/STROKEAHA.114.006348

121. Vest RS, O'Leary H, Coultrap SJ, Kindy MS, Bayer KU. Effective post-insult neuroprotection by a novel Ca^{2+}/calmodulin-dependent protein kinase II (CaMKII) inhibitor. *J Biol Chem.* (2010) 285:20675–82. doi: 10.1074/jbc.M109.088617
122. Ashpole NM, Hudmon A. Excitotoxic neuroprotection and vulnerability with CaMKII inhibition. *Mol Cell Neurosci.* (2011) 46:720–30. doi: 10.1016/j.mcn.2011.02.003
123. Ahmed ME, Dong Y, Lu Y, Tucker D, Wang R, Zhang Q. Beneficial effects of a CaMKIIα inhibitor TatCN21 peptide in global cerebral ischemia. *J Mol Neurosci.* (2017) 61:42–51. doi: 10.1007/s12031-016-0830-8
124. Pei DS, Wang XT, Liu Y, Sun YF, Guan QH, Wang W, et al. Neuroprotection against ischaemic brain injury by a GluR6–9c peptide containing the TAT protein transduction sequence. *Brain.* (2006) 129:465–79. doi: 10.1093/brain/awh700
125. Liu XM, Pei DS, Guan QH, Sun YF, Wang XT, Zhang QX, et al. Neuroprotection of Tat-GluR6–9c against neuronal death induced by kainate in rat hippocampus via nuclear and non-nuclear pathways. *J Biol Chem.* (2006) 281:17432–45. doi: 10.1074/jbc.M513490200
126. Yu CZ, Li C, Pei DS, Zong YY, Shi Q, Wen XR, et al. Neuroprotection against transient focal cerebral ischemia and oxygen-glucose deprivation by interference with GluR6-PSD95 protein interaction. *Neurochem Res.* (2009) 34:2008–21. doi: 10.1007/s11064-009-9990-z
127. Xu W, Wong TP, Chery N, Gaertner T, Wang YT, Baudry M. Calpain-mediated mGluR1alpha truncation: a key step in excitotoxicity. *Neuron.* (2007) 53:399–412. doi: 10.1016/j.neuron.2006.12.020
128. Zhou M, Xu W, Liao G, Bi X, Baudry M. Neuroprotection against neonatal hypoxia/ischemia-induced cerebral cell death by prevention of calpain-mediated mGluR1alpha truncation. *Exp Neurol.* (2009) 218:75–82. doi: 10.1016/j.expneurol.2009.04.006
129. Wang W, Han P, Xie R, Yang M, Zhang C, Mi Q, et al. TAT-mGluR1 attenuation of neuronal apoptosis through prevention of mGluR1α truncation after experimental subarachnoid hemorrhage. *ACS Chem Neurosci.* (2018) 10:746–56. doi: 10.1021/acschemneuro.8b00531
130. Zhang S, Taghibiglou C, Girling K, Dong Z, Lin SZ, Lee W, et al. Critical role of increased PTEN nuclear translocation in excitotoxic and ischemic neuronal injuries. *J Neurosci.* (2013) 33:7997–8008 doi: 10.1523/JNEUROSCI.5661-12.2013
131. Taghibiglou C, Martin HG, Lai TW, Cho T, Prasad S, Kojic L, et al. Role of NMDA receptor-dependent activation of SREBP1 in excitotoxic and ischemic neuronal injuries. *Nat Med.* (2009) 15:1399–406. doi: 10.1038/nm.2064
132. Li LL, Ginet V, Liu X, Vergun O, Tuittila M, Mathieu M, et al. The nNOS-p38MAPK pathway is mediated by NOS1AP during neuronal death. *J Neurosci.* (2013) 33:8185–201. doi: 10.1523/JNEUROSCI.4578-12.2013
133. Li LL, Melero-Fernandez de Mera RM, Chen J, Ba W, Kasri NN, Zhang M, et al. Unexpected heterodivalent recruitment of NOS1AP to nNOS reveals multiple sites for pharmacological intervention in neuronal disease models. *J Neurosci.* (2015) 35:7349–64. doi: 10.1523/JNEUROSCI.0037-15.2015
134. Lee WH, Li LL, Chawla A, Hudmon A, Lai YY, Courtney MJ, et al. Disruption of nNOS-NOS1AP protein-protein interactions suppresses neuropathic pain in mice. *Pain.* (2018) 159:849–63. doi: 10.1097/j.pain.0000000000001152
135. Wang Q, Gou X, Xiong L, Jin W, Chen S, Hou L, et al. Trans-activator of transcription-mediated delivery of NEP1–40 protein into brain has a neuroprotective effect against focal cerebral ischemic injury via inhibition of neuronal apoptosis. *Anesthesiology.* (2008) 108:1071–80. doi: 10.1097/ALN.0b013e318173f66b
136. Wang Q, Gou X, Jin W, Xiong L, Hou L, Chen S, et al. TAT-mediated protein transduction of Nogo extracellular peptide 1–40 and its biological activity. *Cell Mol Neurobiol.* (2009) 29:97–108. doi: 10.1007/s10571-008-9301-2
137. van der Kooij MA, Nijboer CH, Ohl F, Groenendaal F, Heijnen CJ, van Bel F, et al. NF-kappaB inhibition after neonatal cerebral hypoxia-ischemia improves long-term motor and cognitive outcome in rats. *Neurobiol Dis.* (2010) 38:266–72. doi: 10.1016/j.nbd.2010.01.016
138. Sun X, Budas GR, Xu L, Barreto GE, Mochly-Rosen D, Giffard RG. Selective activation of protein kinase Cϵ in mitochondria is neuroprotective *in vitro* and reduces focal ischemic brain injury in mice. *J Neurosci Res.* (2013) 91:799–807. doi: 10.1002/jnr.23186
139. He M, Ding Y, Chu C, Tang J, Xiao Q, Luo ZG. Autophagy induction stabilizes microtubules and promotes axon regeneration after spinal cord injury. *Proc Natl Acad Sci USA.* (2016) 113:11324–9. doi: 10.1073/pnas.1611282113
140. Zhang L, Li Z, Feng D, Shen H, Tian X, Li H, et al. Involvement of Nox2 and Nox4 NADPH oxidases in early brain injury after subarachnoid haemorrhage. *Free Radic Res.* (2017) 51:316–28. doi: 10.1080/10715762.2017.1311015
141. Khayrullina G, Bermudez S, Byrnes KR. Inhibition of NOX2 reduces locomotor impairment inflammation and oxidative stress after spinal cord injury. *J Neuroinflammation.* (2015) 12:172. doi: 10.1186/s12974-015-0391-8
142. Zhang QG, Laird MD, Han D, Nguyen K, Scott E, Dong Y, et al. Critical role of NADPH oxidase in neuronal oxidative damage and microglia activation following traumatic brain injury. *PLoS ONE.* (2012) 7:e34504. doi: 10.1371/journal.pone.0034504
143. Lang BT, Cregg JM, DePaul MA, Tran AP, Xu K, Dyck SM, et al. Modulation of the proteoglycan receptor PTPσ promotes recovery after spinal cord injury. *Nature.* (2015) 518:404–8. doi: 10.1038/nature13974
144. García-Caballero A, Gadotti VM, Stemkowski P, Weiss N, Souza IA, Hodgkinson V, et al. The deubiquitinating enzyme USP5 modulates neuropathic and inflammatory pain by enhancing Cav32 channel activity. *Neuron.* (2014) 83:1144–58. doi: 10.1016/j.neuron.2014.07.036
145. Ozaki T, Ishiguro S, Hirano S, Baba A, Yamashita T, Tomita H, et al. Inhibitory peptide of mitochondrial μ-calpain protects against photoreceptor degeneration in rhodopsin transgenic S334ter and P23H rats. *PLoS ONE.* (2013) 8:e71650. doi: 10.1371/annotation/7a8aaf1d-e968-4b39-abb0-867d6078b2af
146. Ju W, Li Q, Allette YM, Ripsch MS, White FA, Khanna R. Suppression of pain-related behavior in two distinct rodent models of peripheral neuropathy by a homopolyarginine-conjugated CRMP2 peptide. *J Neurochem.* (2013) 124:869–79. doi: 10.1111/jnc.12070
147. Xu J, Kurup P, Zhang Y, Goebel-Goody SM, Wu PH, Hawasli AH, et al. Extrasynaptic NMDA receptors couple preferentially to excitotoxicity via calpain-mediated cleavage of STEP. *J Neurosci.* (2009) 29:9330–43. doi: 10.1523/JNEUROSCI.2212-09.2009
148. Gamir-Morralla A, López-Menéndez C, Ayuso-Dolado S, Tejeda GS, Montaner J, Rosell A, et al. Development of a neuroprotective peptide that preserves survival pathways by preventing Kidins220/ARMS calpain processing induced by excitotoxicity. *Cell Death Dis.* (2015) 6:e1939. doi: 10.1038/cddis.2015.307
149. Disatnik MH, Joshi AU, Saw NL, Shamloo M, Leavitt BR, Qi X, et al. Potential biomarkers to follow the progression and treatment response of Huntington's disease. *J Exp Med.* (2016) 213:2655–69. doi: 10.1084/jem.20160776
150. Guo X, Sesaki H, Qi X. Drp1 stabilizes p53 on the mitochondria to trigger necrosis under oxidative stress conditions *in vitro* and *in vivo*. *Biochem J.* (2014) 461:137–46. doi: 10.1042/BJ20131438
151. Du W, Huang J, Yao H, Zhou K, Duan B, Wang Y. Inhibition of TRPC6 degradation suppresses ischemic brain damage in rats. *J Clin Invest.* (2010) 120:3480–92. doi: 10.1172/JCI43165
152. Wang CL, Qiu TT, Diao YX, Zhang Y, Gu N. Novel endomorphin-1 analogs with C-terminal oligoarginine-conjugation display systemic antinociceptive activity with less gastrointestinal side effects. *Biochimie.* (2015) 116:24–33. doi: 10.1016/j.biochi.2015.06.008
153. Cimini S, Sclip A, Mancini S, Colombo L, Messa M, Cagnotto A, et al. The cell-permeable Aβ1–6A2VTAT(D) peptide reverts synaptopathy induced by Aβ1–42wt. *Neurobiol Dis.* (2016) 89:101–11. doi: 10.1016/j.nbd.2015.12.013
154. Tu J, Zhang X, Zhu Y, Dai Y, Li N, Yang F, et al. Cell-permeable peptide targeting the Nrf2-Keap1 interaction: a potential novel therapy for global cerebral ischemia. *J Neurosci.* (2015) 35:14727–39. doi: 10.1523/JNEUROSCI.1304-15.2015
155. Liu J, Du J, Yang Y, Wang Y. Phosphorylation of TRPV1 by cyclin-dependent kinase 5 promotes TRPV1 surface localization leading to inflammatory thermal hyperalgesia. *Exp Neurol.* (2015) 273:253–62. doi: 10.1016/j.expneurol.2015.09.005
156. Zhang Y, Su P, Liang P, Liu T, Liu X, Liu XY, et al. The DREAM protein negatively regulates the NMDA receptor

through interaction with the NR1 subunit. *J Neurosci.* (2010) 30:7575–86. doi: 10.1523/JNEUROSCI.1312-10.2010
157. Yeh CY, Bulas AM, Moutal A, Saloman JL, Hartnett KA, Anderson CT, et al. Targeting a potassium channel/syntaxin interaction ameliorates cell death in ischemic stroke. *J Neurosci.* (2017) 37 5648–58. doi: 10.1523/JNEUROSCI.3811-16.2017
158. Wattiez AS, Dupuis A, Privat AM, Chalus M, Chapuy E, Aissouni Y, et al. Disruption of 5-HT2A-PDZ protein interaction differently affects the analgesic efficacy of SSRI SNRI and TCA in the treatment of traumatic neuropathic pain in rats. *Neuropharmacology.* (2017) 125:308–18. doi: 10.1016/j.neuropharm.2017.07.034
159. Li X, Zheng L, Xia Q, Liu L, Mao M, Zhou H, et al. A novel cell-penetrating peptide protects against neuron apoptosis after cerebral ischemia by inhibiting the nuclear translocation of annexin A1. *Cell Death Differ.* (2019) 26:260–75. doi: 10.1038/s41418-018-0116-5
160. Moutal A, Li W, Wang Y, Ju W, Luo S, Cai S, et al. Homology-guided mutational analysis reveals the functional requirements for antinociceptive specificity of collapsin response mediator protein 2-derived peptides. *Br J Pharmacol.* (2018) 175:2244–60. doi: 10.1111/bph.13737
161. Kashkin VA, Shekunova EV, Titov MI, Eliseev II, Gureev MA, Porozov YB, et al. A new tridecapeptide with an octaarginine vector has analgesic therapeutic potential and prevents morphine-induced tolerance. *Peptides.* (2018) 99:61–9. doi: 10.1016/j.peptides.2017.11.011
162. Vezzoli E, Caron I, Talpo F, Besusso D, Conforti P, Battaglia E, et al. Inhibiting pathologically active ADAM10 rescues synaptic and cognitive decline in Huntington's disease. *J Clin Invest.* (2019) 130:120616. doi: 10.1172/JCI120616
163. O'Donnell LA, Agrawal A, Sabnekar P, Dichter MA, Lynch DR, Kolson DL. Apelin an endogenous neuronal peptide protects hippocampal neurons against excitotoxic injury. *J Neurochem.* (2007) 102:1905–17. doi: 10.1111/j.1471-4159.2007.04645.x
164. Cook DR, Gleichman AJ, Cross SA, Doshi S, Ho W, Jordan-Sciutto KL, et al. NMDA receptor modulation by the neuropeptide apelin: implications for excitotoxic injury. *J Neurochem.* (2011) 118:1113–23. doi: 10.1111/j.1471-4159.2011.07383.x
165. Sakamoto K, Murakami Y, Sawada S, Ushikubo H, Mori A, Nakahara T, et al. Apelin-36 is protective against N-methyl-D-aspartic-acid-induced retinal ganglion cell death in the mice. *Eur J Pharmacol.* (2016) 791:213–20. doi: 10.1016/j.ejphar.2016.08.036
166. Ishimaru Y, Sumino A, Kajioka D, Shibagaki F, Yamamuro A, Yoshioka Y, et al. Apelin protects against NMDA-induced retinal neuronal death via an APJ receptor by activating Akt and ERK1/2 and suppressing TNF-α expression in mice. *J Pharmacol Sci.* (2017) 133:34–41. doi: 10.1016/j.jphs.2016.12.002
167. Gu Q, Zhai L, Feng X, Chen J, Miao Z, Ren L, et al. Apelin-36 a potent peptide protects against ischemic brain injury by activating the PI3K/Akt pathway. *Neurochem Int.* (2013) 63:535–40. doi: 10.1016/j.neuint.2013.09.017
168. Chen D, Lee J, Gu X, Wei L, Yu SP. Intranasal delivery of apelin-13 is neuroprotective and oromotes angiogenesis after ischemic stroke in mice. *ASN Neuro.* (2015) 7:1–15. doi: 10.1177/1759091415605114
169. Yang Y, Zhang XJ, Li LT, Cui HY, Zhang C, Zhu CH, et al. Apelin-13 protects against apoptosis by activating AMP-activated protein kinase pathway in ischemia stroke. *Peptides.* (2016) 75:96–100. doi: 10.1016/j.peptides.2015.11.002
170. Qiu J, Wang X, Wu F, Wan L, Cheng B, Wu Y, et al. Low dose of apelin-36 attenuates ER stress-associated apoptosis in rats with ischemic stroke. *Front Neurol.* (2017) 8:556. doi: 10.2174/9781681085326117040l
171. Xu N, Wang H, Fan L, Chen Q. Supraspinal administration of apelin-13 induces antinociception via the opioid receptor in mice. *Peptides.* (2009) 30:1153–7. doi: 10.1016/j.peptides.2009.02.011
172. Khaksari M, Aboutaleb N, Nasirinezhad F, Vakili A, Madjd Z. Apelin-13 protects the brain against ischemic reperfusion injury and cerebral edema in a transient model of focal cerebral ischemia. *J Mol Neurosci.* (2012) 48:201–8. doi: 10.1007/s12031-012-9808-3
173. Bao H, Yang X, Huang Y, Qiu H, Huang G, Xiao H, et al. The neuroprotective effect of apelin-13 in a mouse model of intracerebral haemorrhage. *Neurosci Lett.* (2016) 628:219–24. doi: 10.1016/j.neulet.2016.06.046
174. Bao HJ, Zhang L, Han WC, Dai DK. Apelin-13 attenuates traumatic brain injury-induced damage by suppressing autophagy. *Neurochem Res.* (2015) 40:89–97. doi: 10.1007/s11064-014-1469-x
175. Xin Q, Cheng B, Pan Y, Liu H, Yang C, Chen J, et al. Neuroprotective effects of apelin-13 on experimental ischemic stroke through suppression of inflammation. *Peptides.* (2015) 63:55–62. doi: 10.1016/j.peptides.2014.09.016
176. Hajimashhadi Z, Aboutaleb N, Nasirinezhad F. Chronic administration of [Pyr1] apelin-13 attenuates neuropathic pain after compression spinal cord injury in rats. *Neuropeptides.* (2017) 61:15–22. doi: 10.1016/j.npep.2016.08.010
177. Kao TK, Ou YC, Liao SL, Chen WY, Wang CC, Chen SY, et al. Opioids modulate post-ischemic progression in a rat model of stroke. *Neurochem Int.* (2008) 52:1256–65. doi: 10.1016/j.neuint.2008.01.007
178. Liu B, Qin L, Yang SN, Wilson BC, Liu Y, Hong JS. Femtomolar concentrations of dynorphins protect rat mesencephalic dopaminergic neurons against inflammatory damage. *J Pharmacol Exp Ther.* (2001) 298:1133–41.
179. Hall SM, Lee YS, Hruby VJ. Dynorphin A analogs for the treatment of chronic neuropathic pain. *Future Med Chem.* (2016) 8:165–77. doi: 10.4155/fmc.15.164
180. Yamamoto T, Tatsuno I. Antinociceptive effect of intrathecally administered pituitary adenylate cyclase activating polypeptide (PACAP) on the rat formalin test. *Neurosci Lett.* (1995) 184:32–5. doi: 10.1016/0304-3940(94)11161-B
181. Uchida D, Arimura A, Somogyvári-Vigh A, Shioda S, Banks WA. Prevention of ischemia-induced death of hippocampal neurons by pituitary adenylate cyclase activating polypeptide. *Brain Res.* (1996) 736:280–6. doi: 10.1016/0006-8993(96)00716-0
182. Shoge K, Mishima HK, Saitoh T, Ishihara K, Tamura Y, Shiomi H, et al. Attenuation by PACAP of glutamate-induced neurotoxicity in cultured retinal neurons. *Brain Res.* (1999) 839:66–73. doi: 10.1016/S0006-8993(99)01690-X
183. Reglodi D, Borzsei R, Bagoly T, Boronkai A, Racz B, Tamas A, et al. Agonistic behavior of PACAP6–38 on sensory nerve terminals and cytotrophoblast cells. *J Mol Neurosci.* (2008) 36:270–8. doi: 10.1007/s12031-008-9089-z
184. Reglodi D, Lubics A, Tamás A, Szalontay L, Lengvári I. Pituitary adenylate cyclase activating polypeptide protects dopaminergic neurons and improves behavioral deficits in a rat model of Parkinson's disease. *Behav Brain Res.* (2004) 151:303–12. doi: 10.1016/j.bbr.2003.09.007
185. Reglodi D, Tamás A, Somogyvári-Vigh A, Szántó Z, Kertes E, Lénárd L, et al. Effects of pretreatment with PACAP on the infarct size and functional outcome in rat permanent focal cerebral ischemia. *Peptides.* (2002) 23:2227–34. doi: 10.1016/S0196-9781(02)00262-0
186. Sibilia V, Lattuada N, Rapetti D, Pagani F, Vincenza D, Bulgarelli I, et al. Ghrelin inhibits inflammatory pain in rats: involvement of the opioid system. *Neuropharmacology.* (2006) 51:497–505. doi: 10.1016/j.neuropharm.2006.04.009
187. Erşahin M, Toklu HZ, Erzik C, Cetinel S, Akakin D, Velioglu-Ogünç A, et al. The anti-inflammatory and neuroprotective effects of ghrelin in subarachnoid hemorrhage-induced oxidative brain damage in rats. *J Neurotrauma.* (2010) 27:1143–55. doi: 10.1089/neu.2009.1210
188. Andrews ZB Erion D, Beiler R, Liu ZW, Abizaid A, Zigman J, et al. Ghrelin promotes and protects nigrostriatal dopamine function via a UCP2-dependent mitochondrial mechanism. *J Neurosci.* (2009) 29:14057–65. doi: 10.1523/JNEUROSCI.3890-09.2009
189. Hwang S, Moon M, Kim S, Hwang L, Ahn KJ, Park S. Neuroprotective effect of ghrelin is associated with decreased expression of prostate apoptosis response-4. *Endocr J.* (2009) 56:609–17. doi: 10.1507/endocrj.K09E-072
190. Lopez NE, Gaston L, Lopez KR, Coimbra RC, Hageny A, Putnam J, et al. Early ghrelin treatment attenuates disruption of the blood brain barrier and apoptosis after traumatic brain injury through a UCP-2 mechanism. *Brain Res.* (2012) 1489:140–8. doi: 10.1016/j.brainres.2012.10.031
191. Ge T, Yang W, Fan J, Li B. Preclinical evidence of ghrelin as a therapeutic target in epilepsy. *Oncotarget.* (2017) 8:59929–39. doi: 10.18632/oncotarget.18349
192. Eslami M, Sadeghi B, Goshadrou F. Chronic ghrelin administration restores hippocampal long-term potentiation and ameliorates memory

impairment in rat model of Alzheimer's disease. *Hippocampus.* (2018) 28:724–34. doi: 10.1002/hipo.23002
193. Xu X, Chua CC, Gao J, Hamdy RC, Chua BH. Humanin is a novel neuroprotective agent against stroke. *Stroke.* (2006) 37:2613–19. doi: 10.1161/01.STR.0000242772.94277.1f
194. Niikura T, Sidahmed E, Hirata-Fukae C, Aisen PS, Matsuoka Y. A humanin derivative reduces amyloid beta accumulation and ameliorates memory deficit in triple transgenic mice. *PLoS ONE.* (2011) 6:e16259. doi: 10.1371/journal.pone.0016259
195. Wang T, Huang Y, Zhang M, Wang L, Wang Y, Zhang L, et al. [Gly14]-Humanin offers neuroprotection through glycogen synthase kinase-3β inhibition in a mouse model of intracerebral hemorrhage. *Behav Brain Res.* (2013) 247:132–39. doi: 10.1016/j.bbr.2013.03.023
196. Chen J, Sun M, Zhang X, Miao Z, Chua BH, Hamdy RC, et al. Increased oligodendrogenesis by humanin promotes axonal remyelination and neurological recovery in hypoxic/ischemic brains. *Hippocampus.* (2015) 25:62–71. doi: 10.1002/hipo.22350
197. Yang X, Zhang H, Wu J, Yin L, Yan LJ, Zhang C. Humanin attenuates NMDA-induced excitotoxicity by inhibiting ROS-dependent JNK/p38 MAPK pathway. *Int J Mol Sci*. (2018) 19:E2982. doi: 10.3390/ijms19102982
198. Ross CR, Ricevuti G, Scovassi AI. The antimicrobial peptide PR-39 has a protective effect against HeLa cell apoptosis. *Chem Biol Drug Des.* (2007) 70:154–57. doi: 10.1111/j.1747-0285.2007.00540.x
199. Wu J, Parungo C, Wu G, Kang PM, Laham RJ, Sellke FW, et al. PR39 inhibits apoptosis in hypoxic endothelial cells: role of inhibitor apoptosis protein-2. *Circulation.* (2004) 109:1660–7. doi: 10.1161/01.CIR.0000124067.35915.E0
200. Bao J, Sato K, Li M, Gao Y, Abid R, Aird W, et al. PR-39 and PR-11 peptides inhibit ischemia-reperfusion injury by blocking proteasome-mediated I kappa B alpha degradation. *Am J Physiol Heart Circ Physiol.* (2001) 281:2612–18. doi: 10.1152/ajpheart.2001.281.6.H2612
201. Sarko D, Beijer B, Garcia Boy R, Nothelfer EM, Leotta K, Eisenhut M, et al. The pharmacokinetics of cell-penetrating peptides. *Mol Pharm.* (2010) 7:2224–31. doi: 10.1021/mp100223d
202. Stalmans S, Bracke N, Wynendaele E, Gevaert B, Peremans K, Burvenich C, et al. Cell-penetrating peptides selectively cross the blood-brain barrier *in vivo*. *PLoS ONE.* (2015) 10:e0139652. doi: 10.1371/journal.pone.0139652
203. Collado Camps E, Brock R. An opportunistic route to success: towards a change of paradigm to fully exploit the potential of cell-penetrating peptides. *Bioorg Med Chem.* (2018) 26:2780–87. doi: 10.1016/j.bmc.2017.11.004
204. Bechara C, Pallerla M, Zaltsman Y, Burlina F, Alves ID, Lequin O, et al. Tryptophan within basic peptide sequences triggers glycosaminoglycan-dependent endocytosis. *FASEB J.* (2013) 27:738–49. doi: 10.1096/fj.12-216176
205. Bechara C, Pallerla M, Burlina F, Illien F, Cribier S, Sagan S. Massive glycosaminoglycan-dependent entry of Trp-containing cell-penetrating peptides induced by exogenous sphingomyelinase or cholesterol depletion. *Cell Mol Life Sci.* (2015) 72:809–20. doi: 10.1007/s00018-014-1696-y
206. Jobin ML, Blanchet M, Henry S, Chaignepain S, Manigand C, Castano S, et al. The role of tryptophans on the cellular uptake and membrane interaction of arginine-rich cell penetrating peptides. *Biochim Biophys Acta.* (2015) 1848:593–602. doi: 10.1016/j.bbamem.2014.11.013
207. Rydberg HA, Matson M, Amand HL, Esbjörner EK, Nordén B. Effects of tryptophan content and backbone spacing on the uptake efficiency of cell-penetrating peptides. *Biochemistry.* (2012) 51:5531–39. doi: 10.1021/bi300454k
208. Walrant A, Vogel A, Correia I, Lequin O, Olausson BE, Desbat B, et al. Membrane interactions of two arginine-rich peptides with different cell internalization capacities. *Biochim Biophys Acta.* (2012) 1818:1755–63. doi: 10.1016/j.bbamem.2012.02.024
209. Himmel HM, Kiss T, Borvendeg SJ, Gillen C, Illes P. The arginine-rich hexapeptide R4W2 is a stereoselective antagonist at the vanilloid receptor 1: a Ca^{2+} imaging study in adult rat dorsal root ganglion neurons. *J Pharmacol Exp Ther.* (2002) 301:981–6. doi: 10.1124/jpet.301.3.981
210. Schwarze SR, Ho A, Vocero-Akbani A, Dowdy SF. *In vivo* protein transduction: delivery of a biologically active protein into the mouse. *Science.* (1999) 285:1569–72. doi: 10.1126/science.285.5433.1569
211. Mitchell DJ, Kim DT, Steinman L, Fathman CG, Rothbard JB. Polyarginine enters cells more efficiently than other polycationic homopolymers. *J Pept Res.* (2000) 56:318–25. doi: 10.1034/j.1399-3011.2000.00723.x
212. Meloni BP, South SM, Gill DA, Marriott AL Déziel RA, Jacques A, et al. Poly-arginine peptides R18 and R18D improve functional outcomes after endothelin-1 (ET-1)-induced stroke in the Sprague Dawley rat. *J Neuropathol Exp Neurol.* (2019) 78:426–35. doi: 10.1093/jnen/nlz014
213. Bechinger B, Gorr SU. Antimicrobial peptides: mechanisms of action and resistance. *J Dent Res.* (2017) 96:254–60. doi: 10.1177/0022034516679973
214. Leite ML, da Cunha NB, Costa FF. Antimicrobial peptides nanotechnology and natural metabolites as novel approaches for cancer treatment. *Pharmacol Ther.* (2018) 183:160–76. doi: 10.1016/j.pharmthera.2017.10.010
215. Schnaar RL. Gangliosides of the vertebrate nervous system. *J Mol Biol.* (2016) 428:3325–36. doi: 10.1016/j.jmb.2016.05.020
216. Ravindran MS, Tanner LB, Wenk MR. Sialic acid linkage in glycosphingolipids is a molecular correlate for trafficking and delivery of extracellular cargo. *Traffic*. (2013) 14:1182–91. doi: 10.1111/tra.12100
217. Yu RK, Tsai YT, Ariga T, Yanagisawa M. Structures biosynthesis and functions of gangliosides-an overview. *J Oleo Sci.* (2011) 60:537–44. doi: 10.5650/jos.60.537
218. Aliste MP, MacCallum JL, Tieleman DP. Molecular dynamics simulations of pentapeptides at interfaces: salt bridge and cation-pi interactions. *Biochemistry.* (2003) 42:8976–87. doi: 10.1021/bi027001j
219. Dougherty DA. The cation-π interaction. *Acc Chem Res.* (2013) 46:885–93. doi: 10.1021/ar300265y
220. Chauhan A, Tikoo A, Kapur AK, Singh M. The taming of the cell penetrating domain of the HIV Tat: myths and realities. *J Control Release.* (2007) 117:148–62. doi: 10.1016/j.jconrel.2006.10.031
221. Wender PA, Galliher WC, Goun EA, Jones LR, Pillow TH. The design of guanidinium-rich transporters and their internalization mechanisms. *Adv Drug Deliv Rev.* (2008) 60:452–72. doi: 10.1016/j.addr.2007.10.016
222. Tyagi M, Rusnati M, Presta M, Giacca M. Internalization of HIV-1 tat requires cell surface heparan sulfate proteoglycans. *J Biol Chem.* (2001) 276:3254–61. doi: 10.1074/jbc.M006701200
223. Suzuki T, Futaki S, Niwa M, Tanaka S, Ueda K, Sugiura Y. Possible existence of common internalization mechanisms among arginine-rich peptides. *J Biol Chem.* (2002) 277:2437–43. doi: 10.1074/jbc.M110017200
224. Takeuchi T, Futaki S. Current understanding of direct translocation of arginine-rich cell-penetrating peptides and its internalization mechanisms. *Chem Pharm Bull (Tokyo).* (2016) 64:1431–37. doi: 10.1248/cpb.c16-00505
225. Rothbard JB, Kreider E, VanDeusen CL, Wright L, Wylie BL, Wender PA. Arginine-rich molecular transporters for drug delivery: role of backbone spacing in cellular uptake. *J Med Chem.* (2002) 45:3612–18. doi: 10.1021/jm0105676
226. Amand HL, Rydberg HA, Fornander LH, Lincoln P, Nordén B, Esbjörner EK. Cell surface binding and uptake of arginine- and lysine-rich penetratin peptides in absence and presence of proteoglycans. *Biochim Biophys Acta.* (2012) 1818:2669–78. doi: 10.1016/j.bbamem.2012.06.006
227. Rullo A, Qian J, Nitz M. Peptide-glycosaminoglycan cluster formation involving cell penetrating peptides. *Biopolymers.* (2011) 95:722–31. doi: 10.1002/bip.21641
228. MacDougall G, Anderton RS, Edwards AB, Knuckey NW, Meloni BP. The Neuroprotective peptide poly-arginine-12 (R12) reduces cell surface levels of NMDA NR2B receptor subunit in cortical neurons; investigation into the involvement of endocytic mechanisms. *J Mol Neurosci.* (2017) 61:235–46. doi: 10.1007/s12031-016-0861-1
229. Fotin-Mleczek M, Welte S, Mader O, Duchardt F, Fischer R, Hufnagel H, et al. Cationic cell-penetrating peptides interfere with TNF signalling by induction of TNF receptor internalization. *J Cell Sci.* (2005) 118:3339–51. doi: 10.1242/jcs.02460
230. Weng XC, Gai XD, Zheng JQ, Li J. Agmatine blocked voltage-gated calcium channel in cultured rat hippocampal neurons. *Acta Pharmacol Sin.* (2003) 24:746–50.
231. Garcia ML, King VF, Shevell JL, Slaughter RS, Suarez-Kurtz G, Winquist RJ, et al. Amiloride analogs inhibit L-type calcium channels and display calcium entry blocker activity. *J Biol Chem.* (1990) 265:3763–71.

232. Keana JF, McBurney RN, Scherz MW, Fischer JB, Hamilton PN, Smith SM, et al. Synthesis and characterization of a series of diarylguanidines that are noncompetitive N-methyl-D-aspartate receptor antagonists with neuroprotective properties. *Proc Natl Acad Sci USA*. (1989) 86:5631–35. doi: 10.1073/pnas.86.14.5631
233. Goldin SM, Subbarao K, Sharma R, Knapp AG, Fischer JB, Daly D, et al. Neuroprotective use-dependent blockers of Na^+ and Ca^{2+} channels controlling presynaptic release of glutamate. *Ann N Y Acad Sci.* (1995) 765:210–29. doi: 10.1111/j.1749-6632.1995.tb16578.x
234. Kalia J, Swartz KJ. Elucidating the molecular basis of action of a classic drug: guanidine compounds as inhibitors of voltage-gated potassium channels. *Mol Pharmacol.* (2011) 80:1085–95. doi: 10.1124/mol.111.074989
235. Hong L, Kim IH, Tombola F. Molecular determinants of Hv1 proton channel inhibition by guanidine derivatives. *Proc Natl Acad Sci USA*. (2014) 111:9971–6. doi: 10.1073/pnas.1324012111
236. Armstrong CT, Mason PE, Anderson JL, Dempsey CE. Arginine side chain interactions and the role of arginine as a gating charge carrier in voltage sensitive ion channels. *Sci Rep.* (2016) 6:21759. doi: 10.1038/srep21759
237. Durán-Riveroll LM, Cembella AD. Guanidinium toxins and their interactions with voltage-gated sodium ion channels. *Mar Drugs.* (2017) 15:303. doi: 10.3390/md15100303
238. Yang XC, Reis DJ. Agmatine selectively blocks the N-methyl-D-aspartate subclass of glutamate receptor channels in rat hippocampal neurons. *J Pharmacol Exp Ther.* (1999) 288:544–9.
239. Williams K. Interactions of polyamines with ion channels. *Biochem J.* (1997) 325:289–97. doi: 10.1042/bj3250289
240. Szeto HH. Cell-permeable mitochondrial-targeted peptide antioxidants. *AAPS J.* (2006) 8:277–83. doi: 10.1007/BF02854898
241. MacDougall G, Anderton RS, Mastaglia FL, Knuckey NW, Meloni BP. Mitochondria and neuroprotection in stroke: cationic arginine-rich peptides (CARPs) as a novel class of mitochondria-targeted neuroprotective therapeutics. *Neurobiol Dis.* (2019) 121:17–33. doi: 10.1016/j.nbd.2018.09.010
242. Wascher TC, Posch K, Wallner S, Hermetter A, Kostner GM, Graier WF. Vascular effects of L-arginine: anything beyond a substrate for the NO-synthase? *Biochem Biophys Res Commun.* (1997) 234:35–8. doi: 10.1006/bbrc.1997.9994
243. Haklar G, Ulukaya-Durakbaşa C, Yüksel M, Dagli T, Yalçin AS. Oxygen radicals and nitric oxide in rat mesenteric ischaemia-reperfusion: modulation by L-arginine and NG-nitro-L-arginine methyl ester. *Clin Exp Pharmacol Physiol.* (1998) 25:908–12. doi: 10.1111/j.1440-1681.1998.tb02342.x
244. Yildiz G, Demiryürek AT, Sahin-Erdemli I, Kanzik I. Comparison of antioxidant activities of aminoguanidine methylguanidine and guanidine by luminol-enhanced chemiluminescence. *Br J Pharmacol.* (1998) 124:905–10. doi: 10.1038/sj.bjp.0701924
245. Courderot-Masuyer C, Dalloz F, Maupoil V, Rochette L. Antioxidant properties of aminoguanidine. *Fundam Clin Pharmacol.* (1999) 13:535–40. doi: 10.1111/j.1472-8206.1999.tb00358.x
246. Giardino I, Fard AK, Hatchell DL, Brownlee M. Aminoguanidine inhibits reactive oxygen species formation lipid peroxidation and oxidant-induced apoptosis. *Diabetes.* (1998) 47:1114–20. doi: 10.2337/diabetes.47.7.1114
247. Philis-Tsimikas A, Parthasarathy S, Picard S, Palinski W, Witztum JL. Aminoguanidine has both pro-oxidant and antioxidant activity toward LDL. *Arterioscler Thromb Vasc Biol.* (1995) 15:367–76. doi: 10.1161/01.ATV.15.3.367
248. Lawler JM, Barnes WS, Wu G, Song W, Demaree S. Direct antioxidant properties of creatine. *Biochem Biophys Res Commun.* (2002) 290:47–52. doi: 10.1006/bbrc.2001.6164
249. Lass A, Suessenbacher A, Wölkart G, Mayer B, Brunner F. Functional and analytical evidence for scavenging of oxygen radicals by L-arginine. *Mol Pharmacol.* (2002) 61:1081–88. doi: 10.1124/mol.61.5.1081
250. Uemura S, Fathman CG, Rothbard JB, Cooke JP. Rapid and efficient vascular transport of arginine polymers inhibits myointimal hyperplasia. *Circulation.* (2000) 102:2629–35. doi: 10.1161/01.CIR.102.21.2629
251. Suessenbacher A, Lass A, Mayer B, Brunner F. Antioxidative and myocardial protective effects of L-arginine in oxygen radical-induced injury of isolated perfused rat hearts. *Naunyn Schmiedebergs Arch Pharmacol.* (2002) 365:269–76. doi: 10.1007/s00210-001-0523-9
252. Kown MH, Lijkwan MA, Jahncke CL, Murata S, Rothbard JB, Robbins RC. L-Arginine polymers enhance coronary flow and reduce oxidative stress following cardiac transplantation in rats. *J Thorac Cardiovasc Surg.* (2003) 126:1065–70. doi: 10.1016/S0022-5223(03)00354-4
253. Ma H, Ma Y, Zhang Z, Zhao Z, Lin R, Zhu J, et al. l-Arginine enhances resistance against oxidative stress and heat stress in *Caenorhabditis elegans*. *Int J Environ Res Public Health.* (2016) 13:E969. doi: 10.3390/ijerph13100969
254. Mandal SM, Bharti R, Porto WF, Gauri SS, Mandal M, Franco OL, et al. Identification of multifunctional peptides from human milk. *Peptides.* (2014) 56:84–93. doi: 10.1016/j.peptides.2014.03.017
255. Aluganti Narasimhulu C, Selvarajan K, Brown M, Parthasarathy S. Cationic peptides neutralize Ox-LDL prevent its uptake by macrophages and attenuate inflammatory response. *Atherosclerosis.* (2014) 236:133–41. doi: 10.1016/j.atherosclerosis.2014.06.020
256. Akhmedov A, Bonetti NR, Reiner MF, Spescha RD, Amstalden H, Merlini M, et al. Deleterious role of endothelial lectin-like oxidized low-density lipoprotein receptor-1 in ischaemia/reperfusion cerebral injury. *J Cereb Blood Flow Metab.* (2019) 39:2233–45. doi: 10.1177/0271678X18793266
257. Takemura Y, Okamoto M, Hasegawa M, Hatanaka K, Kubota S. Protamine may have anti-atherogenic potential by inhibiting the binding of oxidized-low density lipoprotein to LOX-1. *Biosci Biotechnol Biochem.* (2019) 15:1–8. doi: 10.1080/09168451.2019.1588096
258. Joseph G, Gorzalczany Y, Koshkin V, Pick E. Inhibition of NADPH oxidase activation by synthetic peptides mapping within the carboxyl-terminal domain of small GTP-binding proteins: lack of amino acid sequence specificity and importance of polybasic motif. *J Biol Chem.* (1994) 269:29024–31.
259. Chen Y, Brennan-Minnella AM, Sheth S, El-Benna J, Swanson RA. Tat-NR2B9c prevents excitotoxic neuronal superoxide production. *J Cereb Blood Flow Metab.* (2015) 35:739–42. doi: 10.1038/jcbfm.2015.16
260. Cifuentes-Pagano E, Csanyi G, Pagano PJ. NADPH oxidase inhibitors: a decade of discovery from Nox2ds to HTS. *Cell Mol Life Sci.* (2012) 69:2315–25. doi: 10.1007/s00018-012-1009-2
261. Shi J, Ross CR, Leto TL, Blecha F. PR-39 a proline-rich antibacterial peptide that inhibits phagocyte NADPH oxidase activity by binding to Src homology 3 domains of p47 phox. *Proc Natl Acad Sci USA*. (1996) 93:6014–18. doi: 10.1073/pnas.93.12.6014
262. Allaman I, Bélanger M, Magistretti PJ. Methylglyoxal the dark side of glycolysis. *Front Neurosci.* (2015) 9:23. doi: 10.3389/fnins.2015.00023
263. Su Y, Lei X, Wu L, Liu L. The role of endothelial cell adhesion molecules P-selectin E-selectin and intercellular adhesion molecule-1 in leucocyte recruitment induced by exogenous methylglyoxal. *Immunology.* (2012) 137:65–79. doi: 10.1111/j.1365-2567.2012.03608.x
264. Wang B, Aw TY, Stokes KY. The protection conferred against ischemia-reperfusion injury in the diabetic brain by N-acetylcysteine is associated with decreased dicarbonyl stress. *Free Radic Biol Med.* (2016) 96:89–98. doi: 10.1016/j.freeradbiomed.2016.03.038
265. McDonald DM, Coleman G, Bhatwadekar A, Gardiner TA, Stitt AW. Advanced glycation of the Arg-Gly-Asp (RGD) tripeptide motif modulates retinal microvascular endothelial cell dysfunction. *Mol Vis.* (2009) 15:1509–20.
266. Rabbani N, Thornalley PJ. Dicarbonyl proteome and genome damage in metabolic and vascular disease. *Biochem Soc Trans.* (2014) 42:425–32. doi: 10.1042/BST20140018
267. Morcos M, Du X, Pfisterer F, Hutter H, Sayed AA, Thornalley P, et al. Glyoxalase-1 prevents mitochondrial protein modification and enhances lifespan in *Caenorhabditis elegans*. *Aging Cell.* (2008) 7:260–9. doi: 10.1111/j.1474-9726.2008.00371.x
268. Thornalley PJ. Use of aminoguanidine (Pimagedine) to prevent the formation of advanced glycation endproducts. *Arch Biochem Biophys.* (2003) 419:31–40. doi: 10.1016/j.abb.2003.08.013
269. Kinsky OR, Hargraves TL, Anumol T, Jacobsen NE, Dai J, Snyder SA, et al. Metformin scavenges methylglyoxal to form a novel imidazolinone metabolite in humans. *Chem Res Toxicol.* (2016) 29:227–34. doi: 10.1021/acs.chemrestox.5b00497

270. Dhar I, Dhar A, Wu L, Desai K. Arginine attenuates methylglyoxal- and high glucose-induced endothelial dysfunction and oxidative stress by an endothelial nitric-oxide synthase-independent mechanism. *J Pharmacol Exp Ther.* (2012) 342:196–204. doi: 10.1124/jpet.112.192112
271. Brings S, Fleming T, De Buhr S, Beijer B, Lindner T, Wischnjow A, et al. A scavenger peptide prevents methylglyoxal induced pain in mice. *Biochim Biophys Acta Mol Basis Dis.* (2017) 1863:654–62. doi: 10.1016/j.bbadis.2016.12.001
272. Cameron A, Appel J, Houghten RA, Lindberg I. Polyarginines are potent furin inhibitors. *J Biol Chem.* (2000) 275:36741–9. doi: 10.1074/jbc.M003848200
273. Kacprzak MM, Peinado JR, Than ME, Appel J, Henrich S, Lipkind G, et al. Inhibition of furin by polyarginine-containing peptides: nanomolar inhibition by nona-D-arginine. *J Biol Chem.* (2004) 279:36788–94. doi: 10.1074/jbc.M400484200
274. Peinado JR, Kacprzak MM, Leppla SH, Lindberg I. Cross-inhibition between furin and lethal factor inhibitors. *Biochem Biophys Res Commun.* (2004) 321:601–5. doi: 10.1016/j.bbrc.2004.07.012
275. Fugere M, Appel J, Houghten RA, Lindberg I, Day R. Short polybasic peptide sequences are potent inhibitors of PC5/6 and PC7: use of positional scanning-synthetic peptide combinatorial libraries as a tool for the optimization of inhibitory sequences. *Mol Pharmacol.* (2007) 71:323–32. doi: 10.1124/mol.106.027946
276. Ramos-Molina B, Lick AN, Nasrolahi Shirazi A, Oh D, Tiwari R, El-Sayed NS, et al. Cationic cell-penetrating peptides are potent furin inhibitors. *PLoS ONE.* (2015) 10:e0130417. doi: 10.1371/journal.pone.0130417
277. McMahon S, Grondin F, McDonald PP, Richard DE, Dubois CM. Hypoxia-enhanced expression of the proprotein convertase furin is mediated by hypoxia-inducible factor-1: impact on the bioactivation of proproteins. *J Biol Chem.* (2005) 280:6561–9. doi: 10.1074/jbc.M413248200
278. Yokota N, Uchijima M, Nishizawa S, Namba H, Koide Y. Identification of differentially expressed genes in rat hippocampus after transient global cerebral ischemia using subtractive cDNA cloning based on polymerase chain reaction. *Stroke.* (2001) 32:168–74. doi: 10.1161/01.STR.32.1.168
279. Yang Y, Estrada EY, Thompson JF, Liu W, Rosenberg GA. Matrix metalloproteinase-mediated disruption of tight junction proteins in cerebral vessels is reversed by synthetic matrix metalloproteinase inhibitor in focal ischemia in rat. *J Cereb Blood Flow Metab.* (2007) 27:697–709. doi: 10.1038/sj.jcbfm.9600375
280. Tian S, Huang Q, Fang Y, Wu J. FurinDB: a database of 20-residue furin cleavage site motifs substrates and their associated drugs. *Int J Mol Sci.* (2011) 12:1060–5. doi: 10.3390/ijms12021060
281. Yang Y, Rosenberg GA. Matrix metalloproteinases as therapeutic targets for stroke. *Brain Res.* (2015) 1623:30–8. doi: 10.1016/j.brainres.2015.04.024
282. Turner RJ, Sharp FR. Implications of MMP9 for blood brain barrier disruption and hemorrhagic transformation following ischemic stroke. *Front Cell Neurosci.* (2016) 10:56. doi: 10.3389/fncel.2016.00056
283. Seki M, Soussou W, Manabe S, Lipton SA. Protection of retinal ganglion cells by caspase substrate-binding peptide IQACRG from N-methyl-D-aspartate receptor-mediated excitotoxicity. *Invest Ophthalmol Vis Sci.* (2010) 51:1198–207. doi: 10.1167/iovs.09-4102
284. Horn M, Pavlík M, Dolecková L, Baudys M, Mares M. Arginine-based structures are specific inhibitors of cathepsin C application of peptide combinatorial libraries. *Eur J Biochem.* (2000) 267:3330–6. doi: 10.1046/j.1432-1327.2000.01364.x
285. Gao Y, Lecker S, Post MJ, Hietaranta AJ, Li J, Volk R, et al. Inhibition of ubiquitin-proteasome pathway-mediated I kappa B alpha degradation by a naturally occurring antibacterial peptide. *J Clin Invest.* (2000) 106:439–48. doi: 10.1172/JCI9826
286. Gaczynska M, Osmulski PA, Gao Y, Post MJ, Simons M. Proline- and CARPs constitute a novel class of allosteric inhibitors of proteasome activity. *Biochemistry.* (2003) 42:8663–70. doi: 10.1021/bi034784f
287. Kloss A, Henklein P, Siele D, Schmolke M, Apcher S, Kuehn L, et al. The cell-penetrating peptide octa-arginine is a potent inhibitor of proteasome activities. *Eur J Pharm Biopharm.* (2009) 72:219–25. doi: 10.1016/j.ejpb.2008.10.016
288. Anbanandam A, Albarado DC, Tirziu DC, Simons M, Veeraraghavan S. Molecular basis for proline- and arginine-rich peptide inhibition of proteasome. *J Mol Biol.* (2008) 384:219–27. doi: 10.1016/j.jmb.2008.09.021
289. Karpowicz P, Osmulski PA, Witkowska J, Sikorska E, Gizynska M, Belczyk-Ciesielska A, et al. Interplay between structure and charge as a key to allosteric modulation of human 20S proteasome by the basic fragment of HIV-1 tat protein. *PLoS ONE.* (2015) 10:e0143038. doi: 10.1371/journal.pone.0143038
290. Wojcik C, Di Napoli M. Ubiquitin-proteasome system and proteasome inhibition: new strategies in stroke therapy. *Stroke.* (2004) 35:1506–18. doi: 10.1161/01.STR.0000126891.93919.4e
291. Doeppner TR, Mlynarczuk-Bialy I, Kuckelkorn U, Kaltwasser B, Herz J, Hasan MR, et al. The novel proteasome inhibitor BSc2118 protects against cerebral ischaemia through HIF1A accumulation and enhanced angioneurogenesis. *Brain.* (2012) 135:3282–97. doi: 10.1093/brain/aws269
292. Doeppner TR, Kaltwasser B, Schlechter J, Jaschke J, Kilic E, Bähr M, et al. Systemic proteasome inhibition induces sustained post-stroke neurological recovery and neuroprotection via mechanisms involving reversal of peripheral immunosuppression and preservation of blood-brain-barrier integrity. *Mol Neurobiol.* (2016) 53:6332–41. doi: 10.1007/s12035-015-9533-3
293. Doeppner TR, Doehring M, Kaltwasser B, Majid A, Lin F, Bähr M, et al. Ischemic post-conditioning induces post-stroke neuroprotection via Hsp70-mediated proteasome inhibition and facilitates neural progenitor cell transplantation. *Mol Neurobiol.* (2017) 54:6061–73. doi: 10.1007/s12035-016-0137-3
294. Bieler S, Meiners S, Stangl V, Pohl T, Stangl K. Comprehensive proteomic and transcriptomic analysis reveals early induction of a protective anti-oxidative stress response by low-dose proteasome inhibition. *Proteomics.* (2009) 9:3257–67. doi: 10.1002/pmic.200800927
295. Li J, Post M, Volk R, Gao Y, Li M, Metais C, et al. PR39 a peptide regulator of angiogenesis. *Nat Med.* (2000) 6:49–55. doi: 10.1038/71527
296. Loboda A, Damulewicz M, Pyza E, Jozkowicz A, Dulak J. Role of Nrf2/HO-1 system in development oxidative stress response and diseases: an evolutionarily conserved mechanism. *Cell Mol Life Sci.* (2016) 73:3221–7. doi: 10.1007/s00018-016-2223-0
297. Steel R, Cowan J, Payerne E, O'Connell MA, Searcey M. Anti-inflammatory effect of a cell-penetrating peptide targeting the Nrf2/Keap1 interaction. *ACS Med Chem Lett.* (2012) 3:407–10. doi: 10.1021/ml300041g
298. Kanzaki H, Shinohara F, Kajiya M, Fukaya S, Miyamoto Y, Nakamura Y. Nuclear Nrf2 induction by protein transduction attenuates osteoclastogenesis. *Free Radic Biol Med.* (2014) 77:239–48. doi: 10.1016/j.freeradbiomed.2014.09.006
299. Zhao J, Redell JB, Moore AN, Dash PK. A novel strategy to activate cytoprotective genes in the injured brain. *Biochem Biophys Res Commun.* (2011) 407:501–6. doi: 10.1016/j.bbrc.2011.03.046
300. Liang M, Wang Z, Li H, Cai L, Pan J, He H, et al. L-Arginine induces antioxidant response to prevent oxidative stress via stimulation of glutathione synthesis and activation of Nrf2 pathway. *Food Chem Toxicol.* (2018) 115:315–28. doi: 10.1016/j.fct.2018.03.029
301. Wang YF, Xu X, Fan X, Zhang C, Wei Q, Wang X, et al. A cell-penetrating peptide suppresses inflammation by inhibiting NF-κB signaling. *Mol Ther.* (2011) 19:1849–57. doi: 10.1038/mt.2011.82
302. Lawrence T. The nuclear factor NF-kappaB pathway in inflammation. *Cold Spring Harb Perspect Biol.* (2009) 1:a001651. doi: 10.1101/cshperspect.a001651
303. Korthuis RJ, Gute DC, Blecha F, Ross CR. PR-39 a proline/arginine-rich antimicrobial peptide prevents postischemic microvascular dysfunction. *Am J Physiol.* (1999) 277:1007–13. doi: 10.1152/ajpheart.1999.277.3.H1007
304. Kim H, Moodley S, Liu M. TAT cell-penetrating peptide modulates inflammatory response and apoptosis in human lung epithelial cells. *Drug Deliv Transl Res.* (2015) 5:275–8. doi: 10.1007/s13346-015-0230-6
305. Nankar SA, Pande AH. Properties of apolipoprotein E derived peptide modulate their lipid-binding capacity and influence their anti-inflammatory function. *Biochim Biophys Acta.* (2014) 184:620–9. doi: 10.1016/j.bbalip.2014.01.006

306. Sharifov OF, Xu X, Gaggar A, Tabengwa EM, White CR, Palgunachari MN, et al. L-4F inhibits lipopolysaccharide-mediated activation of primary human neutrophils. *Inflammation.* (2014) 37:1401–12. doi: 10.1007/s10753-014-9864-7
307. Datta G, White CR, Dashti N, Chaddha M, Palgunachari MN, Gupta H, et al. Anti-inflammatory and recycling properties of an apolipoprotein mimetic peptide Ac-hE18A-NH(2). *Atherosclerosis.* (2010) 208:134–41. doi: 10.1016/j.atherosclerosis.2009.07.019
308. Laskowitz DT, Thekdi AD, Thekdi SD, Han SK, Myers JK, Pizzo SV, et al. Downregulation of microglial activation by apolipoprotein E and apoE-mimetic peptides. *Exp Neurol.* (2001) 167:74–85. doi: 10.1006/exnr.2001.7541
309. Pane K, Sgambati V, Zanfardino A, Smaldone G, Cafaro V, Angrisano T, et al. A new cryptic cationic antimicrobial peptide from human apolipoprotein E with antibacterial activity and immunomodulatory effects on human cells. *FEBS J.* (2016) 283:2115–31. doi: 10.1111/febs.13725
310. Singh K, Chaturvedi R, Asim M, Barry DP, Lewis ND, Vitek MP, et al. The apolipoprotein E-mimetic peptide COG112 inhibits the inflammatory response to Citrobacter rodentium in colonic epithelial cells by preventing NF-kappaB activation. *J Biol Chem.* (2008) 283:16752–161. doi: 10.1074/jbc.M710530200
311. Singh K, Chaturvedi R, Barry DP, Coburn LA, Asim M, Lewis ND, et al. The apolipoprotein E-mimetic peptide COG112 inhibits NF-kappaB signaling proinflammatory cytokine expression and disease activity in murine models of colitis. *J Biol Chem.* (2011) 286:3839–50. doi: 10.1074/jbc.M110.176719
312. Neree AT, Nguyen PT, Bourgault S. Cell-penetrating ability of peptide hormones: key role of glycosaminoglycans clustering. *Int J Mol Sci.* (2015) 16:27391–400. doi: 10.3390/ijms161126025
313. Morio H, Tatsuno I, Hirai A, Tamura Y, Saito Y. Pituitary adenylate cyclase-activating polypeptide protects rat-cultured cortical neurons from glutamate-induced cytotoxicity. *Brain Res.* (1996) 741:82–8. doi: 10.1016/S0006-8993(96)00920-1
314. Seki T, Nakatani M, Taki C, Shinohara Y, Ozawa M, Nishimura S, et al. Neuroprotective effect of PACAP against kainic acid-induced neurotoxicity in rat retina. *Ann N Y Acad Sci.* (2006) 1070:531–4. doi: 10.1196/annals.1317.074
315. Werling D, Banks WA, Salameh TS, Kvarik T, Kovacs LA, Vaczy A, et al. Passage through the ocular barriers and beneficial effects in retinal ischemia of topical application of PACAP1–38 in rodents. *Int J Mol Sci.* (2017) 18:E675. doi: 10.3390/ijms18030675
316. Reglodi D, Somogyvari-Vigh A, Vigh S, Kozicz T, Arimura A. Delayed systemic administration of PACAP38 is neuroprotective in transient middle cerebral artery occlusion in the rat. *Stroke.* (2000) 31:1411–7. doi: 10.1161/01.STR.31.6.1411
317. Lazarovici P, Cohen G, Arien-Zakay H, Chen J, Zhang C, Chopp M, et al. Multimodal neuroprotection induced by PACAP38 in oxygen-glucose deprivation and middle cerebral artery occlusion stroke models. *J Mol Neurosci.* (2012) 48:526–40. doi: 10.1007/s12031-012-9818-1
318. Mao SS, Hua R, Zhao XP, Qin X, Sun ZQ, Zhang Y, et al. Exogenous administration of PACAP alleviates traumatic brain injury in rats through a mechanism involving the TLR4/MyD88/NF-κB pathway. *J Neurotrauma.* (2012) 29:1941–59. doi: 10.1089/neu.2011.2244
319. Suk K, Park JH, Lee WH. Neuropeptide PACAP inhibits hypoxic activation of brain microglia: a protective mechanism against microglial neurotoxicity in ischemia. *Brain Res.* (2004) 1026:151–6. doi: 10.1016/j.brainres.2004.08.017
320. Kandler K, Shaykhiev R, Kleemann P, Klescz F, Lohoff M, Vogelmeier C, et al. The anti-microbial peptide LL-37 inhibits the activation of dendritic cells by TLR ligands. *Int Immunol.* (2006) 18:1729–36. doi: 10.1093/intimm/dxl107
321. Yoo SA, Bae DG, Ryoo JW, Kim HR, Park GS, Cho CS, et al. Arginine-rich anti-vascular endothelial growth factor (anti-VEGF) hexapeptide inhibits collagen-induced arthritis and VEGF-stimulated productions of TNF-alpha and IL-6 by human monocytes. *J Immunol.* (2005) 174:5846–55. doi: 10.4049/jimmunol.174.9.5846
322. Chow LN, Choi KY, Piyadasa H, Bossert M, Uzonna J, Klonisch T, et al. Human cathelicidin LL-37-derived peptide IG-19 confers protection in a murine model of collagen-induced arthritis. *Mol Immunol.* (2014) 57:86–92. doi: 10.1016/j.molimm.2013.08.011
323. Marin-Luevano P, Trujillo V, Rodriguez-Carlos A, González-Curiel I, Enciso-Moreno JA, Hancock REW, et al. Induction by innate defence regulator peptide 1018 of pro-angiogenic molecules and endothelial cell migration in a high glucose environment. *Peptides.* (2018) 101:135–44. doi: 10.1016/j.peptides.2018.01.010
324. Scatizzi JC, Hutcheson J, Pope RM, Firestein GS, Koch AE, Mavers M, et al. Bim-Bcl-2 homology 3 mimetic therapy is effective at suppressing inflammatory arthritis through the activation of myeloid cell apoptosis. *Arthritis Rheum.* (2010) 62:441–51. doi: 10.1002/art.27198
325. Ahmed CM, Massengill MT, Brown EE, Ildefonso CJ, Johnson HM, Lewin AS. A cell penetrating peptide from SOCS-1 prevents ocular damage in experimental autoimmune uveitis. *Exp Eye Res.* (2018) 177:12–22. doi: 10.1016/j.exer.2018.07.020
326. Karicherla P, Aras S, Aiyar A, Hobden JA. Nona-D-arginine amide suppresses corneal cytokines in *Pseudomonas aeruginosa* keratitis. *Cornea.* (2010) 29:1308–14. doi: 10.1097/ICO.0b013e3181ca3a69
327. Lee JY, Suh JS, Kim JM, Kim JH, Park HJ, Park YJ, et al. Identification of a cell-penetrating peptide domain from human beta-defensin 3 and characterization of its anti-inflammatory activity. *Int J Nanomedicine.* (2015) 10:5423–34. doi: 10.2147/IJN.S90014
328. Olsen UB, Selmer J, Kahl JU. Complement C5a receptor antagonism by protamine and poly-L-Arg on human leukocytes. *Complement.* (1988) 5:153–62. doi: 10.1159/000463049
329. Zhang T, Garstka MA, Li K. The controversial C5a receptor C5aR2: its role in health and disease. *J Immunol Res.* (2017) 2017:8193932. doi: 10.1155/2017/8193932
330. Yang Y, Wolfram J, Fang X, Shen H, Ferrari M. Polyarginine induces an antitumor immune response through binding to toll-like receptor 4. *Small.* (2014) 10:1250–4. doi: 10.1002/smll.201302887
331. Niyonsaba F, Madera L, Afacan N, Okumura K, Ogawa H, Hancock RE. The innate defense regulator peptides IDR-HH2 IDR-1002 and IDR-1018 modulate human neutrophil functions. *J Leukoc Biol.* (2013) 94:159–70. doi: 10.1189/jlb.1012497
332. Shin K, Chapman NA, Sarker M, Kenward C, Huang SK, Weatherbee-Martin N, et al. Bioactivity of the putative apelin proprotein expands the repertoire of apelin receptor ligands. *Biochim Biophys Acta Gen Subj.* (2017) 1861:1901–12. doi: 10.1016/j.bbagen.2017.05.017
333. Zhou N, Fang J, Acheampong E, Mukhtar M, Pomerantz RJ. Binding of ALX40–4C to APJ a CNS-based receptor inhibits its utilization as a co-receptor by HIV-1. *Virology.* (2003) 312:196–203. doi: 10.1016/S0042-6822(03)00185-5
334. Zhou N, Zhang X, Fan X, Argyris E, Fang J, Acheampong E, et al. The N-terminal domain of APJ a CNS-based coreceptor for HIV-1 is essential for its receptor function and coreceptor activity. *Virology.* (2003) 317:84–94. doi: 10.1016/S0042-6822(03)00638-X
335. Le Gonidec S, Chaves-Almagro C, Bai Y, Kang HJ, Smith A, Wanecq E, et al. Protamine is an antagonist of apelin receptor and its activity is reversed by heparin. *FASEB J.* (2017) 31:2507–19. doi: 10.1096/fj.201601074R
336. Masri B, Morin N, Pedebernade L, Knibiehler B, Audigier Y. The apelin receptor is coupled to Gi1 or Gi2 protein and is differentially desensitized by apelin fragments. *J Biol Chem.* (2006) 281:18317–26. doi: 10.1074/jbc.M600606200
337. Li Y, Chen J, Bai B, Du H, Liu Y, Liu H. Heterodimerization of human apelin and kappa opioid receptors: roles in signal transduction. *Cell Signal.* (2012) 24:991–1001. doi: 10.1016/j.cellsig.2011.12.012
338. Liu J, Liu M, Chen L. Novel pathogenesis: regulation of apoptosis by Apelin/APJ system. *Acta Biochim Biophys Sin (Shanghai).* (2017) 49:471–8. doi: 10.1093/abbs/gmx035
339. O'Carroll AM, Lolait SJ, Harris LE, Pope GR. The apelin receptor APJ: journey from an orphan to a multifaceted regulator of homeostasis. *J Endocrinol.* (2013) 219:13–35. doi: 10.1530/JOE-13-0227
340. Bertrand C, Valet P, Castan-Laurell I. Apelin and energy metabolism. *Front Physiol.* (2015) 6:115. doi: 10.3389/fphys.2015.00115
341. Zeng XJ, Yu SP, Zhang L, Wei L. Neuroprotective effect of the endogenous neural peptide apelin in cultured mouse cortical neurons. *Exp Cell Res.* (2010) 316:1773–83. doi: 10.1016/j.yexcr.2010.02.005

342. Wu Y, Wang X, Zhou X, Cheng B, Li G, Bai B. Temporal expression of apelin/apelin receptor in ischemic stroke and its therapeutic potential. *Front Mol Neurosci.* (2017) 10:1. doi: 10.3389/fnmol.2017.00001
343. Perjés Á, Kilpiö T, Ulvila J, Magga J, Alakoski T, Szabó Z, et al. Characterization of apela, a novel endogenous ligand of apelin receptor, in the adult heart. *Basic Res Cardiol.* (2016) 111:2. doi: 10.1007/s00395-015-0521-6
344. Tomioka H, Nakagami H, Tenma A, Saito Y, Kaga T, Kanamori T, et al. Novel anti-microbial peptide SR-0379 accelerates wound healing via the PI3 kinase/Akt/mTOR pathway. *PLoS ONE.* (2014) 9:e92597. doi: 10.1371/journal.pone.0092597
345. Bowdish DM, Davidson DJ, Speert DP, Hancock RE. The human cationic peptide LL-37 induces activation of the extracellular signal-regulated kinase and p38 kinase pathways in primary human monocytes. *J Immunol.* (2004) 172:3758–65. doi: 10.4049/jimmunol.172.6.3758
346. Vandamme D, Landuyt B, Luyten W, Schoofs L. A comprehensive summary of LL-37 the factotum human cathelicidin peptide. *Cell Immunol.* (2012) 280:22–35. doi: 10.1016/j.cellimm.2012.11.009
347. Lokeshwar VB, Huang SS, Huang JS. Protamine enhances epidermal growth factor (EGF)-stimulated mitogenesis by increasing cell surface EGF receptor number. Implications for existence of cryptic EGF receptors. *J Biol Chem.* (1989) 264:19318–26.
348. Hubler L, Leventhal PS, Bertics PJ. Alteration of the kinetic properties of the epidermal growth factor receptor tyrosine kinase by basic proteins. *Biochem J.* (1992) 281:107–14. doi: 10.1042/bj2810107
349. Baynes BM, Wang DI, Trout BL. Role of arginine in the stabilization of proteins against aggregation. *Biochemistry.* (2005) 44:4919–25. doi: 10.1021/bi047528r
350. Shukla D, Trout BL. Interaction of arginine with proteins and the mechanism by which it inhibits aggregation. *J Phys Chem B.* (2010) 114:13426–38. doi: 10.1021/jp108399g
351. Gibson TJ, Murphy RM. Design of peptidyl compounds that affect beta-amyloid aggregation: importance of surface tension and context. *Biochemistry.* (2005) 44:8898–907. doi: 10.1021/bi050225s
352. Taddei K, Laws SM, Verdile G, Munns S, D'Costa K, Harvey AR, et al. Novel phage peptides attenuate beta amyloid-42 catalysed hydrogen peroxide production and associated neurotoxicity. *Neurobiol Aging.* (2010) 31:203–14. doi: 10.1016/j.neurobiolaging.2008.03.023
353. Kawasaki T, Onodera K, Kamijo S. Identification of novel short peptide inhibitors of soluble 37/48 kDa oligomers of amyloid β42. *Biosci Biotechnol Biochem.* (2011) 75:1496–501. doi: 10.1271/bbb.110198
354. Kawasaki T, Kamijo S. Inhibition of aggregation of amyloid β42 by arginine-containing small compounds. *Biosci Biotechnol Biochem.* (2012) 76:762–6. doi: 10.1271/bbb.110879
355. Parthsarathy V, McClean PL, Hölscher C, Taylor M, Tinker C, Jones G, et al. A novel retro-inverso peptide inhibitor reduces amyloid deposition oxidation and inflammation and stimulates neurogenesis in the APPswe/PS1ΔE9 mouse model of Alzheimer's disease. *PLoS ONE.* (2013) 8:e54769. doi: 10.1371/annotation/57e0a947-8600-4658-b04c-cf7a45c8bd8d
356. Cheng YS, Chen ZT, Liao TY, Lin C, Shen HC, Wang YH, et al. An intranasally delivered peptide drug ameliorates cognitive decline in Alzheimer transgenic mice. *EMBO Mol Med.* (2017) 9:703–15. doi: 10.15252/emmm.201606666
357. Fonar G, Polis B, Meirson T, Maltsev A, Samson AO. Subcutaneous sustained-release of poly-arginine ameliorates cognitive impairment in a transgenic mouse model of Alzheimer's disease. *Adv Alzheimer's Dis.* (2018) 7:153–82. doi: 10.4236/aad.2018.74011
358. Nadimidla K, Ismail T, Kanapathipillai M. Tau peptides and tau mutant protein aggregation inhibition by cationic polyethyleneimine and polyarginine. *Biopolymers.* (2017) 107:e23024. doi: 10.1002/bip.23024
359. Podvin S, Yaksh T, Hook V. The emerging role of spinal dynorphin in chronic pain: a therapeutic perspective. *Annu Rev Pharmacol Toxicol.* (2016) 56:511–33. doi: 10.1146/annurev-pharmtox-010715-103042
360. Reis DJ, Yang XC, Milner TA. Agmatine containing axon terminals in rat hippocampus form synapses on pyramidal cells. *Neurosci Lett.* (1998) 250:185–88. doi: 10.1016/S0304-3940(98)00466-2
361. Dawson VL, Dawson TM, London ED, Bredt DS, Snyder SH. Nitric oxide mediates glutamate neurotoxicity in primary cortical cultures. *Proc Natl Acad Sci USA.* (1991) 88:6368–71. doi: 10.1073/pnas.88.14.6368
362. Víteček J, Lojek A, Valacchi G, Kubala L. Arginine-based inhibitors of nitric oxide synthase: therapeutic potential and challenges. *Mediators Inflamm.* (2012) 2012:318087. doi: 10.1155/2012/318087
363. *Field Randomization of NA-1 Therapy in Early Responders (FRONTIER).* Available online at: https://clinicaltrials.gov/ct2/show/NCT02315443?term=NA-1&draw=2&rank=2
364. *Safety and Efficacy of NA-1 in Subjects Undergoing Endovascular Thrombectomy for Stroke (ESCAPE-NA1).* Available online at: https://clinicaltrials.gov/ct2/show/NCT02930018?term=NA-1&draw=2&rank=1
365. Guptill JT, Raja SM, Boakye-Agyeman F, Noveck R, Ramey S, Tu TM, et al. Phase 1 randomized, double-blind, placebo-controlled study to determine the safety, tolerability, and pharmacokinetics of a single escalating dose and repeated doses of CN-105 in healthy adult subjects. *J Clin Pharmacol.* (2017) 57:770–6. doi: 10.1002/jcph.853
366. Hill MD, Martin RH, Mikulis D, Wong JH, Silver FL, Terbrugge KG, et al. ENACT trial investigators. Safety and efficacy of NA-1 in patients with iatrogenic stroke after endovascular aneurysm repair (ENACT): a phase 2, randomised, double-blind, placebo-controlled trial. *Lancet Neurol.* (2012) 11:942–50. doi: 10.1016/S1474-4422(12)70225-9
367. Doranz BJ, Grovit-Ferbas K, Sharron MP, Mao SH, Goetz MB, Daar ES, et al. Safe use of the CXCR4 inhibitor ALX40–4C in humans. *AIDS Res Hum Retroviruses.* (2001) 17:475–86. doi: 10.1089/08892220151126508
368. Sokolowska E, Kalaska B, Miklosz J, Mogielnicki A. The toxicology of heparin reversal with protamine: past, present and future. *Expert Opin Drug Metab Toxicol.* (2016) 12:897–909. doi: 10.1080/17425255.2016.1194395
369. Willbold D, Kutzsche J. Do we need anti-prion compounds to treat Alzheimer's disease? *Molecules.* (2019) 24:E2237. doi: 10.3390/molecules24122237

Conflict of Interest: BM and NK are named inventors of several patent applications regarding the use of CARPs as neuroprotective agents.

The remaining author declares that the research was conducted in the absence of any commercial or financial relationships that could be construed as a potential conflict of interest.

frontiers in Neurology

ORIGINAL RESEARCH
published: 10 June 2020
doi: 10.3389/fneur.2020.00436

miR-339 Promotes Hypoxia-Induced Neuronal Apoptosis and Impairs Cell Viability by Targeting FGF9/CACNG2 and Mediating MAPK Pathway in Ischemic Stroke

Xiao-Zeng Gao[1], *Ru-Hua Ma*[2] *and Zhao-Xia Zhang*[3]*

[1] Department of Anesthesiology, North China University of Science and Technology, Tangshan, China, [2] Emergency Department, Rizhao Hospital of Traditional Chinese Medicine, Rizhao, China, [3] Department of Geriatrics, Shanxian Central Hospital, Heze, China

OPEN ACCESS

Edited by:
Thiruma Valavan Arumugam, La Trobe University, Australia

Reviewed by:
Steffen Tiedt, Hospital of the University of Munich, Germany
Laura Castiglioni, University of Milan, Italy

***Correspondence:**
Zhao-Xia Zhang
sdzzx369@163.com

Specialty section:
This article was submitted to Stroke, a section of the journal Frontiers in Neurology

Received: *11 February 2020*
Accepted: *23 April 2020*
Published: *10 June 2020*

Citation:
Gao X-Z, Ma R-H and Zhang Z-X (2020) miR-339 Promotes Hypoxia-Induced Neuronal Apoptosis and Impairs Cell Viability by Targeting FGF9/CACNG2 and Mediating MAPK Pathway in Ischemic Stroke. Front. Neurol. 11:436. doi: 10.3389/fneur.2020.00436

Ischemic stroke (IS) is a common cerebrovascular disease characterized by insufficient blood blow to the brain and the second leading cause of death as well as disability worldwide. Recent literatures have indicated that abnormal expression of miR-339 is closely related to IS. In this study, we attempted to assess the biological function of miR-339 and its underlying mechanism in IS. By accessing the GEO repository, the expression of miR-339, FGF9, and CACNG2 in middle cerebral artery occlusion (MCAO) and non-MCAO was evaluated. PC12 cells after oxygen-glucose deprivation/reoxygenation (OGD/R) treatment were prepared to mimic *in vitro* the IS model. The levels of miR-339, FGF9, CACNG2, and MAPK-related markers were quantitatively measured by qRT-PCR and Western blot. CCK-8 and flow cytometry analyses were performed to examine cell viability and apoptosis, respectively. IS-related potential pathways were identified using KEGG enrichment analysis and GO annotations. Bioinformatics analysis and dual-luciferase reporter assay were used to predict and verify the possible target of miR-339. Our results showed that miR-339 expression was significantly increased in MCAO and OGD/R-treated PC12 cells. Overexpression of miR-339 inhibited cell viability of PC12 cells subjected to OGD/R treatment. FGF9 and CACMG2 are direct targets of miR-339 and can reverse the aggressive effect of miR-339 on the proliferation and apoptosis of OGD/R-treated PC12 cells. Moreover, miR-339 mediated the activation of the MAPK pathway, which was inhibited by the FGF9/CACNG2 axis in PC12 cells treated by OGD/R stimulation. In summary, these findings suggested that miR-339 might act as a disruptive molecule to accelerate the IS progression via targeting the FGF9/CACNG2 axis and mediating the MAPK pathway.

Keywords: ischemic stroke, miR-339, oxygen-glucose deprivation/reoxygenation (OGD/R), FGF9/CACNG2, apoptosis, MAPK pathway

INTRODUCTION

Ischemic stroke (IS) is a common neurological disease with high recurrence or disability rate (1, 2). The prevalent symptoms of IS are sudden numbness or weakness of face, arm, or leg; temporary confusion; and trouble walking or loss of balance (1, 3). Increasing statistical evidence has demonstrated that IS accounts for 80% of all strokes and seriously damages human health and life (4). Currently, the most efficacious treatment of IS is thrombolysis with reperfusion at the appropriate time (5). However, this treatment tends to induce cerebral ischemia reperfusion injury through enforcing inflammation and glutamate excitotoxicity (6, 7). Therefore, it is of great significance to decipher potential therapeutic targets and effective treatment options for IS.

microRNAs (miRNAs) have been identified as important regulators to participate in various kinds of diseases. Furthermore, the specific effects of several miRNAs in IS have also been elucidated. For example, miR-384-5p can contribute to endothelial progenitor cell viability and angiogenesis in cerebral IS via delta-like ligand 4-mediated Notch signaling pathway (8). Peng et al. indicated that the progression of IS is driven by miR-221 through mediating PTEN/PI3K/AKT signaling pathway (9). The OGD/R-induced neuronal injury can be alleviated by miR-340-5p through activating PI3/AKT pathway (10). These researches greatly support the point that miRNAs are involved in the progression of IS. Recently, a published investigation suggested that miR-339 presents an early and sustained increase in ischemic models of stroke (11). Altintas et al. discovered that aberrant expression of cerebral miRNAs including miR-339 exert the neuroprotective effect against transient cerebral ischemia in diabetic rats (12). Thus, we speculated that miR-339 might play an important role on the development of IS, but the detailed function and the possible mechanism of it in IS remain unclear.

In this present study, the expression of miR-339 in middle cerebral artery occlusion (MCAO) was determined based on the Gene Expression Omnibus (GEO) repository and OGD/R was used to mimic *in vitro* the IS model in PC12 cells. The effect of miR-339 on cell viability and apoptosis of PC12 cells treated by OGD/R and its underlying mechanism was investigated using functional experiments. This exploration may advance both our knowledge of the IS pathogenesis and possible effective treatment agents.

MATERIALS AND METHODS

Clinical Samples Collection

GEO (http://www.ncbi.nlm.nih.gov/geo) is a public functional genomics data repository and helps user query and download experiments and curated gene expression profiles. The two arrays including GSE29287 and GSE61616 were derived from GEO to be used to analyze the expression levels of subjects.

Cell Culture and OGD/R Model

Rat adrenal medulla-derived pheochromocytoma cell line PC12 was obtained from the American Type Culture Collection (ATCC; Manassas, VA, USA) and maintained in Dulbecco's minimal Eagle's medium (DMEM) containing 10% FBS, 100 mg/ml streptomycin, and 100 U/ml penicillin at 37°C in a conventional atmosphere of 95% O_2 and 5% CO_2. The culture medium was changed every 2–3 days. Briefly, to establish the *in vitro* OGD/R model, PC12 cells were incubated in glucose-free DMEM after washing with glucose-free Earle's balanced salt solution and immediately transferred into the anaerobic chamber (1% O_2, 94% N_2, and 5% CO_2) for 2 h. Then, these cells were seeded in the normal medium supplemented with 10% FBS to be incubated for an additional 12 h. In addition, cells of the control group were continuously cultured in the normal condition.

Transfection

PC12 cells were transfected with specific productions using Lipofectamine 2000 (Invitrogen, Carlsbad, CA, USA) according to the manufacturer's instruction. The productions contain miR-339 mimic, miR-339 inhibitor, and their corresponding negative control (miR-NC), pcDNA3.1-FGF9, pcDNA3.1-CACNG2 and pcDNA3.1 empty vector, si-FGF9 (5′-GACTGGATTTCA CTTAGAAATCT-3′), si-CACNG2 (5′-TGGGTGTTTATA TAATGAAGAAT-3′), and si-con (5′-AATTCTCCGAACGTGT CACGT-3′). They were all synthesized by GenePharma Co., Ltd (Shanghai, China). At 48-h post transfection, transfectants were exposed to OGD/R treatment and collected to perform further experiments the next day.

Cell Viability Analysis

CCK-8 assay was conducted to measure the proliferation capacity of PC12 cells stimulated with OGD/R under various transfection. First, cells (1000 cells/well) were inoculated in a 96-well-plate and cultivated for 0, 24, 48, and 72 h. Ten microliters of CCK-8 reagent was subsequently added to every well for an additional 1.5-h incubation at 37°C. Finally, the measurements of optical density (OD) values were finished at 450 nm using the microplate reader to plot the proliferation curve.

Apoptosis Assay

Following OGD/R treatment and specific transfections, PC12 cells were harvested and suspended using pre-cooled PBS as well as 1 × binding buffer. Then, 100 μl of cell suspension (1–5 × 10^6/ml) was incubated with 5 μl of Annexin V/FITC for 5 min in the dark. Subsequently, cells were stained with 10 μl of PI and apoptosis rate was analyzed by a flow cytometer (Beckman Coulter, USA) and FlowJo (version 7.6.1; FlowJo LLC) software.

Luciferase Activity Assay

The fragments of FGF9/CACNG2-wild type (WT) and FGF9/CACNG2-mutant (MUT) carrying miR-339 binding site or not were amplified into pmiR-RB-REPORT™ (RiboBio Co Ltd., Guangzhou, China) for luciferase activity detection. PC12 cells were co-transfected with FGF9/CACNG2-WT or FGF9/CACNG2-MUT and miR-339 mimic/inhibitor as well as miR-NC using Lipofectamine 2000 (Invitrogen). After 48-h transfection, relative luciferase activity was evaluated using Dual-Luciferase Reporter Assay Kit (Promega, Madison, WI, USA) in accordance with the guideline for users.

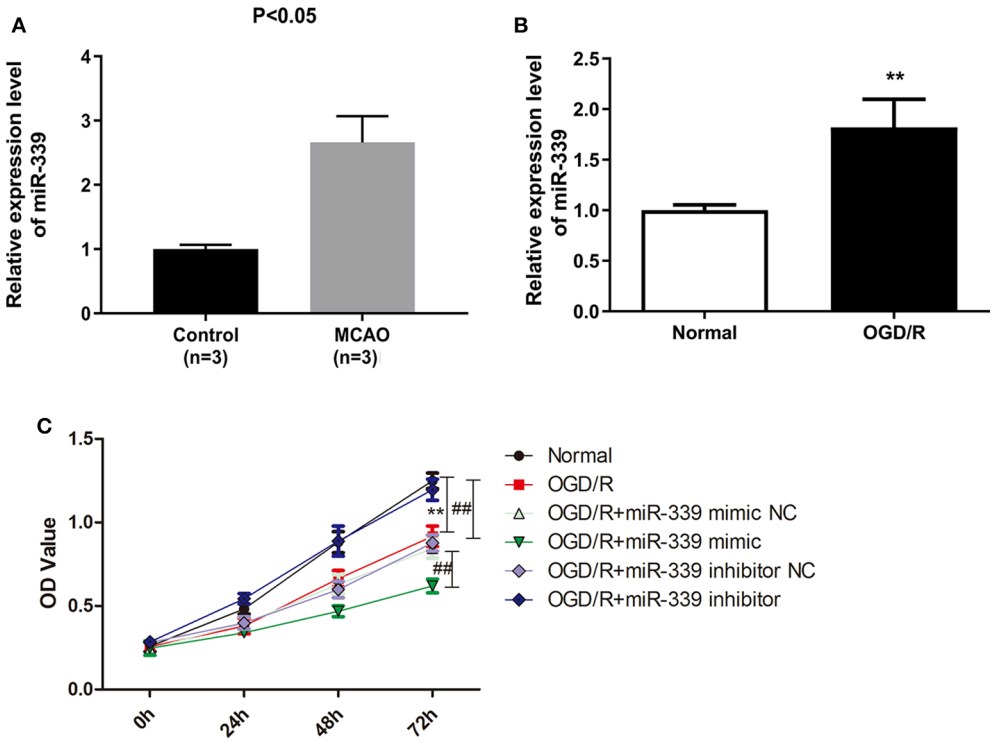

FIGURE 1 | miR-339 plays an aggressive role on IS progression. **(A)** Analysis of miR-339 expression in MCAO patients ($n = 3$) and normal samples ($n = 3$) on the basis of GEO database. Data were presented as the mean (SD), $P < 0.05$ *vs.* control group. **(B)** Measurement of miR-339 expression in PC12 cells after OGD/R treatment using qRT-PCR. Data were presented as the mean (SEM), $n = 3$, $^{**}P < 0.01$ *vs.* normal group. **(C)** CCK-8 assay was performed to detect the proliferation of OGD/R-induced PC12 cells with different transfections, Data were presented as the mean (SEM), $n = 3$, $^{**}P < 0.01$ vs. normal group, $^{\#\#}P < 0.01$ vs. OGD/R group.

qRT-PCR

TRIzol solution was utilized to isolate the total RNA of PC12 cells based on the protocols of the manufacturer. For miR-339, cDNA was reverse transcribed with MiScript Reverse Transcription kit (Qiagen, Hilden, Germany). For FGF9/CACNG2, first-strand cDNA was reverse transcribed by PrimeScript RT kit (Takara biomedical Technology Co., Ltd., Beijing, China). Real-time PCR was implemented on an ABI 7900HT real-time PCR system with MiScript SYBR-Green PCR kit (Qiagen) or SYBR Premix Ex Taq II (TaKaRa, Japan) under indicated conditions (5 min at 95°C followed by 40 cycles of 30 s at 95°C and 45 s at 60°C). All primers were purchased from GenePharma Co., Ltd (Shanghai, China):

miR-339F: 5′-TCCCTGTCCTCCAGGAGCTC-3′,
R: 5′-GAACATGTCTGCGTATCTC-3′;
FGF9F: 5′-CAGCTCCACTGTTGCCAAAC-3′,
R: 5′-ATACAGCTCCCCCTTCTCGT-3′;
CACNG2F: 5′-AATACTCTGCGGTGTCAGCC-3′,
R: 5′-AATACTCTGCGGTGTCAGCC-3′;
U6F: 5′-CTCGCTTCGGCAGCACA-3′,
R: 5′-AACGCTTCACGAATTTGCGT-3′;
GAPDHF: 5′-TGATGGGTGTGAACCACGAG-3′,
R: 5′-AGTGATGGCATGGACTGTGG-3′.

The expression of miR-339 and FGF9/CACNG2 was normalized to U6 or GAPDH using the $2^{-\Delta\Delta CT}$ method for quantification.

Western Blotting

PC12 cells were solubilized in RIPA buffer with protease inhibitor, and the total proteins were extracted. Separated proteins were firstly denatured at 95°C for 10 min and quantified by BCA method. Next, denatured proteins (20 μg) were subjected to the 12% SDS-PAGE and transferred to PVDF membranes (Roche, Basel, Switzerland). Five percentage fat-free milk was used to block the PVDF membranes for 1 h at room temperature. Then, PVDF membranes were incubated with indicated primary antibodies (1:1000; Abcam, Cambridge, UK) against FGF9, CACNG2, p-P38 MAPK, P38 MAPK, p-JNK, JNK, and GAPDH at 4°C overnight. After washing with TBST (3 × 5 min), PVDF membranes were probed with horseradish peroxidase (HRP)-labeled secondary antibody for 1 h at room temperature. The protein bands were visualized using ECL solution, and QUANTITY ONE software was employed to measure the gray values of protein bands.

Statistical Analysis

All statistical analyses were applied using SPSS22.0 (SPSS, Chicago, IL, USA) and GraphPad Prism 6.0 (GraphPad Software, Inc., La Jolla, CA, USA). A Student's *t*-test was conducted to assess the differences of two groups, while the significant differences among multiple groups were performed by one-way ANOVA with Dunnett or Bonferroni *post-hoc* test. KEGG

and GO enrichment analyses were conducted according to the criterion of FDR <0.05. The threshold for statistical significance was considered as $P < 0.05$.

RESULTS

miR-339 Promotes OGD/R-Induced Injury in PC12 Cells

To inquire the biological function of miR-339 in IS, we firstly analyzed the expression of miR-339 in MCAO and normal tissues based on the GEO datasets. miR-339 was expressed at a higher level in MCAO samples compared with the control (**Figure 1A**, $P < 0.05$). To mimic *in vitro* the IS model, PC12 cells were stimulated with OGD/R. As shown in **Figure 1B**, in contrast to the normoxic control, the expression of miR-339 was up-regulated in PC12 cells with OGD/R treatment ($P < 0.01$). Subsequently, we performed CCK-8 test to explore whether miR-339 can regulate the cell viability of OGD/R-induced PC12 cells. The expression of miR-339 in PC12 cells was significantly increased or decreased by the transfection of miR-339 mimic or miR-339 inhibitor, respectively. Results indicated that the OGD/R treatment significantly attenuated the proliferation of PC12 cells; up-regulation of miR-339 further induced a decrease in the proliferation of PC12 cells after OGD/R stimulation compared with miR-339 mimic NC group, whereas down-regulation of miR-339 remarkably elevated the proliferative ability of PC12 cells (**Figure 1C**, $P < 0.01$). Altogether, these findings demonstrated that overexpression of miR-339 might aggravate the OGD/R-induced injury.

miR-339 Directly Targets FGF9 and CACNG2 in IS

To identify the potential targets of miR-339 in IS, the GSE61616 dataset was downloaded to screen out the DEGs of IS and a total of 1,144 DEGs were identified including 1,046 up-regulated genes and 98 down-regulated genes. Then, the down-regulated genes were analyzed for GO annotation and KEGG pathway enrichment in the David database. Under the condition of FDR <0.05, a total of 14 meaningful pathways and 9 GO-BP were obtained (**Figures 2A,B**). Prediction tool Targetscan was used to predict the putative targets of miR-339 and 695 potential target genes were finally obtained. By intersecting with the putative targets and down-regulated genes, a total of 27 common genes was achieved (**Figure 2C**). In addition, given the results of KEGG enrichment analysis, we found that FGF9 and CACNG2 were all enriched in the MAPK signaling pathway; thus, FGF9 and CACNG2 were selected as target genes of miR-339 for further research. Furthermore, data derived from GEO database revealed that the down-regulation of EGF9 and CACNG2 was expressed in MCAO in comparison with that of normal specimens (**Figures 2D,E**, $P < 0.01$).

To further validate the correlation between miR-339 and FGF9/CACNG2, dual-luciferase reporter gene assay was conducted and results displayed that the luciferase activity of the WT FGF9 group was significantly changed (decreased after miR-339 mimic transfection and increased after miR-339 inhibitor transfection) (**Figure 3A**, $P < 0.01$). However, there was no significant difference in the MUT FGF9 group. The consistent results were observed in WT CACNG2 and MUT CACNG2 groups (**Figure 3B**, $P < 0.01$). In addition, qRT-PCR and Western blot were performed to assess whether abnormal expression of miR-339 affects the expression of FGF9 or CACNG2 in PC12 cells. As the results presented, FGF9 and CACNG2 expression were negatively regulated by the expression of miR-339 (**Figures 3C–F**, $P < 0.01$). Compared with the control group, PC12 cells transfected with miR-339 mimic showed a decrease level of FGF9 expression while the co-transfection of miR-339 mimic and pcDNA3.1-FGF9 partially recovered the mimic-induced down-regulation of FGF9. miR-339 inhibitor significantly increased the expression of FGF9 and the addition of si-FGF9 inhibited the promoting effect of miR-339 inhibitor on FGF9 expression. Similarly, CACNG2 expression was also repressed by miR-339 mimic and elevated attributed to the transfection of miR-339 inhibitor. Furthermore, the effect of miR-339 mimic and inhibitor on CACNG2 expression could be reversed by CACNG2 or si-CACNG2, respectively. Collectively, all data suggested that FGF9/CACNG2 were direct targets of miR-339 in IS.

miR-339 Inhibits Cell Proliferation and Induces Apoptosis of OGD/R-Treated PC12 Cells Through Directly Targeting FGF9 and CACNG2

In order to explore whether the regulatory effect of miR-339 on IS progression is associated with FGF9/CACNG2, further experiments containing CCK-8 and flow cytometry analyses were conducted. Interestingly, overexpression of miR-339 intensified the OGD/R-induced injury; up-regulation of FGF9/CACNG2 protected PC12 cells from OGD/R-induced damage; co-transfection of miR-339 mimic and FGF9/CACNG2 recovered cell viability of PC12 cells to normal levels (**Figures 4A**, **5A**, $P < 0.01$). Apoptosis analysis revealed that miR-339 enhancement could promote the apoptosis rate of PC12 cells after OGD/R treatment, while overexpression of FGF9 or CACNG2 significantly inhibited apoptosis. By contrast, co-transfection of miR-339 mimic and FGF9 or CACNG2 recovered the apoptotic ability to the conventional level (**Figures 4C, 5C**, $P < 0.01$). On the contrary, the transfection of miR-339 inhibitor protected PC12 cells from OGD/R treatment, contributed to cell proliferation, and suppressed apoptosis. The knockdown of FGF9 or CACNG2 exhibited a converse role on PC12 cells after OGD/R injury. The co-transfection of miR-339 inhibitor and si-FGF9 or si-CACNG2 overturned their individually effect on cell proliferation as well as apoptosis (**Figures 4B,D, 5B,D**, $P < 0.01$). These results determined that miR-339 aggravated OGD/R-stimulated cell damage via inhibiting the expression of FGF9/CACNG2 in PC12 cells.

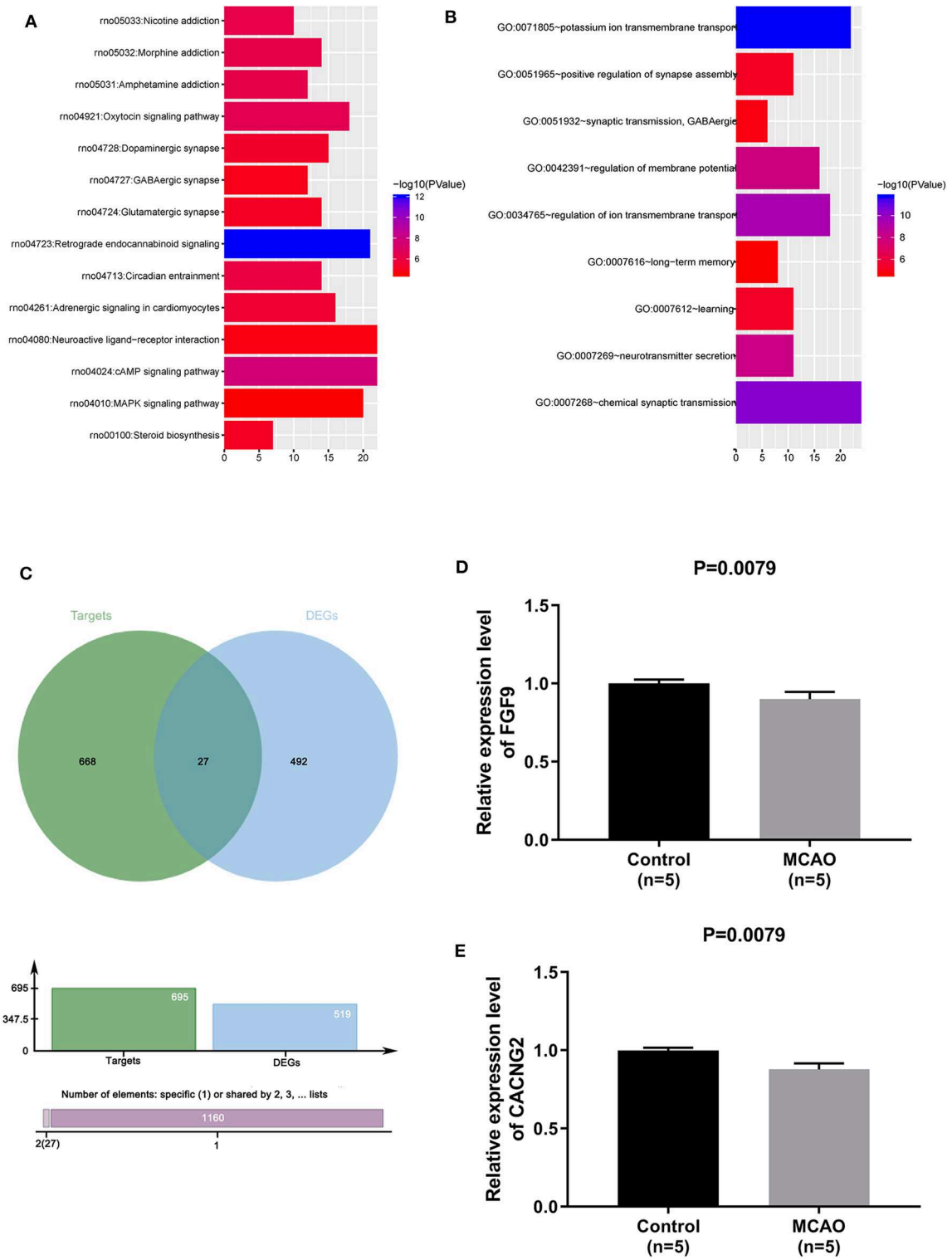

FIGURE 2 | FGF9 and CACNG2 might serve as the potential targets of miR-339 in IS. **(A)** KEGG enrichment analysis and **(B)** GO annotations were conducted to identify the pathways related with down-regulated genes of IS. **(C)** Venn curve of the interaction between the putative targets that predicted by TargetScan and down-regulated genes. **(D)** FGF9 and **(E)** CACNG2 expressions were determined owing to the GEO datasets (accession number: GSE61616, includes five normal controls and five MCAO cases), $P = 0.0079$.

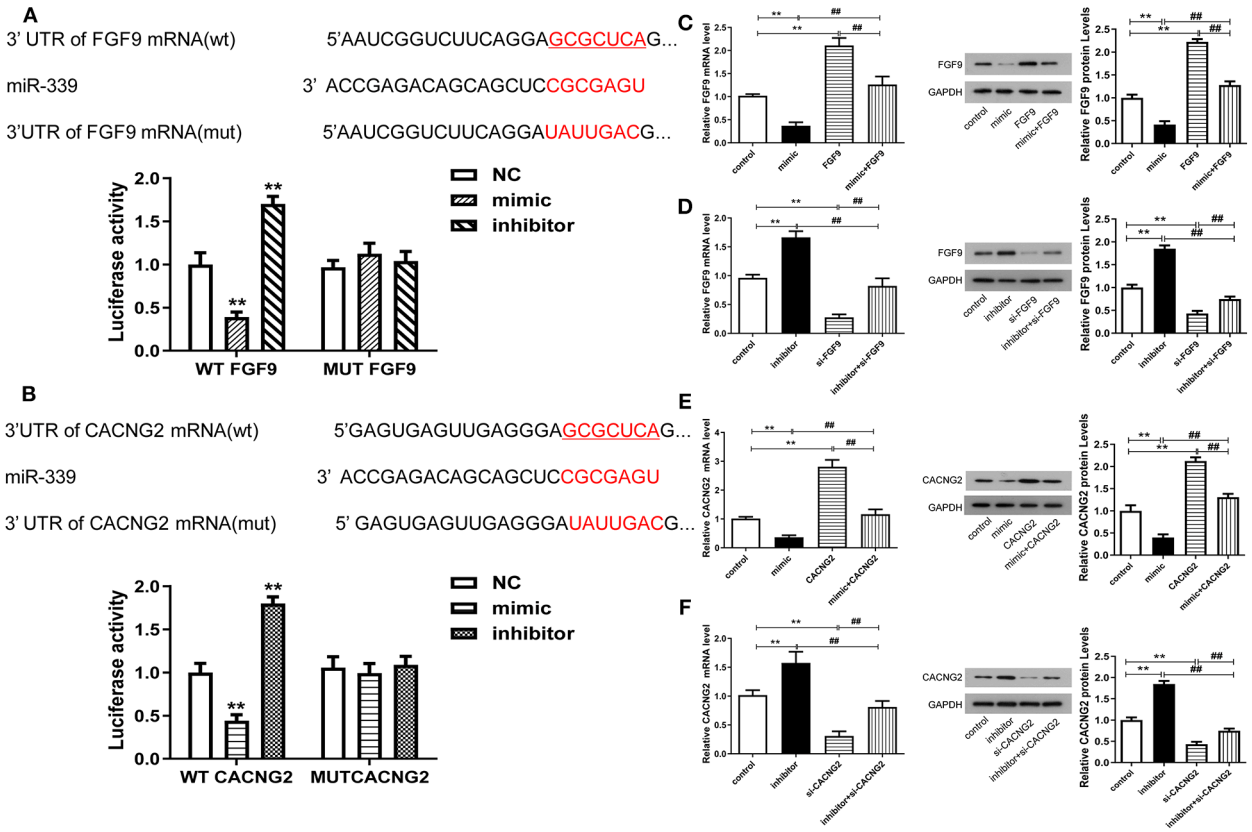

FIGURE 3 | miR-339 can negatively regulate the expression levels of FGF9 and CACNG2. **(A)** The predicted binding site between miR-339 and FGF9. The luciferase activity assay was conducted to examine the luciferase activity of WT FGF9 and MUT FGF9 in PC12 cells transfected with miR-339 mimic or miR-339 inhibitor. Data were presented as the mean (SEM), $n = 3$, $^{**}P < 0.01$ vs. negative control (NC) group. **(B)** Sequence of interaction site between miR-339 and CACNG2. Dual-luciferase reporter assay was implemented to assess the relative luciferase activity of WT CACNG2 and MUT CACNG2 in PC12 cells after miR-339 mimic or miR-339 inhibitor transfection. Data were presented as the mean (SEM), $n = 3$, $^{**}P < 0.01$ vs. NC group. **(C,D)** Detection of FGF9 mRNA and protein levels in PC12 cells with various transfections, including blank control, miR-339 mimic/inhibitor, pcDNA3.1-FGF9/si-FGF9, mimic+FGF9/inhibitor+si-FGF9. Data were presented as the mean (SEM), $n = 3$, $^{**}P < 0.01$ vs. control group, $^{\#\#}P < 0.01$ vs. mimic+FGF9/inhibitor+si-FGF9. **(E,F)** Exploration of CACNG2 mRNA and protein levels in PC12 cells with different transfections, including blank control, miR-339 mimic/inhibitor, pcDNA3.1-CACNG2/si- CACNG2, mimic+CACNG2/inhibitor+si-CACNG2. Data were presented as the mean (SEM), $n = 3$, $^{**}P < 0.01$ vs. control group, $^{\#\#}P < 0.01$ vs. mimic+CACNG2/inhibitor+si-CACNG2.

The miR-339/FGF9/CACNG2 Axis Regulates the MAPK Signaling Pathway in OGD/R-Induced PC12 Cells

Considering that the FGF9 and CACNG2 were all enriched in the MAPK pathway (based on the KEGG enrichment analysis), we speculated that the effect of miR-339/FGF9/CACNG2 in IS may be correlated with the activity of the MAPK pathway. To clarify this potential molecular mechanism, the protein levels of key markers implicated in the MAPK pathway were measured by Western blotting including p-P38, P38, p-JNK, and JNK. As shown in **Figures 6A,C**, in the OGD/R+mimic group, the protein levels of p-P38 and p-JNK were significantly increased compared with the OGD/R group ($P < 0.01$). Overexpression of FGF9 or CACNG2 led to a remarkable decrease in the expression level of p-P38 and p-JNK when compared with the OGD/R group ($P < 0.01$). Furthermore, the co-transfection of miR-339 mimic and FGF9 or CACNG2 recovered the effects of either miR-339 mimic or FGF9/CACNG2 on the expression levels of p-P38 and p-JNK. Compared with the OGD/R group, miR-339 inhibitor induced the reduction of p-P38 and p-JNK expression while silencing of FGF9 or CACNG2 elevated the protein levels of p-P38 and p-JNK. A significant restoration of the attenuation or increase in the protein levels of p-P38 and p-JNK was induced by miR-339 inhibitor or si-FGF9/CACNG2, respectively (**Figures 6B,D**, $P < 0.01$). The results also exhibited that there were no significant changes in the P38 and JNK expression after different treatments (**Figure 6**, $P < 0.01$). In summary, these data indicated that miR-339 could activate the MAPK pathway through inhibiting the FGF9 and CACNG2 expression in IS development.

DISCUSSION

As previously described, cerebral ischemia/reperfusion (I/R) injury is the leading cause of cerebrovascular diseases and the frequent kind being stroke (13). It is well-known that the

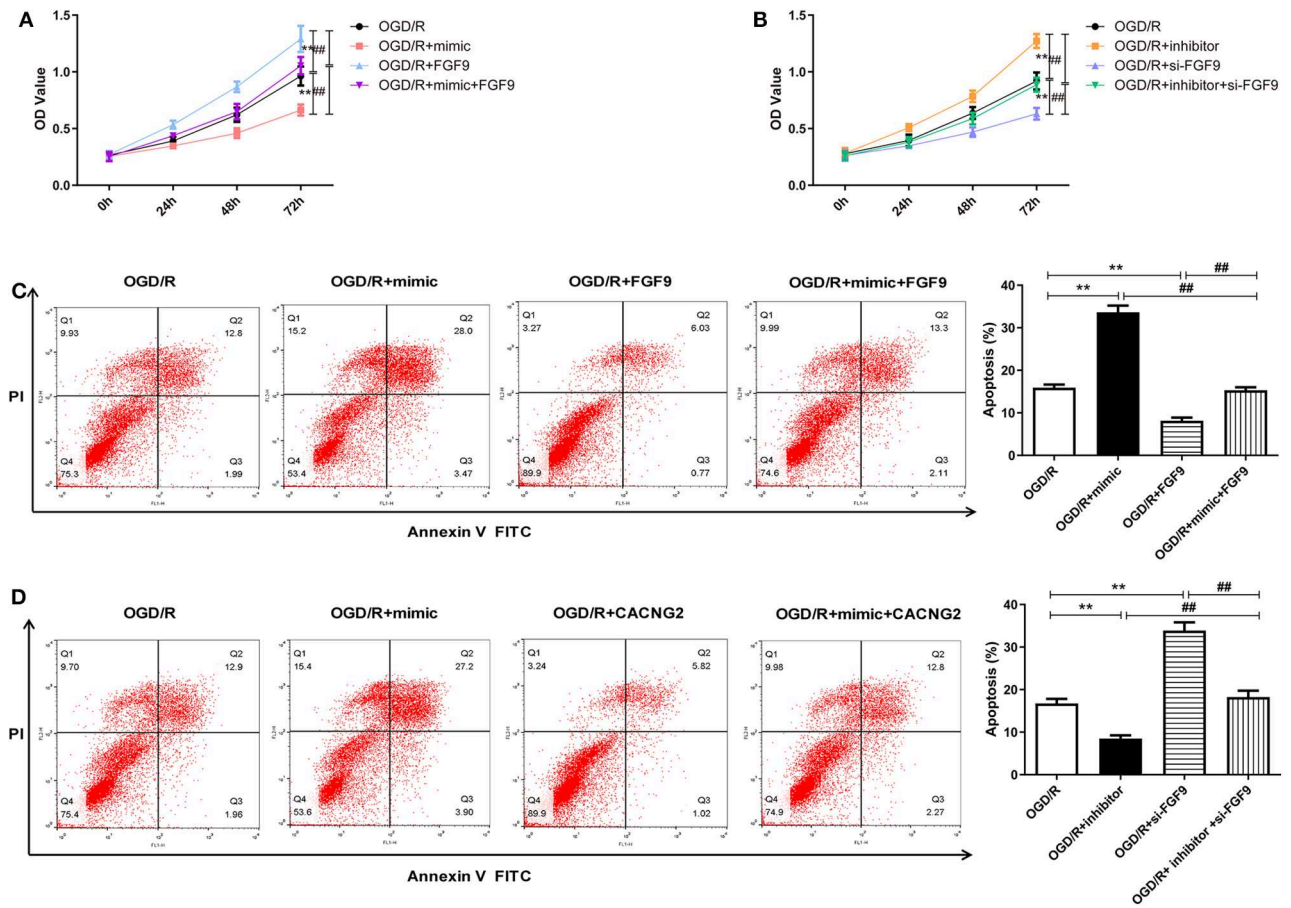

FIGURE 4 | miR-339 aggravated OGD/R-induced injury through targeting FGF9 in PC12 cells. **(A,B)** CCK-8 assays were performed to detect the PC12 cell viability after OGD/R treatment and different transfections. Data were presented as the mean (SEM), $n = 3$, $^{**}P < 0.01$ vs. OGD/R group, $^{\#\#}P < 0.01$ vs. OGD/R+mimic+FGF9 or OGD/R+inhibitor+si-FGF9 group. **(C,D)** Annexin V-fluorescein isothiocynate (FITC)/propidium iodide (PI) staining and flow cytometry analysis were implemented to evaluate cell apoptosis. Data were presented as the mean (SEM), $n = 3$, $^{**}P < 0.01$ vs. OGD/R group, $^{\#\#}P < 0.01$ vs. OGD/R+mimic+FGF9 or OGD/R+inhibitor+si-FGF9 group.

mechanism of cerebral I/R injury is complex, which refers to multiple biological processes, including apoptosis, inflammation, and necrosis (14, 15). Therefore, it is an urgent task to explain the potential mechanism of cerebral I/R injury that mainly induces IS. OGD/R treatment has been widely used to mimic the cell state after I/R injury *in vitro* (16). Our present study demonstrated that miR-339 expression was markedly increased in MCAO. By constructing the OGD/R model, we also found that the expression of miR-339 was elevated in PC12 cells. Through *in vitro* functional analyses, miR-339 could accelerate the progression of IS via targeting FGF9/CACNG2 and mediating the activity of MAPK signaling pathway, indicating that miR-339/FGF9/CACNG2 might act as novel therapeutic targets to improve the grave outcomes of patients with IS.

Accumulating studies have shown that dysregulation of miR-339 is associated with a variety of cancers. Yu et al. have reported that miR-339 inhibits the invasion and migration of pancreatic tumor cells through down-regulating ZNF689 expression (17). Similarly, knockdown of miR-339 in hepatocellular carcinoma cells promotes proliferation and invasion and suppresses apoptosis (18). On the contrary, miR-339 exerts an opposite role to cancer in other diseases. Hu et al. demonstrated that miR-339 is up-regulated in stem cell leukemia/lymphoma syndrome and promotes the development of stem cell leukemia/lymphoma syndrome via suppressing BCL211 and BAX expression (19). Importantly, Dhiraj et al. have profiled miRNAs in the whole ischemic infarct and identified that miR-339 may serve as an essential factor and modulates the salvageable ischemic penumbra-related cellular pathways (11). Consistent with this prior study, miR-339 was found to be overexpressed in MCAO and PC12 cells exposed to OGD/R in our study. Up-regulation of miR-339 could significantly attenuate PC12 cell viability after OGD/R treatment. These data elucidated that miR-339 might aggravate the PC12 cell injury induced by OGD/R.

To explore the mechanism and targets of miR-339 in IS in depth, we screened out the DEGs in MCAO based on GEO repository and predicted the possible target genes of miR-339 using TargetScan website. After enriching DEGs using KEGG

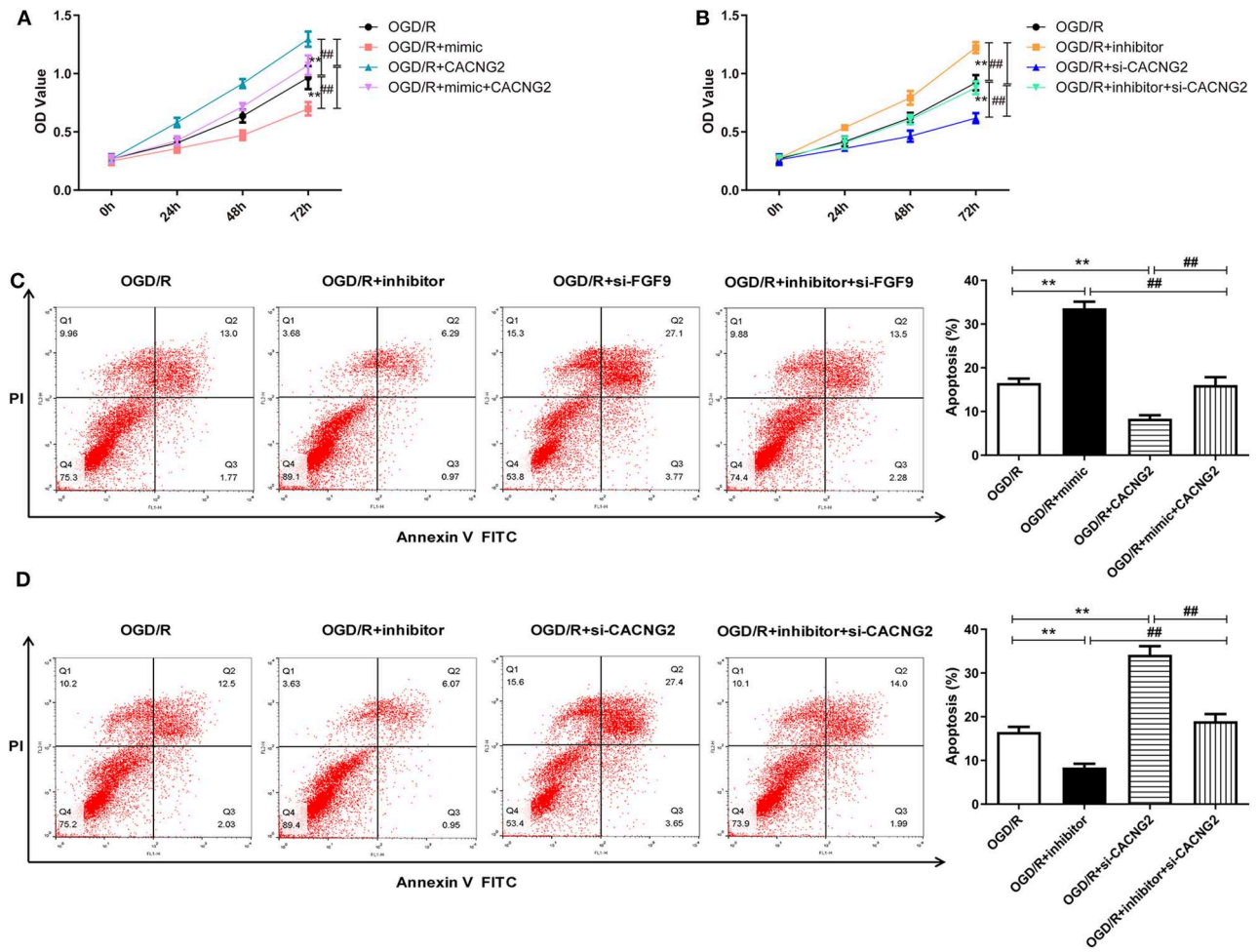

FIGURE 5 | The regulation of miR-339 on OGD/R-induced PC12 cell injury was modulated by CACNG2. **(A,B)** After transfection with various agents, the proliferative ability of PC12 cells stimulated by OGD/R was determined. Data were presented as the mean (SEM), $n = 3$, $^{**}P < 0.01$ vs. OGD/R group, $^{\#\#}P < 0.01$ vs. OGD/R+mimic+CACNG2 or OGD/R+inhibitor+si-CACNG2 group. **(C,D)** The apoptotic potential of OGD/R-treated PC12 cells was measured using flow cytometry analysis. Data were presented as the mean (SEM), $n = 3$, $^{**}P < 0.01$ vs. OGD/R group, $^{\#\#}P < 0.01$ vs. OGD/R+mimic+CACNG2 or OGD/R+inhibitor+si-CACNG2 group.

and GO analysis, a total of 14 pathways including the MAPK pathway were obtained. A previous study indicated that the MAPK pathway is an important pathway stimulated in the early stage of IS (20). Furthermore, the common genes FGF9 and CACNG2 that were identified by intersecting the DEGs and putative targets of miR-339 were enriched in the MAPK pathway. Thus, FGF9 and CACNG2 were selected as the targets of miR-339 for further detection. FGF9 (fibroblast growth factor 9) is located on the chromosome 13q11-q12 and initially considered as a secreted agent revealing a mitogenic role on the glial cells (21, 22). The secretion of FGF9 can improve the survival rate and neurite growth of SH-SY5Y neuroblastoma cells (23). The miR-182/FGF9 axis is associated with nerve injury-caused phenotype (24). CACNG2 (calcium voltage-gated channel auxiliary subunit gamma 2) has been proven to be a pain susceptibility gene. CACNG2 could encode the gamma-2 transmembrane AMPA receptor protein (TARP) stargazing and is involved in the modulation of neuronal Ca^{2+} channels. It plays a central role in the cerebellar function and epilepsy (25–27). Therefore, we reasonably speculated that FGF9/CACNG2 might participate in the development of IS. In this present study, we found that FGF9/CACNG2 were directly targeted by miR-339 and the overexpression of miR-339 could significantly attenuate the expression of FGF9 and CACNG2 in PC12 cells. Rescue experiments in OGD/R-induced PC12 cells further suggested that the promoting effect of miR-339 on the progression of IS was reversed by the overexpressing FGF9/CACNG2.

The role of the MAPK pathway in the pathogenesis of IS uncovered that regulating the activity of the MAPK pathway through ameliorating or intensifying key markers may be an important event for IS development (28). P38 and JNK have been regarded as key markers in the MAPK signaling pathway, which exert pathological and physiological roles when they are phosphorylated (29, 30). Our results demonstrated that

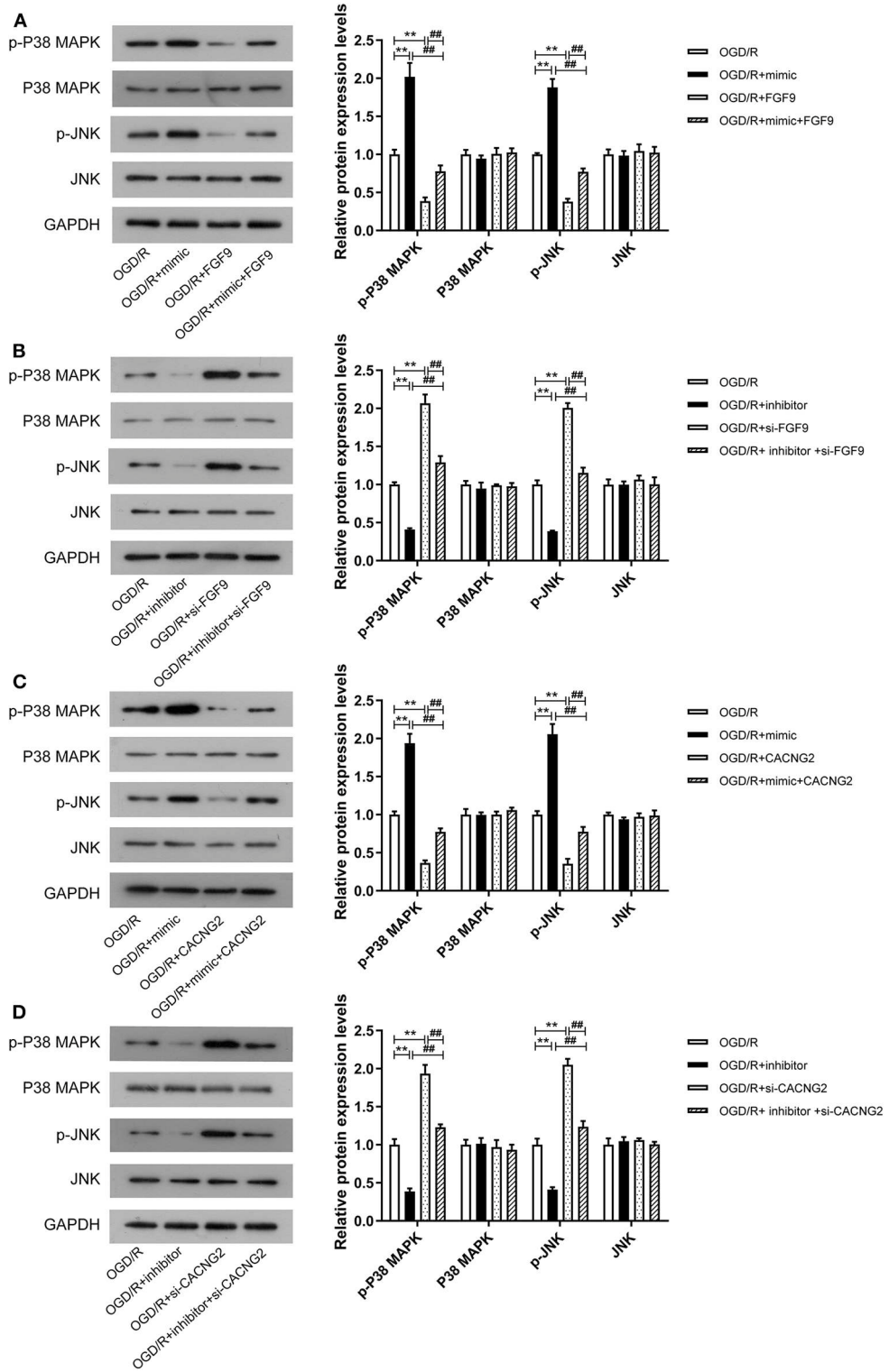

FIGURE 6 | Effects of miR-339 on the MAPK pathway were associated with FGF9/CACNG2 in OGD/R-stimulated PC12 cells. **(A–D)** The immunoblots of p-P38 MAPK, P-38 MAPK, p-KNK, and JNK (left panels), and quantification of the gray values of corresponding protein bands (right panels) in PC12 cells after OGD/R treatment. Data were presented as the mean (SEM), $n = 3$, $^{**}P < 0.01$ vs. OGD/R group, $^{\#\#}P < 0.01$ vs. OGD/R+mimic+FGF9/CACNG2 or OGD/R+inhibitor+si-FGF9/si-CACNG2 group.

abnormal expression of miR-339 affected the protein levels of p-P38 and p-JNK in OGD/R-induced PC12 cells as well as FGF9/CACNG2. Furthermore, the interferences of FGF9 and CACNG2 could rescue the aggressive impacts of miR-339 enhancement on OGD/R-stimulated injury in PC12 cells. Consequently, we summarized that miR-339 could contribute to the development of IS through targeting FGF9/CACNG2 and mediating the activity of the MAPK pathway.

In conclusion, we observed that overexpression of miR-339 in PC12 cells after OGD/R treatment inhibited cell viability and induced apoptosis via mediating the FGF9/CACNG2 axis and the MAPK pathway. Due to the insufficient number of MCAO, it is difficult to strongly conclude the biological effects of miR-339/FGF9/CACNG2 in IS development. Besides, their specific role still needs to be performed *in vivo*. To sum up, this current study sheds new insights into the mechanism of OGD/R injury and provides promising therapeutic targets for IS treatment.

DATA AVAILABILITY STATEMENT

Publicly available datasets were analyzed in this study. This data can be found here: GSE29287 and GSE61616.

AUTHOR CONTRIBUTIONS

X-ZG and R-HM carried out the research, performed the analysis, and participated in the writing of the manuscript. X-ZG and Z-XZ designed and supervised the research, and participated in the writing and reviewing of the manuscript. All authors have read and approved the final manuscript.

REFERENCES

1. Randolph SA. Ischemic stroke. *Workplace Health Safety*. (2016) 64:444–44. doi: 10.1177/2165079916665400
2. Guzik A, Bushnell C. Stroke epidemiology and risk factor management. *Continuum*. (2017) 23:15–39. doi: 10.1212/CON.0000000000000416
3. Lenzer J. Centers for disease control and prevention: protecting the private good? *BMJ*. (2015) 350:h2362. doi: 10.1136/bmj.h2362
4. Ginsberg MD. Neuroprotection for ischemic stroke: past, present and future. *Neuropharmacology*. (2008) 55:363–89. doi: 10.1016/j.neuropharm.2007.12.007
5. Zheng T, Shi Y, Zhang J, Peng J, Zhang X, Chen K, et al. MiR-130a exerts neuroprotective effects against ischemic stroke through PTEN/PI3K/AKT pathway. *Biomed Pharmacother*. (2019) 117:109117. doi: 10.1016/j.biopha.2019.109117
6. Xu W, Zheng J, Gao L, Li T, Zhang J, Shao A. Neuroprotective effects of stem cells in ischemic stroke. *Stem cells Int*. (2017) 2017:4653936–36. doi: 10.1155/2017/4653936
7. Liang Y, Xu J, Wang Y, Tang J-Y, Yang S-L, Xiang H-G, et al. Inhibition of MiRNA-125b decreases cerebral ischemia/reperfusion injury by targeting CK2α/NADPH oxidase signaling. *Cellular Physiol Biochem*. (2018) 45:1818–26. doi: 10.1159/000487873
8. Fan J, Xu W, Nan S, Chang M, Zhang Y. MicroRNA-384-5p promotes endothelial progenitor cell proliferation and angiogenesis in cerebral ischemic stroke through the delta-likeligand 4-mediated notch signaling pathway. *Cerebrovasc Dis*. (2020) 49:39–54. doi: 10.1159/000503950
9. Peng H, Yang H, Xiang X, Li S. MicroRNA-221 participates in cerebral ischemic stroke by modulating endothelial cell function by regulating the PTEN/PI3K/AKT pathway. *Exp Ther Med*. (2020) 19:443–50. doi: 10.3892/etm.2019.8263
10. Zheng Y, Zhao P, Lian Y, Li S, Chen Y, Li L. MiR-340-5p alleviates oxygen-glucose deprivation/reoxygenation-induced neuronal injury via PI3K/Akt activation by targeting PDCD4. *Neurochem Int*. (2019) 134:104650–50. doi: 10.1016/j.neuint.2019.104650
11. Dhiraj DK, Chrysanthou E, Mallucci GR, Bushell M. miRNAs-19b,−29b-2* and−339-5p show an early and sustained up-regulation in ischemic models of stroke. *PLoS ONE*. (2013) 8:e83717–17. doi: 10.1371/journal.pone.0083717
12. Altintas O, Ozgen Altintas M, Kumas M, Asil T. Neuroprotective effect of ischemic preconditioning via modulating the expression of cerebral miRNAs against transient cerebral ischemia in diabetic rats. *Neurol Res*. (2016) 38:1003–11. doi: 10.1080/01616412.2016.1232013
13. Surinkaew P, Sawaddiruk P, Apaijai N, Chattipakorn N, Chattipakorn SC. Role of microglia under cardiac and cerebral ischemia/reperfusion (I/R) injury. *Metab Brain Dis*. (2018) 33:1019–30. doi: 10.1007/s11011-018-0232-4
14. Prabhakaran S, Ruff I, Bernstein RA. Acute stroke intervention: a systematic review. *JAMA*. (2015) 313:1451–62. doi: 10.1001/jama.2015.3058
15. He G, Xu W, Tong L, Li S, Su S, Tan X, et al. Gadd45b prevents autophagy and apoptosis against rat cerebral neuron oxygen-glucose deprivation/reperfusion injury. *Apoptosis*. (2016) 21:390–403. doi: 10.1007/s10495-016-1213-x
16. Ryou M-G, Mallet RT. An *in vitro* oxygen-glucose deprivation model for studying ischemia-reperfusion injury of neuronal cells. *Methods Mol Biol*. (2018) 1717:229–35. doi: 10.1007/978-1-4939-7526-6_18
17. Yu Z, Zhao S, Wang L, Wang J, Zhou J. miRNA-339-5p plays an important role in invasion and migration of pancreatic cancer cells. *Med Sci Monit*. (2019) 25:7509–17. doi: 10.12659/MSM.917038
18. Zeng H, Zheng J, Wen S, Luo J, Shao G, Zhang Y. MicroRNA-339 inhibits human hepatocellular carcinoma proliferation and invasion via targeting ZNF689. *Drug Des Dev Ther*. (2019) 13:435–45. doi: 10.2147/DDDT.S186352
19. Hu T, Chong Y, Lu S, Wang R, Qin H, Silva J, et al. miR-339 promotes development of stem cell leukemia/lymphoma syndrome via downregulation of the BCL2L11 and BAX proapoptotic genes. *Cancer Res*. (2018) 78:3522–31. doi: 10.1158/0008-5472.CAN-17-4049
20. Roy Choudhury G, Ryou M-G, Poteet E, Wen Y, He R, Sun F, et al. Involvement of p38 MAPK in reactive astrogliosis induced by ischemic stroke. *Brain Res*. (2014) 1551:45–58. doi: 10.1016/j.brainres.2014.01.013
21. Chen T-M, Shih Y-H, Tseng JT, Lai M-C, Wu C-H, Li Y-H, et al. Overexpression of FGF9 in colon cancer cells is mediated by hypoxia-induced translational activation. *Nucleic Acids Res*. (2014) 42:2932–44. doi: 10.1093/nar/gkt1286
22. Santos-Ocampo S, Colvin JS, Chellaiah A, Ornitz DM. Expression and biological activity of mouse fibroblast growth factor-9. *J Biol Chem*. (1996) 271:1726–31. doi: 10.1074/jbc.271.3.1726
23. Lee I-S, Koo KY, Jung K, Kim M, Kim I-S, Hwang K, et al. Neurogenin-2-transduced human neural progenitor cells attenuate neonatal hypoxic-ischemic brain injury. *Transl Res*. (2017) 183:121–36.e9. doi: 10.1016/j.trsl.2016.12.010
24. Yu B, Qian T, Wang Y, Zhou S, Ding G, Ding F, et al. miR-182 inhibits schwann cell proliferation and migration by targeting FGF9 and NTM, respectively at an early stage following sciatic nerve injury. *Nucleic Acids Res*. (2012) 40:10356–65. doi: 10.1093/nar/gks750
25. Cokić B, Stein V. Stargazin modulates AMPA receptor antagonism. *Neuropharmacology*. (2008) 54:1062–70. doi: 10.1016/j.neuropharm.2008.02.012
26. Tselnicker I, Tsemakhovich VA, Dessauer CW, Dascal N. Stargazin modulates neuronal voltage-dependent Ca(2+) channel Ca(v)2.2 by a Gbetagamma-dependent mechanism. *J Biol Chem*. (2010) 285:20462–71. doi: 10.1074/jbc.M110.121277
27. Nissenbaum J, Devor M, Seltzer Z e, Gebauer M, Michaelis M, Tal M, et al. Susceptibility to chronic pain following nerve injury is genetically affected by CACNG2. *Genome Res*. (2010) 20:1180–90. doi: 10.1101/gr.104976.110

28. Sun J, Nan G. The Mitogen-Activated Protein Kinase (MAPK) signaling pathway as a discovery target in stroke. *J Mol Neurosci*. (2016) 59:90–8. doi: 10.1007/s12031-016-0717-8
29. Rezatabar S, Karimian A, Rameshknia V, Parsian H, Majidinia M, Kopi TA, et al. RAS/MAPK signaling functions in oxidative stress, DNA damage response and cancer progression. *J Cell Physiol*. (2019) doi: 10.1002/jcp.28334. [Epub ahead of print].
30. Reustle A, Torzewski M. Role of p38 MAPK in atherosclerosis and aortic valve sclerosis. *Int J Mol Sci*. (2018) 19:3761. doi: 10.3390/ijms19123761

Conflict of Interest: The authors declare that the research was conducted in the absence of any commercial or financial relationships that could be construed as a potential conflict of interest.

frontiers in Neurology

REVIEW
published: 31 July 2020
doi: 10.3389/fneur.2020.00703

The Multifaceted Role of Astrocyte Connexin 43 in Ischemic Stroke Through Forming Hemichannels and Gap Junctions

Zhen Liang[1], Xu Wang[1], Yulei Hao[1], Lin Qiu[1], Yingyue Lou[2], Yaoting Zhang[3], Di Ma[1] and Jiachun Feng[1]**

[1] Department of Neurology and Neuroscience Center, The First Hospital of Jilin University, Changchun, China, [2] Department of Plastic and Reconstructive Surgery, The First Hospital of Jilin University, Changchun, China, [3] Department of Cardiology, The First Hospital of Jilin University, Changchun, China

Ischemic stroke is a multi-factorial cerebrovascular disease with high worldwide morbidity and mortality. In the past few years, multiple studies have revealed the underlying mechanism of ischemia/reperfusion injury, including calcium overload, amino acid toxicity, oxidative stress, and inflammation. Connexin 43 (Cx43), the predominant connexin protein in astrocytes, has been recently proven to display non-substitutable roles in the pathology of ischemic stroke development and progression through forming gap junctions and hemichannels. Under normal conditions, astrocytic Cx43 could be found in hemichannels or in the coupling with other hemichannels on astrocytes, neurons, or oligodendrocytes to form the neuro–glial syncytium, which is involved in metabolites exchange between communicated cells, thus maintaining the homeostasis of the CNS environment. In ischemic stroke, the phosphorylation of Cx43 might cause the degradation of gap junctions and the opening of hemichannels, contributing to the release of inflammatory mediators. However, the remaining gap junctions could facilitate the exchange of protective and harmful metabolites between healthy and injured cells, protecting the injured cells to some extent or damaging the healthy cells depending on the balance of the exchange of protective and harmful metabolites. In this study, we review the changes in astrocytic Cx43 expression and distribution as well as the influence of these changes on the function of astrocytes and other cells in the CNS, providing new insight into the pathology of ischemic stroke injury; we also discuss the potential of astrocytic Cx43 as a target for the treatment of ischemic stroke.

Keywords: ischemic stroke, connexin 43, astrocyte, gap junction, hemichannel, syncytium

OPEN ACCESS

Edited by:
Emmanuel Pinteaux, University of Manchester, United Kingdom

Reviewed by:
Jong Eun Lee, Yonsei University, South Korea
Mauricio Antonio Retamal, Universidad del Desarrollo, Chile
Eliseo A. Eugenin, University of Texas Medical Branch at Galveston, United States

****Correspondence:***
Di Ma
april8316@hotmail.com
Jiachun Feng
fengjcfrank@126.com

Specialty section:
This article was submitted to Stroke, a section of the journal Frontiers in Neurology

Received: *20 February 2020*
Accepted: *09 June 2020*
Published: *31 July 2020*

Citation:
Liang Z, Wang X, Hao Y, Qiu L, Lou Y, Zhang Y, Ma D and Feng J (2020) The Multifaceted Role of Astrocyte Connexin 43 in Ischemic Stroke Through Forming Hemichannels and Gap Junctions. Front. Neurol. 11:703. doi: 10.3389/fneur.2020.00703

INTRODUCTION

Ischemic stroke is caused by the stenosis or occlusion of the cerebral blood supply. It is the most common cerebral vascular disease (contributing to ∼80% of strokes) with high morbidity and mortality (1, 2). It was recently reported that ischemic stroke, cardiovascular diseases, and malignant tumors constitute the three major causes of human death (3, 4). Although research into the mechanisms of ischemic stroke injury has made advanced progress in the last few years,

effective strategies for ischemic stroke treatment to protect residual neurons by restoring brain perfusion as soon as possible via intravenous thrombolysis and mechanical thrombectomy (5, 6) remain limited.

Among the glial cells in the brain parenchyma, astrocytes are the most abundant and critical (7, 8) and may modulate the homeostasis of the central nervous system (CNS) environment and support the survival of neurons (8, 9). The roles of astrocytes in the pathology of ischemic stroke are double-edged, while they can help maintain the homeostasis of the CNS micro-environment to protect neurons by maintaining ion and pH balance, transporting metabolic substrates, and clearing neuronal waste. Conversely, the inflammatory mediators and excitatory amino acids produced and released by astrocytes might promote the death of neurons (10). Connexin 43 (Cx43), one of the most abundant Cxs in the brain tissue, is essential for astrocytes to exert their various physiological functions by forming gap junctions and hemichannels (11, 12) and its role in the development and progression of ischemic stroke have received increasing attention in recent years (13, 14). However, the currently available data show that the change in astrocytic Cx43 after ischemic stroke and the roles it plays are controversial (15–17). Therefore, in this study, we reviewed the syncytium structures that astrocytes form with other cells (astrocytes, neurons, and oligodendrocytes), and the change in astrocytic Cx43 expression and distribution after stroke as well as how these changes influence the functions of astrocytes and the neuro–glial syncytium, subsequently regulating ischemic injury. The delineation of the roles of astrocytic Cx43 in ischemic stroke could help elucidate the initiation and spread of inflammation and neuronal damage after ischemic stroke, which might provide some new targets for the treatment of ischemic stroke.

THE STRUCTURE, DISTRIBUTION, AND PHYSIOLOGICAL FUNCTIONS OF Cx43

Cxs in the CNS are important membrane proteins of a family that consist of 21 members that can form gap junctions and hemichannels. Eleven of these Cxs are expressed in the adult mammalian brain and are distributed differently on glial cells and neurons in the CNS (**Table 1**) (31–33). Among these Cxs, astrocytic Cx43 is the most widely expressed and studied in the CNS, playing essential roles in the communication between astrocytes and other cells or with the extracellular milieu, as they form gap junction channels or hemichannels (34).

Structure and Distribution of Cx43

Cx43 in the adult mammalian brain, named after its molecular weight of ∼43 kDa, belongs to the α-Cx family and consists of 382 amino acids (31, 35, 36). The same as other Cxs, Cx43 contains four transmembrane regions, the intracellular N-terminal and C-terminal and two extracellular loops. The two extracellular loops and the N-terminal are relatively conserved, while the intracellular loop and C-terminus determine the different biological characteristics in different species (37, 38).

TABLE 1 | Cellular distribution of connexins expressed by glia and neurons in the adult mammalian central nervous system.

Cell type	Connexins	Gap junctions with astrocytic Cx43	References
Astrocytes	Cx26, Cx30, Cx43	Cx43/Cx43	(18, 19)
Neurons*	Cx30.2, Cx31.1, Cx32, Cx36, Cx40, Cx45, Cx50	Cx36/Cx43	(20–23)
Oligodendrocytes	Cx29, Cx32, Cx47	Cx47/Cx43	(24, 25)
Microglia	Cx32, Cx36, Cx43		(26–28)
Capillary endothelial cells	Cx37, Cx40, Cx43		(29, 30)

**The types of connexins distributed on neurons have not been determined.*

Cx43 is the dominant Cx protein in astrocytes and the main component of astrocytic gap junctions and hemichannels (1). Individual Cx assembles into hexamers around a central pore to form transmembrane channels named connexons, also known as hemichannels (39). They can exist as free, no-junctional channels on the astrocytic membrane and form gap junction channels with other hemichannels on the membrane of adjacent astrocytes or other cells (18). Further studies have shown that hemichannels may be homomeric or heteromeric, depending on the Cx composition. Similarly, gap junctions are homotypic if the paired hemichannels contain the same Cxs, and heterotypic if they contain different Cxs (40).

Hemichannels

Hemichannels are not closed under resting conditions; their opening probability is very low but not zero (41). However, under certain physiological and pathological stimulation conditions (such as the presence pro-inflammatory cytokines, increase in intracellular calcium concentration, and metabolic inhibition), hemichannels might increase their opening probability (42–47). Consequently, activated astrocytic Cx43 hemichannels are critical ion diffusion (including of Ca^{2+}, K^{+}, Na^{+}) from astrocytes to the extracellular milieu as well as for the release of adenosine triphosphate (ATP) and gliotransmitters [including of glutamate (Glu), adenosine, and glutathione], thus forming chemical coupling between cells and the micro-environment through autocrine and paracrine approaches (48–50). The activated hemichannels might play dual roles in the CNS. Recent reports have shown that the opening of hemichannels during resting conditions is involved in basal synaptic transmission and long-term potentiation (51, 52). Other studies have reported that the opening of hemichannels can facilitate the release of D-serine, further enhancing excitatory synaptic transmission in the hippocampus or olfactory bulb (53). However, in pathological situations, the changes in hemichannels

Abbreviations: ATP, Adenosine triphosphate; CBX, carbenoxolone; CNS, central nervous system; Cx, connexin; Glu, glutamate; GLUT, glucose transporters; IL-1β, interleukin-1β; LAD, left anterior descendent; MAPK, mitogen-activated protein kinase; MCAO, middle cerebral artery occlusion; MCT, monocarboxylate transporter; NO, nitric oxide; OGD, oxygen glucose deprivation; ROS, radical oxygen species; TNF-α, tumor necrosis factor-α.

may activate inflammatory signaling, damaging the survival of glial cells and producing excitotoxic molecules (54). After ischemic stroke, inflammation followed by ischemia/reperfusion (I/R) injury could activate the astrocytic hemichannels by increasing extracellular Ca^{2+} and inflammatory cytokine release (15). Then, the opened hemichannels could promote the differentiation of microglia to the M1 phenotype, which could produce pro-inflammatory cytokines including tumor necrosis factor-α (TNF-α) and interleukin-1β (IL-1β), consequently triggering the opening of astrocytic hemichannels (39, 55). The vicious cycle caused the uncontrolled release of ATP, Glu, and Ca^{2+} overload could induce increase in the number of abnormally opened hemichannels, which in turn could lead to tissue excitotoxicity, inflammation amplification, and finally irreversible brain damage (56).

Gap Junction

Astrocytic gap junctions are axially aligned hexamers of connexins, which can connect adjacent cells (57). Thousands of gap junctions clustered into discoid gap junction plaques could further combine with specific protein binding subunits of paired connexons on the membrane of adjacent cells to form the supramolecular gap junction nexus (58). Gap junctions are the major structures of electrical transmission and metabolic and ionic coupling between adjacent cells (41). In contrast to hemichannels, gap junctions are always open under physiological conditions, allowing intercellular communication (59). They allow small molecules, below 1,200 Daltons, to diffuse, including ATP, inositol trisphosphate, and ions (such as K^+, Na^+, and Ca^{2+}), cyclic nucleotides, and oligonucleotides and small peptides, facilitating metabolites exchange and information communication among astrocytes, neurons, and oligodendrocytes, maintaining the intracellular and extracellular homeostasis (60–62). More importantly, astrocytic gap junction channels also transmit chemical signals and metabolites (glucose and lactate) between glial cells, facilitating the function of neuronal, glial, and vascular tissues (63).

THE NEURON–GLIAL SYNCYTIUM STRUCTURE IN THE CENTRAL NERVOUS SYSTEM

As mentioned above, astrocytic Cx43 can both form hemichannels on the cell membrane of astrocytes and form gap junctions with Cx43 or other Cxs on the adjacent astrocytes (18). Considering the hemichannels and gap junctions, astrocytes play a central role in the formation of neuro–glial syncytium structures, where neurons, microglia, oligodendrocytes, and even capillaries could combine to perform various physiological functions (**Figure 1**) (64).

First, astrocytes can be coupled by Cx43 gap junctions to form syncytium structures, which allows groups of cells to synchronously respond to stimuli (61). The coupled astrocytes can differentiate together during the developmental process (65). They also participate in various physiological processes, including clearing K^+ from the extracellular space, synthesizing neurotransmitters, propagating calcium waves, balancing Glu and γ-aminobutyric acid, and the immune response (59, 66, 67). However, in ischemic stroke, gap junctions might also act as channels for the transmission of cytotoxic molecules (including of Ca^{2+}, excessive ATP, and Glu) from dying astrocytes to their coupled cells, amplifying ischemia-induced brain injury (68).

Apart from astrocyte–astrocyte coupling, astrocytes can also couple with neurons and oligodendrocytes through Cx43 (11, 69). Various studies have confirmed that neurons mainly express Cx36, Cx45, and Cx32, all of which can serve as hemichannels (20, 21). Among these Cxs, Cx36 on neurons can couple with astrocytic Cx43, thus forming Cx43/Cx36 heterotypic gap junctions, which facilitate direct metabolic and electrical communication between astrocytes and neurons (20, 70). Additionally, the existence of Cx43/Cx36 gap junctions can combine neurons into the syncytium network. Under physiological conditions, astrocytes can provide energetic substrates (glucose, lactate, citrate, and glutamine) for neurons. Furthermore, Cx32, Cx47, and Cx29 are primarily expressed on oligodendrocytes (24, 25). Among these Cxs on oligodendrocytes, Cx47 participates in the formation of gap junctions with astrocytic Cx43 (19). Recently, studies have revealed that astrocyte–oligodendrocyte gap junctions are essential for CNS myelination and homeostasis (71). Some studies have found that astrocytes can deliver glucose and lactate to oligodendrocytes through gap junctions, which is essential for the survival of neuronal axons (72, 73). Additionally, heterotypic Cx43/Cx47 gap junctions have been shown to mediate the spatial buffering of K^+ and the bi-directional transmission of Ca^{2+} between astrocytes and oligodendrocytes (74). The loss of Cx43/Cx47 gap junctions might disrupt the spatial buffering of K^+, subsequently leading to myelin swelling and axonal degeneration (75, 76).

Although Cxs expressed on capillary endothelial cells (mainly Cx 37, Cx40, and Cx43) can also form hemichannels and gap junctions (29, 30), there is no evidence that astrocytes establish direct contact with endothelial cells, which might account for the obstruction of the basal lamina between these two cell types (77). Astrocytes can attach to capillaries through their end-feet (78, 79). Under normal conditions, capillary endothelial cells can take up blood-borne glucose and lactate by glucose transporter 1 and monocarboxylate transporter (MCT) 1, respectively, which then diffuse through gap junction channels between adjacent endothelial cells. Both glucose and lactate are eventually taken up by the astrocytic end-feet via MCT4 and Cx43 hemichannels, respectively, or released to the extracellular space (80, 81). Thus, glucose and lactate can be transported through astrocytes and their gap junctions with neighboring astrocytes to reach relatively distant areas (82). Furthermore, astrocytes can transfer lactate and glucose to oligodendrocytes through the heterotypic Cx43/Cx47 gap junction channels between them (80). Finally, the lactate in oligodendrocytes can be transported to neuronal axons, inducing axonal degeneration, while the glucose can supply energy for neurons (72, 73).

Taken together, astrocytic Cx43 places astrocytes to a central position in neuron–glial syncytium structures to enroll neurons, oligodendrocytes, microglia, and even capillaries in the CNS into

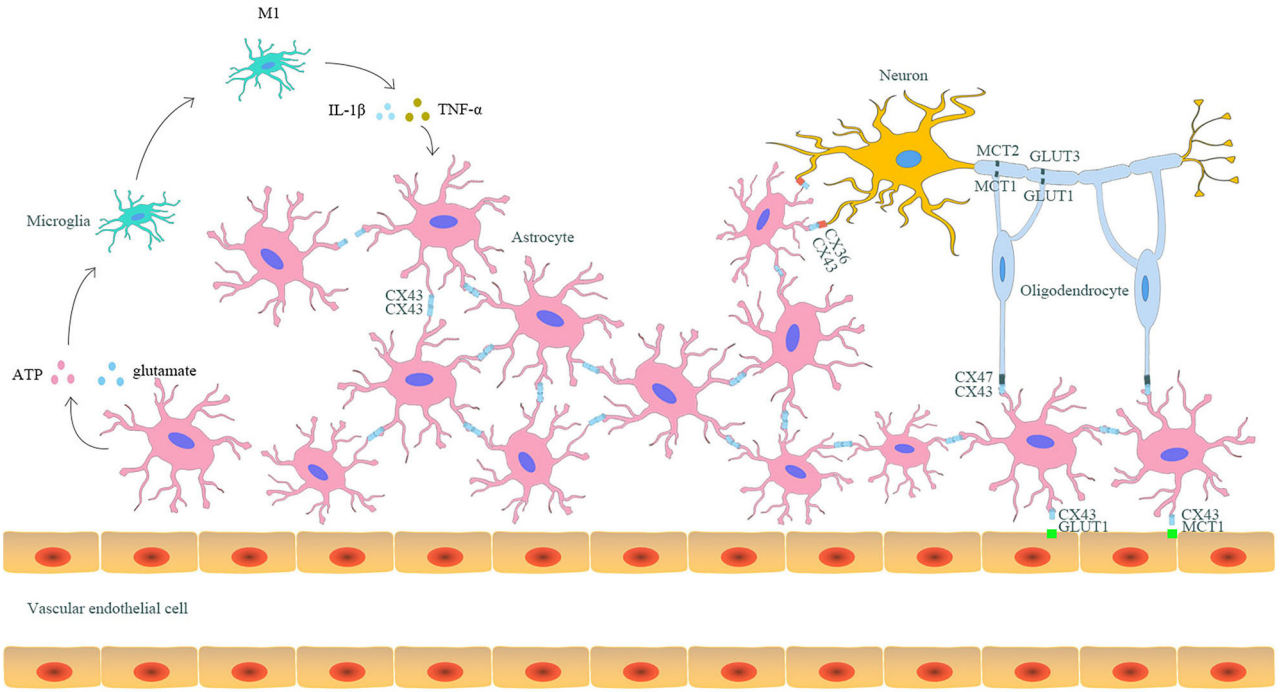

FIGURE 1 | The interaction between astrocytic Cx43 and other parenchymal cells in the CNS. Astrocytes and other parenchyma cells in the CNS form neuro–glial syncytium structures via Cx43/Cx43 gap junctions between astrocytes, Cx43/Cx36 gap junctions between astrocytes and neurons, and Cx43/Cx47 gap junctions between astrocytes and oligodendrocytes. Such structures allow the exchange of metabolites and rapid signal communication, resulting in synergistic response to stimuli. Astrocytic Cx43 is also involved in the capillary-astrocyte-oligodendrocyte-neuron axis and participates in the lactate and glucose transport between capillaries and neurons. Moreover, astrocytes can also indirectly promote the differentiation of microglia to the M1 phenotype through releasing pro-inflammatory mediators via hemichannels. In turn, the differentiated M1 microglia could aggravate the destruction of gap junctions, enhancing injury after ischemic stroke.

this network, facilitating these cells and structures to respond to changes in the CNS micro-environment, thus maintaining the stability of the CNS milieu and regulating the development, differentiation, and function of neurons.

CHANGE IN ASTROCYTIC Cx43 IN ISCHEMIC STROKE

After ischemic stroke, various types of cells in the CNS, including neurons, glial cells, and vascular endothelial cells, sustain different degrees of damage. Astrocytes could be activated and proliferate after ischemic stroke, which is known as reactive astrogliosis (81, 83). Reactive astrogliosis is a type of multistage and pathology-specific reaction, which represents a series of alterations that occur in astrocytes in response to any insult to the CNS (84). At the earlier stage of ischemic stroke, reactive astrocytes can seal the damaged area (85), maintain the balance of the micro-environment, provide nutrients for the neurons, reduce the excitatory toxicity of amino acids, and activate local immune reactions (86). These processes can promote the remodeling of surrounding structural tissues, avoiding secondary damage to neurons (87). However, at the later stage of ischemic stroke, excessive proliferation of reactive astrocytes can change the axon regeneration micro-environment to restrain axonal growth (88), form glial scars, and inhibit the information communication of neurons (89), which can suppress the recovery of nerve function.

Cx43 on astrocytes is an important mediator of CNS ischemic injury, and change in Cx43 expression and distribution has been associated with the outcome of ischemic injury (59). The change in Cx43 expression in the CNS after ischemic stroke remains controversial and depends on ischemia severity, regions, and phase. Cx43 immunoreactivity (Cx43-ir) in the hippocampus and striatum could increase under mild to moderate ischemic conditions (90). However, further studies have indicated that there is an area of reduced Cx43-ir surrounded by a zone of increased Cx43-ir following severe ischemia (66). Another study found that there was a transient downregulation of Cx43 mRNA on day 1 and then upregulation on day 7 after ischemic stroke (91). However, some studies have revealed that there is no significant change in the total amount of Cx43 in *in vitro* and *in vivo* hypoxia models of astrocytes (92). Apart from change in expression, change in Cx43 distribution has also been reported in ischemic stroke. A recent study showed that Cx43 decreased on the astrocytic plasma membrane, whereas it increased in the cytoplasm after ischemic stroke (93). In addition, the reorganization Cx43 gap junctions was also confirmed by immuno-electron microscopy (94).

The C-terminal of astrocytic Cx43 has critical roles in regulating astrocytic functions. Various studies have indicated

that the phosphorylation status of the astrocytic Cx43 C-terminal is an important mediator modulating the gap junction channels and hemichannels after ischemic stroke, thus influencing the functions of astrocytes and neurons (**Figure 2**) (95). It has been reported that the C-terminal of astrocytic Cx43 could be phosphorylated after ischemic stroke via several protein kinases including protein kinase C (96), mitogen-activated protein kinase (MAPK) (97), pp60Src kinase (98), and casein kinase 1δ (99), inducing Cx43 internalization, further contributing to the uncoupling process of astrocytes (100, 101). Interestingly, other studies have found that *in vitro* hypoxia may lead to the dephosphorylation of the C-terminal of astrocytic Cx43, accompanied by the uncoupling of astrocytes (101, 102). This controversy arises because the phosphorylation and dephosphorylation of Cx43 as well as astrocytic uncoupling all occur within a short period after ischemia. Further studies have revealed that astrocytic coupling was significantly reduced by 77% after 15 min of hypoxia, 92% after 30 min of hypoxia, and 97% after 1 h of hypoxia, while subsequent substantial Cx43 dephosphorylation was observed at 30 min or 60 min after hypoxia. In addition, a greater quantity of dephosphorylated Cx43 was observed at 60 min than at 30 min. Moreover, dephosphorylated Cx43 became predominant after 60 min. Subsequent studies have also found that phosphorylated Cx43 remained preponderant from 1 min until 30 min after hypoxia, and the level of preserved astrocytic coupling was 34% after 30 min of hypoxia with addition of phosphatase inhibitors to hypoxic astrocytes (101, 103). These studies indicated that the gap junction uncoupling process of astrocytes lies between the phosphorylation and dephosphorylation of Cx43 and might be the result of the phosphorylation of Cx43 and the cause of Cx43 dephosphorylation on hemichannels. However, the precise phosphorylation and dephosphorylation sites of the astrocytic Cx43 C-terminal remain undetermined. Márquez-Rosado et al. revealed that phosphorylation and dephosphorylation occurred at the serine 325/328/330/365/368 (104) site, while

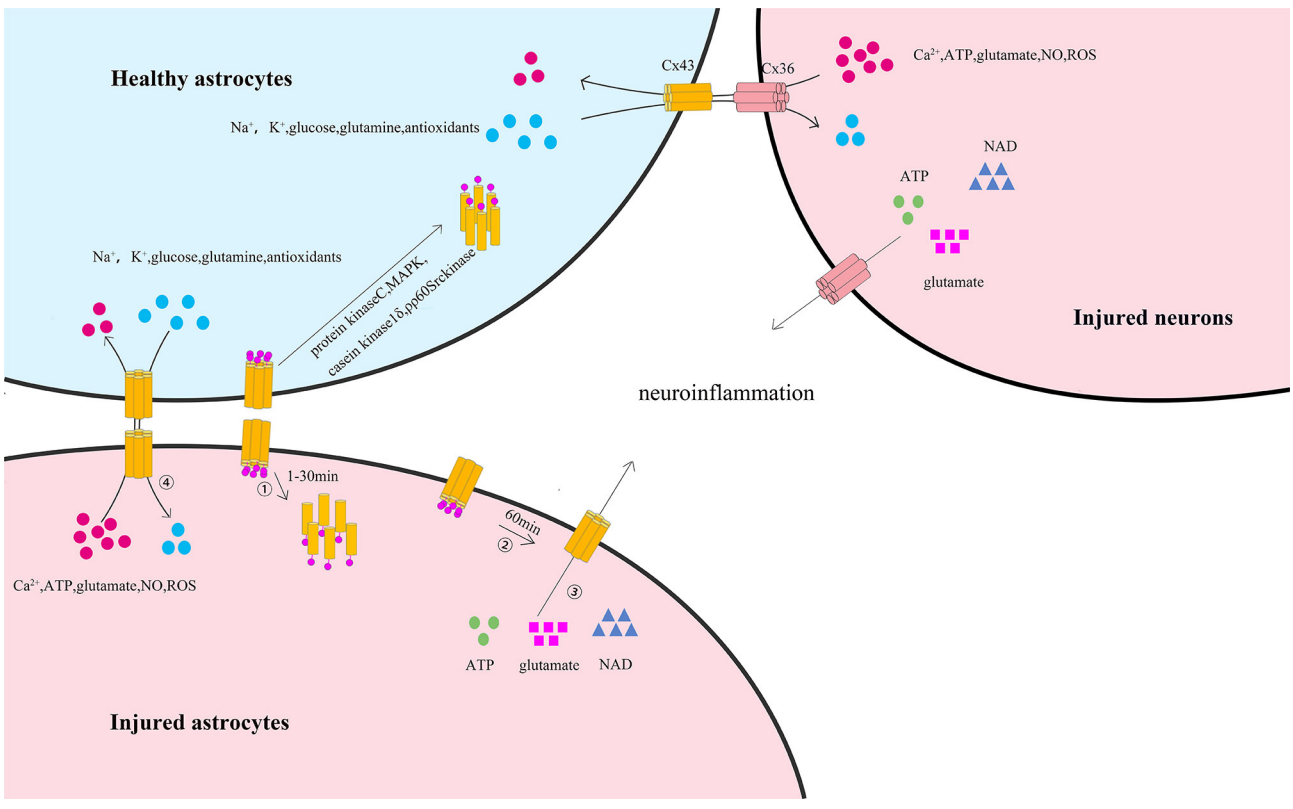

FIGURE 2 | The phosphorylation of astrocytic Cx43 C-terminal and its influence on astrocytes and neurons after ischemic stroke. ① At the early stage of ischemic stroke, astrocytic membrane Cx43, which is involved in the formation of gap junction channels and hemichannels, is phosphorylated at the C-terminal (predominantly from 1 to 30 min) via several protein kinases including protein kinase C, MAPK, pp60Src kinase, and casein kinase 1δ. This process leads to the internalization of membrane Cx43 to the cytoplasm and the degradation of gap junctions. ② At the later stage of ischemic stroke, the remaining astrocytic membrane Cx43 is dephosphorylated (predominantly after 60 min), increasing the permeability of hemichannels. ③ Thus, resulting in the release of ATP, glutamate, and nicotinamide adenine dinucleotide from the cytoplasm of injured astrocytes or injured neurons to the extracellular space, initiating or enhancing neuroinflammation through the remaining gap junctions. ④ In coupled astrocytes, healthy astrocytes could transfer essential ions and metabolites (including Na^+, K^+, glutamine, antioxidants, and glucose) to injured astrocytes by Cx43/Cx43 gap junction channels or injured neurons by Cx43/Cx36 gap junction channels and protect the injured astrocytes. In turn, harmful ions and metabolites (including Ca^{2+}, ATP, glutamate, NO, and ROS) might also be transferred from injured astrocytes or injured neurons to healthy astrocytes, thus spreading the death wave.

Freitas-Andrade et al. demonstrated that phosphorylation and dephosphorylation of serine 255/262/279/282 (105) also occurred. It is unknown whether the phosphorylation and dephosphorylation of astrocytic Cx43 after stroke occurred at the same site and whether the phosphorylation and dephosphorylation of different Cx43 sites might trigger different degrees of Cx43 degradation. Additionally, Cx43 cysteine residues of S-Nitrosylation have been observed in *in vitro* ischemic models induced by nitric oxide (NO) (106). Other *in vitro* studies have found that astrocytic Cx43 was S-Nitrosylated in cultured astrocytes treated with NO for 50 min and that S-Nitrosylated Cx43 could increase the numbers and opening probability of hemichannels (107).

Meanwhile, *in vitro* studies have confirmed that astrocytic Cx43 C-terminal dephosphorylation may increase the opening of hemichannels (108, 109). Previous studies have used astrocytes cultured in *in vitro* ischemia to study the activity of astrocytic Cx43 gap junctions and hemichannels. Among such studies, it has been found that Cx43 gap junctions between dying astrocytes remained functional under ischemic conditions, although Cx43 gap junction coupling decreased (101, 110), signifying that intercellular communication can still occur via astrocytic Cx43 gap junctions under ischemic conditions. Although the opening hemichannels may disrupt the electrochemical and metabolic gradients across the plasma membrane, studies have proven that the remaining gap junctions can protect dying astrocytes to some extent by transferring ions and essential metabolites from healthy astrocytes to dying ones with open hemichannels (107). In contrast, dying astrocytes can also transfer harmful ions and metabolites to neighboring healthy ones with open hemichannels via the remaining gap junctions, which can again cause the death of their neighbors (111). This wave-like spread of the death process is much similar to the extension of infarct regions under ischemic conditions (108, 112, 113).

EFFECTS OF ASTROCYTIC Cx43 IN ISCHEMIC STROKE

Functions of Astrocyte–Astrocyte Coupling

Coupled astrocytes in the astrocytic network share the same fate in ischemic stroke, while the uncoupled ones do not (61, 114). Gap junction communication could positively regulate astrocytic activation and proliferation (115, 116). In permanent right middle cerebral artery occlusion (MCAO) models of $Cx43^{+/-}$ and $Cx43^{+/+}$ mice, $Cx43^{+/-}$ mice showed a significantly larger infarct size but in a smaller area of astrogliosis than did $Cx43^{+/+}$ mice (63), indicating that astrocytic Cx43 gap junctions indeed display a vital role in astrocyte activation and cytotoxic-molecule removal, thus facilitating neuronal survival. Moreover, the astrocytic network formed by gap junctions could also provide energy substrates (glucose and lactate) to neurons (63). Besides, studies with oxygen glucose deprivation (OGD) and MCAO models have found that astrocytic Cx43 is important for astrocytic integrity and stability by activating either astrocytic Cx43 gap junctions or hemichannels (117, 118). Astrocytic Cx43 gap junctions can protect astrocytes by permitting the exit of toxic molecules [including Ca^{2+}, excessive ATP, Glu, NO, and radical oxygen species (ROS)] out of the injured astrocyte and the entrance of neuroprotective metabolites (including Na^{+}, K^{+}, glutamine, antioxidants, glucose) into the astrocytes under ischemic conditions (119, 120). However, if too many toxic molecules are transferred into healthy astrocytes, beyond their bearing load, astrocytic injury might spread to the adjacent astrocytes. Metabolites released by Cx43 hemichannels can also act on the neighboring astrocytes (121). In ischemic stroke, the internalization of astrocytic Cx43 induced by the phosphorylation of the C-terminal might contribute to the uncoupling of astrocytes, thus reducing the mutual support of astrocytes and aggravating their injury (99). In addition, the opening of hemichannels induced by the dephosphorylation of astrocytic Cx43 could promote the release of inflammatory mediators, increasing neuroinflammation after ischemic stroke (108, 109).

Functions of Astrocyte–Neuronal Coupling

Recent studies have found that astrocytes could protect neurons by producing glutathione to exert anti-oxidant effects, reducing inflammatory media, enlarging the gap junctions, regulating energy metabolism, inhibiting apoptosis, uptaking excitatory amino acids, inducing cerebral ischemic tolerance in response to ischemic preconditioning, and other processes (122, 123). Accumulating evidence indicates that the amount of Cx43/Cx36 gap junctions decreases due to Cx43 internalization after ischemic stroke, which reduces the transportation of neurotransmitters and metabolites between astrocytes and neurons (100). However, aerobic metabolism and ATP production declined while toxic ions and molecules, such as Ca^{2+}, glutamate, ROS, and NO, accumulated in damaged neurons after ischemic stroke (124). These toxic metabolites may be released by hemichannels and transmitted from damaged neurons to healthy astrocytes via Cx43/Cx36 gap junctions, thus reducing the load of neurons and activating astrocytes (125). The activated astrocytes could release pro-inflammatory cytokines and chemokines (80), which could in turn lead to changes in the neuronal functions that affect behavior, mood, and cognitive abilities (126). Furthermore, pro-inflammatory cytokines decreased the gap junctions between astrocytes and increased the opening of neuronal Cx36 and astrocytic Cx43 hemichannels, finally causing an increase in the release of ATP, Glu, prostaglandins, and NO (127–129). These molecules are toxic to adjacent cells, which may amplify the inflammation and cause secondary damage to distant cells, leading to tissue excitotoxicity and irreversible brain damage (56, 130).

Functions of Astrocyte–Oligodendrocyte Coupling

Studies have reported that the existence of astrocytic Cx43 is necessary for the functions of oligodendrocytes (71, 131). The loss of astrocytic Cx43, which forms hemichannels and gap junction channels on the astrocytic membrane, could disrupt the Cx43/Cx47 gap junctions, which are harmful for the transmission of ions and nutrients between astrocytes and

oligodendrocytes (132). Studies have found that Cx43 displays multiple metabolic and signaling roles in astrocytes, which can affect oligodendrocytes independently of gap junctions (133). Studies with astrocytic Cx43-deficient mice have revealed that Cx47 was not stabilized and its amount was strongly decreased because of internalization and degradation (131), which lead to the diffusion of Cx47 away from the oligodendrocytic cell membrane, aggravating the post-ischemic inflammatory response and myelin loss of oligodendrocytes (134, 135).

Interaction of Astrocytes and Microglia

Although microglia express Cx36, Cx32, and Cx43 (26, 136), gap junctions between microglia and astrocytes have not been observed. In addition, extracellular ATP released from astrocytes accounting for the opening of hemichannels after ischemic stroke could activate the purine ionotropic receptors on microglia (including $P2X_4R$ and $P2Y_{12}R$), thereby promoting the differentiation of microglia to the M1 subtype (56, 137). Activated microglia could secret TNF-α and IL-1β, which could further aggravate the inflammation (138). Activated microglia could inhibit gap junction communication and downregulate Cx43 expression in astrocytes through the release of TNF-α and IL-1β by mix culturing of astrocytes and activated microglia induced by lipopolysaccharides. Interestingly, Meme et al. found in subsequent experiments that activated microglia treated with lipopolysaccharides were four times more efficient than untreated microglia in inhibiting gap junction communication and Cx43 expression (139). We assume that the reason for this diversity might be that TNF-α and IL-1β are mainly secreted by activated, rather by untreated, microglia. More importantly, TNF-α and IL-1β released by activated microglia could increase astrocytic-hemichannel activity. The increased hemichannels can continuously release ATP, further activating the microglia (38, 128). Thus, abnormally opened astrocytic hemichannels, secondary ATP release, and activated microglia-mediated neuroinflammation may complement each other, leading to a vicious cycle of continuously aggravating post-ischemic tissue damage.

However, the interactions of astrocytes and microglia exert neuroprotective effects under some pathological conditions such as traumatic brain injury (TBI). Microglia in the injury core could be activated after TBI and then release ATP and inflammatory cytokines, and ensuing downregulation of the P2Y1 receptor could then transform the astrocytes to a neuroprotective phenotype (140). Then, reactive astrogliosis would occur in the peri-injured region and accelerate neuroprotective astrocytic scar formation, thus relieving inflammation (141).

Interaction of Astrocytes and Capillaries

The interaction between astrocytes and capillaries is quite meaningful for the energy supply of neurons by astrocytic MCT4 and capillary GLUT. In addition, the lactate in capillaries could also be transported to astrocytes by astrocytic Cx43 hemichannels and capillary MCT1, and further delivered to neuronal axons, inducing axonal degeneration (80, 82). Recent studies have revealed that the opening of astrocytic Cx43 hemichannels could increase after ischemic stroke, contributing to substantial lactate diffusion to astrocytes and neuronal axons (93, 142). Studies have also found that the overexpression of astrocytic MCT4 under hypoxia provides more rapid transmission of glucose, facilitating the energy supply of neurons (82). Furthermore, astrocytes were considered to produce vasoactive factors in response to neuronal activity by their hemichannels, causing rapid and localized changes in cerebral blood flow after ischemic stroke (143, 144). Thus, astrocytes may nourish neurons by controlling the glucose and lactate availability through the regulation of blood flow (81).

THERAPIES AND APPLICATIONS

Nowadays, an increasing number of studies focus on the significance of Cx43 for irreversible injury after ischemic stroke. The influence of the expression and distribution of Cx43 and the block of hemichannels might affect the outcomes of ischemic stroke. Several astrocytic Cx43 targeted reagents or drugs have been considered to be potential therapeutic in cerebral I/R injury (145).

Leptin is a multifunctional hormone secreted by adipocytes and could regulate food intake and energy metabolism (146). Deng et al. found that leptin could also suppress the elevation of Cx43 expression via the ERK/MAPK signaling pathway in MCAO mice *in vivo*, further alleviating cerebral I/R injury. In the same study, the authors also demonstrated that leptin could inhibit Cx43 elevation in SY5Y and U87 cells, thus reducing Glu release by inhibiting the function of Cx43 hemichannels and decreasing cell death in *in vitro* OGD models (147). Carbenoxolone (CBX) is another widely used hemichannel blocker in diverse pathological processes in the brain. It has been proven that CBX can inhibit the release of ATP, further inhibiting or reversing the activation of microglia (148). The latest studies have revealed that CBX can switch the differentiation of activated microglia from M1 to M2, thus providing effective neuroprotection after ischemic stroke (93, 149). Apart from directly blocking hemichannels, a recent study revealed that CBX may influence Cx43 hemichannels and gap junctions by indirect mechanisms such as phosphorylation or internalization of Cx43 subunits (150).

Cx43 mimetic peptides, including Gap 19, Gap 26, Gap 27, peptide 5, and L2 peptide, can also serve as Cx43 hemichannel blockers, further reducing I/R injury (151, 152). In these Cx43 mimetic peptides, Gap26 and Gap27 were found to not only inhibit the opening of hemichannels after ischemic stroke in neonatal rats, but also to modulate gap junction communication due to their poor specificity to Cx43 hemichannels at high concentrations and/or following prolonged exposure (153, 154). Indeed, Gap26 has also been confirmed to protect the heart of rats against myocardial ischemic injury induced by ligation of the left anterior descendent (LAD) by selective inhibition of hemichannels at low concentrations of Gap26 (0.5 μM) (155). Gap27 could also reduce the myocardial infarct size in rat LAD models (156). Interestingly, the function of peptide 5 was shown to be concentration dependent; it could block hemichannels at 5 μM, while blocking gap junctions at 500 μM (157). The L2 sequence is located on the cytoplasmic loop of Cx43, and the

Gap19 sequence is a nine amino acid stretch within the L2 domain (158). The L2 peptide can stabilize the open state of gap junctions while blocking hemichannels (158). Slightly different from the L2 peptide, Gap19 blocks hemichannels while not influencing gap junctions on short exposure (30 min) but slightly inhibits them on longer exposures (24–48 h) (158). In addition, studies with Gap19-treated mice after ischemic stroke induced by MCAO found that Gap19 could attenuate the white matter infarct volume by suppressing the expression of Cx43 and of inflammatory cytokines (TNF-α and IL-1β) as well as inhibiting Toll-like receptor 4 pathway activation; experiments with *in vitro* OGD ischemic stroke models have also confirmed these results (55). Furthermore, treating mouse MCAO models with Gap19 also reduced the myocardial infarct size by blocking Cx43 hemichannels (159). More importantly, Gap19 appeared to be more effective than Gap26/27 in reducing the myocardial infarct volume after heart ischemia (160), possibly because Gap26/27 is less selective to Cx43 gap junctions and hemichannels and it can inhibit channels composed of Cxs other than Cx43 (161).

CONCLUSION

Astrocytes are the central cells in the neuron–glial syncytium, which can combine parenchyma cells in the CNS into a whole to rapidly and synchronously respond to stimuli by forming Cx43/Cx43 gap junctions with other astrocytes, Cx43/Cx36 gap junctions with neurons, Cx43/Cx47 gap junctions with oligodendrocytes, and indirect interactions with microglia. This markedly large network ensures better between-cell communication and increases tolerance to ischemia. The gap junctions between astrocytes and other cells have an important role in substance and metabolite exchange and cell communication. In ischemic stroke, the phosphorylation of astrocytic Cx43 might lead to the uncoupling of gap junctions between astrocytes and other parenchymal cells, reducing the direct communication between these cells. The subsequent dephosphorylation of Cx43 on hemichannels activates the opening of hemichannels, promoting the release of various pro-inflammatory mediators and toxic molecules, such as ATP and Glu. Meanwhile, astrocytic Cx43 could also become S-Nitrosylated after ischemic stroke, increasing the numbers and opening probability of hemichannels. However, the change in astrocytic Cx43 expression and distribution remains controversial and might depend on ischemia duration, region, and severity. Besides, how ischemia induces change in astrocytic Cx43 expression and distribution and the underlying mechanism also need to be delineated.

The destruction of the neuro-glial syncytium structure resulting from the uncoupling of corresponding gap junctions might weaken the mutual support between astrocytes and other cells, and the increase in hemichannel numbers caused by the uncoupling of gap junctions and permeability caused by the dephosphorylation of Cx43 might enhance and spread neuroinflammation and aggravate injury after ischemic stroke. Based on these theories, astrocytic Cx43 might be a potential target for ischemic stroke treatment. However, Cx43 participates both in the formation of gap junctions and of hemichannels. The former is more likely to play a beneficial role, whereas the latter is more likely to be deleterious in ischemic stroke; accordingly, agents that simply target Cx43 might not have the expected therapeutic effect. Therefore, it might be more meaningful to explore agents that can specifically block hemichannels or promote the maintenance of gap junctions. What is more important is that the currently available research that has focused on Cx43-associated agents was conducted using animal and cell models; whether these agents act protectively in patients with ischemia and their safety in the clinic require further exploration.

AUTHOR CONTRIBUTIONS

ZL contributed to the design of the study and wrote the first draft of the manuscript. YH contributed to the design of the study. LQ, YL, and YZ drew the pictures. XW, DM, and JF contributed to the editing of the manuscript. All authors contributed to the article and approved the submitted version.

FUNDING

The work of the authors was supported by the National Science Foundation of China, Grant Nos. 81771257 and 81701158; The science and technology planning project of Jilin Province, Grant No. 20180101161JC and No. 20180520134JH; and National Key Program of China, grant 2017YFC1308401 and 2017YFC0110304.

ACKNOWLEDGMENTS

We would like to thank Editage (www.editage.cn) for English language editing.

REFERENCES

1. Carmichael ST. Rodent models of focal stroke: size, mechanism, and purpose. *NeuroRx.* (2005) 2:396–409. doi: 10.1602/neurorx.2.3.396
2. Lo EH, Dalkara T, Moskowitz MA. Mechanisms, challenges and opportunities in stroke. *Nat Rev Neurosci.* (2003) 4:399–415. doi: 10.1038/nrn1106
3. Lerario MP, Segal AZ. Arterial ischemic stroke prevention and risk factor management. *Prim Care Rep.* (2016) 22. Available online at: https://search.proquest.com/docview/1991845173/abstract/DE6C9BF5333B4807PQ/1?accountid=11718
4. Guzik A, Bushnell C. Stroke epidemiology and risk factor management. *Continuum.* (2017) 23:15–39. doi: 10.1212/CON.0000000000000416
5. Zini A. [Reperfusion therapies in acute ischemic stroke]. *G Ital Cardiol.* (2019) 20:279–88. doi: 10.1186/s12883-017-1007-y
6. Sallustio F, Koch G, Alemseged F, Konda D, Fabiano S, Pampana E, et al. Effect of mechanical thrombectomy alone or in combination with intravenous thrombolysis for acute ischemic stroke. *J Neurol.* (2018) 265:2875–80. doi: 10.1007/s00415-018-9073-7

7. Barres BA. The mystery and magic of glia: a perspective on their roles in health and disease. *Neuron.* (2008) 60:430–40. doi: 10.1016/j.neuron.2008.10.013
8. Xing L, Yang T, Cui S, Chen G. Connexin hemichannels in astrocytes: role in CNS disorders. *Front Mol Neurosci.* (2019) 12:23. doi: 10.3389/fnmol.2019.00023
9. Hirayama Y, Koizumi S. Astrocytes and ischemic tolerance. *Neurosci Res.* (2018) 126:53–9. doi: 10.1016/j.neures.2017.11.013
10. Nedergaard M, Ransom B, Goldman SA. New roles for astrocytes: redefining the functional architecture of the brain. *Trends Neurosci.* (2003) 26:523–30. doi: 10.1016/j.tins.2003.08.008
11. Rash JE, Yasumura T, Dudek FE, Nagy JI. Cell-specific expression of connexins and evidence of restricted gap junctional coupling between glial cells and between neurons. *J Neurosci.* (2001) 21:1983–2000. doi: 10.1523/JNEUROSCI.21-06-01983.2001
12. Ma D, Feng L, Cheng Y, Xin M, You J, Yin X, et al. Astrocytic gap junction inhibition by carbenoxolone enhances the protective effects of ischemic preconditioning following cerebral ischemia. *J Neuroinflammation.* (2018) 15:198. doi: 10.1186/s12974-018-1230-5
13. Davidson JO, Green CR, Nicholson LF, O'Carroll SJ, Fraser M, Bennet L, et al. Connexin hemichannel blockade improves outcomes in a model of fetal ischemia. *Ann Neurol.* (2012) 71:121–32. doi: 10.1002/ana.22654
14. Davidson JO, Green CR, Nicholson LF, Bennet L, Gunn AJ. Deleterious effects of high dose connexin 43 mimetic peptide infusion after cerebral ischaemia in near-term fetal sheep. *Int J Mol Sci.* (2012) 13:6303–19. doi: 10.3390/ijms13056303
15. Davidson JO, Green CR, Bennet L, Nicholson LF, Danesh-Meyer H, O'Carroll SJ, et al. A key role for connexin hemichannels in spreading ischemic brain injury. *Curr Drug Targets.* (2013) 14:36–46. doi: 10.2174/138945013804806479
16. Davidson JO, Drury PP, Green CR, Nicholson LF, Bennet L, Gunn AJ. Connexin hemichannel blockade is neuroprotective after asphyxia in preterm fetal sheep. *PLoS ONE.* (2014) 9:e0096558.doi: 10.1371/journal.pone.0096558
17. Unwin PN, Zampighi G. Structure of the junction between communicating cells. *Nature.* (1980) 283:545–9. doi: 10.1038/283545a0
18. Dermietzel R, Traub O, Hwang TK, Beyer E, Bennett MV, Spray DC, et al. Differential expression of three gap junction proteins in developing and mature brain tissues. *Proc Natl Acad Sci USA.* (1989) 86:10148–52. doi: 10.1073/pnas.86.24.10148
19. Nagy JI, Ionescu AV, Lynn BD, Rash JE. Coupling of astrocyte connexins Cx26, Cx30, Cx43 to oligodendrocyte Cx29, Cx32, Cx47: Implications from normal and connexin32 knockout mice. *Glia.* (2003) 44:205–18. doi: 10.1002/glia.10278
20. Condorelli DF, Belluardo N, Trovato-Salinaro A, Mudo G. Expression of Cx36 in mammalian neurons. *Brain Res Brain Res Rev.* (2000) 32:72–85. doi: 10.1016/S0165-0173(99)00068-5
21. Chapman RJ, Lall VK, Maxeiner S, Willecke K, Deuchars J, King AE. Localization of neurones expressing the gap junction protein connexin45 within the adult spinal dorsal horn: a study using Cx45-eGFP reporter mice. *Brain Struct Func.* (2013) 218:751–65. doi: 10.1007/s00429-012-0426-1
22. Bruzzone R, Hormuzdi SG, Barbe MT, Herb A, Monyer H. Pannexins, a family of gap junction proteins expressed in brain. *Proc Natl Acad Sci USA.* (2003) 100:13644–9. doi: 10.1073/pnas.2233464100
23. Dere E, Zheng-Fischhofer Q, Viggiano D, Gironi Carnevale UA, Ruocco LA, Zlomuzica A, et al. Connexin31.1 deficiency in the mouse impairs object memory and modulates open-field exploration, acetylcholine esterase levels in the striatum, and cAMP response element-binding protein levels in the striatum and piriform cortex. *Neuroscience.* (2008) 153:396–405. doi: 10.1016/j.neuroscience.2008.01.077
24. Scherer SS, Deschenes SM, Xu YT, Grinspan JB, Fischbeck KH, Paul DL. Connexin32 is a myelin-related protein in the PNS and CNS. *J Neurosci.* (1995) 15:8281–94. doi: 10.1523/JNEUROSCI.15-12-08281.1995
25. Odermatt B, Wellershaus K, Wallraff A, Seifert G, Degen J, Euwens C, et al. Connexin 47 (Cx47)-deficient mice with enhanced green fluorescent protein reporter gene reveal predominant oligodendrocytic expression of Cx47 and display vacuolized myelin in the CNS. *J Neurosci.* (2003) 23:4549–59. doi: 10.1523/JNEUROSCI.23-11-04549.2003
26. Eugenin EA, Eckardt D, Theis M, Willecke K, Bennett MV, Saez JC. Microglia at brain stab wounds express connexin 43 and *in vitro* form functional gap junctions after treatment with interferon-gamma and tumor necrosis factor-alpha. *Proc Natl Acad Sci USA.* (2001) 98:4190–5. doi: 10.1073/pnas.051634298
27. Orellana JA, Moraga-Amaro R, Diaz-Galarce R, Rojas S, Maturana CJ, Stehberg J, et al. Restraint stress increases hemichannel activity in hippocampal glial cells and neurons. *Front Cell Neurosci.* (2015) 9:102. doi: 10.3389/fncel.2015.00102
28. Dobrenis K, Chang HY, Pina-Benabou MH, Woodroffe A, Lee SC, Rozental R, et al. Human and mouse microglia express connexin36, and functional gap junctions are formed between rodent microglia and neurons. *J Neurosci Res.* (2005) 82:306–15. doi: 10.1002/jnr.20650
29. Errede M, Benagiano V, Girolamo F, Flace P, Bertossi M, Roncali L, et al. Differential expression of connexin43 in foetal, adult and tumour-associated human brain endothelial cells. *Histochem J.* (2002) 34:265–71. doi: 10.1023/a:1023344106815
30. Little TL, Beyer EC, Duling BR. Connexin 43 and connexin 40 gap junctional proteins are present in arteriolar smooth muscle and endothelium *in vivo*. *Am J Physiol.* (1995) 268:H729–39. doi: 10.1152/ajpheart.1995.268.2.H729
31. Goodenough DA, Paul DL. Gap junctions. *Cold Spring Harbor Perspec Biol.* (2009) 1:a002576. doi: 10.1101/cshperspect.a002576
32. Rash JE, Yasumura T, Davidson KG, Furman CS, Dudek FE, Nagy JI. Identification of cells expressing Cx43, Cx30, Cx26, Cx32 and Cx36 in gap junctions of rat brain and spinal cord. *Cell Commun Adhes.* (2001) 8:315–20. doi: 10.3109/15419060109080745
33. Theis M, Giaume C. Connexin-based intercellular communication and astrocyte heterogeneity. *Brain Res.* (2012) 1487:88–98. doi: 10.1016/j.brainres.2012.06.045
34. Trosko JE. The gap junction as a "biological rosetta stone": implications of evolution, stem cells to homeostatic regulation of health and disease in the barker hypothesis. *J Cell Commun Signal.* (2011) 5:53–66. doi: 10.1007/s12079-010-0108-9
35. Ek Vitorin JF, Pontifex TK, Burt JM. Determinants of Cx43 channel gating and permeation: the amino terminus. *Biophys J.* (2016) 110:127–40. doi: 10.1016/j.bpj.2015.10.054
36. Beyer EC, Paul DL, Goodenough DA. Connexin family of gap junction proteins. *J Membr Biol.* (1990) 116:187–94. doi: 10.1007/BF01868459
37. Leithe E, Mesnil M, Aasen T. The connexin 43 C-terminus: a tail of many tales. *Biochim Biophys Acta Biomembr.* (2018) 1860:48–64. doi: 10.1016/j.bbamem.2017.05.008
38. Faustmann PM, Haase CG, Romberg S, Hinkerohe D, Szlachta D, Smikalla D, et al. Microglia activation influences dye coupling and Cx43 expression of the astrocytic network. *Glia.* (2003) 42:101–8. doi: 10.1002/glia.10141
39. Giaume C, Leybaert L, Naus CC, Saez JC. Connexin and pannexin hemichannels in brain glial cells: properties, pharmacology, and roles. *Front Pharmacol.* (2013) 4:88. doi: 10.3389/fphar.2013.00088
40. Orthmann-Murphy JL, Freidin M, Fischer E, Scherer SS, Abrams CK. Two distinct heterotypic channels mediate gap junction coupling between astrocyte and oligodendrocyte connexins. *J Neurosci.* (2007) 27:13949–57. doi: 10.1523/JNEUROSCI.3395-07.2007
41. Contreras JE, Saez JC, Bukauskas FF, Bennett MV. Gating and regulation of connexin 43 (Cx43) hemichannels. *Proc Natl Acad Sci USA.* (2003) 100:11388–93. doi: 10.1073/pnas.1434298100
42. Li H, Liu TF, Lazrak A, Peracchia C, Goldberg GS, Lampe PD, et al. Properties and regulation of gap junctional hemichannels in the plasma membranes of cultured cells. *J Cell Biol.* (1996) 134:1019–30. doi: 10.1083/jcb.134.4.1019
43. Ebihara L, Liu X, Pal JD. Effect of external magnesium and calcium on human connexin46 hemichannels. *Biophys J.* (2003) 84:277–86. doi: 10.1016/S0006-3495(03)74848-6
44. Valiunas V. Biophysical properties of connexin-45 gap junction hemichannels studied in vertebrate cells. *J Gen Physiol.* (2002) 119:147–64. doi: 10.1085/jgp.119.2.147
45. John SA, Kondo R, Wang SY, Goldhaber JI, Weiss JN. Connexin-43 hemichannels opened by metabolic inhibition. *J Biol Chem.* (1999) 274:236–40. doi: 10.1074/jbc.274.1.236

46. Chever O, Lee CY, Rouach N. Astroglial connexin43 hemichannels tune basal excitatory synaptic transmission. *J Neurosci.* (2014) 34:11228–32. doi: 10.1523/JNEUROSCI.0015-14.2014
47. Ambrosi C, Gassmann O, Pranskevich JN, Boassa D, Smock A, Wang JJ, et al. Pannexin1 and pannexin2 channels show quaternary similarities to connexons and different oligomerization numbers from each other. *J Biol Chem.* (2010) 285:24420–31. doi: 10.1074/jbc.M110.115444
48. Spray DC, Ye ZC, Ransom BR. Functional connexin "hemichannels": a critical appraisal. *GLIA*. (2006) 54:758–73. doi: 10.1002/glia.20429
49. Saez JC, Berthoud VM, Branes MC, Martinez AD, Beyer EC. Plasma membrane channels formed by connexins: their regulation and functions. *Physiol Rev.* (2003) 83:1359–400. doi: 10.1152/physrev.00007.2003
50. Montero TD, Orellana JA. Hemichannels: new pathways for gliotransmitter release. *Neuroscience.* (2015) 286:45–59. doi: 10.1016/j.neuroscience.2014.11.048
51. Meunier C, Wang N, Yi C, Dallerac G, Ezan P, Koulakoff A, et al. Contribution of astroglial Cx43 hemichannels to the modulation of glutamatergic currents by D-serine in the mouse prefrontal cortex. *J Neurosci.* (2017) 37:9064–75. doi: 10.1523/JNEUROSCI.2204-16.2017
52. Stehberg J, Moraga-Amaro R, Salazar C, Becerra A, Echeverria C, Orellana JA, et al. Release of gliotransmitters through astroglial connexin 43 hemichannels is necessary for fear memory consolidation in the basolateral amygdala. *FASEB J.* (2012) 26:3649–57. doi: 10.1096/fj.11-198416
53. Abudara V, Retamal MA, Del Rio R, Orellana JA. Synaptic functions of hemichannels and pannexons: a double-edged sword. *Front Mol Neurosci.* (2018) 11:435. doi: 10.3389/fnmol.2018.00435
54. Beyer EC, Berthoud VM. Gap junction gene and protein families: connexins, innexins, and pannexins. *Biochim Biophys Acta Biomembr.* (2018) 1860:5–8. doi: 10.1016/j.bbamem.2017.05.016
55. Chen Y, Wang L, Zhang L, Chen B, Yang L, Li X, et al. Inhibition of connexin 43 hemichannels alleviates cerebral ischemia/reperfusion injury via the TLR4 signaling pathway. *Front Cell Neurosci.* (2018) 12:372. doi: 10.3389/fncel.2018.00372
56. Kim Y, Davidson JO, Green CR, Nicholson LFB, O'Carroll SJ, Zhang J. Connexins and pannexins in cerebral ischemia. *Biochim Biophys Acta Biomembr.* (2018) 1860:224–36. doi: 10.1016/j.bbamem.2017.03.018
57. Scott CA, Tattersall D, O'Toole EA, Kelsell DP. Connexins in epidermal homeostasis and skin disease. *Biochim Biophys Acta.* (2012) 1818:1952–61. doi: 10.1016/j.bbamem.2011.09.004
58. Duffy HS, Delmar M, Spray DC. Formation of the gap junction nexus: binding partners for connexins. *J Physiol.* (2002) 96:243–9. doi: 10.1016/S0928-4257(02)00012-8
59. Meier C, Rosenkranz K. Cx43 expression and function in the nervous system-implications for stem cell mediated regeneration. *Front Physiol.* (2014) 5:106. doi: 10.3389/fphys.2014.00106
60. Lapato AS, Tiwari-Woodruff SK. Connexins and pannexins: at the junction of neuro-glial homeostasis & disease. *J Neurosci Res.* (2018) 96:31–44. doi: 10.1002/jnr.24088
61. Cronin M, Anderson PN, Cook JE, Green CR, Becker DL. Blocking connexin43 expression reduces inflammation and improves functional recovery after spinal cord injury. *Mol Cell Neurosci.* (2008) 39:152–60. doi: 10.1016/j.mcn.2008.06.005
62. Wallraff A, Kohling R, Heinemann U, Theis M, Willecke K, Steinhauser C. The impact of astrocytic gap junctional coupling on potassium buffering in the hippocampus. *J Neurosci.* (2006) 26:5438–47. doi: 10.1523/JNEUROSCI.0037-06.2006
63. Pereda AE. Electrical synapses and their functional interactions with chemical synapses. *Nat Rev Neurosci.* (2014) 15:250–63. doi: 10.1038/nrn3708
64. Altevogt BM, Paul DL. Four classes of intercellular channels between glial cells in the CNS. *J Neurosci.* (2004) 24:4313–23. doi: 10.1523/JNEUROSCI.3303-03.2004
65. Allen NJ, Eroglu C. Cell biology of astrocyte-synapse interactions. *Neuron.* (2017) 96:697–708. doi: 10.1016/j.neuron.2017.09.056
66. Chew SS, Johnson CS, Green CR, Danesh-Meyer HV. Role of connexin43 in central nervous system injury. *Exp Neurol.* (2010) 225:250–61. doi: 10.1016/j.expneurol.2010.07.014
67. Sohl G, Maxeiner S, Willecke K. Expression and functions of neuronal gap junctions. *Nat Rev Neurosci.* (2005) 6:191–200. doi: 10.1038/nrn1627
68. Spray DC, Hanstein R, Lopez-Quintero SV, Stout RF, Jr, Suadicani SO, et al. Gap junctions and bystander effects: good samaritans and executioners. Wiley interdisciplinary reviews. *Membrane Transport Signal.* (2013) 2:1–15. doi: 10.1002/wmts.72
69. Massa PT, Mugnaini E. Cell junctions and intramembrane particles of astrocytes and oligodendrocytes: a freeze-fracture study. *Neuroscience.* (1982) 7:523–38. doi: 10.1016/0306-4522(82)90285-8
70. Kay CW, Ursu D, Sher E, King AE. The role of Cx36 and Cx43 in 4-aminopyridine-induced rhythmic activity in the spinal nociceptive dorsal horn: an electrophysiological study *in vitro*. *Physiol Rep.* (2016) 4:e12852.doi: 10.14814/phy2.12852
71. Papaneophytou C, Georgiou E, Kleopa KA. The role of oligodendrocyte gap junctions in neuroinflammation. *Channels.* (2019) 13:247–63. doi: 10.1080/19336950.2019.1631107
72. Rinholm JE, Vervaeke K, Tadross MR, Tkachuk AN, Kopek BG, Brown TA, et al. Movement and structure of mitochondria in oligodendrocytes and their myelin sheaths. *Glia.* (2016) 64:810–25. doi: 10.1002/glia.22965
73. Rinholm JE, Hamilton NB, Kessaris N, Richardson WD, Bergersen LH, Attwell D. Regulation of oligodendrocyte development and myelination by glucose and lactate. *J Neurosci.* (2011) 31:538–48. doi: 10.1523/JNEUROSCI.3516-10.2011
74. Parys B, Cote A, Gallo V, De Koninck P, Sik A. Intercellular calcium signaling between astrocytes and oligodendrocytes via gap junctions in culture. *Neuroscience.* (2010) 167:1032–43. doi: 10.1016/j.neuroscience.2010.03.004
75. Zahs KR. Heterotypic coupling between glial cells of the mammalian central nervous system. Glia. (1998) 24:85–96. doi: 10.1002/(SICI)1098-1136(199809)24:1<85::AID-GLIA9>3.0.CO;2-#
76. Menichella DM, Majdan M, Awatramani R, Goodenough DA, Sirkowski E, Scherer SS, et al. Genetic and physiological evidence that oligodendrocyte gap junctions contribute to spatial buffering of potassium released during neuronal activity. *J Neurosci.* (2006) 26:10984–91. doi: 10.1523/JNEUROSCI.0304-06.2006
77. Braet K, Paemeleire K, D'Herde K, Sanderson MJ, Leybaert L. Astrocyte-endothelial cell calcium signals conveyed by two signalling pathways. *Eur J Neurosci.* (2001) 13:79–91. doi: 10.1046/j.1460-9568.2001.01372.x
78. Newman EA. High potassium conductance in astrocyte endfeet. *Science.* (1986) 233:453–4. doi: 10.1126/science.3726539
79. Miyata M, Mandai K, Maruo T, Sato J, Shiotani H, Kaito A, et al. Localization of nectin-2delta at perivascular astrocytic endfoot processes and degeneration of astrocytes and neurons in nectin-2 knockout mouse brain. *Brain Res.* (2016) 1649:90–101. doi: 10.1016/j.brainres.2016.08.023
80. Orellana JA, Saez PJ, Shoji KF, Schalper KA, Palacios-Prado N, Velarde V, et al. Modulation of brain hemichannels and gap junction channels by pro-inflammatory agents and their possible role in neurodegeneration. *Antioxid Redox Sign.* (2009) 11:369–99. doi: 10.1089/ars.2008.2130
81. Pellerin L, Bouzier-Sore AK, Aubert A, Serres S, Merle M, Costalat R, et al. Activity-dependent regulation of energy metabolism by astrocytes: an update. *Glia.* (2007) 55:1251–62. doi: 10.1002/glia.20528
82. Abe T, Takahashi S, Suzuki N. Oxidative metabolism in cultured rat astroglia: effects of reducing the glucose concentration in the culture medium and of D-aspartate or potassium stimulation. *J Cereb Blood Flow Metab.* (2006) 26:153–60. doi: 10.1038/sj.jcbfm.9600175
83. Seifert G, Schilling K, Steinhauser C. Astrocyte dysfunction in neurological disorders: a molecular perspective. *Nat Rev Neurosci.* (2006) 7:194–206. doi: 10.1038/nrn1870
84. Jha MK, Lee WH, Suk K. Functional polarization of neuroglia: implications in neuroinflammation and neurological disorders. *Biochem Pharmacol.* (2016) 103:1–16. doi: 10.1016/j.bcp.2015.11.003
85. Pekny M, Nilsson M. Astrocyte activation and reactive gliosis. *Glia.* (2005) 50:427–34. doi: 10.1002/glia.20207
86. Sofroniew MV. Reactive astrocytes in neural repair and protection. *Neuroscientist.* (2005) 11:400–7. doi: 10.1177/1073858405278321
87. Bush TG, Puvanachandra N, Horner CH, Polito A, Ostenfeld T, Svendsen CN, et al. Leukocyte infiltration, neuronal degeneration, and neurite outgrowth after ablation of scar-forming, reactive

astrocytes in adult transgenic mice. *Neuron.* (1999) 23:297–308. doi: 10.1016/S0896-6273(00)80781-3
88. Faulkner JR, Woo MJ, Sislak MD, Safroniew MV. Genetically targeted astrocyte scar ablation results in modest local growth of axons after spinal cord injury. *J Neurotraum.* (2004) 21:1340. Available online at: http://apps.webofknowledge.com/Search.do?product=UA&SID=7DVluIHdjOnkbar3NOy&search_mode=GeneralSearch&prID=08c6d970-23a1-4778-b550-a8380bec950c
89. Ikeda H, Murase K. Glial nitric oxide-mediated long-term presynaptic facilitation revealed by optical imaging in rat spinal dorsal horn. *J Neurosci.* (2004) 24:9888–96. doi: 10.1523/JNEUROSCI.2608-04.2004
90. Rami A, Volkmann T, Winckler J. Effective reduction of neuronal death by inhibiting gap junctional intercellular communication in a rodent model of global transient cerebral ischemia. *Exp Neurol.* (2001) 170:297–304. doi: 10.1006/exnr.2001.7712
91. Haupt C, Witte OW, Frahm C. Temporal profile of connexin 43 expression after photothrombotic lesion in rat brain. *Neuroscience.* (2007) 144:562–70. doi: 10.1016/j.neuroscience.2006.09.054
92. Haupt C, Witte OW, Frahm C. Up-regulation of connexin43 in the glial scar following photothrombotic ischemic injury. *Mol Cell Neurosci.* (2007) 35:89–99. doi: 10.1016/j.mcn.2007.02.005
93. Yin X, Feng L, Ma D, Yin P, Wang X, Hou S, et al. Roles of astrocytic connexin-43, hemichannels, and gap junctions in oxygen-glucose deprivation/reperfusion injury induced neuroinflammation and the possible regulatory mechanisms of salvianolic acid B and carbenoxolone. *J Neuroinflam.* (2018) 15:97. doi: 10.1186/s12974-018-1127-3
94. Hossain MZ, Peeling J, Sutherland GR, Hertzberg EL, Nagy JI. Ischemia-induced cellular redistribution of the astrocytic gap junctional protein connexin43 in rat brain. *Brain Res.* (1994) 652:311–22. doi: 10.1016/0006-8993(94)90242-9
95. Sosinsky GE, Nicholson BJ. Structural organization of gap junction channels. *Biochim Biophys Acta.* (2005) 1711:99–125. doi: 10.1016/j.bbamem.2005.04.001
96. Lampe PD, TenBroek EM, Burt JM, Kurata WE, Johnson RG, Lau AF. Phosphorylation of connexin43 on serine368 by protein kinase C regulates gap junctional communication. *J Cell Biol.* (2000) 149:1503–12. doi: 10.1083/jcb.149.7.1503
97. Warn-Cramer BJ, Lampe PD, Kurata WE, Kanemitsu MY, Loo LW, Eckhart W, et al. Characterization of the mitogen-activated protein kinase phosphorylation sites on the connexin-43 gap junction protein. *J Biol Chem.* (1996) 271:3779–86. doi: 10.1074/jbc.271.7.3779
98. Loo LW, Berestecky JM, Kanemitsu MY, Lau AF. pp60src-mediated phosphorylation of connexin 43, a gap junction protein. *J Biol Chem.* (1995) 270:12751–61. doi: 10.1074/jbc.270.21.12751
99. Cooper CD, Lampe PD. Casein kinase 1 regulates connexin-43 gap junction assembly. *J Biol Chem.* (2002) 277:44962–8. doi: 10.1074/jbc.M209427200
100. Solan JL, Lampe PD. Connexin43 phosphorylation: structural changes and biological effects. *Biochem J.* (2009) 419:261–72. doi: 10.1042/BJ20082319
101. Li WE, Nagy JI. Connexin43 phosphorylation state and intercellular communication in cultured astrocytes following hypoxia and protein phosphatase inhibition. *Eur J Neurosci.* (2000) 12:2644–50. doi: 10.1046/j.1460-9568.2000.00162.x
102. Beckmann A, Grissmer A, Wolf S, Recktenwald J, Meier C. Oxygen-glucose deprivation in mouse astrocytes is associated with ultrastructural changes in connexin 43 gap junctions. *Neuroscience.* (2019) 397:67–79. doi: 10.1016/j.neuroscience.2018.11.043
103. Moreno AP, Saez JC, Fishman GI, Spray DC. Human connexin43 gap junction channels. Regulation of unitary conductances by phosphorylation. *Circ Res.* (1994) 74:1050–7. doi: 10.1161/01.RES.74.6.1050
104. Marquez-Rosado L, Solan JL, Dunn CA, Norris RP, Lampe PD. Connexin43 phosphorylation in brain, cardiac, endothelial and epithelial tissues. *Biochim Biophys Acta.* (2012) 1818:1985–92. doi: 10.1016/j.bbamem.2011.07.028
105. Freitas-Andrade M, Wang N, Bechberger JF, De Bock M, Lampe PD, Leybaert L, et al. Targeting MAPK phosphorylation of connexin43 provides neuroprotection in stroke. *J Exp Med.* (2019) 216:916–35. doi: 10.1084/jem.20171452
106. Narne P, Pandey V, Phanithi PB. Role of nitric oxide and hydrogen sulfide in ischemic stroke and the emergent epigenetic underpinnings. *Mol Neurobiol.* (2019) 56:1749. doi: 10.1007/s12035-018-1141-6
107. Retamal MA, Cortes CJ, Reuss L, Bennett MVL, Saez JC. S-nitrosylation and permeation through connexin 43 hemichannels in astrocytes: induction by oxidant stress and reversal by reducing agents. *P Natl Acad Sci USA.* (2006) 103:4475–80. doi: 10.1073/pnas.0511118103
108. Contreras JE, Sanchez HA, Eugenin EA, Speidel D, Theis M, Willecke K, et al. Metabolic inhibition induces opening of unapposed connexin 43 gap junction hemichannels and reduces gap junctional communication in cortical astrocytes in culture. *Proc Natl Acad Sci USA.* (2002) 99:495–500. doi: 10.1073/pnas.012589799
109. Ek-Vitorin JF, Pontifex TK, Burt JM. Cx43 channel gating and permeation: multiple phosphorylation-dependent roles of the carboxyl terminus. *Int J Mol Sci.* (2018) 19:1659. doi: 10.3390/ijms19061659
110. Cotrina ML, Kang J, Lin JH, Bueno E, Hansen TW, He L, et al. Astrocytic gap junctions remain open during ischemic conditions. *J Neurosci.* (1998) 18:2520–37. doi: 10.1523/JNEUROSCI.18-07-02520.1998
111. Contreras JE, Sanchez HA, Veliz LP, Bukauskas FF, Bennett MV, Saez JC. Role of connexin-based gap junction channels and hemichannels in ischemia-induced cell death in nervous tissue. *Brain Res Brain Res Rev.* (2004) 47:290–303. doi: 10.1016/j.brainresrev.2004.08.002
112. Rawanduzy A, Hansen A, Hansen TW, Nedergaard M. Effective reduction of infarct volume by gap junction blockade in a rodent model of stroke. *J Neurosurg.* (1997) 87:916–20. doi: 10.3171/jns.1997.87.6.0916
113. Nodin C, Nilsson M, Blomstrand F. Gap junction blockage limits intercellular spreading of astrocytic apoptosis induced by metabolic depression. *J Neurochem.* (2005) 94:1111–23. doi: 10.1111/j.1471-4159.2005.03241.x
114. Hansson E, Muyderman H, Leonova J, Allansson L, Sinclair J, Blomstrand F, et al. Astroglia and glutamate in physiology and pathology: aspects on glutamate transport, glutamate-induced cell swelling and gap-junction communication. *Neurochem Int.* (2000) 37:317–29. doi: 10.1016/S0197-0186(00)00033-4
115. Asklund T, Appelskog IB, Ammerpohl O, Langmoen IA, Dilber MS, Aints A, et al. Gap junction-mediated bystander effect in primary cultures of human malignant gliomas with recombinant expression of the HSVtk gene. *Exp Cell Res.* (2003) 284:185–95. doi: 10.1016/S0014-48270200052-6
116. Giaume C, Tabernero A, Medina JM. Metabolic trafficking through astrocytic gap junctions. *Glia.* (1997) 21:114–23. doi: 10.1002/SICI1098-113619970921:1114::AID-GLIA133.0.CO;2-V
117. Freitas-Andrade M, Naus CC. Astrocytes in neuroprotection and neurodegeneration: the role of connexin43 and pannexin1. *Neuroscience.* (2016) 323:207–21. doi: 10.1016/j.neuroscience.2015.04.035
118. Wu LY, Yu XL, Feng LY. Connexin 43 stabilizes astrocytes in a stroke-like milieu to facilitate neuronal recovery. *Acta Pharmacol Sinica.* (2015) 36:928–38. doi: 10.1038/aps.2015.39
119. Walz W, Hertz L. Functional interactions between neurons and astrocytes. II. Potassium homeostasis at the cellular level. *Prog Neurobiol.* (1983) 20:133–83. doi: 10.1016/0301-0082(83)90013-8
120. Goldberg GS, Lampe PD, Nicholson BJ. Selective transfer of endogenous metabolites through gap junctions composed of different connexins. *Nat Cell Biol.* (1999) 1:457–9. doi: 10.1038/15693
121. Kang J, Kang N, Lovatt D, Torres A, Zhao Z, Lin J, et al. Connexin 43 hemichannels are permeable to ATP. *J Neurosci.* (2008) 28:4702–11. doi: 10.1523/JNEUROSCI.5048-07.2008
122. Barber PA, Demchuk AM, Hirt L, Buchan AM. Biochemistry of ischemic stroke. *Adv Neurol.* (2003) 92:151–64.
123. Aschner M. Astrocytes as mediators of immune inflammatory responses in the CNS. *Neurotoxicology*. (1998) 19:269–81.
124. Alvarez-Maubecin V, Garcia-Hernandez F, Williams JT, Van Bockstaele EJ. Functional coupling between neurons and glia. *J Neurosci.* (2000) 20:4091–8. doi: 10.1523/JNEUROSCI.20-11-04091.2000
125. Takeuchi H, Suzumura A. Gap junctions and hemichannels composed of connexins: potential therapeutic targets for neurodegenerative diseases. *Front Cell Neurosci.* (2014) 8:189. doi: 10.3389/fncel.2014.00189
126. Sofroniew MV. Multiple roles for astrocytes as effectors of cytokines and inflammatory mediators. *Neuroscientist*. (2014) 20:160–72. doi: 10.1177/1073858413504466
127. Avila-Munoz E, Arias C. When astrocytes become harmful: functional and inflammatory responses that contribute to alzheimer's disease. *Ageing Res Rev.* (2014) 18:29–40. doi: 10.1016/j.arr.2014.07.004

128. Retamal MA, Froger N, Palacios-Prado N, Ezan P, Saez PJ, Saez JC, et al. Cx43 hemichannels and gap junction channels in astrocytes are regulated oppositely by proinflammatory cytokines released from activated microglia. *J Neurosci.* (2007) 27:13781–92. doi: 10.1523/JNEUROSCI.2042-07.2007
129. Orellana JA, Froger N, Ezan P, Jiang JX, Bennett MV, Naus CC, et al. ATP and glutamate released via astroglial connexin 43 hemichannels mediate neuronal death through activation of pannexin 1 hemichannels. *J Neurochem.* (2011) 118:826–40. doi: 10.1111/j.1471-4159.2011.07210.x
130. Castellano P, Nwagbo C, Martinez LR, Eugenin EA. Methamphetamine compromises gap junctional communication in astrocytes and neurons. *J Neurochem.* (2016) 137:561–75. doi: 10.1111/jnc.13603
131. May D, Tress O, Seifert G, Willecke K. Connexin47 protein phosphorylation and stability in oligodendrocytes depend on expression of Connexin43 protein in astrocytes. *J Neurosci.* (2013) 33:7985–96. doi: 10.1523/JNEUROSCI.5874-12.2013
132. Basu R, Bose A, Thomas D, Das Sarma J. Microtubule-assisted altered trafficking of astrocytic gap junction protein connexin 43 is associated with depletion of connexin 47 during mouse hepatitis virus infection. *J Biol Chem.* (2017) 292:14747–63. doi: 10.1074/jbc.M117.786491
133. Cotrina ML, Lin JH, Alves-Rodrigues A, Liu S, Li J, Azmi-Ghadimi H, et al. Connexins regulate calcium signaling by controlling ATP release. *Proc Natl Acad Sci USA.* (1998) 95:15735–40. doi: 10.1073/pnas.95.26.15735
134. Papaneophytou CP, Georgiou E, Karaiskos C, Sargiannidou I, Markoullis K, Freidin MM, et al. Regulatory role of oligodendrocyte gap junctions in inflammatory demyelination. *Glia.* (2018) 66:2589–603. doi: 10.1002/glia.23513
135. Giepmans BN. Gap junctions and connexin-interacting proteins. *Cardiovasc Res.* (2004) 62:233–45. doi: 10.1016/j.cardiores.2003.12.009
136. Kielian T. Glial connexins and gap junctions in CNS inflammation and disease. Journal of neurochemistry. (2008) 106:1000–16. doi: 10.1111/j.1471-4159.2008.05405.x
137. Wixey JA, Reinebrant HE, Carty ML, Buller KM. Delayed P2X4R expression after hypoxia-ischemia is associated with microglia in the immature rat brain. *J Neuroimmunol.* (2009) 212:35–43. doi: 10.1016/j.jneuroim.2009.04.016
138. Zhou JJ, Cheng C, Qiu Z, Zhou WH, Cheng GQ. Decreased connexin 43 in astrocytes inhibits the neuroinflammatory reaction in an acute mouse model of neonatal sepsis. *Neurosci Bull.* (2015) 31:763–8. doi: 10.1007/s12264-015-1561-5
139. Meme W, Calvo CF, Froger N, Ezan P, Amigou E, Koulakoff A, et al. Proinflammatory cytokines released from microglia inhibit gap junctions in astrocytes: potentiation by beta-amyloid. *FASEB J.* (2006) 20:494–6. doi: 10.1096/fj.05-4297fje
140. Shinozaki Y, Shibata K, Yoshida K, Shigetomi E, Gachet C, Ikenaka K, et al. Transformation of astrocytes to a neuroprotective phenotype by microglia via P2Y1 receptor downregulation. *Cell Rep.* (2017) 19:1151–64. doi: 10.1016/j.celrep.2017.04.047
141. Anderson MA, Burda JE, Ren Y, Ao Y, O'Shea TM, Kawaguchi R, et al. Astrocyte scar formation aids central nervous system axon regeneration. *Nature.* (2016) 532:195–200. doi: 10.1038/nature17623
142. Abe T, Takahashi S, Suzuki N. Metabolic properties of astrocytes differentiated from rat neurospheres. *Brain Res.* (2006) 1101:5–11. doi: 10.1016/j.brainres.2006.05.009
143. Metea MR, Newman EA. Glial cells dilate and constrict blood vessels: a mechanism of neurovascular coupling. *J Neurosci.* (2006) 26:2862–70. doi: 10.1523/JNEUROSCI.4048-05.2006
144. Zonta M, Angulo MC, Gobbo S, Rosengarten B, Hossmann KA, Pozzan T, et al. Neuron-to-astrocyte signaling is central to the dynamic control of brain microcirculation. *Nat Neurosci.* (2003) 6:43–50. doi: 10.1038/nn980
145. Manjarrez-Marmolejo J, Franco-Perez J. Gap junction blockers: an overview of their effects on induced seizures in animal models. *Curr Neuropharmacol.* (2016) 14:759–71. doi: 10.2174/1570159X14666160603115942
146. Zhang Y, Proenca R, Maffei M, Barone M, Leopold L, Friedman JM. Positional cloning of the mouse obese gene and its human homologue. *Nature.* (1994) 372:425–32. doi: 10.1038/372425a0
147. Deng ZH, Liao J, Zhang JY, Liang C, Song CH, Han M, et al. Inhibition of the connexin 43 elevation may be involved in the neuroprotective activity of leptin against brain ischemic injury. *Cell Mol Neurobiol.* (2014) 34:871–9. doi: 10.1007/s10571-014-0066-5
148. Zhang L, Li YM, Jing YH, Wang SY, Song YF, Yin J. Protective effects of carbenoxolone are associated with attenuation of5 oxidative stress in ischemic brain injury. *Neurosci Bull.* (2013) 29:311–20. doi: 10.1007/s12264-013-1342-y
149. Tamura K, Alessandri B, Heimann A, Kempski O. The effect of a gap-junction blocker, carbenoxolone, on ischemic brain injury and cortical spreading depression. *Neuroscience.* (2011) 194:262–71. doi: 10.1016/j.neuroscience.2011.07.043
150. Goldberg GS, Moreno AP, Bechberger JF, Hearn SS, Shivers RR, MacPhee DJ, et al. Evidence that disruption of connexon particle arrangements in gap junction plaques is associated with inhibition of gap junctional communication by a glycyrrhetinic acid derivative. *Exp Cell Res.* (1996) 222:48–53. doi: 10.1006/excr.1996.0006
151. Evans WH, Leybaert L. Mimetic peptides as blockers of connexin channel-facilitated intercellular communication. *Cell Commun Adhes.* (2007) 14:265–73. doi: 10.1080/15419060801891034
152. Li X, Zhao H, Tan X, Kostrzewa RM, Du G, Chen Y, et al. Inhibition of connexin43 improves functional recovery after ischemic brain injury in neonatal rats. *Glia.* (2015) 63:1553–67. doi: 10.1002/glia.22826
153. Decrock E, De Vuyst E, Vinken M, Van Moorhem M, Vranckx K, Wang N, et al. Connexin 43 hemichannels contribute to the propagation of apoptotic cell death in a rat C6 glioma cell model. *Cell Death Differ.* (2009) 16:151–63. doi: 10.1038/cdd.2008.138
154. Evans WH, De Vuyst E, Leybaert L. The gap junction cellular internet: connexin hemichannels enter the signalling limelight. *Biochem J.* (2006) 397:1–14. doi: 10.1042/BJ20060175
155. Hawat G, Benderdour M, Rousseau G, Baroudi G. Connexin 43 mimetic peptide Gap26 confers protection to intact heart against myocardial ischemia injury. *Pflugers Archiv.* (2010) 460:583–92. doi: 10.1007/s00424-010-0849-6
156. Hawat G, Helie P, Baroudi G. Single intravenous low-dose injections of connexin 43 mimetic peptides protect ischemic heart *in vivo* against myocardial infarction. *J Mol Cell Cardiol.* (2012) 53:559–66. doi: 10.1016/j.yjmcc.2012.07.008
157. O'Carroll SJ, Alkadhi M, Nicholson LF, Green CR. Connexin 43 mimetic peptides reduce swelling, astrogliosis, and neuronal cell death after spinal cord injury. *Cell Commun Adhes.* (2008) 15:27–42. doi: 10.1080/15419060802014164
158. D'Hondt C, Iyyathurai J, Wang N, Gourdie RG, Himpens B, Leybaert L, et al. Negatively charged residues (Asp378 and Asp379) in the last ten amino acids of the C-terminal tail of Cx43 hemichannels are essential for loop/tail interactions. *Biochem Biophys Res Commun.* (2013) 432:707–12. doi: 10.1016/j.bbrc.2013.01.066
159. Wang N, De Vuyst E, Ponsaerts R, Boengler K, Palacios-Prado N, Wauman J, et al. Selective inhibition of Cx43 hemichannels by Gap19 and its impact on myocardial ischemia/reperfusion injury. *Basic Res Cardiol.* (2013) 108:309. doi: 10.1007/s00395-012-0309-x
160. Schulz R, Gorge PM, Gorbe A, Ferdinandy P, Lampe PD, Leybaert L. Connexin 43 is an emerging therapeutic target in ischemia/reperfusion injury, cardioprotection and neuroprotection. *Pharmacol Ther.* (2015) 153:90–106. doi: 10.1016/j.pharmthera.2015.06.005
161. Chaytor AT, Martin PE, Edwards DH, Griffith TM. Gap junctional communication underpins EDHF-type relaxations evoked by ACh in the rat hepatic artery. *Am J Physiol Heart Circ Physiol.* (2001) 280:H2441–50. doi: 10.1152/ajpheart.2001.280.6.H2441

Conflict of Interest: The authors declare that the research was conducted in the absence of any commercial or financial relationships that could be construed as a potential conflict of interest.

frontiers in Neurology

BRIEF RESEARCH REPORT
published: 10 September 2020
doi: 10.3389/fneur.2020.01023

Growth Differentiation Factor-11 Causes Neurotoxicity During Ischemia *in vitro*

Brad A. Sutherland[1,2*], *Gina Hadley*[1], *Zoi Alexopoulou*[3], *Tiffany A. Lodge*[4], *Ain A. Neuhaus*[1], *Yvonne Couch*[1], *Nareg Kalajian*[1], *Karl J. Morten*[4] and *Alastair M. Buchan*[1]

[1] *Acute Stroke Programme, Radcliffe Department of Medicine, University of Oxford, Oxford, United Kingdom,* [2] *Tasmanian School of Medicine, College of Health and Medicine, University of Tasmania, Hobart, TAS, Australia,* [3] *Nuffield Department of Clinical Neurosciences, University of Oxford, Oxford, United Kingdom,* [4] *Nuffield Department of Womens and Reproductive Health, University of Oxford, Oxford, United Kingdom*

Age-related neuronal dysfunction can be overcome by circulating factors present in young blood. Growth differentiation factor-11 (GDF-11), a systemic factor that declines with age, can reverse age-related dysfunction in brain, heart and skeletal muscle. Given that age increases susceptibility to stroke, we hypothesized that GDF-11 may be directly protective to neurons following ischemia. Primary cortical neurons were isolated from E18 Wistar rat embryos and cultured for 7–10 days. Neurons were deprived of oxygen and glucose (OGD) to simulate ischemia. Neuronal death was assessed by lactate dehydrogenase, propidium iodide or CellTox^{TM} green cytotoxicity assays. 40 ng/mL GDF-11 administration during 2 h OGD significantly increased neuronal death following 24 h recovery. However, GDF-11 pre-treatment did not affect neuronal death during 2 h OGD. GDF-11 treatment during the 24 h recovery period after 2 h OGD also did not alter death. Real-time monitoring for 24 h revealed that by 2 h OGD, GDF-11 treatment had increased neuronal death which remained raised at 24 h. Co-treatment of 1 μM SB431542 (ALK4/5/7 receptor inhibitor) with GDF-11 prevented GDF-11 neurotoxicity after 2 h OGD and 24 h OGD. Transforming growth factor beta (TGFβ) did not increase neuronal death to the same extent as GDF-11 following OGD. GDF-11 neurotoxicity was also exhibited following neuronal exposure to hydrogen peroxide. These results reveal for the first time that GDF-11 is neurotoxic to primary neurons in the acute phase of simulated stroke through primarily ALK4 receptor signaling.

Keywords: growth factor, GDF-11, stroke, neuron, ischemia, *in vitro*

OPEN ACCESS

Edited by:
Emmanuel Pinteaux, The University of Manchester, United Kingdom

Reviewed by:
Lorenz Hirt, University of Lausanne, Switzerland
Maria Calvo-Rodriguez, Massachusetts General Hospital and Harvard Medical School, United States

***Correspondence:**
Brad A. Sutherland
brad.sutherland@utas.edu.au

Specialty section:
This article was submitted to Stroke, a section of the journal Frontiers in Neurology

Received: *14 May 2020*
Accepted: *05 August 2020*
Published: *10 September 2020*

Citation:
Sutherland BA, Hadley G, Alexopoulou Z, Lodge TA, Neuhaus AA, Couch Y, Kalajian N, Morten KJ and Buchan AM (2020) Growth Differentiation Factor-11 Causes Neurotoxicity During Ischemia in vitro. Front. Neurol. 11:1023. doi: 10.3389/fneur.2020.01023

INTRODUCTION

The increased life expectancy of twenty-first century living has led to a substantial rise in the number of age-related disorders including stroke. Even in the thrombectomy era where a number of ischemic stroke patients are receiving reperfusion therapy (either pharmacologically with alteplase or mechanically via thrombectomy), the majority of ischemic stroke patients are left with no therapeutic options acutely to limit the damage of ischemia (1). The search continues for both primary and adjunctive neuroprotective therapies that can protect the brain from the resulting injury following an ischemic stroke (2).

Anti-aging factors are hypothesized to slow down the aging process and improve the quality of life of the aged. Recently, it was revealed that age-related neuronal dysfunction can be overcome by circulating factors present in young blood (3). A number of factors exist in young blood that are not found in old blood. One of these factors, considered to be an anti-aging factor is growth differentiation factor-11 (GDF-11) as its levels in blood decline with age (4), though this has been challenged due to problems with detection methods for GDF-11 measurement (5). In addition, systemic (i.p.) administration of recombinant GDF-11 has been shown to reverse age-related dysfunction in the rodent brain (4), heart (6) and skeletal muscle (7). GDF-11 is a growth factor that belongs to the transforming growth factor-beta (TGFβ) family and acts upon a number of TGFβ receptors including ALK4 and ALK5 (8). Previous studies have shown that TGFβ receptor agonists show neuroprotection whereas TGFβ receptor antagonists have exacerbated injury in pre-clinical stroke models (9). Two recent studies have trialed GDF-11 as a neuroprotectant in middle cerebral artery occlusion models, and both showed that recombinant GDF-11 administration reduced neurobehavioural deficits through the augmentation of angiogenesis, endothelial cell proliferation and increased neural precursor proliferation out to 14 days post-stroke (10, 11). Further evidence supporting this was the fact that SB431542, a ALK4/5/7 receptor inhibitor, blocked the protective effects of GDF-11 (10, 11).

Given its effectiveness on the vascular system and the ability of GDF-11 to modulate age-related neuronal dysfunction, we hypothesize that GDF-11 could be an ideal candidate as a neuroprotective agent for ischemic stroke. Therefore, in this study, we sought to determine whether GDF-11 administration to primary neurons could provide direct protection to neurons using an *in vitro* model of ischemia.

MATERIALS AND METHODS

To determine the effects of GDF-11 directly on neurons, we used a primary cortical neuronal culture as we have previously described (12, 13). Neurons were plated onto poly-D-lysine-coated 12 well plates at 10^5 cells per well in complete neurobasal media containing 2% B27 serum-free supplement, 2 mM L-glutamine and 1% penicillin/streptomycin in neurobasal medium (all Invitrogen). Neurons remained in culture for 7–10 days to allow neuronal networks to develop before experiments were conducted.

GDF-11 was purchased from Peprotech (cat#120-11, UK). To determine whether GDF-11 altered basal viability of neurons, GDF-11 was diluted in complete neurobasal media to produce a concentration range of 4–400 ng/mL and added to neuronal cultures for 48 h. Neuronal viability was assessed with a CellTiter 96 assay (Promega, UK) following manufacturer's instructions, with neurons being incubated for 5 h with the reaction reagent.

To determine whether GDF-11 altered neuronal viability under simulated ischemic conditions, we performed OGD experiments. Days *in vitro* (DIV) 7–10 primary cortical neurons were exposed to 0% oxygen using a hypoxic chamber (Coy) coupled with glucose-free neurobasal media (Invitrogen) for 2 h as described previously (12, 13), or using an environmentally-controlled microplate reader (Omega, BMG Labtech) for up to 24 h exposure. Following 2 h OGD in the hypoxic chamber, cultures were returned to normoxic conditions with glucose-containing neurobasal media for 24 h. For all OGD experiments, 40 ng/mL GDF-11 was used due to this being the concentration in which effects in brain capillary endothelial cells have been observed (4) and there was no neurotoxicity under normoxic conditions (**Figure 1A**). Depending on the experiment, GDF-11 was administered for 7 days prior to OGD, during OGD or for 24 h following OGD in the recovery phase.

To assess neuronal death, a lactate dehydrogenase (LDH) activity assay (Cytotoxicity kit, Promega, UK), propidium iodide assay or CellTox^{TM} green cytotoxicity assay (Promega, UK) was used as per manufacturer's instructions. Briefly, for the LDH assessment, media were collected at the end of the relevant period for measurement of LDH release. The cells were then lysed with 1% Triton X-100 in complete neurobasal medium to obtain total LDH released. To get a percentage cell death, the LDH released during the relevant period was divided by the sum of the LDH released during that period and during cell lysis (12, 13). For the propodium iodide assay, cells were plated in 96-well plates at 50,000 cells/well and following the OGD protocol, propidium iodide (final concentration 50 μM, Invitrogen, UK) was added and incubated for 30 min. Plates were then assessed for the level of cell death as indicated by propidium iodide fluorescence (excitation 540 nm emission 620 nm) using a fluorometer (Omega Optima, BMG Labtech, UK). The CellTox^{TM} green cytotoxicity assay was used per manufacturer's instructions for real-time monitoring of cell death as it measures cell free DNA in the media or DNA of dead cells with a compromised plasma membrane (14). After administration of the CellTox^{TM} Green reagent, and placed in the environmentally controlled plate reader (Omega, BMG Labtech), a gas permeable membrane (Breathe-Easy sealing membrane, Sigma) was used to prevent evaporation while still allowing gas exchange. A concurrent positive control was performed using lysis buffer (Promega).

Neurons possess ALK4 and ALK5 receptors (15, 16), and so to determine whether the effects of GDF-11 were mediated by the ALK4/5 receptors on neurons, we performed neuronal OGD experiments in the presence of GDF-11 with or without 1 μM SB431542 (an ALK4/5/7 receptor inhibitor, Tocris) (17). TGFβ is a ligand for ALK5 receptors (15, 18) and so we performed neuronal OGD experiments with 10 ng/mL TGFβ to determine its effect on neurotoxicity.

During ischemia, neurons were exposed to a number of potentially damaging factors including lack of energy supply, oxidative stress and excitotoxicity. We exposed cortical neuronal cultures to 100 μM iodoacetate (to inhibit glycolysis) and 10 μM antimycin A (to inhibit mitochondrial respiration) as a model of chemical ischemia, 500 μM glutamate as a model of excitotoxicity, and 1 mM hydrogen peroxide as a model

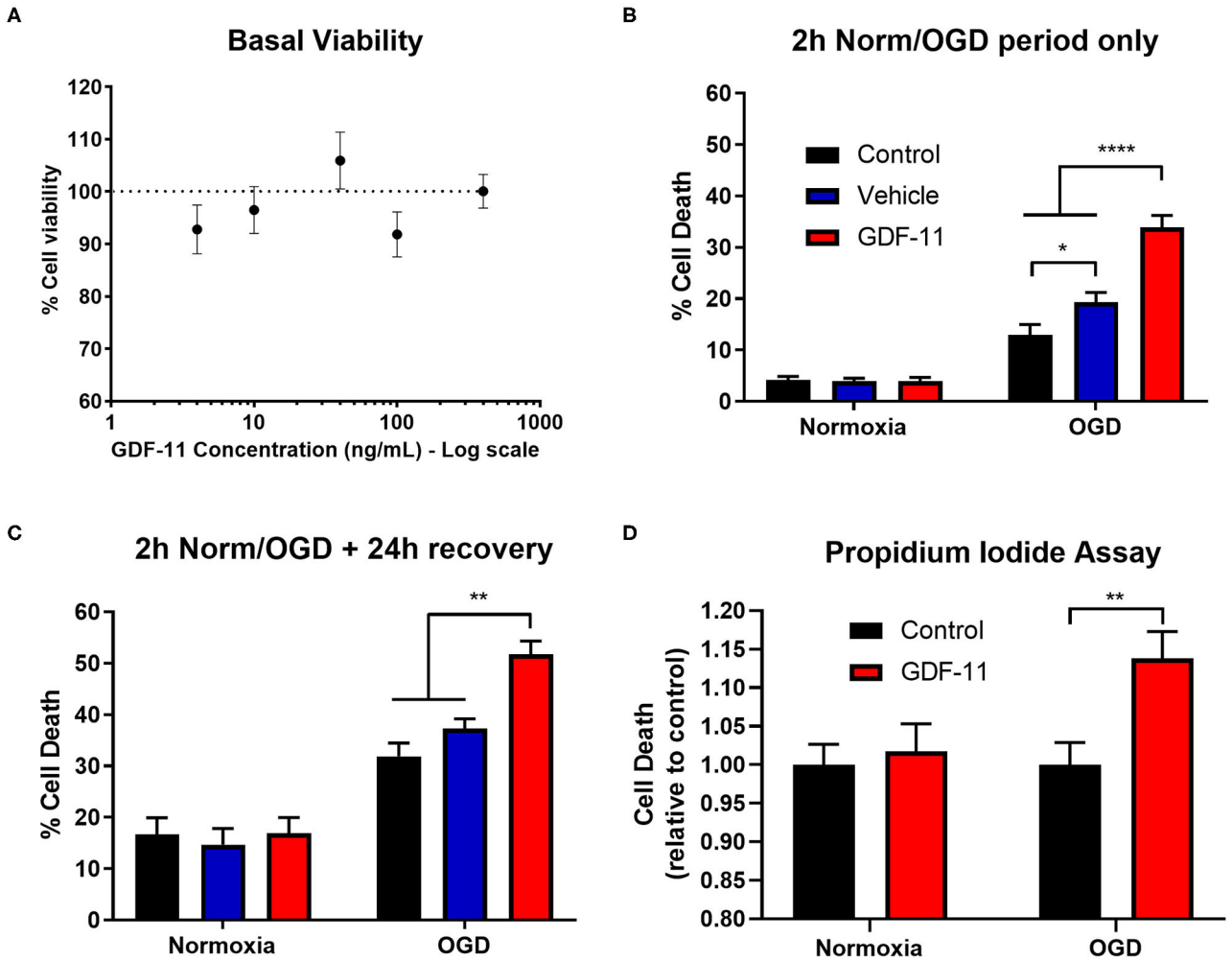

FIGURE 1 | GDF-11 increased neuronal death during OGD. **(A)** Cortical neurons kept under normoxic conditions were exposed to GDF-11 (4–400 ng/mL) for 48 h. Percentage neuronal viability was quantified with the CellTiter 96 assay. N=4 for each condition. 2 h OGD **(B)** and 2 h OGD + 24 h recovery **(C)** increased cortical neuronal death compared to normoxia while GDF-11 increased cell death compared with media and DMSO under OGD conditions. GDF-11 did not affect neuronal death under normoxic conditions. Cell death was quantified by LDH assay. Groups: media (control) ($n = 6$), DMSO (control) ($n = 6$), GDF-11 ($n = 3$). **(D)** GDF-11 increased cell death following 2 h OGD + 24 h recovery, but not under normoxia conditions using a propidium iodide assay. $N = 8$–16 per condition. All data are presented as mean ± SEM. Two-way ANOVA with Tukey's *post-hoc* Test. $^{*}p < 0.05$, $^{**}p < 0.01$, $^{****}p < 0.0001$.

of oxidative stress for 24 h. Experiments were carried out in the absence or presence of GDF-11. Neuronal death was determined by LDH activity of the incubating media during the insults.

Data were analyzed by a two way ANOVA followed by a Tukey's *post-hoc* test when there were two independent variables or a one way ANOVA followed by a Tukey's or Bonferroni's *post-hoc* test when there was only one variable. All analyses were performed using GraphPad Prism v7.0. Data are presented as mean + SEM. All results are from at least three experiments, $p < 0.05$ is considered statistically significant. All data and research materials are available upon request.

RESULTS

48 h GDF-11 Administration Did Not Alter Cellular Viability in Primary Cortical Neurons

Initially, we wished to test whether GDF-11 altered neuronal viability under standard culture conditions. Exposure of 4–400 ng/mL GDF-11 to neurons for 48 h did not affect neuronal viability (all concentrations had >90% viability; **Figure 1A**). Since Katsimpardi et al. had previously shown effects of 40 ng/mL GDF-11 in brain capillary endothelial cells (4), we selected this concentration for subsequent studies.

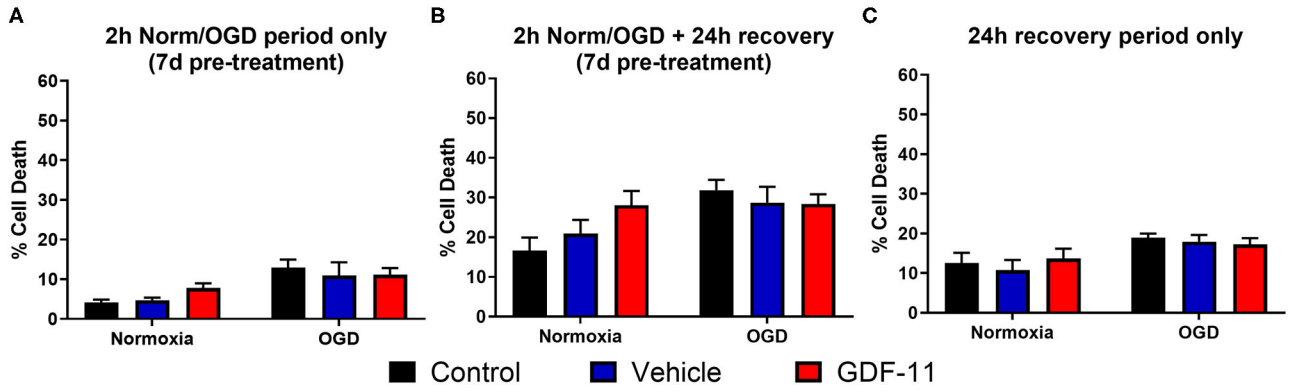

FIGURE 2 | GDF-11 had no effect on neuronal death with treatment prior to OGD and after OGD. **(A)** 7 days pre-treatment with 40 ng/mL GDF-11 had no effect on cortical neuronal death during 2 h normoxia or OGD. GDF-11 was not present during the OGD phase. **(B)** 7 days pre-treatment with 40 ng/mL GDF-11 did not affect cortical neuronal death following 2 h normoxia or OGD and 24 h recovery. GDF-11 was not present during the OGD phase. **(C)** Treatment with GDF-11 during 24 h recovery only did not affect cortical neuronal death following 2 h normoxia or OGD. GDF-11 was not present during the OGD phase. Cell death was quantified by LDH assay. Data presented as mean ± SEM. Groups: control ($n = 6$), DMSO ($n = 3$) and GDF-11 ($n = 3$). Two-way ANOVA with Tukey's *post-hoc* test.

Exposure of 40 ng/mL GDF-11 to Neurons During 2 h OGD Exacerbated Neuronal Death

Given the potential neuroprotective effects of GDF-11 (10, 11), we wished to determine whether GDF-11 could provide direct neuroprotection to ischemic neurons. Following 2 h OGD (**Figure 1B**), there was a significant increase in cell death during OGD compared to normoxia [$F_{(1,48)} = 201.7$, $p < 0.0001$] as detected by an LDH assay. Administration of 40 ng/mL GDF-11 to neurons during 2 h OGD significantly increased neuronal death (vehicle: 19.3% ± 1.9% cell death, GDF-11: 33.9% ± 2.3%; Tukey's $p < 0.0001$). At 24 h recovery following 2 h OGD (**Figure 1C**), the OGD group continued to have significantly increased cell death compared to normoxia [$F_{(1,48)} = 111.1$, $p < 0.0001$], with GDF-11 increasing cell death compared to OGD alone (vehicle: 37.3% ± 1.9% cell death, GDF-11: 51.7% ± 2.6%; Tukey's $p = 0.0019$). This neurotoxicity by GDF-11 following OGD was replicated using a propidium iodide assay (1.14 ± 0.04 fold over control, Tukey's $p = 0.003$; **Figure 1D**). There was no significant effect of GDF-11 treatment on neuronal death under normoxic conditions (**Figure 1**).

GDF-11 Treatment Prior to OGD or After OGD Did Not Alter Neuronal Death

Given that GDF-11 administration to ischemic neurons worsened cell death, we then carried out experiments to determine whether treatment with GDF-11 prior to OGD or after OGD could alter this neurotoxic effect. Again, there was a significant increase in cell death with OGD compared to normoxia [**Figure 2A**, $F_{(1,36)} = 17.0$, $p = 0.0002$]. However, 7 days of pre-treatment with GDF-11 did not affect neuronal death during 2 h OGD compared to vehicle pre-treatment (vehicle: 11.0% ± 3.3%, GDF-11: 11.1% ± 1.7%; Tukey's $p = 0.998$). Similar results were observed at 24 h recovery following 2 h OGD (**Figure 2B**; vehicle: 28.7% ± 4.0%, GDF-11: 28.4% ± 2.4%; Tukey's $p = 0.998$). When measuring cell death during 24 h recovery after 2 h OGD or normoxia (**Figure 2C**), there was a small but significant increase in neuronal death following OGD [$F_{(1,48)} = 11.1$, $p = 0.0017$]. When GDF-11 was administered during the 24 h recovery period only following 2 h OGD (**Figure 2C**), there was no significant effect of GDF-11 treatment on the ability of OGD to kill neurons (vehicle: 17.9% ± 1.7%, GDF-11: 17.2% ± 1.6%; Tukey's $p = 0.970$). GDF-11 treatment had no effect on neuronal death at any timepoint following normoxia (**Figure 2**).

Increase in Ischemic Neuronal Death by GDF-11 Could Be Blocked by an ALK4/5 Receptor Inhibitor

GDF-11 caused neurotoxicity when administered during OGD and so we sought to identify a mechanism by which this is occurring. Neurons are known to possess a range of TGFβ receptors including ALK4/5 receptors (15, 16) and GDF-11 is known to bind to these receptors (8). We exposed OGD neurons to GDF-11 in the presence or absence of SB431542, an ALK4/5/7 receptor inhibitor (17), and performed real-time monitoring of cell death under OGD or normoxic conditions over a 24 h period (**Figures 3A,D**). After 2 h OGD (**Figure 3E**), GDF-11 treatment had increased neuronal death (GDF-11: 1.27 ± 0.03 fold over control; vehicle: 1.15 ± 0.02 over control; Tukey's $p = 0.0258$) which remained raised at 24 h (**Figure 3F**; GDF-11: 1.36 ± 0.08 fold over control; vehicle: 1.11 ± 0.01 fold over control; Tukey's $p < 0.0001$). Co-treatment of 1 μM SB431542 with GDF-11 prevented GDF-11 neurotoxicity after 2 h OGD (1.03 ± 0.04 fold over control; Tukey's $p < 0.0001$) and 24 h OGD (1.00 ± 0.04 fold over vehicle, Tukey's $p < 0.0001$). No significant effects with GDF-11 nor SB431542 were observed during normoxic conditions (**Figures 3B,C**). We replicated this experiment using the LDH assay (**Figure 4A**) and showed that the addition of SB431542 to GDF-11 could restrict cell death (0.72 ± 0.05 fold under control) compared to GDF-11 alone

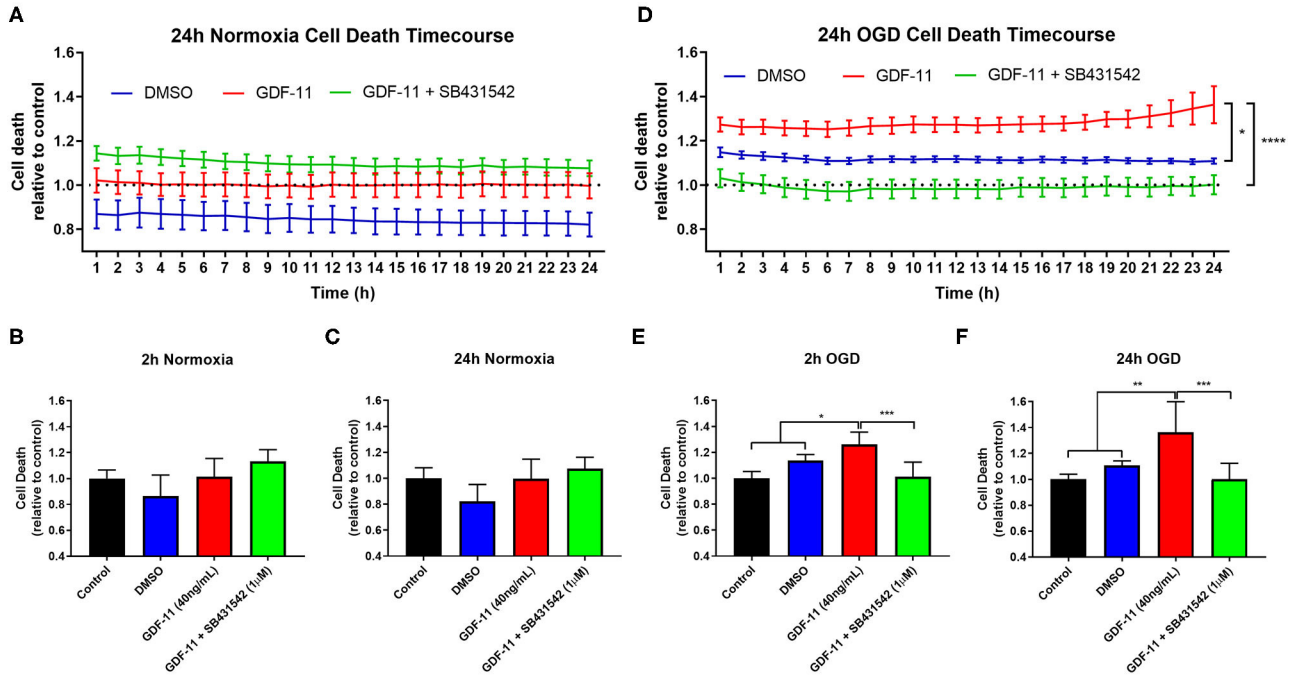

FIGURE 3 | GDF-11 neuronal toxicity during OGD was prevented by a ALK4/5/7 receptor inhibitor. **(A)** GDF-11 +/− SB431542 (ALK4/5/7 receptor inhibitor) had no effect on neuronal death during 24 h of normoxia. **(B)** At 2 h of normoxia, there was no effect of GDF-11 on neuronal death. **(C)** At 24 h of normoxia, GDF-11 did not affect neuronal death. **(D)** GDF-11 enhanced cortical neuronal death throughout 24 h of OGD which was prevented fully by the administration of SB431542. **(E)** At 2 h OGD, GDF-11 increased neuronal death which was reversed by SB431542. **(F)** At 24 h OGD, GDF-11 increased neuronal death which was reversed by SB431542. Cell death was measured by the CellTox™ Green Assay. Data presented as mean ± SEM. $n = 3$ per group except media control which was $n = 6$. One-way ANOVA with Tukey's *post-hoc* test. $^{*}p < 0.05$; $^{**}p < 0.01$; $^{***}p < 0.001$.

(1.28 ± 0.08, Bonferroni's $p = 0.0017$) following 2 h OGD + 24 h recovery. We also assessed whether administration of TGFβ could replicate the neurotoxicity exhibited by GDF-11 following OGD. **Figure 4A** demonstrated that while GDF-11 increased cell death compared to control (1.28 ± 0.08 fold over control, Bonferroni's $p = 0.0743$), TGFβ had no significant effect compared to control (1.18 ± 0.06 fold over control, Bonferroni's $p = 0.349$).

GDF-11 Worsened Neuronal Viability During Oxidative Stress but Not Chemical Ischemia or Excitotoxicity

Other types of stressors occur during an ischemic injury to the brain such as a lack of energy supply, excitotoxicity and oxidative stress all of which can impact on neuronal survival. We modeled these conditions *in vitro* to determine whether GDF-11 could also alter neuronal death under these conditions (**Figure 4B**). Exposure of neurons for 24 h to a combination of 100 μM iodoacetate (glycolysis inhibitor) and 10 μM antimycin A (mitochondrial respiration inhibitor) to mimic a reduction in energy supply led to increased neuronal death (control: 8.0% ± 1.0%, iodoacetate/antimycin: 22.0% ± 0.9%; Tukey's $p < 0.0001$), but this was not influenced by GDF-11 administration (iodoacetate/antimycin + GDF-11: 23.4% ± 1.0%, Tukey's $p = 0.9812$). Neurons that were subjected to 500 μM glutamate had increased neuronal death (control: 8.0% ± 1.0%, glutamate: 17.2% ± 0.7%; Tukey's $p = 0.0032$), but again this was not influenced by GDF-11 administration (glutamate + GDF-11: 20.5% ± 2.2%, Tukey's $p = 0.5455$). 1 mM hydrogen peroxide indicative of oxidative stress showed a substantial increase in neuronal death (control: 8.0% ± 1.0%, H_2O_2: 55.3% ± 1.3%; Tukey's $p < 0.0001$), and interestingly GDF-11 exacerbated neuronal death by hydrogen peroxide (H_2O_2 + GDF-11: 64.0% ± 2.0%, Tukey's $p = 0.0005$).

DISCUSSION

The aging brain is susceptible to a number of different stressors, and the effect of ischemia on the aged brain can cause irreversible damage and subsequent mortality. Recent studies have pointed toward factors that are present in young blood such as GDF-11, that could have potential neuroprotective effects (4, 10, 11). Circulating GDF-11 levels have been shown to decrease with age (4, 6, 19), though this is controversial (5, 20), but this could leave the brain in a susceptible state. Here, we wished to determine whether GDF-11 could have direct protective effects on neurons under simulated ischemic conditions. On the contrary, we discovered that GDF-11 had neurotoxic effects when administered during OGD, and that this neurotoxicity appeared to be due to its activation of the

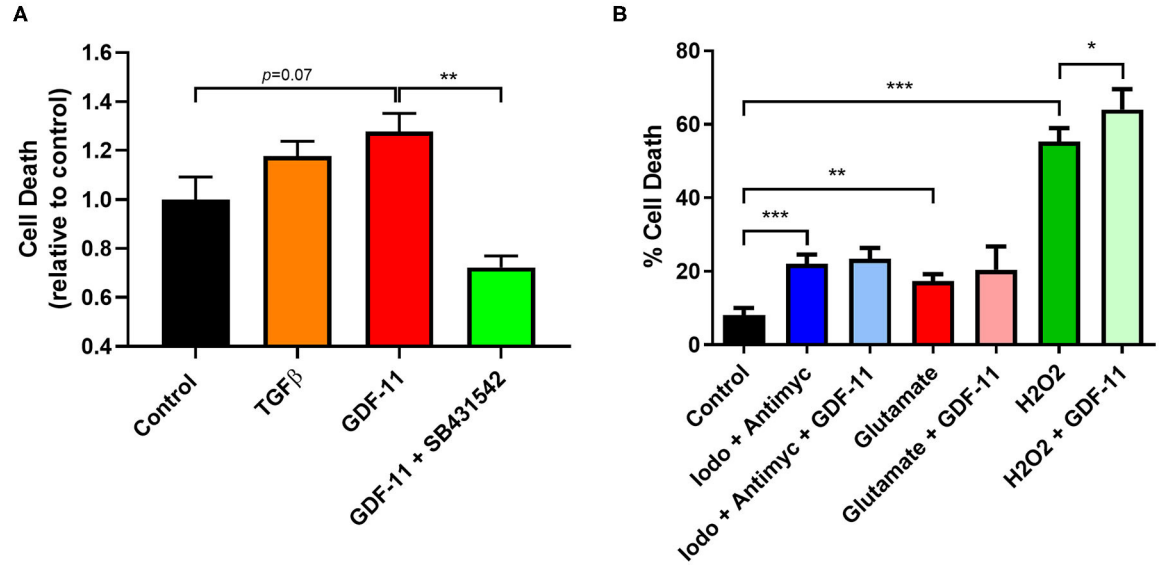

FIGURE 4 | GDF-11 neuronal toxicity occurred under OGD and oxidative stress. **(A)** Neurons were exposed to 2 h OGD followed by 24 h recovery. GDF-11 increased neuronal death while TGFβ did not increase death to the same extent. GDF-11 neurotoxicity was blocked by the ALK4/5/7 inhibitor SB431542. **(B)** Exposure to chemical ischaemia (iodoacetate + antimycin A), excitotoxicity (glutamate) and oxidative stress (H_2O_2) for 24 h enhanced neuronal death. GDF-11 increased neuronal death only during oxidative stress (H_2O_2) exposure. Data presented as mean ± SEM and were calculated from an LDH assay. $n = 3$–8 per group. One-way ANOVA with Bonferroni *post-hoc* test. $^*p < 0.05$, $^{**}p < 0.01$, $^{***}p < 0.001$.

ALK4/5 receptors. GDF-11 neurotoxicity was also observed under oxidative stress conditions. Confining GDF-11 to the bloodstream will help prevent any direct neurotoxic effects of GDF-11 under ischemic conditions.

Under normal conditions, GDF-11 is found in the bloodstream, with a limited amount crossing an intact blood-brain barrier (21). GDF-11 has been shown to have multiple beneficial effects on the vasculature including promotion of angiogenesis, maintaining the blood-brain barrier and providing vascular stability (4, 10, 11, 21). Under *in vivo* stroke conditions, GDF-11 has been shown to reduce infarct volume and improve behavioral outcomes mainly due to both angiogenesis and endothelial cell proliferation (10, 11). However, our evidence suggests that if GDF-11 made it out of the bloodstream and into the brain during ischemia, either through BBB leakage or via some mode of active transport, then it could potentially be harmful to neurons. Therefore, limiting the amount of neuronal exposure to GDF-11 during a stroke could restrict its neurotoxic effects while maintaining their vasculoprotective effects to help improve recovery of the brain.

It is important to note that there was no indication that GDF-11 was neurotoxic under normoxic conditions suggesting that this neurotoxicity was only present when neurons were exposed to ischemia. Likewise, experiments where GDF-11 administration took place prior to or after OGD did not affect neuronal death. This indicates that the susceptibility of neurons to GDF-11-induced neurotoxicity is during ischemia only, but the effects of this can last during the recovery phase. The mechanisms behind why this occurs are unclear, however RNAseq data showed that primary hippocampal neurons subject to OGD increased the expression of both the ALK4 receptor and Smad3 (22). This suggests that the neurotoxic effects of GDF-11 are limited to when the cell becomes stressed, which may augment the activation of the ALK4/Smad3 signaling cascade in neurons.

The type of stress that leads to GDF-11 neurotoxicity is important as there are multiple stressors that can occur during an ischemic episode *in vivo*. Our results suggest that when neurons are oxygen and glucose deprived (limiting energy substrates) and are exposed to oxidative stress (hydrogen peroxide), then GDF-11-induced neurotoxicity ensues, whereas under excitotoxic (excessive glutamate) and chemical ischemia (limiting energy production), GDF-11 neurotoxicity was not observed. However, a recent study showed that under conditions where oxidative stress was increased such as in intracerebral hemorrhage among other pathologies, administration of GDF-11 intraperitoneally promoted production of heme oxygenase-1, an important antioxidant, as well as protecting mitochondrial capacity suggesting indirect effects on neuronal survival (23). This highlights important differences between *in vitro* modeling of neurons and how neurons may react to a stressor *in vivo*, which can be influenced by different cell types in the brain which are not present in single cell type cultures.

GDF-11 is a member of the TGFβ signaling family and has been shown to act at specific TGFβ superfamily receptors including ALK4 and ALK5 (8, 18). Both of these receptors are expressed in neurons and can be activated by Activin A and TGFβ1, respectively (15, 18, 24). Previous studies using Activin A as an agonist at ALK4 receptors and TGFβ1 as an agonist at ALK5 receptors have shown neuroprotective properties in *in*

vivo models of stroke (9, 25). While our data showing direct GDF-11 neurotoxicity under ischemic conditions is in contrast to the neuroprotective effects of these agonists, the exposure of TGFβ1 to neurons subjected chronically to glutamate led to neurotoxicity (26). Our data suggest that GDF-11 neurotoxicity was due to its action on the ALK4 receptor. TGFβ administration (which only activates ALK5 receptors) did not increase neuronal death to the same extent as GDF-11. This is further supported by the evidence that the ALK4/5/7 inhibitor SB431542 could block the neurotoxic effects of GDF-11 during OGD. Moreover, RNAseq analysis of hippocampal neurons following OGD and recovery has demonstrated that there was an increase in both ALK4 receptor expression and Smad3 signaling following OGD (22). Therefore, GDF-11 administration may put greater stress on the Smad signaling cascade through ALK4 activation leading to detrimental outcomes to neurons.

Exposure of hydrogen peroxide to neurons led to exacerbation of neuronal death by GDF-11 which suggests that free radical formation may be an important mechanism of cell death by GDF-11. OGD of neuronal cultures can directly lead to reactive oxygen species generation, which can be blocked by free radical scavengers (27). Interestingly, a traditional pro-survival factor, neurotrophin-3, unexpectedly showed damaging effects on neurons following OGD due to increased reactive oxygen species formation (28). Furthermore, there is evidence in other disease conditions that activation of TGFβ and Smad signaling can lead to reactive oxygen species formation (29). Confirmation with pharmacological studies, using agents such as SB431542, would be valuable to confirm that these effects are mediated through the ALK4/5 receptors. Overall, there appears to be a link between the TGFβ signaling cascade and free radical formation, which could mediate GDF-11 neurotoxicity under ischemic and oxidative stress conditions, but further experiments investigating mitochondrial changes by GDF-11 under these conditions are needed to confirm these effects.

There are some limitations to this study. One limitation was the utilization of only one concentration of GDF-11 in the neurotoxicity experiments (40 ng/mL). We showed that GDF-11 at a range of concentrations (4–400 ng/mL) had no effects on neuronal viability under normoxic conditions, and so we carefully chose a concentration within this range that had exhibited effects in previous studies (4) and had a concentration above the half maximal effective concentration (EC_{50}) to activate Smad signaling in other cell types (30). However, we cannot rule out the possibility that effects, beneficial or neurotoxic, could be observed at other concentrations of GDF-11 following OGD. Another limitation is that the isolated neuronal culture method may not reflect the effects of GDF-11 in the complex brain environment. However, determining direct effects of GDF-11 on neurons *in vivo* or in *ex vivo* brain slices is difficult, particularly due to the strong vascular effects that GDF-11 are known to have (4, 10, 11, 21), meaning that the viability of neurons will be influenced by the effects of GDF-11 on other cell types in experiments using these methodologies.

These results reveal for the first time that GDF-11 is neurotoxic to primary neurons in the acute phase of simulated stroke through primarily ALK4 receptor signaling. Therefore, limiting GDF-11 access to the brain during ischemia could prevent its neurotoxicity. Future studies will further characterize the neurotoxic vs. protective properties of GDF-11 in the brain and whether the protection of the brain is solely mediated through the vascular system.

DATA AVAILABILITY STATEMENT

The raw data supporting the conclusions of this article will be made available by the authors upon request.

AUTHOR CONTRIBUTIONS

BS, GH, AN, YC, and AB conceived and designed the study. BS, GH, ZA, TL, and NK carried out the experiments. BS, ZA, TL, and KM analyzed the data. BS wrote the manuscript. All authors edited and approved the final version.

FUNDING

This work was supported by a Fondation Leducq Transatlantic Network of Excellence (AB) and Medical Research Council grant (MR/M022757/1; BS, YC, and AB). BS was supported by a National Health and Medical Research Council Fellowship (APP1137776). GH was supported by the Oxford University Clinical Academic Graduate School. AN was supported by a Radcliffe Department of Medicine Scholarship.

REFERENCES

1. Hankey GJ. Stroke. *Lancet.* (2017) 389:641–654. doi: 10.1016/S0140-6736(16)30962-X
2. Neuhaus AA, Couch Y, Hadley G, Buchan AM. Neuroprotection in stroke: the importance of collaboration and reproducibility. *Brain.* (2017) 140:2079–92. doi: 10.1093/brain/awx126
3. Villeda SA, Plambeck KE, Middeldorp J, Castellano JM, Mosher KI, Luo J, et al. Young blood reverses age-related impairments in cognitive function and synaptic plasticity in mice. *Nat Med.* (2014) 20:659–63. doi: 10.1038/nm.3569
4. Katsimpardi L, Litterman NK, Schein PA, Miller CM, Loffredo FS, Wojtkiewicz GR, et al. Vascular and neurogenic rejuvenation of the aging mouse brain by young systemic factors. *Science.* (2014) 344:630–4. doi: 10.1126/science.1251141
5. Egerman MA, Cadena SM, Gilbert JA, Meyer A, Nelson HN, Swalley SE, et al. GDF11 increases with age and inhibits skeletal muscle regeneration. *Cell Metab.* (2015) 22:164–74. doi: 10.1016/j.cmet.2015.05.010
6. Loffredo FS, Steinhauser ML, Jay SM, Gannon J, Pancoast JR, Yalamanchi P, et al. Growth differentiation factor 11 is a circulating factor that reverses age-related cardiac hypertrophy. *Cell.* (2013) 153:828–39. doi: 10.1016/j.cell.2013.04.015
7. Sinha M, Jang YC, Oh J, Khong D, Wu EY, Manohar R, et al. Restoring systemic GDF11 levels reverses age-related dysfunction in mouse skeletal muscle. *Science.* (2014) 344:649–52. doi: 10.1126/science.1251152
8. Andersson O, Reissmann E, Ibanez CF. Growth differentiation factor 11 signals through the transforming growth factor-beta receptor ALK5 to regionalize the anterior-posterior axis. *EMBO Rep.* (2006) 7:831–7. doi: 10.1038/sj.embor.7400752

9. Dhandapani KM, Brann DW. Transforming growth factor-beta: a neuroprotective factor in cerebral ischemia. *Cell Biochem Biophys.* (2003) 39:13–22. doi: 10.1385/CBB:39:1:13
10. Ma J, Zhang L, Niu T, Ai C, Jia G, Jin X, et al. Growth differentiation factor 11 improves neurobehavioral recovery and stimulates angiogenesis in rats subjected to cerebral ischemia/reperfusion. *Brain Res Bull.* (2018) 139:38–47. doi: 10.1016/j.brainresbull.2018.02.011
11. Lu L, Bai X, Cao Y, Luo H, Yang X, Kang L, et al. Growth differentiation factor 11 promotes neurovascular recovery after stroke in mice. *Front Cell Neurosci.* (2018) 12:205. doi: 10.3389/fncel.2018.00205
12. Hadley G, Beard DJ, Alexopoulou Z, Sutherland BA, Buchan AM. Investigation of the novel mTOR inhibitor AZD2014 in neuronal ischemia. *Neurosci Lett.* (2019) 706:223–30. doi: 10.1016/j.neulet.2019.05.023
13. Hadley G, Neuhaus AA, Couch Y, Beard DJ, Adriaanse BA, Vekrellis K, et al. The role of the endoplasmic reticulum stress response following cerebral ischemia. *Int J Stroke.* (2018) 13:379–90. doi: 10.1177/1747493017724584
14. Riss T, Niles A, Moravec R, Karassina N, Vidugiriene J. Cytotoxicity assays: *in vitro* methods to measure dead cells. In: Markossian M, Sittampalam GS, Grossman A, Brimacombe K, Arkin M, Auld D, Austin C, Baell J, Bejcek B, Caaveiro JMM, Chung TDY, Coussens NP, Dahlin JL, Devanaryan V, Foley TL, Glicksman M, Hall MD, Haas JV, Hoare SRJ, Inglese J, Iversen PW, Kahl SD, Kales SC, Kirshner S, Lal-Nag M, Li Z, McGee J, McManus O, Riss T, Trask OJ, Jr., Weidner JR, Wildey MJ, Xia M, Xu X, editors. *The Assay Guidance Manual*. Bethesda, MD: Assay Guidance Manual (2019).
15. Konig HG, Kogel D, Rami A, Prehn JH. TGF-{beta}1 activates two distinct type I receptors in neurons: implications for neuronal NF-{kappa}B signaling. *J Cell Biol.* (2005) 168:1077–86. doi: 10.1083/jcb.200407027
16. Zhang Y, Chen K, Sloan SA, Bennett ML, Scholze AR, O'Keeffe S, et al. An RNA-sequencing transcriptome and splicing database of glia, neurons, and vascular cells of the cerebral cortex. *J Neurosci.* (2014) 34:11929–47. doi: 10.1523/JNEUROSCI.1860-14.2014
17. Inman GJ, Nicolas FJ, Callahan JF, Harling JD, Gaster LM, Reith AD, et al. SB-431542 is a potent and specific inhibitor of transforming growth factor-beta superfamily type I activin receptor-like kinase (ALK) receptors ALK4, ALK5, and ALK7. *Mol Pharmacol.* (2002) 62:65–74. doi: 10.1124/mol.62.1.65
18. Heldin CH, Moustakas A. Signaling receptors for TGF-beta family members. *Cold Spring Harb Perspect Biol.* (2016) 8:a022053. doi: 10.1101/cshperspect.a022053
19. Poggioli T, Vujic A, Yang P, Macias-Trevino C, Uygur A, Loffredo FS, et al. Circulating growth differentiation factor 11/8 levels decline with age. *Circ Res.* (2016) 118:29–37. doi: 10.1161/CIRCRESAHA.115.307521
20. Schafer MJ, Atkinson EJ, Vanderboom PM, Kotajarvi B, White TA, Moore MM, et al. Quantification of GDF11 and myostatin in human aging and cardiovascular disease. *Cell Metab.* (2016) 23:1207–15. doi: 10.1016/j.cmet.2016.05.023
21. Ozek C, Krolewski RC, Buchanan SM, Rubin LL. Growth Differentiation Factor 11 treatment leads to neuronal and vascular improvements in the hippocampus of aged mice. *Sci Rep.* (2018) 8:17293. doi: 10.1038/s41598-018-35716-6
22. Shi J, Chen X, Li H, Wu Y, Wang S, Shi W, et al. Neuron-autonomous transcriptome changes upon ischemia/reperfusion injury. *Sci Rep.* (2017) 7:5800. doi: 10.1038/s41598-017-05342-9
23. Anqi X, Ruiqi C, Yanming R, Chao Y. Neuroprotective potential of GDF11 in experimental intracerebral hemorrhage in elderly rats. *J Clin Neurosci.* (2019) 63:182–8. doi: 10.1016/j.jocn.2019.02.016
24. Suzuki K, Kobayashi T, Funatsu O, Morita A, Ikekita M. Activin A induces neuronal differentiation and survival via ALK4 in a SMAD-independent manner in a subpopulation of human neuroblastomas. *Biochem Biophys Res Commun.* (2010) 394:639–45. doi: 10.1016/j.bbrc.2010.03.039
25. Mukerji SS, Rainey RN, Rhodes JL, Hall AK. Delayed activin A administration attenuates tissue death after transient focal cerebral ischemia and is associated with decreased stress-responsive kinase activation. *J Neurochem.* (2009) 111:1138–48. doi: 10.1111/j.1471-4159.2009.06406.x
26. Prehn JH, Krieglstein J. Opposing effects of transforming growth factor-beta 1 on glutamate neurotoxicity. *Neuroscience.* (1994) 60:7–10. doi: 10.1016/0306-4522(94)90198-8
27. Abramov AY, Scorziello A, Duchen MR. Three distinct mechanisms generate oxygen free radicals in neurons and contribute to cell death during anoxia and reoxygenation. *J Neurosci.* (2007) 27:1129–38. doi: 10.1523/JNEUROSCI.4468-06.2007
28. Bates B, Hirt L, Thomas SS, Akbarian S, Le D, Amin-Hanjani S, et al. Neurotrophin-3 promotes cell death induced in cerebral ischemia, oxygen-glucose deprivation, and oxidative stress: possible involvement of oxygen free radicals. *Neurobiol Dis.* (2002) 9:24–37. doi: 10.1006/nbdi.2001.0458
29. Liu RM, Desai LP. Reciprocal regulation of TGF-beta and reactive oxygen species: A perverse cycle for fibrosis. *Redox Biol.* (2015) 6:565–577. doi: 10.1016/j.redox.2015.09.009
30. Walker RG, Czepnik M, Goebel EJ, McCoy JC, Vujic A, Cho M, et al. Structural basis for potency differences between GDF8 and GDF11. *BMC Biol.* (2017) 15:19. doi: 10.1186/s12915-017-0350-1

Conflict of Interest: AB is a senior medical science advisor and co-founder of Brainomix, a company that develops electronic ASPECTS (e-ASPECTS), an automated method to evaluate ASPECTS in stroke patients.

The remaining authors declare that the research was conducted in the absence of any commercial or financial relationships that could be construed as a potential conflict of interest.

frontiers in Neurology

STUDY PROTOCOL
published: 25 September 2020
doi: 10.3389/fneur.2020.569696

REMOTE Ischemic Perconditioning Among Acute Ischemic Stroke Patients in Catalonia: REMOTE-CAT PROJECT

Francisco Purroy[1,2†], Gloria Arque[2†], Gerard Mauri[1,2], Cristina García-Vázquez[2], Mikel Vicente-Pascual[1,2], Cristina Pereira[2], Daniel Vazquez-Justes[1,2], Coral Torres-Querol[2], Ana Vena[1,2], Sònia Abilleira[3], Pere Cardona[4], Carles Forné[5†], Xavier Jiménez-Fàbrega[6], Jorge Pagola[7], Manuel Portero-Otin[8], Ana Rodríguez-Campello[9], Àlex Rovira[10] and Joan Martí-Fàbregas[11]*

[1] Stroke Unit, Department of Neurology, Hospital Universitari Arnau de Vilanova de Lleida, Lleida, Spain, [2] Clinical Neurosciences Group, Institut de Recerca Biomèdica de Lleida (IRBLleida), Universitat de Lleida, Lleida, Spain, [3] Stroke Programme, Agency for Health Quality and Assessment of Catalonia, CIBER Epidemiología y Salud Pública (CIBERESP), Barcelona, Spain, [4] Stroke Unit, Hospital de Bellvitge, Hospitalet de Llobregat, Spain, [5] Department of Basic Medical Sciences, Universitat de Lleida, Lleida, Spain, [6] Servei d'Emergències Mèdiques, Hospitalet de Llobregat, Spain, [7] Stroke Unit, Neurology Department, Vall d'Hebron Hospital, Barcelona, Spain, [8] Department of Experimental Medicine, NUTREN-Nutrigenomics, Biomedical Institut de Recerca Biomèdica de Lleida (IRBLleida), Universitat de Lleida, Lleida, Spain, [9] Neurovascular Research Group, Neurology Department, Institut Hospital del Mar d'Investigacions Mèdiques-Hospital del Mar, Departament de Medicina, Universitat Autònoma de Barcelona, Barcelona, Spain, [10] Section of Neuroradiology and MRI Unit, Department of Radiology, Hospital Universitari Vall d'Hebron, Universitat Autònoma de Barcelona, Barcelona, Spain, [11] Stroke Unit, Hospital de Sant Pau, Barcelona, Spain

Rationale: Remote ischemic perconditioning during cerebral ischemia (RIPerC) refers to the application of brief episodes of transient limb ischemia commonly to a limb, it represents a new safe, simple and low-cost paradigm in neuroprotection.

Aim and/or Hypothesis: To evaluate the effects of RIPerC on acute ischemic stroke (AIS) patients, applied in the ambulance, to improve functional outcomes compared with standard of care.

Sample Size Estimates: A sample size of 286 patients in each arm achieves 80% power to detect treatment differences of 14% in the outcome, using a two-sided binomial test at significance level of 0.05, assuming that 40% of the control patients will experience good outcome and an initial misdiagnosis rate of 29%.

Methods and Design: We aim to conduct a multicentre study of pre-hospital RIPerC application in AIS patients. A total of 572 adult patients diagnosed of suspected clinical stroke within 8 h of symptom onset and clinical deficit >0 according to prehospital rapid arterial occlusion evaluation (RACE) scale score will be randomized, in blocks of size 4, to RIPerC or sham. Patients will be stratified by RACE score scale. RIPerC will be started in the ambulance before hospital admission and continued in the hospital if necessary. It will consist of five cycles of electronic tourniquet inflation and deflation (5 min each). The cuff pressure for RIPerC will be 200 mmHg during inflation. Sham will only simulate vibration of the device.

OPEN ACCESS

Edited by:
Bruno Meloni,
University of Western Australia, Australia

Reviewed by:
Craig S. Anderson,
University of New South Wales, Australia
Vasileios-Arsenios Lioutas,
Beth Israel Deaconess Medical Center and Harvard Medical School, United States

***Correspondence:**
Francisco Purroy
fpurroygarcia@gmail.com

†ORCID:
Francisco Purroy
orcid.org/0000-0002-1808-5968
Gloria Arque
orcid.org/0000-0002-8039-3726
Carles Forné
orcid.org/0000-0002-8133-3274

Specialty section:
This article was submitted to Stroke, a section of the journal Frontiers in Neurology

Received: 04 June 2020
Accepted: 27 August 2020
Published: 25 September 2020

Citation:
Purroy F, Arque G, Mauri G, García-Vázquez C, Vicente-Pascual M, Pereira C, Vazquez-Justes D, Torres-Querol C, Vena A, Abilleira S, Cardona P, Forné C, Jiménez-Fàbrega X, Pagola J, Portero-Otin M, Rodríguez-Campello A, Rovira À and Martí-Fàbregas J (2020) REMOTE Ischemic Perconditioning Among Acute Ischemic Stroke Patients in Catalonia: REMOTE-CAT PROJECT. Front. Neurol. 11:569696. doi: 10.3389/fneur.2020.569696

Study Outcome(s): The primary outcome will be the difference in the proportion of patients with good outcomes as defined by a mRS score of 2 or less at 90 days. Secondary outcomes to be monitored will include early neurological improvement rate, treatment related serious adverse event rates, size of the infarct volume, symptomatic intracranial hemorrhage, metabolomic and lipidomic response to RIPerC and Neuropsychological evaluation at 90 days.

Discussion: Neuroprotective therapies could not only increase the benefits of available reperfusion therapies among AIS patients but also provide an option for patients who are not candidates for these treatments. REMOTE-CAT will investigate the clinical benefit of RIC as a new neuroprotective strategy in AIS.

Clinical Trial Registration: www.ClinicalTrials.gov, identifier: NCT03375762.

Keywords: ischemic stroke, remote ischemic perconditioning (rPerC), neuroprotection, infarct size (IS), metabolomics (OMICS)

INTRODUCTION AND RATIONALE

Stroke is one of the leading causes of death worldwide and the main cause of disability (1). Currently, the only therapies for acute ischemic stroke (AIS) patients are the administration of rt-PA (2) and/or endovascular treatment (3). Unfortunately, many patients cannot benefit from these therapies due to their contraindications or evolution time. Neuroprotective therapies could not only increase the benefits of available reperfusion therapies but also provide an option for patients who are not candidates for these treatments (4). However, most neuroprotection trials have so far failed to demonstrate their efficacy in AIS patients, despite promising results in animal studies (4). Remote ischemic perconditioning (RIPerC) represents a new paradigm in neuroprotection (5). It potential upregulates endogenous defense systems to achieve ischemic tolerance in brain ischemia (6). It consists of brief episodes of transient limb ischemia. According to studies in coronary ischemia, RIPerC during the ischemic event is safe, feasible, and related to a decrease in myocardial injury (7). However, there is limited data about the clinical utility of RIPerC in AIS patients. Only four randomized clinical trials (RCTs) have been completed and published (8–11). All of them demonstrated that RIC is safe and feasible in AIS. One has been conducted to test RIPerC in a prehospital setting in AIS patients and as an adjunct treatment with intravenous alteplase (11). Two other small-size studies were only designed to evaluate the safety and feasibility of RIC in AIS patients recruited within 24 h of onset of symptoms (8) and in alteplase treated patients (9). The last and the largest study included 188 patients with confirmed carotid ischemic stroke within 6 h of symptoms onset (10). None of them demonstrated a significant clinical effect or a significant effect on brain infarction volume growth.

We aim to conduct a multicentre study of pre-hospital RIPerC in AIS patients applied within 8 h of stroke onset. Our hypothesis is that RIPerC would be safe and would induce endogenous neuroprotective phenomena associated with good outcomes in AIS patients treated with revascularization therapies or not.

METHODS

Design

REMOTE-CAT is a prospective randomized controlled multicentre clinical trial that follows CONSORT statement (12). The study will be performed in accordance with the standards of good clinical practice (International committee on Harmonization of E6 Guideline for Good Clinical Practice) and the latest revision of the Declaration of Helsinki. The study has been approved by the Ethics Committee on Clinical Research of the Hospital Universitari Arnau de Vilanova of Lleida (approval code 1744). All patients will provide written informed consent. The protocol is registered in ClinicalTrials.gov identifier is NCT03375762.

Patient Population

Inclusion and exclusion criteria are detailed in **Table 1**. Summarizing, REMOTE-CAT focuses on patients with suspected acute stroke identified in the pre-hospital setting by emergency medical services (EMS). The EMS is a public company responsible for urgent prehospital care including Code Stroke (CS) patients. We will include consecutive adult subjects (age $\geq$18 years old) with CS activation will be included. CS activation criteria include neurologic impairment suggestive of acute stroke according to FAST criteria (13), time from symptom onset of $<$8 h and previous functional independence (modified Rankin Scale, mRS$\leq$2). Patients should have at least motor impairment (**Figure 1**). Baseline assessments and study procedures are reported in **Table 2**.

Randomization

First, patients will be stratified using the rapid arterial occlusion evaluation (RACE) scale score (14) and then, they will be randomly allocated in blocks of size four, to either receive remote ischemic conditioning (RIPerC group) or sham in the ambulance. An on-call physician not involved in the study will perform the randomization using a computer program located in a web server.

TABLE 1 | Inclusion and exclusion criteria.

Inclusion criteria
• Age above 18 years old
• Suspected clinical stroke within 8 h of onset of neurological symptoms
• Stroke code (SC) activation
• Independent in daily living before the acute onset of symptoms (mRs ≤ 2)
• RACE score>0 and RACE motor score>0
• Written informed consent (patient or legal representative)
Exclusion criteria
• Unknown onset of symptoms
• Coma (GCS< 8)
• Malignancy or significant comorbidity thought to limit life expectancy to <6 months
• Pregnancy
• Participation in other clinical trial related with a research medical product/device

RACE, The rapid arterial occlusion evaluation scale; mRs, Modified Rankin scale; GCS, Glasgow Coma Scale.

Intervention

RIPerC will consist of automatically delivered five cycles of electronic tourniquet inflation to the upper non-paretic limb, each lasting 5 min and separated by 5 min of cuff deflation. The cuff will be inflated to 200 mmHg and it will be applied to the opposite arm to the one experiencing motor and/or sensory deficit in order to reduce the risk of phlebitis and to maintain the somatosensory stimuli. RIPerC will be initiated by the ambulance staff during transportation and it will be finished for all patients in the ambulance or during Hospital admission. All patients in both groups will be treated according to conventional care procedures following international guidelines. Thus, mechanical thrombectomy and intravenous fibrinolysis will be allowed. Revascularization therapies will not be delayed due to the study. The non-interventionist group will use a sham device. It will simulate vibration of the device but no inflation will be performed. Discomfort and complications related to RIPerC will be recorded.

Primary Outcome

The primary outcome will be the difference in the proportion of patients with good outcomes as defined by a mRS score of 2 or less at 90 days.

Secondary Outcomes

The secondary outcomes will be: (1) a decrease in the National Institutes of Health Stroke Scale (NIHSS) score greater or equal than 4 between baseline and day one, 5 ± 1 days and 90 ± 7 days; (2) a mRS score of 2 or less at 5 ± 1 days; (3) the rate of serious adverse events related to the intervention; (4) the rate of symptomatic intracerebral hemorrhage (SICH) defined by the Safe Implementation of Thrombolysis in Stroke Monitoring Study protocol at 24–36 hours (15); (5) acute infarct volume; (6) metabolomic and lipidomic response to RIC; and, (7) neuropsychological evaluation of cognitive and affective domains.

In all eligible patients, a brain MRI will be performed within 3–4 days of the onset of symptoms, including the following sequences: (1) transverse T2-FLAIR; (2) transverse T2*-weighted gradient-echo; (3) transverse diffusion-weighted (DWI) single-shot echo-planar spin-echo; and, (4) axial 3D time-of-flight MR angiography (through the circle of Willis). All participating centers will follow the same protocol. A neuroradiologist blinded to clinical features and intervention will review the MRI images. Infarct volume will be defined as the hyperintense area on the initial isotropic DWI acquired with a b value of 1,000 sec/mm2.

In addition, we will use metabolomic and lipidomic analyses to define a panel of serum biomarkers accurately related to RIC phenomenon. For these purposes, in 100 patients (50 sham and 50 RIPerC), blood samples for further determination of metabolomics and lipidomics will be drawn at arrival to hospital, at days 3 and 5 as previously performed (16, 17). As we did not have preliminary data and no metabolites have yet been defined we will performed a non-targeted metabolomics and lipidomic profiling in order to identify differential molecules found in the intervention group.

The neuropsychological evaluation will include Montreal cognitive assessment, trail making test part a and b, the Wechsler adult intelligence scale, the free and cued selective reminding test, the apathy evaluation scale and the Rey complex figure test. We also performed the Health-related quality of life assessment questionnaire (EQ-5D) at 90 days.

Data Monitoring Body

An independent data safety monitoring board (DSMB) will look after the safety of the study. It will ensure that the rate of SICH and serious adverse events is similar in the two groups. An interim analysis will be performed after the inclusion of the first 100 patients for early stopping due to safety reasons. Moreover, the DSMB could recommend stopping the study for safety reasons at any moment and make recommendations to the Executive Committee regarding efficacy, quality and feasibility of the study.

Sample Size Estimates

A sample size of 280 subjects in each arm achieves 80% power to detect treatment differences of 14% between the intervention and the control groups, using a two-sided binomial test at significance level of 0.05, assuming that 40% of the control patients will experience good outcome defined by a mRS score of 2 or less at 90 days, and allowing a misdiagnosis rate of 29% (15% of haemorrhagic strokes and 14% of mimic stroke conditions). Two extra interim analyses will be performed at 33 and 67% of recruitment on the primary outcome. Early stopping is planned if large differences between the study groups are observed in order to reduce study participants' exposure to the inferior study arm and saving time and resources. Since repeated significance testing on accumulating data will be performed, adjustment of the usual hypothesis testing procedure to maintain the overall significance level of 0.05 will be done by using the flexible type I error spending function (18, 19). Due to the interim analyses, the sample size must be increased by an inflation factor of 1.02, resulting in 572 patients (286 per group).

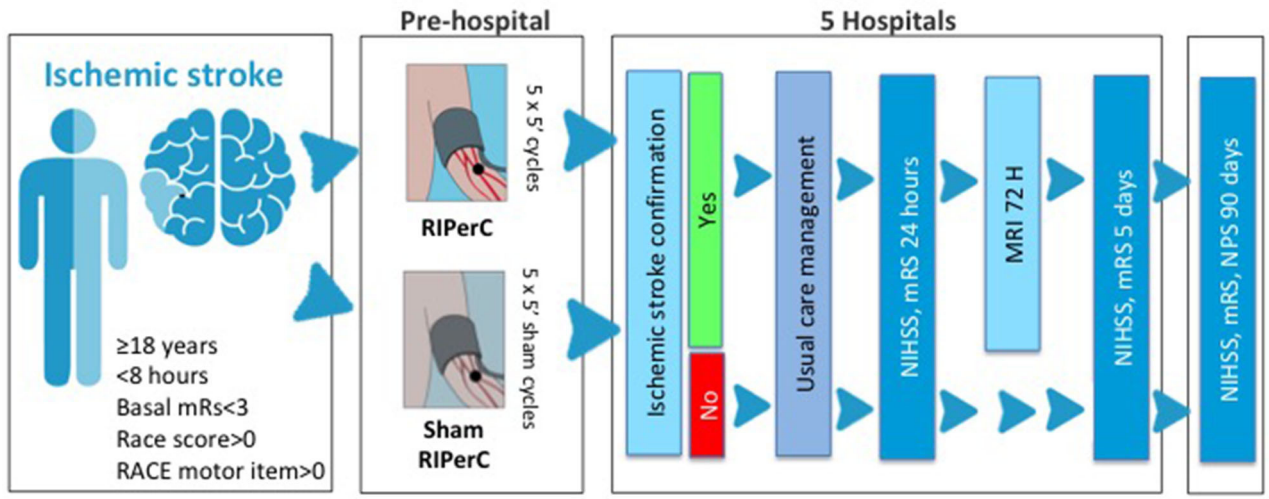

FIGURE 1 | Graphical representation of REMOTE-CAT clinical trial procedures. After Stroke Code activation in the ambulance, remote ischemic perconditioning (RIPerC) is applied by an automatic device during transportion to the nearest Stroke care center. Usual medical care will be performed in the stroke center.

Statistical Analyses

Included patients will be described with respect to demographic and clinical characteristics, according to the study arm. Continuous variables will be summarized using means and standard deviations for normally distributed data; or median and 25–75% percentiles for non-normally distributed data. Normal distribution will be assessed by means of the Shapiro–Wilks test, rejecting normality when $p < 0.05$. Categorical data will be summarized using counts and percentages. Comparisons will be performed by means of the Pearson's chi-squared test for categorical variables; the *t*-test for normally distributed data; and the Mann–Whitney *U*-test for non-normally distributed data.

Primary analysis will be performed by means of the binomial test. If the study groups are unbalanced, the primary outcome will be compared using a logistic regression model that will include the variables exhibiting baseline differences as covariates.

Secondary outcomes will be compared using the most appropriate test according to the distribution of the data. As with the primary analysis, secondary outcomes and safety outcome analyses will be conducted using multivariable generalized linear models with suitable links.

The analysis will be performed on the intention-to-treat set and will be repeated on the per-protocol set as a sensitivity analysis.

Stratified Analysis

All objectives will be assessed in the following stratified analyses: (i) by sex; (ii) depending on whether patients have undergone thrombectomy; (iii) depending on whether patients have undergone thrombectomy and treated with rtPA; (iv) whether patients have undergone thrombectomy or treated with rtPA; and (v) number of cycles of inflation and deflation finished to evaluate a possible dose-response effect.

Handling Missing Data

If there are missing data, they will be reported for each variable and missingness mechanism will be explored. Missing values could depend on other observed data. We will consider these missing values as missing at random (MAR). If there is no correlation between the missing values and other observed data (i.e., the Little's test is not statistically significant, $p > 0.05$) missing values will be considered missing completely at random (MCAR) (20). If missing values are MAR, a series of multiple imputations by chained equations will be performed and the Rubin's rules will be used to combine variable estimates and standard errors (21). If missing values are MCAR, complete case analysis will be performed.

Current Status of the Trial

The study started recruitment in August 2019 in one Hospital, and the estimated completion date is August 2022. At 1st August 2020: 76 patients have been recruited.

Study Organization and Funding

FP is the coordinating investigator of the study, which is funded by a grant from the Spanish National Ministry of Heath—PI17/01725.

DISCUSSION

RIPerC emerges as an interesting neuroprotective strategy (5). Our study improves the previous limited experience in humans (8, 11). It includes all AIS with symptom onset within 8 h and not only intravenous alteplase treated patients (11). According to the animal model, it is effective when applied both alone and in combination with revascularization therapies (22, 23). Although few studies have been published about the effect of RIC in AIS, some important issues have been learned (8–11). As in Hougaard's trial (11) and in most of the trials involving

TABLE 2 | Study procedures for eligible patients with AIS.

Time points	Prehospital	Admission	24 h	3 days	5 days	3 months
Enrollment						
Eligibility screen	✓					
Patient/family information	✓	✓				
Acute waiver of consent	✓					
Randomization	✓					
RACE scale	✓					
Blood pressure	✓	✓‡				
Informed consent		✓				
AIS confirmation		✓*			✓*	
Demographics and medical history		✓				
Reperfusion therapies		✓				
Intervention						
RIC/Sham application	✓					
Complications related to RIC		✓	✓		✓	✓
Assessment						
NIHSS		✓	✓		✓	✓
Modified Rankin scale		✓			✓	✓
Neuroimaging		✓	✓#			
MRI				✓		
Blood biomarkers		✓		✓	✓	
Stroke etiology					✓	
Quality of life						✓
Neuropsychological evaluation						✓
Safety measurement						
Intrahospital complications					✓	✓
SICH			✓		✓	

RACE, rapid arterial occlusion evaluation; AIS, acute ischemic stroke; RIC, remote ischemic conditioning; MRI, magnetic resonance imaging; NIHSS, National Institutes of Health Stroke Scale. ‡*Blood pressure will be reported at the end of RIC/Sham application and 1 h after.* **Patients with intracranial hemorrhage will complete the 90 days follow-up. Patients without evidence of brain ischemia will be followed until discharge and through registries.* #*Patients treated with intravenous rtPA and/or EVT will undergo neuroimaging at 24 h.*

patients with myocardial infarction (7, 24) it is applied it in the ambulance, as soon as possible, in order to induce the maximum effect. This action seems to be safe although the definitive diagnosis will not be established until the arrival at the hospital. To date, no serious adverse effects have been reported in RIC studies (5, 7–11, 25). The recent RCT published by Pico et al. failed to demonstrate an effect of RIC in the final infarction size in AIS. One explanation of their neutral results was that the treatment with RIC was performed too late during or after the receipt of reperfusion therapies (10). In addition, we will increase the number of cycles to five. Most RIC trials use the four-cycle protocol (7, 11) due to tradition. The ischemic conditioning phenomena was first demonstrated using this protocol in an animal model of myocardial infarction (26). Recent studies in animal models address the need to increase the number of cycles in order to optimize the efficacy of RIPerC (27). Some other recent successes in remote ischemic preconditioning (28) and chronic postconditioning (29) in AIS patients have used the 5-cycle protocol. Increasing the duration of the cycle to 10 min does not offer any further protection (27). Although the quantity of muscle mass affects the efficacy of the intervention, we decided to perform the RIPerC on an upper arm rather than on a leg for safety reasons as up to one in four AIS patients have silent peripheral arterial disease defined by a low ankle-brachial index (30). One of the main shortcomings of the previously mentioned Hougaard's trial (11) was that fewer than one out of three patients complete the four cycles of limb ischemia. We will therefore use an automatic device. To avoid misdiagnosis only subjects with RACE score of >0 and RACE motor items >0 will be included. Finally, according to the stroke treatment academic industry roundtable (STAIR) recommendations a clinical endpoint would clearly evaluate the utility of applying RIPerC in AIS patients.

SUMMARY AND CONCLUSIONS

RIPerC represents a new paradigm in neuroprotection with limited data in AIS patients. According to previous preclinical and clinical studies of acute ischemia, a clinical RIPerC trial should include both candidates and non-candidates for reperfusion therapies. As the RIPerC effect decreases with time, RIPerC should be started during the transfer of stroke code patients. The size of the trial should be large enough to detect differences in clinical outcomes and not only neuroimaging endpoints. Finally, the RIC device should be automatic to not only ensure that

patients finish all of the programmed cycles but also to interfere as little as possible with the work of paramedics during the transfer and of nurses and physicians during the admission.

ETHICS STATEMENT

The studies involving human participants were reviewed and approved by the Ethics Committee on Clinical Research of the Hospital Universitari Arnau de Vilanova de Lleida. The patients/participants provided their written informed consent to participate in this study.

AUTHOR CONTRIBUTIONS

FP conceived the study and wrote the paper. FP, GM, CG-V, MV-P, DV-J, and GA were involved in protocol development and study conduct. GA, CF, and SA substantively revised the manuscript. All authors read and approved the final manuscript.

FUNDING

This study was supported by the Government of Catalonia-Agència de Gestió d'Ajuts Universitaris i de Recerca (FP: 2017 SGR 1628), Instituto de Salud Carlos III and co-funded by European Union (ERDF A way to make Europe) (FP: Project PI17-01725) and the INVICTUS plus Research Network (Carlos III Health Institute).

ACKNOWLEDGMENTS

The content of this manuscript has been presented in part at the European Stroke Organization Conference in 2018, European Stroke Journal 2018, Vol. 3(1S) 160.

REFERENCES

1. Mozaffarian D, Benjamin EJ, Go AS, Arnett DK, Blaha MJ, Cushman M, et al. American heart association statistics and stroke statistics, heart disease and stroke statistics-2016 update: a report from the American heart association. *Circulation.* (2016) 133:e38–360. doi: 10.1161/CIR.0000000000000350
2. Demaerschalk BM, Kleindorfer DO, Adeoye OM, Demchuk AM, Fugate JE, Grotta JC, et al. American heart association stroke, council on and prevention, scientific rationale for the inclusion and exclusion criteria for intravenous alteplase in acute ischemic stroke: a statement for healthcare professionals from the American heart association/American stroke association. *Stroke.* (2016) 47:581–641. doi: 10.1161/STR.0000000000000086
3. Saver JL, Goyal M, van der Lugt A, Menon BK, Majoie CB, Dippel DW, et al. Time to treatment with endovascular thrombectomy and outcomes from ischemic stroke: a meta-analysis. *JAMA.* (2016) 316:1279–88. doi: 10.1001/jama.2016.13647
4. Chamorro A, Dirnagl U, Urra X, Planas AM. Neuroprotection in acute stroke: targeting excitotoxicity, oxidative and nitrosative stress, and inflammation. *Lancet Neurol.* (2016) 15:869–81. doi: 10.1016/S1474-4422(16)00114-9
5. Hess DC, Blauenfeldt RA, Andersen G, Hougaard KD, Hoda MN, Ding Y, et al. Remote ischaemic conditioning-a new paradigm of self-protection in the brain. *Nat Rev Neurol.* (2015) 11:698–710. doi: 10.1038/nrneurol.2015.223
6. Purroy F, Garcia C, Mauri G, Pereira C, Torres C, Vazquez-Justes D, et al. Induced neuroprotection by remote ischemic perconditioning as a new paradigm in ischemic stroke at the acute phase, a systematic review. *BMC Neurol.* (2020) 20:266. doi: 10.1186/s12883-020-01836-8
7. Man C, Gong D, Zhou Y, Fan Y. Meta-analysis of remote ischemic conditioning in patients with acute myocardial infarction. *Sci Rep.* (2017) 7:43529. doi: 10.1038/srep43529
8. England TJ, Hedstrom A, O'Sullivan S, Donnelly R, Barrett DA, Sarmad S, et al. RECAST (Remote ischemic conditioning after stroke trial): a pilot randomized placebo controlled phase II trial in acute ischemic stroke. *Stroke.* (2017) 48:1412–15. doi: 10.1161/STROKEAHA.116.016429
9. Che R, Zhao W, Ma Q, Jiang F, Wu L, Yu Z, et al. rt-PA with remote ischemic postconditioning for acute ischemic stroke. *Ann Clin Transl Neurol.* (2019) 6:364–72. doi: 10.1002/acn3.713
10. Pico F, Lapergue B, Ferrigno M, Rosso C, Meseguer E, Chadenat ML, et al. Effect of in-hospital remote ischemic perconditioning on brain infarction growth and clinical outcomes in patients with acute ischemic stroke: the RESCUE BRAIN randomized clinical trial. *JAMA Neurol.* (2020) 77:1–11. doi: 10.1001/jamaneurol.2020.0326
11. Hougaard KD, Hjort N, Zeidler D, Sørensen L, Nørgaard A, Hansen TM, et al. Remote ischemic perconditioning as an adjunct therapy to thrombolysis in patients with acute ischemic stroke: a randomized trial. *Stroke.* (2014) 45:159–67. doi: 10.1161/STROKEAHA.113.001346
12. Schulz KF, Altman DG, Moher D, Group C. CONSORT 2010 statement: updated guidelines for reporting parallel group randomised trials. *BMJ.* (2010) 340:c332. doi: 10.1136/bmj.c332
13. Harbison J, Hossain O, Jenkinson D, Davis J, Louw SJ, Ford GA. Diagnostic accuracy of stroke referrals from primary care, emergency room physicians, and ambulance staff using the face arm speech test. *Stroke.* (2003) 34:71–6. doi: 10.1161/01.STR.0000044170.46643.5E
14. Perez de la Ossa N, Carrera D, Gorchs M, Querol M, Millan M, Gomis M, et al. Design and validation of a prehospital stroke scale to predict large arterial occlusion: the rapid arterial occlusion evaluation scale. *Stroke.* (2014) 45:87–91. doi: 10.1161/STROKEAHA.113.003071
15. Wahlgren N, Ahmed N, Davalos A, Ford GA, Grond M, Hacke W, et al. Thrombolysis with alteplase for acute ischaemic stroke in the safe implementation of thrombolysis in stroke-monitoring study (SITS-MOST): an observational study. *Lancet.* (2007) 369:275–82. doi: 10.1016/S0140-6736(07)60149-4
16. Purroy F, Cambray S, Mauri-Capdevila G, Jove M, Sanahuja J, Farre J, et al. Metabolomics predicts neuroimaging characteristics of transient ischemic attack patients. *EBioMed.* (2016) 3964:30514–X. doi: 10.1016/j.ebiom.2016.11.010
17. Jove M, Mauri-Capdevila G, Suarez I, Cambray S, Sanahuja J, Quilez A, et al. Metabolomics predicts stroke recurrence after transient ischemic attack. *Neurology.* (2015) 84:36–45. doi: 10.1212/WNL.0000000000001093
18. Kim K, DeMets DL. Confidence intervals following group sequential tests in clinical trials. *Biometrics.* (1987) 43:857–64. doi: 10.2307/2531539
19. Lan KKG, DeMets DL. Discrete sequential boundaries for clinical trials. *Biometrika.* (1983) 70:659–63. doi: 10.1093/biomet/70.3.659
20. Jakobsen JC, Gluud C, Wetterslev J, Winkel P. When and how should multiple imputation be used for handling missing data in randomised clinical trials - a practical guide with flowcharts. *BMC Med Res Methodol.* (2017) 17:162. doi: 10.1186/s12874-017-0442-1
21. White IR, Royston P, Wood AM. Multiple imputation using chained equations: issues and guidance for practice. *Stat Med.* (2011) 30:377–99. doi: 10.1002/sim.4067
22. Hoda MN, Siddiqui S, Herberg S, Periyasamy-Thandavan S, Bhatia K, Hafez SS, et al. Remote ischemic perconditioning is effective alone and in combination with intravenous tissue-type plasminogen activator in murine model of embolic stroke. *Stroke.* (2012) 43:2794–9. doi: 10.1161/STROKEAHA.112.660373
23. Hahn CD, Manlhiot C, Schmidt MR, Nielsen TT, Redington AN. Remote ischemic per-conditioning: a novel therapy for acute stroke? *Stroke.* (2011) 42:2960–2. doi: 10.1161/STROKEAHA.111.622340

24. McLeod SL, Iansavichene A, Cheskes S. Remote ischemic perconditioning to reduce reperfusion injury during acute st-segment-elevation myocardial infarction: a systematic review and meta-analysis. *J Am Heart Assoc.* (2017) 6:e005522. doi: 10.1161/JAHA.117.005522
25. Zhao W, Che R, Li S, Ren C, Li C, Wu C, et al. Remote ischemic conditioning for acute stroke patients treated with thrombectomy. *Ann Clin Transl Neurol.* (2018) 5:850–6. doi: 10.1002/acn3.588
26. Murry CE, Jennings RB, Reimer KA. Preconditioning with ischemia: a delay of lethal cell injury in ischemic myocardium. *Circulation.* (1986) 74:1124–36. doi: 10.1161/01.CIR.74.5.1124
27. Johnsen J, Pryds K, Salman R, Lofgren B, Kristiansen SB, Botker HE. The remote ischemic preconditioning algorithm: effect of number of cycles, cycle duration and effector organ mass on efficacy of protection. *Basic Res Cardiol.* (2016) 111:10. doi: 10.1007/s00395-016-0529-6
28. Zhao W, Meng R, Ma C, Hou B, Jiao L, Zhu F, et al. Safety and efficacy of remote ischemic preconditioning in patients with severe carotid artery stenosis before carotid artery stenting: a proof-of-concept, randomized controlled trial. *Circulation.* (2017) 135:1325–35. doi: 10.1161/CIRCULATIONAHA.116.024807
29. Meng R, Asmaro K, Meng L, Liu Y, Ma C, Xi C, et al. Upper limb ischemic preconditioning prevents recurrent stroke in intracranial arterial stenosis. *Neurology.* (2012) 79:1853–61. doi: 10.1212/WNL.0b013e318271f76a
30. Purroy F, Coll B, Oró M, Setó E, Piñol-Ripoll G, Plana A, et al. Predictive value of ankle brachial index in patients with acute ischaemic stroke. *Eur J Neurol.* (2010) 17:602–6. doi: 10.1111/j.1468-1331.2009.02874.x

Conflict of Interest: The authors declare that the research was conducted in the absence of any commercial or financial relationships that could be construed as a potential conflict of interest.

frontiers in Neurology

SYSTEMATIC REVIEW
published: 27 October 2020
doi: 10.3389/fneur.2020.566124

The Role of DNA Methylation in Ischemic Stroke: A Systematic Review

Minyan Zeng[1], Juanying Zhen[1,2], Xiaodan Zheng[1,2], Hongyan Qiu[1], Xiaonan Xu[1], Jun Wu[1], Zhijian Lin[1] and Jun Hu[1]**

[1] Department of Neurology, Peking University Shenzhen Hospital, Shenzhen, China, [2] Department of Clinical Medicine, Shantou University Medical College, Shantou, China

Background: Knowledge about the classic risk and protective factors of ischemic stroke is accumulating, but the underlying pathogenesis has not yet been fully understood. As emerging evidence indicates that DNA methylation plays a role in the pathological process of cerebral ischemia, this study aims to summarize the evidence of the association between DNA methylation and ischemic stroke.

Methods: MEDLINE, EMBASE, PubMed, and Cochrane Central Register of Controlled Trials were searched for eligible studies. The results reported by each study were summarized narratively.

Results: A total of 20 studies with 7,014 individuals finally met the inclusion criteria. Three studies focused on global methylation, 11 studies on candidate-gene methylation, and six on epigenome-wide methylation analysis. Long-interspersed nuclear element 1 was found to be hypomethylated in stroke cases in two studies. Another 16 studies reported 37 genes that were differentially methylated between stroke cases and controls. Individuals with ischemic stroke were also reported to have higher acceleration in Hanuum 's epigenetic age compared to controls.

Conclusion: DNA methylation might be associated with ischemic stroke and play a role in several pathological pathways. It is potentially a promising biomarker for stroke prevention, diagnosis and treatment, but the current evidence is limited by sample size and cross-sectional or retrospective design. Therefore, studies on large asymptomatic populations with the prospective design are needed to validate the current evidence, explore new pathways and identify novel risk/protective loci.

Keywords: DNA, methylation, ischemic, stroke, systematic, review

OPEN ACCESS

Edited by:
Bruno Meloni, University of Western Australia, Australia

Reviewed by:
Zheng Gang Zhang, Henry Ford Hospital, United States
Amery Treble-Barna, University of Pittsburgh, United States

***Correspondence:**
Zhijian Lin
linzjpush@pkuszh.com
Jun Hu
dochj@163.com

Specialty section:
This article was submitted to Stroke, a section of the journal Frontiers in Neurology

Received: *27 May 2020*
Accepted: *28 September 2020*
Published: *27 October 2020*

Citation:
Zeng M, Zhen J, Zheng X, Qiu H, Xu X, Wu J, Lin Z and Hu J (2020) The Role of DNA Methylation in Ischemic Stroke: A Systematic Review. Front. Neurol. 11:566124. doi: 10.3389/fneur.2020.566124

INTRODUCTION

Stroke is one of the major causes of death and disability worldwide, leading to substantial public health issues and medical costs. Currently, the global burden of stroke remains high with 80.1 million prevalent cases and 5.5 million deaths in 2016 (1). Besides, stroke burden has also been increasing in adults aged under 64 years (2, 3), suggesting that scaled-up prevention strategies with wider coverage are needed.

The knowledge of the classic factors which are associated with ischemic stroke (IS) is accumulating, mostly in the aspects of demographic characteristics, psychosocial status, cognitive function, health behavior, medication use, and cardiometabolic comorbidities (4). However, the underlying pathogenesis has not yet been fully understood. The substantial advance in the research of epigenetic modifications might provide new insights into this field and help understand additional pathological mechanisms (5, 6). DNA methylation is one of the most understood epigenetic mechanisms (7). It refers to the process of one or more methyl groups being added to a cytosine residual without changing the DNA sequence, which thereby modulates gene transcription and expression as well as many other cellular processes (8). Since DNA methylation is influenced by many environmental exposures throughout the life course (9, 10), it reflects the environment-gene interaction. It has been proved to be associated with some common diseases such as cancer (11–14), psychiatric disorders (15), and dementia (16). Emerging evidence indicated the multi-faceted role of DNA methylation in various pathological mechanisms of cerebral ischemia (6). One of the mechanisms might be its promoting effects on neuronal cell death, as researchers observed that mice who expressed lower levels of DNA methyltransferase, a catalyst of DNA methylation, were protected from cerebral ischemia (17). Other possible mechanisms include deficiency of methylenetetrahydrofolate reductase (*MTHFR*), X chromosome inactivation, aberrant homeostasis regulation, increasing oxidative stress, and abnormal modulation of synaptic plasticity (6, 18, 19). Since DNA methylation is modifiable by lifestyle factors and medical intervention, such as mental, social, and dietary factors (20, 21) it might be a promising biomarker for stroke prevention, diagnosis, and targeted neuroprotective therapy.

We aimed to conduct a systematic review according to current research literature to investigate the association of DNA methylation with the occurrence of IS. This will help update the latest evidence of the potential role of DNA methylation in cerebral ischemia and provide new insights for future research.

METHODS

Literature Search

The systematic review was conducted in line with the Preferred Reporting Items for Systematic Review and Meta-Analyses (PRISMA) guidelines (22). We conducted the literature search systematically in four databases—MEDLINE, EMBASE, PubMed, and Cochrane Central Register of Controlled Trials from inception to April 29th, 2020. To supplement the searching result of electronic databases, we manually searched the included studies' references and unpublished studies from The Preprint Server for Biology as well as The Preprint Server for Health Science. A series of text terms and thesaurus related to DNA methylation and IS were used, with the detailed search strategies included in **Supplementary Table 1**. To make the search results more comprehensive, "s-adenosylmethionine," a unique methyl donor in DNA methylation, was included in the search terms. We also included "CpG islands" as these are regions in gene promotor in which methylation is associated with epigenetic silencing (23, 24). The literature search was restricted to human studies.

Study Selection

Two reviewers (MZ and JZ) independently screened the titles and abstracts to initially assess the relevance of studies to this systematic review. Studies meeting the inclusion criteria were subsequently assessed by full-text reading. Studies were included if they quantitatively assessed the association between the level of DNA methylation (global, candidate-gene, or genome-wide) and the diagnosis of IS. Only the studies that involved at least one or more individuals with a diagnosis of IS, or followed individuals until such a diagnosis was made were eligible. No restrictions on methods/approaches for IS diagnosis or DNA methylation measures were imposed. Studies were excluded if they: (1) were animal studies, editorials, erratum, letters, reviews, and case reports; (2) investigated irrelevant outcomes, exposures, or comparisons. A third reviewer (ZL or JH) was involved for consensus after discussion if there was a discrepancy between the results from the two reviewers in the initial screening.

Data Extraction

Two reviewers (MZ and JZ) independently extracted the relevant data from the full-texts and supplementary materials from the eligible articles using a standardized extraction form. Data extracted included study design, characteristics of the study subjects, IS diagnostic approach, tissue sources of DNA, genes of interest, platforms of DNA methylation analysis, methylation patterns, and main findings relevant to the aim of this review. Discrepancies between the two reviewers were resolved through discussion and consultation with a third reviewer (ZL or JH).

Assessment of Methodological Quality

The Newcastle-Ottawa Scale (NOS) was used to assess the risk of bias and quality of the studies (25). This scale is focused on several aspects, including the selection of study participants, comparability, and the measurement of exposure and outcome. The score of NOS ranges from 0 to 9 for case-control, cohort studies, and cross-sectional studies. A study with 6 stars or lower was regarded as a high risk of bias; 7 or 8 stars as medium risk of bias; 9 stars as low risk of bias. Two reviewers (MZ and JZ) independently conducted the quality assessment, and disagreements were resolved by discussion and reconfirmation with a third reviewer (ZL or JH).

Data Synthesis

Results were summarized narratively. Data synthesis was not conducted due to the heterogeneity across studies.

RESULTS

Search Results

As shown in **Figure 1**, a total of 2,398 articles were identified via the initial search. Subsequently, 1,577 articles, including editorials, erratum, letters, reviews, case reports, animal studies,

and irrelevant articles, were further excluded. After full-text assessment of the remaining 115 articles, 20 articles with 7,014 individuals fulfilled the inclusion criteria and were finally included in this systematic review.

Summary of Findings

The characteristics of eligible studies were shown in **Supplementary Table 2**. Of the 20 studies, 17 were case-control studies (26–42), two were prospective cohort studies (43, 44), and one was a cross-sectional study (45). Participants of the included studies were mostly older adults, with mean age ranging from 47.4 to 75.0 years. Nineteen studies recruited both male and female participants, while one study included males only (44). Eighteen studies had an independent evaluation for the diagnosis of IS and claimed the use of imaging tests such as brain computed tomography, magnetic resonance imaging, or magnetic resonance diffusion weighted imaging (26–42, 44). Nineteen out of 20 studies assessed DNA methylation from acute/subacute stroke patients (26–44). Seventeen studies were assessed as high or medium-quality, and three studies were evaluated as low-quality (**Supplementary Table 3** for case-control studies, **Supplementary Table 4** for cohort studies and cross-sectional studies).

Tables 1–3 summarizes the main relevant findings from the eligible studies. Fourteen studies extracted DNA from whole peripheral blood and the rest from peripheral blood leukocytes ($n = 6$). Eighteen studies reported differential patterns of DNA methylation between individuals with and without IS, but results were unable to be synthesized for a meta-analysis due to high heterogeneity across studies. Therefore, relevant results are narratively summarized below.

Global Methylation

A total of three studies measured global methylation level in relation to IS, with two using *LINE-1* repetitive elements and one using *ALU* plus *Satellite 2* repetitive elements. Among these three studies, one used a cross-sectional study design (35), and the other two used prospective study designs (43, 44) (**Supplementary Table 2**). However, one of prospective studies did not report the follow-up results of DNA methylation with IS (43). All three studies adjusted for risk factors to control the bias (**Supplementary Table 2**).

Findings of the association between global methylation and IS were summarized in **Table 1**. Two of the studies found that *LINE-1* was hypomethylated in IS patients. Specifically, Baccarelli et al. (44) indicated that lower *LINE-1* methylation level was associated with higher IS prevalence (every 2.5% 5-methylcytosine decrease in *LINE-1* methylation, OR = 1.90, 95%CI = 1.16–3.10), but this association did not reach statistical significance for IS incidence in follow-up analyses(every 2.5% 5-methylcytosine decrease in *LINE-1* methylation, OR = 1.80, 95%CI = 0.72–4.46). Lin et al. (35) also found that IS patients had lower *LINE-1* methylation level (IS vs. control: 75.9 vs. 77.0%, $p = 0.0024$). After the adjustment for risk factors, this association still existed in male patients (every 1% decrease in *LINE-1* methylation, OR = 1.20, 95%CI = 1.10–1.32). No associations were observed in the study estimating *ALU* and *Satellite 2* in relation to IS (43).

Candidate Gene Methylation

The main findings from studies of candidate gene methylation were summarized in **Table 2**. There were 11 studies (case-control studies) that compared the methylation levels of candidate genes between the IS cases and controls. Eight studies measured DNA methylation in the promoter region and three measured in the gene body. Nine studies adjusted for risk factors to control the bias (**Supplementary Table 2**).

Overall, IS cases showed lower methylation levels in the promoter region of four genes, including human tumor necrosis factor (*TNF-α*) (26), estrogen receptor α (*ERα*) (28), matrix metalloproteinase-2 (*MMP-2*) (29), and microRNA223 (*MIR-223*) (33). In contrast, seven genes showed higher methylation levels in IS cases compared to controls. These include the promoter regions of apolipoprotein E (*APOE*) (30), tumor protein p53 (*TP53*) (32), thrombomodulin (*TM*) (34), and Cystathionine β-synthase (*CBS*) (41) and gene body of methylenetetrahydrofolate reductase (*MTHFR*) (31), ATP-binding cassette G1 (*ABCG1*) (38), and S-adenosylhomocysteine hydrolase (*AHCY*) (42). The methylation level of Paraoxonase (*PON*) promoter was observed to be interacting with energy intake in IS cases (26). No associations were observed in the gene body of *APOE* methylation and IS (38). Furthermore, two studies conducted sub-analyses according to stroke subtypes. One found that women with large-artery atherosclerosis and cardio-embolic (LAA/CE) had lower methylation levels of *ERα* promoter (28), and the other one found *MMP-2* promoter being hypomethylated in men with small-vessel stroke (29).

Epigenome-Wide Methylation

The main findings of the epigenome-wide association studies (EWAS) were summarized in **Table 3**. Six studies (five case-control studies and one cross-sectional study) used this hypothesis-free approach. Specifically, one case-control study investigated IS in relation to two types of DNA methylation age, which were calculated according to the methylation level of 353 and 71 CpG probes across the genome, respectively (36). It found that individuals with an IS diagnosis had higher age acceleration (the residual results from regressing DNA methylation age on chronological age) in the epigenetic clock calculated by Hannum's method. However, no associations were observed when using Havorth's method. The other five studies identified potential DNA methylation sites without a pre-specified hypothesis that they were related to IS. Among which, a maximum of 438 CpG sites were identified to be differentially methylated in IS cases compared to controls. Four studies conducted validation tests, and 26 candidate genes were detected to be associated with IS (27, 37, 39, 40). However, one study observed no association between methylation and IS (45). Three studies conducted enrichment analyses showing that the identified loci were related to several biological pathways including, inflammation, angiogenesis, metabolic, and immune-related function (27, 39, 40).

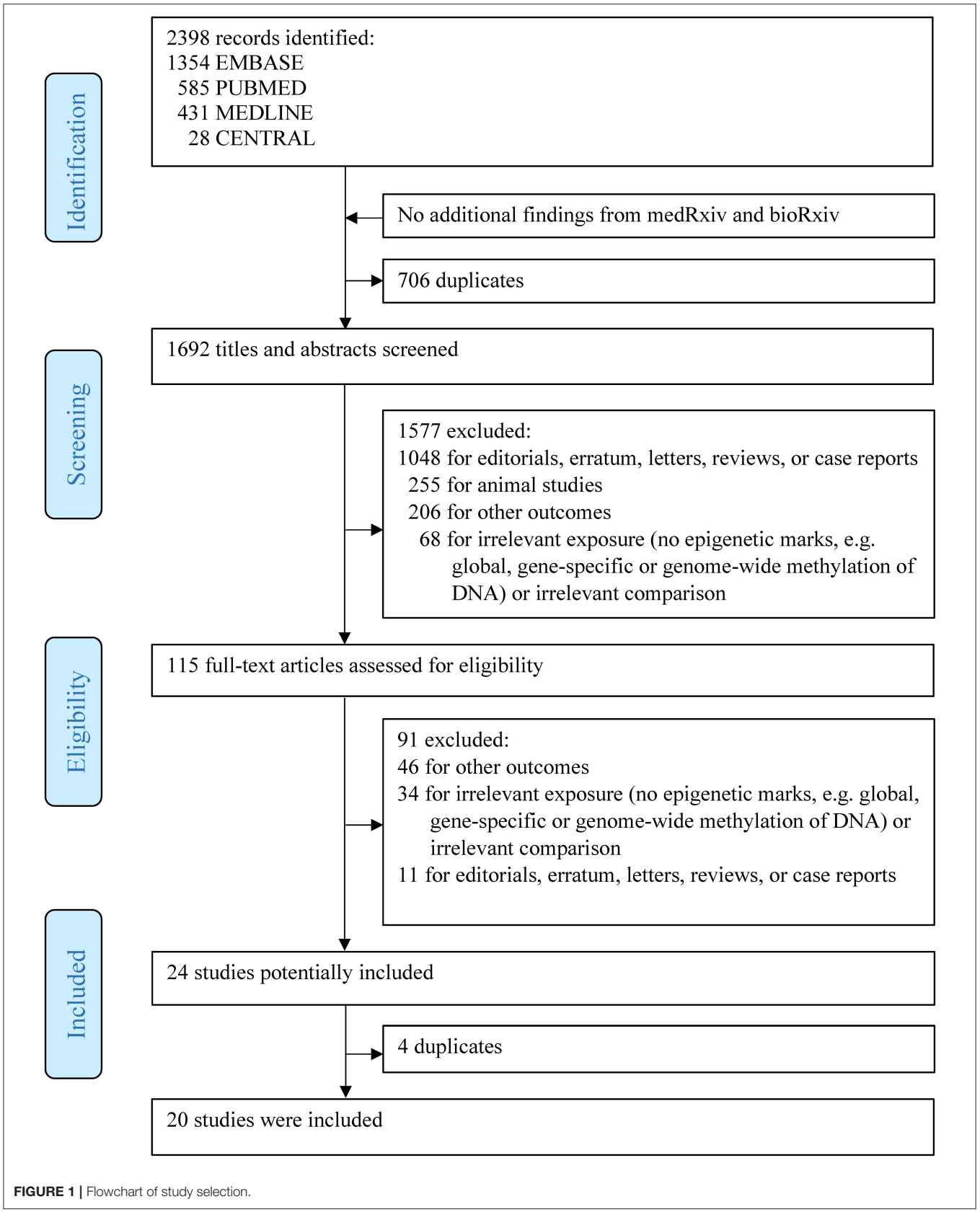

FIGURE 1 | Flowchart of study selection.

TABLE 1 | Global methylation analysis for ischemic stroke.

Study	Sample size	Tissue	Methylation sites, platform	Methylation pattern*	Main relevant findings
(35)[a]	Case: $n = 280$ Control: $n = 280$	Peripheral blood leukocytes	*LINE-1* repetitive elements, pyrosequencing	Hypomethylation	• Mean methylation level: case vs. control, 75.9 vs. 77.0%, $p = 0.0024$; male: case vs. control, 75.7 vs. 77.3%, $p = 0.0012$; female, case vs. control, 76.2 vs. 76.7%, $p = 0.3010$. • Men: per 1% decrease in *LINE-1* methylation level, OR = 1.20, 95% CI: 1.10–1.32, $p < 0.0001$; women: not stated.
(43)	Cohort: $n = 286$ (Stroke: $n = 4$)	Peripheral blood leukocytes	*ALU* and *Satellite 2* repetitive elements, MethyLight-based assay	No association	• Prevalence stroke (baseline): no difference was observed in geometric mean methylation level between cases and controls (215 vs. 147, $p = 0.15$). • Incident stroke (follow-up): not analyzed.
(44)	Cohort: $n = 712$ (Stroke: Baseline: $n = 51$, Follow-up: $n = 8$)	Peripheral blood leukocytes	*LINE-1* repetitive elements, pyrosequencing	Hypomethylation	• Prevalent stroke (baseline): per 2.5% decrease in methylation level, OR = 1.90, 95% CI: 1.16–3.10. • Incident stroke (follow-up): per 2.5% decrease in methylation level, OR = 1.80; 95% CI, 0.72–4.46.

LINE-1, long-interspersed nuclear element 1; OR, odds ratio; CI, confidence interval.
**Methylation pattern refers to the methylation alteration of the site(s) in stroke cases compared to non-stroke controls.*
[a]*Overlapping participant.*

DISCUSSION

This systematic review involving 7,014 individuals suggested that DNA methylation appeared to be associated with the occurrence of IS. Thirty-two genes were found to be hypermethylated and five were hypomethylated in stroke cases compared to controls. *LINE-1* methylation and epigenetic clock also showed an association with IS. Gender might influence the differences of DNA methylation levels in stroke subtypes, such as LAA/CE and small-vessel stroke. Energy taking and obesity were found to be interacting with the methylation level of specific loci in IS cases.

Methods of DNA Methylation Analysis

According to different laboratory processes, conditions, and methods of data analysis, DNA methylation analysis can be categorized into three main types, including global, gene-specific, and epigenome-wide methylation analysis (46). All studies included in this review used one of the methods to measure the DNA methylation accordingly and explored their relationship with IS.

Global methylation refers to the overall level of 5-methylcytosine content in the genome. This is mostly measured using repetitive elements which constitute approximately 55% of the human genome and account for a significant fraction of DNA methylation in human (47–49). Analyses of candidate gene methylation, on the other hand, are focused on the methylation level of one or more specific sites which were pre-selected based on their possible involvement in the pathological mechanism (50). This analysis approach investigates the role of epigenetic modifications according to the functions of these candidate genes. In terms of epigenome-wide methylation, studies of this type utilize wide arrays to quantify the DNA methylation level of particular sites across the genome, in order to discover disease-associated methylated sites without a predilection on specific loci using a hypothesis-free approach. Due to such heterogeneity in analysis methodologies, it is difficult to directly compare the results of previous studies, especially for external validation, even though great efforts have been made to help standardize the analysis approach and improve the reliability of the findings (51).

Global DNA Methylation

Global DNA Methylation and Stroke

Methylation levels of *LINE-1*, *ALU* and *Satellite 2* repeats were found to be significantly associated with global DNA methylation as measured by high-performance liquid chromatography (52). Therefore, the average methylation levels of these elements are commonly considered as surrogates to express the methylation level of total cytosine in the genome (53, 54). Two studies included in the present review found that individuals with IS had lower methylation level of LINE-1, and it is worth noting that one of them observed this association prospectively. The consistent trend of association found in the robust cohort study could provide stronger evidence that *LINE-1* hypomethylation plays an important role in the pathogenesis of IS at a pre-clinical stage in the asymptomatic individuals and thus might be considered as an early etiologic factor.

Possible Pathological Mechanisms of Global Methylation

LINE-1 accounts for approximately 17% of the genome sequence, and it is the only type of elements that can be activated in *LINE* families (49). Hypomethylated alternation of *LINE-1* in somatic cells may trigger genomic instability and gene deregulation, which then alters gene coding and expression (55, 56). Although the biological function of *LINE-1* has not been fully understood, there have been a few studies suggesting that its hypomethylated alternation is associated with risk factors of stroke. According

TABLE 2 | Candidate-gene methylation analysis for ischemic stroke.

Study	Sample size	Tissue	Methylation sites, platform	Methylation pattern*	Main relevant findings
(26)[b]	Case: $n = 12$ Control: $n = 12$	Whole peripheral blood	*TNF-α* promoter (19 CpG sites), *PON* promoter (22 CpG sites), Sequenom EpiTYPER	Promoter hypomethylation	• Lower methylation level of *TNF-α* promoter was positively associated with stroke (OR = 9.0, 95% CI, 1.4–57.1, $p = 0.020$). • Methylation level of *PON* promoter was found to be interacting with energy intake in stroke cases ($p = 0.017$).
(28)[a]	Case: $n = 201$ Control: $n = 217$	Whole peripheral blood	*ERα* promoter (14 CpG sites), pyrosequencing	Promoter hypomethylation	• Mean methylation level: site 13, case vs. control, 2.60 vs. 3.05%, $p = 0.035$; site 14, case vs. control, 6.95 vs. 7.87%, $p = 0.026$. • Stroke subtypes, LAA/CE: site 5, case vs. control, 3.55 vs. 4.34%; site 9, case vs. control, 2.40 vs. 2.93%; site 12, case vs. control, 3.60 vs. 4.40%; site 13, case vs. control, 2.48 vs. 3.05%; site 14, case vs. control, 6.68 vs. 7.87%. (All $p < 0.05$).
(29)[a]	Case: $n = 298$ Control: $n = 258$	Whole peripheral blood	*MMP-2* promoter (8 CpG sites), pyrosequencing	Promoter hypomethylation	• Mean methylation level: all 8 sites, case vs. control, 3.24 vs. 3.64%; site 1, case vs. control, 1.88 vs. 2.13%; site 5, case vs. control, 1.92 vs. 2.25%; site 7, case vs. control, 2.70 vs. 3.02%; site 8, case vs. control, 4.46 vs. 4.98%. (All $p < 0.05$). • Stroke subtypes, small-vessel stroke: men, case vs. control, 3.01 vs. 3.65%, $p = 0.018$; women, not stated.
(30)	Case: $n = 26$ Control: $n = 26$	Whole peripheral blood	*APOE* promoter (17 CpG sites), pyrosequencing	Promoter hypermethylation	• Higher methylation level of site 16 was positively associated with ACI (OR = 16.1, 95% CI, 1.2–225.8, $p = 0.039$).
(31)	Case: $n = 446$ Control: $n = 159$	Whole peripheral blood	*MTHFR* gene (2 CpG sites), pyrosequencing	Hypermethylation	• Higher methylation level of CpG A was positively associated with stroke (OR = 4.73, 95% CI, 2.56–8.75, $p < 0.001$).
(32)	Case: $n = 78$ Control: $n = 86$	Whole peripheral blood	*TP53* promoter, Sanger sequencing	Promoter hypermethylation	• Mean methylation level: case vs. control, 32.1 vs. 16.3%; $p < 0.001$.
(33)	Case: $n = 23$ Control: $n = 32$	Peripheral blood leukocytes	*MIR-223* promoter (9 CpG sites), methylation-specific PCR	Promoter hypomethylation	• Lower mean methylation levels of a total of 7 CpG sites (sites 2, 3, 4, 6, 7, 8, 9) as well as island 1 and 2 of MIR-223 promoter were found in ACI cases compared to controls. (all $p < 0.05$).
(34)	Case: $n = 120$ Control: $n = 80$	Whole peripheral blood	*TM* promoter, methylation-specific PCR	Promoter hypermethylation	• Mean methylation level: case vs. control, 74.2 vs. 47.5%, $p < 0.01$.
(38)	Case: $n = 55$ Control: $n = 55$	Peripheral blood leukocytes	*ABCG1* gene, *APOE* gene, pyrosequencing	Hypermethylation	• Higher DNA methylation at the *cg02494239* site in *ABCG1* was positively associated with stroke (OR = 2.416, 95% CI: 1.024–5.700, $p = 0.044$). • No associations were observed for the *cg06500161* site in *ABCG1* and the *cg14123992* site in *APOE*.
(41)	Case: $n = 132$ Control: $n = 218$	Whole peripheral blood	*CBS* promoter, methylation-specific PCR	Promoter hypermethylation	• Median methylation level: case vs. control, 38.05 vs. 30.53%, $p < 0.001$. • Higher methylation level of *CBS* promoter was positively associated with stroke. (OR = 1.015 95% CI: 1.003–1.028).
(42)	Case: $n = 64$ Control: $n = 138$	Whole peripheral blood	*AHCY* gene, methylation-specific PCR	Hypermethylation	• Median methylation level: case vs. control, 0.13 vs. 0.06%, $p < 0.0001$.

ABCG1, ATP-binding cassette G1; AHCY, S-adenosylhomocysteine hydrolase; APOE, Apolipoprotein E; CBS, Cystathionine β-synthase; ERα, estrogen receptor alpha; MIR-223, microRNA223; MMP-2, Matrix metalloproteinase-2; MTHFR, methylenetetrahydrofolate reductase; PON, paraoxonase; TM, thrombomodulin; TNF-α, human tumor necrosis factor; TP53, tumor protein p53; LAA/CE, large-artery atherosclerosis and cardioembolism; ACI, atherosclerotic cerebral infarction; OR, odds ratio; CI, confidence interval.

**Methylation pattern refers to the methylation alteration of the site(s) in stroke cases compared to non-stroke controls.*

[a]*Overlapping participant;* [b]*Overlapping participant.*

TABLE 3 | Epigenome-wide methylation analysis for ischemic stroke.

Study	Sample size	Tissue	Methylation site, platform	Methylation pattern*	Main relevant findings
(36)[c]	Case: $n = 82$ Control: $n = 41$	Whole peripheral blood	DNA methylation age: Horvath's method: 353 methylation probes; Hannum's method: 71 methylation probes, Illumina HM450K	Differentially methylated	• Hannum age acceleration was positively associated with stroke (OR = 1.13, 95%CI: 1.00–1.26, $p = 0.045$). • No association was observed between Horvath age acceleration and stroke.
(27)	Case: $n = 161$ Control: $n = 161$	Whole peripheral blood	485,578 CpG sites, Illumina HM450K, pyrosequencing and Sequenom EpiTYPER	Hypermethylation	• In the validation study, higher methylation levels of *HLA-DRB1* and *HLA-DQB1* were found in stroke cases compared to control (both $p < 0.05$).
(37)[b]	Case: $n = 72$ Control: $n = 67$	Peripheral blood leukocytes	27,578 CpG sites, Illumina HM27K	Hypermethylation	• 80 CpG sites were found to be differentially methylated in stroke cases compared to controls, and 56 CpG sites were found to be interacting with obesity in stroke cases. • In validation study, higher methylate on levels at CpG site 19_20 in *WT1*, at the CpG site 1_2_10, 11, 12, 13, 14, 16_17, 18, 22 in *PM20D1* promoter were found in stroke cases compared to controls (all $p < 0.05$). • In the validation study, CpG site 1 and 8 in *CALD1* and CpG site 8_9 in *KCNQ1* were found to be interacting with obesity in stroke cases. • In the subgroup analysis, higher methylation levels of CPG 1_2_3 was found to be correlated with NIHSS ($P = 0.016$, $r = 0.371$).
(40)[c]	Case: $n = 548$ Control: $n = 245$	Whole peripheral blood	358,709 CpG sites, Infinium MethylationEPIC Beadchip and Illumina HM450K	Hypermethylation	• In validation study, higher methylation levels of 22 CpGs in 21 loci (*CAMSAP3*, *SLC35E1*, *ZFHX3*, *PIM3*, *MAPK1*, *LRRC26*, *HIF1A*, *RNF126*, *SENP3*, *ANAPC11*, *PLBD2*, *CCNL2*, *PUM1*, *ITPKB*, *NAPA*, *IL15RA*, *ACSL1*, *JMY*, *PUF60*, *CHSY1*, and *BAMBI*) were found in stroke cases compared to controls (all $p < 0.000$).
(39)	Case: $n = 301$ Control: $n = 313$	Whole peripheral blood	482,360 sites CpG sites, Illumina HM450K	Differentially methylated	• In the validation study, lower methylation levels of 438 CpG loci were found in stroke cases (mean difference, −7%, 95%CI, −5 to −38.7%). • In the validation study, higher methylation levels of 574 CpG loci were found in stroke cases (mean methylation, 6.8%, 95%CI, 5 to 28.9%). • In the validation study, lower average methylation level of 7 CpG sites (including CpG_3, CpG_4.5, CpG_8, CpG_9, CpG_10, CpG_11, CpG_13.14, and CpG_16) in *MTRNR2L8* was found in LAA stroke cases (mean difference: −13.01%, $p < 0.000$).
(45)	Cohort: $n = 729$ (Stroke: $n = 27$)	Whole peripheral blood	470,789 CpG sites, Illumina HM450K	No association	• No association between CpG methylation level and stroke was reported.

ACSL1, Long-chain-fatty-acid–CoA ligase 1; ANAPC11, Anaphase-promoting complex subunit 11; BAMBI, BMP and activin membrane-bound inhibitor homolog; CALD1, Caldesmon 1; CAMSAP3, Calmodulin-regulated spectrin-associated protein 3; CCNL2, Cyclin-L2; CHSY1, Chondroitin sulfate synthase 1; HLA-DRB1, human leukocyte antigen DR beta 1; HLA-DQB1, human leukocyte antigen DQ beta 1; HIF1A, Hypoxia-inducible factor 1-alpha; ITPKB, Inositol-trisphosphate 3-kinase B; IL15RA, Interleukin-15 receptor subunit alpha; JMY, Junction-mediating and -regulatory; LRRC26, Leucine-rich repeat-containing protein 26; KCNQ1, potassium voltage-gated channel, KQT-like subfamily,member 1; MAPK1, Mitogen-activated protein kinase 1; PIM3, Serine/threonine-protein kinase pim-3; PM20D1, peptidase M20 domain containing 1; PLBD2, Putative phospholipase B-like 2; PUM1, Pumilio homolog 1; PUF60, Poly(U)-binding-splicing factor PUF60; RNF126, RING finger protein 126; SENP3, Sentrin-specific protease 3; SLC35E1, Solute carrier family 35 member E1; WT1, wilms' tumor 1; ZFHX3, Zinc finger homeobox protein 3; HM450K, Infinium HumanMethylation450 BeadChip; HM27K, Infinium HumanMethylation27 BeadChip; NIHSS, the National Institute of Health Stroke Scale; OR, odds ratio; CI, confidence interval.

** Methylation pattern refers to the methylation alteration of the site(s) in stroke cases compared to non-stroke controls.*

[b] Overlapping participant; [c] Overlapping participant.

to previous studies, *LINE-1* hypomethylation could modify the metabolism of lipid and carbohydrate and cause aberrant lipid profile and impaired glucose metabolism, which might further lead to the formation of atherosclerotic plaques (55, 57–61). Additionally, *LINE-1* methylation was reported to become lower with age, which might reflect the cumulated effects of age-related environmental risk factors on the onset of stroke (55). The other study focusing on the methylation of *ALU* and *Satellite 2* repetitive elements, on the other hand, failed to observe an association. *ALU* and *Satellite 2* were also reported to be associated with risk factors of IS, including higher BMI and blood pressure in previous studies (54, 61). The non-significant association might be due to the underpowered analysis since there were only four stroke cases included in the analysis. On the other hand, a combined measurement of *ALU* and Satellite for global DNA methylation analysis differs from the measurement of *LINE-1* in the assay and genetic position. Previous studies indicated that the methylation levels of *ALU* and *LINE-1* were correlated only in cancer cells rather than peripheral blood cells, and their regulatory mechanisms regarding DNA methylation might be different (62, 63). Therefore, *ALU* and *Satellite 2* might show different traits and patterns in relation to cerebral ischemia.

Global DNA methylation of repetitive elements can be a novel marker for stroke as standardized assays of DNA methylation are available, and they can nicely reflect global DNA methylation changes. However, there are concerns to be considered. The methylation alternation of the promoter and gene body might have different effects on gene expression. For example, hypermethylation in the gene body normally increases gene expression, while higher methylation in CpG islands of a promoter mostly leads to lower gene expression (54). Global DNA methylation of repetitive elements could only provide a rough measurement of methylation patterns. Some correlations between methylation of repetitive elements and specific genes were found, but the majority of these studies focused on other diseases, such as gastritis and glioma (64–66). Therefore, further studies are encouraged to expand the mechanisms of global methylation to specific loci and investigate their inter-relationship.

Genome-Wide and Candidate Gene Methylation

Genome-Wide and Gene-Specific DNA Methylation and Stroke

Genome-wide and candidate gene methylation studies identified a total of 37 genes that were differentially methylated between stroke cases and controls. Twenty-five genes identified in genome-wide association studies were validated in replication samples, while none of the findings in candidate-gene studies was validated by other studies.

Possible Pathological Mechanisms of Genome-Wide and Gene-Specific DNA Methylation

The influence of DNA methylation alternations on the pathogenesis of IS has been studied in the past few years. Generally, methylation alternations of these genes regulate gene expression and risk factors of IS via a variety of pathological processes, such as disorders of the coagulation cascade, higher plasma homocysteine, dyslipidemia, atherosclerosis, and inflammatory response (54). For example, *APOE* controls an essential enzyme for lipid profile, and it was found that *APOE* genotype, especially the E4 allele, was associated with a higher level of LDL-C and carotid intima-media thickness (67–69). The hypermethylation of the *APOE* promoter can cause aberrant expression of the *APOE* gene, eventually leading to dyslipidemia and earlier onset of stroke.

DNA methylation alternations might also be involved in the pathway of the inflammatory response and cell death. For example, *TNF-α* has detrimental effects on both neuronal and glial cells by disrupting the blood-brain barrier or activating cell death signaling pathways (70). The lower methylation level of *TNF-α* promoter might increase the expression of *TNF-α* in stroke patients, causing glutamate excitotoxicity and apoptosis on neurons (71). Likewise, the genes of *TP53*, *HLA-DRB1*, and *HLA-DQB1* were also found to be associated with early neurological deterioration in IS for its function of regulating cell proliferation in atherosclerotic plaques (72, 73). Aberrant methylation on these genes might lead to an inflammatory response in arteries and the formation of arterial plaques, which accelerates the formation of atherosclerosis.

DNA methylation might also elevate the level of plasma homocysteine, which is one of the most established risk factors for stroke (74). *CBS* is a major enzyme in the metabolism of homocysteine converting to cysteine, and its deficiency could cause hyperhomocysteinemia (74). Hypermethylated *CBS* promoter might silence *CBS* gene expression and subsequently reduce enzyme activity, leading to plasma homocysteine accumulation and increased risk of stroke (75). Another possible mechanism is related to disorders of coagulation cascade. *TM* gene acts as a cofactor of thrombin and reduces blood coagulation, and its deficiency might cause cerebral thrombosis for less inhibited coagulation and fibrinolysis (76).

However, the biological mechanism affected by gene expression might only partially explain the mechanisms of stroke onset. For example, *MTHFR* is a major enzyme in the metabolism of vitamin folate, and its deficiency caused by hypermethylation might lead to hyperhomocysteinemia and subsequently increase the risk of stroke (6, 77). Meanwhile, hypermethylated *MTHFR* gene might function as a mediator on a broader pathological pathway, synergistically leading to hypermethylation of the *TM* gene promoter and further inducing *TM* gene silencing (34). On the other hand, Wei et al. (31) failed to observe an association of *MTHFR* methylation with plasma homocysteine despite its association with IS in this study. Therefore, there are still some underlying mechanisms unexplored, suggesting that new biological pathways as well as new loci related to the risk factors and onset of IS are needed to be explored.

Epigenetic Clock and Stroke

One of the included studies found that age acceleration using Hannum's method was positively associated with stroke (36). As the epigenetic clock is an algorithm calculated by the methylation level at a number of age-related loci across the human genome (78), it works as a marker of biological age against chronological age. Acceleration in biological age is probably a better scale for aging than the chronological age, and it is associated with many

diseases as well as mortality risk (79). Since aging is an extremely chronic process influenced complicatedly by a large number of environmental factors (80, 81), Hannum's epigenetic clock could be a marker for the interaction between brain aging and the environment in relation to stroke.

Limitations of the Current Evidence

First, among the included studies in the present review, only one study used prospective data to identify the association of DNA methylation with IS while the other studies basically used case-control or cross-sectional study design. Such study designs could not provide robust evidence for the temporality or causality of associations presented as reverse causations might have existed. Although some of the pathological processes mentioned above could provide evidence for the biological function, these are not enough to demonstrate the causal relationship due to the complexity of the pathological mechanisms. Second, in terms of the collection of bio-samples, all studies collected DNA from the blood while it is unclear if DNA methylation in blood could accurately reflect its level in brain tissues. Moreover, given the dynamic nature of the epigenetic modification, the level of DNA methylation might change as the disease progresses. Therefore, the amount of time between the onset of stroke and collection of bio-sample is an important factor that reflects the potentially changeable role of DNA methylation in different phases before and after stroke. The majority of the included studies assessed DNA methylation at an acute/subacute stage of stroke. No study measured DNA methylation longitudinally or recorded the exact time interval between stroke and bio-sample collection, leaving an open question of how DNA methylation would change through the course of the disease. This could be an important consideration for future studies. Third, the homogeneity of the study sample might have limited the generalizability of the results. For example, 13 out of 20 studies used samples which are comprised exclusively of Asians. Also, several studies used the data from overlapping participants.

Prospective

In order to improve the quality of evidence, it is preferable to investigate this research question by a large-scale prospective cohort study with comprehensive data collection in a well-defined healthy population. First, longitudinal observation of the trajectory of DNA methylation might help to reflect the environment-gene interaction, especially the cumulated environmental effects on DNA methylation over time. Also, such a study design with a baseline as well as multiple measurements of DNA methylation during follow-up in healthy individuals provides evidence for the longitudinal properties of DNA methylation and its complex interaction with cerebral ischemia. It delineates a more comprehensive epigenetic pathway for stroke prevention and recovery. For example, in addition to only focusing on the association between DNA methylation and occurrence of stroke, one study also found that methylation at the baseline was correlated with stroke severity at hospital admission, suggesting that it might be predictive of the functional loss/recovery after admission (37). Therefore, it is a promising direction for future studies to investigate how DNA methylation at the early stage of stroke is associated with the short- or long-term functional outcome of IS using a patient sample. Second, studies with large sample size and sufficient length of follow-up are important, as the prospective study included in this review only observed eight IS cases during follow-up, which might have caused underpowered analysis. Third, it is crucial to standardize the methods of DNA methylation measure for reliable comparison of results across different studies. Fourth, a large number of covariates have been adjusted in data analyses of the previous studies, which is done most likely to control for the confounding effects. For example, many risk factors of IS that were adjusted in the included studies, such as BMI/obesity, blood pressure/hypertension, and smoking are proved to be associated with both cerebral ischemia (82) and the level of methylation (60, 83–85). However, the covariates considered in previous studies have been highly heterogeneous, possibly due to data availability. Some studies collected the data of physical examination and history of disease from the study participants (31, 41, 44), while some only had basic information (32). For future studies, it is important to adequately collect and adjust a wide range of potential confounders, including demographic, lifestyle, and health data at both baseline and follow-up, to avoid residual confounding bias.

The clinical utility of epigenetic biomarker is promising as techniques in epigenome-sequencing is rapidly developing. Since DNA methylation is involved in many pathological pathways related to the well-established risk/protective factors of stroke, epigenetic biomarker has the potential to become a prediction tool to identify people at risk of stroke at the asymptomatic stage. Also, a better understanding of how DNA methylation interplays with metabolism, inflammation, or other pathways will help supplement the current treatment of IS. Epigenetic therapies that target the post-translational stage by modifying DNA methylation might be of huge clinical value for stroke patients, as aforementioned evidence has indicated genetic causes of cerebral ischemia and potential effects of DNA methylation. Some epigenetic therapies have already been used clinically for cancer patients (86). It is possible to prioritize and explore epigenetic therapies for ischemic stroke.

Strengths and Limitations of this Review

To our knowledge, this study involving more than 7,000 participants, is the first study systematically and comprehensively summarizing the current evidence of the relationship of DNA methylation with IS. We identified the studies from four major databases as well as other sources manually and extracted all the relevant information from these studies. Also, we performed quality assessments for these studies using an established tool. However, two limitations need to be acknowledged. First, we only focus on ischemic stroke, which might cause the omission hemorrhagic stroke. Second, due to high heterogeneity, we were unable to perform meta-analyses and use Begg's funnel plot and Egger's test to examine publication bias.

CONCLUSION

This review systematically integrated current evidence for the role of DNA methylation in IS. Epigenetic clock and methylation

of *LINE-1* repetitive elements, as well as a number of genes, were found to be associated with IS. However, conclusive evidence has not yet been drawn due to high heterogeneity across studies, uncertain causal relationship, and complex process of the pathogenesis of IS. Future studies with a large-scale, prospective design, comprehensive data collection, and robust methylation measures, might help answer the research question.

DATA AVAILABILITY STATEMENT

All datasets generated for this study are included in the article/**Supplementary Material**.

AUTHOR CONTRIBUTIONS

MZ was involved in study conception and design, collection and analysis of data, and draft writing. JZ carried out study design, collection and analysis of data, and critical revision of the manuscript. XZ, HQ, XX, and JW performed study design and critical revision of the manuscript. ZL and JH were involved in study conception and design, collection and analysis of data, and critical revision of the manuscript. All authors contributed to the article and approved the submitted version.

FUNDING

This study was supported by Shenzhen High-level Hospital Construction Fund.

SUPPLEMENTARY MATERIAL

The Supplementary Material for this article can be found online at: https://www.frontiersin.org/articles/10.3389/fneur.2020.566124/full#supplementary-material

REFERENCES

1. GBD 2016 Neurology Collaborators. Global, regional, and national burden of stroke, 1990-2016: a systematic analysis for the Global Burden of Disease Study 2016. *Lancet Neurol.* (2019) 18:439–58. doi: 10.1016/s1474-4422(19)30034-1
2. Krishnamurthi RV, Moran AE, Feigin VL, Barker-Collo S, Norrving B, Mensah GA, et al. Stroke prevalence, mortality and disability-adjusted life years in adults aged 20-64 years in 1990-2013: data from the global burden of disease 2013 study. *Neuroepidemiology.* (2015) 45:190–202. doi: 10.1159/000441098
3. Feigin VL, Norrving B, Mensah GA. Global Burden of Stroke. *Circ Res.* (2017) 120:439–48. doi: 10.1161/CIRCRESAHA.116.308413
4. Singer J, Gustafson D, Cummings C, Egelko A, Mlabasati J, Conigliaro A, et al. Independent ischemic stroke risk factors in older Americans: a systematic review. *Aging (Albany NY).* (2019) 11:3392–407. doi: 10.18632/aging.101987
5. Dichgans M, Pulit SL, Rosand J. Stroke genetics: discovery, biology, clinical applications. *Lancet Neurol.* (2019) 18:587–99. doi: 10.1016/S1474-4422(19)30043-2
6. Qureshi IA, Mehler MF. Emerging role of epigenetics in stroke: part 1: DNA methylation and chromatin modifications. *Arch Neurol.* (2010) 67:1316–22. doi: 10.1001/archneurol.2010.275
7. Feinberg A. Epigenetics at the epicenter of modern medicine. *JAMA.* (2008) 299:1345–50. doi: 10.1001/jama.299.11.1345
8. Robertson KD. DNA methylation and human disease. *Nat Rev Genet.* (2005) 6:597–610. doi: 10.1038/nrg1655
9. Martin EM, Fry RC. Environmental influences on the epigenome: exposure-associated DNA methylation in human populations. *Annu Rev Public Health.* (2018) 39:309–33. doi: 10.1146/annurev-publhealth-040617-014629
10. Alegria-Torres JA, Baccarelli A, Bollati V. Epigenetics and lifestyle. *Epigenomics. Jun.* (2011) 3:267–77. doi: 10.2217/epi.11.22
11. Lam K, Pan K, Linnekamp JF, Medema JP, Kandimalla R. DNA methylation based biomarkers in colorectal cancer: a systematic review. *Biochim Biophys Acta.* (2016) 1866:106–20. doi: 10.1016/j.bbcan.2016.07.001
12. Jiang D, Hong Q, Shen Y, Xu Y, Zhu H, Li Y, et al. The diagnostic value of DNA methylation in leukemia: a systematic review and meta-analysis. *PLoS One.* (2014) 9:e96822. doi: 10.1371/journal.pone.0096822
13. Guan Z, Yu H, Cuk K, Zhang Y, Brenner H. Whole-blood DNA methylation markers in early detection of breast cancer: a systematic literature review. *Cancer Epidemiol Biomarkers Prev.* (2019) 28:496–505. doi: 10.1158/1055-9965.EPI-18-0378
14. Gurung PMS, Barnett AR, Wilson JS, Hudson J, Ward DG, Messing EM, et al. Prognostic DNA methylation biomarkers in high-risk non-muscle-invasive bladder cancer: a systematic review to identify loci for prospective validation. *Eur Urol Focus.* (2020) 6:683–97. doi: 10.1016/j.euf.2019.02.012
15. Teroganova N, Girshkin L, Suter CM, Green MJ. DNA methylation in peripheral tissue of schizophrenia and bipolar disorder: a systematic review. *BMC Genet.* (2016) 17:27. doi: 10.1186/s12863-016-0332-2
16. Fransquet PD, Lacaze P, Saffery R, McNeil J, Woods R, Ryan J. Blood DNA methylation as a potential biomarker of dementia: a systematic review. *Alzheimers Dement.* (2018) 14:81–103. doi: 10.1016/j.jalz.2017.10.002
17. Endres M, Fan G, Meisel A, Dirnagl U, Jaenisch R. Effects of cerebral ischemia in mice lacking DNA methyltransferase 1 in post-mitotic neurons. *Neuroreport.* (2001) 12:3763–6. doi: 10.1097/00001756-200112040-00032
18. Gapp K, Woldemichael BT, Bohacek J, Mansuy IM. Epigenetic regulation in neurodevelopment and neurodegenerative diseases. *Neuroscience.* (2014) 264:99–111. doi: 10.1016/j.neuroscience.2012.11.040
19. Casas JP, Hingorani AD, Bautista LE, Sharma P. Meta-analysis of genetic studies in ischemic stroke: thirty-two genes involving approximately 18,000 cases and 58,000 controls. *Arch Neurol.* (2004) 61:1652–61. doi: 10.1001/archneur.61.11.1652
20. Ghosh J, Coutifaris C, Sapienza C, Mainigi M. Global DNA methylation levels are altered by modifiable clinical manipulations in assisted reproductive technologies. *Clin Epigenet.* (2017) 9:14. doi: 10.1186/s13148-017-0318-6
21. Lim U, Song MA. Dietary and lifestyle factors of DNA methylation. *Cancer Epigenet.* (2012) 863:359–76. doi: 10.1007/978-1-61779-612-8_23
22. Moher D, Shamseer L, Clarke M, Ghersi D, Liberati A, Petticrew M, et al. Preferred reporting items for systematic review and meta-analysis protocols (PRISMA-P) 2015 statement. *Syst Rev.* (2015) 4:1. doi: 10.1186/2046-4053-4-1
23. Pfalzer AC, Choi SW, Tammen SA, Park LK, Bottiglieri T, Parnell LD, et al. S-adenosylmethionine mediates inhibition of inflammatory response and changes in DNA methylation in human macrophages. *Physiol Genomics.* (2014) 46:617–23. doi: 10.1152/physiolgenomics.00056.2014
24. Feltus FA, Lee EK, Costello JF, Plass C, Vertino PM. Predicting aberrant CpG island methylation. *Proc Natl Acad Sci U S A.* (2002) 100:12253–8. doi: 10.1073/pnas.2037852100
25. Wells G, Shea B, O'Connell D. *The Newcastle-Ottawa Scale (NOS) for Assessing the Quality of Nonrandomised Studies in Meta-Analyses.* (2015) Available online at: http://www.ohri.ca/programs/clinical_epidemiology/nos_manual.pdf.
26. Gomez-Uriz AM, Goyenechea E, Campion J, Arce A, Martinez MT, Puchau B, et al. Epigenetic patterns of two gene promoters (TNF-alpha and PON) in stroke considering obesity condition and dietary intake. *J Physiol Biochem.* (2014) 70:603–14. doi: 10.1007/s13105-014-0316-5
27. Deng GX, Xu N, Huang Q, Tan JY, Zhang Z, Li XF, et al. Association between promoter DNA methylation and gene expression in

the pathogenesis of ischemic stroke. *Aging (Albany NY).* (2019) 11:7663–77. doi: 10.18632/aging.102278
28. Lin HF, Hsi E, Liao YC, Chhor B, Hung J, Juo SHH, et al. Demethylation of circulating estrogen receptor alpha gene in cerebral ischemic stroke. (2015) *PLoS One*. 10:e0139608. doi: 10.1371/journal.pone.0139608
29. Lin HF, Hsi E, Huang LC, Liao YC, Juo SH, Lin RT. Methylation in the matrix metalloproteinase-2 gene is associated with cerebral ischemic stroke. *J Investig Med.* (2017) 65:794–9. doi: 10.1136/jim-2016-000277
30. Zhang H, Zhao X, Wang C, Du R, Wang X, Fu J, et al. A Preliminary Study of the association between apolipoprotein E promoter methylation and atherosclerotic cerebral infarction. *J Stroke Cerebrovasc Dis.* (2019) 28:1056–61. doi: 10.1016/j.jstrokecerebrovasdis.2018.12.027
31. Wei LK, Sutherland H, Au A, Camilleri E, Haupt LM, Gan HS, et al. A potential epigenetic marker mediating serum folate and vitamin B12 levels contributes to the risk of ischemic stroke. *Biomed Res Int.* (2015) 2015:167976. doi: 10.1155/2015/167976
32. Wei Y, Sun Z, Wang Y, Xie Z, Xu S, Xu Y, et al. Methylation in the TP53 promoter is associated with ischemic stroke. *Mol Med Rep.* (2019) 20:1404–10. doi: 10.3892/mmr.2019.10348
33. Li Z, Yu F, Zhou X, Zeng S, Zhan Q, Yuan M, et al. Promoter hypomethylation of microRNA223 gene is associated with atherosclerotic cerebral infarction. *Atherosclerosis.* (2017) 263:237–43. doi: 10.1016/j.atherosclerosis.2017.06.924
34. Yang Z, Wang L, Zhang W, Wang X, Zhou S. Plasma homocysteine involved in methylation and expression of thrombomodulin in cerebral infarction. *Biochem Biophys Res Commun.* (2016) 473:1218–22. doi: 10.1016/j.bbrc.2016.04.042
35. Lin RT, Hsi E, Lin HF, Liao YC, Wang YS, Juo SH. LINE-1 methylation is associated with an increased risk of ischemic stroke in men. *Curr Neurovasc Res.* (2014) 11:4–9. doi: 10.2174/1567202610666131202145530
36. Soriano-Tarraga C, Giralt-Steinhauer E, Mola-Caminal M, Vivanco-Hidalgo RM, Ois A, Rodríguez-Campello A, et al. Ischemic stroke patients are biologically older than their chronological age. *Aging (Albany NY).* (2016) 8:2655–66. doi: 10.18632/aging.101028
37. Gomez-Uriz AM, Milagro FI, Mansego ML, Cordero P, Abete I, Arce AD, et al. Obesity and ischemic stroke modulate the methylation levels of KCNQ1 in white blood cells. *Hum Mol Genet.* (2015) 24:1432–40. doi: 10.1093/hmg/ddu559
38. Qin X, Li J, Wu T, Wu Y, Tang X, Gao P, et al. Overall and sex-specific associations between methylation of the ABCG1 and APOE genes and ischemic stroke or other atherosclerosis-related traits in a sibling study of Chinese population. *Clin Epigenet.* (2019) 11:189. doi: 10.1186/s13148-019-0784-0
39. Shen Y, Peng C, Bai Q, Ding Y, Yi X, Du H, et al. Epigenome-wide association study indicates hypomethylation of MTRNR2L8 in large-artery atherosclerosis stroke. *Stroke.* (2019) 50:1330–8. doi: 10.1161/STROKEAHA.118.023436
40. Soriano-Tarraga C, Lazcano U. Identification of 20 novel loci associated with ischaemic stroke. Epigenome-wide association study. *Epigenetics.* (2020) 6:1–0. doi: 10.1101/2019.12.11.872945
41. Wang C, Xu G, Wen Q, Peng X, Chen H, Zhang J, et al. CBS promoter hypermethylation increases the risk of hypertension and stroke. *Clinics (São Paulo).* (2019) 74:e630. doi: 10.6061/clinics/2019/e630
42. Zhao L, Chen X, Zhou S, Lin Z, Yu X, Huang Y. DNA methylation of AHCY may increase the risk of ischemic stroke. *Bosn J Basic Med Sci.* (2020) 20:471–6. doi: 10.17305/bjbms.2020.4535
43. Kim M, Long TI, Arakawa K, Wang R, Yu MC, Laird PW. DNA methylation as a biomarker for cardiovascular disease risk. *PLoS One.* (2010) 5:e9692. doi: 10.1371/journal.pone.0009692
44. Baccarelli A, Wright R, Bollati V, Litonjua A, Zanobetti A, Tarantini L, et al. Ischemic heart disease and stroke in relation to blood DNA methylation. *Epidemiology.* (2010) 21:819–28. doi: 10.1097/EDE.0b013e3181f20457
45. Rask-Andersen M, Martinsson D, Ahsan M, Enroth S, Ek WE, Gyllensten U, et al. Epigenome-wide association study reveals differential DNA methylation in individuals with a history of myocardial infarction. *Hum Mol Genet.* (2016) 25:4739–48. doi: 10.1093/hmg/ddw302
46. Rakyan VK, Down TA, Balding DJ, Beck S. Epigenome-wide association studies for common human diseases. *Nat Rev Genet.* (2011) 12:529–41. doi: 10.1038/nrg3000
47. Hwu HR, Roberts JW, Davidson EH, Britten RJ. Insertion and/or deletion of many repeated DNA sequences in human and higher ape evolution. *Proc Natl Acad Sci U S A.* (1986) 83:3875–9. doi: 10.1073/pnas.83.11.3875
48. Gu Z, Wang H, Nekrutenko A, Li WH. Densities, length proportions and other distributional features of repetitive sequences in the human genome estimated from 430 megabases of genomic sequence. *Gene.* (2000) 259:81–8. doi: 10.1016/S0378-1119(00)00434-0
49. Consortium* IHGS. Initial sequencing and analysis of the human genome. *Nature.* (2001) 409:860–921. doi: 10.1038/35057062
50. Shabalin AA, Aberg KA, van den Oord EJCG. Candidate gene methylation studies are at high risk of erroneous conclusions. *Epigenomics.* (2015) 7:13–5. doi: 10.2217/epi.14.70
51. Michels KB, Binder AM, Dedeurwaerder S, Epstein CB, Greally JM, Gut I, et al. Recommendations for the design and analysis of epigenome-wide association studies. *Nat Methods.* (2013) 10:949–55. doi: 10.1038/nmeth.2632
52. Weisenberger DJ, Campan M, Long TI, Kim M, Woods C, Fiala E, et al. Analysis of repetitive element DNA methylation by MethyLight. *Nucleic Acids Res.* (2005) 33:6823–36. doi: 10.1093/nar/gki987
53. Vryer R, Saffery R. What's in a name? Context-dependent significance of global methylation measures in human health and disease. *Clin Epigenet.* (2017) 9:1–4. doi: 10.1186/s13148-017-0311-0
54. Muka T, Koromani F, Portilla E, O'Connor A, Bramer WM, Troup J, et al. The role of epigenetic modifications in cardiovascular disease: A systematic review. *Int J Cardiol.* (2016) 212:174–83. doi: 10.1016/j.ijcard.2016.03.062
55. Li W, Shuchuan L, Zhendong S, Rongchao C, Xiuping B, Xueqi L. LINE-1 hypomethylation is associated with the risk of coronary heart disease in Chinese population. *Arq Bras Cardiol.* (2014) 102:481–8. doi: 10.5935/abc.20140054
56. Schulz WA, Steinhoff C, AR F. Methylation of endogenous human retroelements in health and disease. *Curr Top Microbiol Immunol.* (2006) 310:211–50. doi: 10.1007/3-540-31181-5_11
57. Martin-Nunez GM, Rubio-Martin E, Cabrera-Mulero R, Rojo-Martínez G, Olveira G, Valdés S, et al. Type 2 diabetes mellitus in relation to global LINE-1 DNA methylation in peripheral blood: a cohort study. *Epigenetics.* (2014) 9:1322–8. doi: 10.4161/15592294.2014.969617
58. Perng W, Mora-Plazas M, Marin C, Rozek LS, Baylin A, Villamor E. A prospective study of LINE-1DNA methylation and development of adiposity in school-age children. *PLoS One.* (2013) 8:e62587. doi: 10.1371/journal.pone.0062587
59. Valérie T, André T, Yves D, Pérusse L, Bélisle A, Marceau S, et al. LINE-1 methylation in visceral adipose tissue of severely obese individuals is associated with metabolic syndrome status and related phenotypes. *Clinical Epigenet.* (2012) 4:10. doi: 10.1186/1868-7083-4-10
60. Cash HL, McGarvey ST, Houseman EA, Marsit CJ, Hawley NL, Lambert-Messerlian GM, et al. Cardiovascular disease risk factors and DNA methylation at the LINE-1 repeat region in peripheral blood from Samoan Islanders. *Epigenetics.* (2011) 6:1257–64. doi: 10.4161/epi.6.10.17728
61. Alexeeff SE, Baccarelli AA, Halonen J, Coull BA, Wright RO, Tarantini L, et al. Association between blood pressure and DNA methylation of retrotransposons and pro-inflammatory genes. *Int J Epidemiol.* (2013) 42:270–80. doi: 10.1093/ije/dys220
62. Hou L, Wang H, Sartori S, Gawron A, Lissowska J, Bollati V, et al. Blood leukocyte DNA hypomethylation and gastric cancer risk in a high-risk Polish population. *Int J cancer.* (2010) 127:1866–74. doi: 10.1002/ijc.25190
63. Choi JY, James SR, Link PA, McCann SE, Hong CC, Warren D, et al. Association between global DNA hypomethylation in leukocytes and risk of breast cancer. *Carcinogenesis.* (2009) 30:1889–97. doi: 10.1093/carcin/bgp143
64. Yamamoto E, Toyota M, Suzuki H, Kondo Y, Sanomura T, Murayama Y, et al. LINE-1 hypomethylation is associated with increased CpG island methylation in Helicobacter pylori-related enlarged-fold gastritis. *Cancer Epidemiol Biomarkers Prev.* (2008) 17:2555–64. doi: 10.1158/1055-9965.EPI-08-0112
65. Martin-Nunez GM, Cabrera-Mulero R, Rubio-Martin E, Rojo-Martinez G, Olveira G, Valdes S, et al. Methylation levels of the SCD1 gene promoter and LINE-1 repeat region are associated with weight change: an intervention study. *Mol Nutr Food Res.* (2014) 58:1528–36. doi: 10.1002/mnfr.201400079
66. Fumiharu O, Atsushi N, Kazuya M, Yugo K, Yutaka K, Tatsuya A, et al. The global DNA methylation surrogate LINE-1 methylation is correlated with

MGMT promoter methylation and is a better prognostic factor for glioma. *PLoS One.* (2011) 6:e23332. doi: 10.1371/journal.pone.0023332
67. Lagging C, Lorentzen E, Stanne TM, Pedersen A, Soderholm M, Cole JW, et al. APOE epsilon4 is associated with younger age at ischemic stroke onset but not with stroke outcome. *Neurology.* (2019) 93:849–53. doi: 10.1212/WNL.0000000000008459
68. Khan TA, Shah T, Prieto D, Zhang W, Price J, Fowkes GR, et al. Apolipoprotein E genotype, cardiovascular biomarkers and risk of stroke: systematic review and meta-analysis of 14,015 stroke cases and pooled analysis of primary biomarker data from up to 60,883 individuals. *Int J Epidemiol.* (2013) 42:475–92. doi: 10.1093/ije/dyt034
69. Satizabal CL, Samieri C, Davis-Plourde KL, Voetsch B, Aparicio HJ, Pase MP, et al. APOE and the Association of Fatty Acids With the Risk of Stroke, Coronary Heart Disease, and Mortality. *Stroke.* (2018) 49:2822–9. doi: 10.1161/STROKEAHA.118.022132
70. Watters O, O'Connor JJ. A role for tumor necrosis factor-alpha in ischemia and ischemic preconditioning. *J Neuroinflammation.* (2011) 8:87. doi: 10.1186/1742-2094-8-87
71. Jones P. Functions of DNA methylation: islands, start sites, gene bodies and beyond. *Nat Rev Genet.* (2012) 13:484–92. doi: 10.1038/nrg3230
72. Gomez-Sanchez JC, Delgado-Esteban M, Rodriguez-Hernandez I, Sobrino T, Ossa NP, Reverte S, et al. The human Tp53 Arg72Pro polymorphism explains different functional prognosis in stroke. *J Exp Med.* (2011) 208:429–37. doi: 10.1084/jem.20101523
73. Li J, Chen G, Gao X, Shen C, Zhou P, Wu X, et al. p53 participates in the protective effects of ischemic post-conditioning against OGD-reperfusion injury in primary cultured spinal cord neurous. *Neurosci Lett.* (2017) 638:129–34. doi: 10.1016/j.neulet.2016.12.037
74. Stanzione R, Cotugno M, Bianchi F, Marchitti S, Forte M, Volpe M, et al. Pathogenesis of ischemic stroke: role of epigenetic mechanisms. *Genes.* (2020) 11:89. doi: 10.3390/genes11010089
75. Ding R, Lin S, Chen D. The association of cystathionine beta synthase (CBS) T833C polymorphism and the risk of stroke: a meta-analysis. *J Neurol Sci.* (2012) 312:26–30. doi: 10.1016/j.jns.2011.08.029
76. Boffa MC, Karmochkine M. Thrombomodulin: an overview and potential implications in vascular disorders. *Lupus.* (1998) 7(Suppl. 2):S120–5. doi: 10.1177/096120339800700227
77. Parnetti L, Caso V, Santucci A, Corea F, Lanari A, Floridi A, et al. Mild hyperhomocysteinemia is a risk-factor in all etiological subtypes of stroke. *Neurol Sci.* (2004) 25:13–7. doi: 10.1007/s10072-004-0219-5
78. Armstrong NJ, Mather KA TA, Wright MJ, Trollor JN, Ames D, Brodaty H, et al. Aging, exceptional longevity and comparisons of the Hannum and Horvath epigenetic clocks. *Epigenomics.* (2017) 9:689–700. doi: 10.2217/epi-2016-0179
79. Fransquet PD, Wrigglesworth J, Woods RL, Ernst ME, Ryan J. The epigenetic clock as a predictor of disease and mortality risk: a systematic review and meta-analysis. *Clin Epigenetics.* (2019) 11:62. doi: 10.1186/s13148-019-0656-7
80. Blagosklonny M. Answering the ultimate question "What is the Proximal Cause of Aging?" *Aging (Albany NY).* (2012) 4:861–77. doi: 10.18632/aging.100525
81. Fraga MF, Esteller M. Epigenetics and aging: the targets and the marks. *Trends Genet.* (2007) 23:413–8. doi: 10.1016/j.tig.2007.05.008
82. Boehme AK, Esenwa C, Elkind MSV. Stroke risk factors, genetics, and prevention. *Circ Res.* (2017) 120:472–95. doi: 10.1161/CIRCRESAHA.116.308398
83. Wang X, Falkner B, Zhu H, Shi H, Su S, Xu X, et al. A genome-wide methylation study on essential hypertension in young african american males. *PLoS One.* (2013) 8:e53938. doi: 10.1371/journal.pone.0053938
84. Hironobu S, Yoshifumi B, Masayuki W, Shiro I, Keisuke M, Takatsugu I, et al. LINE-1 hypomethylation in noncancerous esophageal mucosae is associated with smoking history. *Ann Surg Oncol.* (2012) 19:4238–43. doi: 10.1245/s10434-012-2488-y
85. Pearce MS, McConnell JC, Potter C, Barrett LM, Parker L, Mathers JC, et al. Global LINE-1 DNA methylation is associated with blood glycaemic and lipid profiles. *Int J Epidemiol.* (2012) 41:210–7. doi: 10.1093/ije/dys020
86. Karimi M, Johansson S, Ekstrom TJ. Using LUMA: a Luminometric-based assay for global DNA-methylation. *Epigenetics.* (2006) 1:45–8. doi: 10.4161/epi.1.1.2587

Conflict of Interest: The authors declare that the research was conducted in the absence of any commercial or financial relationships that could be construed as a potential conflict of interest.

frontiers in Neurology

ORIGINAL RESEARCH
published: 23 November 2020
doi: 10.3389/fneur.2020.577927

Ablation of GSDMD Improves Outcome of Ischemic Stroke Through Blocking Canonical and Non-canonical Inflammasomes Dependent Pyroptosis in Microglia

Kankai Wang[1,2], *Zhezhe Sun*[1,3], *Junnan Ru*[1,2], *Simin Wang*[1,2], *Lijie Huang*[1,2], *Linhui Ruan*[1,2], *Xiao Lin*[1,2], *Kunlin Jin*[4], *Qichuan Zhuge*[1,2*] *and Su Yang*[1,2*]

[1] *Zhejiang Provincial Key Laboratory of Aging and Neurological Disorder Research, The First Affiliated Hospital of Wenzhou Medical University, Wenzhou, China,* [2] *Department of Neurosurgery, The First Affiliated Hospital of Wenzhou Medical University, Wenzhou, China,* [3] *Department of Cerebrovascular, The Affiliated Hospital of Medical School of Ningbo University, Ningbo, China,* [4] *Department of Pharmacology and Neuroscience, University of North Texas Health Science Center, Fort Worth, TX, United States*

OPEN ACCESS

Edited by:
Emmanuel Pinteaux, The University of Manchester, United Kingdom

Reviewed by:
Hiroaki Ooboshi, Fukuoka Dental College, Japan
Xiaoying Wang, Tulane University, United States

***Correspondence:**
Qichuan Zhuge
zhugeqichuan@vip.163.com
Su Yang
yangsu@wmu.edu.cn

Specialty section:
This article was submitted to Stroke, a section of the journal Frontiers in Neurology

Received: *30 June 2020*
Accepted: *12 October 2020*
Published: *23 November 2020*

Citation:
Wang K, Sun Z, Ru J, Wang S, Huang L, Ruan L, Lin X, Jin K, Zhuge Q and Yang S (2020) Ablation of GSDMD Improves Outcome of Ischemic Stroke Through Blocking Canonical and Non-canonical Inflammasomes Dependent Pyroptosis in Microglia. Front. Neurol. 11:577927. doi: 10.3389/fneur.2020.577927

Ischemia/reperfusion (I/R) injury is a significant cause of mortality and long-term disability worldwide. Recent evidence has proved that pyroptosis, a novel cell death form, contributes to inflammation-induced neuron death and neurological function impairment following ischemic stroke. Gasdermin D (GSDMD) is a newly discovered key molecule of cell pyroptosis, but its biological function and precise role in ischemic stroke are still unclear. The present study investigates the cleavage activity of GSDMD, localization of pyroptotic cells, and global neuroinflammation in *gsdmd*$^{-/-}$ mice after I/R. The level of cell pyroptosis around the infarcted area was significantly increased in the acute phase of cerebral I/R injury. The ablation of GSDMD reduced the infraction volume and improved neurological function against cerebral I/R injury. Furthermore, we confirmed I/R injury induced cell pyroptosis mainly in microglia. Knockdown of GSDMD effectively inhibited the secretion of mature IL-1β and IL-18 from microglia cells but did not affect the expression of caspase-1/11 *in vitro* and *in vivo*. In summary, blocking GSDMD expression might serve as a potential therapeutic strategy for ischemic stroke.

Keywords: ischemia/reperfusion injury, pyroptosis, neuroinflammation, gasdermin D, microglia, neurological outcome

INTRODUCTION

According to systematic analysis studies of the global burden of disease (GBD) between 1990 and 2017, acute ischemic stroke has become the leading cause of mortality and disability worldwide (1–3), causing severe economic and healthy burdens. Intravenous thrombolysis and selective mechanical thrombectomy are the optimal therapeutic measures for ischemic stroke up till now (4, 5); however, the applicable proportion of intravenous thrombolysis only accounts for 3% of total ischemic stroke patients. Therefore, further research on the pathogenesis and interventions of ischemic stroke is urgently needed.

The primary injury of ischemic stroke is mainly caused by vascular occlusion which leads to neuron death and release of damage-associated molecular patterns (DAMPs) in focal ischemic

tissue. A secondary immune response is subsequently induced in the injury area, characterized by activation of resident cells (mainly microglia), recruitment of peripheral cells (neutrophils, monocytes/macrophages, and other cells) (6, 7), and rapid induction of cascaded events, including the release of pro-inflammatory mediators, blood-brain barrier (BBB) damage, brain edema, and nerve cell death (6, 8). It is reasonable to speculate that blocking the release of inflammatory mediators may be beneficial for stroke recovery.

Pyroptosis, a newly discovered proinflammatory programmed cell death, has drawn increasing attention for its unique characteristics, such as cell swelling, bulging of the plasma membrane, secretion of inflammatory cytokines, and cell lysis (9). The pyroptotic process is dependent on caspase cleavage and accompanied by the maturity and release of pro-inflammatory mediators such as IL-1β and IL-18 (10, 11). The morphological characteristics, occurrence, and regulation mechanisms of pyroptosis are different from other types of cell death such as apoptosis and necrosis. Nucleotide-binding oligomerization domain like receptor (NLR) family proteins serve as sensors that recognize DAMPs and pathogen-associated molecular patterns (PAMPs), including high cytosolic Ca^{2+} with reduced K^+ concentrations, extracellular ATP, mitochondrial dysfunction, and lysosomal rupture (10). These stimuli initiate caspase-dependent canonical or non-canonical inflammasome assembly (12), which subsequently cleaves gasdermin, a recently discovered pyroptosis effector. The N-terminal of gasdermin forms pores on the cell membrane, causing the release of mature inflammatory mediators into the extracellular matrix, and eventually leading to a severe inflammatory cascade reaction (13). Increasing evidence indicates that pyroptosis is induced in central nervous system disease including ischemic stroke (14, 15), traumatic brain injury (TBI) (16, 17), multiple sclerosis (MS) (18), Alzheimer's Disease (AD) (19), and Parkinson's disease (PD) (20). Illuminating the pyroptotic procedure would speed up the development of a cure for those diseases.

Gasdermin D (GSDMD), a 487 amino acid cytoplasmic protein, has been discovered to form membrane pore and act as a key effector for pyroptosis. N-terminal of GSDMD (GSDMD-N) is responsible for pore-forming activity, while the C-terminal domain (GSDMD-C) exerts autoinhibition on GSDMD-induced pyroptosis by binding to the N-terminal (21–23). Studies have confirmed that GSDMD participates in a series of pathologically pyroptotic events (21, 23), including ischemia/reperfusion (I/R) injury-induced pyroptosis. Experimental findings by Lee et al. showed that increased expression of NLRP3 inflammasome components and GSDMD peaked at 48 h after penetrating ballistic-like brain injury (24). Inhibition of caspase-1 mediated pyroptosis by limiting apoptosis-associated speck-like protein containing a CRAD (ASC) oligomerization and GSDMD cleavage resulted in suppressed expression of IL-1β and IL-18, and subsequent alleviation of BBB-disruption and brain injury (16, 17). Many studies have revealed the involvement of pyroptosis in cerebral injury (25, 26). However, the main cell type for pyroptosis, as well as the detailed information regarding GSDMD cleavage and its contribution to global inflammatory profile, still needs to be clarified. This study, utilizing *gsdmd*$^{-/-}$ mice and *gsdmd*$^{-/-}$ microglia cells, highlights the precise function of GSDMD, main pyroptotic effector cell, and canonical or non-canonical inflammasome-dependent pyroptosis pathway in cerebral I/R injury, aiming to elucidate the mechanisms underlying GSDMD-mediated pyroptosis and to exploit new therapeutic targets for ischemic stroke.

MATERIALS AND METHODS

Animals and Stroke Model

Wild type C57BL/6 mice (n = 80, 8–10 weeks old, 20–25 g) were purchased from the Shanghai Laboratory Animal Center, Chinese Academy of Science (SLACCAS, Shanghai, China). All mice were housed in a standardized animal care center under a 12-h light-dark cycle with free access to food and water. All experimental operations were approved by the Ethics Committee of Wenzhou Medical University and were carried out in strict accordance with the animal care and use guidelines of the National Institutes of Health. GSDMD knockout (*gsdmd*$^{-/-}$) mice (n = 20) were purchased from the Nanjing Biomedical Research Institute of Nanjing University (SCXK 2015-0001). All the *gsdmd*$^{-/-}$ mice were generated from heterozygous breeding pairs of C57BL/6 mice.

The wild type C57BL/6 mice were randomized into a Sham group (n = 20), an MCAO model group (n = 40), and *gsdmd*$^{-/-}$ group (n = 20). The middle cerebral artery occlusion (MCAO) model was established by intraluminal suture as described previously (27). Briefly, wild type C57BL/6 mice in the model group and the *gsdmd*$^{-/-}$ mice inhaled 8% isoflurane. The inhalation anesthesia was maintained using a face mask with 4% isoflurane in a 5-l/min oxygen flow. The mice were then placed on a heating device to sustain a constant body temperature of 37°C. The right common, internal, and external carotid arteries (CCA, ICA, and ECA) were gently dissected and exposed. With a blockage of ICA at the proximal cranial end and the proximal end of the CCA, a suitable nylon thread was then inserted into the anterior cerebral artery to block the blood flow of the middle cerebral artery (MCA). After blockage for 1 h, the nylon thread was pulled out to allow reperfusion. The sham operated mice accepted the same operations, except for the occlusion of CCA. The mortality of the Sham group was around 5%. Mortality of the model group and *gsdmd*$^{-/-}$ group was 13 and 10%, respectively at 24 h and reached 22 and 16% at 72 h.

Cell Culture and OGD/R

BV2 microglia cells were purchased from iCell Bioscience Inc. (iCell-m011) and cultured in Dulbecco's minimal essential medium (DMEM) with 10% FBS (Gbico, USA), 100 U/ml penicillin, and 100 U/ml streptomycin under standard conditions. Oxygen and glucose deprivation/reperfusion (OGD/R) were conducted using an anaerobic incubator. Briefly, cells were incubated in a glucose-free DMEM (Thermo Fisher Scientific, USA) in a humidified 37°C anaerobic incubator supplied with a gas mixture of 94% N_2, 5% CO_2, and 1% O_2 for 2-6 h. Reperfusion was allowed in normal conditions at 37°C for 12 h.

Detection of Local Cerebral Blood Flow (CBF), Body Temperature, Blood Gas, and Blood Glucose

Mice were anesthetized by intraperitoneal injection of ketamine (90 mg/kg) and xylazine (10 mg/kg). The anesthetized mice were fixed on a stereotaxic apparatus and given local anesthesia on the top of the head with lidocaine. The skull was exposed by a median incision. Tissues adhering to the skull were removed by 3% H_2O_2. A probe was fixed at the core blood supply area of MCA (2.0 mm posterior to anterior fontanelle and 6.0 mm left from midline) to monitor local CBF. The MCAO model was established 10 min later. CBF value was recorded after 1 h of MCAO and 20 min of reperfusion. Taken the baseline value of CBF as 100%, the ratio of the CBF after MCAO/reperfusion to the baseline value represents the variation rate of CBF. The blood sample was taken from the submandibular vein of the mice. The body temperature, PH value of venous blood, oxygen partial pressure (PO_2), carbon dioxide partial pressure (PCO_2), and blood glucose of the mice were monitored 5 min before and after the operation. The CBF was monitored by a laser Doppler monitor (moorVMS-LDF, Wilmington, Delaware, USA). The body temperature of the mice was kept at 36 to 37°C by the 69001 temperature maintenance instrument (RWD Life Science Co., Ltd., Shenzhen, China). The blood gas of the venous blood was analyzed by the ABL80basic blood gas analyzer (Denmark Leidow). The blood glucose was measured by a One-touch blood glucose meter (Johnson & Johnson, US).

TTC Staining

The brains of the mice were removed and cut into 2 mm sections 24 h after MCAO/reperfusion. The sections were then placed in 2% saline-dissolved 2,3,5-Triphenyltetrazolium chloride (TTC, sigma) for 30 min at room temperature. After washing with PBS, the sections were placed from the frontal pole and photographed. Ultimately, the infarct volume was calculated by Image J software.

Neurobehavioral Training and Evaluation

The neurobehaviors of the mice were evaluated using a modified neurological severity score (mNSS) after training as previously described (28). Briefly, the neurological symptoms were scored at 9 a.m. on day 1, 7, 14, 21, and 28 after ischemia. A higher score indicates a more severe neurological dysfunction. All mice were pre-trained for 14 days before operation until their performances reached a steady state. The scoring was performed in strict accordance with double blinding principles. Scoring of the same mouse was performed with a time interval of more than 20 min.

Immunohistochemical Analysis

Mice were anesthetized and perfused with normal saline (NS) and 4% paraformaldehyde. After that, the brain was rapidly taken out and placed in 4% paraformaldehyde for 2 days followed by paraffin embedding and sectioning. After continuous rehydration with 30% sucrose solution and washing with PBS, endogenous peroxidase activity in the tissue sections was blocked by 3% H_2O_2 for 25 min at room temperature. Antigen crosslinking was then conducted followed by two PBS washes. After being blocked in blocking solution (5% Goat Serum Albumin; Sigma) for 1 h, the sections were then incubated with the primary antibody against MAP2 (1:20, Proteintech) overnight. After two PBS washes and subsequent incubation with secondary antibody (ASS3403; Abgent, San Diego, CA, USA) for 30 min, the sections were then incubated with DAB (Solarbio, DA1010) till proper color appeared.

Immunofluorescence Assays

Brain sections were fixed with 4% paraformaldehyde at room temperature (RT) for 30 min and then incubated in PBST (0.4% triton in PBS) containing 5% bovine serum albumin solution (BSA, Sigma-Aldrich) for 30 min at 37°C to rupture cell membrane and block non-specific staining. After that, incubation with the primary antibodies against cleaved caspase-1 (1:25, CST), cleaved caspase-11 (1:25, Abcam), MAP2 (1:50, Santa Cruz), and TMEM119 (1:200, Abcam) was then conducted at 4°C overnight followed by crosslink with the corresponding secondary antibody at RT for 1 h. After the unbound antibodies were washed off, the nuclei were then stained with DAPI (Abcam) and photographed with a fluorescence microscope (Leica). The data were analyzed from 3 randomly selected microscope fields using Image J software.

Western Blot Analysis

Brain tissue was removed from euthanized mice and lysed in a RIPA buffer containing a protease inhibitor cocktail. After protein quantification with a bicinchoninic acid (BCA) protein assay kit (Thermo Fisher Scientific, USA), the sodium dodecyl sulfate polyacrylamide gel electrophoresis (SDS-PAGE) was then conducted. After the protein was transferred to a 0.22- or 0.45-μm polyvinylidene fluoride membrane (pre-activated with methanol; Milli-pore, Billerica, MA, USA), the membrane was blocked with 5% milk for 2 h, followed by incubation at 4°C for 24 h with primary antibodies against the following proteins: NLRP3 (1:1,000, CST), GSDMD (1:1,000, Abcam), caspase-1 (p20, 1:1,000, CST), caspase-11 (1:1,000, affinity), IL-1β (p17, 1:400, Proteintech), and IL-18 (1:500, Affinity). Glyceraldehyde 3-phosphate dehydrogenase (GAPDH; 1:1,000, CST), α-tubulin (1:1,000, CST), or β-actin (1:1,000, CST) was used as an internal reference. After that, the membrane was washed and the protein was incubated with the corresponding secondary antibody (1:5,000) at RT for 2 h. Image J software was used to analyze immunoreactive bands. The intensity of the targeted protein signal was compared to GAPDH or β-actin intensity.

Enzyme-Linked Immunosorbent Assay (ELISA)

Cortical tissues of the brain taken from mice at 12, 24, 48, and 72 h were used for ELISA. The secretion levels of IL-1β and IL-18 in cortical tissues and cell culture medium were measured by ELISA kits (Elabscience Biotechnology, Wuhan, China) according to the manufacturer's instructions.

Construction of Lentiviral Vectors for GSDMD Knockdown and Overexpression

The lentiviral vector pLent-U6-GFP-puro was applied for knockdown of GSDMD. Briefly, the shRNA-GSDMD

oligonucleotides were designed and annealed through primers (N-shRNA: 5′- GATCCCACCGCAGCATGAAAGGCACCTT CACGAATGAAGGTGCCTTTCATGCTGCA−3′; C-shRNA: 5′- CGCGTAAAAGCAGCATGAAAGGCACCTTCATTCGTG AAGGTGCCTTTCATGCTGCG−3′). The lentiviral plasmid carrying shRNA-GSDMD fragment together with packaging plasmids were co-transfected into 293T cells for packaging. Virus-containing media were then collected, filtered, and concentrated for targeted suppression. For overexpression of GSDMD, the full length of GSDMD was amplified, enzyme digested, and conjoined with plasmid vector pCDH-CMV-MCS-EF1-Puro (Genepharma, Shanghai, China), followed by co-transfection into lentivirus. Microglia BV2 cells were infected with lenti-GSDMD. Western blotting was applied to assess the effectiveness of GSDMD knockdown or overexpression.

RNA Extraction and PCR

Total RNA was isolated by TRIzol (Invitrogen) and cDNA was obtained from reverse transcription of the total RNA by RevertAid First Strand cDNA Synthesis Kit. PCR amplification assay was conducted with primers (GSDMD-gtF1: CGATGG AACGTAGTGCTGTG; GSDMD-gtR1: TCCTTCCCAACCTGC TGTTG).

Statistical Analysis

All data analysis is based on at least three independent experiments. The data are present as mean ± standard deviation (SD). Data analysis at different time points was carried out using two-way analysis of variance (ANOVA) followed by least significant difference (LSD) *post-hoc* analysis. For other data comparisons, one-way ANOVA was used, followed by LSD *post-hoc* analysis or Student's *t*-tests. We considered a *p*-value lower than 0.05 as significant.

RESULT

Ischemic Reperfusion Stroke Induces GSDMD-Mediated Pyroptosis

In order to study the pyroptosis in I/R, we firstly constructed the model of cerebral I/R in mice using the MCAO method. After the model had been establishment for 24 h, TTC staining showed that the subcortical tissue of the I/R ipsilateral brain was partially infarcted, and the infarcted area was approximately 51.35 ± 13.92% of the unilateral brain (**Figures 1A,B**). The neurological deficit score revealed that the MCAO group had a higher neurological deficit score (**Figure 1C**). The immunohistochemical staining also showed a significant infarcted area in the MCAO group (**Figures 1D,E**). These results indicate the successful construction of the cerebral I/R model in the mice.

GSDMD serves as a key response component in pyroptosis. To investigate the pyroptotic process during I/R injury, we detected the cleavage of GSDMD at different time points after the MCAO model was established. As shown in **Figures 2A,B**, cleaved GSDMD appeared at 12 h post I/R injury, and peaked at 24 h, indicating the initiation and development of GSDMD-mediated pyroptosis during I/R injury. As cleavage effectors of GSDMD, caspase-1, and caspase-11 regulate in canonical and non-canonical inflammasomes-dependent pathways. Through detecting the expression of active caspase-1 and caspase-11 by immunoblotting in the ischemic penumbra, we found that both caspase-1 and caspase-11 were activated and exhibited the same expression tendency as cleaved GSDMD (**Figures 2C,D**), which subsequently resulted in the production of mature IL-1β and IL-18 (**Figures 2E,F**). These results indicated that both canonical and non-canonical inflammasomes were involved in I/R induced pyroptosis.

Pyroprosis Occurs Mainly in the Microglia

To further detect which type of cells in the brain were involved in I/R injury induced pyroptosis, double-immunofluorescence staining of MAP2 plus cleaved caspase-1, MAP2 plus cleaved caspase-11, TMEM119 pus cleaved caspase-1, and TMEM119 pus cleaved caspase-11 was applied to locate pyroptosis. **Figure 3** shows that after brain I/R injury, $MAP2^+$ cells were significantly reduced while $TMEM119^+$ cells were increased significantly, indicating the death of neurons and activation of microglia cells post MCAO. We also found that cleaved caspase-$1/11^+$ cells increased significantly and well-overlapped with $TMEM119^+$ cells, whereas the surviving neurons displayed negligible positive staining of caspase-1 and caspase-11. Taken together, these results suggested that microglia might be the main effector cell to activate pyroptosis in I/R injury.

GSDMD Promotes Pyroptosis in Microglia Cells

After cerebral pyroptosis was confirmed in microglia post stroke induction, we next investigated the precise role of GSDMD in stroke-induced microglia. An OGD/R model of BV2 microglia was established to mimic I/R injury *in vitro*. As shown in **Figures 4A,B**, cleaved GSDMD (p30) was significantly elevated 2 h after OGD/R, and peaked at 4 h, indicating GSDMD-mediated pyroptosis was induced in microglia by OGD/R injury. However, BV2 microglia cells showed a high death rate after 6 h of OGD/R treatment, which might be attributed to the decreased expression of GSDMD. The expression of caspase-1 and caspase-11 was also detected and exhibited the same increasing tendency as GSDMD expression (**Figures 4A,C,D**). These results determined that GSDMD-mediated pyroptosis was activated in microglia by OGD/R injury.

To further clarify the mechanism of GSDMD in pyroptosis and related inflammatory responses in microglia, we detected the relevant factors after interfering with the expression of GSDMD. As shown in **Figures 4E,F**, the addition of exogenous GSDMD increased the content of GSDMD protein in microglia, while shRNA-GSDMD caused a decrease in GSDMD-p30 protein content 4 h after OGD/R injury. Neither exogenous GSDMD nor shRNA-GSDMD influenced the expression of caspase-1 and caspase-11 in microglia (**Figures 4G,H**; $P > 0.05$). The secretion changes of IL-1β and IL-18 were measured by ELISA. OGD/R treatment increased the media secretion of IL-1β and IL-18 from 38.81 ± 6.311 pg/ml, 11.25 ± 2.125 pg/ml to 104.9 ± 12.92 pg/ml, and 27.48 ± 2.104 pg/ml, respectively. Overexpression of GSDMD significantly promoted the secretion levels of IL-1β

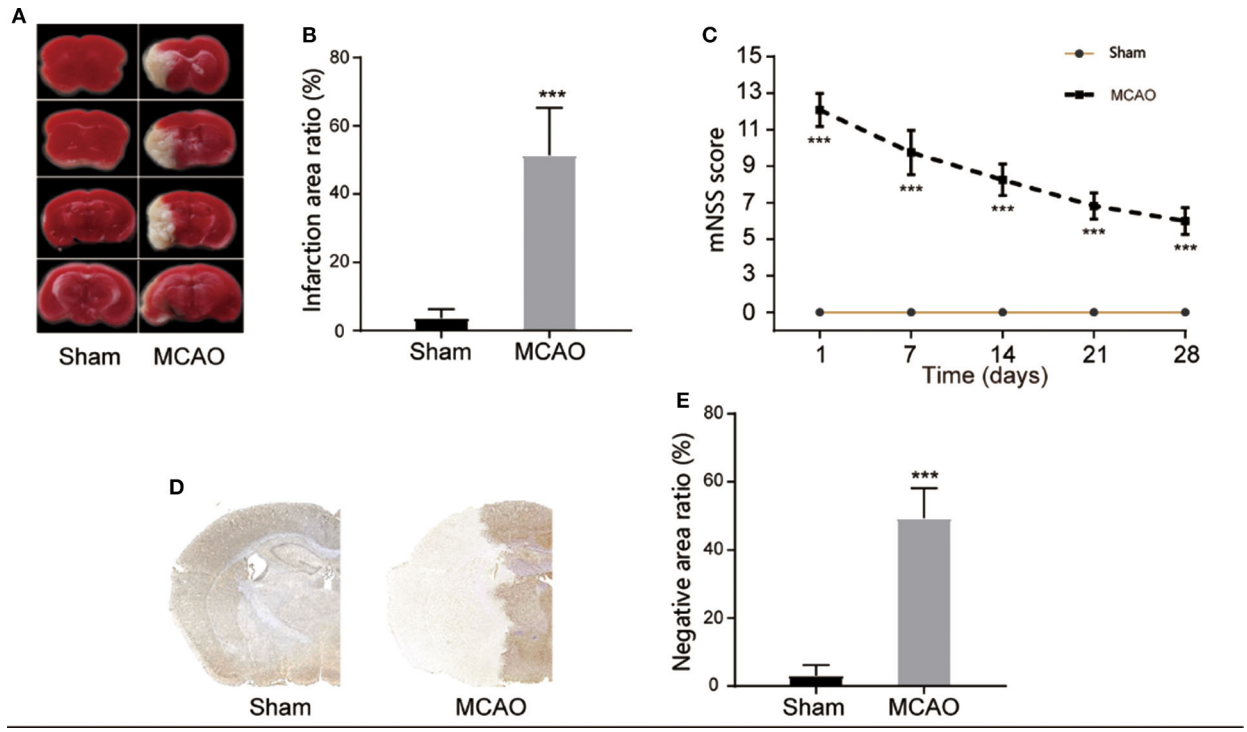

FIGURE 1 | Construction of cerebral I/R model. **(A,B)** Representative images of TTC staining in four sequential brain slices from the mice in each group. $n = 5$. **(C)** Neurological recovery was evaluated by the mNSS scoring system on days 1, 7, 14, 21, and 28 post MCAO/R. $n = 12$. **(D,E)** Immunohistochemical staining of brain tissue at day 1 post MCAO/R. $n = 5$. $^{***}P < 0.001$, vs. the Sham group. I/R, ischemia reperfusion; MCAO, middle cerebral artery occlusion; mNSS, modified neurological severity score.

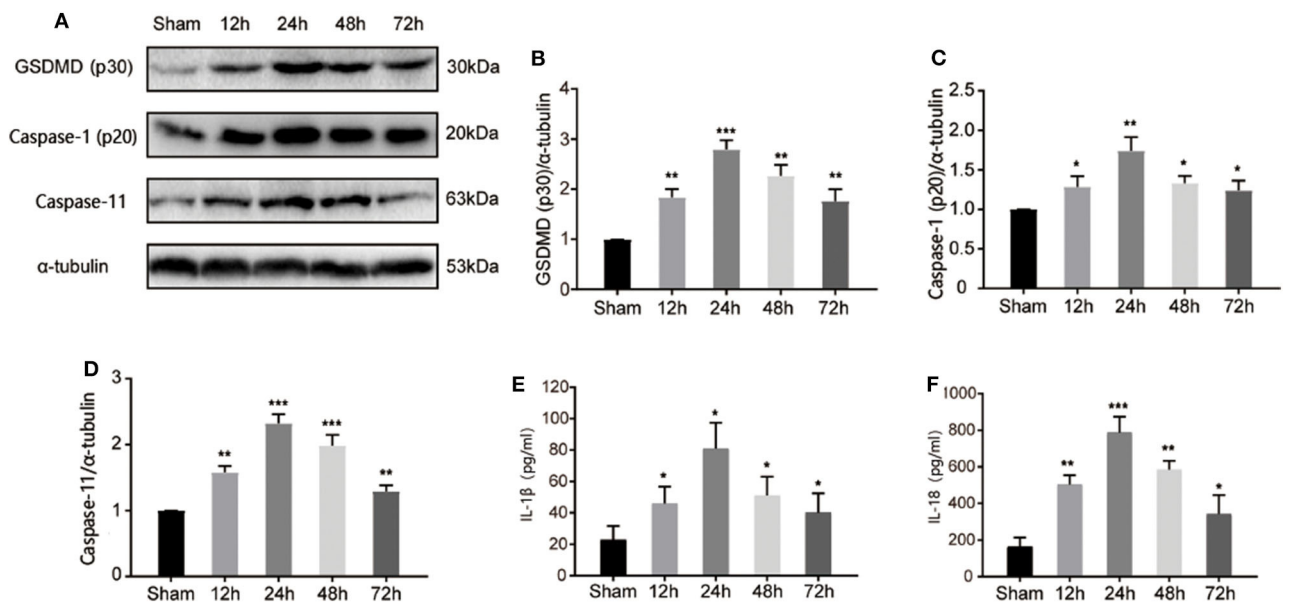

FIGURE 2 | I/R injury induced canonical and non-canonical inflammasome dependent pyroptosis in ischemic cortex. **(A)** Band intensity of cleaved-GSDMD, active caspase-1, and caspase-11 at 12, 24, 48, 72 h post I/R injury. **(B–D)** Relative expression of cleaved-GSDMD **(B)**, active caspase-1 (p20) **(C)**, and caspase-11 **(D)** at 12, 24, 48, 72 h post I/R injury. $n = 5$. **(E,F)** The levels of IL-1β and IL-18 in the cortex were measured by ELISA at 12, 24, 48, 72 h post I/R injury. $n = 5$. $^{*}P < 0.05$, $^{**}P < 0.01$, $^{***}P < 0.001$, vs. the Sham group. I/R, ischemia reperfusion; GSDMD, gasdermin D.

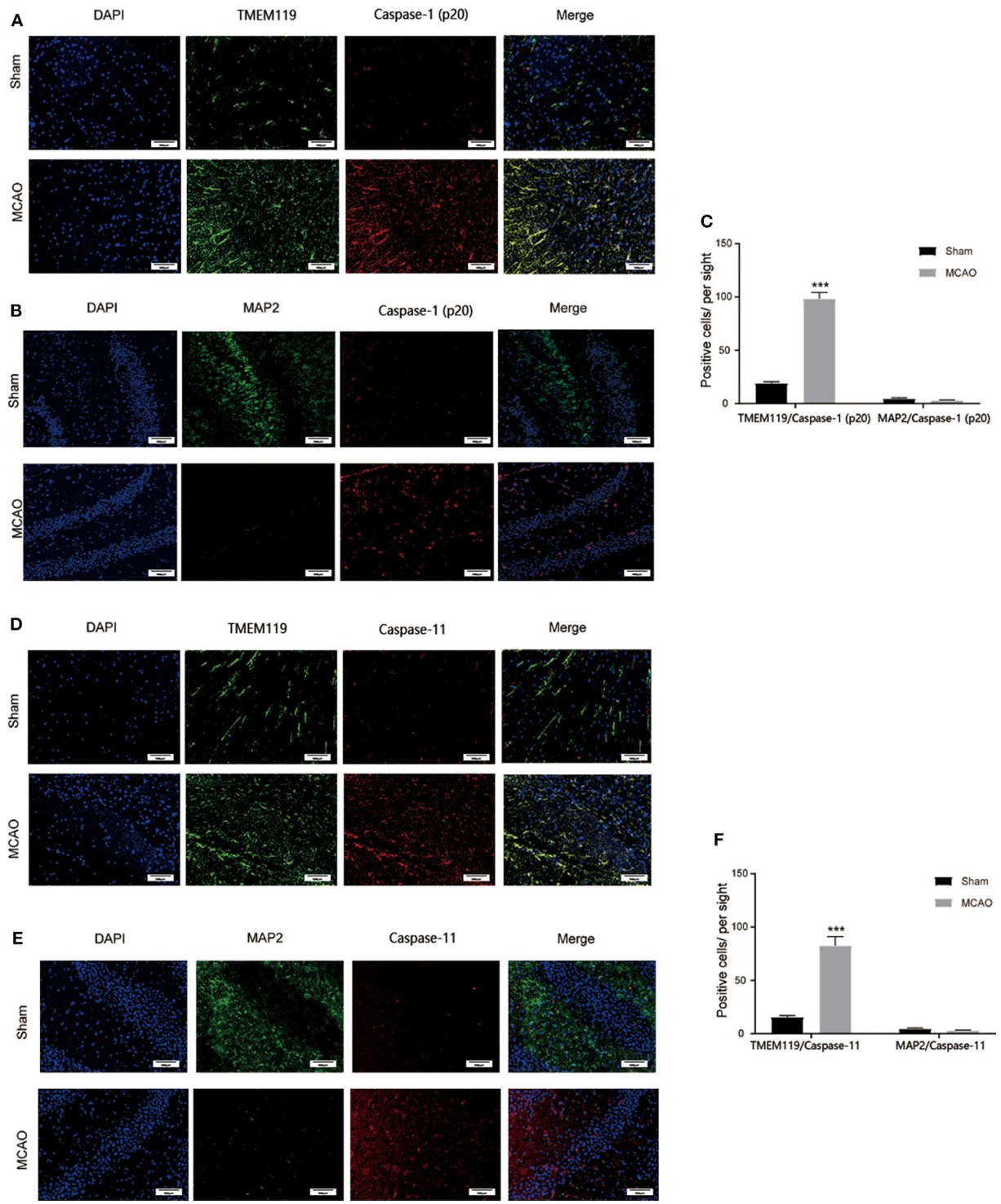

FIGURE 3 | Main cell type for pyroptosis post I/R injury. **(A)** Caspase-1$^+$ (red) and TMEM119$^+$ (green) cells were significantly induced in the cortex at 24 h post I/R injury. **(B)** Caspase-1$^+$ (red) cells were largely induced while MAP2$^+$ (green) neurons were rarely detected in the cortex at 24 h post I/R injury. **(C)** Statistical analysis of immunofluorescence-positive cells. **(D)** Caspase-11$^+$ (red) and TMEM119$^+$ (green) cells were significantly induced in the cortex at 24 h post I/R injury. **(E)** Caspase-11$^+$ (red) cells were largely induced while MAP2$^+$ (green) stained neurons were rarely detected in the cortex at 24 h post I/R injury. **(F)** Statistical analysis of immunofluorescence-positive cells. Scale bars: 100 μm. $n = 5$. Data are presented as mean ± SD. $^{***}P < 0.001$, vs. the Sham group. I/R, ischemia reperfusion.

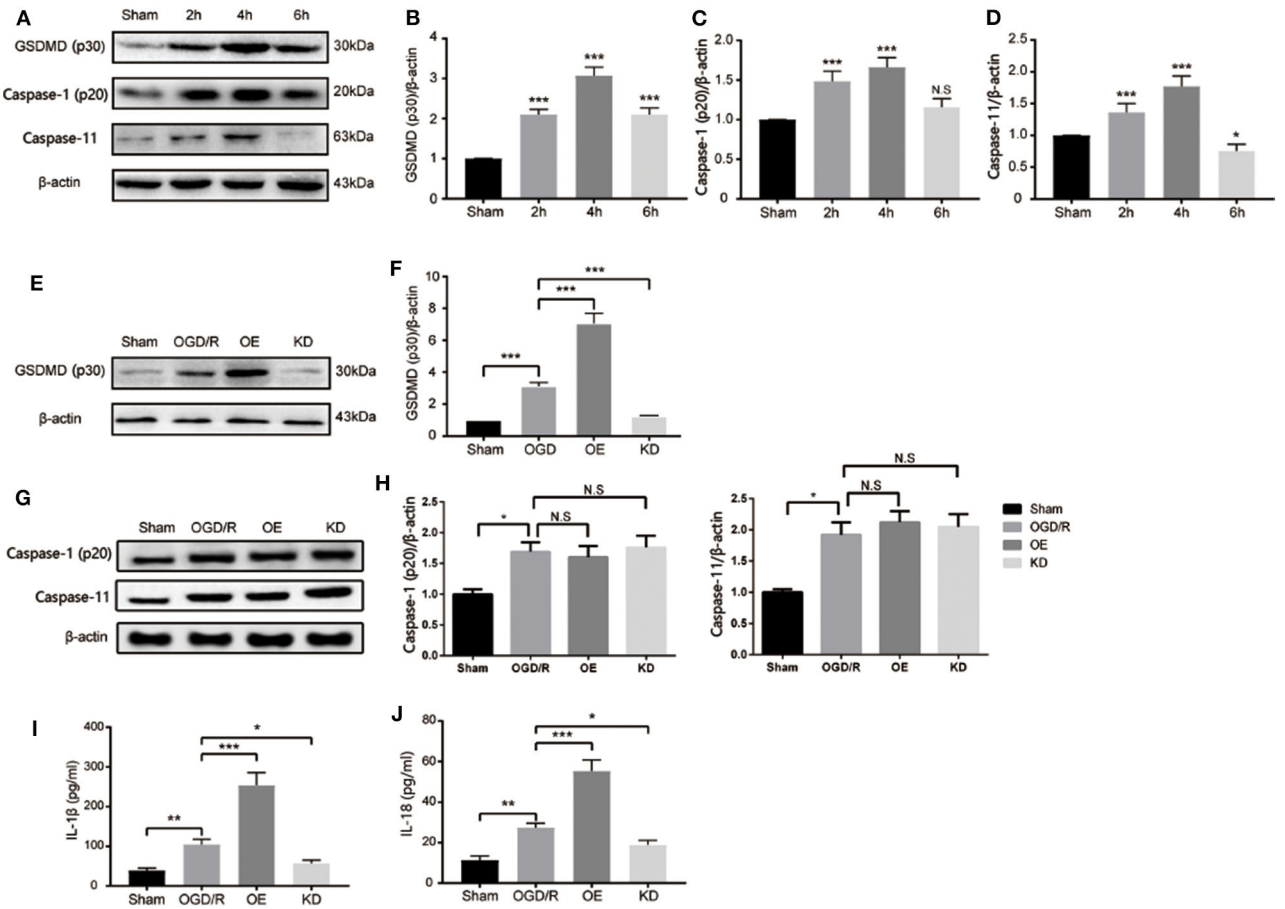

FIGURE 4 | GSDMD is necessary for I/R induced pyroptosis and proinflammatory cytokine secretion in microglia BV2 cells. **(A–D)** Western blot analysis of the relative expression of cleaved-GSDMD **(B)**, active caspase-1 (p20) **(C)**, and caspase-11 **(D)** in microglia after OGD/R. **(E,F)** Relative expression of cleaved-GSDMD post shRNA-GSDMD interference or GSDMD overexpression in microglia. $n = 5$. **(G,H)** Relative expression of caspase-1 and caspase-11 in microglia post GSDMD silence or GSDMD overexpression. $n = 5$. **(I,J)** The expression of mature IL-1β and IL-18 in microglia BV2 cells were measured by ELISA at 4 h post OGD/R. $n = 3$. Data are presented as mean ± SD. $^{*}P < 0.05$, $^{**}P < 0.01$, $^{***}P < 0.001$ vs. the Sham group or relative group. GSDMD, gasdermin D; I/R, ischemia reperfusion; OGD, oxygen glucose deprivation.

and IL-18 to approximately 254 ± 31.88 and 55.3 ± 5.397 pg/ml (**Figures 4I,J**). However, the absence of GSDMD attenuated the increased secretion levels of IL-1β and IL-18 (**Figures 4I,J**). Taken together, GSDMD mediated pyroptosis-dependent inflammation reaction in microglia.

Knockout of GSDMD Accelerates Neurological Recovery From I/R Injury

To further validate the effective role of GSDMD protein in I/R induced pyroptosis *in vivo*, we constructed *gsdmd*$^{-/-}$ C57BL/6 mice by CRISPR-Cas9 technology. Firstly, the cerebral I/R model was established in wide type (WT) and *gsdmd*$^{-/-}$ C57BL/6 mice. The local CBF was monitored according to the technical standards of the Stroke Treatment Academic Industry Roundtable (STAIR). The local CBF of WT mice dropped from 100% to about 20% after MCAO, while returned to 100% after the thread plug was removed. The CBF of *gsdmd*$^{-/-}$ mice which were treated in the same way as the WT mice had similar variations (**Figure 5A**, $P > 0.05$). The body temperature, blood gas, and blood glucose of WT and *gsdmd*$^{-/-}$ mice were also measured before and after modeling and showed no significant differences in these two groups of mice (**Figures 5B–D**; $P > 0.05$). Therefore, it was appropriate to compare the groups in the following experiments. TTC staining showed that 24 h after I/R, the cerebral infarction of the *gsdmd*$^{-/-}$ group reduced to 25.37 ± 9.074% compared to 44.55 ± 5.834% in the WT group (**Figures 5E,F**; $P < 0.01$). Twenty-eight days after stroke, the mNSS scores of the *gsdmd*$^{-/-}$ group and WT group were 3.75 ± 0.4523 and 6.25 ± 0.6216, respectively (**Figure 5G**, $P < 0.001$), indicating that the absence of GSDMD significantly promoted neurological recovery from I/R injury. The result of immunohistochemical staining was consistent with that of the TTC staining (**Figures 5H,I**), suggesting that the absence of GSDMD effectively reduced the infarct volume.

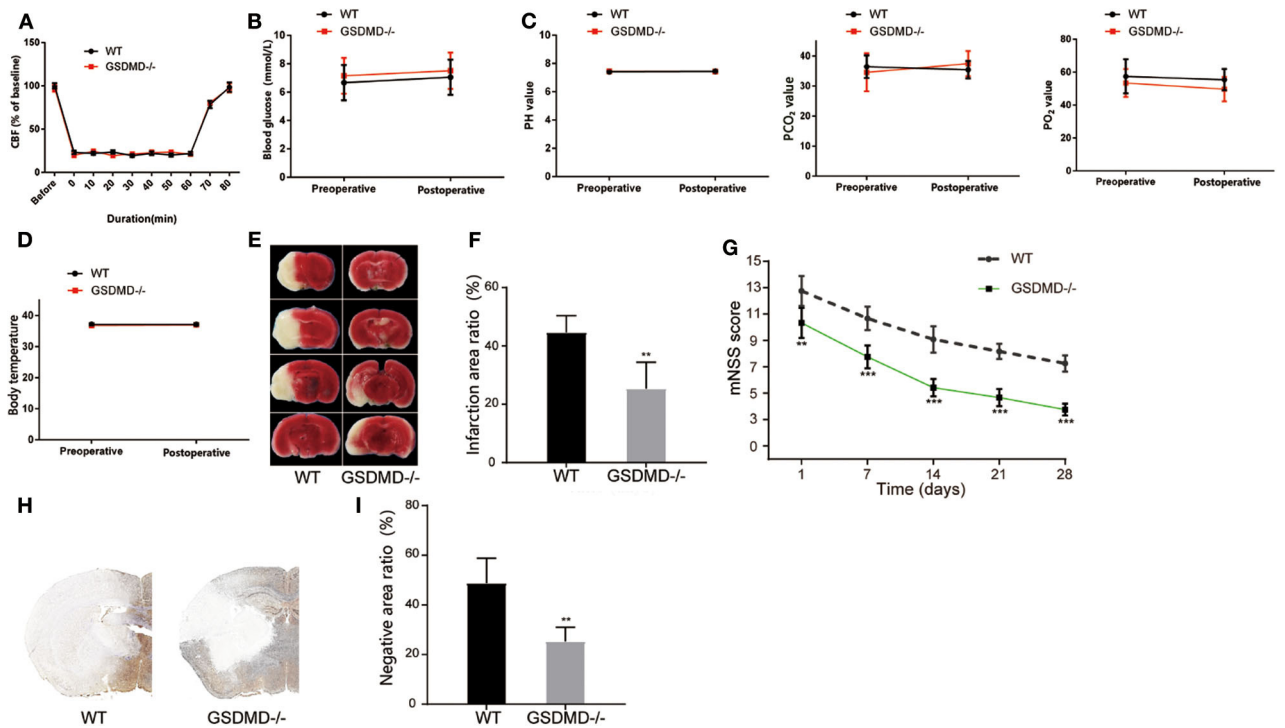

FIGURE 5 | Ablation of GSDMD improves neurological outcome post I/R injury. **(A)** CBF in the MCAO modeling. $n = 5$. **(B–D)** Blood glucose **(B)**, blood gas **(C)**, and body temperature **(D)** of the mice before and after MCAO modeling. $n = 5$. **(E,F)** Representative images of TTC staining in four sequential brain slices from WT and *gsdmd*$^{-/-}$ mice. $n = 5$. **(G)** Neurological recovery was evaluated by mNSS on days 1, 7, 14, 21, and 28 post MCAO/R. $n = 12$. **(H,I)** Immunohistochemical staining of brain tissue on day 1 post MCAO/R. $n = 5$. $^{**}P < 0.01$, $^{***}P < 0.001$, vs. the WT group. GSDMD, gasdermin D; I/R, ischemia reperfusion; MCAO, middle cerebral artery occlusion; CBF, cerebral blood flow; mNSS, modified neurological severity score; WT, wild type.

Knockout of GSDMD Prevents Caspase-1 and Caspase-11 Mediated Inflammatory Response

To further validate the role of GSDMD protein in the global inflammatory response during I/R injury, the secretion of IL-1β and IL-18 was detected through ELISA. As shown in **Figures 6A,B**, the expressions of plasma IL-1β and IL-18 were significantly attenuated in the *gsdmd*$^{-/-}$ group, approximately from 88.35 ± 5.993 pg/ml and 793.3 ± 87.35 pg/ml to 49.12 ± 7.224 pg/ml and 524.8 ± 86.33 pg/ml, respectively. The immunofluorescence staining of cleaved caspase-1 (**Figure 6C**) showed that blockage of GSDMD did not affect the expression or cleavage of caspase-1, suggesting that the knockout of GSDMD had no influence on the upstream process of pyroptosis but that it significantly blocked the release of inflammatory cytokines. Furthermore, through detecting caspase-1 and caspase-11 mediated pyroptosis pathways post I/R injury, the expression of caspase-1 (p20), caspase-11, mature IL-1β, IL-18, and NLRP3 proteins in the ischemic cortex showed no significant changes in the absence of GSDMD (**Figures 6D–J**). These results suggested that knockout of the GSDMD gene blocked the release of mature IL-1β and IL-18, but did not affect the process of maturation, which was consistent with other studies (13).

DISCUSSION

In this study, we demonstrated that cerebral pyroptosis was significantly induced around the infarcted area in the acute I/R injury. Our results revealed that knockdown of GSDMD exhibited promising therapeutic effects, including improving neural function, reducing cortical lesion volume, and attenuating global inflammation *in vitro* and *in vivo*. In addition, we confirmed that microglia might be the main pyroptotic effector cell in the ischemic brain. Moreover, the ablation of GSDMD could effectively reduce the secretion of mature IL-1β and IL18. Brain damage following I/R injury is a complicated pathophysiological problem, accompanied by a variety of interrelated cellular and molecular changes. These changes include neuronal apoptosis, BBB disruption, mitochondrial dysregulation, reactive oxygen species (ROS) accumulation, and inflammatory reaction (25, 29). Overall, cerebral ischemic injury causes a large number of irreversible neuron deaths. Although timely reperfusion prevents further neuron deaths, the ongoing reperfusion triggers secondary brain injuries, including neural inflammation, oxidative damage, cell apoptosis, and necroptosis, which finally leads to cerebral infarct and neurological deficit (30, 31). In this study, WT mice exhibited a significant neurological deficit and plentiful nerve cell deaths after I/R, while

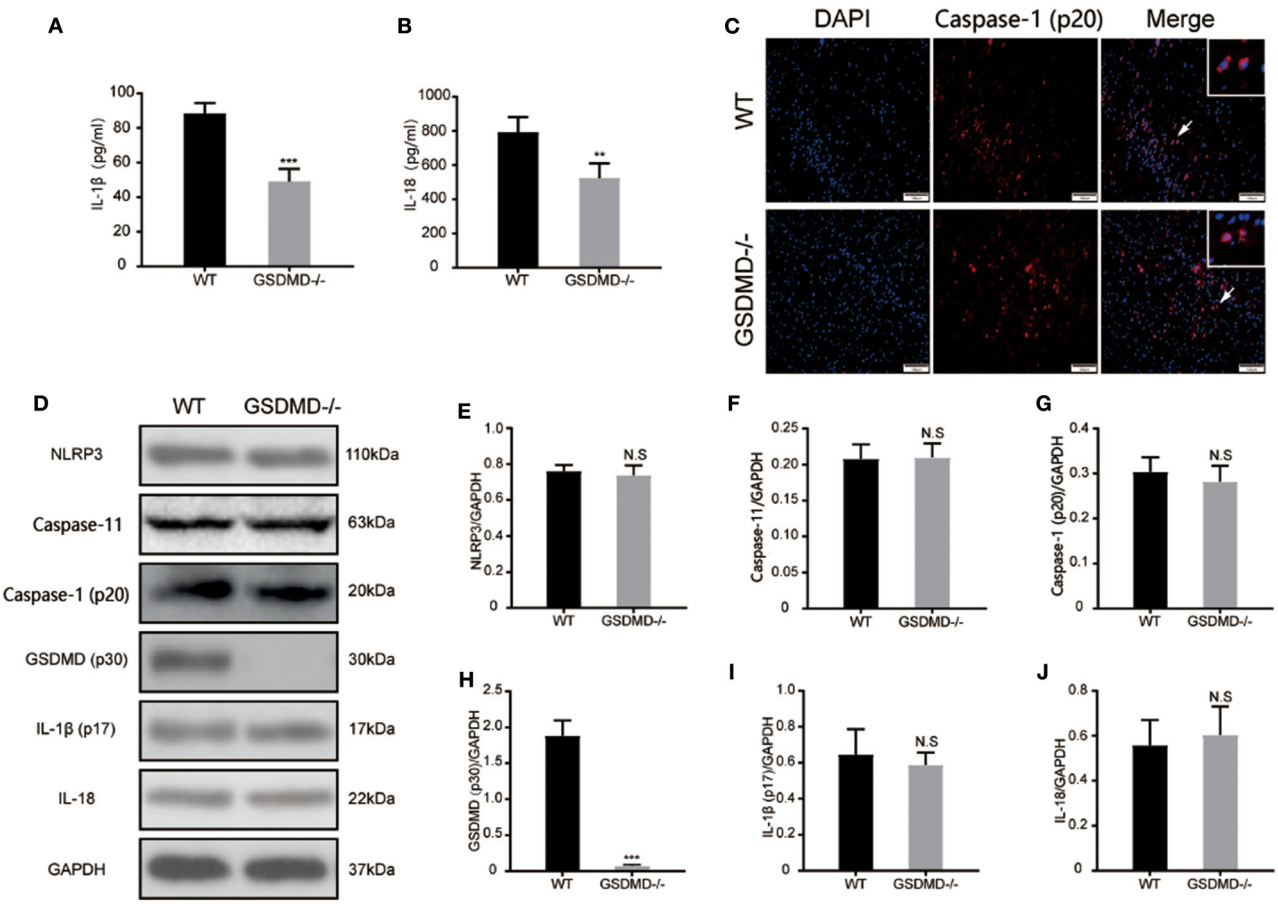

FIGURE 6 | Ablation of GSDMD reduces pyroptosis and global neuroinflammation post I/R injury. **(A,B)** Secretion of mature IL-1β and IL-18 into plasma was measured by ELISA at 24 h post I/R injury. $n = 5$. **(C)** Representative photographs of immunofluorescence staining for cleaved caspase-1 (red) in the cortex at 24 h post-injury. $n = 5$. **(D–J)** Western blotting assay and statistical analysis of the relative expression of NLRP3 **(E)**, caspase-11 **(F)**, active caspase-1**(G)**, cleaved GSDMD **(H)**, active mature IL-1β **(I)**, and IL-18 **(J)**. $n = 5$. $^{**}P < 0.01$, $^{***}P < 0.001$ vs. the WT group. GSDMD, gasdermin D; I/R, ischemia reperfusion; WT, wild type.

gsdmd$^{-/-}$ mice gained a neural recovery, suggesting GSDMD acted as a crucial protein in I/R induced secondary injury.

Pyroptosis has been identified as a programmed cell necroptosis associated with inflammatory and antimicrobial responses. Pyroptosis is featured by cell membrane perforation and disintegration, which eventually result in cell lysis (32). The initiation of pyroptosis is caused by recognition of PAMPS and DAMPs through NLRand Toll-like receptor (TLR) family proteins which trigger caspase-dependent cleavage of GSDMD. GSDMD-N binds to lipids in the plasma membrane and forms large oligomeric pores with a diameter of 10–20 nm, causing the release of pro-inflammatory mediators IL-1β and IL-18 (33, 34). Therefore, preventing GSDMD cleavage and membrane pore formation might terminate cell pyroptosis. To date, caspase-1 dependent canonical inflammasomes and caspase-4/5/11 dependent non-canonical inflammasomes are found to be involved in the cleavage of the GSDM family (34, 35). In our study, canonical inflammasome and non-canonical inflammasome mediated pyroptosis was detected during I/R injury, evidenced by increased expression of NLRP3, caspase-1/11, GSDMD, and IL-1β/18 (**Supplementary Figure 1**). Further investigations into the process of inflammasome assembly may provide new insights into I/R injury induced pyroptosis.

Neuroinflammation is considered as the main cause of secondary brain injury during I/R. Immune cells recognize certain danger signals which boost production and the release of cytokines like TNF-α, IL-1β, IL-6, MCP-1, and MIP-1α, leading to activation of inflammatory pathways and neural damage (36, 37). As a pro-inflammatory process, pyroptosis causes not only rapid loss of membrane integrity but also the release of mature IL-1β and IL-18, which induces the strong pro-inflammatory activity of immune cells. A pore of about 20 nm was created in the cell membrane, allowing for water influx and leading to cell swelling and cellular breakdown (38). In our study, through interrupting I/R injury induced pyroptosis by inhibition of GSDMD, we successfully reduced expression of IL-1β and IL-18 in plasma but not in ischemic tissue, suggesting that GSDMD pore formation contributed to the release of proinflammatory cytokines from immune cells. Since GSDMD activity can influence the secretion

of mature IL-1β and IL-18, further investigation could be made into the potential of GSDMD inhibition for inflammation expansion and neuron protection.

Consistent with our study, Zhang et al. have identified GSDMD as a key executioner in caspase-1-mediated pyroptosis during I/R injury (26). However, the cell candidate for I/R induced pyroptosis remains unclear. As the main immune cells resident in brain tissue, it has been proposed that microglia play an essential role in the progression of neuroinflammation (39). A recent study demonstrated that microglia acquired an M1 phenotype and secreted abundant pro-inflammatory cytokines during I/R injury (40). Immunofluorescence assay in this study showed that the microglia was activated in I/R injury induced cerebral pyroptosis. Aggregated intracellular proinflammatory mediators are released into the extracellular matrix during microglia pyroptosis, causing neuronal inflammation around the ischemic penumbra (41, 42). As the inflammation continues, necrosis of the ischemia penumbra is aggravated. Based on *in vivo* and *in vitro* experiments, GSDMD knockout resulted in less pyroptotic microglia cells and attenuated global cerebral neuroinflammation, which was caused by blockage of pore formation in the cell membrane and reduction of the subsequent secretion of proinflammatory mediators. We also found massive neuron deaths in the ischemic penumbra even though GSDMD was inhibited, suggesting that ischemia induced neuron death was irreversible. Therefore, rescuing neurons nearby the ischemic penumbra is still of great importance.

There are some limitations to this study. Firstly, apart from NLRP3-driven inflammasome assembly, we did not dig into other NLRs or TLRs which also trigger the initiation of pyroptosis during I/R injury. Secondly, we only performed immunofluorescence of GSDMD and cleaved caspase-1 in neurons and microglia to find out that ischemic stroke induced pyroptosis mainly occurs in microglia that resides in the brain tissue, but did not exclude the possibility of other immune cells like astrocytes, neutrophils, and permeated macrophages being the candidate for stroke induced pyroptosis. Despite these limitations, this study provides new insights into neurological recovery and stroke treatment. Since pyroptosis is not responsible for neuron death during ischemic stroke, the rescue of neurons may be of great significance to neurological recovery. Other forms of cell death, including apoptosis, necrosis, and ferroptosis, may also play certain roles in secondary cerebral injury. Future

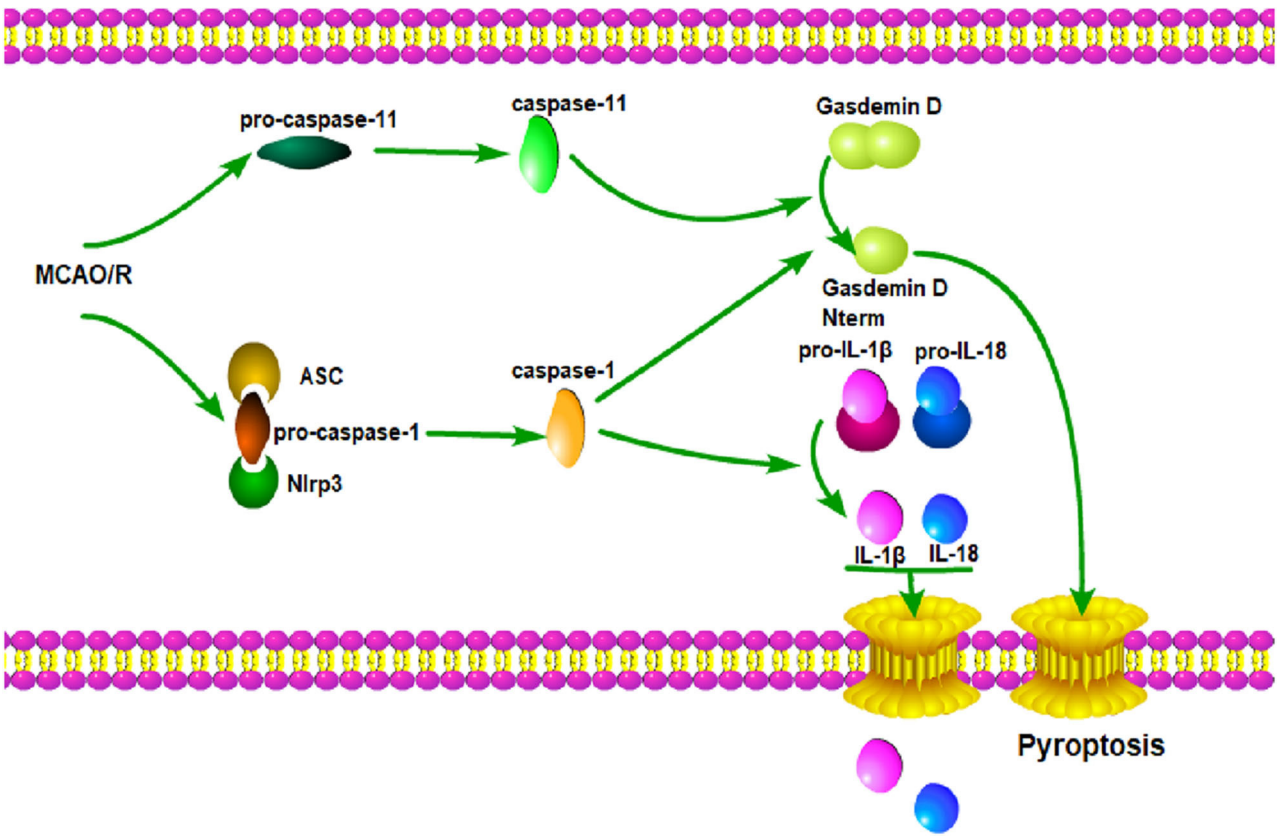

FIGURE 7 | GSDMD mediated pyroptosis pathways. Cerebral I/R damage induces the activation of caspase-1 and caspase-11; caspase-1 leads to the maturation of IL-1β and IL-18; caspase-1 and caspase-11 induce the cleavage of GSDMD and release of GSDMD-N; GSDMD-N forms a large pore in the plasma membrane; IL-1β and IL-18 are released through the pore; membrane integrity is disrupted, which ultimately leads to pyroptosis.

research may focus on immune cell death during cerebral I/R injury.

CONCLUSION

In summary, our results indicate that the knockout of GSDMD exerts a neuroprotective effect by inhibiting microglia pyroptosis and global neuroinflammation in mice with I/R injury. Therefore, a miRNA modulator and/or genetic regulator targeting GSDMD might serve as a promising alternative molecular drug for the treatment of ischemic stroke. Here, a diagram depicting the working mode of microglia pyroptosis signaling after cerebral I/R is supplemented (**Figure 7**).

DATA AVAILABILITY STATEMENT

All datasets generated for this study are included in the article/**Supplementary Material**.

ETHICS STATEMENT

The animal study was reviewed and approved by the Ethics Committee of Wenzhou Medical University.

AUTHOR CONTRIBUTIONS

SY, LH, and QZ designed the experiments and edited the manuscript. KJ gave guidance to the experiments. KW, ZS, JR, and XL performed the experiments and analyzed the data. KW, SW, and LR interpreted the data and prepared the figures. SY and KW wrote the manuscript. All authors contributed to the article and approved the submitted version.

FUNDING

This study was financially supported by the National Natural Science Foundation of China (81771262), International (Regional) Cooperation and Exchange Projects of the National Natural Science Foundation of China (81820108011), and Key Project of Science Technology Department of Zhejiang Province (2017C03027 and 2020C03022).

SUPPLEMENTARY MATERIAL

The Supplementary Material for this article can be found online at: https://www.frontiersin.org/articles/10.3389/fneur.2020.577927/full#supplementary-material

REFERENCES

1. Kaji R. Global burden of neurological diseases highlights stroke. *Nat Rev Neurol*. (2019) 15:371–2. doi: 10.1038/s41582-019-0208-y
2. Murray CJ, Lopez AD. Measuring the global burden of disease. *N Engl J Med*. (2013) 369:448–57. doi: 10.1056/NEJMra1201534
3. Zhou M, Wang H, Zeng X, Yin P, Zhu J, Chen W, et al. Mortality, morbidity, and risk factors in China and its provinces, 1990-2017: a systematic analysis for the Global Burden of Disease Study 2017. *Lancet*. (2019) 394:1145–58. doi: 10.1016/S0140-6736(19)30427-1
4. Powers WJ, Rabinstein AA, Ackerson T, Adeoye OM, Bambakidis NC, Becker K, et al. 2018 guidelines for the early management of patients with acute ischemic stroke: a guideline for Healthcare Professionals From the American Heart Association/American Stroke Association. *Stroke*. (2018) 49:e46–110. doi: 10.1161/STR.0000000000000158
5. Prabhakaran S, Ruff I, Bernstein RA. Acute stroke intervention: a systematic review. *JAMA*. (2015) 313:1451–62. doi: 10.1001/jama.2015.3058
6. Jiang X, Andjelkovic AV, Zhu L, Yang T, Bennett MVL, Chen J, et al. Blood-brain barrier dysfunction and recovery after ischemic stroke. *Prog Neurobiol*. (2018) 163–4, 144–71. doi: 10.1016/j.pneurobio.2017.10.001
7. Jin R, Yang G, Li G. Inflammatory mechanisms in ischemic stroke: role of inflammatory cells. *J Leukoc Biol*. (2010) 87:779–89. doi: 10.1189/jlb.1109766
8. Fann DY, Lee SY, Manzanero S, Chunduri P, Sobey CG, Arumugam TV. Pathogenesis of acute stroke and the role of inflammasomes. *Ageing Res Rev*. (2013) 12:941–66. doi: 10.1016/j.arr.2013.09.004
9. Sarhan M, Land WG, Tonnus W, Hugo CP, Linkermann A. Origin and consequences of necroinflammation. *Physiol Rev*. (2018) 98:727–80. doi: 10.1152/physrev.00041.2016
10. He Y, Hara H, Nunez G. Mechanism and regulation of NLRP3 inflammasome activation. *Trends Biochem Sci*. (2016) 41:1012–21. doi: 10.1016/j.tibs.2016.09.002
11. Liu YG, Chen JK, Zhang ZT, Ma XJ, Chen YC, Du XM, et al. NLRP3 inflammasome activation mediates radiation-induced pyroptosis in bone marrow-derived macrophages. *Cell Death Dis*. (2017) 8:e2579. doi: 10.1038/cddis.2016.460
12. Mamik MK, Power C. Inflammasomes in neurological diseases: emerging pathogenic and therapeutic concepts. *Brain*. (2017) 140:2273–85. doi: 10.1093/brain/awx133
13. He WT, Wan H, Hu L, Chen P, Wang X, Huang Z, et al. Gasdermin D is an executor of pyroptosis and required for interleukin-1beta secretion. *Cell Res*. (2015) 25:1285–98. doi: 10.1038/cr.2015.139
14. An P, Xie J, Qiu S, Liu Y, Wang J, Xiu X, et al. Hispidulin exhibits neuroprotective activities against cerebral ischemia reperfusion injury through suppressing NLRP3-mediated pyroptosis. *Life Sci*. (2019) 232:116599. doi: 10.1016/j.lfs.2019.116599
15. Caso JR, Moro MA, Lorenzo P, Lizasoain I, Leza JC. Involvement of IL-1beta in acute stress-induced worsening of cerebral ischaemia in rats. *Eur Neuropsychopharmacol*. (2007) 17:600–7. doi: 10.1016/j.euroneuro.2007.02.009
16. Ge X, Li W, Huang S, Yin Z, Xu X, Chen F, et al. The pathological role of NLRs and AIM2 inflammasome-mediated pyroptosis in damaged blood-brain barrier after traumatic brain injury. *Brain Res*. (2018) 1697:10–20. doi: 10.1016/j.brainres.2018.06.008
17. Liu W, Chen Y, Meng J, Wu M, Bi F, Chang C, et al. Ablation of caspase-1 protects against TBI-induced pyroptosis *in vitro* and *in vivo*. *J Neuroinflamm*. (2018) 15:48. doi: 10.1186/s12974-018-1083-y
18. McKenzie BA, Mamik MK, Saito LB, Boghozian R, Monaco MC, Major EO, et al. Caspase-1 inhibition prevents glial inflammasome activation and pyroptosis in models of multiple sclerosis. *Proc Natl Acad Sci USA*. (2018) 115:E6065–74. doi: 10.1073/pnas.1722041115
19. Yap JKY, Pickard BS, Chan EWL, Gan SY. The role of neuronal NLRP1 inflammasome in Alzheimer's disease: bringing neurons into the neuroinflammation game. *Mol Neurobiol*. (2019) 56:7741–53. doi: 10.1007/s12035-019-1638-7
20. Zeng R, Luo DX, Li HP, Zhang QS, Lei SS, Chen JH. MicroRNA-135b alleviates MPP(+)-mediated Parkinson's disease in *in vitro* model through suppressing FoxO1-induced NLRP3 inflammasome and pyroptosis. *J Clin Neurosci*. (2019) 65:125–33. doi: 10.1016/j.jocn.2019.04.004
21. Kayagaki N, Stowe IB, Lee BL, O'Rourke K, Anderson K, Warming S, et al. Caspase-11 cleaves gasdermin D for non-canonical inflammasome signalling. *Nature*. (2015) 526:666–71. doi: 10.1038/nature15541

22. Man SM, Kanneganti TD. Gasdermin D: the long-awaited executioner of pyroptosis. *Cell Res*. (2015) 25:1183–4. doi: 10.1038/cr.2015.124
23. Shi J, Zhao Y, Wang K, Shi X, Wang Y, Huang H, et al. Cleavage of GSDMD by inflammatory caspases determines pyroptotic cell death. *Nature*. (2015) 526:660–5. doi: 10.1038/nature15514
24. Lee SW, Gajavelli S, Spurlock MS, Andreoni C, de Rivero Vaccari JP, Bullock MR, et al. Microglial inflammasome activation in penetrating ballistic-like brain injury. *J Neurotrauma*. (2018) 35:1681–93. doi: 10.1089/neu.2017.5530
25. Datta A, Sarmah D, Mounica L, Kaur H, Kesharwani R, Verma G, et al. Cell death pathways in ischemic stroke and targeted pharmacotherapy. *Transl Stroke Res.* (2020) 11:1185–202. doi: 10.1007/s12975-020-00806-z
26. Zhang D, Qian J, Zhang P, Li H, Shen H, Li X, et al. Gasdermin D serves as a key executioner of pyroptosis in experimental cerebral ischemia and reperfusion model both *in vivo* and *in vitro*. *J Neurosci Res*. (2019) 97:645–60. doi: 10.1002/jnr.24385
27. Dong X, Gao J, Zhang CY, Hayworth C, Frank M, Wang Z. Neutrophil membrane-derived nanovesicles alleviate inflammation to protect mouse brain injury from ischemic stroke. *ACS Nano*. (2019) 13:1272–83. doi: 10.1021/acsnano.8b06572
28. Longa EZ, Weinstein PR, Carlson S, Cummins R. Reversible middle cerebral artery occlusion without craniectomy in rats. *Stroke*. (1989) 20:84–91. doi: 10.1161/01.STR.20.1.84
29. Catanese L, Tarsia J, Fisher M. Acute ischemic stroke therapy overview. *Circ Res*. (2017) 120:541–58. doi: 10.1161/CIRCRESAHA.116.309278
30. Borgens RB, Liu-Snyder P. Understanding secondary injury. *Q Rev Biol*. (2012) 87:89–127. doi: 10.1086/665457
31. Soriano SG, Piva S. Central nervous system inflammation. *Eur J Anaesthesiol Suppl*. (2008) 42:154–9. doi: 10.1017/S0265021507003390
32. Orning P, Lien E, Fitzgerald KA. Gasdermins and their role in immunity and inflammation. *J Exp Med.* (2019) 16:2453–65. doi: 10.1084/jem.20190545
33. Broz P, Pelegrin P, Shao F. The gasdermins, a protein family executing cell death and inflammation. *Nat Rev Immunol*. (2020) 20:143–57. doi: 10.1038/s41577-019-0228-2
34. Van Opdenbosch N, Lamkanfi M. Caspases in cell death, inflammation, and disease. *Immunity*. (2019) 50:1352–64. doi: 10.1016/j.immuni.2019.05.020
35. Yuan J, Najafov A, Py BF. Roles of caspases in necrotic cell death. *Cell*. (2016) 167:1693–704. doi: 10.1016/j.cell.2016.11.047
36. Chen AQ, Fang Z, Chen XL, Yang S, Zhou YF, Mao L, et al. Microglia-derived TNF-alpha mediates endothelial necroptosis aggravating blood brain-barrier disruption after ischemic stroke. *Cell Death Dis*. (2019) 10:487. doi: 10.1038/s41419-019-1716-9
37. Hummitzsch L, Albrecht M, Zitta K, Hess K, Parczany K, Rusch R, et al. Human monocytes subjected to ischaemia/reperfusion inhibit angiogenesis and wound healing *in vitro*. *Cell Prolif*. (2020) 53:e12753. doi: 10.1111/cpr.12753
38. Sborgi L, Ruhl S, Mulvihill E, Pipercevic J, Heilig R, Stahlberg H, et al. GSDMD membrane pore formation constitutes the mechanism of pyroptotic cell death. *EMBO J*. (2016) 35:1766–78. doi: 10.15252/embj.201694696
39. Hu X, Leak RK, Shi Y, Suenaga J, Gao Y, Zheng P, et al. Microglial and macrophage polarization-new prospects for brain repair. *Nat Rev Neurol*. (2015) 11:56–64. doi: 10.1038/nrneurol.2014.207
40. Li G, Xiao L, Qin H, Zhuang Q, Zhang W, Liu L, et al. Exosomes-carried microRNA-26b-5p regulates microglia M1 polarization after cerebral ischemia/reperfusion. *Cell Cycle*. (2020) 19:1022–35. doi: 10.1080/15384101.2020.1743912
41. Lv Y, Sun B, Lu XX, Liu YL, Li M, Xu LX, et al. The role of microglia mediated pyroptosis in neonatal hypoxic-ischemic brain damage. *Biochem Biophys Res Commun*. (2020) 521:933–8. doi: 10.1016/j.bbrc.2019.11.003
42. Voet S, Srinivasan S, Lamkanfi M, van Loo G. Inflammasomes in neuroinflammatory and neurodegenerative diseases. *EMBO Mol Med*. (2019) 11: e10248. doi: 10.15252/emmm.201810248

Conflict of Interest: The authors declare that the research was conducted in the absence of any commercial or financial relationships that could be construed as a potential conflict of interest.

frontiers in Neurology

REVIEW
published: 23 December 2020
doi: 10.3389/fneur.2020.608610

The Role of Mitophagy in Ischemic Stroke

Ziqi Shao[1], Shanshan Dou[2], Junge Zhu[1], Huiqing Wang[1], Dandan Xu[1], Chunmei Wang[2], Baohua Cheng[2] and Bo Bai[2]**

[1] Cheeloo College of Medicine, Shandong University, Jinan, China, [2] Neurobiology Institute, Jining Medical University, Jining, China

Mitochondria are important places for eukaryotes to carry out energy metabolism and participate in the processes of cell differentiation, cell information transmission, and cell apoptosis. Autophagy is a programmed intracellular degradation process. Mitophagy, as a selective autophagy, is an evolutionarily conserved cellular process to eliminate dysfunctional or redundant mitochondria, thereby fine-tuning the number of mitochondria and maintaining energy metabolism. Many stimuli could activate mitophagy to regulate related physiological processes, which could ultimately reduce or aggravate the damage caused by stimulation. Stroke is a common disease that seriously affects the health and lives of people around the world, and ischemic stroke, which is caused by cerebral vascular stenosis or obstruction, accounts for the vast majority of stroke. Abnormal mitophagy is closely related to the occurrence, development and pathological mechanism of ischemic stroke. However, the exact mechanism of mitophagy involved in ischemic stroke has not been fully elucidated. In this review, we discuss the process and signal pathways of mitophagy, the potential role of mitophagy in ischemic stroke and the possible signal transduction pathways. It will help deepen the understanding of mitophagy and provide new ideas for the treatment of ischemic stroke.

Keywords: molecular mechanisms, signaling pathway, ischemia-reperfusion injury, ischemic stroke, mitophagy

OPEN ACCESS

Edited by:
Emmanuel Pinteaux, The University of Manchester, United Kingdom

Reviewed by:
Luigi Sironi, University of Milan, Italy
Laura Castiglioni, University of Milan, Italy

***Correspondence:**
Baohua Cheng
chengbh1979@163.com
Bo Bai
bbai@mail.jnmc.edu.cn

Specialty section:
This article was submitted to Stroke, a section of the journal Frontiers in Neurology

Received: *21 September 2020*
Accepted: *04 December 2020*
Published: *23 December 2020*

Citation:
Shao Z, Dou S, Zhu J, Wang H, Xu D, Wang C, Cheng B and Bai B (2020) The Role of Mitophagy in Ischemic Stroke. Front. Neurol. 11:608610. doi: 10.3389/fneur.2020.608610

INTRODUCTION

Stroke refers to a group of diseases that cause brain tissue damage due to the sudden rupture of blood vessels or the blockage of blood flow into the brain, including hemorrhagic and ischemic stroke. It has the characteristics of high morbidity and high mortality. Ischemic stroke accounts for ∼87% of the total number of stroke patients (1). Ischemic stroke refers to a type of disease in which brain tissue necrosis is caused by a narrowing or occlusion of the blood supply arteries (carotid and vertebral arteries) of the brain and insufficient blood supply to the brain. At present, thrombolysis is considered to be the most important method for the treatment of ischemic stroke (2). However, due to the limitations of current thrombolytic therapy such as an optimal treatment time window of only 4.5 h (3), enhancing the self-resistance and protection of neurons has become the focus which has attracted more researchers (4).

Mitochondria are where the oxidative metabolism of eukaryotes takes place, and the major producers of intracellular reactive oxygen species (ROS). They can also regulate membrane potential and control programmed cell death (5). Based on the complex structure and important functions of mitochondria, they are closely related to many diseases including ischemic stroke. When ischemic stroke occurs, the dynamic balance maintained by mitochondria is broken, and

related signaling pathways are activated, which lead to cascade damage to nerve cells (6). In the ischemic period of ischemic stroke, mitochondria cannot synthesize enough ATP or cause energy disorders due to lack of oxygen and energy substances. During the reperfusion period, the increase of ROS and mitochondrial membrane lipid peroxidation lead to oxidative stress damage. Increased ROS also disrupts the calcium pump on the mitochondrial membrane, which induces calcium overload and inflammatory response. In addition to these pathological changes, cell death in ischemic stroke including apoptosis and autophagy are all related to the loss of mitochondrial function (7). Therefore, the research on the correlation between mitochondria and ischemic stroke can not only fully explain the mechanism of the occurrence and development of ischemic stroke, but also provide potential guidance and help for the innovative treatment of ischemic stroke.

Autophagy is a biological process in which organelles and proteins are degraded by lysosomes in eukaryotic cells (8). One of the main functions of autophagy is to keep cells alive when they are threatened by stressful death (9). This is an important evolutionary conservation mechanism for eukaryotic cells to maintain homeostasis and achieve renewal (10). Although autophagy in a broad sense includes macroautophagy, microautophagy and chapeon-mediated autophagy (11), it is commonly referred to as macroautophagy. Mitophagy is a type of macroautophagy by which cells selectively clear impaired or dysfunctional mitochondria through the mechanism of autophagy (12). It plays an important role in mitochondrial quality control and cell survival (13). More and more studies have shown that mitophagy is associated with neurodegenerative diseases such as Parkinson's disease (PD), Alzheimer disease (AD) and Huntington's (HD) and brain injury (14). Although there have been studies showing that mitophagy is closely related to ischemic stroke (4, 15), the exact roles of mitophagy still need to be studied further. In this review, we focus on the research progress in the occurrence and regulation of mitophagy in ischemic stroke.

MITOCHONDRIAL DYNAMICS AND MITOPHAGY

The Molecular Mechanism of Mitochondrial Dynamics

Mitochondria are highly dynamic organelles that adapt to various stress conditions to meet the energy metabolism and other biological needs through continuous fusion and fission to change their shape (16). This biological process is called mitochondrial dynamics, which is an important basis for maintaining cell homeostasis (17). Mitochondrial fusion is a multi-step process in a certain order: (1) mitochondrial trans-tethering; (2) mitochondrial outer membrane fusion; (3) mitochondrial inner membrane fusion (16). The fusion process of mitochondria is mainly completed by activating three GTPases: mitofusins 1(Mfn1), mitofusins 2 (Mfn2) and optic atrophy 1 (OPA1) (18). Among them, Mfn1 and Mfn2 mainly mediate mitochondrial outer membrane fusion, and OPA1 mainly participates in the mitochondrial inner membrane fusion process (19). The fission process is mainly mediated by dynamin-related protein 1 (Drp1) and fission protein 1 (Fis1) (18). Under the stimulus, Fis1 mediates the translocation of Drp1 in the cytoplasm to the outer mitochondrial membrane. Drp1 accumulates at the mitochondrial fission site to form a "ring" structure and then combines with Fis1 to form a complex, which is gradually compressed until the mitochondria ruptures. Finally, two independent mitochondria are produced (20) (**Figure 1**).

Disturbance of mitochondrial dynamics is an important phenomenon in cerebral ischemia/reperfusion injury. Studies have found that there is a loss of OPA1 complex during reperfusion (21). In the rat model of cerebral ischemia/reperfusion injury, the expression of Mfn2 in the cerebral cortex is significantly reduced (22). Research has indicated that activating Mfn1 could reduce cerebral ischemia/reperfusion injury (23). In addition, the fission of mitochondria in the hippocampus is found to be activated, and the mitochondria become more and more fragmented with time (24). Previous studies have shown that inhibiting Drp1-dependent mitochondrial fission could protect against cerebral ischemia/reperfusion injury (25). Similarly, the inhibition of Fis1 could also achieve the protective effect (26).

Interplay Between Mitochondrial Dynamics and Mitophagy

Mitochondrial fusion could repair slightly damaged mitochondria. And mitochondrial fission could not only achieve normal number of proliferation, but also selectively distribute the damaged components of mitochondria to the offspring, which result in healthy mitochondria and severely damaged mitochondria (27). The membrane potential of severely damaged mitochondria cannot be restored. Therefore, the severely damaged mitochondria are unable to participate in fusion, which will be cleared through mitophagy (28). The interaction and mutual regulation between mitochondrial dynamics and mitophagy are important mechanisms for maintaining mitochondrial homeostasis and ensuring mitochondrial quality. In the early stage of ischemia, Drp1-dependent mitophagy is found to contribute to the clearance of damaged mitochondria (29). Studies have shown that mitochondrial fragmentation could regulate mitophagy and apoptosis in cerebral ischemia/reperfusion injury (30). It is also found that OPA1 and Mfn2 are reduced in cerebral ischemia, thereby inducing mitophagy (31). These findings indicate that mitochondrial dynamics is closely related to mitophagy in cerebral ischemia/reperfusion injury.

Mechanisms and Regulatory Pathways of Mitophagy

The Process of Mitophagy

The process of mitophagy is similar to ordinary autophagy. First, permeability changes occur after mitochondria are damaged, which leads to mitochondrial depolarization, and induces the activation of mitophagy-related proteins. Then, the isolation membrane wraps the damaged mitochondria and

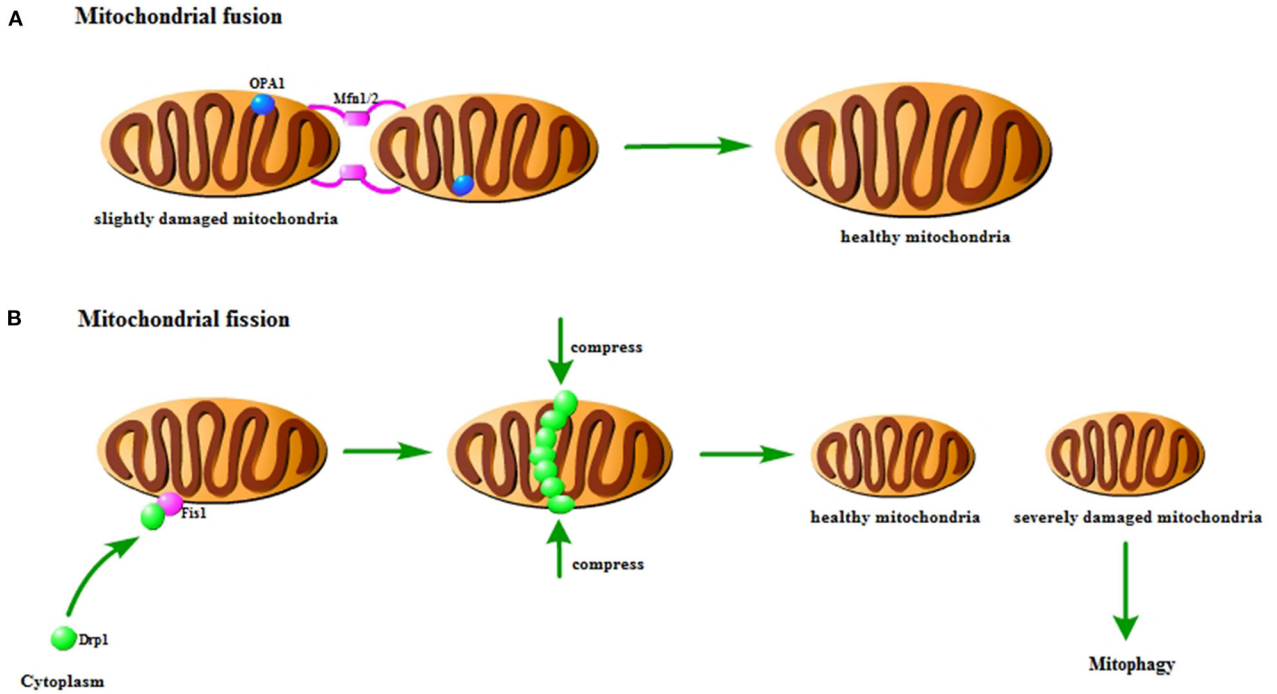

FIGURE 1 | Pattern diagram of mitochondrial fusion and fission. **(A)** Mitochondrial fusion. The Mfn1/2 interaction causes the outer membrane to fuse, and then the Opa1 interaction causes the inner membrane to fuse. It could repair slightly damaged mitochondria. **(B)** Mitochondrial fission. Fis1 on the mitochondria recruits Drp1 to the mitochondria to form a finger ring structure, which squeezes and ruptures the mitochondria. It could distribute the damaged components of mitochondria to the offspring. The severely damaged mitochondria will be cleared by mitophagy.

forms mitophagosomes. After the formation of mitophagosomes, fusion with lysosomes to form mitolysosomes results in the degradation of damaged mitochondria. This process requires the participation of microtubule-associated protein light chain 3 (LC3) and the linker proteins p62, NBR1 and optineurin connecting mitochondria and LC3. In addition, Nix/BNIP3, FUNDC1 also play an important role in this process (32).

Mitophagy Signaling Pathway

The mechanisms of mitophagy in cells mainly include Parkin-dependent pathways and Parkin-independent pathways. There are multiple signals involved in the regulation of mitophagy, as showed in **Figure 2**. The current review focuses on PINK1/Parkin, BNIP3/NIX, and FUNDC1 pathway.

Parkin-Dependent Mitophagy Pathway

At the beginning of the 21st century, the laboratory of Richard Youle found that Parkin, an E3 ubiquitin ligase, could mediate mitochondria to be wrapped by autophagosomes, which creates a new breakthrough for the study of mitophagy (33). Then, subsequent research found that PINK1 (phosphatase and tensin homolog (PTEN)-induced putative protein kinase (1), a serine/threonine kinase, is located upstream of Parkin (34–36). PINK1 can phosphorylate Parkin and promote the translocation of Parkin from cytoplasm to mitochondria (37). PINK1/Parkin is the clearest pathway for the research of mitophagy.

In healthy mitochondria, the PINK1 protein exists on the outer mitochondrial membrane. It can be introduced into the mitochondrial membrane space and degraded by proteases on the inner mitochondrial membrane to maintain the basic level (38). However, when mitochondria are damaged and depolarized, their ability to degrade PINK1 is weakened, and PINK1 can stably exist on the outer mitochondrial membrane (39). Then, it can phosphorylate both ubiquitin and Parkin to recruit Parkin from the cytoplasm to the outer mitochondrial membrane (40). The stability of PINK1 on the outer mitochondrial membrane is necessary for Parkin to be recruited to damaged mitochondria and to stimulate mitophagy. Activated Parkin can ubiquitinate the voltage-dependent anion channels 1 (VDAC1) of damaged mitochondria. Then, Parkin is recognized and bound by the signal adaptor protein p62/SQSTM1. P62 could recruit ubiquitinated substances into autophagosomes by binding to LC3, which ultimately leads to mitochondria degraded by lysosome (41–43). In the penumbra of rat cortex, fluorescence results show that PINK1 accumulates on the outer mitochondrial membrane and Parkin mitochondrial translocation occurs following ischemia and reperfusion, and the levels of other related autophagy proteins such as LC3 and Beclin1 are elevated. These results

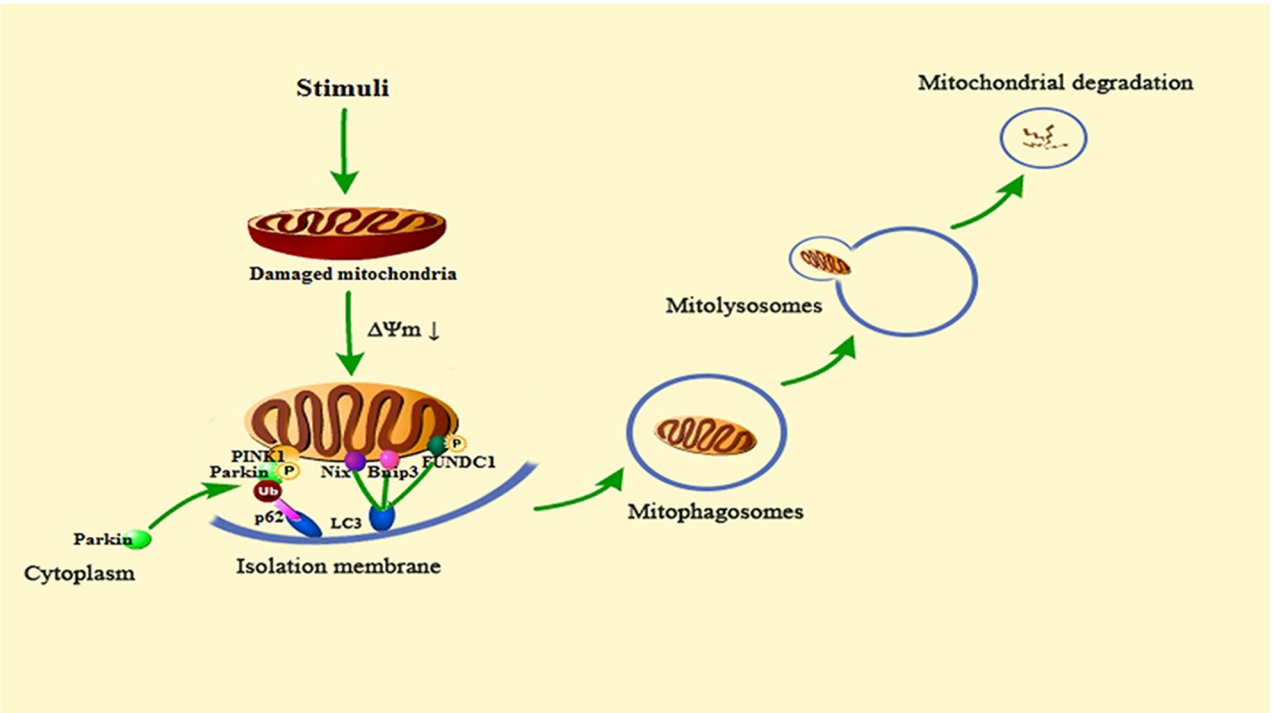

FIGURE 2 | Summary of the mitophagy signaling pathway. When the cell is stimulated, the mitochondria will be damaged. Then the mitochondrial transmembrane potential (ΔΨm) drops, and mitophagy will be activated. PINK1 accumulates on the outer mitochondrial membrane, phosphorylates Parkin and recruits Parkin from the cytoplasm to the mitochondria. Activated Parkin can ubiquitinate the voltage-dependent anion channels 1 (VDAC1) of damaged mitochondria, Then, Parkin is recognized and bound by the signal adaptor protein p62/SQSTM1. P62 could recruit ubiquitinated substances into autophagosomes by binding to microtubule-associated protein light chain 3 (LC3). Bnip3, Nix and phosphorylated FUNDC1 can also connect to LC3 to promote mitophagy. Subsequent mitophagosomes are formed, which bind to lysosomes, and finally lyse damaged mitochondria.

may demonstrate that mitophagy is activated in ischemic stroke (44).

Parkin-Independent Mitophagy Pathway

Different from PINK1/Parkin-mediated mitophagy, some proteins on the outer mitochondrial membrane can directly recognize and bind LC3. Then, targeted mitochondria are connected with autophagic vesicles, which directly induces mitophagy (45). In this review, we focus on the Nix/Bnip3 and FUNDC1 signaling pathways. They are the most important pathways in Parkin-independent mitophagy.

Nix/Bnip3-Mediated Mitophagy Pathway

Bnip3 and Nix (BNIP3L) have about 56% amino acid sequence identity, and both are located in mitochondria (46). Bnip3 is a pro-apoptotic mitochondrial protein. And it is also an important participant in the process of autophagy and even mitophagy (47, 48). Bnip3 is the target gene of HIF1α (hypoxia inducible factor 1α). Under hypoxic conditions, Bnip3 could activate autophagy (49). Similarly, in ischemia and reperfusion, Bnip3 could clear damaged mitochondria by activating mitophagy (49, 50). In the process of red blood cell maturation and development, Nix is essential for the removal of mitochondria. Mitochondrial depolarization, increased production of ROS and hypoxia can induce Nix to regulate mitophagy (51, 52). Bnip3 and Nix could competitively bind to the anti-apoptotic Bc1-2, dissociate the Bc1-Beclin1 complex and release Beclin1, and then activate autophagy and mitophagy (53). In cerebral ischemia/reperfusion injury, Bnip3 and Nix could participate in the induction of mitophagy (54). However, Studies have found that the up-regulation of Nix cannot restore the mitophagy defect caused by Bnip3 deletion in stroke (55). This may indicate that Bnip3 could activate excessive mitophagy leading to cell death, whereas Nix may only regulate basal levels of mitophagy in physiological conditions. Therefore, Bnip3 may be a potential target for the treatment of ischemic stroke in the future.

FUNDC1-Mediated Mitophagy Pathway

FUNDC1 is a tertiary transmembrane protein on the outer mitochondrial membrane. The FUNDC1 protein contains a N-terminal LC3 interaction region motif, which plays an important role in mitophagy (56). Under normal conditions, FUNDC1 can stably exist on the outer mitochondrial membrane without mediating mitophagy. When mitochondria are damaged or dysfunctional, the affinity of FUNDC1 and LC3 will increase. Then FUNDC1 can be dephosphorylated to activate, which will induce mitophagy (57). In myocardial ischemia/reperfusion, studies have found that hypoxic preconditioning could induce

FUNDC1-dependent mitophagy to resist ischemia/reperfusion injury (58). However, some studies have shown that inhibition of mitophagy mediated by the mTORC1-ULK1-FUNDC1 pathway can protect myocardium from ischemia/reperfusion injury (59). This indicates that similar mechanisms may exist in cerebral ischemia/reperfusion.

Roles of Mitophagy in Ischemic Stroke

The brain is the main organ of energy metabolism, and the content of mitochondria in the brain is much higher than other tissues (60). Even if short-term ischemia and hypoxia may cause serious injury to the brain, overproduction of free radicals and calcium overload after reperfusion also cause more extensive damage to cells and tissues of the brain. Current research suggests that cerebral ischemia/reperfusion injury is related to the production of free radicals, excitatory amino acid toxicity, mitochondrial dysfunction, and activation of apoptosis-related genes (7, 61–63). Mitochondrial dysfunction is an important part of cerebral ischemia/reperfusion injury, and mitophagy plays a significant role in it. Elimination of abnormal mitochondria through mitophagy is essential for maintaining normal cell function in ischemic stroke.

More than 50 years ago, transmission electron microscopy first discovered the existence of autophagosomes (64–66). As the research on autophagy gets deeper, research methods on autophagy are becoming more and more abundant. Accumulated evidence indicated that autophagy is activated in brain tissue in many nervous system diseases including ischemic stroke (67–70). And mitophagy, as a special type of autophagy, is also found to be activated in ischemic stroke (44). In cerebral ischemia/reperfusion injury, early ischemia and hypoxia damage the structure and function of mitochondria in brain cells. After the oxygen supply and energy supply are restored, the mitochondrial permeability transition pore opens (mPTP) and the mitochondrial membrane potential (MMP) decreases, and then mitochondrial damage is followed by activation of mitochondrial autophagy (71).

Like macroautophagy, we are not sure whether mitophagy is beneficial or harmful in ischemic stroke. The degree of mitochondrial permeability transition (MPT) may play an important role in it (72). Under mild starvation or hypoxia, limited MPT can only damage a small part of mitochondria and then activate mitophagy. At this time, mitophagy not only provides energy by degrading proteins, but also removes damaged mitochondria to protect the cells. In the case of severe starvation or hypoxia, mitophagy is insufficient to clear the damaged mitochondria, and then the autophagy system will be overloaded, which will activate apoptosis-related regulatory proteins and promote the occurrence of apoptosis. When excessive stress causes drastic changes in the MPT of all mitochondria in the cell, cell necrosis will occur.

Neuronal Mitophagy in Ischemic Stroke

Enhancing Mitophagy Reduced Cerebral Ischemic-Reperfusion Injury

Studies have shown that rapamycin could protect against cerebral ischemia/reperfusion injury by activating mitophagy and reducing mitochondrial dysfunction in transient middle cerebral artery occlusion (tMCAO) model. And these protective effects can be reversed by 3-methyladenine, an autophagy inhibitor (73). There are similar findings in the oxygen-glucose deprivation model of hippocampal neurons (74). And activating mitophagy to clear excessively aggregated and damaged mitochondria can reduce neuronal damage caused by cerebral ischemia/reperfusion injury (75–79). Knockout of the mitophagy-related gene Bnip3L could aggravate cerebral ischemia/reperfusion injury, and overexpression of this gene could rescue (54). Studies have also found that activating Parkin-dependent mitophagy could inhibit the activation of NLRP3 inflammasome to reduce cerebral ischemia/reperfusion injury (80). Activation of PARK2-mediated mitophagy may be the basis for protecting endoplasmic reticulum stress in cerebral ischemia/reperfusion injury (81) and extending the limited reperfusion window (82).

Inhibiting Mitophagy Reduced Cerebral Ischemic-Reperfusion Injury

However, there are still some studies showing that inhibiting excessive mitophagy can play a protective role in cerebral ischemia/reperfusion injury. In the middle cerebral artery occlusion model (MCAO) of ischemic stroke, studies have found that inhibiting mitophagy can protect against cerebral ischemia/reperfusion injury (83). In the oxygen glucose deprivation model of SH-SY5Y cells, inhibition of mitochondrial calcium uniporter and the influx of Ca^{2+} into mitochondria could inhibit excessive mitophagy and reduce neuronal damage (84). And inhibiting Peroxynitrite-mediated mitochondrial activation could reduce neuronal damage in ischemic stroke (85, 86). In neuronal death caused by chronic cerebral hypoperfusion, it is also found that inhibiting excessive mitophagy could exert neuroprotective effects (87). Similarly, inhibition of AMPK-mediated mitophagy could reduce the ischemic and hypoxic damage of neurons in ischemic hypoxic encephalopathy (88).

Although the differences in the above results may be caused by different ischemia or reperfusion time, different cell types, or even different experimental environments, it is undeniable that mitophagy plays an important role in the pathological mechanism of cerebral ischemia/reperfusion injury. When it is at the basic level, it may be beneficial to cell homeostasis and neuron survival. But it can be harmful when it reaches excess or deficiency. Therefore, the role of mitophagy in ischemic stroke should be studied more deeply to provide novel ideas and targets for clinical treatment.

Glial Mitophagy in Ischemic Stroke

Glial cells can not only support, nourish, and protect neurons, but also receive signals from neurons. Through their own function, metabolism and morphological changes, glial cells could affect the function and activity of neurons (89). After cerebral ischemic injury, glial cells are activated. In the early stage of cerebral ischemic injury, the activation of glial cells can play a certain neuroprotective effect, but the excessive activation of glial cells can produce a series of inflammatory factors or mediators to mediate neuronal degeneration (90). Previous study has found

that hypoxia and reoxygenation of astrocytes caused increased mitochondrial fission and mitophagy (91). In the rat cortex after cerebral ischemia and reperfusion, the activation of mitophagy in astrocytes is also found (83). There are many studies on glial cells autophagy in ischemic stroke while mitophagy-related reports are few. More investigations on astrocytes or microglial mitophagy are needed.

Interplay Between Mitophagy and Other Cellular Processes in Ischemic Stroke

Mitochondria are the most important organelles involved in energy metabolism in cells. They play a key role in cell signal transduction, free radical generation and apoptosis induction, and determine the survival and death of cells. In the occurrence and development of ischemic stroke, mitophagy is closely related to many biological processes in the cell, such as apoptosis, oxidative stress, and inflammation (**Figure 3**). These biological processes interact with mitophagy to regulate mitochondrial quality, which could affect the survival and death of nerve cells.

Mitophagy and Apoptosis

Unlike mitophagy, apoptosis only has a one-way effect on cell fate. It removes aging and severely damaged cells through a programmed death regulation mechanism. Mitophagy and apoptosis have obvious differences in biochemical metabolic pathways and morphology, but they are functionally antagonistic, coordinated, and promote each other, and participate in the regulation of mitochondrial quality (92–95).

Mitophagy and apoptosis are mostly mutually antagonistic to achieve mutual regulation. Under stress conditions such as ischemia and hypoxia, the phosphorylation of the anti-apoptotic protein Bcl-2 could destroy its binding to autophagy-related protein Beclin1 and activate mitophagy. At the same time, Bcl-2 could prevent the release of pro-apoptotic proteins by maintaining the integrity of the mitochondrial membrane, which finally inhibits the occurrence of cell apoptosis (96). When the cell is under continuous and severe stress, apoptosis can inhibit the occurrence of mitophagy by cleaving the key autophagy protein Beclin1 by activated Caspase and avoid the mitochondrial dysfunction caused by excessive mitophagy (97, 98). However, other studies have shown that mitophagy and apoptosis are functionally coordinated and mutually promoted. Excessive induction of mitophagy can cause the leakage of cathepsin and other hydrolytic enzymes in lysosomes or autophagic lysosomes, and promote the occurrence of apoptosis (99).

Studies have reported that activating mitophagy could inhibit cell apoptosis in ischemic stroke. During the reperfusion phase, mitophagy could inhibit neuronal apoptosis by removing damaged mitochondria (100), and remote ischemic post conditioning could promote Parkin/DJ-1-mediated mitophagy to attenuate apoptosis in MCAO rats (101). Similarly, enhancing Parkin /PINK1-mediated mitophagy could inhibit apoptosis caused by cerebral ischemia/reperfusion injury in hippocampal neurons (74). However, there are still some studies indicating that inhibiting excessive mitophagy can reduce apoptosis. Mitophagy-related protein Bnip3 and Nix could induce excessive mitophagy to promote cell apoptosis in ischemic stroke (55). And inhibition of PINK1/Parkin-mediated mitophagy could reduce the number of apoptotic cells in the cortex of the model group in cerebral ischemia/reperfusion injury (86).

Mitophagy and Oxidative Stress

Oxidative stress is caused by free radicals to produce oxidative damage to deoxyribonucleic acid (DNA), lipids and proteins, which leads to aging and neurodegenerative diseases. The oxidation of proteins, lipids and DNA are all related to ROS (102). ROS can lead to mitochondrial lipid peroxidation, membrane potential collapse and ATP synthesis disorder. Mitochondria are the main source of ROS production (103). Mitophagy is closely related to oxidative stress. And it also plays a dual role in oxidative stress.

Under physiological conditions, low levels of ROS can usually be degraded by some antioxidant enzymes or substances. Maintaining the balance between ROS production and degradation is very important for the normal physiological functions. If the anti-oxidant substances in the cell cannot effectively degrade ROS, it will make ROS accumulate in the cell and then cause oxidative stress (104). Excessive ROS and other substances can preferentially activate mitophagy, allowing it to selectively degrade damaged mitochondria, which could reduce damage to cells (105). There are studies showing that activating mitophagy could reduce oxidative stress damage in ischemia/reperfusion injury. In renal ischemia/reperfusion injury, ischemic preconditioning can protect mitochondrial function by activating mitophagy and inhibit the production of ROS (106), and activation of ROS-dependent autophagy promotes the survival of liver endothelial cells in liver ischemia/reperfusion injury (107). Also, in cerebral ischemia/reperfusion injury, enhancing mitophagy could reduce excessive accumulation of ROS (74). However, mitophagy also can directly induce the death of oxidized cells. In myocardial ischemia/reperfusion injury, inhibiting PINK1/Parkin-mediated mitophagy could reduce ROS production and protect against neurons damage (108). Likely, there may be a similar mechanism in cerebral ischemia/reperfusion injury.

Mitophagy and Inflammation

Inflammation is an important self-defense mechanism of the body, and mitochondria play a significant role in the occurrence and development of inflammation (109). After being stimulated by factors such as infection, trauma, lipopolysaccharide, high temperature, and hypoxia, the body's innate immune cells activate and trigger an inflammatory response. Under the stimulation of inflammatory factors, ROS and other inflammatory mediators released by neutrophils can induce mitochondrial structural and functional damage (110), including decreased activity of electron transport chain complexes, decreased membrane potential, ATP depletion, and decreased mitochondrial DNA. Mitophagy is of great significance for removing damaged mitochondria and maintaining the function of cellular mitochondrial network. It can remove

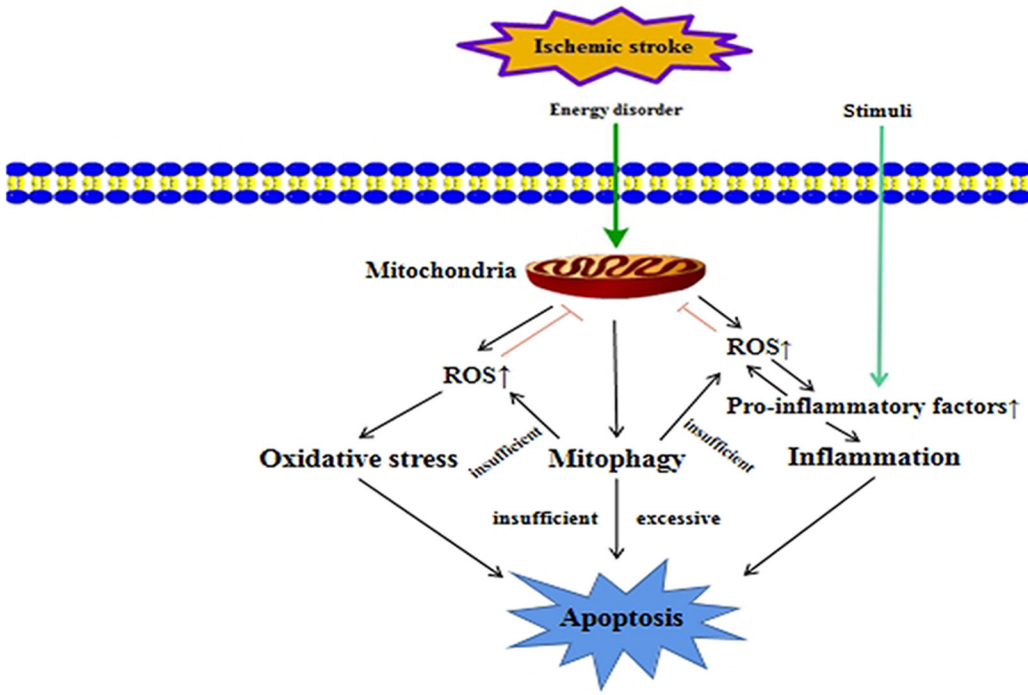

FIGURE 3 | Crosstalk between mitophagy and other cellular processes in ischemic stroke. In ischemic stroke, ischemia and hypoxia can cause energy disorders, which will damage mitochondria. Mitophagy is activated when mitochondria are damaged. When mitophagy is insufficient or excessive, it can lead to apoptosis. Mitochondrial damage will also release a large amount of ROS, leading to oxidative stress damage. At the same time, excessive ROS will promote the release of pro-inflammatory factors, which lead to inflammation. When mitophagy is not enough to clear over-produced ROS, it will aggravate oxidative stress damage and inflammation, which could promote apoptosis.

damaged mitochondria, promote healthy mitochondrial proliferation and other processes, improve mitochondrial homeostasis and function, and exert anti-inflammatory effects (111).

In recent years, a large number of studies have shown that autophagy is inhibited or weakened in inflammatory diseases, and the body is manifested as excessive inflammation or excessive activation of inflammasomes (112–114). And the related mechanisms of mitophagy and inflammation have also been studied in depth (110, 115). In cerebral ischemia/reperfusion injury, the relationship between NLRP3 inflammasome activation and mitophagy has been the most studied. In the rat model of ischemic stroke, studies have found that Parkin-dependent mitophagy could effectively inhibit the activation of NLRP3 inflammasome (80). And in myocardial ischemia/reperfusion injury, activation of PINK1/Parkin-mediated mitophagy could reduce cell apoptosis and inflammatory response (116). At present, the interaction and relationship between the specific mechanisms and pathways of mitophagy and inflammation in ischemic stroke are not fully understood. Uncovering the complex regulatory network mechanism between them can provide a theoretical basis for finding new treatment methods of ischemic stroke.

CONCLUSION AND PROSPECTS

Obviously, mitophagy plays an important role in ischemic stroke through many regulatory factors and other related cellular processes. Although the role of mitophagy has not been unified yet, most studies have proved that in cerebral ischemia/reperfusion injury, mitophagy as an early defense mechanism could clear damaged mitochondria in time, thereby reducing the further damage to normal mitochondria caused by stimulation. However, when the process of mitophagy is blocked or excessive it will aggravate cerebral ischemia/reperfusion injury. Mitophagy may have different effects on neurons with changes in different pathological stages of ischemia and reperfusion, but the reasons for this change have not been clearly studied. These mechanisms need to be further investigated.

This review summarizes the occurrence and development of mitophagy, the related regulatory factors and signal pathways of mitophagy, and the correlation between mitophagy and other cellular processes after cerebral ischemia/reperfusion, which could help to discover new treatment targets and strategies for ischemic stroke. There are still controversies about the mechanism of mitophagy in cerebral ischemia/reperfusion injury. Exploring mitophagy and its regulation mechanism in cerebral ischemia/reperfusion injury will help to

grasp the relationship between mitophagy and cerebral ischemia/reperfusion injury and various diseases, and provide new ideas for clinical treatment. The role of mitophagy in the different stages and cells of cerebral ischemia/reperfusion and the reasons for this change, from beneficial to harmful, need to be further studied.

AUTHOR CONTRIBUTIONS

ZS wrote the manuscript and generated the figures. SD helped to design the figures. JZ, HW, and DX proposed suggestions for revisions. CW revised the manuscript. BB and BC designed the content. All authors read and approved the final manuscript.

FUNDING

The study was supported by the National Natural Science Foundation of China, Nos. 81870948 (to BB), 81671276 (to BC), 81501018 (to CW) the Natural Science Foundation of Shandong Province of China, No. ZR2014HL040 (to BC); Program Supporting Foundation for Teachers' Research of Jining Medical University of China, No. JYFC2018KJ003 (to SD).

REFERENCES

1. Benjamin EJ, Muntner P, Alonso A, Bittencourt MS, Callaway CW, Carson AP, et al. Heart disease and stroke statistics-2019 update: a report from the American heart association. *Circulation.* (2019) 139:e56–e528. doi: 10.1161/CIR.0000000000000659
2. Berkowitz AL, Mittal MK, McLane HC, Shen GC, Muralidharan R, Lyons JL, et al. Worldwide reported use of IV tissue plasminogen activator for acute ischemic stroke. *Int J Stroke.* (2014) 9:349–55. doi: 10.1111/ijs.12205
3. Ferrell AS, Britz GW. Developments on the horizon in the treatment of neurovascular problems. *Surg Neurol Int.* (2013) 4:S31–7. doi: 10.4103/2152-7806.109194
4. Guan R, Zou W, Dai X, Yu X, Liu H, Chen Q, et al. Mitophagy, a potential therapeutic target for stroke. *J Biomed Sci.* (2018) 25:87. doi: 10.1186/s12929-018-0487-4
5. Oyewole AO, Birch-Machin MA. Mitochondria-targeted antioxidants. *FASEB J.* (2015) 29:4766–71. doi: 10.1096/fj.15-275404
6. Ham PB 3rd, Raju R. Mitochondrial function in hypoxic ischemic injury and influence of aging. *Prog Neurobiol.* (2017) 157:92–116. doi: 10.1016/j.pneurobio.2016.06.006
7. Yang JL, Mukda S, Chen SD. Diverse roles of mitochondria in ischemic stroke. *Redox Biol.* (2018) 16:263–75. doi: 10.1016/j.redox.2018.03.002
8. Menzies FM, Fleming A, Rubinsztein DC. Compromised autophagy and neurodegenerative diseases. *Nat Rev Neurosci.* (2015) 16:345–57. doi: 10.1038/nrn3961
9. Ravanan P, Srikumar IF, Talwar P. Autophagy: the spotlight for cellular stress responses. *Life Sci.* (2017) 188:53–67. doi: 10.1016/j.lfs.2017.08.029
10. Bialik S, Dasari SK, Kimchi A. Autophagy-dependent cell death—where, how and why a cell eats itself to death. *J Cell Sci.* (2018) 131:jcs.215152. doi: 10.1242/jcs.215152
11. Galluzzi L, Green DR. Autophagy-independent functions of the autophagy machinery. *Cell.* (2019) 177:1682–99. doi: 10.1016/j.cell.2019.05.026
12. Tolkovsky AM. Mitophagy. *Biochim Biophys Acta.* (2009) 1793:1508–15. doi: 10.1016/j.bbamcr.2009.03.002
13. Pickles S, Vigie P, Youle RJ. Mitophagy and quality control mechanisms in mitochondrial maintenance. *Curr Biol.* (2018) 28:R170–85. doi: 10.1016/j.cub.2018.01.004
14. Fivenson EM, Lautrup S, Sun N, Scheibye-Knudsen M, Stevnsner T, Nilsen H, et al. Mitophagy in neurodegeneration and aging. *Neurochem Int.* (2017) 109:202–9. doi: 10.1016/j.neuint.2017.02.007
15. Tang YC, Tian HX, Yi T, Chen HB. The critical roles of mitophagy in cerebral ischemia. *Protein Cell.* (2016) 7:699–713. doi: 10.1007/s13238-016-0307-0
16. Garone C, Minczuk M, Tilokani L, Nagashima S, Paupe V, Prudent J. Mitochondrial dynamics: overview of molecular mechanisms. *Essays Biochem.* (2018) 62:341–60. doi: 10.1042/ebc20170104
17. Whitley BN, Engelhart EA, Hoppins S. Mitochondrial dynamics and their potential as a therapeutic target. *Mitochondrion.* (2019) 49:269–83. doi: 10.1016/j.mito.2019.06.002
18. Chan DC. Mitochondria: dynamic organelles in disease, aging, and development. *Cell.* (2006) 125:1241–52. doi: 10.1016/j.cell.2006.06.010
19. Otera H, Ishihara N, Mihara K. New insights into the function and regulation of mitochondrial fission. *Biochim Biophys Acta.* (2013) 1833:1256–68. doi: 10.1016/j.bbamcr.2013.02.002
20. Yoon Y, Krueger EW, Oswald BJ, McNiven MA. The mitochondrial protein hFis1 regulates mitochondrial fission in mammalian cells through an interaction with the dynamin-like protein DLP1. *Mol Cell Biol.* (2003) 23:5409–20. doi: 10.1128/mcb.23.15.5409-5420.2003
21. Kumar R, Bukowski MJ, Wider JM, Reynolds CA, Calo L, Lepore B, et al. Mitochondrial dynamics following global cerebral ischemia. *Mol Cell Neurosci.* (2016) 76:68–75. doi: 10.1016/j.mcn.2016.08.010
22. Klacanova K, Kovalska M, Chomova M, Pilchova I, Tatarkova Z, Kaplan P, et al. Global brain ischemia in rats is associated with mitochondrial release and downregulation of Mfn2 in the cerebral cortex, but not the hippocampus. *Int J Mol Med.* (2019) 43:2420–8. doi: 10.3892/ijmm.2019.4168
23. Gao J, Wang H, Li Y, Li W. Resveratrol attenuates cerebral ischaemia reperfusion injury via modulating mitochondrial dynamics homeostasis and activating AMPK-Mfn1 pathway. *Int J Exp Pathol.* (2019) 100:337–49. doi: 10.1111/iep.12336
24. Owens K, Park JH, Gourley S, Jones H, Kristian T. Mitochondrial dynamics: cell-type and hippocampal region specific changes following global cerebral ischemia. *J Bioenerg Biomembr.* (2014) 47:13–31. doi: 10.1007/s10863-014-9575-7
25. Flippo KH, Gnanasekaran A, Perkins GA, Ajmal A, Merrill RA, Dickey AS, et al. AKAP1 protects from cerebral ischemic stroke by inhibiting Drp1-dependent mitochondrial fission. *J Neurosci.* (2018) 38:8233–42. doi: 10.1523/jneurosci.0649-18.2018
26. Wang M-S, Tang Y-N, Zhang G-F, Chen H-L, Sun X-P, Qin W-W, et al. Selective brain hypothermia-induced neuroprotection against focal cerebral ischemia/reperfusion injury is associated with Fis1 inhibition. *Neural Regen Res.* (2020) 15:903–11. doi: 10.4103/1673-5374.268973
27. Vásquez-Trincado C, García-Carvajal I, Pennanen C, Parra V, Hill JA, Rothermel BA, et al. Mitochondrial dynamics, mitophagy and cardiovascular disease. *J Physiol.* (2016) 594:509–25. doi: 10.1113/jp271301
28. Dorn GW, Kitsis RN. The mitochondrial dynamism-mitophagy-cell death interactome. *Circ Res.* (2015) 116:167–82. doi: 10.1161/circresaha.116.303554
29. Zuo W, Zhang S, Xia C-Y, Guo X-F, He W-B, Chen N-H. Mitochondria autophagy is induced after hypoxic/ischemic stress in a Drp1 dependent manner: the role of inhibition of Drp1 in ischemic brain damage. *Neuropharmacology.* (2014) 86:103–15. doi: 10.1016/j.neuropharm.2014.07.002
30. Xu B, Zhu L, Chu J, Ma Z, Fu Q, Wei W, et al. Esculetin improves cognitive impairments induced by transient cerebral ischaemia and reperfusion in mice via regulation of mitochondrial fragmentation and mitophagy. *Behav Brain Res.* (2019) 372. doi: 10.1016/j.bbr.2019.112007
31. Kumari S, Anderson L, Farmer S, Mehta SL, Li PA. Hyperglycemia alters mitochondrial fission and fusion proteins in mice subjected to cerebral ischemia and reperfusion. *Transl Stroke Res.* (2012) 3:296–304. doi: 10.1007/s12975-012-0158-9

32. Yoshii SR, Mizushima N. Autophagy machinery in the context of mammalian mitophagy. *Biochim Biophys Acta.* (2015) 1853:2797–801. doi: 10.1016/j.bbamcr.2015.01.013
33. Narendra D, Tanaka A, Suen DF, Youle RJ. Parkin is recruited selectively to impaired mitochondria and promotes their autophagy. *J Cell Biol.* (2008) 183:795–803. doi: 10.1083/jcb.200809125
34. Narendra DP, Jin SM, Tanaka A, Suen DF, Gautier CA, Shen J, et al. PINK1 is selectively stabilized on impaired mitochondria to activate Parkin. *PLoS Biol.* (2010) 8:e1000298. doi: 10.1371/journal.pbio.1000298
35. Geisler S, Holmstrom KM, Skujat D, Fiesel FC, Rothfuss OC, Kahle PJ, et al. PINK1/Parkin-mediated mitophagy is dependent on VDAC1 and p62/SQSTM1. *Nat Cell Biol.* (2010) 12:119–31. doi: 10.1038/ncb2012
36. Matsuda N, Sato S, Shiba K, Okatsu K, Saisho K, Gautier CA, et al. PINK1 stabilized by mitochondrial depolarization recruits Parkin to damaged mitochondria and activates latent Parkin for mitophagy. *J Cell Biol.* (2010) 189:211–21. doi: 10.1083/jcb.200910140
37. Barodia SK, Creed RB, Goldberg MS. Parkin and PINK1 functions in oxidative stress and neurodegeneration. *Brain Res Bull.* (2017) 133:51–9. doi: 10.1016/j.brainresbull.2016.12.004
38. Rasool S, Soya N, Truong L, Croteau N, Lukacs GL, Trempe JF. PINK1 autophosphorylation is required for ubiquitin recognition. *EMBO Rep.* (2018) 19:e44981. doi: 10.15252/embr.201744981
39. Guardia-Laguarta C, Liu Y, Lauritzen KH, Erdjument-Bromage H, Martin B, Swayne TC, et al. PINK1 content in mitochondria is regulated by ER-associated degradation. *J Neurosci.* (2019) 39:7074–85. doi: 10.1523/JNEUROSCI.1691-18.2019
40. Koyano F, Okatsu K, Kosako H, Tamura Y, Go E, Kimura M, et al. Ubiquitin is phosphorylated by PINK1 to activate parkin. *Nature.* (2014) 510:162–6. doi: 10.1038/nature13392
41. Georgakopoulos ND, Wells G, Campanella M. The pharmacological regulation of cellular mitophagy. *Nat Chem Biol.* (2017) 13:136–46. doi: 10.1038/nchembio.2287
42. Eiyama A, Okamoto K. PINK1/Parkin-mediated mitophagy in mammalian cells. *Curr Opin Cell Biol.* (2015) 33:95–101. doi: 10.1016/j.ceb.2015.01.002
43. Ashrafi G, Schwarz TL. The pathways of mitophagy for quality control and clearance of mitochondria. *Cell Death Differ.* (2013) 20:31–42. doi: 10.1038/cdd.2012.81
44. Lan R, Wu J-T, Wu T, Ma Y-Z, Wang B-Q, Zheng H-Z, et al. Mitophagy is activated in brain damage induced by cerebral ischemia and reperfusion via the PINK1/Parkin/p62 signalling pathway. *Brain Res Bull.* (2018) 142:63–77. doi: 10.1016/j.brainresbull.2018.06.018
45. Villa E, Marchetti S, Ricci J-E. No parkin zone: mitophagy without parkin. *Trends Cell Biol.* (2018) 28:882–95. doi: 10.1016/j.tcb.2018.07.004
46. Zhang J, Ney PA. Role of BNIP3 and NIX in cell death, autophagy, and mitophagy. *Cell Death Differ.* (2009) 16:939–46. doi: 10.1038/cdd.2009.16
47. Chourasia AH, Macleod KF. Tumor suppressor functions of BNIP3 and mitophagy. *Autophagy.* (2015) 11:1937–8. doi: 10.1080/15548627.2015.1085136
48. Ney PA. Mitochondrial autophagy: origins, significance, and role of BNIP3 and NIX. *Biochim Biophys Acta.* (2015) 1853:2775–83. doi: 10.1016/j.bbamcr.2015.02.022
49. Liu XW, Lu MK, Zhong HT, Wang LH, Fu YP. Panax notoginseng saponins attenuate myocardial ischemia-reperfusion injury through the HIF-1alpha/BNIP3 pathway of autophagy. *J Cardiovasc Pharmacol.* (2019) 73:92–9. doi: 10.1097/FJC.0000000000000640
50. Tang C, Han H, Liu Z, Liu Y, Yin L, Cai J, et al. Activation of BNIP3-mediated mitophagy protects against renal ischemia-reperfusion injury. *Cell Death Dis.* (2019) 10:677. doi: 10.1038/s41419-019-1899-0
51. Ding WX, Ni HM, Li M, Liao Y, Chen X, Stolz DB, et al. Nix is critical to two distinct phases of mitophagy, reactive oxygen species-mediated autophagy induction and Parkin-ubiquitin-p62-mediated mitochondrial priming. *J Biol Chem.* (2010) 285:27879–90. doi: 10.1074/jbc.M110.119537
52. Jung J, Zhang Y, Celiku O, Zhang W, Song H, Williams BJ, et al. Mitochondrial NIX promotes tumor survival in the hypoxic niche of glioblastoma. *Cancer Res.* (2019) 79:5218–32. doi: 10.1158/0008-5472.CAN-19-0198
53. Bellot G, Garcia-Medina R, Gounon P, Chiche J, Roux D, Pouyssegur J, et al. Hypoxia-induced autophagy is mediated through hypoxia-inducible factor induction of BNIP3 and BNIP3L via their BH3 domains. *Mol Cell Biol.* (2009) 29:2570–81. doi: 10.1128/MCB.00166-09
54. Yuan Y, Zheng Y, Zhang X, Chen Y, Wu X, Wu J, et al. BNIP3L/NIX-mediated mitophagy protects against ischemic brain injury independent of PARK2. *Autophagy.* (2017) 13:1754–66. doi: 10.1080/15548627.2017.1357792
55. Shi RY, Zhu SH, Li V, Gibson SB, Xu XS, Kong JM. BNIP3 interacting with LC3 triggers excessive mitophagy in delayed neuronal death in stroke. *CNS Neurosci Ther.* (2014) 20:1045–55. doi: 10.1111/cns.12325
56. Liu L, Feng D, Chen G, Chen M, Zheng Q, Song P, et al. Mitochondrial outer-membrane protein FUNDC1 mediates hypoxia-induced mitophagy in mammalian cells. *Nat Cell Biol.* (2012) 14:177–85. doi: 10.1038/ncb2422
57. Chen G, Han Z, Feng D, Chen Y, Chen L, Wu H, et al. A regulatory signaling loop comprising the PGAM5 phosphatase and CK2 controls receptor-mediated mitophagy. *Mol Cell.* (2014) 54:362–77. doi: 10.1016/j.molcel.2014.02.034
58. Zhang W, Siraj S, Zhang R, Chen Q. Mitophagy receptor FUNDC1 regulates mitochondrial homeostasis and protects the heart from I/R injury. *Autophagy.* (2017) 13:1080–1. doi: 10.1080/15548627.2017.1300224
59. Zhou H, Wang J, Zhu P, Zhu H, Toan S, Hu S, et al. NR4A1 aggravates the cardiac microvascular ischemia reperfusion injury through suppressing FUNDC1-mediated mitophagy and promoting Mff-required mitochondrial fission by CK2alpha. *Basic Res Cardiol.* (2018) 113:23. doi: 10.1007/s00395-018-0682-1
60. Belanger M, Allaman I, Magistretti PJ. Brain energy metabolism: focus on astrocyte-neuron metabolic cooperation. *Cell Metab.* (2011) 14:724–38. doi: 10.1016/j.cmet.2011.08.016
61. Sun MS, Jin H, Sun X, Huang S, Zhang FL, Guo ZN, et al. Free radical damage in ischemia-reperfusion injury: an obstacle in acute ischemic stroke after revascularization therapy. *Oxid Med Cell Longev.* (2018) 2018:3804979. doi: 10.1155/2018/3804979
62. Malik AR, Willnow TE. Excitatory amino acid transporters in physiology and disorders of the central nervous system. *Int J Mol Sci.* (2019) 20:5671. doi: 10.3390/ijms20225671
63. Uzdensky AB. Apoptosis regulation in the penumbra after ischemic stroke: expression of pro- and antiapoptotic proteins. *Apoptosis.* (2019) 24:687–702. doi: 10.1007/s10495-019-01556-6
64. Ashford TP, Porter KR. Cytoplasmic components in hepatic cell lysosomes. *J Cell Biol.* (1962) 12:198–202. doi: 10.1083/jcb.12.1.198
65. Deter RL, Baudhuin P, De Duve C. Participation of lysosomes in cellular autophagy induced in rat liver by glucagon. *J Cell Biol.* (1967) 35:C11–6. doi: 10.1083/jcb.35.2.c11
66. Fedorko M. Effect of chloroquine on morphology of cytoplasmic granules in maturing human leukocytes–an ultrastructural study. *J Clin Invest.* (1967) 46:1932–42. doi: 10.1172/JCI105683
67. Yamamoto A, Yue Z. Autophagy and its normal and pathogenic states in the brain. *Annu Rev Neurosci.* (2014) 37:55–78. doi: 10.1146/annurev-neuro-071013-014149
68. Bingol B. Autophagy and lysosomal pathways in nervous system disorders. *Mol Cell Neurosci.* (2018) 91:167–208. doi: 10.1016/j.mcn.2018.04.009
69. Geronimo-Olvera C, Massieu L. Autophagy as a homeostatic mechanism in response to stress conditions in the central nervous system. *Mol Neurobiol.* (2019) 56:6594–608. doi: 10.1007/s12035-019-1546-x
70. Wang P, Shao BZ, Deng Z, Chen S, Yue Z, Miao CY. Autophagy in ischemic stroke. *Prog Neurobiol.* (2018) 163–4:98–117. doi: 10.1016/j.pneurobio.2018.01.001
71. Wang Y, Nartiss Y, Steipe B, McQuibban GA, Kim PK. ROS-induced mitochondrial depolarization initiates PARK2/PARKIN-dependent mitochondrial degradation by autophagy. *Autophagy.* (2012) 8:1462–76. doi: 10.4161/auto.21211
72. Mijaljica D, Prescott M, Devenish RJ. Different fates of mitochondria: alternative ways for degradation? *Autophagy.* (2007) 3:4–9. doi: 10.4161/auto.3011
73. Li Q, Zhang T, Wang J, Zhang Z, Zhai Y, Yang GY, et al. Rapamycin attenuates mitochondrial dysfunction via activation of mitophagy in experimental ischemic stroke. *Biochem Biophys Res Commun.* (2014) 444:182–8. doi: 10.1016/j.bbrc.2014.01.032
74. Wu X, Li X, Liu Y, Yuan N, Li C, Kang Z, et al. Hydrogen exerts neuroprotective effects on OGD/R damaged neurons in rat hippocampal

by protecting mitochondrial function via regulating mitophagy mediated by PINK1/Parkin signaling pathway. *Brain Res.* (2018) 1698:89–98. doi: 10.1016/j.brainres.2018.06.028
75. Di Y, He YL, Zhao T, Huang X, Wu KW, Liu SH, et al. Methylene blue reduces acute cerebral ischemic injury via the induction of mitophagy. *Mol Med.* (2015) 21:420–9. doi: 10.2119/molmed.2015.00038
76. Li F, Tan J, Zhou F, Hu Z, Yang B. Heat shock protein B8 (HSPB8) reduces oxygen-glucose deprivation/reperfusion injury via the induction of mitophagy. *Cell Physiol Biochem.* (2018) 48:1492–504. doi: 10.1159/000492259
77. Wang H, Chen S, Zhang Y, Xu H, Sun H. Electroacupuncture ameliorates neuronal injury by Pink1/Parkin-mediated mitophagy clearance in cerebral ischemia-reperfusion. *Nitric Oxide.* (2019) 91:23–34. doi: 10.1016/j.niox.2019.07.004
78. Wang W, Xu J. Curcumin attenuates cerebral ischemia-reperfusion injury through regulating mitophagy and preserving mitochondrial function. *Curr Neurovasc Res.* (2020) 17:113–22. doi: 10.2174/1567202617666200225122620
79. Wu M, Lu G, Lao YZ, Zhang H, Zheng D, Zheng ZQ, et al. Garciesculenxanthone B induces PINK1-parkin-mediated mitophagy and prevents ischemia-reperfusion brain injury in mice. *Acta Pharmacol Sin.* (2020). doi: 10.1038/s41401-020-0480-9. [Epub ahead of print].
80. He Q, Li Z, Meng C, Wu J, Zhao Y, Zhao J. Parkin-dependent mitophagy is required for the inhibition of ATF4 on NLRP3 inflammasome activation in cerebral ischemia-reperfusion injury in rats. *Cells.* (2019) 8:897. doi: 10.3390/cells8080897
81. Zhang X, Yuan Y, Jiang L, Zhang J, Gao J, Shen Z, et al. Endoplasmic reticulum stress induced by tunicamycin and thapsigargin protects against transient ischemic brain injury: involvement of PARK2-dependent mitophagy. *Autophagy.* (2014) 10:1801–13. doi: 10.4161/auto.32136
82. Shen Z, Zheng Y, Wu J, Chen Y, Wu X, Zhou Y, et al. PARK2-dependent mitophagy induced by acidic postconditioning protects against focal cerebral ischemia and extends the reperfusion window. *Autophagy.* (2017) 13:473–85. doi: 10.1080/15548627.2016.1274596
83. Lan R, Zhang Y, Wu T, Ma YZ, Wang BQ, Zheng HZ, et al. Xiao-Xu-Ming decoction reduced mitophagy activation and improved mitochondrial function in cerebral ischemia and reperfusion injury. *Behav Neurol.* (2018) 2018:4147502. doi: 10.1155/2018/4147502
84. Yu S, Zheng S, Leng J, Wang S, Zhao T, Liu J. Inhibition of mitochondrial calcium uniporter protects neurocytes from ischemia/reperfusion injury via the inhibition of excessive mitophagy. *Neurosci Lett.* (2016) 628:24–9. doi: 10.1016/j.neulet.2016.06.012
85. Feng J, Chen X, Lu S, Li W, Yang D, Su W, et al. Naringin attenuates cerebral ischemia-reperfusion injury through inhibiting peroxynitrite-mediated mitophagy activation. *Mol Neurobiol.* (2018) 55:9029–42. doi: 10.1007/s12035-018-1027-7
86. Feng J, Chen X, Guan B, Li C, Qiu J, Shen J. Inhibition of peroxynitrite-induced mitophagy activation attenuates cerebral ischemia-reperfusion injury. *Mol Neurobiol.* (2018) 55:6369–86. doi: 10.1007/s12035-017-0859-x
87. Su SH, Wu YF, Wang DP, Hai J. Inhibition of excessive autophagy and mitophagy mediates neuroprotective effects of URB597 against chronic cerebral hypoperfusion. *Cell Death Dis.* (2018) 9:733. doi: 10.1038/s41419-018-0755-y
88. Cai CC, Zhu JH, Ye LX, Dai YY, Fang MC, Hu YY, et al. Glycine protects against hypoxic-ischemic brain injury by regulating mitochondria-mediated autophagy via the AMPK pathway. *Oxid Med Cell Longev.* (2019) 2019:4248529. doi: 10.1155/2019/4248529
89. Durkee CA, Araque A. Diversity and specificity of astrocyte–neuron communication. *Neuroscience.* (2019) 396:73–8. doi: 10.1016/j.neuroscience.2018.11.010
90. Li L, Stary CM. Targeting glial mitochondrial function for protection from cerebral ischemia: relevance, mechanisms, and the role of microRNAs. *Oxid Med Cellu Longev.* (2016) 2016:1–11. doi: 10.1155/2016/6032306
91. Quintana DD, Garcia JA, Sarkar SN, Jun S, Engler-Chiurazzi EB, Russell AE, et al. Hypoxia-reoxygenation of primary astrocytes results in a redistribution of mitochondrial size and mitophagy. *Mitochondrion.* (2019) 47:244–55. doi: 10.1016/j.mito.2018.12.004
92. Cheng Y, Yang JM. Autophagy and apoptosis: rivals or mates? *Chin J Cancer.* (2013) 32:103–5. doi: 10.5732/cjc.013.10022
93. Kaminskyy VO, Zhivotovsky B. Free radicals in cross talk between autophagy and apoptosis. *Antioxid Redox Signal.* (2014) 21:86–102. doi: 10.1089/ars.2013.5746
94. Wu HJ, Pu JL, Krafft PR, Zhang JM, Chen S. The molecular mechanisms between autophagy and apoptosis: potential role in central nervous system disorders. *Cell Mol Neurobiol.* (2015) 35:85–99. doi: 10.1007/s10571-014-0116-z
95. Praharaj PP, Naik PP, Panigrahi DP, Bhol CS, Mahapatra KK, Patra S, et al. Intricate role of mitochondrial lipid in mitophagy and mitochondrial apoptosis: its implication in cancer therapeutics. *Cell Mol Life Sci.* (2019) 76:1641–52. doi: 10.1007/s00018-018-2990-x
96. Mukhopadhyay S, Panda PK, Sinha N, Das DN, Bhutia SK. Autophagy and apoptosis: where do they meet? *Apoptosis.* (2014) 19:555–66. doi: 10.1007/s10495-014-0967-2
97. Wirawan E, Vande Walle L, Kersse K, Cornelis S, Claerhout S, Vanoverberghe I, et al. Caspase-mediated cleavage of Beclin-1 inactivates Beclin-1-induced autophagy and enhances apoptosis by promoting the release of proapoptotic factors from mitochondria. *Cell Death Dis.* (2010) 1:e18. doi: 10.1038/cddis.2009.16
98. Choubey V, Cagalinec M, Liiv J, Safiulina D, Hickey MA, Kuum M, et al. BECN1 is involved in the initiation of mitophagy: it facilitates PARK2 translocation to mitochondria. *Autophagy.* (2014) 10:1105–19. doi: 10.4161/auto.28615
99. Chen Y, Chen HN, Wang K, Zhang L, Huang Z, Liu J, et al. Ketoconazole exacerbates mitophagy to induce apoptosis by downregulating cyclooxygenase-2 in hepatocellular carcinoma. *J Hepatol.* (2019) 70:66–77. doi: 10.1016/j.jhep.2018.09.022
100. Zhang X, Yan H, Yuan Y, Gao J, Shen Z, Cheng Y, et al. Cerebral ischemia-reperfusion-induced autophagy protects against neuronal injury by mitochondrial clearance. *Autophagy.* (2013) 9:1321–33. doi: 10.4161/auto.25132
101. Zhou M, Xia ZY, Lei SQ, Leng Y, Xue R. Role of mitophagy regulated by Parkin/DJ-1 in remote ischemic postconditioning-induced mitigation of focal cerebral ischemia-reperfusion. *Eur Rev Med Pharmacol Sci.* (2015) 19:4866–71.
102. Yaribeygi H, Panahi Y, Javadi B, Sahebkar A. The underlying role of oxidative stress in neurodegeneration: a mechanistic review. *CNS Neurol Disord Drug Targets.* (2018) 17:207–15. doi: 10.2174/1871527317666180425122557
103. Diebold L, Chandel NS. Mitochondrial ROS regulation of proliferating cells. *Free Radic Biol Med.* (2016) 100:86–93. doi: 10.1016/j.freeradbiomed.2016.04.198
104. Angelova PR, Abramov AY. Role of mitochondrial ROS in the brain: from physiology to neurodegeneration. *FEBS Lett.* (2018) 592:692–702. doi: 10.1002/1873-3468.12964
105. Fan P, Xie XH, Chen CH, Peng X, Zhang P, Yang C, et al. Molecular regulation mechanisms and interactions between reactive oxygen species and mitophagy. *DNA Cell Biol.* (2019) 38:10–22. doi: 10.1089/dna.2018.4348
106. Livingston MJ, Wang J, Zhou J, Wu G, Ganley IG, Hill JA, et al. Clearance of damaged mitochondria via mitophagy is important to the protective effect of ischemic preconditioning in kidneys. *Autophagy.* (2019) 15:2142–62. doi: 10.1080/15548627.2019.1615822
107. Bhogal RH, Weston CJ, Velduis S, Leuvenink HGD, Reynolds GM, Davies S, et al. The reactive oxygen species-mitophagy signaling pathway regulates liver endothelial cell survival during ischemia/reperfusion injury. *Liver Transpl.* (2018) 24:1437–52. doi: 10.1002/lt.25313
108. Feng Y, Madungwe NB, da Cruz Junho CV, Bopassa JC. Activation of G protein-coupled oestrogen receptor 1 at the onset of reperfusion protects the myocardium against ischemia/reperfusion injury by reducing mitochondrial dysfunction and mitophagy. *Br J Pharmacol.* (2017) 174:4329–44. doi: 10.1111/bph.14033
109. Green DR, Galluzzi L, Kroemer G. Mitochondria and the autophagy-inflammation-cell death axis in organismal aging. *Science.* (2011) 333:1109–12. doi: 10.1126/science.1201940
110. Zhao Y, Huang S, Liu J, Wu X, Zhou S, Dai K, et al. Mitophagy contributes to the pathogenesis of inflammatory diseases. *Inflammation.* (2018) 41:1590–600. doi: 10.1007/s10753-018-0835-2
111. Tschopp J. Mitochondria: sovereign of inflammation? *Eur J Immunol.* (2011) 41:1196–202. doi: 10.1002/eji.201141436

112. Matsuzawa-Ishimoto Y, Hwang S, Cadwell K. Autophagy and inflammation. *Annu Rev Immunol.* (2018) 36:73–101. doi: 10.1146/annurev-immunol-042617-053253
113. Deretic V, Levine B. Autophagy balances inflammation in innate immunity. *Autophagy.* (2018) 14:243–51. doi: 10.1080/15548627.2017.1402992
114. Joven J, Guirro M, Marine-Casado R, Rodriguez-Gallego E, Menendez JA. Autophagy is an inflammation-related defensive mechanism against disease. *Adv Exp Med Biol.* (2014) 824:43–59. doi: 10.1007/978-3-319-07320-0_6
115. Gkikas I, Palikaras K, Tavernarakis N. The role of mitophagy in innate immunity. *Front Immunol.* (2018) 9:1283. doi: 10.3389/fimmu.2018.01283
116. Yao L, Chen H, Wu Q, Xie K. Hydrogen-rich saline alleviates inflammation and apoptosis in myocardial I/Rinjury via PINK-mediated autophagy. *Int J Mol Med.* (2019) 44:1048–62. doi: 10.3892/ijmm.2019.4264

Conflict of Interest: The authors declare that the research was conducted in the absence of any commercial or financial relationships that could be construed as a potential conflict of interest.

frontiers in Neurology

ORIGINAL RESEARCH
published: 06 January 2021
doi: 10.3389/fneur.2020.618765

Effect of Oxygen Extraction (Brush-Sign) on Baseline Core Infarct Depends on Collaterals (HIR)

*Adrien Guenego[1], Matthew Leipzig[1], Robert Fahed[2], Eric S. Sussman[1], Tobias D. Faizy[1], Blake W. Martin[1], David G. Marcellus[1], Max Wintermark[1], Jean-Marc Olivot[3], Gregory W. Albers[4], Maarten G. Lansberg[4] and Jeremy J. Heit[1]**

[1] Interventional and Diagnostic Neuroradiology, Stanford Medical Center, Palo Alto, CA, United States, [2] Division of Neurology, Department of Medicine, Ottawa Hospital, Ottawa, ON, Canada, [3] Toulouse Stroke Center, Toulouse, France, [4] Stanford Stroke Center, Stanford University School of Medicine, Stanford, CA, United States

OPEN ACCESS

Edited by:
Rajiv Ram Ratan,
Burke Neurological Institute (BNI),
United States

Reviewed by:
Yingxin Chen,
Burke Neurological Institute (BNI),
United States
Nikoloz Tsiskaridze,
Pineo Medical Ecosystem, Georgia

***Correspondence:**
Jeremy J. Heit
jheit@stanford.edu

Specialty section:
This article was submitted to Stroke,
a section of the journal Frontiers in Neurology

Received: 18 October 2020
Accepted: 07 December 2020
Published: 06 January 2021

Citation:
Guenego A, Leipzig M, Fahed R, Sussman ES, Faizy TD, Martin BW, Marcellus DG, Wintermark M, Olivot J-M, Albers GW, Lansberg MG and Heit JJ (2021) Effect of Oxygen Extraction (Brush-Sign) on Baseline Core Infarct Depends on Collaterals (HIR). Front. Neurol. 11:618765. doi: 10.3389/fneur.2020.618765

Objectives: Baseline-core-infarct volume is a critical factor in patient selection and outcome in acute ischemic stroke (AIS) before mechanical thrombectomy (MT). We determined whether oxygen extraction efficiency and arterial collaterals, two different physiologic components of the cerebral ischemic cascade, interacted to modulate baseline-core-infarct volume in patients with AIS-LVO undergoing MT triage.

Methods: Between January 2015 and March 2018, consecutive patients with an AIS and M1 occlusion considered for MT with a baseline MRI and perfusion-imaging were included. Variables such as baseline-core-infarct volume [mL], arterial collaterals (HIR: TMax > 10 s volume/TMax > 6 s), high oxygen extraction (HOE, presence of the brush-sign on T2*) were assessed. A linear-regression was used to test the interaction of HOE and HIR with baseline-core-infarct volume, after including potential confounding variables.

Results: We included 103 patients. Median age was 70 (58–78), and 63% were female. Median baseline-core-infarct volume was 32 ml (IQR 8–74.5). Seventy six patients (74%) had HOE. In a multivariate analysis both favorable HIR collaterals ($p = 0.02$) and HOE ($p = 0.038$) were associated with lower baseline-core-infarct volume. However, HOE significantly interacted with HIR ($p = 0.01$) to predict baseline-core-infarct volume, favorable collaterals (low HIR) with HOE was associated with small baseline-core-infarct whereas patients with poor collaterals (high HIR) and HOE had large baseline-core-infarct.

Conclusion: While HOE under effective collateral blood-flow has the lowest baseline-core-infarct volume of all patients, the protective effect of HOE reverses under poor collateral blood-flow and may be a maladaptive response to ischemic stroke as measured by core infarctions in AIS-LVO patients undergoing MT triage.

Keywords: stroke, interventional, MRI perfusion imaging, MRI susceptibility weighted imaging, thrombectomy

INTRODUCTION

Mechanical thrombectomy (MT) is an effective treatment for acute ischemic stroke due to large-vessel occlusion (AIS-LVO) (1–5). MT eligible patients have a relatively small baseline-core-infarct volume at the time of imaging evaluation, and patients with favorable arterial collaterals are more likely to present with a small core infarction (6, 7) and to have less core infarction growth (8). Up to 40% of AIS-LVO patients may experience rapid early core infarct expansion, which often renders patients ineligible for MT at the time of imaging evaluation (9). Therefore, imaging biomarkers that would help to a better understanding of the physiologic response to ischemic challenge or that are predictive of core infarct growth would be beneficial in AIS patients undergoing MT triage.

The hypoperfusion intensity ratio (HIR) is derived from computed tomography (CT) or magnetic resonance (MR) perfusion imaging and has emerged as a powerful imaging predictor of favorable collaterals, decreased core infarction growth, and favorable clinical outcomes (8, 10–12). HIR is defined as the ratio of the brain tissue volume with a Time-to-Maximum delay (TMax, in seconds) $>$ 10 s divided by that with a TMax $>$ 6 s, such that a lower HIR ratio indicates a less severe perfusion delay and more robust collaterals (10, 13). Therefore, a low HIR ($<$0.4 or $<$0.5 according to studies) is a favorable imaging biomarker of MT eligibility (12) and outcome after treatment (14, 15).

Although cerebral collateral assessment by HIR or CT angiogram techniques provide important information to determine MT treatment eligibility, these techniques do not provide a complete understanding of the brain's physiologic response to ischemic challenge. For example, how well ischemic brain tissue extracts oxygen may influence core infarction size, penumbral volumes, and patient outcome. High oxygen extraction (HOE) in AIS-LVO patients may be measured by the presence of prominent hypointense signal within the medullary veins within ischemic tissue, which has been termed the Brush sign (16, 17). However, the relationship of these variables, especially the degree of oxygen extraction, to cerebral arterial collaterals is not clearly established in humans with AIS-LVO.

We hypothesized that the degree of oxygen extraction interacts with the ability of arterial collaterals to maintain small core infarct volumes and prevent core infarct growth in AIS-LVO patients. We determined whether HOE (Brush sign presence) interacted with arterial collaterals (HIR) to modulate baseline core infarction volume in patients with AIS-LVO undergoing MT triage.

METHODS

The study protocol was approved by the institutional review board and complied with the Health Insurance Portability and Accountability Act (HIPAA). Patient informed consent was waived by our review board for this single center retrospective analysis of anonymized data acquired prospectively. Adherence to the STROBE criteria (18) was enforced.

Population and Clinical Data

Between January 2015 and March 2018, consecutive AIS-LVO patients with a M1 occlusion who underwent MT triage at our comprehensive stroke center were retrospectively reviewed in this single-center study. Included patients underwent MT triage by MRI that included an axial T2* sequence, MR angiogram and MR perfusion. Patient clinical and treatment data were extracted from a prospectively maintained stroke database and the electronic medical record.

Imaging Data and Evaluation

All imaging were performed on either a 1.5T GE Signa or 3.0T GE MR750 MRI scanner using standard departmental protocols, using an eight channel GE HR brain coil (GE Healthcare, Milwaukee, Wisconsin). Technical details and parameters for the sequences used in this study were as follows.

Diffusion Weighted Imaging parameters: TR = 6,000 ms, TE = 78.2 ms; *b*-value = 0 and 1,000 s/mm^2; flip angle 90°, and slice thickness of 5 mm.

Perfusion-weighted imaging was performed using a dynamic susceptibility contrast technique following the intravenous administration of Multihance (529 mg/ml; Bracco, Milan, Italy) at a dose of 0.2 ml/kg body weight into an antecubital vein at a rate of 4.0 mL/s using a power injector (19). Perfusion parameters were: TR = 1,800 ms, TE = 35 ms; flip angle 80°, and slice thickness of 5 mm. Standard perfusion maps, including time-to-maximum of the residue function (TMax), were generated using the automated RAPID software (iSchemaView, Menlo Park, CA) (20). Quantitative perfusion delays were assessed as the volumes of cerebral tissue with TMax delays of $>$6 and 10 s using RAPID.

The ischemic penumbra was defined as the volume of brain tissue with a TMax $>$6 s on gadolinium-based dynamic-contrast susceptibility imaging.

Collaterals were measured by HIR, which was defined as the volume of brain tissue with TMax $>$10 s volume divided by the volume of tissue with TMax $>$6 s (10). A lower HIR ratio indicates a less severe perfusion delay and more robust collaterals (8, 10, 12, 13).

Core infarction and TMax volume measurements were quantified by an automatic software (RAPID, iSchemaView, Menlo Park, CA, USA). The core-penumbra mismatch volume and ratio was determined by a comparison of core infarction and penumbra volumes (21).

T2* gradient-echo axial sequences were mostly performed as: TR 650.0 ms, TE 15.0 ms, slice was 5 mm, slice gap of 0.0, FOV of 24.0 × 24.0. Brush-sign was defined as an asymmetric hypo-intense area along the course of the sub-ependymal and medullary veins in the deep white matter (16, 17) and was assessed as present or absent on baseline T2* imaging by two neuro-radiologists, XX. and XX., with respectively 4 and 7 years of practice. Disagreements were resolved by consensus readings.

Abbreviations: AIS-LVO, Acute Ischemic Stroke due to Large-Vessel Occlusion; CT, Computed Tomography; HIR, Hypoperfusion Intensity Ratio; HOE, High Oxygen Extraction; M1, Proximal Middle Cerebral Artery; MR, Magnetic Resonance imaging; MT, Mechanical Thrombectomy; NIHSS, National Institute of Health Stroke Scale; TMax, Time-to-Maximum (seconds).

TABLE 1 | Baseline demographic and clinical data in the population, association with baseline-core-infarct volume.

	All ($n = 103$)	p-value
Age, median (IQR)	70 (58–78)	0.04
Female, *n* (%)	65 (63%)	0.07
Mean Systolic Blood Pressure, mmHg (SD)	142 (32)	0.63
Median LDL (mg/dL, IQR)	105 (72–125)	0.18
Median Hemoglobin A1c% (IQR)	5.7 (5.4–6.5)	0.13
Median Admission Blood Glucose (mg/dL, IQR)	135 (111–180)	<0.0001
Medical history		
Hypertension, *n* (%)	77 (77%)	0.04
Diabetes, *n* (%)	33 (35%)	0.03
Hyperlipidemia, *n* (%)	52 (54%)	0.13
Atrial Fibrillation, *n* (%)	48 (52%)	0.4
Coronary Artery Disease, *n* (%)	22 (24%)	0.63
Prior Stroke, *n* (%)	11 (11.6%)	0.12
Smoking		
Never, *n* (%)	55 (56.7%)	0.85
Prior, *n* (%)	26 (26.8%)	
Current, *n* (%)	16 (16.5%)	
Stroke details		
Median time since LSN to imaging, min (IQR)	334 (238–430)	0.02
Median NIHSS (IQR)	17 (12–22)	0.0009
Intravenous Thrombolysis, *n* (%)	60 (58%)	0.78

SD, standard deviation; IQR, interquartile range; CAD, coronary artery disease; LSN, last seen normal; NIHSS, National Institute of Health stroke scale.

Outcomes and Statistical Analyses

Primary outcome was the interaction of brush-sign on T2* and collaterals as defined by their HIR with baseline-core-infarct volume on Diffusion Weighted Imaging.

A descriptive analysis of the data was performed. Nominal variables were summarized using frequency descriptive analysis then compared using Fisher's exact test. Continuous variables were treated using mean, standard deviation, 95% confidence interval (IC95), median, quartiles and inter-quartile ranges, then tested on univariate analysis using the Mann-Whitney test. Normality of the variables was tested by the Shapiro-Wilk test.

A linear regression was used to analyze the interaction of brush-sign with the full scale of HIR values and their interaction to predict baseline-core-infarct volume in these patients. We also included potential confounding variables in the model based on published literature, such as age, presentation National Institute of Health Stroke Scale (NIHSS), onset to imaging time, and admission blood glucose. Initial agreement between the two interventional neuroradiologists was measured using Kappa of Cohen, then disagreements were resolved by consensus reading.

All statistical analyses were performed with R version 3.6.2 (22). P-value < 0.05 was set for significance.

Data Availability Statement

The data that support the findings of this study are available from the corresponding author upon reasonable request.

TABLE 2 | Imaging characteristics in the population, association with baseline-core-infarct volume.

	All ($n = 103$)	p-value
Imaging characteristics		
Baseline infarct core volume, ml, median (IQR)	32 (8–74.5)	
HOE (Brush sign presence) *n* (%)	76 (74%)	0.18
TMax 6 s volume, ml median (IQR)	39 (19.5–74)	<0.0001
TMax 10 s volume, ml median (IQR)	100 (64.3–132)	<0.0001
HIR median (IQR)	0.43 (0.27–0.625)	<0.0001
Mismatch volume, ml median (IQR)	54.9 (20.25–81)	<0.0001
Mismatch ratio median (IQR)	3 (1.4–9.95)	0.0007
1.5 Tesla MRI, *n* (%)	58 (56%)	0.38
Vessel occlusion		
MCA–M1, *n* (%)	103 (100%)	1
Vessel occlusion side		
Left, *n* (%)	56 (54%)	0.07

SD, standard deviation; ICA, internal carotid artery; MCA, middle cerebral artery; M1, first segment of MCA; HOE, high oxygen extraction; TMax, Time-to-Maximum (seconds).

RESULTS

A total of 103 patients were included (see Flow-Chart in **Supplementary Figure 1**). Median patient age was 70 (58–78) years, baseline NIHSS was 17 (12–22), 65/103 patients (63%) were female, and 60 (58.3%) received intravenous thrombolysis. Patient clinical and imaging baseline characteristics are presented in **Tables 1**, **2**.

Median baseline-core-infarct volume was 32 mL (IQR, 8–74.5) and HIR was 0.43 (0.27–0.625). HOE, which was indicated by the Brush-sign, was present in 76 patients (74%), reader agreement was substantial (Cohen's Kappa 0.731) (23).

The linear regression model of HIR, HOE, their interaction, age, presentation NIHSS, onset to imaging delay, and admission blood glucose as confounding variables revealed not only significant effects of HOE ($p = 0.038$) and HIR ($p = 0.026$), but also a significant association between HIR and HOE to predict baseline-core-infarct volume ($p = 0.017$) (**Figure 1**, **Table 3**). In patients with favorable collaterals (lower HIR), poor oxygen extraction (absent HOE [brush sign]) was associated with larger infarct core volumes compared to patients with HOE (brush sign present). By contrast, in patients with unfavorable collaterals (high HIR), HOE (brush sign present) was associated with larger infarct core volumes compared to patients with poor oxygen extraction (no HOE [brush sign]) (examples in **Figure 2**).

DISCUSSION

In this study of AIS-LVO patients undergoing MT triage, we found that HOE in patients with favorable collaterals is associated with small core infarctions at the time of presentation. By contrast, HOE in patients with poor collaterals was associated

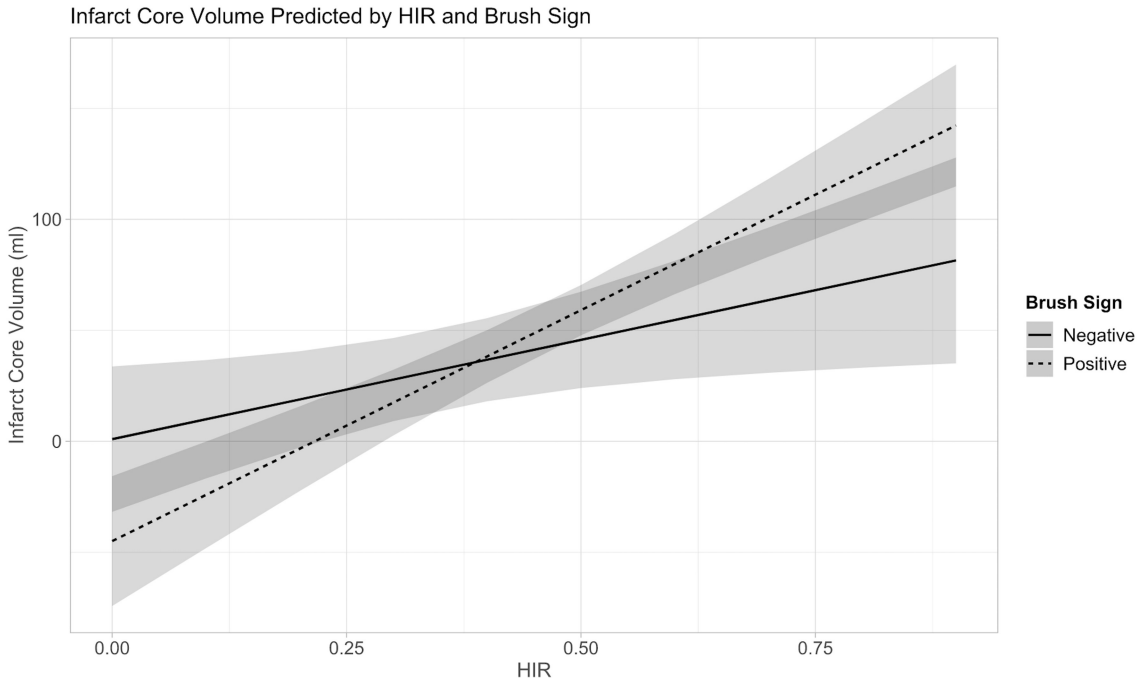

FIGURE 1 | Interaction between Collateral Flow (HIR) and Oxygen Extraction (Brush-Sign) with Baseline-Core-Infarct Volume.

TABLE 3 | Multivariate model for interactions with baseline-core-infarct volume.

	Core volume (ml)		
Predictors	**Estimates**	**CI**	***p***
(Intercept)	33.17	−35.14–101.48	0.337
HOE (Brush Sign)	−45.92	−89.25 – −2.58	**0.038**
HIR	89.47	10.95–168.00	**0.026**
Age	−0.96	−1.63 – −0.30	**0.005**
Presentation NIHSS	0.48	−1.10–2.05	0.550
Onset imaging	0.05	0.00–0.09	**0.039**
Admission blood glucose	0.08	−0.07–0.22	0.287
HOE (Brush sign) * HIR	118.55	21.67–215.44	**0.017**
Observations	103		

Bold values are p-values with a statistical significance <0.05.

with larger core infarctions. Interestingly, HOE was not significantly associated with baseline-core-infarct volume in univariate but in multivariate analysis, these findings indicate the oxygen extraction and collateral blood flow are important modulators of brain tissue preservation during ischemic challenge due to AIS-LVO.

AIS-LVO results in the sudden disruption of blood flow to the brain, which must adapt to this ischemic challenge by maximizing blood flow to the brain to prevent irreversible core infarction. Patients with favorable collaterals are able to deliver blood to the ischemic brain and minimize core infarction growth. Patients who are able to maximally extract oxygen from the blood delivered by favorable collaterals are likely to further protect against core infarction growth due to increased oxygen delivery to ischemic brain tissue. Our findings support this hypothesis and interpretation of the ischemic cascade. Moreover, our findings suggest that neuroprotective agents that augment oxygen extraction might be beneficial in preventing core infarction growth in patients with robust collaterals, which has implications for AIS-LVO patients undergoing transfer from a primary stroke center to a comprehensive stroke center, where MT may be performed.

Our finding that HOE (brush sign presence) in patients with poor collaterals correlates with large core infarction volumes suggests that even a maximal physiologic response to ischemia with high levels of oxygen extraction are unable to prevent core infarction growth. Thus, the ability of collaterals to deliver blood to ischemic tissue may be more important for the preservation of brain tissue than effective oxygen extraction. This finding is consistent with prior MT trials that have found collaterals to be an important predictor of core infarction volume and outcome after MT (8, 12, 15, 24–27). The identification of neuroprotective agents that augment collateral blood flow are therefore of paramount importance for these patients.

Our results might also explain discrepant findings in prior studies that have evaluated oxygen extraction in the context of AIS. One study found that HOE in AIS patients is associated with larger baseline core infarctions and a greater risk of hemorrhagic transformation (16). However, the interaction between oxygen extraction and collateral robustness was not examined, which likely explains why increased oxygen extraction

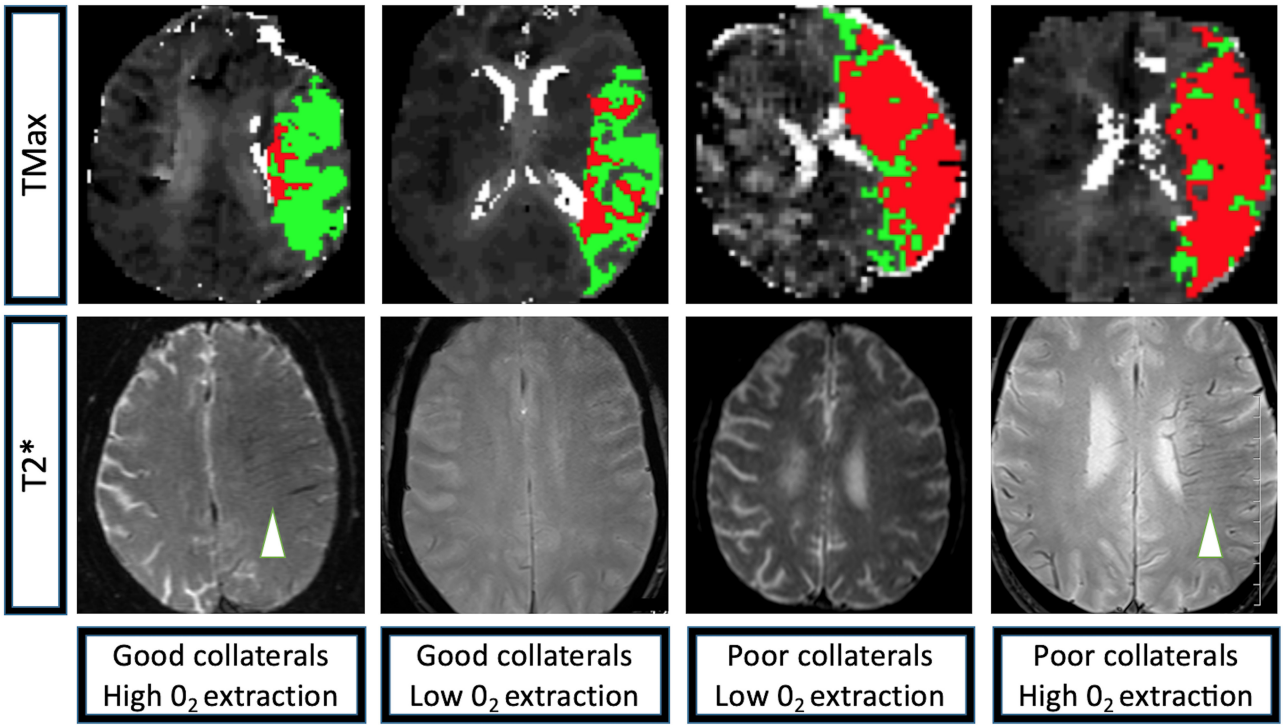

FIGURE 2 | Perfusion and T2* characteristics of the four extreme imaging profiles with a left M1 occlusion. Group 1: Left M1 occlusion, HIR≤0.40 (good collaterals, low volume of tissue with TMax > 10 s [depicted in red] compared to the volume of tissue with TMax > 6 s [depicted in green]), high 0_2 extraction (brush-sign on T2*, white arrowhead); Group 2: Left M1 occlusion, HIR≤0.40 (good collaterals), low 0_2 extraction (no brush-sign on T2*); Group 3: Left M1 occlusion, HIR > 0.40 (poor collaterals, high volume of tissue with TMax>10 s [depicted in red] compared to the volume of tissue with TMax > 6 s [depicted in green]), low 0_2 extraction (no brush-sign on T2*); Group 4: Left M1 occlusion, HIR > 0.40 (poor collaterals), high 0_2 extraction (brush-sign on T2*, white arrowhead). TMax: Axial images of a magnetic resonance perfusion sequence depicting in red the volume of tissue with a TMax>10 s and in green the volume of tissue with TMax > 6 s. T2*: Axial images of a magnetic resonance GRE sequence, brush-sign is defined as an asymmetric hypo-intense area along the course of the sub-ependymal and medullary veins in the deep white matter and is outlined by a white circle.

was correlated with larger baseline core infarctions (16) and poor clinical outcomes after intravenous-thrombolysis and MT treatment (28, 29).

By contrast, Derdeyn and colleagues showed that increased oxygen extraction in patients with cervical carotid artery occlusion may occur in the absence of cerebral blood volume elevation (a marker of collateral blood flow) (30). Furthermore, patients who were maximally adapted to augment blood flow to an ischemic hemisphere (increased oxygen extraction and cerebral blood volume) were at an increased risk for subsequent cerebral infarction (30). These findings are similar to our study, both of which indicate that oxygen extraction and cerebral perfusion due to collaterals might be uncoupled depending upon an individual patient's physiology and ability to respond to ischemic challenge. Our results and those of Derdeyn and colleagues also suggest that patients with poor collaterals and high rates of oxygen extraction are at the highest risk for core infarction and core infarction growth, as brain tissue damage related to oxidative stress may be maximized.

Limitations

Our study is limited by its retrospective and single center design, which may introduce bias and limit the generalizability of our findings. We did not include patients without perfusion imaging, with CT imaging or with SWI imaging which may further limit the generalizability of our findings. The use of both 1.5 and 3.0 Tesla MRIs in our study might affect the detection of the brush-sign due to differences in technique, which may also introduce bias in our study.

CONCLUSION

Robust collateral blood flow and high oxygen extraction are associated with small core infarctions in AIS-LVO patients undergoing MT triage. However, in patients with poor collaterals, increased oxygen extraction does not protect against core infarction growth prior to presentation. Maximal oxygen extraction and cerebral perfusion are variables that may be uncoupled depending upon an individual patient's physiologic adaptation to cerebral ischemia.

DATA AVAILABILITY STATEMENT

The datasets used and analyzed during the current study will be made available by the corresponding author upon reasonable request.

ETHICS STATEMENT

The studies involving human participants were reviewed and approved by Stanford Ethics committee. Written informed consent for participation was not required for this study in accordance with the national legislation and the institutional requirements.

AUTHOR CONTRIBUTIONS

AG, ML, RF, ES, TF, BM, DM, MW, J-MO, GA, MGL, and JH contributed to study conception and design, data collection, analysis and interpretation of results, and manuscript preparation. ML conducted all the statistical analyses. All authors contributed to the article and approved the submitted version.

SUPPLEMENTARY MATERIAL

The Supplementary Material for this article can be found online at: https://www.frontiersin.org/articles/10.3389/fneur.2020.618765/full#supplementary-material

Supplementary Figure 1 | Patients flow-chart. **352** (186 patients without an M1 occlusion) → **166** (61 patients had a CT as baseline imaging) → **105** (two patients had major artifacts on the baseline T2* sequence, or the T2* was not available) → **103** patients included.

REFERENCES

1. Berkhemer OA, Fransen PS, Beumer D, Van Den Berg LA, Lingsma HF, Yoo AJ, et al. A randomized trial of intraarterial treatment for acute ischemic stroke. *N Engl J Med.* (2015) 372:11–20. doi: 10.1056/NEJMoa1411587
2. Goyal M, Menon BK, Van Zwam WH, Dippel DW, Mitchell PJ, Demchuk AM, et al. Endovascular thrombectomy after large-vessel ischaemic stroke: a meta-analysis of individual patient data from five randomised trials. *Lancet.* (2016) 387:1723–31. doi: 10.1016/S0140-6736(16)00163-X
3. Saver JL, Goyal M, Van Der Lugt A, Menon BK, Majoie CB, Dippel DW, et al. Time to treatment with endovascular thrombectomy and outcomes from ischemic stroke: a meta-analysis. *JAMA.* (2016) 316:1279–88. doi: 10.1001/jama.2016.13647
4. Albers GW, Marks MP, Kemp S, Christensen S, Tsai JP, Ortega-Gutierrez S, et al. Thrombectomy for stroke at 6 to 16 hours with selection by perfusion imaging. *N Engl J Med.* (2018) 378:708–18. doi: 10.1056/NEJMoa1713973
5. Nogueira RG, Jadhav AP, Haussen DC, Bonafe A, Budzik RF, Bhuva P, et al. Thrombectomy 6 to 24 hours after stroke with a mismatch between deficit and infarct. *N Engl J Med.* (2018) 378:11–21. doi: 10.1056/NEJMoa1706442
6. Aoki J, Tateishi Y, Cummings CL, Cheng-Ching E, Ruggieri P, Hussain MS, et al. Collateral flow and brain changes on computed tomography angiography predict infarct volume on early diffusion-weighted imaging. *J Stroke Cerebrovasc Dis.* (2014) 23:2845–50. doi: 10.1016/j.jstrokecerebrovasdis.2014.07.015
7. Seyman E, Shaim H, Shenhar-Tsarfaty S, Jonash-Kimchi T, Bornstein NM, Hallevi H. The collateral circulation determines cortical infarct volume in anterior circulation ischemic stroke. *BMC Neurol.* (2016) 16:206. doi: 10.1186/s12883-016-0722-0
8. Guenego A, Mlynash M, Christensen S, Kemp S, Heit JJ, Lansberg MG, et al. Hypoperfusion ratio predicts infarct growth during transfer for thrombectomy. *Ann Neurol.* (2018) 84:616–20. doi: 10.1002/ana.25320
9. Rocha M, Desai SM, Jadhav AP, Jovin TG. Prevalence and temporal distribution of fast and slow progressors of infarct growth in large vessel occlusion stroke. *Stroke.* (2019) 50:2238–40. doi: 10.1161/STROKEAHA.118.024035
10. Olivot JM, Mlynash M, Inoue M, Marks MP, Wheeler HM, Kemp S, et al. Hypoperfusion intensity ratio predicts infarct progression and functional outcome in the DEFUSE 2 cohort. *Stroke.* (2014) 45:1018–23. doi: 10.1161/STROKEAHA.113.003857
11. Christensen S, Mlynash M, Kemp S, Yennu A, Heit JJ, Marks MP, et al. Persistent target mismatch profile >24 hours after stroke onset in DEFUSE 3. *Stroke.* (2019) 50:754–7. doi: 10.1161/STROKEAHA.118.023392
12. Guenego A, Marcellus DG, Martin BW, Christensen S, Albers GW, Lansberg MG, et al. Hypoperfusion intensity ratio is correlated with patient eligibility for thrombectomy. *Stroke.* (2019) 50:917–22. doi: 10.1161/STROKEAHA.118.024134
13. Arenillas JF, Cortijo E, Garcia-Bermejo P, Levy EI, Jahan R, Goyal M, et al. Relative cerebral blood volume is associated with collateral status and infarct growth in stroke patients in SWIFT PRIME. *J. Cereb. Blood Flow Metab.* (2017) 38:1839–47. doi: 10.1177/0271678X17740293
14. Heit JJ, Mlynash M, Kemp SM, Lansberg MG, Christensen S, Marks MP, et al. Rapid neurologic improvement predicts favorable outcome 90 days after thrombectomy in the DEFUSE 3 study. *Stroke.* (2019) 50:1172–7. doi: 10.1161/STROKEAHA.119.024928
15. De Havenon A, Mlynash M, Kim-Tenser MA, Lansberg MG, Leslie-Mazwi T, Christensen S, et al. Results from DEFUSE 3: good collaterals are associated with reduced ischemic core growth but not neurologic outcome. *Stroke.* (2019) 50:632–8. doi: 10.1161/STROKEAHA.118.023407
16. Hermier M, Nighoghossian N, Derex L, Adeleine P, Wiart M, Berthezene Y, et al. Hypointense transcerebral veins at T2*-weighted MRI: a marker of hemorrhagic transformation risk in patients treated with intravenous tissue plasminogen activator. *J Cereb Blood Flow Metab.* (2003) 23:1362–70. doi: 10.1097/01.WCB.0000091764.61714.79
17. Morita N, Harada M, Uno M, Matsubara S, Matsuda T, Nagahiro S, et al. Ischemic findings of T2*-weighted 3-tesla MRI in acute stroke patients. *Cerebrovasc Dis.* (2008) 26:367–75. doi: 10.1159/000151640
18. Von Elm E, Altman DG, Egger M, Pocock SJ, Gotzsche PC, Vandenbroucke JP, et al. The Strengthening the reporting of observational studies in epidemiology (STROBE) statement: guidelines for reporting observational studies. *Lancet.* (2007) 370:1453–7. doi: 10.1016/S0140-6736(07)61602-X
19. Lansberg MG, Straka M, Kemp S, Mlynash M, Wechsler LR, Jovin TG, et al. MRI profile and response to endovascular reperfusion after stroke (DEFUSE 2): a prospective cohort study. *Lancet Neurol.* (2012) 11:860–7. doi: 10.1016/S1474-4422(12)70203-X
20. Straka M, Albers GW, Bammer R. Real-time diffusion-perfusion mismatch analysis in acute stroke. *J Magn Reson Imaging.* (2010) 32:1024–37. doi: 10.1002/jmri.22338
21. Olivot JM, Mlynash M, Thijs VN, Kemp S, Lansberg MG, Wechsler L, et al. Optimal Tmax threshold for predicting penumbral tissue in acute stroke. *Stroke.* (2009) 40:469–75. doi: 10.1161/STROKEAHA.108.526954
22. R Core Team. *R Statistical Software*. Vienna: Foundation for Statistical Computing.
23. Landis JR, Koch GG. The measurement of observer agreement for categorical data. *Biometrics.* (1977) 33:159–74. doi: 10.2307/2529310
24. Bang OY, Saver JL, Kim SJ, Kim GM, Chung CS, Ovbiagele B, et al. Collateral flow averts hemorrhagic transformation after endovascular therapy for acute ischemic stroke. *Stroke.* (2011) 42:2235–9. doi: 10.1161/STROKEAHA.110.604603
25. Liebeskind DS, Tomsick TA, Foster LD, Yeatts SD, Carrozzella J, Demchuk AM, et al. Collaterals at angiography and outcomes in the interventional management of stroke (IMS) III trial. *Stroke.* (2014) 45:759–64. doi: 10.1161/STROKEAHA.113.004072
26. Berkhemer OA, Jansen IG, Beumer D, Fransen PS, Van Den Berg LA, Yoo AJ, et al. Collateral status on baseline computed tomographic angiography and intra-arterial treatment effect in patients with proximal anterior circulation stroke. *Stroke.* (2016) 47:768–76. doi: 10.1161/STROKEAHA.115.011788
27. Tan BY, Wan-Yee K, Paliwal P, Gopinathan A, Nadarajah M, Ting E, et al. Good intracranial collaterals trump poor ASPECTS (alberta stroke program early CT score) for intravenous thrombolysis in anterior circulation acute ischemic stroke. *Stroke.* (2016) 47:2292–8. doi: 10.1161/STROKEAHA.116.013879

28. Yu X, Yuan L, Jackson A, Sun J, Huang P, Xu X, et al. Prominence of medullary veins on susceptibility-weighted images provides prognostic information in patients with subacute stroke. *AJNR Am J Neuroradiol.* (2016) 37:423–9. doi: 10.3174/ajnr.A4541
29. Wang Y, Shi T, Chen B, Lin G, Xu Y, Geng Y. Prominent hypointense vessel sign on susceptibility-weighted imaging is associated with clinical outcome in acute ischaemic stroke. *Eur Neurol.* (2018) 79:231–9. doi: 10.1159/000488587
30. Derdeyn CP, Videen TO, Yundt KD, Fritsch SM, Carpenter DA, Grubb RL, et al. Variability of cerebral blood volume and oxygen extraction: stages of cerebral haemodynamic impairment revisited. *Brain.* (2002) 125:595–607. doi: 10.1093/brain/awf047

Conflict of Interest: The authors declare that the research was conducted in the absence of any commercial or financial relationships that could be construed as a potential conflict of interest.

frontiers in Neurology

SYSTEMATIC REVIEW
published: 06 January 2021
doi: 10.3389/fneur.2020.588479

A Systematic Review and Meta-Analysis of Animal Studies Testing Intra-Arterial Chilled Infusates After Ischemic Stroke

*Lane J. Liddle[1], Christine A. Dirks[1], Brittany A. Fedor[2], Mohammed Almekhlafi[3] and Frederick Colbourne[1,2]**

[1] Department of Psychology, University of Alberta, Edmonton, AB, Canada, [2] Neuroscience and Mental Health Institute, University of Alberta, Edmonton, AB, Canada, [3] Calgary Stroke Program, Calgary, AB, Canada

Background: As not all ischemic stroke patients benefit from currently available treatments, there is considerable need for neuroprotective co-therapies. Therapeutic hypothermia is one such co-therapy, but numerous issues have hampered its clinical use (e.g., pneumonia risk with whole-body cooling). Some problems may be avoided with brain-specific methods, such as intra-arterial selective cooling infusion (IA-SCI) into the arteries supplying the ischemic tissue.

Objective: Our research question was about the efficacy of IA-SCI in animal middle cerebral artery occlusion models. We hypothesized that IA-SCI would be beneficial, but translationally-relevant study elements may be missing (e.g., aged animals).

Methods: We completed a systematic review of the PubMed database following the PRISMA guidelines on May 21, 2020 for animal studies that administered IA-SCI in the peri-reperfusion period and assessed infarct volume, behavior (primary meta-analytic endpoints), edema, or blood-brain barrier injury (secondary endpoints). Our search terms included: "focal ischemia" and related terms, "IA-SCI" and related terms, and "animal" and related terms. Nineteen studies met inclusion criteria. We adapted a methodological quality scale from 0 to 12 for experimental design assessment (e.g., use of blinding/randomization, *a priori* sample size calculations).

Results: Studies were relatively homogenous (e.g., all studies used young, healthy animals). Some experimental design elements, such as blinding, were common whereas others, such as sample size calculations, were infrequent (median methodological quality score: 5; range: 2–7). Our analyses revealed that IA-SCI provides benefit on all endpoints (mean normalized infarct volume reduction = 23.67%; 95% CI: 19.21–28.12; mean normalized behavioral improvement = 35.56%; 95% CI: 25.91–45.20; mean standardized edema reduction = 0.95; 95% CI: 0.56–1.34). Unfortunately, blood-brain barrier assessments were uncommon and could not be analyzed. However, there was substantial statistical heterogeneity and relatively few studies. Therefore, exploration of heterogeneity *via* meta-regression using saline infusion parameters, study quality, and ischemic duration was inconclusive.

OPEN ACCESS

Edited by:
Geoffrey Alan Donnan, University of Melbourne, Australia

Reviewed by:
Yuchuan Ding, Wayne State University, United States
Marios K. Georgakis, LMU Munich University Hospital, Germany

***Correspondence:**
Frederick Colbourne
fcolbour@ualberta.ca

Specialty section:
This article was submitted to Stroke, a section of the journal Frontiers in Neurology

Received: *28 July 2020*
Accepted: *04 December 2020*
Published: *06 January 2021*

Citation:
Liddle LJ, Dirks CA, Fedor BA, Almekhlafi M and Colbourne F (2021) A Systematic Review and Meta-Analysis of Animal Studies Testing Intra-Arterial Chilled Infusates After Ischemic Stroke. Front. Neurol. 11:588479. doi: 10.3389/fneur.2020.588479

Conclusion: Despite convincing evidence of benefit in ischemic stroke models, additional studies are required to determine the scope of benefit, especially when considering additional elements (e.g., dosing characteristics). As there is interest in using this treatment alongside current ischemic stroke therapies, more relevant animal studies will be critical to inform patient studies.

Keywords: therapeutic hypothermia (TH), meta-analysis, intraarterial cooling, neuroprotection, focal ischemia, MCAO (middle cerebral artery occlusion)

INTRODUCTION

Ischemic stroke is one of the leading global causes of death and disability (1). Acute therapies, namely, tissue plasminogen activator (tPA) and mechanical thrombectomy (MT) are the only clinically-proven therapies for acute ischemic stroke (2–4). As a thrombolytic agent, tPA can reduce neurological deficits and improve functional outcomes when given to patients shortly after ictus [within ∼4.5 h; (2, 3, 5)]. Similarly, clot retrieval *via* MT devices can improve patient outcomes within 6–24 h of symptom onset, depending on patient condition (6, 7). Unfortunately, not all patients that receive these treatments become functionally independent (8). For example, in some cases, <50% of the tPA-treated patient population may have successful recanalization after ischemic stroke (2). In other cases, patients do not benefit despite successful recanalization for several reasons [e.g., older age, delayed presentation, poor collateral status; (9–11)]. Without additional treatment options or co-therapies, disability rates in such patients will remain unchanged.

Therapeutic hypothermia (TH) is a long-studied approach for treating ischemic injury (12, 13). Indeed, TH provides demonstrable benefit in cardiac arrest and hypoxic-ischemic encephalopathy (14, 15). However, clinical application of TH in ischemic stroke has proven to be difficult, with multiple clinical trials prematurely ended owing to safety and feasibility concerns (16, 17). Thus, the limitations of current cooling techniques must be addressed. Until recently, TH methods have been limited to systemic cooling by use of cooling blankets and endovascular approaches, or *via* exogenous regional cooling through cooling helmets or nasopharyngeal approaches (3, 18). Systemic cooling often takes hours to reach target temperatures and frequently results in complications [e.g., shivering, pneumonia; (3, 19, 20)]. Despite avoiding systemic complications, exogenous regional cooling may not penetrate subcortical brain regions that are commonly affected after ischemic stroke, and prolonged cooling with these methods is not yet feasible (3). Therefore, although efficacious in similar brain injuries, the use of TH in ischemic stroke will remain limited without advancements in TH methodologies.

Intra-arterial selective cooling infusion [IA-SCI; (21)] is a newer TH method that directly targets the injured parenchyma by infusing cool (i.e., <35°C) substances into the arteries supplying the infarcted region (22, 23). The infusate may be physiologically inert (e.g., saline, Ringer's solution) or active (e.g., magnesium sulfate), and may be a useful co-therapy to current endovascular approaches. Current studies commonly infuse saline into the common carotid artery or internal carotid artery following middle cerebral artery occlusion (MCAO) with a hollow microcatheter or intraluminal filament (24, 25). With the feasibility and efficacy of IA-SCI shown in multiple preclinical studies, recent pilot trials have shown that IA-SCI is feasible in focal ischemia patients (21, 26). Accordingly, IA-SCI may avoid complications observed with other TH techniques, as localizing TH effects limits systemic complications and allows for faster temperature reductions (19). In addition to the benefits of brief hypothermia [e.g., decreased cellular metabolism, blood-brain barrier improvement (22, 27)], IA-SCI studies have shown that flushing the ischemic vasculature improves cerebral blood flow, clears the vasculature of inflammatory mediators, and reduces oxidative stress (25, 28, 29). Many of these mechanisms may provide benefit as a supplemental therapy for endovascular therapies, particularly for those that do not benefit from endovascular therapies alone (21). In sum, IA-SCI is a pluripotent treatment that may be an eligible co-therapy for patients who may not benefit from current therapies.

In order to reduce the substantial disability rates associated with ischemic stroke, current preclinical research aims to generate and test neuroprotective treatments that are clinically relevant to reduce disease burden and improve patient outcomes (30, 31). Initially, exploratory studies are conducted to identify target mechanisms and establish safety and efficacy of putative neuroprotectants, and later confirmatory elements are added (32, 33). In the early stages, research is often conducted in young, healthy, male animals for cost and simplicity reasons. Later studies are expected to introduce clinically-relevant and more rigorous experimental design elements [e.g., all features of good laboratory practice, comparison of sex differences, use of aged animals, use of animals with comorbidities; (34–36)]. Translational rigor is critical to consider as some studies have shown that experiments failing to consider these elements result in biased outcome assessments [i.e., inflated effect sizes; (37, 38)]. Moreover, high-quality experimental reporting is critical to reproducibility and ethical, cost-effective use of laboratory animals (39, 40). Altogether, effective translation of putative neuroprotectants is thought to be predicated on high quality experimental design and reporting.

While the feasibility and efficacy of the IA-SCI protocol has been examined in animal studies (18), no meta-analysis exists with a focus on IA-SCI. Thus, through systematic review and meta-analysis, we quantified the efficacy of IA-SCI, analyzed the translational quality of IA-SCI studies, and highlighted future opportunities. Our efficacy assessment is based on histological

and behavioral outcomes, as recommended by the STAIR and RIGOR publications regarding translational rigor in stroke neuroprotection research (41, 42). As TH commonly reduces blood-brain barrier disruption and edema, secondary analysis centered on blood-brain barrier improvement and edema reduction, which are both key issues, especially in severe strokes. Experimental design parameters (e.g., randomization, blinding) were qualitatively assessed and combined into a methodological quality scale (MQS) for study quality assessment. Altogether, this study provides an updated and focused review on the use of IA-SCI as a supplemental therapy to current endovascular approaches for ischemic stroke and the efficacy of IA-SCI administered at the time of reperfusion.

METHODS

Search Terms and Inclusion Criteria

Although we did not pre-register this study, we upheld PRISMA standards (meeting all other aspects of the PRISMA checklist) during our systematic search of the PubMed database from Canada for all published English-language literature on May 21, 2020 using the following terms: (focal ischemia OR stroke OR ischemic stroke OR MCAO OR middle cerebral artery occlusion) AND (intra-arterial saline OR saline infusion OR IACS OR SI-AC OR ICSI OR carotid infusion OR LCI OR local cooling infusion OR LEVI OR local endovascular infusion) AND (hypothermia OR local cooling OR focal hypothermia OR focal cooling OR cooling OR therapy OR therapeutic hypothermia OR stroke therapy OR efficacy OR translation) AND (rat OR mouse OR gerbil OR rodent OR primate OR monkey OR dog OR cat OR lamb OR patient OR human) NOT [coronary (Text Word) OR myocardial (Text Word)]. All studies that were identified during the systematic review were included in the meta-analysis.

For our inclusion criteria we followed the PICOS framework using English-language only studies (43). Our population of interest was any animal study of MCAO. Our inclusion criteria for the intervention included any study using IA-SCI within 1 h before, during, or after reperfusion. Our inclusion criteria for the comparator group was the following hierarchy: sham catheter insertion but no infusion, sham procedure without catheter insertion, pure MCAO without infusion or sham procedure, carotid catheterization with homeothermic (37°C) saline infusion. We selected this hierarchy because some studies have discovered histological and/or behavioral benefit with normothermic carotid saline infusion and thus this procedure may not be an adequate "null effect" control (25, 44). Our inclusion criteria for outcomes were infarct volume and/or behavior and/or edema and/or blood-brain barrier assessment. If histology or behavior was assessed at multiple time points, only the comparison at the latest time point was extracted [long-term outcomes are recommended by the STAIR guidelines; (41)]. In terms of study design, we accepted prospective studies with concurrent control groups. Studies that did not meet the above criteria were excluded. Article screening and data extraction were completed by 2 reviewers using Covidence software, as recommended by the Cochrane Handbook for Systematic Reviews of Interventions and others (45–47). Outcome data were extracted into a shared spreadsheet by one reviewer and all data were validated by a second reviewer. In general, we collected descriptive statistics, experimental parameters, and specific treatment parameters for any study that assessed infarct volume, behavior, edema, or the blood-brain barrier (see **Supplementary Material** for all variables extracted). All ordinal behavioral rating scales were converted to represent low scores indicating less deficit by subtracting the mean value by the value of the maximum score (e.g., Garcia behavioral assessment scale). Finally, one study reported no behavioral benefit using IA-SCI, but the data were not presented and could not be obtained from the authors (no response). Therefore, we assumed a conservative effect size estimate of Cohen's $d = 0$ and an average variability estimate.

TABLE 1 | Methodological quality scale reporting elements for preclinical IA-SCI research in ischemic stroke and % adherence.

Element	% Adherence
Control of body temperature	100
Blinding to outcome(s)	89
Complete reporting of infusion parameters	89
Group randomization	63
Exclusion statement	58
Conflict of interest statement	47
Blinding to ischemia/IA-SCI	21
Use of male and female animals	5
Use of aged animals	0
Use of animals with comorbid conditions	0
Sample size calculation	0
A priori study registration	0

Study Quality Assessment

We adapted previously used study quality scales to analyze study quality and possible bias risk. The elements of our scale are informed by guidelines and publications for translationally-rigorous neuroprotection research [e.g., STAIR and RIGOR; (38, 39, 41, 48)]. For study quality assessment, we considered: study pre-registration, exclusion statement, inclusion of both sexes, aged and/or comorbid animals, *a priori* sample size calculations, randomization, blinding to outcomes and/or treatment, control of body temperature, clear description of infusion parameters (e.g., rate and/or duration, temperature), and conflict of interest statements. The characteristics of interest were ranked by most prevalent to least prevalent to give a snapshot of the current literature characteristics, and directions for future research (**Table 1**). In **Table 2**, we broke down the use of each characteristic at the level of the individual study.

Statistical Analysis

Data were analyzed using R statistical software (version 3.5.1, Vienna, Austria). Because of the varying MCAO durations and infusion parameters, we chose to use random-effects

TABLE 2 | Statistical summary comparison and total % of reported MQS elements (✓ = yes, χ = no).

References	Pre-registration	Exclusion statement	Both sexes	Old age	Sample size calculation	Randomization	Comorbidities	Outcome(s) blinding	Ischemia/ IA-SCI blinding	Control body temp.	Infusion parameters	Conflict of interest	Total score (max. 12)
Chen et al. (44)	χ	χ	χ	χ	χ	✓	χ	✓	✓	✓	χ	✓	5
Chen et al. (27)	χ	✓	χ	χ	χ	✓	χ	✓	χ	✓	✓	✓	6
Corey et al. (49)	χ	χ	✓	χ	χ	✓	χ	✓	χ	✓	✓	χ	5
Ding et al. (23)	χ	✓	χ	χ	χ	χ	χ	✓	χ	✓	✓	χ	4
Ding et al. (25)	χ	χ	χ	χ	χ	χ	χ	✓	χ	✓	✓	χ	3
Ding et al. (22)	χ	χ	χ	χ	χ	χ	χ	χ	χ	✓	✓	χ	2
Duan et al. (50)	χ	✓	χ	χ	χ	✓	χ	✓	✓	✓	✓	✓	7
Ji et al. (51)	χ	✓	χ	χ	χ	✓	χ	✓	χ	✓	✓	✓	6
Ji et al. (28)	χ	✓	χ	χ	χ	✓	χ	✓	χ	✓	✓	χ	5
Kim et al. (52)	χ	χ	χ	χ	χ	χ	χ	✓	χ	✓	✓	χ	3
Kurisu et al. (53)	χ	✓	χ	χ	χ	χ	χ	✓	χ	✓	✓	✓	5
Kurisu et al. (54)	χ	✓	χ	χ	χ	✓	χ	✓	χ	✓	✓	✓	6
Li et al. (55)	χ	✓	χ	χ	χ	χ	χ	✓	χ	✓	✓	χ	4
Song et al. (24)	χ	χ	χ	χ	χ	✓	χ	✓	χ	✓	χ	χ	3
Wang et al. (56)	χ	χ	χ	χ	χ	✓	χ	✓	χ	✓	✓	✓	5
Wei et al. (57)	χ	✓	χ	χ	χ	✓	χ	✓	✓	✓	✓	✓	7
Wu et al. (58)	χ	χ	χ	χ	χ	✓	χ	χ	χ	✓	✓	χ	3
Wu et al. (59)	χ	✓	χ	χ	χ	✓	χ	✓	✓	✓	✓	✓	7
Zhao et al. (60)	χ	✓	χ	χ	χ	χ	χ	✓	χ	✓	✓	χ	4
Total (%)	0	58	5	0	0	63	0	89	21	100	89	47	

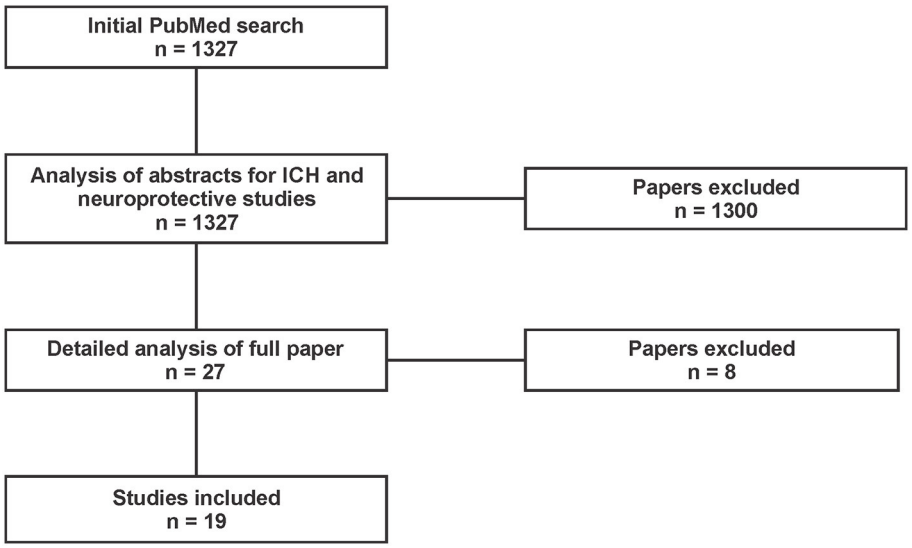

FIGURE 1 | PRISMA diagram of studies returned by our PubMed search conducted on May 21, 2020. Inclusion criteria limited studies to those in animal models of intracarotid cooling after ischemic stroke that assessed infarct volume and/or behavior and/or edema (English only). Our search included the following terms: (focal ischemia OR stroke OR ischemic stroke OR MCAO OR middle cerebral artery occlusion) AND (intra-arterial saline OR saline infusion OR IACS OR SI-AC OR ICSI OR carotid infusion OR LCI OR local cooling infusion OR LEVI OR local endovascular infusion) AND (hypothermia OR local cooling OR focal hypothermia OR focal cooling OR cooling OR therapy OR therapeutic hypothermia OR stroke therapy OR efficacy OR translation) AND (rat OR mouse OR gerbil OR rodent OR primate OR monkey OR dog OR cat OR lamb OR patient OR human) NOT [coronary (Text Word) OR myocardial (Text Word)].

meta-analysis models for all endpoints with the Dersimonian-Laird estimator. In cases when one control group serviced multiple treatment groups, the sample size of the control group was divided by the number of treatment groups serviced [described in (61)]. Whenever possible, we normalized our data to sham or baseline values [recommended and used in (61, 62)]. The normalization procedure yielded normalized mean difference effect sizes that were expressed as a percentage of sham or baseline performance, and our data were converted in this way only if sham or baseline data were available or could be reasonably assumed (61). In our analysis, we considered the latest infarct volume measurement for each study. We statistically combined the effect sizes from the latest assessment of each behavioral test within each study by weighing the outcome from each behavioral task using the inverse variance weighting method (61). There was little variability in the timing of edema measurement across studies. However, varied edema measurement methodologies (i.e., tissue wet-dry weight or histological measurement) meant that we had to use standardized mean differences as our effect size measure rather than normalized effect sizes. Hedge's G [advantageous in the context of relatively small sample sizes; (61)] was used when standardized mean differences were used. Meta-regression was used to investigate heterogeneity, and MCAO duration, saline infusion parameters (temperature, rate, volume), and methodological quality were parameters in the meta-regression model. Planned sensitivity analyses were conducted if unexpected or extreme results were obtained in the forest plots.

RESULTS

Search Results

Of the 1,327 studies returned for title and abstract screening, 1,300 were omitted for irrelevance. Following full-text screening of the remaining 27 studies, we excluded 3 for incorrect study design, 2 for incorrect comparator, 2 for incorrect outcomes, and 1 for non-English language. This left 19 studies for data analysis and extraction (**Figure 1**).

Study Characteristics

A modified PE-50 microcatheter occlusion model of MCAO (25) was the most commonly used ischemia model (58% of studies), with the classic Longa (63) suture occlusion model being used in fewer studies (37%). One study (5%) permanently occluded the MCA *via* craniotomy. Sixty-three percent of studies reported randomization, 58% exclusions, 47% conflict of interest statement, 26% complete blinding (i.e., during IA-SCI infusion and outcome assessment), and 11% stated the mortality rate (**Tables 1**, **2**). No studies were pre-registered, used rats with comorbidities, or conducted *a priori* group size calculations. Studies infused a median of 6 mL of saline (range 2.5–10 mL; **Figure 2A**). The most common anesthetic used was halothane (42%) (**Figure 2B**). All studies used young, male Sprague-Dawley rats, except for one study which included females, but did not consider biological sex as a variable or detail the distribution of females per group (**Figure 2C**). All studies regulated body temperature during surgery. Eighty-four percent of studies measured the impact of IA-SCI on brain temperature. One study

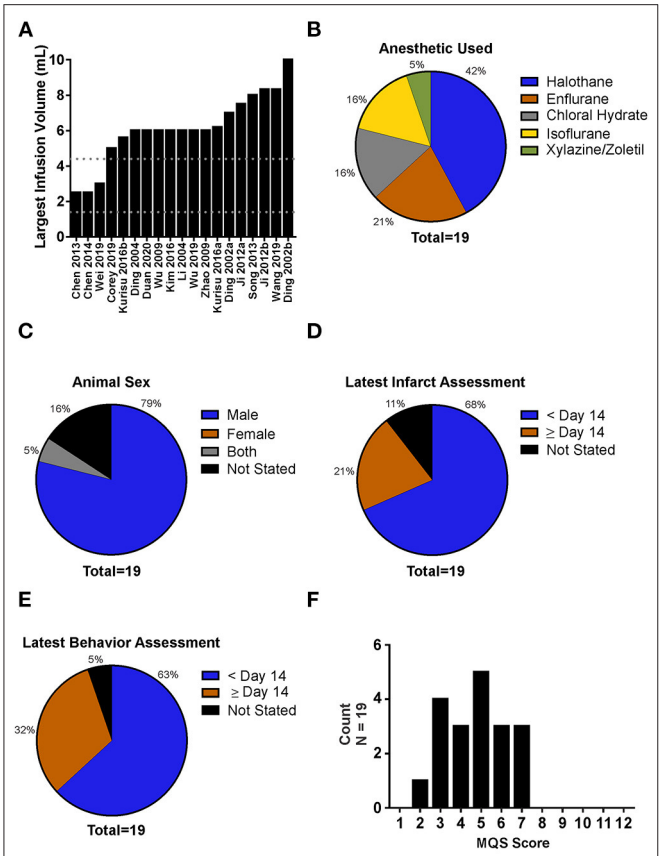

FIGURE 2 | Analysis of experimental characteristics used in intra-arterial selective cooling infusion (IA-SCI) literature. **(A)** Distribution of saline infusion volumes used in IA-SCI studies. Upper and lower dotted lines represent our calculated limits for saline infusion volumes. Calculations are based on 1 L of saline being infused into a patient and scaled to brain mass (1.4 mL; lower line) and body mass (4.4 mL; upper line). **(B)** Breakdown of anesthetics used in IA-SCI neuroprotection studies. **(C)** Animal sexes used in IA-SCI neuroprotection literature. No studies used exclusively female animals. **(D)** Analysis of infarct assessment timing. A majority of studies investigated infarct volume between 0 and 14 days post-MCAO (median = 2 days post-MCAO). **(E)** Analysis of behavioral assessment timing. Similar to infarct volume assessment, a majority of studies assessed behavior between 0 and 14 days post-MCAO (median = 2 days post-MCAO). **(F)** Evaluation of methodological quality score for IA-SCI studies (max score = 12). MQS, Methodological Quality Score.

used multiple ischemia lengths. All studies used saline in the IA-SCI infusion.

Tissue and Behavioral Endpoints

Out of the 19 studies analyzed, 17 assessed infarct volume, 17 assessed behavioral outcomes, and 9 assessed edema. The latest date of infarct volume and behavioral assessment was 28 days (median = 2; **Figures 2D,E**). Only 4 studies analyzed blood-brain-barrier integrity.

Analysis of Methodological Quality

For an overview of our methodological quality scale and analysis of studies making use of the experimental elements included in our methodological quality scale, see **Tables 1**, **2**. Overall, the median methodological quality score was 5, indicating low to moderate study quality, with a range from 2 to 7 (12 points maximum; **Figure 2F**).

Characteristics of IA-SCI

The median IA-SCI temperature was 10°C and ranged from 0 to 23°C. Infusion volume characteristics are listed in Study Characteristics section. All studies administered the IA-SCI treatment immediately following MCAO (i.e., immediately after the occluding filament was removed), with the exception of one study that administered IA-SCI 1 h after bilateral carotid occlusion and distal occlusion of the MCAO with surgical clips *via* craniotomy. In studies that used the modified PE-50 microcatheter as an occlusion device, IA-SCI was administered immediately before reperfusion (i.e., monofilament withdrawn 1–2 mm following MCAO and IA-SCI occurred), whereas in studies using the Longa suture occlusion method, IA-SCI occurred post-reperfusion, following removal of the occluding filament, and advancement of the IA-SCI catheter. Also, in studies that used the modified PE-50 microcatheter, the infusion took place closer to the infarct (∼1–2 mm from MCA origin). In studies that used the Longa suture method, infusions were closer to the internal carotid artery origin (within 5 mm of the carotid bifurcation).

Impact of IA-SCI on Body Temperature

All 19 studies measured body temperature intraoperatively, and maintained body temperature between 36.5 and 37.5°C. Despite this, only 10 studies remarked on, tabulated, or graphically depicted the change in body temperature during and after the IA-SCI infusion. Studies reported an average nadir body temperature reduction of 0.28°C from baseline, within 5 min of IA-SCI. Thus, the average minimum body temperature achieved by IA-SCI was ∼36.72°C during the infusion, with most studies indicating small, non-significant body temperature changes from baseline (range: 36.09–37.5°C). Body temperature quickly returned to baseline values after IA-SCI within 10 min, however one study reported reduced body temperature for up to 50 min.

Impact of IA-SCI on Brain Temperature

Sixteen out of 19 studies measured brain temperature. Fourteen out of 16 studies measured brain temperature using implantable needle thermistor probes, and 2 studies did not specify their brain temperature measurement method. None performed or mentioned contralateral brain temperature measurement, an important internal control. Thirteen out of the 16 studies measured ipsilesional brain temperature in more than 1 region of interest (i.e., striatum and cortex). Studies reported an average nadir brain temperature reduction of 4°C from baseline, within 3–5 min of IA-SCI start. Thus, the average minimum brain temperature achieved by IA-SCI was ∼33°C during the infusion (range: 30.5–34.8°C). Brain temperature decreases were

TABLE 3 | Descriptive characteristics of studies that assessed infarct volume.

References	Latest assessment (*d*)	Control (*n*)	IA-SCI (*n*)	Normalized effect size	95% confidence interval
Duan et al. (50)	1	14	14	−14.2	−14.36, −14.04
Kurisu et al. (53)	1	12	12	−38.8	−48.04, −29.56
Wei et al. (57)	1	8	10	−13.9	−22.94, −4.86
Chen et al. (44)	2	8	12	−19.9	−44.51, 4.71
Chen et al. (27)	2	10	10	−26.1	−45.9, −6.3
Ding et al. (25)	2	10	10	−35	−40.54, −29.46
Ding et al. (22)	2	13	12	−33.9	−41.7, −26.1
Ding et al. (23)	2	8	8	−50.4	−56.71, −44.09
Ji et al. (51)	2	13	13	−16.7	−29.48, −3.92
Ji et al. (28)	2	13	13	−26.2	−36.21, −16.19
Kurisu et al. (54)	2	8	8	−19.26	−26.77, −11.75
Song et al. (24)	2	12	12	−23.32	−38.4, −8.24
Wang et al. (56)	2	24	26	−23.54	−39.93, −7.15
Wu et al. (58)	2	7.5 (shared)	15	−28	−58.11, 2.11
Wu et al. (58)	2	7.5 (shared)	15	−14	−45.85, 17.85
Zhao et al. (60)	2	7	7	−13.01	−15.48, −10.54
Zhao et al. (60)	2	7	7	−11.2	−14.98, −7.42
Zhao et al. (60)	2	7	7	−22.12	−28.89, −15.35
Zhao et al. (60)	2	7	7	−6.87	−13.16, −0.58
Wu et al. (59)	21	6	6	−48	−73.3, −22.7
Li et al. (55)	28	8	8	−26	−34.32, −17.68
Summary statistic	**Median = 2**	**$\Sigma = 210$**	**$\Sigma = 232$**	**$\bar{X}_{Weighted} = -23.67$**	**$\bar{X}_{Weighted} = -28.12, -19.21$**

similar in the cortex and striatum. At the cessation of IA-SCI, brain temperature often quickly returned to baseline values within 5–10 min, however some studies reported reduced brain temperatures for longer than 10 min, up to 50 min.

Infarct Volume Results

Seventeen studies assessed infarct volume; of these, 16 measured infarct volume as a "% infarction" using the contralesional hemisphere as control tissue. The remaining study analyzed infarct volume as an absolute value in cubic millimeters. Descriptive characteristics of each infarct volume assessment can be found in **Table 3**, with all data available in the **Supplementary Material**. The results of our analysis can be found in **Figure 3A**. In brief, our random-effects model revealed that IA-SCI significantly reduced infarct volume compared to controls [$p < 0.0001$; normalized mean reduction: 23.66 (95% CI: 19.21, 28.12)]. However, there was substantial heterogeneity among studies ($I^2 = 93\%$; $P < 0.0001$). Additionally, the funnel plot, Egger regression analysis, and trim-and fill bias analyses revealed that the current literature may be missing null or negative data, as the trim-and-fill analysis primarily filled the right side of the plot (Egger regression $p = 0.01$; **Figure 3B**). More specifically, after the trim-and-fill analysis, the normalized mean difference was 14.94%, dropping almost 10%. In an attempt to explain some heterogeneity and investigate the impact of various model parameters, we performed meta-regression using MCAO duration, saline infusion parameters, and MQS as predictors. We did not find effects of MCAO duration ($p = 0.42$), saline temperature ($p = 0.59$), saline volume ($p = 1.0$), saline rate ($p = 0.26$), nor MQS ($p = 0.88$) on infarct volume reduction.

Behavioral Results

Seventeen studies assessed behavior using a variety of behavioral tests. The most commonly used behavioral assessment methods were neurological deficit rating scales. Overall, studies used 1–5 behavioral tasks (median = 1), with a grand total of 41 tasks used across all studies. Data were analyzed and expressed as normalized mean differences if baseline/sham data were available or could be assumed. Two tests from one study did not provide baseline/sham data and were thus excluded. If studies used multiple tasks, their data were combined into a cumulative normalized behavioral score using a method described by Vesterinen et al. (61). Descriptive characteristics of the studies that conducted behavioral assessments can be found in **Table 4**, and more specific information regarding behavioral tests used (and their timing) can be found in the **Supplementary Material** document. Our random-effects model revealed that chilled saline infusion significantly improved behavioral outcomes compared to controls [$p < 0.0001$; normalized mean difference: 35.56 (95% CI: 25.91–45.20); **Figure 4A**]. However, there was substantial heterogeneity among studies ($I^2 = 60\%$, $p < 0.0001$). Trim-and-fill analysis and Egger regression revealed that some studies on the left side of the distribution may be missing from the literature, though the result from the Egger regression was only a trend toward significance (Egger regression $p = 0.06$; **Figure 4B**). However, the trim-and-fill model suggested only a small (3%) change in the normalized mean difference would occur if the

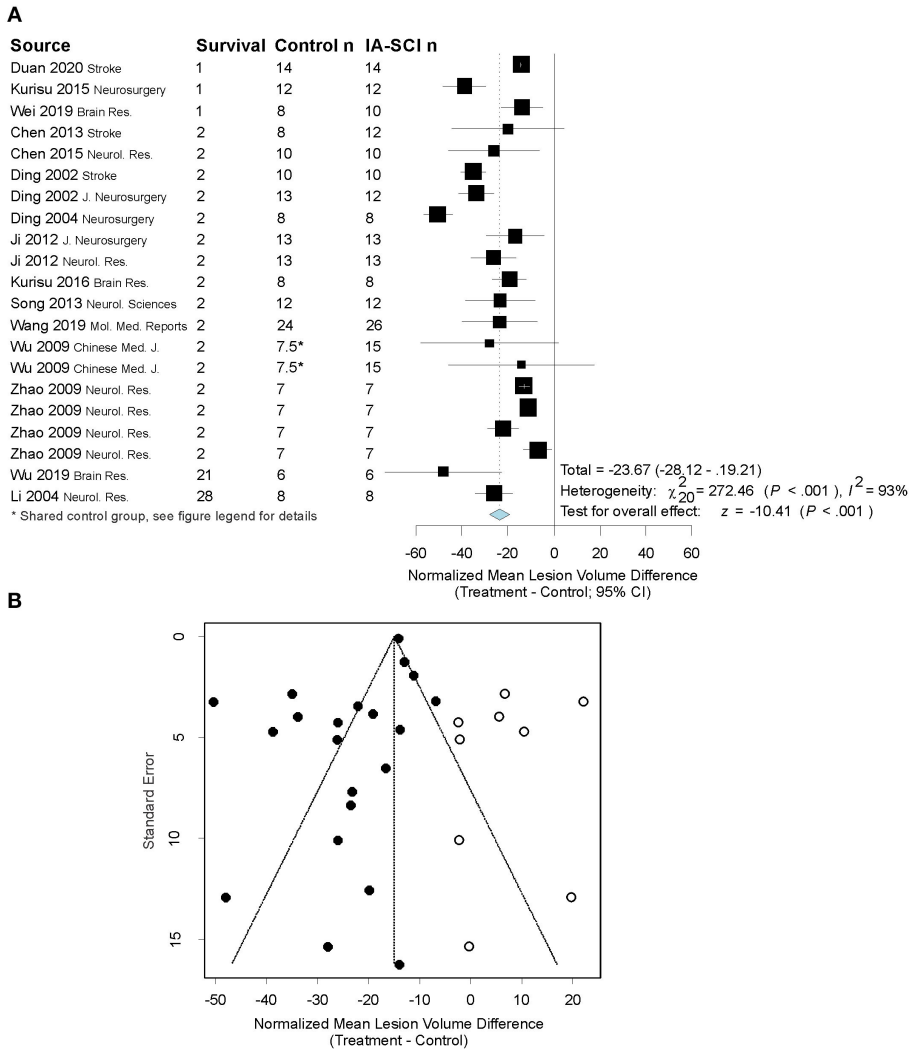

FIGURE 3 | Quantitative analysis of studies that assessed infarct volume using random-effects meta-analysis. **(A)** Forest plot of studies investigating infarct volume (normalized mean difference ± 95% CI). Effect size estimates were heterogeneous, likely owing to study design differences. *Control group in (58) serviced 2 treatment groups, and thus to avoid outcome dependence, we divided the control group in half [procedure described in (61)]. **(B)** Funnel plot with trim-and-fill analysis to assess publication bias. Closed circles represent actual studies whereas open circles represent results of the trim-and-fill analysis. These results suggest that null and negative studies may be missing from the distribution (i.e., the left side of the funnel is more filled out, favoring beneficial effects of the treatment on infarct volume). Note that the effect size in Panel B is smaller than in Panel A, as this has been corrected for in the trim-and-fill analysis.

filled studies were included. The meta-regression model did not find any predictive value of MCAO duration ($p = 0.59$), saline infusion parameters ($p \geq 0.27$), or methodological quality ($p = 0.81$) on behavioral benefit after IA-SCI.

Edema Data

Nine studies assessed edema: 5 used the tissue wet-dry weight method, and 4 used histological methods. Our observed outcome was converted to the standardized mean difference, rather than the normalized, due to the absence of sham data in some studies and discrepancies between measurement techniques (61). Descriptive characteristics of studies that assessed edema can be found in **Table 5**. Our model revealed a significant effect of chilled saline infusion on edema ($p = 0.04$). However, the meta-analytic data were relatively heterogeneous ($I^2 = 85\%$; $p < 0.0001$). Upon inspection of the data, there was one extreme outlier (miniscule variability estimate leading to extremely high standardized effect size estimate; Hedge's G = 57) that appeared to affect heterogeneity in the model and meta-regression model when sensitivity analysis was conducted. With the outlier removed, the model still revealed a significant effect of IA-SCI on edema ($p < 0.0001$), however, our random effects model no longer returned statistical heterogeneity ($I^2 = 16\%$; $p = 0.30$). Additionally, our analysis of bias did not reveal remarkable publication bias by investigating funnel plots, and using Egger regression ($p = 0.98$) or trim-and-fill methods (**Figure 5B**).

TABLE 4 | Descriptive characteristics of studies that assessed behavior.

References	Control (*n*)	IA-SCI (*n*)	Normalized effect size	95% confidence interval	# of tests combined
Chen et al. (44)	8	12	59.74	−24.04, 143.52	5
Chen et al. (27)	10	10	74.58	19.81, 129.35	1
Corey et al. (49)	3	4	11.95	0.23, 23.67	1
Ding et al. (25)	10	10	83.84	−56.66, 224.34	1
Ding et al. (22)	12	11	75.52	−20.26, 171.3	4
Ding et al. (23)	8	8	61.76	21.84, 101.68	4
Duan et al. (50)	8	8	32.89	−71.49, 137.27	4
Ji et al. (51)	13	13	4.97	−31.09, 41.03	1
Ji et al. (28)	13	13	44.33	8.51, 80.16	1
Kim et al. (52)	10	10	0	−47.47, 47.47	1
Kurisu et al. (53)	7	7	55.56	20.87, 90.24	1
Kurisu et al. (54)	8	8	35.97	25.76, 46.18	1
Li et al. (55)	8	8	60.83	36.22, 85.45	5
Song et al. (24)	8	8	28.71	−16.06, 73.47	1
Wei et al. (57)	8	10	32.04	−9.63, 73.72	4
Wu et al. (59)	6	6	20.16	7.82, 32.49	2
Zhao et al. (60)	7	7	41.4	0.28, 82.51	1
Zhao et al. (60)	7	7	51.64	29.92, 73.36	1
Zhao et al. (60)	7	7	58.22	33.54, 82.9	1
Zhao et al. (60)	7	7	15.69	5.2, 26.18	1
Summary statistic	**$\Sigma = 147$**	**$\Sigma = 153$**	**$\bar{X}_{Weighted} = 35.56$**	**$\bar{X}_{Weighted} = 25.91, 26.18$**	**$\Sigma = 41$**

Finally, our meta-regression did not reveal a significant impact of MCAO duration ($p = 0.91$), saline infusion volume (0.82), saline temperature ($p = 0.96$), nor methodological quality ($p = 0.49$) on edema reduction. Due to limited degrees of freedom, saline rate could not be considered in the model fitting.

DISCUSSION

Our meta-analysis showed that IA-SCI is beneficial when administered at the time of reperfusion in rat MCAO models. However, there are several considerations that must be made when interpreting these results. For example, the meta-analyses for our primary endpoints yielded significant and substantial heterogeneity, likely owing to a number of differing study characteristics (e.g., inter-lab variability, MCAO duration, saline infusion parameters). In contrast, aside from the MCAO and treatment parameters, experimental models appear to be relatively homogenous, as young and healthy rats are the most common model employed to study the efficacy of IA-SCI (with concurrent control groups). On average, the duration of MCAO was 2 h (range: 1 h–permanent MCAO). In all studies, the MCAO duration resulted in $\geq$ 30% hemispheric infarction in all control animals (range 30–64% hemispheric infarction), and this injury size is proportionally comparable to malignant infarction seen clinically (64). Thus, these models have face validity in that they represent severe stroke cases, including patients that benefit little from reperfusion therapy alone. Our trim-and-fill analyses revealed that our primary endpoints may be subjected to publication bias, as indicated by few null results in the published literature. During our analysis, we noticed a paucity of safety studies regarding IA-SCI, and few authors clearly justified the model choice and dosing parameters used in their study. Altogether, IA-SCI has demonstrable efficacy in animal models of MCAO, but there are limitations of the current literature that carry significant implications.

Our methodological quality analysis revealed that more studies are required to better predict the efficacy of IA-SCI treatment in clinical settings. We developed our scale in alignment with STAIR and RIGOR guidelines (41, 42), with the understanding that IA-SCI is relatively novel. Therefore, particular translational elements (i.e., age, sex) may not have been extensively explored. Accordingly, no studies investigated whether IA-SCI had similar efficacy in females compared to males, or aged compared to young animals. These results are pertinent, as multiple studies have shown that treatment efficacy may be reduced when experimentally considering age and comorbidities (34, 65). Indeed, age and certain comorbidities (e.g., hypertension) predict both stroke incidence and outcome, and thus future studies with these conditions are critical in understanding the impact of this treatment in its primary demographic. Moreover, as females are underrepresented in preclinical and clinical stroke research, future studies on this issue are critical (41, 42, 66). Finally, because neuroprotective efficacy has mostly been shown in the current literature using short-term (median = 48 h) assessments, future

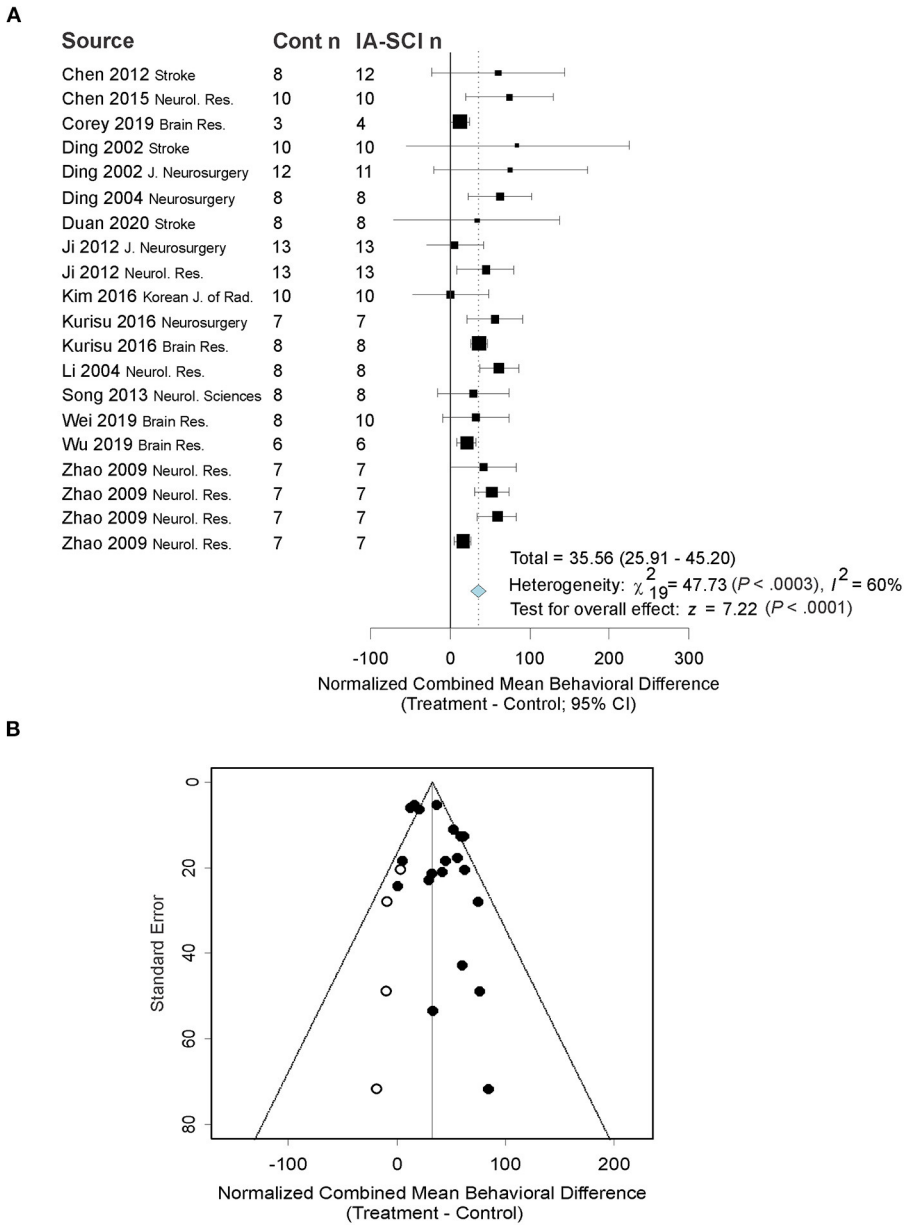

FIGURE 4 | Quantitative analysis of studies that assessed behavioral outcomes using random-effects meta-analysis. **(A)** Forest plot of studies investigating behavioral outcomes (normalized mean difference ± 95% CI). Effect size estimates were very heterogeneous, likely owing to differences in MCAO duration, treatment parameters, and timing of assessment. Note: as behavioral results were combined across a number of tests, the test date could not be presented in the figure because behavioral tasks often had differing timing. **(B)** Funnel plot with trim-and-fill analysis to assess publication bias. Closed circles represent actual studies whereas open circles represent results of the trim-and-fill analysis. These results suggest that null and negative studies may be missing from the distribution (i.e., the right side of the funnel is more filled out, favoring beneficial effects of the treatment on behavioral outcomes). As in **Figure 3**, the effect size in Panel B is smaller than in Panel A, because of trim-and-fill correction.

studies should consider comprehensive, long-term outcome assessments in order to complete our understanding of the neuroprotective efficacy of IA-SCI [e.g., shed light on persistence of neuroprotection, residual deficits; (42, 67)]. In sum, our analysis of methodological quality revealed a few opportunities for future study that are essential to understanding the parameters under which IA-SCI is efficacious. Because multiple studies have shown that treatment efficacy decreases in translationally-rigorous research, one might predict that IA-SCI may be less effective than the current literature suggests (34, 37, 65).

Importantly, few studies stated the assumptions used in determining their "dose" of infused saline. In our previous study, we assumed that humans could tolerate no more than

TABLE 5 | Descriptive characteristics of studies that assessed edema.

References	Latest assessment (d)	Control (*n*)	IA-SCI (*n*)	Standardized effect size (Hedge's G)	95% confidence interval	Edema method
Chen et al. (27)	2	10	10	−0.79	−1.71, 0.13	Histology
Kurisu et al. (54)	2	8	8	−1.62	−2.79, −0.45	Histology
Kurisu et al. (53)	1	7	7	−1.64	−2.9, −0.37	Histology
Wang et al. (56)	2	24	26	−1.12	−1.72, −0.52	Histology
Wu et al.(58)	2	4 (shared)	8	0.03	−1.17, 1.23	Tissue wet-dry weight
Wu et al. (58)	2	4 (shared)	8	−0.11	−1.31, 1.09	Tissue wet-dry weight
Ji et al. (28)	2	5	5	−1.74	−3.32, −0.16	Tissue wet-dry weight
Ji et al. (28)	2	5	5	−1.48	−2.98, 0.01	Tissue wet-dry weight
Song et al. (24)	2	6	6	−0.42	−1.57, 0.73	Tissue wet-dry weight
Duan et al. (50)*	2	14	14	−57.12	−73.28, −40.97	Histology
Summary statistic	**Median = 2**	**$\Sigma = 232$**	**$\Sigma = 210$**	**$\bar{X}_{Weighted} = -23.67$**	**$\bar{X}_{Weighted} = -28.12, -19.21$**	

Study marked (*) was excluded because it is an extreme outlier with influential statistical leverage.

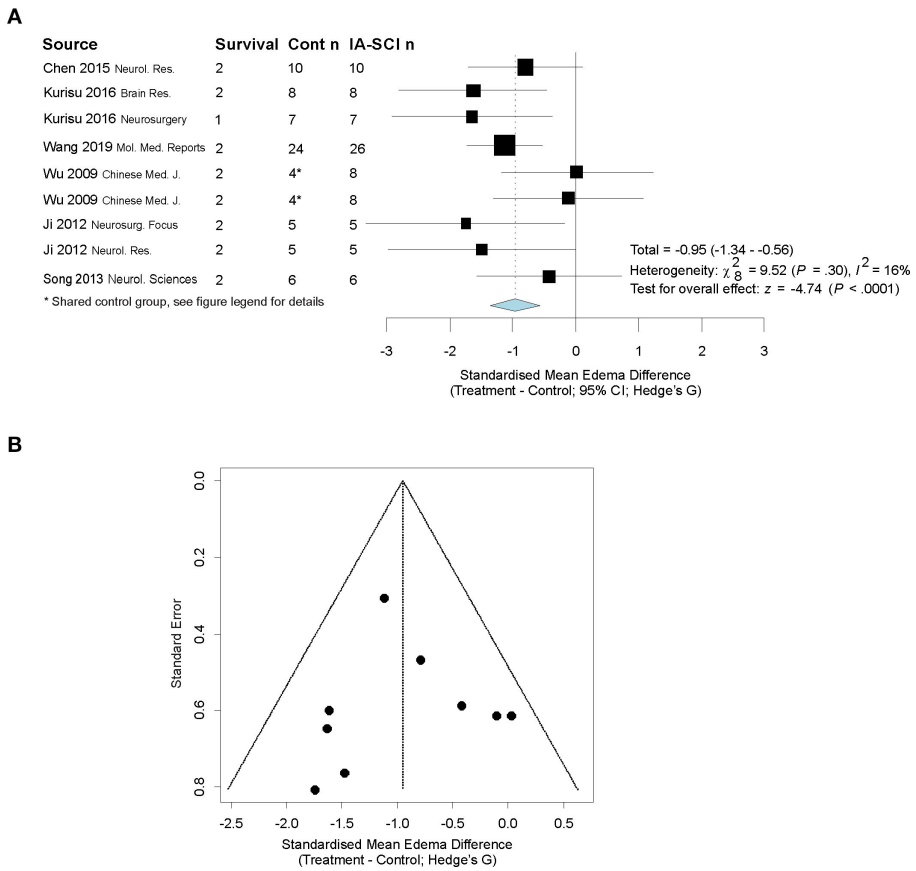

FIGURE 5 | Quantitative analysis of studies that assessed edema using random-effects meta analysis. Random-effects meta-analysis was conducted because of the variability in MCAO durations and treatment infusion parameters. **(A)** Forest plot of studies investigating behavioral outcomes (Hedge's G standardized mean difference ± 95% CI). One study was not included in the final analysis owing to the exceptionally large effect size observed therein, which caused a high amount of heterogeneity in the meta-analytic model and statistical leverage in the meta-regression model. With the exceptional study removed, study heterogeneity was reduced substantially and the meta-regression model no longer showed signs of statistical leverage. *Control group in (58) serviced 2 treatment groups, and thus to avoid outcome dependence, we divided the control group in half [procedure described in (61)]. Cont *n* = control group sample size; IA-SCI *n* = IA-SCI group sample size. **(B)** Funnel plot with trim-and-fill analysis. There did not appear to be publication bias for studies using this endpoint in our analysis.

1 L of saline, infused at a rate of ∼30 mL/min (68). Our initial calculations revealed an approximate range of saline infusion volumes that may be clinically applicable: 1.4 mL (scaled to brain weight), 4 mL (scaled to blood volume) and 4.4 mL (scaled to body mass). The results of our calculations were similar to those obtained by Ding et al. (23), however their group suggested that perhaps less saline (500–750 mL) could be given to patients at a faster rate (50–70 mL/min) (23). Our calculated infusion volumes are almost 3-fold greater than what has been used clinically with this method [e.g., in (21, 69) where ∼350 mL of saline was infused]. Scaling to what has been done clinically so far, we calculate an IA-SCI volume of between 0.5 mL (scaled to brain weight) and 1.4 mL (scaled to body mass), which is notably lower than all of the animal studies reviewed here. In this meta-analysis, the average infusion volume across studies was 6 mL. Accordingly, animal studies may be overestimating benefit. Other parameters of the infusion procedure are critical to consider while modeling this treatment approach. For example, 17 of the studies (∼89%) infused saline that was 20°C or cooler (median: 10°C; range: 0–23°C). IA-SCI in animal models involves direct catheterization of the external carotid artery (near the carotid bifurcation), whereas in patients, endovascular therapies are performed *via* femoral catheterization and the catheter is advanced to the injured brain region. Thus, in patient studies, the saline within the catheter is warmed by surrounding blood [minimized as catheter insulation is improved, e.g., (70)]. Indeed, a phantom model constructed by Choi et al. (69) showed that saline infused by a femoral catheter, running to the "internal carotid artery," warmed to ∼25°C at the catheter tip. Such warming is less likely to occur in animal studies of IA-SCI (69, 71). These results are important for investigators to consider given the current methodology of ischemic stroke treatment and limitations with current medical equipment and experimental modeling.

Interestingly, our meta-regression models were relatively ineffective at identifying factors that are known to contribute to the efficacy of TH (e.g., hypothermic depth and duration driven by saline temperature, volume, and rate). Of note, we expected our meta-regression model to identify MCAO duration as a contributor to treatment efficacy, as preclinical and clinical studies have repeatedly identified this to be an important modifier of efficacy (72–74). In line with our expectations, only one study in our data set investigated treatment efficacy in the context of multiple MCAO durations, and found waning treatment efficacy as MCAO durations increased, with no effect of this treatment following a 2.5 and 3 h MCAO duration (60). We expect that our meta-regression models were not successful (i.e., are inconsistent with current literature) for a few reasons. First, meta-regression models do not have sufficient statistical power if the number of studies are relatively low (75). Indeed, the number of studies that assessed edema were so low that we could not analyze the full meta-regression model, due to limited degrees of freedom. Second, meta-regression power is undermined when between study variance is large (i.e., τ^2-values are high). In our study, between-study variation was common, as the model for our primary endpoints returned significant heterogeneity statistics. Third, our analysis may also suggest that the actual cooling effect of IA-SCI is less important than other mechanisms or a ceiling effect has been reached. However, at this time, there is not enough data to discern the key treatment parameters from the existing literature.

Pre-clinical research is well-suited for studying adverse events associated with disease, and thorough investigation of these events provide critical clinical information. During our analysis, we noticed that 58% of studies mentioned exclusions for a variety of reasons. Of particular interest were exclusions related to adverse bleeding events. Theoretically, TH may induce coagulopathy, highlighting the need for future studies to emphasize this complication (76, 77). Often, bleeding events were attributed to vascular perforation by the occluding device used in the MCAO model. To our knowledge, no studies have included bleeding complications related to chilled saline treatment as a primary endpoint in models of MCAO. Our previous study in ICH investigated the safety and efficacy of IA-SCI in the collagenase model of ICH, where bleeding evolves over hours (68). We found that IA-SCI did not appear to worsen bleeding when administered shortly (∼30–60 min) after collagenase infusion, and did not improve long-term (day 28 post-ICH) behavioral or histological outcomes. However, our treatment was relatively mild compared to some studies included in this meta-analysis, because it was scaled to an infusion volume that would be clinically tolerable in patients [3 mL of room temperature (22°C) saline infused over 20 min in rat; (68)]. Although collagenase-induced hemorrhage shares some pathophysiological overlap with hemorrhagic transformation in ischemic stroke (e.g., blood-brain barrier breakdown *via* matrix metalloproteinases), future studies in focal ischemia with clinically-relevant elements (e.g., age, hypertension, coagulopathy) will be important to more definitively establish the safety of this treatment.

The only clinically-established neuroprotective interventions for focal cerebral ischemia are endovascular therapies [i.e., tPA administration, and/or MT; (4)]. To our knowledge, only one study has administered chilled saline in tandem with endovascular therapies, and that was in a non-human primate embolic MCAO model (78). However, this study did not meet our *a priori* inclusion criteria because it only investigated the combined effects of IA-SCI + tPA vs. tPA, without a sham IA-SCI or IA-SCI only treatment group. Thus, this study would be difficult to combine with the studies included in our meta-analysis. The authors thoroughly investigated the incremental benefit of IA-SCI with respect to reperfusion status and concluded that IA-SCI appears to provide acute histological benefit in animals with complete and partial reperfusion, though to a lesser degree in animals with partial reperfusion. In animals with no reperfusion, IA-SCI was unsuccessful at providing neuroprotection, and mortality was high in both groups. Animals that received IA-SCI treatment had better behavioral outcomes following a long-term (30-day) survival (main effect), but histological benefit could not be shown at this time. Given the ethical complexity and cost in the use of non-human primates, the typical control groups used in IA-SCI literature would be difficult to justify, but would be necessary in understanding the individual mechanistic contributions of IA-SCI alone and

potential interactions with endovascular therapies. Thus, future rodent studies should consider a factorial design to investigate whether IA-SCI enhances behavioral and histological outcomes when administered alongside endovascular therapy and these studies will be foundational, as IA-SCI will likely be administered as an adjunct therapy to endovascular therapies, rather than a stand-alone treatment. Additionally, the safety and efficacy of this combinatorial treatment will be critical to establish, as tPA is known to increase hemorrhage risk, which may interact with IA-SCI (79, 80). Moreover, because tPA is a thrombolytic enzyme, hypothermia methods such as IA-SCI may hinder the effectiveness of tPA through kinetic inhibition (81). Very few humans have received IA-SCI so our understanding of its safety profile is relatively poor (26, 69). Although these early studies showed that IA-SCI appears to be safe and feasible, future preclinical safety and efficacy studies may shed light on possible contraindications and eligibility with this treatment.

Limitations and Future Directions

One major question that remains following this meta-analysis is whether the depth and duration of TH offered by IA-SCI is sufficient to promote neuroprotection following severe ischemic insults (82). Indeed, MCAO duration is a well-known modifier of treatment efficacy, and often more aggressive treatments (e.g., longer and deeper TH protocols) are required to achieve persistent neuroprotection following greater intervention delays (42, 83), though this area is controversial as others have claimed that brief hypothermia is similarly effective, highlighting the need for rigorous dose-response studies for optimal TH protocols (84). IA-SCI offers a relatively short TH duration (<1 h) that is limited by saline volumes that are physiologically tolerable. Currently, it is unknown whether supplemental TH methods may provide incremental benefit beyond that observed with IA-SCI, especially following severe insults [e.g., those in (60)]. Future studies may feature an IA-SCI protocol to rapidly induce cooling, and further prolong cooling by TH methods that last for hours or days [e.g., nasopharyngeal methods; (19)].

Our endpoint selection criteria was limited to three endpoints, two of which are recommended by published guidelines [i.e., the STAIR and RIGOR guidelines; (41, 42)]. Although we initially planned to investigate long-term behavioral and histological outcomes, we found a heavy reliance on short-term histological and behavioral analysis (i.e., median latest assessment time = 48 h). Future studies must consider chronic [minimum 1 month; (42)] behavioral and histological analysis, as long-term outcomes are critical for understanding the persistence of neuroprotection, possible residual deficits, and potential complications.

Our *a priori* study inclusion criteria were relatively strict, with the conditions that studies used concurrent control groups in their statistical comparisons, and that IA-SCI was compared to a sham IA-SCI control group. This resulted in the exclusion of a few noteworthy studies. First, as mentioned above, Wu et al. (78) conducted a study in non-human primates where tPA-treated animals were compared to tPA + IA-SCI animals, but because this design is relatively unique in the IA-SCI literature, without a sham IA-SCI infusion group and pure IA-SCI treatment group, the results are difficult to compare to existing studies. Caroff et al. (70) performed IA-SCI in canines, but due to a small sample size in their control group, historical controls were used to boost the sample size, ultimately leading to the conclusion that IA-SCI appears to provide benefit in treated animals compared to controls. This study represents one of the few IA-SCI studies that we are aware of that have been conducted in non-rodent species. Altogether however, due to the general paucity of non-rodent animal species used in IA-SCI studies, combining these studies *via* meta-analysis with their relatively unique methodologies [e.g., embolic stroke in (78), and novel insulated catheter in (70)] would likely add to the already great statistical heterogeneity we observed in our meta-analysis. Nonetheless, those studies certainly add to the growing weight of evidence supporting the use of IA-SCI in focal ischemia.

Our qualitative analysis suggested that study designs used to investigate the efficacy of chilled saline treatment are relatively homogenous. For example, only one study used female animals, but did not consider sex as a biological variable (49). No studies considered age or comorbidities in their analysis of IA-SCI efficacy on ischemic stroke outcomes. Recent studies have shown that effect sizes are severely reduced (and risk of complications are increased) when age and comorbid conditions are considered, emphasizing a key area for future investigations (34, 37).

Our study focused specifically on the use of chilled saline administered into the carotid artery at the time of reperfusion. Therefore, we did not consider intra-arterially delivered treatments such as magnesium sulfate, stem cells, or other therapies. However, these have been recently reviewed by Link et al. (85).

Meta-analysis is an ever-changing method, evolving as new studies are published. As such, our data should not be taken as definitive evidence to support or refute the use of IA-SCI in the context of cerebral ischemia. Of note, our analysis of publication bias (i.e., Egger regression and trim-and-fill methods) suggested that our meta-analysis lacked null data that may have been found in so-called "gray literature." However, our inclusion criteria were limited to peer-reviewed publications and thus null results available in alternative formats were not actively sought out. The limited number of null results in the context of relatively small sample sizes does suggest a positive publication bias, and several authors stress the importance of publishing results that are null (and negative) in order to inform the evidence-base surrounding a treatment (86).

SUMMARY

Translational pre-clinical research is conducted with the goal of developing and testing therapies for patient use (40). Because current therapies for focal ischemia do not improve outcomes for all that receive them, we sought to quantify whether a potential co-therapy, IA-SCI, could reduce brain damage and functional disability in animal models of MCAO. Our results suggest that IA-SCI is effective at reducing brain damage and improving behavioral outcomes when administered at the time of reperfusion in MCAO. Currently, studies have been performed in homogenous models, providing an

excellent foundation for future study. Thus, future studies should consider integrating heterogeneous experimental design elements and longer survival times to establish the scope and magnitude of benefits observed with IA-SCI to inform its use in clinic.

DATA AVAILABILITY STATEMENT

The original contributions generated in the study are included in the article/**Supplementary Materials**, further inquiries can be directed to the corresponding author.

AUTHOR CONTRIBUTIONS

LL and FC were involved in study conceptualization and project administration. LL and CD were involved in data curation and analysis. LL, CD, and FC wrote the original draft. LL, FC, CD, BF, and MA were involved in expert review and editing. All authors contributed to the article and approved the submitted version.

FUNDING

FC was supported by the Canadian Institutes of Health Research Grant (166087) and holds a Canada Research Chair in Intracerebral Hemorrhagic Stroke. LL was supported by the Canadian Graduate Studies—Master's Award from the Canadian Institutes of Health Research. CD was supported by the Alberta Innovates Health Solutions Summer Studentship.

SUPPLEMENTARY MATERIAL

The Supplementary Material for this article can be found online at: https://www.frontiersin.org/articles/10.3389/fneur.2020.588479/full#supplementary-material

REFERENCES

1. Alharbi AS, Alhayan MS, Alnami SK, Traad RS, Aldawsari MA, Alharbi SA, et al. Epidemiology and risk factors of stroke. *Arch Pharm Pract*. (2019) 10:60–6.
2. Tomkins AJ, Hood RJ, Levi CR, Spratt NJ. Tissue plasminogen activator for preclinical stroke research: neither "rat" nor "human" dose mimics clinical recanalization in a carotid occlusion model. *Sci Rep*. (2015) 5:16026. doi: 10.1038/srep16026
3. Wang F, Luo Y, Ling F, Wu H, Chen J, Yan F, et al. Comparison of neuroprotective effects in ischemic rats with different hypothermia procedures. *Neurol Res*. (2010) 32:378–83. doi: 10.1179/016164110X12670144526183
4. Powers WJ, Rabinstein AA, Ackerson T, Adeoye OM, Bambakidis NC, Becker K, et al. Guidelines for the early management of patients with acute ischemic stroke: 2019 update to the 2018 guidelines for the early management of acute ischemic stroke: a guideline for healthcare professionals from the American Heart Association/American Stroke. *Stroke*. (2019) 50:e344–18. doi: 10.1161/STR.0000000000000211
5. Eissa A, Krass I, Levi C, Sturm J, Ibrahim R, Bajorek B. Understanding the reasons behind the low utilisation of thrombolysis in stroke. *Australas Med J*. (2013) 6:152. doi: 10.4066/AMJ.2013.1607
6. Vidale S, Longoni M, Valvassori L, Agostoni E. Mechanical thrombectomy in strokes with large-vessel occlusion beyond 6 hours: a pooled analysis of randomized trials. *J Clin Neurol*. (2018) 14:407–12. doi: 10.3988/jcn.2018.14.3.407
7. Lambrinos A, Schaink AK, Dhalla I, Krings T, Casaubon LK, Sikich N, et al. Mechanical thrombectomy in acute ischemic stroke: a systematic review. *Can J Neurol Sci*. (2016) 43:455–60. doi: 10.1017/cjn.2016.30
8. McDermott M, Skolarus LE, Burke JF. A systematic review and meta-analysis of interventions to increase stroke thrombolysis. *BMC Neurol*. (2019) 19:86. doi: 10.1186/s12883-019-1298-2
9. Goyal M, Menon BK, Van Zwam WH, Dippel DW, Mitchell PJ, Demchuk AM, et al. Endovascular thrombectomy after large-vessel ischaemic stroke: a meta-analysis of individual patient data from five randomised trials. *Lancet*. (2016) 387:1723–31. doi: 10.1016/S0140-6736(16)00163-X
10. Leng X, Fang H, Leung TWH, Mao C, Miao Z, Liu L, et al. Impact of collaterals on the efficacy and safety of endovascular treatment in acute ischaemic stroke: a systematic review and meta-analysis. *J Neurol Neurosurg Psychiatry*. (2016) 87:537–44. doi: 10.1136/jnnp-2015-310965
11. Saver JL, Goyal M, Van der Lugt AAD, Menon BK, Majoie CBLM, Dippel DW, et al. Time to treatment with endovascular thrombectomy and outcomes from ischemic stroke: a meta-analysis. *JAMA*. (2016) 316:1279–89. doi: 10.1001/jama.2016.13647
12. Yenari MA, Han HS. Neuroprotective mechanisms of hypothermia in brain ischaemia. *Nat Rev Neurosci*. (2012) 13:267–78. doi: 10.1038/nrn3174
13. Dumitrascu OM, Lamb J, Lyden PD. Still cooling after all these years: meta-analysis of pre-clinical trials of therapeutic hypothermia for acute ischemic stroke. *J Cereb Blood Flow Metab*. (2016) 36:1157–64. doi: 10.1177/0271678X16645112
14. Group H after CAS. Mild therapeutic hypothermia to improve the neurologic outcome after cardiac arrest. *N Engl J Med*. (2002) 346:549–56. doi: 10.1056/NEJMoa012689
15. Davidson JO, Wassink G, van den Heuij LG, Bennet L, Gunn AJ. Therapeutic hypothermia for neonatal hypoxic-ischemic encephalopathy-where to from here? *Front Neurol*. (2015) 6:198. doi: 10.3389/fneur.2015.00198
16. Geurts M, Petersson J, Brizzi M, Olsson-Hau S, Luijckx G-J, Algra A, et al. COOLIST (Cooling for Ischemic Stroke Trial) a multicenter, open, randomized, phase II, clinical trial. *Stroke*. (2017) 48:219–21. doi: 10.1161/STROKEAHA.116.014757
17. van der Worp HB, Macleod MR, Bath PMW, Bathula R, Christensen H, Colam B, et al. Therapeutic hypothermia for acute ischaemic stroke. Results of a European multicentre, randomised, phase III clinical trial. *Eur Stroke J*. (2019) 4:254–62. doi: 10.1177/2396987319844690
18. Wu L, Wu D, Yang T, Xu J, Chen J, Wang L, et al. Hypothermic neuroprotection against acute ischemic stroke: the 2019 update. *J Cereb Blood Flow Metab*. (2020) 40:461–81. doi: 10.1177/0271678X19894869
19. Almekhlafi MA, Colbourne F, Al Sultan AS, Goyal M, Demchuk AM. Selective brain cooling: let us have a moment of science. *J Cereb Blood Flow Metab*. (2019) 39:182–3. doi: 10.1177/0271678X18800274
20. Kuczynski AM, Marzoughi S, Al Sultan AS, Colbourne F, Menon BK, van Es A, et al. Therapeutic hypothermia in acute ischemic stroke-a systematic review and meta-analysis. *Curr Neurol Neurosci Rep*. (2020) 20:13. doi: 10.1007/s11910-020-01029-3
21. Wu C, Zhao W, An H, Wu L, Chen J, Hussain M, et al. Safety, feasibility, and potential efficacy of intraarterial selective cooling infusion for stroke patients treated with mechanical thrombectomy. *J Cereb Blood Flow Metab*. (2018) 38:2251–60. doi: 10.1177/0271678X18790139
22. Ding Y, Yao B, Zhou Y, Park H, McAllister JP, Diaz FG. Prereperfusion flushing of ischemic territory: a therapeutic study in which histological and behavioral assessments were used to measure ischemia-reperfusion injury in rats with stroke. *J Neurosurg*. (2002) 96:310–9. doi: 10.3171/jns.2002.96.2.0310
23. Ding Y, Li J, Luan X, Lai Q, McAllister JP, Phillis JW, et al. Local saline infusion into ischemic territory induces regional brain cooling and neuroprotection in rats with transient middle cerebral artery occlusion. *Neurosurgery*. (2004) 54:956–65. doi: 10.1227/01.NEU.0000114513.96704.29

24. Song W, Wu Y-M, Ji Z, Ji Y-B, Wang S-N, Pan S-Y. Intra-carotid cold magnesium sulfate infusion induces selective cerebral hypothermia and neuroprotection in rats with transient middle cerebral artery occlusion. *Neurol Sci*. (2013) 34:479–86. doi: 10.1007/s10072-012-1064-3
25. Ding Y, Li J, Rafols JA, Phillis JW, Diaz FG. Prereperfusion saline infusion into ischemic territory reduces inflammatory injury after transient middle cerebral artery occlusion in rats. *Stroke*. (2002) 33:2492–8. doi: 10.1161/01.STR.0000028237.15541.CC
26. Chen J, Liu L, Zhang H, Geng X, Jiao L, Li G, et al. Endovascular hypothermia in acute ischemic stroke: pilot study of selective intra-arterial cold saline infusion. *Stroke*. (2016) 47:1933–5. doi: 10.1161/STROKEAHA.116.012727
27. Chen J, Fredrickson V, Ding Y, Jiang L, Luo Y, Ji X. The effect of a microcatheter-based selective intra-arterial hypothermia on hemodynamic changes following transient cerebral ischemia. *Neurol Res*. (2015) 37:263–8. doi: 10.1179/1743132814Y.0000000451
28. Ji Y, Hu Y, Wu Y, Ji Z, Song W, Wang S, et al. Therapeutic time window of hypothermia is broader than cerebral artery flushing in carotid saline infusion after transient focal ischemic stroke in rats. *Neurol Res*. (2012) 34:657–63. doi: 10.1179/1743132812Y.0000000061
29. Ding Y, Young CN, Li J, Luan X, McAllister II JP, Clark JD, et al. Reduced inflammatory mediator expression by pre-reperfusion infusion into ischemic territory in rats: a real-time polymerase chain reaction analysis. *Neurosci Lett*. (2003) 353:173–6. doi: 10.1016/j.neulet.2003.09.055
30. Rajah GB, Ding Y. Experimental neuroprotection in ischemic stroke: a concise review. *Neurosurg Focus*. (2017) 42:E2. doi: 10.3171/2017.1.FOCUS16497
31. Bosetti F, Koenig JI, Ayata C, Back SA, Becker K, Broderick JP, et al. Translational stroke research: vision and opportunities. *Stroke*. (2017) 48:2632–7. doi: 10.1161/STROKEAHA.117.017112
32. Dirnagl U. Resolving the tension between exploration and confirmation in preclinical biomedical research. In: Bespalov A, Michel MC, Steckler T, editors. *Handbook of Experimental Pharmacology*. Cham: Springer (2019). p. 71–8.
33. Dirnagl U. Thomas Willis lecture: is translational stroke research broken, and if so, how can we fix it? *Stroke*. (2016) 47:2148–53. doi: 10.1161/STROKEAHA.116.013244
34. Schmidt-Pogoda A, Bonberg N, Koecke MHM, Strecker J, Wellmann J, Bruckmann N, et al. Why most acute stroke studies are positive in animals but not in patients: a systematic comparison of preclinical, early phase, and phase 3 clinical trials of neuroprotective agents. *Ann Neurol*. (2020) 87:40–51. doi: 10.1002/ana.25643
35. Miller LR, Marks C, Becker JB, Hurn PD, Chen W-J, Woodruff T, et al. Considering sex as a biological variable in preclinical research. *FASEB J*. (2016) 31:29–34. doi: 10.1096/fj.201600781r
36. Hankivsky O, Springer KW, Hunting G. Beyond sex and gender difference in funding and reporting of health research. *Res Integr Peer Rev*. (2018) 3:6. doi: 10.1186/s41073-018-0050-6
37. O'Collins VE, Macleod MR, Donnan GA, Horky LL, van der Worp BH, Howells DW. 1,026 experimental treatments in acute stroke. *Ann Neurol*. (2006) 59:467–77. doi: 10.1002/ana.20741
38. Macleod MR, Fisher M, O'collins V, Sena ES, Dirnagl U, Bath PMW, et al. Good laboratory practice: preventing introduction of bias at the bench. *Stroke*. (2009) 40:e50–2. doi: 10.1161/STROKEAHA.108.525386
39. Kilkenny C, Browne WJ, Cuthill IC, Emerson M, Altman DG. Improving bioscience research reporting: the ARRIVE guidelines for reporting animal research. *PLoS Biol*. (2010) 8:e1000412. doi: 10.1371/journal.pbio.1000412
40. Liddle LJ, Ralhan S, Ward DL, Colbourne F. Translational intracerebral hemorrhage research: has current neuroprotection research ARRIVEd at a standard for experimental design and reporting? *Transl Stroke Res*. (2020) 11:1203–13. doi: 10.1007/s12975-020-00824-x
41. Saver JL, Albers GW, Dunn B, Johnston KC, Fisher M. Stroke therapy academic industry roundtable (STAIR) recommendations for extended window acute stroke therapy trials. *Stroke*. (2009) 40:2594–600. doi: 10.1161/STROKEAHA.109.552554
42. Lapchak PA, Zhang JH, Noble-Haeusslein LJ. RIGOR guidelines: escalating STAIR and STEPS for effective translational research. *Transl Stroke Res*. (2013) 4:279–85. doi: 10.1007/s12975-012-0209-2
43. Saaiq M, Ashraf B. Modifying "Pico" question into "Picos" model for more robust and reproducible presentation of the methodology employed in a scientific study. *World J Plast Surg*. (2017) 6:390.
44. Chen J, Fredrickson V, Ding Y, Cheng H, Wang N, Ling F, et al. Enhanced neuroprotection by local intra-arterial infusion of human albumin solution and local hypothermia. *Stroke*. (2013) 44:260–2. doi: 10.1161/STROKEAHA.112.675462
45. Edwards P, Clarke M, DiGuiseppi C, Pratap S, Roberts I, Wentz R. Identification of randomized controlled trials in systematic reviews: accuracy and reliability of screening records. *Stat Med*. (2002) 21:1635–40. doi: 10.1002/sim.1190
46. Waffenschmidt S, Knelangen M, Sieben W, Bühn S, Pieper D. Single screening versus conventional double screening for study selection in systematic reviews: a methodological systematic review. *BMC Med Res Methodol*. (2019) 19:132. doi: 10.1186/s12874-019-0782-0
47. Higgins JPT, Thomas J, Chandler J, Cumpston M, Li T, Page MJ, et al. *Cochrane Handbook for Systematic Reviews of Interventions*. Hoboken, NJ: John Wiley & Sons (2019).
48. Macleod MR, Michie S, Roberts I, Dirnagl U, Chalmers I, Ioannidis JPA, et al. Biomedical research: increasing value, reducing waste. *Lancet*. (2014) 383:101–4. doi: 10.1016/S0140-6736(13)62329-6
49. Corey S, Abraham DI, Kaneko Y, Lee J-Y, Borlongan C V. Selective endovascular cooling for stroke entails brain-derived neurotrophic factor and splenic IL-10 modulation. *Brain Res*. (2019) 1722:146380. doi: 10.1016/j.brainres.2019.146380
50. Duan Y, Wu D, Huber M, Shi J, An H, Wei W, et al. New endovascular approach for hypothermia with intrajugular cooling and neuroprotective effect in ischemic stroke. *Stroke*. (2020) 51:628–36. doi: 10.1161/STROKEAHA.119.026523
51. Ji Y-B, Wu Y-M, Ji Z, Song W, Xu S-Y, Wang Y, et al. Interrupted intracarotid artery cold saline infusion as an alternative method for neuroprotection after ischemic stroke. *Neurosurg Focus*. (2012) 33:E10. doi: 10.3171/2012.5.FOCUS1215
52. Kim ES, Lee S-K, Kwon MJ, Lee PH, Ju Y-S, Yoon DY, et al. Assessment of blood-brain barrier permeability by dynamic contrast-enhanced MRI in transient middle cerebral artery occlusion model after localized brain cooling in rats. *Korean J Radiol*. (2016) 17:715–24. doi: 10.3348/kjr.2016.17.5.715
53. Kurisu K, Abumiya T, Nakamura H, Shimbo D, Shichinohe H, Nakayama N, et al. Transarterial regional brain hypothermia inhibits acute aquaporin-4 surge and sequential microvascular events in ischemia/reperfusion injury. *Neurosurgery*. (2016) 79:125–34. doi: 10.1227/NEU.0000000000001088
54. Kurisu K, Abumiya T, Ito M, Gekka M, Osanai T, Shichinohe H, et al. Transarterial regional hypothermia provides robust neuroprotection in a rat model of permanent middle cerebral artery occlusion with transient collateral hypoperfusion. *Brain Res*. (2016) 1651:95–103. doi: 10.1016/j.brainres.2016.09.017
55. Li J, Luan X, Lai Q, Clark JC, McAllister JP, Fessler R, et al. Long-term neuroprotection induced by regional brain cooling with saline infusion into ischemic territory in rats: a behavioral analysis. *Neurol Res*. (2004) 26:677–83. doi: 10.1179/016164104225015903
56. Wang D, Huang Z, Li L, Yuan Y, Xiang L, Wu X, et al. Intracarotid cold saline infusion contributes to neuroprotection in MCAO-induced ischemic stroke in rats *via* serum and glucocorticoid-regulated kinase 1. *Mol Med Rep*. (2019) 20:3942–50. doi: 10.3892/mmr.2019.10599
57. Wei W, Wu D, Duan Y, Elkin KB, Chandra A, Guan L, et al. Neuroprotection by mesenchymal stem cell (MSC) administration is enhanced by local cooling infusion (LCI) in ischemia. *Brain Res*. (2019) 1724: 146406. doi: 10.1016/j.brainres.2019.146406
58. Wu H, Jiang L, Wrede KH, Ji X, Zhao X, Tian X, et al. Local hypothermia and optimal temperature of stroke therapy in rats. *Chin Med J*. (2009) 122:1558–63.
59. Wu D, Zhi X, Duan Y, Zhang M, An H, Wei W, et al. Inflammatory cytokines are involved in dihydrocapsaicin (DHC) and regional cooling infusion (RCI)-induced neuroprotection in ischemic rat. *Brain Res*. (2019) 1710:173–80. doi: 10.1016/j.brainres.2018.12.033
60. Zhao W-H, Ji X-M, Ling F, Ding Y-C, Xing C-H, Wu H, et al. Local mild hypothermia induced by intra-arterial cold saline infusion prolongs the time

window of onset of reperfusion injury after transient focal ischemia in rats. *Neurol Res*. (2009) 31:43–51. doi: 10.1179/174313208X327982
61. Vesterinen HM, Sena ES, Egan KJ, Hirst TC, Churolov L, Currie GL, et al. Meta-analysis of data from animal studies: a practical guide. *J Neurosci Methods*. (2014) 221:92–102. doi: 10.1016/j.jneumeth.2013.09.010
62. Sena ES, Currie GL, McCann SK, Macleod MR, Howells DW. Systematic reviews and meta-analysis of preclinical studies: why perform them and how to appraise them critically. *J Cereb Blood Flow Metab*. (2014) 34:737–42. doi: 10.1038/jcbfm.2014.28
63. Longa EZ, Weinstein PR, Carlson S, Cummins R. Reversible middle cerebral artery occlusion without craniectomy in rats. *Stroke*. (1989) 20:84–91. doi: 10.1161/01.STR.20.1.84
64. Carmichael ST. Rodent models of focal stroke: size, mechanism, and purpose. *NeuroRx*. (2005) 2:396–409. doi: 10.1602/neurorx.2.3.396
65. McCann SK, Lawrence CB. Comorbidity and age in the modelling of stroke: are we still failing to consider the characteristics of stroke patients? *BMJ Open Sci*. (2020) 4:e100013. doi: 10.1136/bmjos-2019-100013
66. Liberale L, Carbone F, Montecucco F, Gebhard C, Lüscher TF, Wegener S, et al. Ischemic stroke across sexes: what is the status quo? *Front Neuroendocrinol*. (2018) 50:3–17. doi: 10.1016/j.yfrne.2018.05.001
67. Freret T, Schumann-Bard P, Boulouard M, Bouet V. On the importance of long-term functional assessment after stroke to improve translation from bench to bedside. *Exp Transl Stroke Med*. (2011) 3:6. doi: 10.1186/2040-7378-3-6
68. Liddle LJ, Prokop BJ, Dirks CA, Demchuk A, Almekhlafi M, Colbourne F. Infusion of cold saline into the carotid artery does not affect outcome after intrastriatal hemorrhage. *Ther Hypothermia Temp Manag*. (2020) 10:171–8. doi: 10.1089/ther.2020.0010
69. Choi JH, Marshall RS, Neimark MA, Konstas AA, Lin E, Chiang YT, et al. Selective brain cooling with endovascular intracarotid infusion of cold saline: a pilot feasibility study. *Am J Neuroradiol*. (2010) 31:928–34. doi: 10.3174/ajnr.A1961
70. Caroff J, King RM, Mitchell JE, Marosfoi M, Licwinko JR, Gray-Edwards HL, et al. Focal cooling of brain parenchyma in a transient large vessel occlusion model: proof-of-concept. *J Neurointerv Surg*. (2020) 12:209–13. doi: 10.1136/neurintsurg-2019-015179
71. Merrill TL, Smith BF, Mitchell JE, Merrill DR, Pukenas BA, Konstas AA. Infusion warm during selective hypothermia in acute ischemic stroke. *Brain Circ*. (2019) 5:218. doi: 10.4103/bc.bc_48_19
72. dela Peña I, Borlongan C, Shen G, Davis W. Strategies to extend thrombolytic time window for ischemic stroke treatment: an unmet clinical need. *J stroke*. (2017) 19:50. doi: 10.5853/jos.2016.01515
73. Sifat AE, Vaidya B, Abbruscato TJ. Blood-brain barrier protection as a therapeutic strategy for acute ischemic stroke. *AAPS J*. (2017) 19:957–72. doi: 10.1208/s12248-017-0091-7
74. Krieger DW, Yenari MA. Therapeutic hypothermia for acute ischemic stroke: what do laboratory studies teach us? *Stroke*. (2004) 35:1482–9. doi: 10.1161/01.STR.0000126118.44249.5c
75. Viechtbauer W, López-López JA, Sánchez-Meca J, Marín-Martínez F. A comparison of procedures to test for moderators in mixed-effects meta-regression models. *Psychol Methods*. (2015) 20:360–74. doi: 10.1037/met0000023
76. John RF, Williamson MR, Dietrich K, Colbourne F. Localized hypothermia aggravates bleeding in the collagenase model of intracerebral hemorrhage. *Ther Hypothermia Temp Manag*. (2015) 5:19–25. doi: 10.1089/ther.2014.0020
77. Polderman KH. Hypothermia and coagulation. *Crit Care*. (2012) 16:A20. doi: 10.1186/cc11278
78. Wu D, Chen J, Hussain M, Wu L, Shi J, Wu C, et al. Selective intra-arterial brain cooling improves long-term outcomes in a non-human primate model of embolic stroke: efficacy depending on reperfusion status. *J Cereb Blood Flow Metab*. (2020) 40:1415–26. doi: 10.1177/0271678X20903697
79. Lansberg MG, Thijs VN, Bammer R, Kemp S, Wijman CAC, Marks MP, et al. Risk factors of symptomatic intracerebral hemorrhage after tPA therapy for acute stroke. *Stroke*. (2007) 38:2275–8. doi: 10.1161/STROKEAHA.106.480475
80. Zhang J, Yang Y, Sun H, Xing Y. Hemorrhagic transformation after cerebral infarction: current concepts and challenges. *Ann Transl Med*. (2014) 2:81. doi: 10.3978/j.issn.2305-5839.2014.08.08
81. Shaw GJ, Dhamija A, Holland CK, Wagner KR. Temperature dependence of tPA thrombolysis in an *in-vitro* clot model. *Acad Emerg Med*. (2003) 10:438. doi: 10.1197/aemj.10.5.438-c
82. Kuczynski AM, Ospel JM, Demchuk AM, Goyal M, Mitha AP, Almekhlafi MA. Therapeutic hypothermia in patients with malignant ischemic stroke and hemicraniectomy-a systematic review and meta-analysis. *World Neurosurg*. (2020) 141:e677–85. doi: 10.1016/j.wneu.2020.05.277
83. Clark DL, Penner M, Orellana-Jordan IM, Colbourne F. Comparison of 12, 24 and 48 h of systemic hypothermia on outcome after permanent focal ischemia in rat. *Exp Neurol*. (2008) 212:386–92. doi: 10.1016/j.expneurol.2008.04.016
84. Lyden PD, Lamb J, Kothari S, Toossi S, Boitano P, Rajput PS. Differential effects of hypothermia on neurovascular unit determine protective or toxic results: toward optimized therapeutic hypothermia. *J Cereb Blood Flow Metab*. (2019) 39:1693–709. doi: 10.1177/0271678X18814614
85. Link TW, Santillan A, Patsalides A. Intra-arterial neuroprotective therapy as an adjunct to endovascular intervention in acute ischemic stroke: a review of the literature and future directions. *Interv Neuroradiol*. (2020) 26:405–15. doi: 10.1177/1591019920925677
86. Dirnagl U, Lauritzen M. Fighting publication bias: introducing the negative results section. *J Cereb Blood Flow Metab*. (2010) 30:1263–4. doi: 10.1038/jcbfm.2010.51

Conflict of Interest: The authors declare that the research was conducted in the absence of any commercial or financial relationships that could be construed as a potential conflict of interest.

frontiers in Neurology

REVIEW
published: 05 February 2021
doi: 10.3389/fneur.2021.619721

Acute Stroke Biomarkers: Are We There Yet?

Marie Dagonnier[1,2]*, *Geoffrey A. Donnan*[1,3], *Stephen M. Davis*[3], *Helen M. Dewey*[1,4] and *David W. Howells*[1,5]

[1] Stroke Division, Melbourne Brain Centre, The Florey Institute of Neuroscience and Mental Health, Melbourne, VIC, Australia, [2] Department of Neurology, Ambroise Paré Hospital, Mons, Belgium, [3] Melbourne Brain Centre at the Royal Melbourne Hospital and University of Melbourne, Melbourne, VIC, Australia, [4] Eastern Health Clinical School, Monash University, Melbourne, VIC, Australia, [5] Faculty of Health, School of Medicine, University of Tasmania, Hobart, TAS, Australia

Background: Distinguishing between stroke subtypes and knowing the time of stroke onset are critical in clinical practice. Thrombolysis and thrombectomy are very effective treatments in selected patients with acute ischemic stroke. Neuroimaging helps decide who should be treated and how they should be treated but is expensive, not always available and can have contraindications. These limitations contribute to the under use of these reperfusion therapies.

Aim: An alternative approach in acute stroke diagnosis is to identify blood biomarkers which reflect the body's response to the damage caused by the different types of stroke. Specific blood biomarkers capable of differentiating ischemic from hemorrhagic stroke and mimics, identifying large vessel occlusion and capable of predicting stroke onset time would expedite diagnosis and increase eligibility for reperfusion therapies.

Summary of Review: To date, measurements of candidate biomarkers have usually occurred beyond the time window for thrombolysis. Nevertheless, some candidate markers of brain tissue damage, particularly the highly abundant glial structural proteins like GFAP and S100β and the matrix protein MMP-9 offer promising results. Grouping of biomarkers in panels can offer additional specificity and sensitivity for ischemic stroke diagnosis. Unbiased "omics" approaches have great potential for biomarker identification because of greater gene, protein, and metabolite coverage but seem unlikely to be the detection methodology of choice because of their inherent cost.

Conclusion: To date, despite the evolution of the techniques used in their evaluation, no individual candidate or multimarker panel has proven to have adequate performance for use in an acute clinical setting where decisions about an individual patient are being made. Timing of biomarker measurement, particularly early when decision making is most important, requires urgent and systematic study.

Keywords: stroke, biomarker, review, microarray, acute

OPEN ACCESS

Edited by:
Emmanuel Pinteaux, The University of Manchester, United Kingdom

Reviewed by:
Theodoros Karapanayiotides, Aristotle University of Thessaloniki, Greece
Jialing Liu, University of California, San Francisco, United States

***Correspondence:**
Marie Dagonnier
marie.dagonnier@hotmail.com

Specialty section:
This article was submitted to Stroke, a section of the journal Frontiers in Neurology

Received: *21 October 2020*
Accepted: *14 January 2021*
Published: *05 February 2021*

Citation:
Dagonnier M, Donnan GA, Davis SM, Dewey HM and Howells DW (2021) Acute Stroke Biomarkers: Are We There Yet? Front. Neurol. 12:619721. doi: 10.3389/fneur.2021.619721

BIOMARKERS

Use of the term "biomarker" describes measures of biological function was first seen in Medline is 1977 and has exploded in the last decade (1). A US National Institutes of Health working group defined a biomarker as: "a characteristic that is objectively measured and evaluated as an indicator of normal biological processes, pathogenic processes, or pharmacologic responses to a therapeutic

intervention" (2). While the term "biomarker" can include clinical or imaging measurements, it is usually reserved for describing molecules found in bodily fluids (1).

Biomarkers such as cardiac troponin, creatine kinase, or D-dimer are used in practice in the emergency department for the diagnosis and early management of the life-threatening conditions including myocardial infarction or pulmonary embolism. Indeed, D-dimer measurements are used for the exclusion of a diagnosis of pulmonary embolism with a sensitivity of 96%. A negative D-dimer test will virtually rule out thromboembolism (3). Cardiac troponin (and especially the I isoform) is used routinely to diagnose myocardial infarction with a sensitivity of more than 90% for a cut off value of 0.04 ng/ml (4).

Other biomarkers are used as tools for disease stating (e.g., carcinoembryonic antigen-125 for cancers), for classification of disease severity (e.g., blood prostate-specific antigen concentration to indicate prostate cancer growth and metastasis), to assess disease prognosis (e.g., measurement of tumor shrinkage) or to aid therapeutic monitoring (e.g., blood cholesterol concentrations during therapy to reduce the risk of heart disease) (2).

THE NEED FOR ACUTE STROKE BIOMARKERS

Five interventions improve outcome in patients with ischemic stroke. These are thrombolysis with recombinant tissue plasminogen activator (rt-PA) (5), aspirin given within 48 h (6), management of the patients within a dedicated stroke unit (7), hemicraniectomy (8), and more recently endovascular clot retrieval (9).

Thrombolysis is currently recommended for IS patients that present within 4.5 h of stroke onset. Advanced neuroimaging allows extension of this time window up to 9 h and inclusion of patients that wake up with stroke symptoms if salvageable brain tissue can be identified (10, 11). Nevertheless, thrombolysis is disappointingly infrequent in patients with acute ischemic stroke. Indeed, <10% of ischemic stroke patients receive this therapy in most centers and no more than a third in the best performing centers (12–16). The main reasons for this underuse are uncertainty about stroke type, how long the ischemia has been present diagnosis and the associated risks of cerebral bleeding (17–21).

Thrombectomy is currently recommended in IS patients (after or independently from rt-PA) with evidence of large vessel proximal anterior circulation occlusion and within 6 (or 24 h with advanced imaging selection) of symptoms onset (9, 22–24). This revolutionary treatment is unfortunately not in more widespread use than thrombolysis as it is estimated that fewer than 10% of acute IS patients would meet the eligibility criteria and not all stroke centers have sufficient resources and expertise to deliver this therapy (25, 26).

Brain imaging currently plays a critical biomarker role in acute stroke management as it is the only proven way to differentiate ischemic from hemorrhagic stroke. Advanced perfusion imaging can also be used to help select patients that might benefit from rt-PA or thrombectomy under specific circumstances (10, 11, 23, 24). Nevertheless, imaging cost, availability, contraindications, as well as the level of expertise required to interpret advanced imaging results, restricts the global use of reperfusion therapies.

Other less expensive more and accessible stroke biomarkers detected in the blood would be an important addition to the stroke clinician's armory.

An ideal stroke biomarker(s) should be able, with high specificity and sensitivity, to differentiate hemorrhagic and ischemic stroke (and clearly distinguish them from stroke mimics). They should predict stroke prognosis, facilitate therapeutic stratification and therapeutic monitoring, for example by indicating risk of hemorrhagic transformation after stroke or after rt-PA treatment. Moreover, if repeated measures can be made in a clinically useful time frame, specific stroke biomarkers could act as a "stroke clock" to aid in assessing time of stroke onset to increase the number of IS able to benefit from treatment with rt-PA, especially those who wake-up with stroke.

With the advent of mechanical thrombectomy, brain imaging with vascular sequences has become a *de facto* standard in the management of an acute stroke. Nevertheless, a biomarker that provides the same information would facilitate and fasten the access to therapies. It would have the potential to aid early identification and pre-hospital stratification of ischemic stroke patients. Indeed, biomarker stratification of the different classes of stroke patients in a pre-hospital setting would facilitate directing them to a hospital where thrombectomy is performed without losing crucial time by performing brain imaging in the nearest hospital and then transferring the patient to the comprehensive stroke center. It is known that substantial delays of 110–128 min are associated with secondary transfer vs. the direct approach (27).

Over 150 candidate stroke biomarkers have been studied for roles ranging from diagnosis to long term prognosis (28–35).

The following literature review highlights those biomarkers with the potential to have an impact in the acute clinical setting, especially with regard to reperfusion therapy. Moreover, in this acute context, the review has been focused on studies using blood as a substrate for biomarker research because of the ease with which this biological fluid can be accessed in the emergency setting. **Table 1** summarizes the most relevant results of this review. **Table 2** highlights the main clinical uses ascribed to the potential biomarkers and **Figure 1** illustrates the sources of the major candidate biomarkers.

CANDIDATE DIAGNOSTIC BIOMARKERS

S100B

S100B, a glial protein, highly specific to nervous tissue, was one of the first molecules suggested as a candidate to aid IS diagnosis. Hill and colleagues reported a specificity of more than 95% for S100B measured on the first day of admission in 28 non-consecutive stroke patients but the measurement had poor sensitivity (71). More recently, Zhou et al. reported that measuring S100B within the first 6 h of stroke helped differentiate IS from ICH (sensitivity of 95.7%, specificity of 70.4%, using a cut-off of 67 pg/ml) (36). Unfortunately, these

TABLE 1 | Summary of the most relevant studies and results of stroke biomarkers.

Biomarker	Function tested	Timing of sampling	Sensitivity (%)	Specificity (%)	Cut off value	*n*	References
S100B	Differentiation between IS and ICH	Within 6 h of symptom onset	95.7	70.4	67 pg/ml	71 IS and 46 ICH	(36)
	Differentiation between stroke and mimics	24 h after symptom onset	94.4	31.8	0.0415 ng/ml	31 IS and 22 mimics	(37)
	Risk of hemorrhagic transformation after rt-PA	Within 6 h of symptom onset	82	46	>0.23 g/l	275 rt-PA treated IS	(38)
	Risk of malignant oedema	At 8, 12, 16, 20, and 24 h after symptom onset	75 (at 12 h) 94 (at 24 h)	80 (at 12 h) 83 (at 24 h)	>0.35 g/l (at 12 h) >1.03 g/l (at 24 h)	16 malignant, 35 non-malignant	(39)
GFAP	Differentiation between IS and ICH	Within 4.5 h of symptom onset	84.2	96.3	2.9 ng/l	163 IS, 39 ICH and 3 mimics	(40)
	Differentiation between IS and ICH	Between 2 and 6 h of symptom onset	86	76.9	0.7 ng/ml	65 IS and 43 ICH	(41)
	Differentiation between IS and ICH	Within 4.5 h of symptom onset	61	96	34 ng/ml	79 IS and 45 ICH	(42)
	Differentiation between IS and ICH	Within 6 h of symptom onset	77.8	94.2	0.03 g/l	146 I and 46 ICH	(43)
	Differentiation between IS, ICH and mimics	Within 6 h of symptom onset	91	97	0.43 ng/ml	121 IS, 34 ICH, 31 mimics, 5 SAH, and 79 controls	(44)
NSE	Favorable outcome after rt-PA	Within 4.5 h of symptom onset	77.1	59.4	13.90 ng/ml	67 rt-PA treated IS	(45)
MMP-9	Risk of hemorrhagic transformation after rt-PA	Within 3 h of symptom onset	92	74	>140 ng/ml	134 rt-PA treated IS	(46)
NR2A/2B aAbs	Differentiation between stroke and controls	Within 3 h of symptom onset	95	97	2.0 μg/l	31 IS, 56 TIAs, and 255 controls	(47)
NR2	Differentiation between stroke, mimics and controls	Within 72 h of symptom onset	92	96	1.0 μg/l	101 IS, 91 non-stroke and 52 controls	(48)
Apo C-III	Differentiation between IS and ICH	Within 6 h of symptom onset	94	87	36	16 IS and 15 ICH	(49)
Apo C-I	Differentiation between IS and ICH	Within 6 h of symptom onset	94	73	60	16 IS and 15 ICH	(49)
Apo B	Differentiation between stroke and controls	After a period of overnight fasting for 12 h	96	94	144 mg/dl	50 strokes and 50 controls	(50)
Apo A-I	Differentiation between stroke and controls	After a period of overnight fasting for 12 h	88	86	114 mg/dl	50 strokes and 50 controls	(50)
Apo B/Apo A-I	Differentiation between stroke and controls	After a period of overnight fasting for 12 h	98	96	1.2	50 strokes and 50 controls	(50)
PARK 7	Differentiation between stroke and controls	On admission (median of 17 h after symptom onset)	AUC = 0.897; OR = 1.087		–	72 strokes and 78 controls	(51)
NDKA	Differentiation between stroke and controls	On admission (median of 17 h after symptom onset)	AUC = 0.462; OR = 0.882		–	72 strokes and 78 controls	(51)
Glycogen phosphorylase isoenzyme BB	Differentiation between stroke and controls	Within 12 h of symptom onset	93	93	7.0 ng/ml	172 IS and 133 controls	(52)
c-Fn	Risk of hemorrhagic transformation after rt-PA	Within 3 h of symptom onset	100	60	3.6 μg/ml	27 rt-PA treated IS	(46)
	Risk of malignant oedema	On admission (mean time of 6–7 h after symptom onset)	90	100	>16.6 μg/ml	40 malignant and 35 non-malignant	(53)

(Continued)

TABLE 1 | Continued

Biomarker	Function tested	Timing of sampling	Sensitivity (%)	Specificity (%)	Cut off value	*n*	References
PAI-1 and TAFI	Risk of hemorrhagic transformation after rt-PA	Within 3 h of symptom onset	75	97.6	PAI-1 <21.4 ng/mL and TAFI >180%	77 rt-PA treated IS	(54)
Glutamate	Risk of early neurological deterioration	On admission (mean time of 9–10 h after symptom onset)	81	87	>200 μmol/l	27 progressing and 86 non-progressing lacunar strokes	(55)
GABA	Risk of early neurological deterioration	On admission (mean time of 9–10 h after symptom onset)	96	94	<240 nmol/l	27 progressing and 86 non-progressing lacunar strokes	(55)
Combination of S100B, BNGF, vWF, MMP-9, and MCP-1	Differentiation between stroke and controls	Within 12 h of symptom onset	91	97	–	223 strokes and 214 controls	(56)
Combination of S100B, vWF, MMP-9, and VCAM	Differentiation between stroke and controls	Within 24 h of symptom onset	90	90	–	65 IS and 157 controls	(57)
Combination of S100B, MMP-9, D-dimer, BNP, and CRP	Differentiation between stroke and controls	Within 6 h of symptom onset	81	70	–	130 patients with focal neurological deficit	(58)
Combination of S100B, MMP-9, D-dimer, and BNP	Differentiation between stroke and controls	Within 24 h of symptom onset	86	37	–	1,100 patients with focal neurological deficit	(59)
Combination of MMP-9, D-Dimer, sRAGE, caspase-3, chimerin, and secretagogin	Differentiation between stroke and mimics	Within 24 h of symptom onset	Overall accuracy of the model: 0.91		–	915 strokes and 90 mimics	(60)
S100B and sRAGE	Differentiation between IS and ICH	Within 3 and 6 h of symptom onset	22.7	80.2	S100B >96 pg/ml and sRAGE <0.97 ng/ml	776 IS and 139 ICH	(61)
GFAP and RBP4	Differentiation between IS and ICH	Within 6 h of symptom onset	–	100	GFAP <0.07 ng/ml and RBP4 >61 lg/mL	38 IS and 28 ICH	(62)
Panel of 22 genes	Differentiation between stroke and controls	<24, 24–48, >48 h after symptom onset	78	80	–	20 IS and 20 controls	(63)
Panel of 18 genes	Differentiation between stroke and controls	Within 3 h, at 5 h and at 24 h after symptom onset	With accuracy in 66% within 3 h, 86% at 5 h and 100% at 24 h		–	15 IS and 8 controls	(64)
Panel of 23 genes	Differentiation between stroke etiologies	Within 3 h, at 5 h and at 25 h after symptom onset	95.2	95.2	–	15 IS	(65)
Panel of 40 genes	Differentiation between cardio-embolic and large vessel strokes	At 3 h, at 5 h and at 25 h after symptom onset	>90	>90	–	76 IS	(66)
Panel of 34 genes	Differentiation between TIA and patient with CVD	From 9 to 68 h (mean 35 h) after symptom onset	100	100	–	26 TIAs and 26 controls	(67)
Panel of 26 genes	Differentiation between IS or TIA and controls	Within 72 h of symptom onset	89	89	–	94 IS, 26 TIAs, and 44 controls	(68)
Panel of 41 genes	Differentiation between lacunar and non-lacunar strokes	Within 72 h of symptom onset	>90	>90	–	30 lacunar and 86 non-lacunar strokes	(69)
GST-π	Discrimination between early (<3 h) and late (3 h) presentation of stroke	Within 3 h and after 3 h of symptom onset	AUC = 0.79; OR = 10		17.7 μg/l	103 IS and 132 controls	(70)

TABLE 2 | Main clinical uses and their linked potential biomarkers.

Differentiation between stroke and controls	S100B NSE NR2A/2B aAbs Apo B, Apo A-I, and Apo B/Apo A-I ratio CRP P-Selectin Homocysteine BNP D-dimer Combination of S100B, MMP-9, vWF, BNGF, and MCP-1 Combination of S100B, MMP-9, vWF, and VCAM Combination of S100B, MMP-9, D-dimer, BNP, and CRP Combination of S100B, MMP-9, D-dimer, and BNP Combination of MMP-9, D-Dimer, sRAGE, caspase-3, chimerin, and secretagogin Panel of genes
Differentiation between IS and ICH	S100B GFAP Apo C-I and Apo C-III BNP S100B and sRAGE GFAP and RBP4
Risk of hemorrhage after rt-PA	S100B NSE MMP-9 c-Fn PAI-1 and TAFI
Correlation with hemorrhage volume	GFAP
Correlation with stroke severity and infarct size	S100B NSE MMP-9
Correlation with favorable neurological outcome	NSE
Acting as a stroke clock	NSE NR2 GST-π PARK7 NDKA
Risk of early neurological deterioration	MMP-9 Glutamate IL-6 TNF-α ICAM-1
Risk of malignant oedema	S100B MMP-9 c-Fn
Stroke etiology	Panel of genes

results were not substantiated by Gonzalez-García's 2012 study where S100B, measured between 8 and 48 h of symptom onset was significantly elevated in stroke compared to controls but failed to differentiate between IS and ICH and did not correlate with stroke severity on admission (72) despite other studies suggesting that S100B concentrations correlated with stroke severity and size of infarction (73–75).

Serum S100B concentration measured 24 h after symptom onset is significantly higher in stroke patients (posterior circulation IS or infratentorial ICH, no distinction was made in the analysis) than in controls or in patients with vertigo from non-vascular causes (37). However, in addition to prolonged and delayed release into the blood after stroke, S100B levels are also increased in other neurological pathologies such as traumatic brain injuries and extracranial malignancies (76, 77).

Never-the-less, elevated S100B concentration (>0.23 g/l) has been associated with hemorrhage risk due to rt-PA treatment (specificity of 82%, sensitivity 46%) (38) suggesting with further work, this biomarker may have some utility.

GFAP

GFAP (glial fibrillary acidic protein), another glial protein specific to astrocytes (78), is the best candidate to date for differentiating hemorrhage and ischemic stroke. Based on detection of delayed GFAP release in patients with ischemic stroke (maximum concentration reached 2–4 days after ischemic stroke onset), Foerch and his team studied this molecule in different clinical settings and showed promising results (79–81). In a multicenter clinical study of 205 patients (163 with IS, 39 with ICH and three stroke mimics) diagnostic accuracy was high for differentiating intracerebral hemorrhage from ischemic stroke by GFAP immunoassay on a single blood sample obtained within 4.5 h of symptom onset. Using GFAP cut-off of 2.9 ng/l provided a specificity of 96.3% and a sensitivity of 84.2% for distinguishing ICH, IS and stroke mimics (40). In addition, the levels of GFAP were shown to be correlated with the hemorrhage volume (40, 79, 80).

Several studies have confirmed the potential for serum GFAP to distinguish IS and ICH. Xiong et al. showed that the GFAP concentration in blood collected within 2–6 h after symptom onset was significantly higher in ICH ($n = 43$) than IS ($n = 65$) patients, with 86 and 76.9% sensitivity and specificity of, respectively, using a cut-off point of 0.7 ng/ml) (41). Ren et al. replicated these findings using a GFAP cut off value of 0.34 ng/ml with 61% sensitivity and 96% specificity in a 4.5 h time window from symptoms onset (42). A later study measuring serum GFAP in 46 ICH and 146 IS patients reported 77.8 and 94.2% sensitivity and specificity distinguishing the two stroke subtypes using a cut-off value of 0.03 g/l within 6 h of diagnosis (43).

Similarly, Katsanos et al. reported that in samples from patients presenting within 6 h from symptoms onset, significantly raised median plasma GFAP concentrations detected in ICH vs. IS, stroke mimetics, and controls. A cut-off of 0.43 ng/mL provided the best threshold for differentiation between ICH and AIS (sensitivity of 91% and specificity of 97%). They also described that the best timing of sampling to allow optimal differential diagnostic between IS and ICH was in the second hour from symptom onset (44).

A meta-analysis including nearly 1,300 patients confirmed the potential of measuring GFAP in the blood in the early phase of stroke (samples drawn <3 h from symptoms onset), to discriminate IS, ICH and mimics. Interestingly, there was no significant difference in diagnosis accuracy when patients were

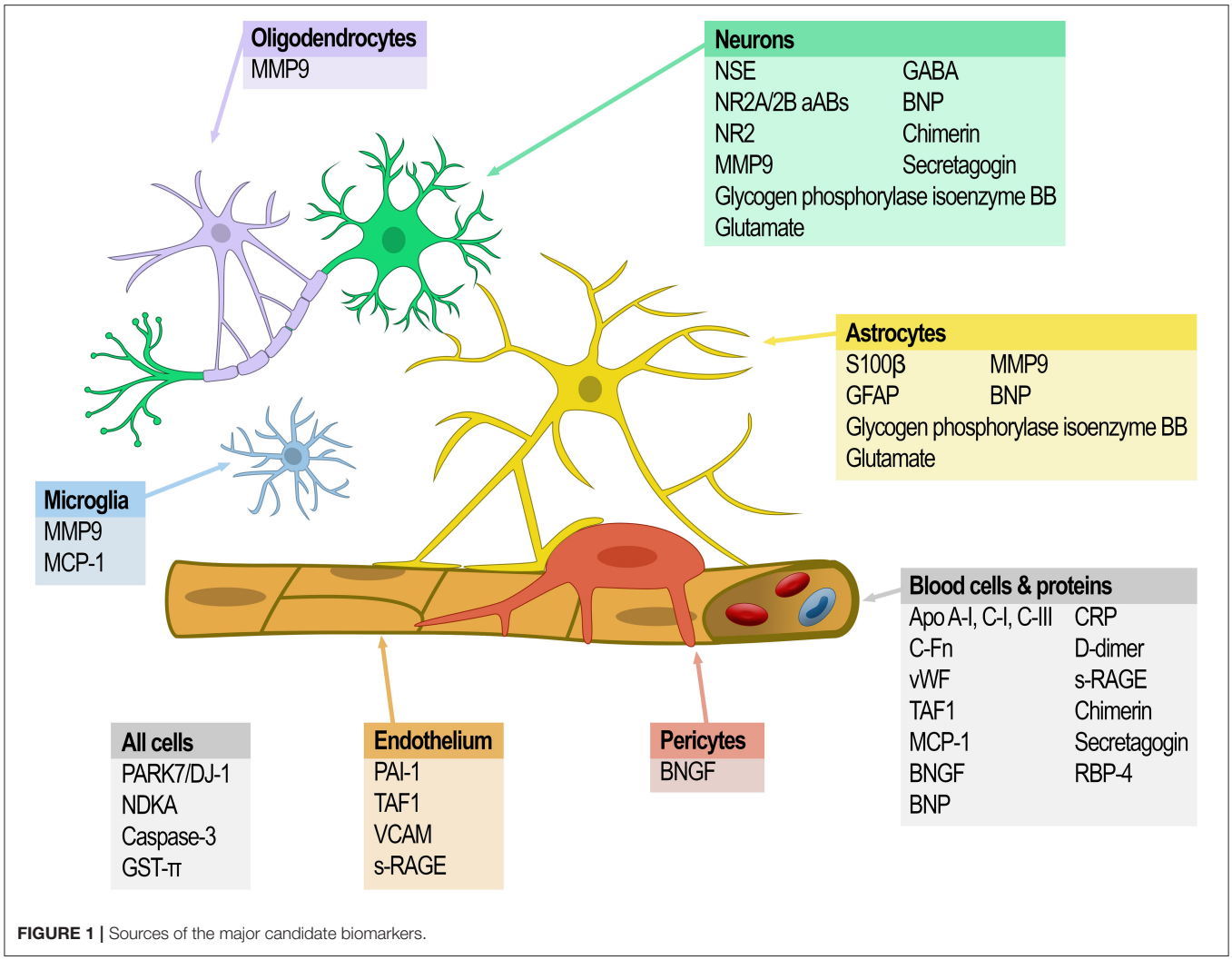

FIGURE 1 | Sources of the major candidate biomarkers.

classified in three subgroups according to time of sampling (0–60, 60–120, 120–180 min after stroke onset) (82).

More recently, in a smaller meta-analysis including 340 patients (236 acute IS and 104 ICH) from four studies, Cabezas et al. confirmed that standardized levels of GFAP blood levels were significantly elevated in ICH compared with IS. Here again, the analysis showed no correlation of GFAP concentration with time of sampling (83).

Controversially, it was previously reported that when measured early (<1 h after stroke onset), serum GFAP did not distinguish ICH and IS (80).

Nevertheless, GFAP measurement is not part of routine clinical practice. The results described above need to be replicated by different groups in larger studies with standardization of detection methodologies and diagnostic cut-offs. This is especially important with respect to the differentiation of stroke mimics as GFAP has also been found in the serum from high-grade glioma patient (84) and is considered as a potential biomarker for diagnosis of traumatic brain injuries (85) which are both potential stroke mimics. Ideally GFAP sensitivity and specificity to distinguish hemorrhagic from ischemic stroke would need to be consistent across time, especially in the earliest time point from symptoms onset when the distinction is most important prior to initiation of thrombolytic therapy. If this is not the case, it will constitute a major barrier for therapeutic triage, especially in a prehospital setting, where timing of stroke evolution may still be uncertain. Refinement of GFAP measurement technologies and application strategies will be required.

NSE

Serum concentrations of NSE (neuron-specific enolase) have been reported to be as significantly raised in stroke patients compared to controls and to correlate with infarct size and stroke symptom severity (75, 86–88). Serum NSE levels assessed prospectively within 4.5 h of IS symptom onset in rt-PA threated patients ($n = 67$) correlates with NIHSS at 24 h ($R = 0.342$), and lower serum NSE levels and NIHSS scores were detected in patients with favorable neurological outcomes after 90 days (45).

Overall, NSE has a similar discriminatory profile to S100B (high specificity and low sensitivity) (71–73, 88). This may in part be due variable kinetics of release, sometimes peaking 24 h after

stroke (89, 90). Interestingly, Kim et al. showed that IS patients identified as having a second peak of serum NSE (20% of the studied population) were more at risk of developing hemorrhagic transformation (OR = 6.8) (90). Therefore, while NSE is not currently recommended for the diagnosis of acute stroke it may still have clinical potential.

MMP-9

Expectations have been high for MMP-9 (matrix metalloproteinase-9) as a stroke diagnostic biomarker because of its role in response to brain injury *via* its involvement in extracellular matrix degradation. MMP-9 concentrations measured acutely have been linked increased to infarct size, worse neurological outcome, and complications of hemorrhagic transformation (46, 91–96). Serum MMP-9 concentrations ≥140 ng/ml were shown to predict hemorrhagic transformation in rt-PA treated ischemic stroke patients (sensitivity 92%, specificity 74%) (46). Six other studies confirmed the correlation between MMP-9 concentration and increased bleeding risk after rt-PA (96). Similarly, Barr et al. identified an association between elevated serum concentrations of MMP-9 and blood brain barrier disruption which is a key feature of hemorrhagic transformation (97). However, the rise of MMP-9 is not specific to ischemic stroke, moreover its concentration is reported to peak at 24 h post stroke (96), too late for making decisions about thrombolysis, and standardization of MMP-9 measurements and experimental replication are still required.

NMDA-R

Autoantibodies to the glutamate NMDA-R (N-methyl-D aspartate receptors; NR2A/NR2B subunits) associated with neurotoxicity are elevated after stroke and distinguish IS patients ($n = 31$) from controls 3 h after symptoms onset with 97% sensitivity and 98% specificity (47). In a different cohort, plasma levels of NMDA-R NR2A were also shown to be elevated in ischemic strokes when there was no difference observed in patients with cerebral hemorrhage in comparison to controls (98). Criticism for the potential use of NMDA-R antibodies for the diagnosis of ischemic stroke were raised as NMDA-R antibodies have also been detected in patients with prior stroke hypertension, atherosclerosis, epilepsy, systemic lupus erythematous, and encephalitis (47, 98–100). Nevertheless, more recently, NR2 peptide (a product of degradation of NMDA-R) in blood has been reported to distinguish IS from stroke mimetics, patients with vascular risk factors and controls with 92 and 96% sensitivity and specificity, respectively (48). On the negative side, NR2 levels might not be increased in lacunar and small cortical strokes (48). Interestingly, detection of NMDA-R NR2A antibodies and NR2 concentrations might have a temporal profile after ischemic stroke (with a peak after 12 h) (48, 98) that might contribute to pinpointing a patients stage of stroke evolution but these results need to be validated in specifically designed studies.

Apo-lipoproteins

Some members of the apo-lipoprotein family have also been tested as potential biomarkers for IS diagnosis. Apo C-I and Apo C-III concentrations were found to be increased in IS compared to ICH within 6 h of symptom onset and both were reported to have the potential to discriminate IS from ICH. For Apo C-III this was achieved with 94 and 87% sensitivity and specificity, respectively (49). A panel of nine apo-lipoproteins was tested as a tool to distinguish IS and ICH patients within the first week after symptom onset using a mass spectrometry assay. Apo C-I and Apo C-III reported to provide the best classification power as individual markers but combining Apo C-III and Apo A-I provided the best discrimination overall (AUC = 0.92) (101). Unfortunately, these results were not confirmed by Walsh and colleagues who looked at a broader panel which included paraoxonase-1, MMP- 3 and 9 and Apo A-I, C-I, and C-III for their ability to distinguish between IS, ICH patients and controls on blood samples obtained within 12 h of symptom onset. In this cohort, the levels of Apo A-I, Apo C-I, and paraoxonase-1, were shown to be lower in IS than in ICH patients with the other candidates having no discriminatory value (102). It is intriguing to speculate that this stark difference might be accounted for by a temporal component to the expression profile that might itself be useful.

Others have taken a ratio-metric approach to the use of apo-lipoprotein family members as stroke biomarkers. As et al. reported that Apo B concentrations and the Apo B/Apo A-I ratio were significantly elevated while levels of Apo A-I was significantly decreased in IS patients compared to controls. All three-potential biomarker tests were reported to have a high specificity and sensitivity to discriminate stroke patients (between 86 and 98%) (50). The Apo B/Apo A-I ratio has also been associated with early neurological deterioration in large artery atherosclerotic stroke, this was not found for other stroke subtypes (103).

Others

Other less well-studied candidates may also have merit. For example, Allard et al. described first in 2005 the potential of PARK7 and NDKA (nucleoside diphosphate kinase A) as biomarkers for stroke diagnosis as their plasma concentrations increased early after symptom onset (29, 104). However, their specificity and sensitivity as markers were dependent on the diagnostic cut-off values used (104) and the results still need to be replicated. Tulantched et al. later specified that PARK7 seemed to have a better prognostic value than NDKA, both in sensitivity and specificity. Once more, collection time in this prospective study was late after stroke onset with a median of 17 h (51).

More recently, a prospective study found that glycogen phosphorylase isoenzyme BB measurements were able to discriminate between 172 IS and 133 controls with 93% sensitivity and specificity (cut-off of 7.0 ng/mL and sample drawn within 12 h of onset) (52). Nevertheless, glycogen phosphorylase which metabolizes glycogen to provide glucose-1-phosphate to restore energy stores has also been identified as a potential marker of ischemic myocardial injury (105, 106).

A meta-analysis interrogating over 130 biomarkers published by Hasan et al. in 2012, concluded that C-reactive protein (CRP), P-selectin and homocysteine were the only three biomarkers able to significantly differentiate ischemic stroke from healthy

patients (28). Nevertheless, once more, these three molecules have a low specificity for ischemic stroke and therefore preclude their diagnostic use in acute stroke situations.

A systematic review performed by Misra et al. identified 10 single biomarkers and seven biomarker panels with a potential for differentiating IS and ICH. Once more, GFAP appeared to perform well, either as a single marker or in association either with the Activated Protein C- Protein C Inhibitor Complex (APC-PCI) or with the Retinol Binding Protein 4 (RBP4). Nevertheless, because the time of sampling was outside of the time window for practical acute stroke intervention (31), their clinical utility is still unclear. In another systematic review, Monbailliu and colleagues identified a different pairing of diagnostic biomarkers for consideration. BNP and S100 were the only two blood-based proteins biomarkers in their study that could differentiate IS from ICH, stroke mimetics and healthy control subjects (32).

The most recent meta-analysis published in 2020 analyzed 25 biomarkers across 40 studies and over 5,000 IS, 750 ICH, 550 mimics, and 1,770 healthy controls on samples collected within 24 h of symptoms onset. BNP, MMP-9, D-Dimer were identified to significantly differentiate the different patient groups while GFAP was successful to differentiate IS from ICH within 6 h. S100B, caspase-3 and NSE only distinguished IS from stroke mimics. Nevertheless, the authors highlighted that 67% of the studies included had only moderate study quality suggesting the need for further well-conducted studies (107).

While these markers all offer promise as diagnostic aids, until larger validation studies tease out the reproducibility of diagnosis, specificity in different patient groups and the role of sampling window in the value of the measurements, the current level of uncertainty does not recommend their immediate clinical use.

BIOMARKERS OF DISEASE PROGRESSION

In addition to the previously mentioned MMP-9, NSE, and S100B, other molecules are linked with increased bleeding risk after IS. Plasma levels of c-Fn (cellular-fibronectin), which reflect vascular damage, have been associated with the development of hemorrhagic transformation following t-PA use (108). When evaluated in a second cohort of 27 subjects, serum c-Fn $\geq$3.6 μg/ml identified hemorrhagic transformation with a sensitivity of 100% but specificity of 60% (46). Combining c-Fn with MMP-9 allowed detection of hemorrhagic transformation with 92% sensitivity, 87% specificity, and a positive predictive value of 41% (46). Reduced levels of PAI-1 (plasminogen activator inhibitor) and higher levels of TAFI (thrombin-activated fibrinolysis inhibitor), two endogenous fibrinolysis inhibitors, have been associated with symptomatic intracranial hemorrhage after thrombolysis therapy. When combined, PAI-1 level <21.4 ng/ml and a TAFI level >180% predicted symptomatic intracranial hemorrhage after rt-PA (sensitivity and specificity of 75 and 97.6%, respectively) (54).

Several biomarkers have been associated with early neurological deterioration (END). This has been defined as neurological worsening between 48 and 72 h after admission and occurs in one third ischemic stroke patients (109). Cytotoxic mechanisms mediated by glutamate, nitric oxide, and cytokines and endothelial-leukocyte adhesion molecules have been proposed as mediators of progression of tissue damage (110).

High plasma glutamate concentrations have been correlated with neurological worsening and infarct growth at 72 h after stroke onset (55, 110). Plasma glutamate concentrations of >200 μmol/l on admission have a positive predictive value for neurological deterioration at 48 h after lacunar infarction of 67% (55). Plasma GABA levels <240 nmol/l on admission also had a positive predictive value for neurological deterioration at 48 h after lacunar infarction of 84% (55). Higher levels of inflammatory markers such as ferritin, IL-6 (interleukine-6), TNF-α (tumor necrosis factor-α) and ICAM-1 (intercellular adhesion molecule-1) were also shown to be associated with early neurological worsening (110–112).

Space-occupying brain oedema (also called malignant oedema), an early life-threatening problem in patients with large hemispheric stroke, has been shown to be predicted by an elevated plasma S100B level (>0.35 g/l) with a 75% sensitivity and a 80% specificity at 12 h after stroke and even more at 24 h (94 and 83% sensitivity and specificity, respectively) (39). c-Fn and MMP-9 concentrations have also been found to be significantly higher in patients with malignant MCA (m-MCA) infarction than in controls. c-Fn concentrations of >16.6 μg/ml provided a 90% sensitivity and 100% specificity with 89 and 100% negative and positive predictive values, respectively, for prediction of m-MCA infarction (53).

While more work is needed to determine precisely when in a patient's clinical course these measurements first provide valuable information about that individual's likely outcome, their generally high sensitivity and specificity suggest they will find clinical utility.

BIOMARKERS PANELS

To better account for the molecular complexity of the ischemic cascade and increase the sensitivity and specificity of biomarkers as diagnosis tools, many researchers have also investigated biomarker panels, evaluating multiple molecules simultaneously instead of looking for a single biomarker. In a systematic review, Whiteley et al. identified seven panels of biomarkers tested as ischemic stroke diagnostic tools. The main criticisms were that the multimarker panel studies did not provide regression equations for stroke prediction and that a variety of cut-off values were used for the same biomarker. Moreover, the sample collection time points usually occurred outside the window where treatment was possible (29).

Reynolds et al. assessed plasma from 223 stroke patients (including IS, ICH and subarachnoid hemorrhage) and 214 healthy controls for more than 50 serum biomarkers using ELISAs (enzyme-linked immunosorbent assay). The combination of S100B, B-type neurotrophic growth factor (BNGF), von Willebrand factor (vWF), MMP-9, and monocyte chemotactic protein-1 (MCP-1) provided diagnosis of stroke

within 12 h after symptom onset with a 91% sensitivity and a 97% specificity (56). A related panel of S100B, MMP-9, vWF, and vascular cell adhesion molecule (VCAM) studied by the same group of researchers in 65 suspected ischemic stroke patients and 157 controls within 24 h of symptoms provided a sensitivity and specificity of 90% (57).

In 130 patients with acute focal neurologic deficits admitted within 6 h of onset of symptoms, a panel including D-dimer, CRP, B-type natriuretic protein (BNP), MMP-9, and S100B was predictive of ischemic stroke with sensitivity and specificity of 81 and 70%, respectively (58). While less specific and sensitive than the preceding panels, its time window of application is more appropriate to the acute stroke setting (6 vs. 24 h). However, when the same panel of markers, excluding CRP, was tested in a prospective multicenter trial of more than 1,100 patients who presented with symptoms suggestive of stroke, a 86% sensitivity and 37% specificity were achieved for distinguishing stroke from mimics in the first 24 h after symptom onset (59).

In a study published in 2011, Montaner et al. tested, in an ED setting, a panel of blood biomarkers including CRP, S100B, MMP-9, a soluble receptor for advanced glycation end products (sRAGE), D-Dimer, brain natriuretic peptide (BNP), caspase-3, neurotrophin-3, chimerin, and secretagogin. They identified levels of caspase-3, D-dimer, sRAGE, chimerin, secretagogin, and MMP-9 as independent predictors of stroke vs. mimics. Moreover, they reported a predictive probability for identifying stroke of 99.01% by combining set cut-off values of these six biomarkers (60). The same team have also demonstrated, in a cohort of 915 stroke patients, that just S100B and sRAGE, could distinguish between IS and ICH with an AUC of 0.76 for blood samples obtained within 3 h after symptom onset. This was confirmed in blood samples obtained within 6 h of symptom onset (61).

More recently, measurement of retinol binding protein 4 (RBP4) (with a cut off value >61 g/ml) and GFAP (with a cut off value of <0.07 ng/ml) was shown to distinguish IS from ICH with a specificity of 100% in a cohort of 38 IS and 28 ICH samples (62).

In the STROKE-CHIP study, a prospective multicenter study of over 1,300 patients, published in 2017, Bustamante et al. studied a panel of 21 biomarkers selected from prior studies and published literature (including S100B, cFn, NSE, MMP-9 e.g.) on blood samples collected immediately upon arrival of patients presenting within 6 h after symptom onset. None of these biomarkers were able to provide an accurate hyperacute differential diagnosis of stroke (113).

While adding complexity to the laboratory work required, panels of markers appear to have the potential to offer significant improvements in specificity and sensitivity. However, further validation is still clearly required.

THE mRNA REVOLUTION

The development of oligonucleotide microarray techniques, and more recently RNAseq, opened new perspectives in the quest for discovery of specific acute stroke biomarkers. These techniques allow unbiased investigation of the entire transcriptome as RNA shed from damaged or communicating cells, or contained within the cells of the immune system, the body's own "first responders" to injury. In addition, changes in mRNA expression occur very quickly often before changes of protein expression can be detected (114). This suits perfectly the acute ischemic stroke setting where "time is brain."

Tang and colleagues reported a blood genomic response specific to ischemic stroke on blood samples collected at 24 h from rats subject to MCAo, sham surgery, and naïve controls. Twenty five genes were shown to be significantly (more than 2-fold) over expressed in rat blood 24 h after induction of ischemia while 98 had decreased significantly in comparison to controls (115).

Using blood samples collected from 20 patients with ischemic stroke and in 20 controls and stratified for sampling time (<24 h $n = 7$, 24–48 h $n = 10$, and >48 h $n = 3$), Moore and colleagues found that, after correction for multiple comparisons, 190 genes were differentially expressed (comparing stroke and control). Moreover, a panel of 22 genes identified as coming from peripheral mononuclear cells differentiated ischemic stroke from controls with 78 and 80% sensitivity and specificity, respectively (63).

When bloods were sequentially collected within 3 h, at 5 h and at 24 h from eight controls and 15 ischemic stroke patients [initially enrolled in the Combination approach to Lysis utilizing Eptifibatide And Recombinant tissue-type plasminogen Activator (CLEAR) trial], 104 genes were identified to have a 1.5-fold change between ischemic stroke and controls at 3 h, 1,106 at 5 h and 906 at 24 h. An 18-gene panel distinguished between ischemic stroke and controls with accuracy in 75% of the cases or more at all 3 different time points (64). Genes included in this panel reflected the involvement of inflammation in the ischemic pathway but were different from those identified by Moore.

When samples from the CLEAR trial were used to explore RNA expression after different ischemic stroke etiologies, 77 genes showed at least a 1.5-fold change in expression between large vessel occlusion and cardioembolic strokes. Twenty three of these genes could distinguish these etiologies with >95% sensitivity and specificity (65).

However, when RNA isolated from the peripheral blood mononuclear cells of acute ischemic stroke patients, stroke survivors and patients with acute traumatic brain injury was analyzed (cohort $n = 15$–20, sampling time: 24–27 h after event onset), no significant differences in single genes expression were identified between these groups. Nevertheless, expression of PDE4D (phosphodiesterase 4 D), an enzyme metabolizing cyclic adenosine monophosphate in inflammatory cells, was significantly different between acute ischemic stroke patients and healthy controls with cardiovascular risk factors (116).

A retrospective case-control study of 39 ischemic stroke patients and 25 controls (sampling time 10 ± 6.5 h), identified nine genes whose expression was significantly different in stroke patients and involvement of toll-like receptor signaling in the ischemic cascade (117). Five of these nine genes; MMP9, ARG1, CA4, LY96, and S100A12, had previously been reported as specific for stroke (64).

In a larger cohort of 194 blood samples collected at 3, 5, and 24 h after stroke from 76 patients with acute IS, a 40-gene panel distinguished cardio-embolic from large vessel strokes with >95% sensitivity and specificity. In addition, a 37-gene panel was identified to be able to differentiate atrial fibrillation from non-atrial fibrillation causes of cardioembolic stroke with >90% sensitivity and specificity (66).

Zhan and colleagues took a different approach and compared TIA with ischemic stroke. In rats they showed that only brief focal ischemia was needed to induce the majority of changes caused by ischemic stroke (118). When the same group compared the blood expression profiles of TIA patients ($n = 26$) and control subjects with vascular risk factor but without symptomatic cardiovascular disease ($n = 26$), they identified 449 genes that distinguished between the two groups. Thirty-four genes separated TIAs from controls with 100% sensitivity and specificity. In addition, two different patterns of gene expression were identified by cluster analysis for the TIA patients suggesting a heterogeneous response to the event between patients and a possible relation with a higher risk of stroke (67).

These findings were soon tested in a bigger cohort by Jickling and colleagues. In 164 blood samples collected within 72 h of symptom onset from stroke, TIA and control patients, 145 genes were differentially expressed between TIA and controls and 413 genes were significantly different between IS and controls. More importantly, 74 of the 145 genes identified in the TIA group were also found in ischemic stroke patients. Twenty six of these 74 common genes were used as a panel to distinguish stroke and TIA from controls with 89% sensitivity and specificity. Pathways analysis revealed that the genes common to stroke and TIA were involved in innate and adaptive immune systems activation involving B-cells and granulocytes (68). Unfortunately, the authors did not reveal the composition of their 26-gene panel, so comparison with the 34-genes panel identified earlier by Zhan et al. is not possible.

Jickling et al. also evaluated the gene expression profile of lacunar strokes. In a cohort of 30 lacunar and 86 non-lacunar strokes (with blood sampling within 72 h of stroke onset), they identified a 41 genes discriminating lacunar and non-lacunar stroke with >90% sensitivity and specificity (69).

In 2012, Oh et al. performed microarray analysis on blood samples collected from 12 ischemic stroke patients and 12 controls (sampling time 12.7 ± 5.3 h after stroke onset). They identified 88 transcripts with a 1.5-fold change in ischemic stroke compared to controls and 11 transcripts with 2-fold difference (including MMP9, Il1R2). Then, they validated the expression of the three most differently expressed genes (MMP9, Il18RAP, and GNLY) by quantitative polymerase chain reaction (qPCR). In another cohort of 120 ischemic stroke patients and 82 controls (sampling time 10.4 ± 9.7 h). MMP9 concentrations measured using ELISA were significantly greater in IS compared to controls but did not to correlate with infarct volume (119).

When quantitative PCR was used validate the expression profiles of 40 candidate biomarkers identified in previous studies (63, 64, 117) in 18 ischemic stroke patients and 15 controls (median time of blood sampling 36 h), 16 genes were significantly upregulated in ischemic stroke patients in comparison to controls. Six gene clusters were reported to discriminate between stroke and controls and one of them, containing seven transcripts, was reported to show high accuracy for stroke classification (120).

In common with the candidate protein biomarker studies described earlier, the investigators for the transcriptome studies summarized above have tended (samples from the CLEAR trial are an obvious exception) to perform analyses relatively late in stroke evolution, when diagnosis is generally already certain and decisions about therapy already made. Moreover, there has been little emphasis on distinguishing ischemic and hemorrhagic stroke, or identifying genes that might identify a heightened risk of bleeding. These gaps in the analysis are surprising. Array technologies also lend themselves to collaborative re-analysis, indeed many publishers stipulate that array data be made freely available. It is therefore also surprising that pooled analysis of the available data has not yet been performed.

BIOMARKERS OF A STROKE CLOCK

As mentioned above, stroke biomarker discovery has rarely focused on early temporal change, despite the dynamic characteristics of stroke. The possibility that changes in expression of candidate biomarkers with time might help predict stroke evolution and act as a biological stroke clock which could allow more patients to be recruited to thrombolysis is largely unstudied.

In serial blood samples collected at 3, 6, 12, 18, 24, 48, 72, 96, and 120 h after onset of stroke symptoms, NSE concentration, measured by immune-assay, rose in the first 2–3 h, then fell until 12 h before a second elevation that was maintained until measurement ended on day 5. Tau concentration showed a continuous increase from admission onward (87).

During a study evaluating the diagnostic performance of 29 pre-selected molecules within the therapeutic window for thrombolysis in 103 stroke and 132 control patients, glutathione S-transferase-π (GST-π), an enzyme providing protection against oxidative stress, was the most significantly elevated molecule in stroke patient blood. Importantly, GST-π measurement allowed the discrimination of early (<3 h) and late (>3 h) presentations of stroke in 90% of the cases with a cut-off value of 17.7 μg/l. Indeed, GST-π concentration was almost immediately after stroke with increases detected within 3 h after symptom onset and within 1 h in some. Importantly, GST-π concentration decreased rapidly after 3 h reaching a concentration close to normal levels by 6 h after stroke symptoms onset. When GST-π was measured in a cohort of thrombolysed stroke patients (blood collected within 3 h after stroke onset, $n = 100$), its concentration was elevated above the threshold of 17.7 μg/l in 98% of the cases. A similar but less striking pattern was observed for PARK7and NDKA (70).

Conversely, in plasma samples collected at 12, 24, and 48 h after symptoms onset in 39 patients with ischemic stroke, while MMP-9 concentrations were greater in stroke patients than the reference interval for healthy controls, no significant changes were reported over time (95).

Others have collected human blood samples sequentially in the same patient early after stroke, but the analysis focused on creation of a diagnostic tool able to differentiate IS patients from controls and blood samples were not collected within 3 h after the ischemic event (results presented previously) (64).

To date, these are the only investigations identifying blood born biomarkers with a potential to contribute to development of a stroke clock and a potential ability to discriminate eligible vs. ineligible patients for reperfusion therapy.

Nevertheless, clinical trials for the discovery of diagnostic stroke biomarkers suitable for use in the hyperacute phase of the disease are underway. Some of these trials hope to identify biomarkers that will aid stroke diagnosis on admission to the clinic.

The multicenter, observational Biomarkers of Acute Stroke Etiology (BASE) study aims to identify biomarkers defining acute IS etiology and is recruited patients presenting within 24 h of symptom onset. Blood samples are being obtained on arrival and 24, and 48 h later, and gene expression profiling is being used to identify biomarker candidates of stroke (121).

Results of the innovative Blood And Clot Thrombectomy Registry And Collaboration (BACTRAC) trial could also lead to new findings in the stroke biomarker field. Fraser et al. aim to collect intracranial thrombus material and arterial blood collected before, after and during mechanical thrombectomy to allow gene expression and proteomic analysis of the early human molecular response to ischemic stroke (122).

The Helsinki Ultra-acute Stroke Biomarker Study even sampled in a pre-hospital setting *via* blood samples taken by emergency medical service clinicians during transit to analyze GFAP and NR2 peptide levels explore novel markers. The recruitment phase is over but the study has yet to report on the primary outcomes (123).

CONCLUSIONS

Improving in patient outcomes in acute stroke requires a rapid and accurate diagnosis of stroke and its subtypes. A biomarker that could differentiate between hemorrhagic and ischemic stroke or risk of subsequent bleeding would, in theory, permit widespread initiation of thrombolysis in the ambulance and save valuable time and brain tissue.

Markers of brain tissue damage, particularly the highly abundant glial structural proteins like GFAP and S100β and the matrix protein MMP-9 offer this promise but have not yet been systematically evaluated at the earliest time points which matter most. To date, other highly abundant structural proteins such as those characteristic of axons, dendrites, and synapses or oligodendrocyte processes have rarely been considered for this role with the exception of the NR2 degradation product of the NMDA receptor and PARK7 which has a specific anti-oxidant role.

Whether such molecules will be able to rule out stroke mimics which also damage the structure of the brain remains to be determined. In this regard, the circulating apolipoproteins (Apo A1, Apo C1, and Apo C111) and c-FN, PAI-1, and TAFI which may specifically react to the hematological changes of a hemorrhagic stroke or hemorrhagic transformation, respectively, require further study. Accurate prediction of poor outcome after stroke would help patients, their families and clinicians to make early and informed decision about choices between rehabilitation and palliative care.

The suggestion that autoantibodies to NMDA receptors might help in this task raises the question of whether their presence in ischemic stroke signifies previous undetected ischemic events and thus heightened stroke risk. Patients with acute minor IS or TIA are at risk of further occlusive vascular events, particularly recurrence of stroke (124, 125). Prognostic scores based on clinical characteristics observed when first assessed, such as the $ABCD^2$ score (126), tend to predict early stroke recurrence risk but they do not discriminate perfectly between those individuals who will have a recurrent stroke and those who will not (127). Specific biomarkers which helped stratify this risk would be of considerable value but might be of little use in diagnosis of first ever stroke.

If selecting candidate biomarkers based on prior knowledge of involvement in stroke pathophysiology has yet to prove successful, the high costs of "omic" discovery strategies has limited the scope of their use and is still in its infancy. Developing panels of markers from either source and developing ratiometric approaches to analysis seem to offer the hope of significantly better specificity and sensitivity.

For both strategies, most measurements made to date have been performed later than the clinically critical thrombolysis and thrombectomy time window. Timing of biomarker measurement, particularly early when decision making is most important, requires urgent and systematic study. The kinetics of change may be revealing in their own right and, if a biomarker stroke clock can be constructed, might dramatically broaden the utility of thrombolysis and thrombectomy.

The recent discoveries in advanced cerebral imaging and the subsequent extension of time window for both thrombolysis and thrombectomy highlight that specific biomarkers of penumbra would be even more crucial than biomarkers of time for therapeutic decision making in the acute setting. Research combining imaging and biological biomarkers is needed.

The ultimate aim of the stroke biomarker research is the development of a point of care device. A quick and reliable bedside biomarker assessment would revolutionize the acute stroke management. It could potentially expedite the diagnosis of ischemic stroke by making the imaging step redundant and aid the clinical decision-making (even in a prehospital setting). It will reduce time from symptoms to initiation of reperfusion therapies. Specific biomarkers could also be used for pre-hospital stratification of important subgroups. Indeed, they might help identify patients with large vessel occlusion and facilitate direct access to comprehensive stroke centers and timely thrombectomy. Stroke biomarkers could help to resolve the mothership vs. drip and ship dilemma.

Most of the candidate biomarkers described in this review have been detected by what are best described as research tools (e.g., ELISA, Western Blotting, Mass Spectrometry, Gene array, RNASeq) which have inherently long lead times before a result

might be available for a clinician to use. However, a range of assay systems are capable of providing results within minutes, both in a laboratory and point of care setting.

Good examples of rapid assays that could be adapted for stroke biomarker detection include a range of widely used clinical tests based on the principles of sandwich ELISA, in which a target protein is first captured to the surface of the assay device and then detected by a second antibody bearing an easily detected label (128). Perhaps the best known of these are pregnancy tests that detect human chorionic gonadotrophin within a few minutes of sample application (129). Numerous point of care immune assays for biomarker detection are currently under evaluation (130).

Other assay methodologies also have potential for rapid detection of stroke biomarkers. For example, blood glucose can be detected even more rapidly (5 s) by using electrochemical detection of the reaction products of glucose oxidase activity (131). Miniaturization now also makes highly sensitive and selective and rapid analyte detection by a range of mass spectrometry protocols possible, even at the bedside (132). Even nucleic acid biomarkers can now be detected within minutes, with recent publications reporting completion of 30 qPCR cycles within 54 s (133), certainly fast enough for stroke diagnostics if the promise of portable devices that might be used at the bedside (134) are realized. Moreover, nanotechnology offers the promise of highly multiplexed biosensors capable of rapid simultaneous analysis of large panels of biomarkers (135), an important consideration if multiple analytes must be assessed to provide stroke diagnosis and prognosis.

However, it has to be concluded that none of the candidate markers described in this review have entered routine clinical use despite their obvious promise. More work is required before lives can depend on such measurements.

AUTHOR CONTRIBUTIONS

DH conceived the manuscript. MD wrote the original draft. MD, GD, SD, HD, and DH edited the document. All authors contributed to the article and approved the submitted version.

ACKNOWLEDGMENTS

The authors would like to thank Dr. Jo-Maree Courtney (University of Tasmania) for the figure illustration.

REFERENCES

1. Whiteley W, Tian Y, Jickling GC. Blood biomarkers in stroke: research and clinical practice. *Int J Stroke*. (2012) 7:435–9. doi: 10.1111/j.1747-4949.2012.00784.x
2. Biomarkers Definitions Working Group. Biomarkers and surrogate endpoints: preferred definitions and conceptual framework. *Clin Pharmacol Ther*. (2001) 69:89–95. doi: 10.1067/mcp.2001.113989
3. Quinn DA, Fogel RB, Smith CD, Laposata M, Taylor Thompson B, Johnson SM, et al. D-dimers in the diagnosis of pulmonary embolism. *Am J Respir Crit Care Med*. (1999) 159:1445–9. doi: 10.1164/ajrccm.159.5.9808094
4. Daubert MA, Jeremias A. The utility of troponin measurement to detect myocardial infarction: review of the current findings. *Vasc Health Risk Manage*. (2010) 7:691–9. doi: 10.2147/VHRM.S5306
5. Hacke W, Donnan G, Fieschi C, Kaste M, von Kummer R, Broderick J, et al. Association of outcome with early stroke treatment: pooled analysis of ATLANTIS, ECASS, and NINDS rt-PA stroke trials. *Lancet*. (2004) 363:768–74. doi: 10.1016/S0140-6736(04)15692-4
6. Chen ZM, Sandercock P, Pan HC, Counsell C, Collins R, Liu LS, et al. Indications for early aspirin use in acute ischemic stroke: a combined analysis of 40 000 randomized patients from the chinese acute stroke trial and the international stroke trial. *Stroke*. (2000) 31:1240–9. doi: 10.1161/01.STR.31.6.1240
7. Langhorne P, Williams BO, Gilchrist W, Howie K. Do stroke units save lives? *Lancet*. (1993) 342:395–8. doi: 10.1016/0140-6736(93)92813-9
8. Hofmeijer J, Kappelle LJ, Algra A, Amelink GJ, van Gijn J, van der Worp HB. Surgical decompression for space-occupying cerebral infarction (the Hemicraniectomy After Middle Cerebral Artery infarction with Life-threatening Edema Trial [HAMLET]): a multicentre, open, randomised trial. *Lancet Neurol*. (2009) 8:326–33. doi: 10.1016/S1474-4422(09)70047-X
9. Goyal M, Menon BK, van Zwam WH, Dippel DWJ, Mitchell PJ, Demchuk AM, et al. Endovascular thrombectomy after large-vessel ischaemic stroke: a meta-analysis of individual patient data from five randomised trials. *Lancet*. (2016) 387:1723–31. doi: 10.1016/S0140-6736(16)00163-X
10. Ma H, Campbell BCV, Parsons M, Churilov L, Levi C, Hsu CY, et al. Thrombolysis guided by perfusion imaging up to 9 hours after onset of stroke. *N Engl J Med*. (2019) 380:1795–803. doi: 10.1056/NEJMoa1813046
11. Thomalla G, Simonsen CZ, Boutitie F, Andersen G, Berthezene Y, Cheng B, et al. MRI-guided thrombolysis for stroke with unknown time of onset. *N Engl J Med*. (2018) 379:611–22. doi: 10.1056/NEJMoa1804355
12. Minnerup J, Wersching H, Ringelstein EB, Schilling M, Schäbitz WR, Wellmann J, et al. Impact of the extended thrombolysis time window on the proportion of recombinant tissue-type plasminogen activator-treated stroke patients and on door-to-needle time. *Stroke*. (2011) 42:2838–43. doi: 10.1161/STROKEAHA.111.616565
13. Moradiya Y, Levine S. Comparison of short-term outcomes of thrombolysis for in-hospital stroke and out-of-hospital stroke in United States. *Stroke*. (2013) 44:1903–8. doi: 10.1161/STROKEAHA.113.000945
14. Dalloz MA, Bottin L, Muresan IP, Favrole P, Foulon S, Levy P, et al. Thrombolysis rate and impact of a stroke code: a French hospital experience and a systematic review. *J Neurol Sci*. (2012) 314:120–5. doi: 10.1016/j.jns.2011.10.009
15. Krogias C, Bartig D, Kitzrow M, Weber R, Eyding J. Trends of hospitalized acute stroke care in Germany from clinical trials to bedside. Comparison of nation-wide administrative data 2008-2012. *J Neurol Sci*. (2014) 345:202–8. doi: 10.1016/j.jns.2014.07.048
16. Moey A, Hamilton-Bruce M, Howell S, Leyden J, Chong W, Dodd L, et al. Significant increase in thrombolysis therapy rates for stroke in South Australia. *Int J Stroke*. (2015) 10:E49. doi: 10.1111/ijs.12498
17. Howells DW, Donnan GA. Where will the next generation of stroke treatments come from? *PLoS Med*. (2010) 7:e1000224. doi: 10.1371/journal.pmed.1000224
18. Barber PA, Zhang J, Demchuk AM, Hill MD, Buchan AM. Why are stroke patients excluded from TPA therapy? An analysis of patient eligibility. *Neurology*. (2001) 56:1015–20. doi: 10.1212/WNL.56.8.1015
19. Fink JN, Kumar S, Horkan C, Linfante I, Selim MH, Caplan LR, et al. The stroke patient who woke up. Clinical and radiological features, including diffusion and perfusion MRI. *Stroke*. (2002) 33:988–93. doi: 10.1161/01.STR.0000014585.17714.67
20. Faiz KW, Sundseth A, Thommessen B, Ronning OM. Reasons for low thrombolysis rate in a Norwegian ischemic stroke population. *Neurol Sci*. (2014) 35:1977–82. doi: 10.1007/s10072-014-1876-4
21. Albers GW, Amarenco P, Easton JD, Sacco RL, Teal P. Antithrombotic and thrombolytic therapy for ischemic stroke: American College of Chest

Physicians evidence-based clinical practice guidelines (8th Edition). *Chest*. (2008) 133(6 Suppl):630S−69S. doi: 10.1378/chest.08-0720
22. Powers WJ, Derdeyn CP, Biller J, Coffey CS, Hoh BL, Jauch EC, et al. 2015 American Heart Association/American Stroke Association focused update of the 2013 guidelines for the early management of patients with acute ischemic stroke regarding endovascular treatment: a guideline for healthcare professionals from the American Heart Association/American Stroke Association. *Stroke*. (2015) 46:3020–35. doi: 10.1161/STR.0000000000000074
23. Nogueira RG, Jadhav AP, Haussen DC, Bonafe A, Budzik RF, Bhuva P, et al. Thrombectomy 6 to 24 hours after stroke with a mismatch between deficit and infarct. *N Engl J Med*. (2018) 378:11–21. doi: 10.1056/NEJMoa1706442
24. Albers GW, Marks MP, Kemp S, Christensen S, Tsai JP, Ortega-Gutierrez S, et al. Thrombectomy for stroke at 6 to 16 hours with selection by perfusion imaging. *N Engl J Med*. (2018) 378:708–18. doi: 10.1056/NEJMoa1713973
25. Chia NH, Leyden JM, Newbury J, Jannes J, Kleinig TJ. Determining the number of ischemic strokes potentially eligible for endovascular thrombectomy: a population-based study. *Stroke*. (2016) 47:1377–80. doi: 10.1161/STROKEAHA.116.013165
26. McMeekin P, White P, James MA, Price CI, Flynn D, Ford GA. Estimating the number of UK stroke patients eligible for endovascular thrombectomy. *Euro Stroke J*. (2017) 2:319–26. doi: 10.1177/2396987317733343
27. Froehler MT, Saver JL, Zaidat OO, Jahan R, Aziz-Sultan MA, Klucznik RP, et al. Interhospital transfer before thrombectomy is associated with delayed treatment and worse outcome in the STRATIS registry (systematic evaluation of patients treated with neurothrombectomy devices for acute ischemic stroke). *Circulation*. (2017) 136:2311–21. doi: 10.1161/CIRCULATIONAHA.117.028920
28. Hasan N, McColgan P, Bentley P, Edwards RJ, Sharma P. Towards the identification of blood biomarkers for acute stroke in humans: a comprehensive systematic review. *Br J Clin Pharmacol*. (2012) 74:230–40. doi: 10.1111/j.1365-2125.2012.04212.x
29. Whiteley W, Tseng MC, Sandercock P. Blood biomarkers in the diagnosis of ischemic stroke: a systematic review. *Stroke*. (2008) 39:2902–9. doi: 10.1161/STROKEAHA.107.511261
30. Whiteley W, Chong WL, Sengupta A, Sandercock P. Blood markers for the prognosis of ischemic stroke: a systematic review. *Stroke*. (2009) 40:e380–9. doi: 10.1161/STROKEAHA.108.528752
31. Misra S, Kumar A, Kumar P, Yadav AK, Mohania D, Pandit AK, et al. Blood-based protein biomarkers for stroke differentiation: a systematic review. *Proteomics Clin Appl*. (2017) 11. doi: 10.1002/prca.201700007
32. Monbailliu T, Goossens J, Hachimi-Idrissi S. Blood protein biomarkers as diagnostic tool for ischemic stroke: a systematic review. *Biomark Med*. (2017) 11:503–12. doi: 10.2217/bmm-2016-0232
33. Simats A, Garcia-Berrocoso T, Montaner J. Neuroinflammatory biomarkers: from stroke diagnosis and prognosis to therapy. *Biochim Biophys Acta*. (2016) 1862:411–24. doi: 10.1016/j.bbadis.2015.10.025
34. Glushakova O, Glushakov A, Miller E, Valadka A, Hayes R. Biomarkers for acute diagnosis and management of stroke in neurointensive care units. *Brain Circ*. (2016) 2:28. doi: 10.4103/2394-8108.178546
35. Kamtchum-Tatuene J, Jickling GC. Blood biomarkers for stroke diagnosis and management. *NeuroMolecular Med*. (2019) 21:344–68. doi: 10.1007/s12017-019-08530-0
36. Zhou S, Bao J, Wang Y, Pan S. S100beta as a biomarker for differential diagnosis of intracerebral hemorrhage and ischemic stroke. *Neurol Res*. (2016) 38:327–32. doi: 10.1080/01616412.2016.1152675
37. Purrucker JC, Herrmann O, Lutsch JK, Zorn M, Schwaninger M, Bruckner T, et al. Serum protein S100beta is a diagnostic biomarker for distinguishing posterior circulation stroke from vertigo of nonvascular causes. *Euro Neurol*. (2014) 72:278–84. doi: 10.1159/000363569
38. Foerch C, Wunderlich M, Dvorak F, Humpich M, Kahles T, Goertler M, et al. Elevated serum S100B levels indicate a higher risk of hemorrhagic transformation after thrombolytic therapy in acute stroke. *Stroke*. (2007) 38:2491–5. doi: 10.1161/STROKEAHA.106.480111
39. Foerch C, Otto B, Singer OC, Neumann-Haefelin T, Yan B, Berkefeld J, et al. Serum S100B predicts a malignant course of infarction in patients with acute middle cerebral artery occlusion. *Stroke*. (2004) 35:2160–4. doi: 10.1161/01.STR.0000138730.03264.ac
40. Foerch C, Niessner M, Back T, Bauerle M, De Marchis GM, Ferbert A, et al. Diagnostic accuracy of plasma glial fibrillary acidic protein for differentiating intracerebral hemorrhage and cerebral ischemia in patients with symptoms of acute stroke. *Clin Chem*. (2012) 58:237–45. doi: 10.1373/clinchem.2011.172676
41. Xiong L, Yang Y, Zhang M, Xu W. The use of serum glial fibrillary acidic protein test as a promising tool for intracerebral hemorrhage diagnosis in Chinese patients and prediction of the short-term functional outcomes. *Neurol Sci*. (2015) 36:2081–7. doi: 10.1007/s10072-015-2317-8
42. Ren C, Kobeissy F, Alawieh A, Li N, Li N, Zibara K, et al. Assessment of serum UCH-L1 and GFAP in acute stroke patients. *Sci Rep*. (2016) 6:24588. doi: 10.1038/srep24588
43. Luger S, Witsch J, Dietz A, Hamann GF, Minnerup J, Schneider H, et al. Glial fibrillary acidic protein serum levels distinguish between intracerebral hemorrhage and cerebral ischemia in the early phase of stroke. *Clin Chem*. (2017) 63:377–85. doi: 10.1373/clinchem.2016.263335
44. Katsanos AH, Makris K, Stefani D, Koniari K, Gialouri E, Lelekis M, et al. Plasma glial fibrillary acidic protein in the differential diagnosis of intracerebral hemorrhage. *Stroke Res Treat*. (2017) 48:2586–88. doi: 10.1161/STROKEAHA.117.018409
45. Lu K, Xu X, Cui S, Wang F, Zhang B, Zhao Y. Serum neuron specific enolase level as a predictor of prognosis in acute ischemic stroke patients after intravenous thrombolysis. *J Neurol Sci*. (2015) 359:202–6. doi: 10.1016/j.jns.2015.10.034
46. Castellanos M, Sobrino T, Millan M, Garcia M, Arenillas J, Nombela F, et al. Serum cellular fibronectin and matrix metalloproteinase-9 as screening biomarkers for the prediction of parenchymal hematoma after thrombolytic therapy in acute ischemic stroke: a multicenter confirmatory study. *Stroke*. (2007) 38:1855–9. doi: 10.1161/STROKEAHA.106.481556
47. Dambinova S, Khounteev G, Izykenova G, Zavolokov I, Ilyukhina A, Skoromets A. Blood test detecting autoantibodies to N-methyl-D-aspartate neuroreceptors for evaluation of patients with transient ischemic attack and stroke. *Clin Chem*. (2003) 49:1752–62. doi: 10.1373/49.10.1752
48. Dambinova S, Bettermann K, Glynn T, Tews M, Olson D, Weissman J, et al. Diagnostic potential of the NMDA receptor peptide assay for acute ischemic stroke. *PLoS ONE*. (2012) 7:e42362. doi: 10.1371/journal.pone.0042362
49. Allard L, Lescuyer P, Burgess J, Leung KY, Ward M, Walter N, et al. ApoC-I and ApoC-III as potential plasmatic markers to distinguish between ischemic and hemorrhagic stroke. *Proteomics*. (2004) 4:2242–51. doi: 10.1002/pmic.200300809
50. As S, Sahukar S, Murthy J, Kumar K. A study of serum apolipoprotein A1, apolipoprotein B and lipid profile in stroke. *J Clin Diagnostic Res*. (2013) 7:1303–6. doi: 10.7860/JCDR/2013/5269.3123
51. Tulantched MDS, Min Z, Feng WX. Comparison of plasma PARK7 and NDKA diagnostic value in acute stroke. *Future Sci OA*. (2019) 5:FSO375. doi: 10.2144/fsoa-2018-0080
52. Park KY, Ay I, Avery R, Caceres JA, Siket MS, Pontes-Neto OM, et al. New biomarker for acute ischaemic stroke: plasma glycogen phosphorylase isoenzyme BB. *J Neurol Neurosurg Psychiatry*. (2018) 89:404–9. doi: 10.1136/jnnp-2017-316084
53. Serena J, Blanco M, Castellanos M, Silva Y, Vivancos J, Moro MA, et al. The prediction of malignant cerebral infarction by molecular brain barrier disruption markers. *Stroke*. (2005) 36:1921–6. doi: 10.1161/01.STR.0000177870.14967.94
54. Ribo M, Montaner J, Molina CA, Arenillas JF, Santamarina E, Quintana M, et al. Admission fibrinolytic profile is associated with symptomatic hemorrhagic transformation in stroke patients treated with tissue plasminogen activator. *Stroke*. (2004) 35:2123–7. doi: 10.1161/01.STR.0000137608.73660.4c
55. Serena J, Leira R, Castillo J, Pumar J, Castellanos M, Dávalos A. Neurological deterioration in acute lacunar infarctions: the role of excitatory and inhibitory neurotransmitters. *Stroke*. (2001) 32:1154–61. doi: 10.1161/01.STR.32.5.1154
56. Reynolds MA, Kirchick HJ, Dahlen JR, Anderberg JM, McPherson PH, Nakamura KK, et al. Early biomarkers of stroke. *Clin Chem*. (2003) 49:1733–9. doi: 10.1373/49.10.1733

57. Lynch JR, Blessing R, White WD, Grocott HP, Newman MF, Laskowitz DT. Novel diagnostic test for acute stroke. *Stroke*. (2004) 35:57–63. doi: 10.1161/01.STR.0000105927.62344.4C
58. Laskowitz DT, Blessing R, Floyd J, White WD, Lynch JR. Panel of biomarkers predicts stroke. *Ann N Y Acad Sci*. (2005) 30. doi: 10.1111/j.1749-6632.2005.tb00006.x
59. Laskowitz DT, Kasner SE, Saver J, Remmel KS, Jauch EC. Clinical usefulness of a biomarker-based diagnostic test for acute stroke: the Biomarker Rapid Assessment in Ischemic Injury (BRAIN) study. *Stroke*. (2009) 40:77–85. doi: 10.1161/STROKEAHA.108.516377
60. Montaner J, Mendioroz M, Ribo M, Delgado P, Quintana M, Penalba A, et al. A panel of biomarkers including caspase-3 and D-dimer may differentiate acute stroke from stroke-mimicking conditions in the emergency department. *J Internal Med*. (2011) 270:166–74. doi: 10.1111/j.1365-2796.2010.02329.x
61. Montaner J, Mendioroz M, Delgado P, Garcia-Berrocoso T, Giralt D, Merino C, et al. Differentiating ischemic from hemorrhagic stroke using plasma biomarkers: the S100B/RAGE pathway. *J Proteomics*. (2012) 75:4758–65. doi: 10.1016/j.jprot.2012.01.033
62. Llombart V, Garcia-Berrocoso T, Bustamante A, Giralt D, Rodriguez-Luna D, Muchada M, et al. Plasmatic retinol-binding protein 4 and glial fibrillary acidic protein as biomarkers to differentiate ischemic stroke and intracerebral hemorrhage. *J Neurochem*. (2016) 136:416–24. doi: 10.1111/jnc.13419
63. Moore DF, Li H, Jeffries N, Wright V, Cooper RA Jr, Elkahloun A, et al. Using peripheral blood mononuclear cells to determine a gene expression profile of acute ischemic stroke: a pilot investigation. *Circulation*. (2005) 111:212–21. doi: 10.1161/01.CIR.0000152105.79665.C6
64. Tang Y, Xu H, Du X, Lit L, Walker W, Lu A, et al. Gene expression in blood changes rapidly in neutrophils and monocytes after ischemic stroke in humans: a microarray study. *J Cereb Blood Flow Metab*. (2006) 26:1089–102. doi: 10.1038/sj.jcbfm.9600264
65. Xu H, Tang Y, Liu DZ, Ran R, Ander BP, Apperson M, et al. Gene expression in peripheral blood differs after cardioembolic compared with large-vessel atherosclerotic stroke: biomarkers for the etiology of ischemic stroke. *J Cereb Blood Flow Metab*. (2008) 28:1320–8. doi: 10.1038/jcbfm.2008.22
66. Jickling GC, Xu H, Stamova B, Ander BP, Zhan X, Tian Y, et al. Signatures of cardioembolic and large-vessel ischemic stroke. *Ann Neurol*. (2010) 68:681–92. doi: 10.1002/ana.22187
67. Zhan X, Jickling G, Tian Y, Stamova B, Xu H, Ander B, et al. Transient ischemic attacks characterized by RNA profiles in blood. *Neurology*. (2011) 77:1718–24. doi: 10.1212/WNL.0b013e318236eee6
68. Jickling GC, Zhan X, Stamova B, Ander BP, Tian Y, Liu D, et al. Ischemic transient neurological events identified by immune response to cerebral ischemia. *Stroke*. (2012) 43:1006–12. doi: 10.1161/STROKEAHA.111.638577
69. Jickling GC, Stamova B, Ander BP, Zhan X, Tian Y, Liu D, et al. Profiles of lacunar and nonlacunar stroke. *Ann Neurol*. (2011) 70:477–85. doi: 10.1002/ana.22497
70. Turck N, Robin X, Walter N, Fouda C, Hainard A, Sztajzel R, et al. Blood glutathione S-transferase-pi as a time indicator of stroke onset. *PLoS ONE*. (2012) 7:e43830. doi: 10.1371/journal.pone.0043830
71. Hill MD, Jackowski G, Bayer N, Lawrence M, Jaeschke R. Biochemical markers in acute ischemic stroke. *CMAJ*. (2000) 162:1139–40.
72. Gonzalez-Garcia S, Gonzalez-Quevedo A, Fernandez-Concepcion O, Pena-Sanchez M, Menendez-Sainz C, Hernandez-Diaz Z, et al. Short-term prognostic value of serum neuron specific enolase and S100B in acute stroke patients. *Clin Biochem*. (2012) 45:1302–7. doi: 10.1016/j.clinbiochem.2012.07.094
73. Jauch EC, Lindsell C, Broderick J, Fagan SC, Tilley BC, Levine SR. Association of serial biochemical markers with acute ischemic stroke: the National Institute of Neurological Disorders and Stroke recombinant tissue plasminogen activator Stroke Study. *Stroke*. (2006) 37:2508–13. doi: 10.1161/01.STR.0000242290.01174.9e
74. Foerch C, Singer O, Neumann-Haefelin T, du Mesnil de Rochemont R, Steinmetz H, Sitzer M. Evaluation of serum S100B as a surrogate marker for long-term outcome and infarct volume in acute middle cerebral artery infarction. *Arch Neurol*. (2005) 62:1130–4. doi: 10.1001/archneur.62.7.1130
75. Wunderlich MT, Wallesch CW, Goertler M. Release of neurobiochemical markers of brain damage is related to the neurovascular status on admission and the site of arterial occlusion in acute ischemic stroke. *J Neurol Sci*. (2004) 227:49–53. doi: 10.1016/j.jns.2004.08.005
76. Ishiguro Y, Kato K, Ito T, Nagaya M. Determination of three enolase isozymes and S-100 protein in various tumors in children. *Cancer Res*. (1983) 42:6080–4.
77. Raabe A, Grolms C, Keller M, Döhnert J, Sorge O, Seifert V. Correlation of computed tomography findings and serum brain damage markers following severe head injury. *Acta Neurochir*. (1998) 140:787–91. doi: 10.1007/s007010050180
78. Eng LF, Ghirnikar RS, Lee YL. Glial fibrillary acidic protein: GFAP-thirty-one years (1969-2000). *Neurochem Res*. (2000) 25:1439–51. doi: 10.1023/A:1007677003387
79. Foerch C, Curdt I, Yan B, Dvorak F, Hermans M, Berkefeld J, et al. Serum glial fibrillary acidic protein as a biomarker for intracerebral haemorrhage in patients with acute stroke. *J Neurol Neurosurg Psychiatry*. (2006) 77:181–4. doi: 10.1136/jnnp.2005.074823
80. Dvorak F, Haberer I, Sitzer M, Foerch C. Characterisation of the diagnostic window of serum glial fibrillary acidic protein for the differentiation of intracerebral haemorrhage and ischaemic stroke. *Cerebrovasc Dis*. (2009) 27:37–41. doi: 10.1159/000172632
81. Herrmann M, Vos P, Wunderlich MT, de Bruijn CHMM, Lamers KJB. Release of glial tissue-specific proteins after acute stroke: a comparative analysis of serum concentrations of protein S-100B and glial fibrillary acidic protein. *Stroke*. (2000) 31:2670–7. doi: 10.1161/01.STR.31.11.2670
82. Perry LA, Lucarelli T, Penny-Dimri JC, McInnes MD, Mondello S, Bustamante A, et al. Glial fibrillary acidic protein for the early diagnosis of intracerebral hemorrhage: systematic review and meta-analysis of diagnostic test accuracy. *Int J Stroke*. (2019) 14:390–9. doi: 10.1177/1747493018806167
83. Cabezas JA, Bustamante A, Giannini N, Pecharroman E, Katsanos AH, Tsivgoulis G, et al. Discriminative value of glial fibrillar acidic protein (GFAP) as a diagnostic tool in acute stroke. Individual patient data meta-analysis. *J Investig Med*. (2020) 68:1379–85. doi: 10.1136/jim-2020-001432
84. Jung CS, Foerch C, Schanzer A, Heck A, Plate KH, Seifert V, et al. Serum GFAP is a diagnostic marker for glioblastoma multiforme. *Brain*. (2007) 130(Pt 12):3336–41. doi: 10.1093/brain/awm263
85. Schiff L, Hadker N, Weiser S, Rausch C. A literature review of the feasibility of glial fibrillary acidic protein as a biomarker for stroke and traumatic brain injury. *Mol Diagn Ther*. (2012) 16:79–92. doi: 10.1007/BF03256432
86. Missler U, Wiesmann M, Friedrich C, Kaps M. S-100 protein and neuron-specific enolase concentrations in blood as indicators of infarction volume and prognosis in acute ischemic stroke. *Stroke*. (1997) 28:1956–60. doi: 10.1161/01.STR.28.10.1956
87. Wunderlich MT, Lins H, Skalej M, Wallesch CW, Goertler M. Neuron-specific enolase and tau protein as neurobiochemical markers of neuronal damage are related to early clinical course and long-term outcome in acute ischemic stroke. *Clin Neurol Neurosurg*. (2006) 108:558–63. doi: 10.1016/j.clineuro.2005.12.006
88. Singh HV, Pandey A, Shrivastava AK, Raizada A, Singh SK, Singh N. Prognostic value of neuron specific enolase and IL-10 in ischemic stroke and its correlation with degree of neurological deficit. *Clin Chim Acta*. (2013) 419:136–8. doi: 10.1016/j.cca.2013.02.014
89. Anand N, Stead LG. Neuron-specific enolase as a marker for acute ischemic stroke: a systematic review. *Cerebrovasc Dis*. (2005) 20:213–9. doi: 10.1159/000087701
90. Kim BJ, Kim YJ, Ahn SH, Kim NY, Kang DW, Kim JS, et al. The second elevation of neuron-specific enolase peak after ischemic stroke is associated with hemorrhagic transformation. *J Stroke Cerebrovasc Dis*. (2014) 23:2437–43. doi: 10.1016/j.jstrokecerebrovasdis.2014.05.020
91. Montaner J, Alvarez-Sabin J, Molina CA, Angles A, Abilleira S, Arenillas J, et al. Matrix metalloproteinase expression is related to hemorrhagic transformation after cardioembolic stroke. *Stroke*. (2001) 32:2762–7. doi: 10.1161/hs1201.99512
92. Rosell A, Alvarez-Sabin J, Arenillas JF, Rovira A, Delgado P, Fernandez-Cadenas I, et al. A matrix metalloproteinase protein array reveals a strong relation between MMP-9 and MMP-13 with diffusion-weighted

image lesion increase in human stroke. *Stroke*. (2005) 36:1415–20. doi: 10.1161/01.STR.0000170641.01047.cc
93. Alvarez-Sabin J, Delgado P, Abilleira S, Molina CA, Arenillas J, Ribo M, et al. Temporal profile of matrix metalloproteinases and their inhibitors after spontaneous intracerebral hemorrhage: relationship to clinical and radiological outcome. *Stroke*. (2004) 35:1316–22. doi: 10.1161/01.STR.0000126827.69286.90
94. Montaner J, Molina CA, Monasterio J, Abilleira S, Arenillas JF, Ribó M, et al. Matrix metalloproteinase-9 pretreatment level predicts intracranial hemorrhagic complications after thrombolysis in human stroke. *Circulation*. (2003) 107:598–603. doi: 10.1161/01.CIR.0000046451.38849.90
95. Montaner J, Alvarez-Sabín J, Molina C, Anglés A, Abilleira S, Arenillas J, et al. Matrix metalloproteinase expression after human cardioembolic stroke: temporal profile and relation to neurological impairment. *Stroke*. (2001) 32:1759–66. doi: 10.1161/01.STR.32.8.1759
96. Ramos-Fernandez M, Bellolio MF, Stead LG. Matrix metalloproteinase-9 as a marker for acute ischemic stroke: a systematic review. *J Stroke Cerebrovasc Dis*. (2011) 20:47–54. doi: 10.1016/j.jstrokecerebrovasdis.2009.10.008
97. Barr TL, Latour LL, Lee KY, Schaewe TJ, Luby M, Chang GS, et al. Blood-brain barrier disruption in humans is independently associated with increased matrix metalloproteinase-9. *Stroke*. (2010) 41:e123–8. doi: 10.1161/STROKEAHA.109.570515
98. Dambinova S, Khounteev G, Skoromets A. Multiple panel of biomarkers for TIA/stroke evaluation. *Stroke*. (2002) 33:1181–2. doi: 10.1161/01.STR.0000014922.83673.86
99. Ganor Y, Goldberg-Stern H, Lerman-Sagie T, Teichberg V, Levite M. Autoimmune epilepsy: distinct subpopulations of epilepsy patients harbor serum autoantibodies to either glutamate/AMPA receptor GluR3, glutamate/NMDA receptor subunit NR2A or double-stranded DNA. *Epilepsy Res*. (2005) 65:11–22. doi: 10.1016/j.eplepsyres.2005.03.011
100. Husebye E, Sthoeger Z, Dayan M, Zinger H, Elbirt D, Levite M, et al. Autoantibodies to a NR2A peptide of the glutamate/NMDA receptor in sera of patients with systemic lupus erythematosus. *Ann Rheum Dis*. (2005) 64:1210–3. doi: 10.1136/ard.2004.029280
101. Lopez MF, Sarracino DA, Prakash A, Athanas M, Krastins B, Rezai T, et al. Discrimination of ischemic and hemorrhagic strokes using a multiplexed, mass spectrometry-based assay for serum apolipoproteins coupled to multi-marker ROC algorithm. *Proteomics Clin Appl*. (2012) 6:190–200. doi: 10.1002/prca.201100041
102. Walsh KB, Hart K, Roll S, Sperling M, Unruh D, Davidson WS, et al. Apolipoprotein A-I and paraoxonase-1 are potential blood biomarkers for ischemic stroke diagnosis. *J Stroke Cerebrovasc Dis*. (2016) 25:1360–5. doi: 10.1016/j.jstrokecerebrovasdis.2016.02.027
103. Ryu WS, Schellingerhout D, Jeong SW, Nahrendorf M, Kim DE. Association between serum lipid profiles and early neurological deterioration in acute ischemic stroke. *J Stroke Cerebrovasc Dis*. (2016) 25:2024–30. doi: 10.1016/j.jstrokecerebrovasdis.2016.05.009
104. Allard L, Burkhard PR, Lescuyer P, Burgess JA, Walter N, Hochstrasser DF, et al. PARK7 and nucleoside diphosphate kinase A as plasma markers for the early diagnosis of stroke. *Clin Chem*. (2005) 51:2043–51. doi: 10.1373/clinchem.2005.053942
105. Krause EG, Rabitzsch G, Noll F, Mair J, Puschendorf B. Glycogen phosphorylase isoenzyme BB in diagnosis of myocardial ischaemic injury and infarction. *Mol Cell Biochem*. (1996) 160–1:289–95. doi: 10.1007/BF00240061
106. Lippi G, Mattiuzzi C, Comelli I, Cervellin G. Glycogen phosphorylase isoenzyme BB in the diagnosis of acute myocardial infarction: a meta-analysis. *Biochem Med*. (2013) 23:78–82. doi: 10.11613/BM.2013.010
107. Misra S, Montaner J, Ramiro L, Arora R, Talwar P, Nath M, et al. Blood biomarkers for the diagnosis and differentiation of stroke: a systematic review and meta-analysis. *Int J Stroke*. (2020) Aug 3:1747493020946157.
108. Castellanos M, Leira R, Serena J, Blanco M, Pedraza S, Castillo J, et al. Plasma cellular-fibronectin concentration predicts hemorrhagic transformation after thrombolytic therapy in acute ischemic stroke. *Stroke*. (2004) 35:1671–6. doi: 10.1161/01.STR.0000131656.47979.39
109. Davalos M, Toni D, Iweins F, Lesaffre E, Bastianello S, Castillo J. Neurological deterioration in acute ischemic stroke potential predictors and associated factors in the European Cooperative Acute Stroke Study (ECASS) I. *Stroke*. (1999) 30:2631–6. doi: 10.1161/01.STR.30.12.2631
110. Castellanos M, Sobrino T, Pedraza S, Moldes O, Pumar J, Silva Y, et al. High plasma glutamate concentrations are associated with infarct growth in acute ischemic stroke. *Neurology*. (2008) 71:1862–8. doi: 10.1212/01.wnl.0000326064.42186.7e
111. Castellanos M, Castillo J, García M, Leira R, Serena J, Chamorro A, et al. Inflammation-mediated damage in progressing lacunar infarctions: a potential therapeutic target. *Stroke*. (2002) 33:982–7. doi: 10.1161/hs0402.105339
112. Dávalos A, Castillo J, Marrugat J, Fernandez-Real J, Armengou A, Cacabelos P, et al. Body iron stores and early neurologic deterioration in acute cerebral infarction. *Neurology*. (2000) 54:1568–74. doi: 10.1212/WNL.54.8.1568
113. Bustamante A, López-Cancio E, Pich S, Penalba A, Giralt D, García-Berrocoso T, et al. Blood biomarkers for the early diagnosis of stroke: the stroke-chip study. *Stroke*. (2017) 48:2419–25. doi: 10.1161/STROKEAHA.117.017076
114. Sharp FR, Jickling GC, Stamova B, Tian Y, Zhan X, Liu D, et al. Molecular markers and mechanisms of stroke: RNA studies of blood in animals and humans. *J Cereb Blood Flow Metab*. (2011) 31:1513–31. doi: 10.1038/jcbfm.2011.45
115. Tang Y, Lu A, Aronow BJ, Sharp FR. Blood genomic responses differ after stroke, seizures, hypoglycemia, and hypoxia: blood genomic fingerprints of disease. *Ann Neurol*. (2001) 50:699–707. doi: 10.1002/ana.10042
116. Grond-Ginsbach C, Hummel M, Wiest T, Horstmann S, Pfleger K, Hergenhahn M, et al. Gene expression in human peripheral blood mononuclear cells upon acute ischemic stroke. *J Neurol*. (2008) 255:723–31. doi: 10.1007/s00415-008-0784-z
117. Barr TL, Conley Y, Ding J, Dillman A, Warach S, Singleton A, et al. Genomic biomarkers and cellular pathways of ischemic stroke by RNA gene expression profiling. *Neurology*. (2010) 75:1009–14. doi: 10.1212/WNL.0b013e3181f2b37f
118. Zhan X, Ander BP, Jickling G, Turner R, Stamova B, Xu H, et al. Brief focal cerebral ischemia that simulates transient ischemic attacks in humans regulates gene expression in rat peripheral blood. *J Cereb Blood Flow Metab*. (2010) 30:110–8. doi: 10.1038/jcbfm.2009.189
119. Oh SH, Kim OJ, Shin DA, Song J, Yoo H, Kim YK, et al. Alteration of immunologic responses on peripheral blood in the acute phase of ischemic stroke: blood genomic profiling study. *J Neuroimmunol*. (2012) 249:60–5. doi: 10.1016/j.jneuroim.2012.04.005
120. Adamski MG, Li Y, Wagner E, Yu H, Seales-Bailey C, Soper SA, et al. Expression profile based gene clusters for ischemic stroke detection. *Genomics*. (2014) 104:163–9. doi: 10.1016/j.ygeno.2014.08.004
121. Jauch EC, Barreto AD, Broderick JP, Char DM, Cucchiara BL, Devlin TG, et al. Biomarkers of acute stroke etiology (BASE) study methodology. *Transl Stroke Res*. (2017) 8:424–8. doi: 10.1007/s12975-017-0537-3
122. Fraser JF, Collier LA, Gorman AA, Martha SR, Salmeron KE, Trout AL, et al. The blood and clot thrombectomy registry and collaboration (BACTRAC) protocol: novel method for evaluating human stroke. *J Neurointerv Surg*. (2019) 11:265–70. doi: 10.1136/neurintsurg-2018-014118
123. Mattila OS, Harve H, Pihlasviita S, Ritvonen J, Sibolt G, Pystynen M, et al. Ultra-acute diagnostics for stroke: large-scale implementation of prehospital biomarker sampling. *Acta Neurol Scand*. (2017) 136:17–23. doi: 10.1111/ane.12687
124. Rothwell PM, Giles MF, Chandratheva A, Marquardt L, Geraghty O, Redgrave JN, et al. Effect of urgent treatment of transient ischaemic attack and minor stroke on early recurrent stroke (EXPRESS study): a prospective population-based sequential comparison. *Lancet*. (2007) 370:1432–342. doi: 10.1016/S0140-6736(07)61448-2
125. Ois A, Gomis M, Rodriguez-Campello A, Cuadrado-Godia E, Jimenez-Conde J, Pont-Sunyer C, et al. Factors associated with a high risk of recurrence in patients with transient ischemic attack or minor stroke. *Stroke*. (2008) 39:1717–21. doi: 10.1161/STROKEAHA.107.505438
126. Johnston SC, Rothwell PM, Nguyen-Huynh MN, Giles MF, Elkins JS, Bernstein AL, et al. Validation and refinement of scores to predict very early stroke risk after transient ischaemic attack. *Lancet*. (2007) 369:283–92. doi: 10.1016/S0140-6736(07)60150-0

127. Chandratheva A, Geraghty OC, Rothwell PM. Poor performance of current prognostic scores for early risk of recurrence after minor stroke. *Stroke*. (2011) 42:632–7. doi: 10.1161/STROKEAHA.110.593301
128. Alhajj M, Farhana A. *Enzyme Linked Immunosorbent Assay*. *StatPearls*. Treasure Island, FL: StatPearls Publishing (2020).
129. Legoupil C, Enderle I, Le Baccon FA, Bendavid C, Peltier L, Bauville E, et al. Performance of a quick pregnancy test on whole blood in early pregnancy units: a prospective cohort study. *Euro J Emerg Med*. (2019) 26:105–11. doi: 10.1097/MEJ.0000000000000501
130. Pecoraro V, Banfi G, Germagnoli L, Trenti T. A systematic evaluation of immunoassay point-of-care testing to define impact on patients' outcomes. *Ann Clin Biochem*. (2017) 54:420–31. doi: 10.1177/0004563217694377
131. Setford S, Grady M, Phillips S, Miller L, Mackintosh S, Cameron H, et al. Seven-year surveillance of the clinical performance of a blood glucose test strip product. *J Diabetes Sci Technol*. (2017) 11:1155–62. doi: 10.1177/1932296817703133
132. Banerjee S. Empowering clinical diagnostics with mass spectrometry. *ACS Omega*. (2020) 5:2041–8. doi: 10.1021/acsomega.9b03764
133. Roche PJR, Najih M, Lee SS, Beitel LK, Carnevale ML, Paliouras M, et al. Real time plasmonic qPCR: how fast is ultra-fast? 30 cycles in 54 seconds. *Analyst*. (2017) 142:1746–55. doi: 10.1039/C7AN00304H
134. Jie J, Hu S, Liu W, Wei Q, Huang Y, Yuan X, et al. Portable and battery-powered PCR device for DNA amplification and fluorescence detection. *Sensors*. (2020) 20:2627. doi: 10.3390/s20092627
135. Liu R, Ye X, Cui T. Recent progress of biomarker detection sensors. *Research*. (2020) 2020:7949037. doi: 10.34133/2020/7949037

Conflict of Interest: The authors declare that the research was conducted in the absence of any commercial or financial relationships that could be construed as a potential conflict of interest.

frontiers in Neurology

REVIEW
published: 15 March 2021
doi: 10.3389/fneur.2021.593582

Stroke Treatment With PAR-1 Agents to Decrease Hemorrhagic Transformation

Patrick D. Lyden[1], Kent E. Pryor[2], Jennifer Minigh[3], Thomas P. Davis[4], John H. Griffin[5], Howard Levy[6] and Berislav V. Zlokovic[1]*

[1] Department of Physiology and Neuroscience, Keck School of Medicine, Zilkha Neurogenetic Institute, University of Southern California, Los Angeles, CA, United States, [2] ZZ Biotech LLC, Houston, TX, United States, [3] inSeption Group LLC, Lansdale, PA, United States, [4] Department of Medical Pharmacology, University of Arizona College of Medicine, Tucson, AZ, United States, [5] Department of Molecular Medicine, The Scripps Research Institute, La Jolla, CA, United States, [6] Howard Levy Consulting LLC, Hopewell, NJ, United States

Ischemic stroke is the most widespread cause of disability and a leading cause of death in developed countries. To date, the most potent approved treatment for acute stroke is recanalization therapy with thrombolytic drugs such as tissue plasminogen activator (rt-PA or tPA) or endovascular mechanical thrombectomy. Although tPA and thrombectomy are widely available in the United States, it is currently estimated that only 10–20% of stroke patients get tPA treatment, in part due to restrictive selection criteria. Recently, however, tPA and thrombectomy selection criteria have loosened, potentially allowing more patients to qualify. The relatively low rate of treatment may also reflect the perceived risk of brain hemorrhage following treatment with tPA. In translational research and a single patient study, protease activated receptor 1 (PAR-1) targeted therapies given along with thrombolysis and thrombectomy appear to reduce hemorrhagic transformation after recanalization. Such adjuncts may likely enhance the availability of recanalization and encourage more physicians to use the recently expanded selection criteria for applying recanalization therapies. This narrative review discusses stroke therapies, the role of hemorrhagic transformation in producing poor outcomes, and presents the data suggesting that PAR-1 acting agents show promise for decreasing hemorrhagic transformation and improving outcomes.

Keywords: hemorrhagic transformation, ischemic stroke, tissue plasminogen activator, intracranial hemorrhage, activated protein C, stroke therapy, thrombectomy, bleeding

OPEN ACCESS

Edited by:
Thiruma Valavan Arumugam, La Trobe University, Australia

Reviewed by:
Asaf Honig, University of British Columbia, Canada
David Howells, University of Tasmania, Australia

****Correspondence:***
Patrick D. Lyden
plyden@usc.edu

Specialty section:
This article was submitted to Stroke, a section of the journal Frontiers in Neurology

Received: *11 August 2020*
Accepted: *08 February 2021*
Published: *15 March 2021*

Citation:
Lyden PD, Pryor KE, Minigh J, Davis TP, Griffin JH, Levy H and Zlokovic BV (2021) Stroke Treatment With PAR-1 Agents to Decrease Hemorrhagic Transformation. Front. Neurol. 12:593582. doi: 10.3389/fneur.2021.593582

INTRODUCTION

Each year about 795,000 people in the United States experience a stroke (1). Of all types of stroke, 87% are ischemic (i.e., caused by an interruption of blood supply), 10% are intracerebral hemorrhage strokes (i.e., caused by a ruptured blood vessel), and 3% are subarachnoid hemorrhage strokes (bleeding into the outermost layer of the brain) (2). Ischemic stroke is the most widespread cause of disability and a leading cause of death in developed countries (3).

The most potent treatment for stroke is recanalization, that is, treatment with intravenous thrombolytics, mechanical revascularization (removal of the clot) known as intra-arterial thrombectomy (IAT), or both. Not all patients respond fully to recanalization; therefore, adjunctive

cytoprotective treatments are needed and many development efforts are ongoing to overcome the long history of failed neuroprotection trials (likely due to lack of recanalization documentation). Agents acting on the protease activated receptor 1 (PAR-1) exhibit pleiotropic actions on neurons, glia, and cerebral vascular cells, including cytoprotection and anti-inflammation (4). In the RHAPSODY trial, the PAR-1 acting drug 3K3A-APC appeared to reduce hemorrhagic transformation (5).

In 2015, several successful trials proved the efficacy of IAT for acute ischemic stroke with large vessel occlusions (6–10). Then, it was shown that multimodal imaging permits clinicians to select patients for IAT with great success. Recently, the feasibility of combining IAT with a putative cytoprotectant has been shown in 2 trials. The RHAPSODY trial was the first to include IAT in the clinical trial of a cytoprotectant (5). A larger recent trial allowed IAT use, but only in patients with evidence of good collateral flow (11). These results confirm that recanalization may powerfully influence the effect of putative cytoprotectants.

Stroke continues to be a major public health concern despite significant previous research that has produced treatment approaches addressing acute reperfusion and revascularization (12–14), neuronal protection (12), and regeneration of damaged brain tissue (15, 16). All these tactics were based on scientific principles and preclinical data, yet no candidate cytoprotective therapy has successfully entered clinical practice (15). It is now clear that single-action, single-target agents fail to treat stroke because ischemia produces a combination of pathologic pathways proceeding in parallel that damage neural tissue (17).

This narrative review presents a discussion of stroke therapies, the role of hemorrhagic transformation in producing poor outcomes, and presents the data suggesting that PAR-1 acting agents show promise for decreasing hemorrhagic transformation and improving outcomes.

STROKE THERAPY

Recanalization therapy with thrombolytic drugs such as recombinant tissue plasminogen activator (rt-PA or tPA) is the most common treatment for acute stroke. tPA is approved for intravenous administration within 3 h of onset of acute ischemic stroke in the United States and for up to 4.5 h following the stroke in Europe (1, 18). Thrombolytic therapy with intravenous tPA beyond 4.5 h in select subjects with diffusion/fluid attenuated inversion recovery mismatch on magnetic resonance imaging (MRI) is also recommended, but less frequently possible (19). The most widely feared adverse effect of tPA is symptomatic intracranial hemorrhage (SICH; 3–6%); other risks include systemic bleeding, myocardial rupture (when used to treat acute myocardial infarction), and, in rare cases, anaphylaxis, or angioedema (20). Although tPA is widely available in the United States, only 10–20% of stroke patients receive such treatment (21, 22), primarily because patients may present with mild deficits, are beyond 4.5 h after onset, have conditions or concomitant medications that increase bleeding risk, or for other reasons.

Another effective (however, less frequently used) recanalization therapy for stroke is mechanical thrombectomy (7–9, 23). Use of mechanical thrombectomy (with or without tPA) is considered standard-of-care treatment in patients with documented large vessel occlusion, defined as thromboembolic blockage of the distal internal carotid artery, the M1 or proximal M2 portions of the middle cerebral artery, or the proximal anterior cerebral artery. As shown in **Table 1**, several well-controlled randomized clinical trials showed benefit following combination therapy of thrombectomy and tPA. In some of these trials, however, patients benefited who were ineligible for tPA and were treated with thrombectomy alone. With careful imaging selection, recanalization with thrombolysis or thrombectomy may be successful as late as 16 or 24 h after last known well time (12, 25, 26).

Although recent trials suggest that recanalization therapy for stroke offers great promise, there remains a very large unmet need to reduce stroke-related deficit and ensure improved outcomes. First, not all patients treated with thrombolysis or thrombectomy recover full function. Second, the risk of hemorrhage after recanalization therapies dissuades some practitioners from using them. Thus, adjuvant cytoprotectants are needed to complement recanalization therapies in such patients, or to provide improved outcomes in patients unable to receive thrombolytic or thrombectomy therapy. In past clinical trials that did not include mechanical thrombectomy as a treatment option, it is likely that many patients failed to reperfuse; the candidate adjuvant cytoprotectants may therefore have appeared less likely to benefit the patients. In modern clinical stroke trial design, candidate adjuvant therapy is studied in concert with recanalization. In patients with large vessel occlusion, more than 80% receiving mechanical thrombectomy do recanalize. In patients without documented large vessel occlusion, thrombolytic therapy alone is generally sufficient to reperfuse the microvasculature.

HEMORRHAGIC TRANSFORMATION

Hemorrhagic transformation (HT) is a consequence of ischemic blood–brain barrier breakdown that occurs mainly within 2 weeks of ischemic stroke (27). Following an acute stroke, the cerebral vasculature is damaged, which increases the risk for HT.

The presentation of HT includes minor petechial bleeding (hemorrhagic infarct) and large mass-producing hemorrhages (parenchymal hematoma). Intracranial hemorrhages are classified by both imaging characteristics and the presentation of clinical worsening.

Radiologic classification uses the location and extent of hemorrhage to distinguish among hemorrhage subtypes (see **Table 2**).

Symptomatic vs. Asymptomatic Hemorrhagic Transformation

In addition to radiologic classification, intracranial hemorrhages are labeled asymptomatic, or symptomatic based on an accompaniment of observable neurologic decline.

TABLE 1 | Summary of mechanical thrombectomy study outcomes.

Study	Percent achieving reperfusion	mRS 0–2	SICH	Mortality
ESCAPE (7) $N = 238$	72.4%[a] [31.2%][b]	53% [29.3%] $p < 0.001$	3.6% [2.7%] $p = 0.75$	10.4% [19.0%] $p = 0.04$
EXTEND-IA (8) $N = 70$	89%[c] [34%][c] $p < 0.001$	71% [40%] $p = 0.01$	0% [6%]	9% [20%]
MR CLEAN (9) $N = 500$	58.7%[a] [57.5][b]	32.6% [19.1%] (95% CI: 5.9–21.2)	7.7% [6.4%]	21% [22%]
REVASCAT (10) $N = 206$	65.7%[a] [Not Reported]	43.7% [28.2%][e] (95% CI: 1.1–4.0)	1.9% [1.9%][e] $p = 1.00$	18.4% [15.5%][e] $p = 0.60$
SWIFT PRIME (23) $N = 196$	82.8%[d] [40.4%][d] $p < 0.0001$	60.2% [35.5%] $p = 0.0008$	1.0% [3.1%] $p = 0.37$	9.2% [12.4%] $p = 0.50$
THRACE (24) $N = 414$	-	-	3 (2%) of 192 [f]; $p = 0.71$	27 (13%) of 206; $p = 0.70$

IV, intravenous; mRS, modified Rankin Scale; SICH, symptomatic intracranial hemorrhage; tPA, tissue plasminogen activator. Data are displayed as Mechanical Thrombectomy Arm [tPA-only Control Arm].

[a]Defined as achieving thrombolysis in cerebral infarction score of 2b or 3.

[b]Defined as achieving modified arterial occlusive lesion score of 2 or 3.

[c]Defined as reperfusion >90% without SICH.

[d]Defined as reperfusion ≥90%.

[e]23 of 103 control subjects did NOT receive IV tPA treatment.

[f]SICH at 24 h.

TABLE 2 | Anatomic descriptions of intracranial hemorrhages according to the heidelberg bleeding classification (28).

Class	Type and description
1	**Hemorrhagic transformation of infarcted brain tissue**
1a	HI1 Scattered small petechia, no mass effect
1b	HI2 Confluent petechia, no mass effect
1c	PH1 Hematoma within infarcted tissue, occupying <30%, no substantive mass effect
2	**Intracerebral hemorrhage within and beyond the infarcted brain tissue**
	PH2 Hematoma occupying ≥30% of the infarcted tissue, with obvious mass effect
3	**Intracerebral hemorrhage outside the infarcted brain tissue or intracranial-extracerebral hemorrhage**
3a	Parenchymal hematoma remote from infarcted brain tissue
3b	Intraventricular hemorrhage
3c	Subarachnoid hemorrhage
3d	Subdural hemorrhage

HI, hemorrhagic infarction; PH, parenchymatous hematoma.

The term SICH was first used by Levy et al. (29). The National Institute of Neurological Disorders and Stroke (NINDS) trials, defined SICH as "any hemorrhagic transformation temporally related to any worsening in neurologic condition (30)."Over the next 2 decades, this definition was recognized as over-inclusive. Other groups such as the Safe Implementation of Thrombolysis in Stroke-Monitoring Study (SITS-MOST) investigators (31), the European Cooperative Acute Stroke Study (ECASS) II and III investigators (18, 32), and the International Stroke Trial-3 (IST-3) investigators (33) have sought more comprehensive definitions of SICH. Widely used definitions are the SITS-MOST and ECASS II:

- SITS-MOST definition of SICH: Local or remote parenchymatous hematoma (PH)-2 with a worsening (i.e., increase of ≥4) on the National Institutes of Health Stroke Scale (NIHSS) score.
- ECASS II definition of SICH: Any intracranial hemorrhage with a clinical worsening (indicated by clinical deterioration or adverse events) or causing a worsening (i.e., increase of ≥4) in NIHSS score.

Asymptomatic intracranial hemorrhage (AICH) does not have a rigorous definition like SICH. In general, it is described as an imaging-documented brain bleed without a concomitant marked deterioration in the patient's neurologic state observable using a neurological rating scale. Thus, the descriptor "asymptomatic" is a misnomer, as the patient very well may exhibit subtle findings, or more robust findings were they to be examined weeks or months later. In many studies, AICH classification is generally not included so that when meta-analyses are performed, those patients with AICH can only be identified as those patients not having SICH. To complicate matters, there are only a handful of studies that specifically enroll subjects with AICH.

Symptomatic Hemorrhage—Clearly a Detriment

Regardless of how SICH is defined, it is consistently associated with worse clinical outcomes (34, 35). Hao et al. (34) reported that patients with and without SICH differed significantly using the modified Rankin score (mRS) scores (odds ratio: 1.45; 95% confidence interval [CI]: 1.10–1.81), 90-day mortality (higher in patients with SICH [65.3%] vs. without [18.8%]; $p < 0.001$); furthermore, favorable neurological outcome (defined as mRS 0–2) at 90 days was proportionally lower in patients with SICH (8.9%) than without (51.2%) ($p < 0.001$).

Asymptomatic Hemorrhage—Likely a Detriment as Well

Whether AICH fosters a negative prognosis remains controversial. Some studies confirmed that AICH has a negative effect on functional outcome. Although there is little clinical trial information regarding possible adverse effects of AICH, the limited available evidence indicates it may not be harmless.

In a study by Kent et al. (36), patients with AICH tended toward worse outcomes, even after adjusting for other prognostic variables (odds ratio: 0.69); however, this trend did not reach statistical significance. The investigators cautioned against concluding that AICH are clinically innocuous based on a lack of statistical effect.

Dzialowski et al. (37) used data obtained from the Canadian Alteplase for Stroke Effectiveness Study to investigate the association between HT type and functional outcome. The authors concluded that the likelihood of a poor outcome following thrombolysis was associated with the extent of hemorrhage. The proportion of patients with a good outcome was 41% with no HT, 30% with HI-1, 17% with HI-2, 15% with PH-1, and 7% with PH-2 ($p < 0.0001$). Although HI-1 was not a predictor of outcome, other types of bleeds were after adjusting for covariates: HI-2 (odds ratio: 0.38; 95% CI: 0.17–0.83), PH-1 (odds ratio: 0.32; 95% CI: 0.12–0.80), and PH-2 (odds ratio: 0.14; 95% CI: 0.04–0.48), thereby suggesting that HI grades of hemorrhagic transformation may not be benign.

Park et al. (38) who sought to determine the impact of asymptomatic hemorrhage transformation on the 3-month outcome, found the odds of a worse outcome were increased by a factor of 2 in patients with AICH compared with those without after acute ischemic stroke. The crude and adjusted odds ratios of AICH for an increment of mRS score at 3 months were 2.94 (95% CI: 2.05–4.24) and 1.90 (95% CI: 1.27–2.82), respectively.

Lei et al. (39) examined whether AICH affects risk of stroke recurrence and a long-term poor outcome. Both SICH and AICH post acute ischemic stroke impacted long-term clinical outcomes. Moreover, patients with SICH or AICH suffered a lower survival rate than did patients without HT in the 1st year following stroke ($p < 0.001$). The investigators suggested that AICH should not be considered clinically innocuous.

In acute ischemic stroke patients undergoing thrombectomy, AICH appeared to be associated with high mortality and worse functional outcomes (40). Specifically, AICH appeared to result in lower odds of functional independence (61.9% of patients without AICH and 35.9% with AICH achieved functional independence at the 3-month follow-up; adjusted $p = 0.117$) and higher odds of deaths (35.9% of patients with AICH vs. 11.1% without AICH died; adjusted $p = 0.015$).

Hao et al. (41) reported that in an Asian population, patients with AICH after endovascular treatment had a lower ratio of excellent outcome (odds ratio: 0.53; 95% CI: 0.33–0.84; $p = 0.007$) compared with patients without ICH. According to the researchers: "Considering the relatively higher incidence (33.5%) and negative impacts on functional outcomes in this study, AICH after endovascular treatment may not be innocuous."

In a recent study, Li et al. (42) evaluated the prevalence of previous chronic cerebral hemorrhage, especially asymptomatic cases, and the associated factors in patients who experienced an acute ischemic stroke. Overall, 9.4% of patients were determined to have had a previous chronic cerebral hemorrhage, with almost half of these being asymptomatic, indicating that previous chronic cerebral hemorrhage is not uncommon in acute ischemic stroke patients. Furthermore, there were no differences in the clinical characteristics of symptomatic vs. asymptomatic previous chronic cerebral hemorrhage, which complicates the detection of asymptomatic hemorrhage, and according to the authors, could increase the risk of re-bleeding.

While AICH may not be associated with acute observable neurologic deterioration, its presence may undermine long-term neurological functions. As the red blood cells in the microbleeds break down over the following days to weeks, neural toxic effects can emerge including heme-induced cerebral inflammation, neuronal apoptosis, and demyelination (43, 44).

Although many studies report the rate of AICH to be ∼10% (30, 45, 46), other studies indicate the rate may be as high as 30–40% when using CT scan (24, 34, 47). AICH occurs at a sufficient frequency such that hemorrhages initially presenting as asymptomatic can eventually result in substantial complications, cause an increase in hospital length of stay, lead to poorer long-term outcomes, and incur higher healthcare costs (48); thus, any bleeding, asymptomatic or not, is a concern following stroke.

APC AND APC ANALOGS

A promising approach for stroke therapy is based on recently discovered biological properties of APC, which is an endogenous plasma protease with multiple properties including antithrombotic action, cytoprotective propensity, and anti-inflammatory activity in the brain and spinal cord (4). Based on known cellular and molecular mechanisms, an APC approach showed promise in experiments consistent with Stroke Therapy Academic Industry Roundtable and other guidelines (49). Wildtype APC shows potent anticoagulant effects along with cytoprotection and reduced inflammation, and anticoagulants often carry an increased risk for serious bleeding. Therefore, protein engineering of APC was undertaken to reduce bleeding risk.

Signaling-selective APC analogs were engineered to retain normal cell-signaling activity (50–53) but to have greatly

diminished anticoagulant activity (<10%) (54), thereby reducing *in vivo* risk for bleeding compared with wildtype APC (55–57).

An engineered form of APC, called 3K3A-APC reflecting lysine to alanine substitutions at positions 191, 192, and 193, offers advantages over wildtype APC (4, 53, 58, 59). 3K3A-APC is a 405-residue APC variant engineered to maximize neuroprotective and cytoprotective activities and minimize anticoagulant activity. It was developed by altering factor Va binding exosites (reducing anticoagulation) on APC without modifying the exosites that recognize and bind to the G-protein coupled receptors, protease-activated receptor 1 (PAR-1), and PAR-3. This mutant retains the cytoprotective cell-signaling effects of native (wildtype) APC but has >90% less of the wildtype anticoagulant effects (54). Glycosylation of recombinant 3K3A-APC differs from wildtype APC because it is expressed in Chinese hamster ovary cells.

Anticoagulants do not improve outcome following stroke (60–62). Thus, the residual anticoagulant activity of 3K3A-APC is not responsible for the benefits seen in animal models (63).

RATIONALE FOR APC AND APC ANALOGS IN TREATING STROKE

APC is an endogenous serine protease with systemic anticoagulant activity as well as cell-signaling actions that convey endothelial stabilizing, anti-inflammatory, and anti-apoptotic activities, and that promote neurogenesis (59, 64–67). APC is normally generated *in vivo* from zymogen protein C through activation by thrombin on the surface of endothelial cells. This activation requires 2 membrane receptors: the thrombomodulin receptor (which binds thrombin) and the endothelial protein C receptor (which binds protein C). The

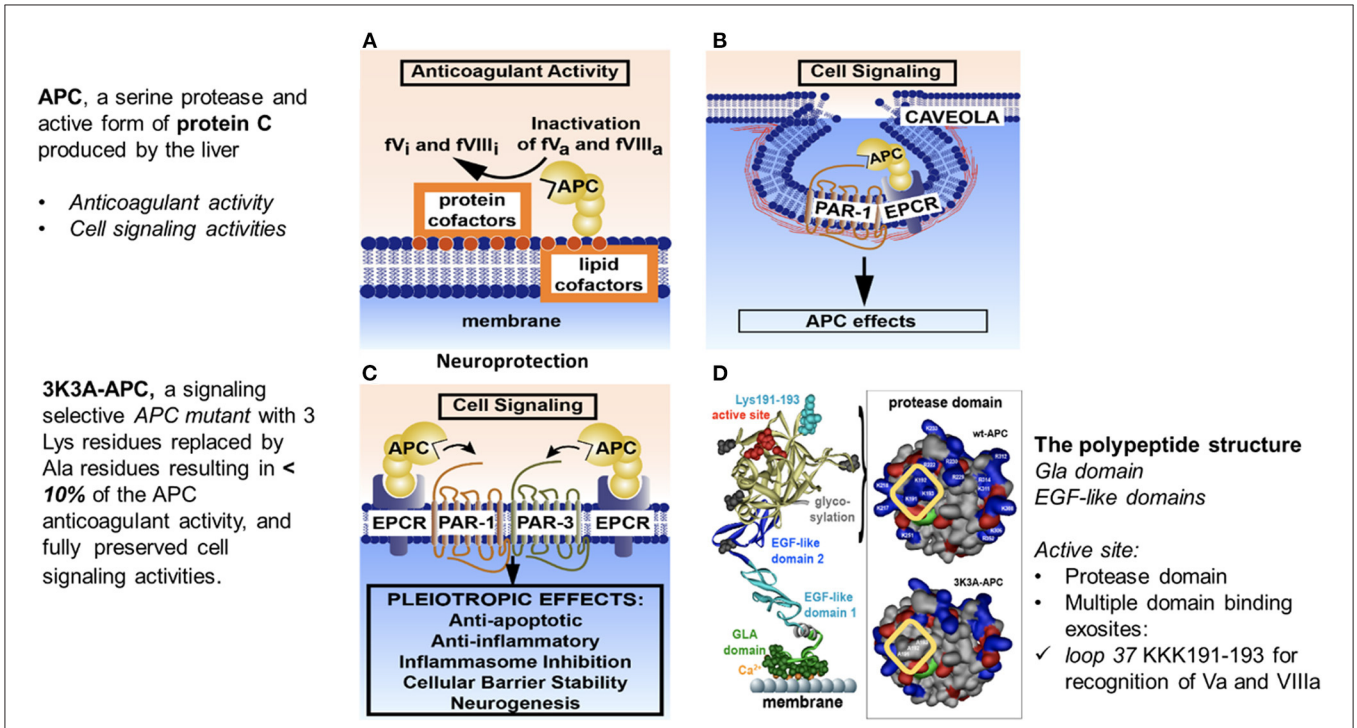

FIGURE 1 | Anticoagulant and cell-signaling pathways of APC and the structure of signaling-selective 3K3A-APC. APC, activated protein C; BBB, blood–brain barrier; EGF, endothelial growth factor; EPCR, endothelial protein C receptor; GLA, gamma-carboxyglutamic acid; PAR, protease-activated receptor. Reprinted from blood, vol. 132(2), Griffin et al. (67) activated protein C, protease activated receptor 1 and neuroprotection; 159–169, 2018, with permission from the American Society of Hematology. **(A)** Anticoagulant activity of APC involves the proteolytic inactivation of factors Va and VIIIa on membrane surfaces containing phospholipids that are derived from cells, platelets, lipoproteins, or cellular microparticles. The irreversible inactivation of factors Va and VIIIa to yield inactive factors Vi and VIIIi by APC is accelerated by a variety of lipid and protein cofactors (e.g., glucosyl ceramide, protein S, etc). **(B)** Beneficial direct effects of APC on cells require the EPCR and PAR-1. One distinction between pro-inflammatory thrombin signaling and cytoprotective APC signaling is the localization of APC signaling in the caveolin-1–rich microdomains (caveolae). **(C)** Neuroprotective mechanisms for APC effects on cells may also involve other receptors including PAR-3. APC-initiated signaling effects on cells can include anti-apoptotic activities, anti-inflammatory activities, inhibition of the inflammasome, stabilization of endothelial barrier functions, including the BBB, and neurogenesis. **(D)** The polypeptide structure of APC comprises an N-terminal GLA domain (green) that binds to negatively charged lipids and EPCR, 2 EGF-like domains (light blue and dark blue), and the protease domain containing the active site triad of serine, histidine, and aspartic acid residues (red). Four glycosylation sites are indicated by gray-shaded moieties. Substrate selectivity of this protease is determined by interactions between the targeted substrates and the active site and also by multiple unique binding exosites on APC that vary for different substrates. The protease domain space–filled model (see insert in D) highlights in the yellow box 3 positively charged lysine (K) residues within the so-called 37 loop (KKK 191–193), which is an exosite for APC's recognition of factors Va and VIIIa. Mutation of these 3 lysine residues to alanine (3K3A-APC) reduces APC's anticoagulant activity by >90% but does not affect its interactions with the cytoprotective substrates, PAR-1, PAR-3, or its other known cell-signaling receptors. Thus, 3K3A-APC is very "signaling-selective".

multiple properties of APC should combine in reversing the effects of an ischemic stroke and in protecting ischemic brain tissue from further damage.

The anticoagulant activity of APC is independent of its direct cellular effects and is mediated by irreversible proteolytic degradation of factors Va and VIIIa with contributions by other cofactors. Its cytoprotective cell-signaling activities require multiple cell-surface receptors and, in most cases, proteolytic activation of PAR-1 (**Figure 1**) (51, 59, 65–68).

The cellular signaling by APC gives rise to cytoprotective alterations in gene expression profiles resulting in multiple cytoprotective actions due to anti-inflammatory and anti-apoptotic activities, as well as a reduction of endothelial barrier disruption (**Figures 1**, **2**) (70–74). APC crosses the blood brain barrier *via* an active transport mechanism (75).

For 3K3A-APC cytoprotective actions in murine preclinical ischemic stroke studies, not only is PAR-1 required but also the arginine 46 residue in PAR-1. The requirement for arginine 46 strongly supports the concept that APC cytoprotection requires "biased" signaling initiated by the G-protein coupled receptor PAR-1 (50, 68). Activation of PAR-1 by APC occurs after proteolysis of the PAR-1 extracellular N-terminal domain at arginine 46, producing a tethered ligand peptide that begins at asparagine 47 causing APC biased, β-arrestin-2-dependent cytoprotective signaling (**Figure 3**) (50, 68, 76–79). In contrast, activation of PAR-1 by thrombin involves cleavage at arginine 16, which generates thrombin-receptor activated peptide, a tethered ligand peptide that begins at residue 42, initiating cytotoxic effects *via* G-protein-dependent signaling and causing human platelet activation, pro-inflammatory changes, endothelial vascular leakage and CNS toxicity (67, 68, 80). PAR-1-tethered ligand peptides beginning at asparagine 47, but not those beginning at amino acid 42, exert cytoprotective effects (**Figure 3**) (68). Similarly, APC activates human PAR-3 by non-canonical cleavage at arginine 41, whereas thrombin cleaves PAR-3 at lysine 38 (81). PAR-3-tethered ligand peptides beginning at amino acid 42, but not those beginning at amino acid 39, exert cytoprotective effects (82), suggesting that human PAR-3 cleavage at arginine 41 by APC causes cytoprotection, whereas PAR-3 cleavage at lysine 38 initiates thrombin-like cytotoxic pro-inflammatory effects (82).

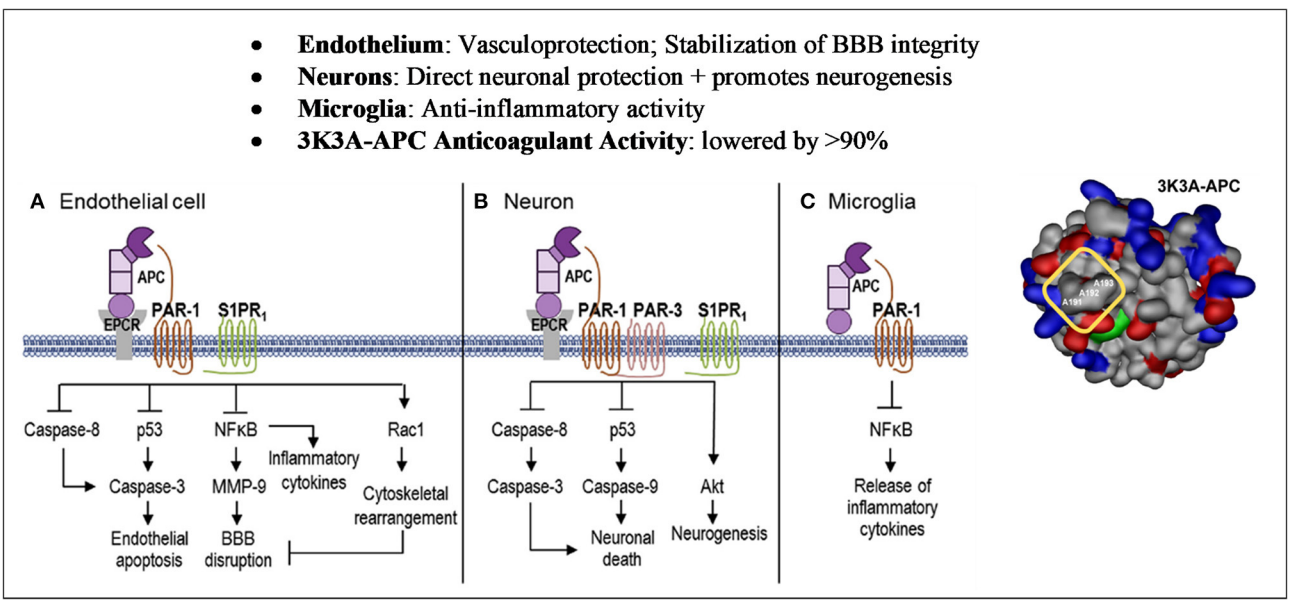

FIGURE 2 | Cell-Specific APC protective signaling pathways. Akt, protein kinase B; APC, activated protein C; BBB, blood–brain barrier; EPCR, endothelial protein C receptor; MMP, matrix metallopeptidase; NFkB, nuclear factor kappa-light-chain-enhancer of activated B cells; PAR, protease-activated receptor; Rac1, Ras-related C3 botulinum toxin substrate 1; S1PR1, sphingosine 1-phosphate receptor 1. Reprinted from neuropharmacology, vol. 134, Amar et al. (69) can adjunctive therapies augment the efficacy of endovascular thrombolysis? A potential role for activated protein C, 293–301, 2018, with permission from Elsevier. 3D structure reprinted from blood, vol. 132(2), Griffin et al. (67) activated protein C, protease activated receptor 1 and neuroprotection; 159–169, 2018, with permission from the American Society of Hematology. **(A)** In endothelial cells, APC helps to seal the BBB and is vasculoprotective. APC/EPCR activates PAR-1 and inhibits caspase-8 activation of caspase-3, thereby limiting the extrinsic apoptotic pathway in endothelium. APC/EPCR-dependent PAR-1 activation suppresses the pro-apoptotic p53 transcription factor inhibiting caspase-3 activation blocking the intrinsic apoptotic pathway. Also, APC suppresses the NFkB-dependent transcriptional activation of MMP-9, thereby blocking degradation of the BBB basement membrane. Furthermore, APC blocks the expression of pro-inflammatory cytokines, limiting inflammation by controlling NFkB nuclear translocation. APC's cytoprotective effects on endothelial cells require EPCR and PAR-1 to cross-activate S1PR1. Cross-activation of S1PR1 activates Rac1, leading to stabilization of the BBB cytoskeleton, thereby supporting the integrity of the BBB. **(B)** In neurons, APC/EPCR is cytoprotective *via* PAR-1 and PAR-3, which inhibits caspase-8 upstream of caspase-3 and thereby limits the extrinsic apoptotic pathway. Also, an APC-PAR-1-PAR-3 pathway blocks p53 activation in injured neurons, thereby blocking the caspase-9-dependent intrinsic apoptotic pathway. Furthermore, APC promotes neurogenesis *via* a PAR-1-PAR-3-S1PR1-Akt pathway. **(C)** APC's inhibition of NFkB-dependent transcriptional expression of different pro-inflammatory cytokines suppresses microglial activation. Suppression of NLRP3 inflammasome development by APC is another activity but is not shown in this figure.

STUDIES WITH THE APC ANALOG 3K3A-APC

Signaling-selective APC analogs, such as 3K3A-APC, were engineered to retain normal cell-signaling activity (50–53) but to have greatly diminished anticoagulant activity (54), thereby reducing *in vivo* risk for bleeding compared with wildtype APC (55–57). In *in vitro* assays, 3K3A-APC retains the cytoprotective activity of recombinant wildtype APC but has <10% of its anticoagulant activity (e.g., see **Table 3**) (54).

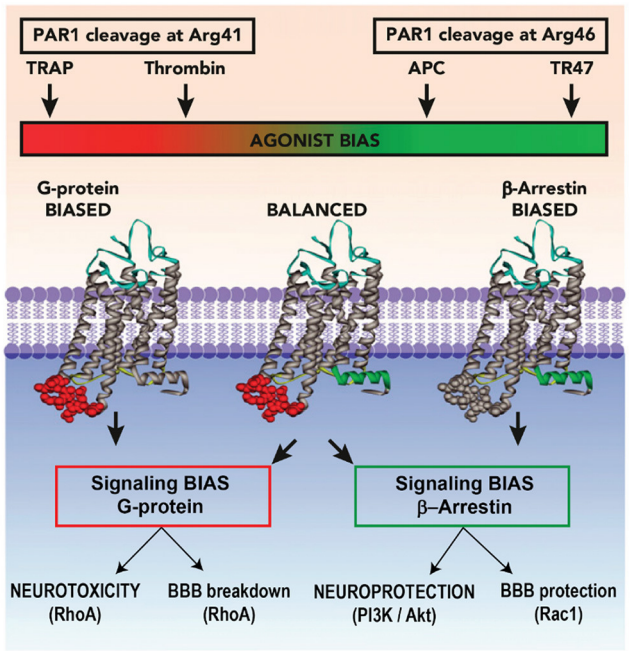

FIGURE 3 | Biased Agonism of PAR-1 by APC. Akt, protein kinase B; APC, activated protein C; BBB, blood–brain barrier; PAR, protease-activated receptor; P13K, phosphoinositide 3-kinase; Rac, Ras-related C3 botulinum toxin substrate; RhoA, ras homolog gene family member A; TRAP, thrombin-receptor activated peptide. Reprinted from Blood, vol. 120(26), Mosnier et al. (68) biased agonism of protease-activated receptor 1 by activated protein C caused by noncanonical cleavage at Arg46; 5237–5246, 2012, with permission from the American Society of Hematology. Activation of PAR-1 by APC and its cytoprotective analogs involves cleavage of PAR-1 N-terminal domain at Arg46, which reveals a tethered ligand peptide that begins at Asn47 causing APC's biased, β-arrestin-2-dependent cytoprotective signaling. Activation of PAR-1 by thrombin involves cleavage at Arg41, which generates a tethered ligand that begins at Thr42, initiating cytotoxic effects *via* G-protein-dependent signaling causing human platelet activation, inflammatory changes, vascular leakage, and CNS toxicity.

The effects of 3K3A-APC on the fibrinolytic activity of tPA has also been studied *in vitro*; no statistically significant effects were noted when rt-PA was applied to induce clot lysis in the presence of either wildtype APC or 3K3A-APC (83).

3K3A-APC has beneficial effects in rodent models of stroke (50, 55–57, 72, 84–89), brain trauma (90, 91), amyotrophic lateral sclerosis (92–94), multiple sclerosis (95) and Alzheimer's disease (96), as well as ischemic injury of heart, kidney or liver, organ transplant, total body radiation, diabetes, sepsis, and wound healing (59, 67). In the CNS, PAR-1 and PAR-3 are both necessary for neuronal protection by APC (84, 85, 92), PAR-1 and endothelial protein C receptor for vasculoprotection and stabilization of the blood–brain barrier (4, 67, 69, 71–73, 84, 85, 97, 98), and PAR-1 for suppression of microglia activation and anti-inflammatory activity.[4,66,91,94] The extensive preclinical studies of the cytoprotective actions of APC and 3K3A-APC have been summarized in several reviews (**Figure 2**) (4, 59, 65–67, 69, 99).

In studies with human progenitor and fetal neural cells, 3K3A-APC promoted neurogenesis *in vitro* (52) as well as *in vivo* using a mouse middle cerebral artery occlusion (MCAO) stroke model (57).

3K3A-APC acts synergistically with tPA in both mouse and rat stroke models (55). tPA alone or in combination with 3K3A-APC, was administered 4 h after MCAO, followed by 3K3A-APC for 3–4 consecutive days afterward. In this delayed treatment paradigm, tPA alone had no beneficial effects on infarct volume, or behavior (neurological score, foot-fault, forelimb asymmetry, adhesive removal) compared with controls. In contrast, the combination of tPA plus 3K3A-APC as compared with control significantly reduced infarct volume at 24 h (65% reduction) and at 7 days (63% reduction) following MCAO in mice and at 7 days (52% reduction) after embolic stroke in rats ($p < 0.05$). Furthermore, the combination significantly improved behavioral outcomes and eliminated tPA-related intracerebral microhemorrhages ($p < 0.01$–0.05).

These positive effects of 3K3A-APC extend to elderly animals and animals with comorbidities such as might be seen in the target patient population of this study. 3K3A-APC alone

TABLE 3 | Cytoprotective and anticoagulant activity of recombinant wildtype APC vs. 3K3A-APC.

APC type	Anticoagulant activity (% rwt)[a]	Cytoprotective activity (% rwt)[b]	Cytoprotective to anticoagulant ratio
Recombinant wildtype APC	100	100	1.0
3K3A-APC	4.6[c]	114[c]	25

APC, activated protein C; rwt, recombinant wildtype.
[a] *Based on the activated partial thromboplastin time dose-response.*
[b] *Derived from the concentrations of APC required for half-maximal inhibition of apoptosis induced by the protein kinase inhibitor, staurosporine.*
[c] *From Mosnier et al. (54).*
Numbers for recombinant wildtype APC are definitional and represent the standard.

or with tPA was given 4 h after transient MCAO in aged female mice and 4 h after embolic stroke in spontaneously hypertensive rats (56). 3K3A-APC was then administered from 3 to 7 days afterward. Assessments included neurological scores, foot-fault, forelimb asymmetry, and adhesive removal. In both models, tPA alone given 4 h after stroke had no effect on infarct volume or behavior. Treatment with 3K3A-APC alone or 3K3A-APC in combination with tPA reduced the infarct volume determined at 7 days by 62–66% (MCAO in aged mice) and 50–53%, (embolic stroke in spontaneously hypertensive rats), as well as improved behavior ($p < 0.05$) and significantly reduced tPA-induced intracerebral microhemorrhages (**Figure 4**).

Overall, in preclinical studies, 3K3A-APC appears to have a reduced risk for bleeding and provides at least equivalent if not greater cytoprotection compared with recombinant wildtype APC in mouse models of stroke. When 3K3A-APC is combined with tPA, infarct volumes are reduced and intracerebral microhemorrhages are greatly reduced and/or eliminated. At the same time, behavioral outcomes in both mouse and rat models of

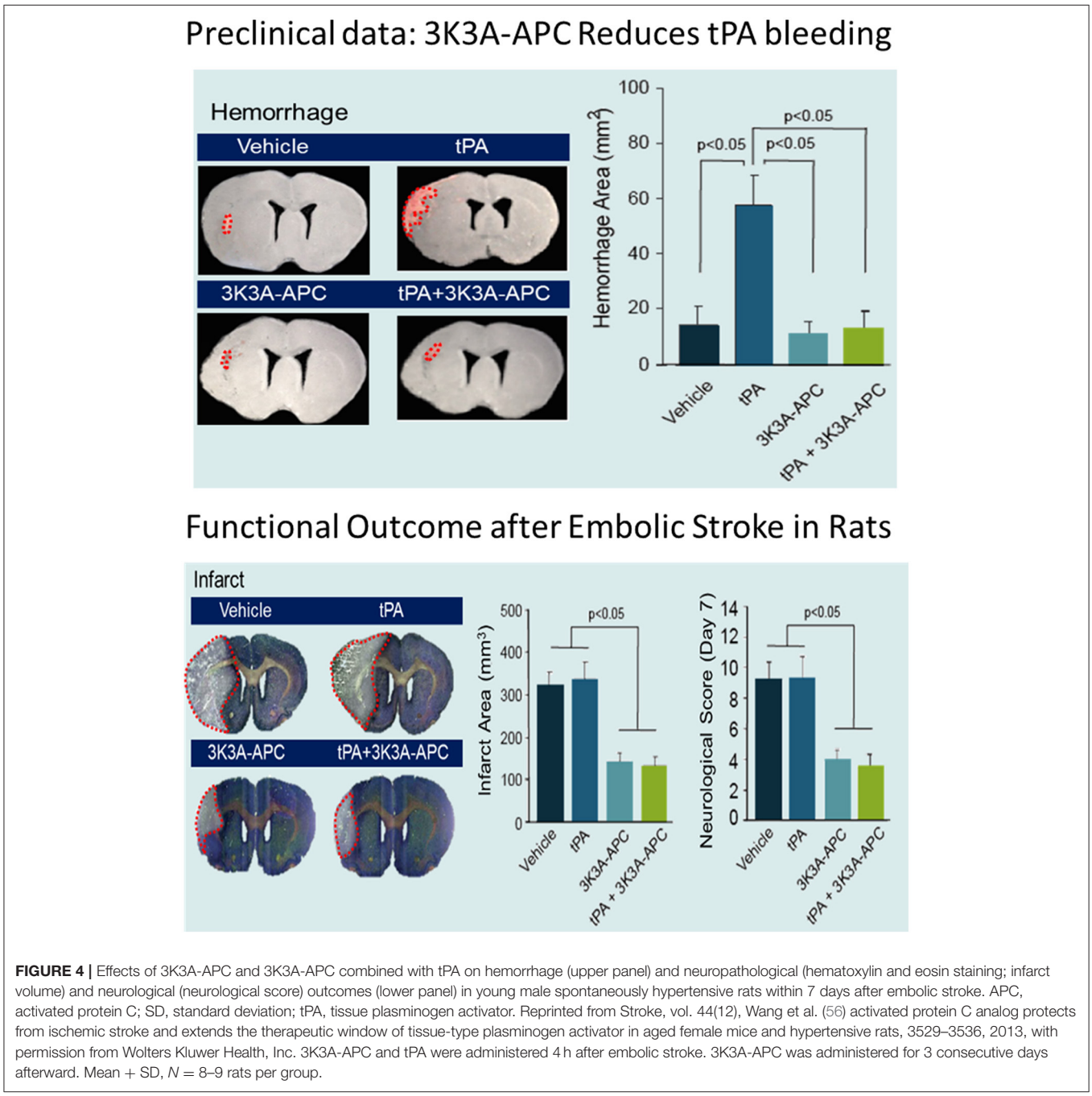

FIGURE 4 | Effects of 3K3A-APC and 3K3A-APC combined with tPA on hemorrhage (upper panel) and neuropathological (hematoxylin and eosin staining; infarct volume) and neurological (neurological score) outcomes (lower panel) in young male spontaneously hypertensive rats within 7 days after embolic stroke. APC, activated protein C; SD, standard deviation; tPA, tissue plasminogen activator. Reprinted from Stroke, vol. 44(12), Wang et al. (56) activated protein C analog protects from ischemic stroke and extends the therapeutic window of tissue-type plasminogen activator in aged female mice and hypertensive rats, 3529–3536, 2013, with permission from Wolters Kluwer Health, Inc. 3K3A-APC and tPA were administered 4 h after embolic stroke. 3K3A-APC was administered for 3 consecutive days afterward. Mean + SD, $N = 8$–9 rats per group.

stroke are improved. Furthermore, 3K3A-APC expands the tPA therapeutic window, supporting further development of tPA and 3K3A-APC combination therapy (69, 99). Of note, the transient suture model of stroke that has been used in several of these studies closely mimics the clinical procedure of thrombectomy as recently reviewed (69, 99). This implies the combination of thrombectomy and 3K3A-APC for focal ischemic stroke in humans may be efficacious.

Currently, 3K3A-APC is in clinical development for stroke therapy and other indications (5).

NEED FOR A STROKE THERAPY WITH DECREASED BLEEDING

As previously mentioned, bleeding is a risk following stroke therapies. In a randomized, controlled trial in patients who had had an arterial occlusion, the control group received standard care alone (including the use of tPA) and the thrombectomy group received mechanical thrombectomy in addition to standard care (100). AICH was more common in the thrombectomy group (51%) compared with the control group (25%).

Although mechanical thrombectomy is associated with greater bleeding and despite tPA being widely available in the United States, it is currently estimated that only 10–20% of stroke patients get tPA treatment (21, 22). According to von Kummer in 2002 (101): "The risk of brain hemorrhage is the main argument of the European authorities not to approve rt-PA, and the fear of hurting patients with rt-PA explains some of its limited use in North America. The common argument is, 'Treatment with rt-PA may have some beneficial effect, but that is traded off by a considerable risk of symptomatic hemorrhage.'"

Fear of thrombolytic-related hemorrhage influences physicians away from treating stroke (102). To quantify the effect on physicians' prescribing behavior from fear that tPA will cause intracerebral bleeding, a biopharmaceutical company obtained focus group and survey data from a private polling service for its developmental therapy for stroke, 3K3A-APC. The market research firm interviewed 34 key opinion leaders and high-volume practitioners who were practicing stroke specialists, split evenly between the United States and Europe. The majority of interviewees were neurologists who routinely treat stroke patients at a comprehensive stroke center. Each interviewee received an honorarium for his or her time. The interviewees remained anonymous to the company and to each

TABLE 4 | Market research survey data from stroke specialists about stroke therapies.

Question	Unites States neurologists	Unites States ER physicians	Unites States total	Europe total	Total
What percentage of patients in your personal practice who are eligible for tPA receive tPA?	84%	54%	79%	87%	83%
What percentage of patients in your geographic area currently receiving tPA would receive 3K3A-APC?	93%	98%	94%	81%	88%
What percentage of patients in your personal practice currently not receiving tPA would receive the combination of tPA + 3K3A-APC were it available?	8%	13%	9%	5%	7%
What percentage of patients in your nation currently not receiving tPA would receive the combination of tPA + 3K3A-APC were it available?	17%	13%	16%	13%	15%

ER, emergency room; tPA, tissue plasminogen activator.

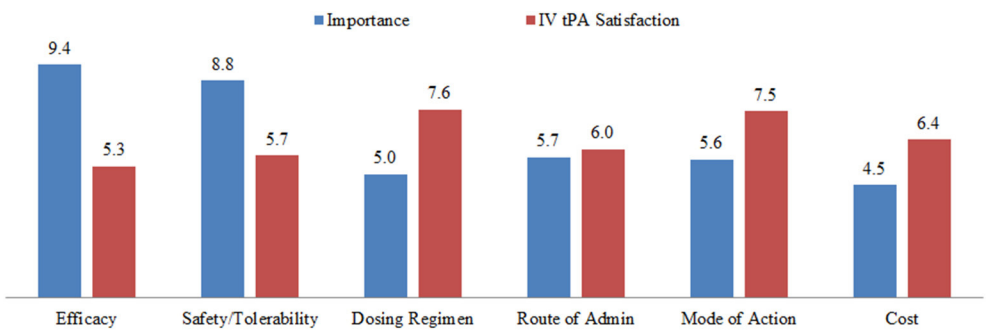

FIGURE 5 | Unmet medical needs concerning physician satisfaction with tPA therapy in the United States and Europe. IV, intravenous; tPA, tissue plasminogen activator. The terms in the figure were provided to the physician interviewees without further definitions, and interviewees were asked to rank each term on a 10-point scale. For importance: 0 = unimportant and 10 = essential. For satisfaction: 0 = fully unsatisfactory and 10 = entirely satisfactory. The numbers are mean responses of the 32 interviewees.

other. They were interviewed one-on-one over the telephone in November, 2014, using a formatted target product profile and standardized questionnaire. The interviews were digitally recorded for subsequent data capture and aggregation. See **Table 4** and **Figure 5**.

The interviews provided insights into physicians' perceptions of the relative importance of several aspects of tPA treatment, compared with their perceived satisfaction with the therapy (**Figure 5**). The data revealed that physicians perceive the "efficacy" of tPA to be very important (9.4/10) but not fully satisfactory (5.3/10). In contrast, the cost of the treatment was rated less important (4.5/10). Of most relevance to the present discussion, the "safety" of the drug was perceived to be very important, and rated an 8.8/10, but physicians are not satisfied with the current safety profile, giving a rating of 5.7/10. These data suggest that physicians perceive there to be a critical need for improving the safety of tPA for acute ischemic stroke.

Approximately 20% of interviewed physicians' patients eligible for intravenous (IV) tPA were not being prescribed IV tPA (**Table 4**) because of patient, family, or physician assessment that bleeding risk outweighed benefit (**Table 4**). However, the percentage of eligible patients not administered tPA was much higher in the emergency room setting (46%) relative to stroke centers (16%) (**Table 4**).

Physician responses suggest ∼90% of patients currently being prescribed IV tPA would also be prescribed 3K3A-APC (**Table 4**); according to the interviewers, many physicians stated it would be a requirement in their opinion to prescribe 3K3A-APC to those patients who received IV tPA.

CONCLUSION

Hemorrhagic transformation after ischemic stroke—even if labeled "asymptomatic"—may lead to long term disability and cognitive impairment. Fear of hemorrhagic transformation leads some physicians to hesitate to use indicated recanalization therapies. The PAR-1 acting agent, 3K3A-APC, reduces hemorrhagic transformation, and in animal models appears to improve long term outcomes after ischemic stroke. Agents that reduce hemorrhagic transformation may lead to wider acceptance of recanalization therapies and improved long-term outcome for ischemic stroke patients.

AUTHOR CONTRIBUTIONS

All authors contributed to the creation and revision of the manuscript, as well as read and approved the submitted version.

FUNDING

This work was supported by U24 NS113452 and R01 NS075930 (to PL), R01 HL142975 and R01 HL133728 (to JG), and R01 NS090904 and NS117827 (to BZ).

REFERENCES

1. Lloyd-Jones D, Adams RJ, Brown TM, Carnethon M, Dai S, De Simone G, et al. Heart disease and stroke statistics-2010 update: a report from the American Heart Association. *Circulation*. (2010) 121:e46–215. doi: 10.1161/CIRCULATIONAHA.109.192667
2. Benjamin EJ, Blaha MJ, Chiuve SE, Cushman M, Das SR, Deo R, et al. Heart disease and stroke statistics-2017 update: a report from the American Heart Association. *Circulation*. (2017) 135:e146–603. doi: 10.1161/CIR.0000000000000491
3. Thom T, Haase N, Rosamond W, Howard VJ, Rumsfeld J, Manolio T, et al. Heart disease and stroke statistics-2006 update: a report from the American Heart Association Statistics Committee and Stroke Statistics Subcommittee. *Circulation*. (2006) 113:e85–151. doi: 10.1161/CIRCULATIONAHA.105.171600
4. Zlokovic BV, Griffin JH. Cytoprotective protein C pathways and implications for stroke and neurological disorders. *Trends Neurosci*. (2011) 34:198–209. doi: 10.1016/j.tins.2011.01.005
5. Lyden P, Pryor KE, Coffey CS, Cudkowicz M, Conwit R, Jadhav A, et al. Final results of the RHAPSODY trial: a multi-center, phase 2 trial using a continual reassessment method to determine the safety and tolerability of 3K3A-APC, a recombinant variant of human activated protein C, in combination with tissue plasminogen activator, mechanical thrombectomy or both in moderate to severe acute ischemic stroke. *Ann Neurol*. (2019) 85:125–36. doi: 10.1002/ana.25383
6. Saver JL, Goyal M, Bonafe A, DienerHC, Levy EI, Pereira VM, et al. Stent-retriever thrombectomy after intravenous t-PA vs. t-PA alone in stroke. *N Engl J Med*. (2015) 372:2285–95. doi: 10.1056/NEJMoa1415061
7. Goyal M, Demchuk AM, Menon BK, Eesa M, Rempel JL, Thornton J, et al. Randomized assessment of rapid endovascular treatment of ischemic stroke. *N Engl J Med*. (2015) 372:1019–30. doi: 10.1056/NEJMoa1414905
8. Campbell BC, Mitchell PJ, Kleinig TJ, Dewey HM, Churilov L, Yassi N, et al. Endovascular therapy for ischemic stroke with perfusion-imaging selection. *N Engl J Med*. (2015) 372:1009–18. doi: 10.1056/NEJMoa1414792
9. Berkhemer OA, Fransen PS, Beumer D, van den Berg LA, Lingsma HF, Yoo AJ, et al. A randomized trial of intraarterial treatment for acute ischemic stroke. *N Engl J Med*. (2015) 372:11–20. doi: 10.1056/NEJMoa1411587
10. Jovin TG, Chamorro A, Cobo E, de Miquel MA, Molina CA, Rovira A, et al. Thrombectomy within 8 hours after symptom onset in ischemic stroke. *N Engl J Med*. (2015) 372:2296–306. doi: 10.1056/NEJMoa1503780
11. Hill MD, Goyal M, Menon BK, Nogueira RG, McTaggart RA, Demchuk AM, et al. Efficacy and safety of nerinetide for the treatment of acute ischaemic stroke (ESCAPE-NA1): a multicentre, double-blind, randomised controlled trial. *Lancet*. (2020) 395:878–87. doi: 10.1016/S0140-6736(20)30258-0
12. Albers GW, Marks MP, Kemp S, Christensen S, Tsai JP, Ortega-Gutierrez S, et al. Thrombectomy for stroke at 6 to 16 hours with selection by perfusion imaging. *N Engl J Med*. (2018) 378:708–18. doi: 10.1056/NEJMoa1713973
13. Mullen MT, Pisapia JM, Tilwa S, Messe SR, Stein SC. Systematic review of outcome after ischemic stroke due to anterior circulation occlusion treated with intravenous, intra-arterial, or combined intravenous+intra-arterial thrombolysis. *Stroke*. (2012) 43:2350–5. doi: 10.1161/STROKEAHA.111.639211
14. Ellis JA, Youngerman BE, Higashida RT, Altschul D, Meyers PM. Endovascular treatment strategies for acute ischemic stroke. *Int J Stroke*. (2011) 6:511–22. doi: 10.1111/j.1747-4949.2011.00670.x
15. Tymianski M. Can molecular and cellular neuroprotection be translated into therapies for patients? Yes, but not the way we tried it before. *Stroke*. (2010) 41:S87–90. doi: 10.1161/STROKEAHA.110.595496
16. Xiong Y, Mahmood A, Chopp M. Angiogenesis, neurogenesis and brain recovery of function following injury. *Curr Opin Investig Drugs*. (2010) 11:298–308.

17. Lapchak PA. Emerging therapies: pleiotropic multi-target drugs to treat stroke victims. *Transl Stroke Res*. (2011) 2:129–35. doi: 10.1007/s12975-011-0074-4
18. Hacke W, Kaste M, Bluhmki E, Brozman M, Dávalos A, Guidetti D, et al. Thrombolysis with alteplase 3 to 4.5 hours after acute ischemic stroke. *N Engl J Med*. (2008) 359:1317–29. doi: 10.1056/NEJMoa0804656
19. Thomalla G, Simonsen CZ, Boutitie F, Andersen G, Berthezene Y, Cheng B, et al. MRI-guided thrombolysis for stroke with unknown time of onset. *N Engl J Med*. (2018) 379:611–22. doi: 10.1056/NEJMoa1804355
20. National Institute of Neurological Disorders and Stroke rt-PA Stroke Study Group. Tissue plasminogen activator for acute ischemic stroke. *N Engl J Med*. (1995) 333:1581–7. doi: 10.1056/NEJM199512143332401
21. Grotta JC, Burgin WS, El-Mitwalli A, Long M, Campbell M, Morgenstern LB, et al. Intravenous tissue-type plasminogen activator therapy for ischemic stroke: houston experience 1996 to 2000. *Arch Neurol*. (2001) 58:2009–13. doi: 10.1001/archneur.58.12.2009
22. Stemer A, Lyden P. Evolution of the thrombolytic treatment window for acute ischemic stroke. *Curr Neurol Neurosci Rep*. (2010) 10:29–33. doi: 10.1007/s11910-009-0076-8
23. Saver JL, Goyal M, Bonafe A, Diener HC, Levy EI, Pereira VM, et al. Solitaire^{TM} with the Intention for thrombectomy as primary endovascular treatment for acute ischemic stroke (SWIFT PRIME) trial: protocol for a randomized, controlled, multicenter study comparing the Solitaire revascularization device with IV tPA with IV tPA alone in acute ischemic stroke. *Int J Stroke*. (2015) 10:439–48. doi: 10.1111/ijs.12459
24. Bracard S, Ducrocq X, Mas JL, Soudant M, Oppenheim C, Moulin T, et al. Mechanical thrombectomy after intravenous alteplase vs. alteplase alone after stroke (THRACE): a randomised controlled trial. *Lancet Neurol*. (2016) 15:1138–47. doi: 10.1016/S1474-4422(16)30177-6
25. Dankbaar JW, Bienfait HP, van den Berg C, Bennink E, Horsch AD, van Seeters T, et al. Wake-up stroke vs. stroke with known onset time: clinical and multimodality CT imaging characteristics. *Cerebrovasc Dis*. (2018) 45:236–44. doi: 10.1159/000489566
26. Nogueira RG, Jadhav AP, Haussen DC, Bonafe A, Budzik RF, Bhuva P, et al. Thrombectomy 6 to 24 hours after stroke with a mismatch between deficit and infarct. *N Engl J Med*. (2018) 378:11–21. NEJMoa1706442. doi: 10.1056/NEJMoa1706442
27. del Zoppo GJ, von Kummer R, Hamann GF. Ischaemic damage of brain microvessels: inherent risks for thrombolytic treatment in stroke. *J Neurol Neurosurg Psychiatry*. (1998) 65:1–9. doi: 10.1136/jnnp.65.1.1
28. von Kummer R, Broderick JP, Campbell BC, Demchuk A, Goyal M, Hill MD, et al. The Heidelberg bleeding classification: classification of bleeding events after ischemic stroke and reperfusion therapy. *Stroke*. (2015) 46:2981–6. doi: 10.1161/STROKEAHA.115.010049
29. Levy DE, Brott TG, Haley EC Jr, Marler JR, Sheppard GL, Barsan W, et al. Factors related to intracranial hematoma formation in patients receiving tissue-type plasminogen activator for acute ischemic stroke. *Stroke*. (1994) 25:291–7. doi: 10.1161/01.STR.25.2.291
30. Trouillas P, von Kummer R. Classification and pathogenesis of cerebral hemorrhages after thrombolysis in ischemic stroke. *Stroke*. (2006) 37: 556–61. doi: 10.1161/01.STR.0000196942.84707.71
31. Wahlgren N, Ahmed N, Dávalos A, Ford GA, Grond M, Hacke W, et al. Thrombolysis with alteplase for acute ischaemic stroke in the safe implementation of thrombolysis in stroke-monitoring study (SITS-MOST): an observational study. *Lancet*. (2007) 369:275–82. doi: 10.1016/S0140-6736(07)60149-4
32. Hacke W, Kaste M, Fieschi C, von Kummer R, Davalos A, Meier D, et al. Randomised double-blind placebo-controlled trial of thrombolytic therapy with intravenous alteplase in acute ischaemic stroke (ECASS II). Second European-Australasian Acute Stroke Study Investigators. *Lancet*. (1998) 352:1245–51. doi: 10.1016/S0140-6736(98)08020-9
33. Emberson J, Lees KR, Lyden P, Blackwell L, Albers G, Bluhmki E, et al. Effect of treatment delay, age, and stroke severity on the effects of intravenous thrombolysis with alteplase for acute ischaemic stroke: a meta-analysis of individual patient data from randomised trials. *Lancet*. (2014) 384:1929–35. doi: 10.1016/S0140-6736(14)60584-5
34. Hao Y, Yang D, Wang H, Zi W, Zhang M, Geng Y, et al. Predictors for symptomatic intracranial hemorrhage after endovascular treatment of acute ischemic stroke. *Stroke*. (2017) 48:1203–09. doi: 10.1161/STROKEAHA.116.016368
35. Powers WJ, Rabinstein AA, Ackerson T, Adeoye OM, Bambakidis NC, Becker K, et al. 2018 Guidelines for the early management of patients with acute ischemic stroke: a guideline for healthcare professionals from the American Heart Association/American Stroke Association. *Stroke*. (2018) 49:e46–110. doi: 10.1161/STR.0000000000000158
36. Kent DM, Hinchey J, Price LL, Levine SR, Selker HP. In acute ischemic stroke, are asymptomatic intracranial hemorrhages clinically innocuous? *Stroke*. (2004) 35:1141–6. doi: 10.1161/01.STR.0000125712.02090.6e
37. Dzialowski I, Pexman JH, Barber PA, Demchuk AM, Buchan AM, Hill MD, et al. Asymptomatic hemorrhage after thrombolysis may not be benign: prognosis by hemorrhage type in the Canadian Alteplase for Stroke Effectiveness Study registry. *Stroke*. (2007) 38:75–9. doi: 10.1161/01.STR.0000251644.76546.62
38. Park JH, Ko Y, Kim W-J, Jang MS, Yang MH, Han M-K, et al. Is asymptomatic hemorrhagic transformation really innocuous? *Neurology*. (2012) 78:421–6. doi: 10.1212/WNL.0b013e318245d22c
39. Lei C, Wu B, Liu M, Chen Y. Asymptomatic hemorrhagic transformation after acute ischemic stroke: is it clinically innocuous? *J Stroke Cerebrovasc Dis*. (2014) 23:2767–72. doi: 10.1016/j.jstrokecerebrovasdis.2014.06.024
40. Jiang F, Zhao W, Wu C, Zhang Z, Li C, Che R, et al. Asymptomatic intracerebral hemorrhage may worsen clinical outcomes in acute ischemic stroke patients undergoing thrombectomy. *J Stroke Cerebrovasc Dis*. (2019) 28:1752–8. doi: 10.1016/j.jstrokecerebrovasdis.2019.02.006
41. Hao Y, Liu W, Wang H, Zi W, Yang D, Wang W, et al. Prognosis of asymptomatic intracranial hemorrhage after endovascular treatment. *J Neurointerv Surg*. (2019) 11:123–6. doi: 10.1136/neurintsurg-2018-013848
42. Li GF, Wu YL, Wang S, Shi YH, Zhao R, Liu FD, et al. Previous chronic symptomatic and asymptomatic cerebral hemorrhage in patients with acute ischemic stroke. *Neuroradiology*. (2019) 61:103–7. doi: 10.1007/s00234-018-2141-y
43. Wang X, Lo EH. Triggers and mediators of hemorrhagic transformation in cerebral ischemia. *Mol Neurobiol*. (2003) 28:229–44. doi: 10.1385/MN:28:3:229
44. Gáll T, Balla G, Balla J. Heme, heme oxygenase, and endoplasmic reticulum stress-a new insight into the pathophysiology of vascular diseases. *Int J Mol Sci*. (2019) 20:3675. doi: 10.3390/ijms20153675
45. Kernan WN, Ovbiagele B, Black HR, Bravata DM, Chimowitz MI, Ezekowitz MD, et al. Guidelines for the prevention of stroke in patients with stroke and transient ischemic attack: a guideline for healthcare professionals from the American Heart Association/American Stroke Association. *Stroke*. (2014) 45:2160–236. doi: 10.1161/STR.0000000000000024
46. Tan S, Wang D, Liu M, Zhang S, Wu B, Liu B. Frequency and predictors of spontaneous hemorrhagic transformation in ischemic stroke and its association with prognosis. *J Neurol*. (2014) 261:905–12. doi: 10.1007/s00415-014-7297-8
47. Zhao W, Che R, Shang S, Wu C, Li C, Wu L, et al. Low-dose tirofiban improves functional outcome in acute ischemic stroke patients treated with endovascular thrombectomy. *Stroke*. (2017) 48:3289–94. doi: 10.1161/STROKEAHA.117.019193
48. Boccuzzi SJ, Martin J, Stephenson J, Kreilick C, Fernandes J, Beaulieu J, et al. Retrospective study of total healthcare costs associated with chronic nonvalvular atrial fibrillation and the occurrence of a first transient ischemic attack, stroke, or major bleed. *Curr Med Res Opin*. (2009) 25:2853–64. doi: 10.1185/03007990903196422
49. O'Collins VE, Macleod MR, Cox SF, Van Raay L, Aleksoska E, Donnan GA, et al. Preclinical drug evaluation for combination therapy in acute stroke using systematic review, meta-analysis, and subsequent experimental testing. *J Cereb Blood Flow Metab*. (2011) 31:962–75. doi: 10.1038/jcbfm.2010.184
50. Sinha RK, Wang Y, Zhao Z, Xu X, Burnier L, Gupta N, et al. PAR1 biased signaling is required for activated protein C *in vivo* benefits in sepsis and stroke. *Blood*. (2018) 131:1163–71. doi: 10.1182/blood-2017-10-810895
51. Mosnier LO, Zlokovic BV, Griffin JH. The cytoprotective protein C pathway. *Blood*. (2007) 109:3161–72. doi: 10.1182/blood-2006-09-003004
52. Guo H, Zhao Z, Yang Q, Wang M, Bell RD, Wang S, et al. An activated protein C analog stimulates neuronal production by human neural

progenitor cells *via* a PAR1-PAR3-S1PR1-Akt pathway. *J Neurosci*. (2013) 33:6181–90. doi: 10.1523/JNEUROSCI.4491-12.2013
53. Mosnier LO, Zlokovic BV, Griffin JH. Cytoprotective-selective activated protein C therapy for ischaemic stroke. *Thromb Haemost*. (2014) 112:883–92. doi: 10.1160/th14-05-0448
54. Mosnier LO, Gale AJ, Yegneswaran S, Griffin JH. Activated protein C variants with normal cytoprotective but reduced anticoagulant activity. *Blood*. (2004) 104:1740–4. doi: 10.1182/blood-2004-01-0110
55. Wang Y, Zhang Z, Chow N, Davis TP, Griffin JH, Chopp M, et al. An activated protein C analog with reduced anticoagulant activity extends the therapeutic window of tissue plasminogen activator for ischemic stroke in rodents. *Stroke*. (2012) 43:2444–9. doi: 10.1161/STROKEAHA.112.658997
56. Wang Y, Zhao Z, Chow N, Rajput PS, Griffin JH, Lyden PD, et al. An activated protein C analog protects from ischemic stroke and extends the therapeutic window of tissue-type plasminogen activator in aged female mice and hypertensive rats. *Stroke*. (2013) 44:3529–36. doi: 10.1161/STROKEAHA.113.003350
57. Wang Y, Zhao Z, Rege SV, Wang M, Si G, Zhou Y, et al. 3K3A-activated protein C stimulates postischemic neuronal repair by human neural stem cells in mice. *Nat Med*. (2016) 22:1050–5. doi: 10.1038/nm.4154
58. Williams PD, Zlokovic BV, Griffin JH, Pryor KE, Davis TP. Preclinical safety and pharmacokinetic profile of 3K3A-APC, a novel, modified activated protein C for stroke. *Curr Pharm Des*. (2012) 18:4215–22. doi: 10.2174/138161212802430413
59. Griffin JH, Zlokovic BV, Mosnier LO. Activated protein C: biased for translation. *Blood*. (2015) 125:2898–907. doi: 10.1182/blood-2015-02-355974
60. Whiteley WN, Adams HP Jr, Bath PM, Berge E, Sandset PM, Dennis M, et al. Targeted use of heparin, heparinoids, or low-molecular-weight heparin to improve outcome after acute ischaemic stroke: an individual patient data meta-analysis of randomised controlled trials. *Lancet Neurol*. (2013) 12:539–45. doi: 10.1016/S1474-4422(13)70079-6
61. Bath PM, Lindenstrom E, Boysen G, De Deyn P, Friis P, Leys D, et al. Tinzaparin in acute ischaemic stroke (TAIST): a randomised aspirin-controlled trial. *Lancet*. (2001) 358:702–10. doi: 10.1016/S0140-6736(01)05837-8
62. Lyden PD, Zivin JA, Soll M, Sitzer M, Rothrock JF, Alksne J. Intracerebral hemorrhage after experimental embolic infarction: anticoagulation. *Arch Neurol*. (1987) 44:848–50. doi: 10.1001/archneur.1987.00520200052018
63. Rajput PS, Lamb JA, Fernández JA, Bai J, Pereira BR, Lei I, et al. Neuroprotection and vasculoprotection using genetically targeted protease-ligands. *Brain Res*. (2019) 1715:13–20. doi: 10.1016/j.brainres.2019.03.010
64. Mosnier LO, Yang XV, Griffin JH. Activated protein C mutant with minimal anticoagulant activity, normal cytoprotective activity, and preservation of thrombin activable fibrinolysis inhibitor-dependent cytoprotective functions. *J Biol Chem*. (2007) 282:33022–33. doi: 10.1074/jbc.M705824200
65. Griffin JH, Fernández JA, Lyden PD, Zlokovic BV. Activated protein C promotes neuroprotection: mechanisms and translation to the clinic. *Thromb Res*. (2016) 141(Suppl. 2):S62–4. doi: 10.1016/S0049-3848(16)30368-1
66. Griffin JH, Mosnier LO, Fernández JA, Zlokovic BV. 2016 scientific sessions Sol Sherry distinguished lecturer in thrombosis: thrombotic stroke: neuroprotective therapy by recombinant-activated protein C. *Arterioscler Thromb Vasc Biol*. (2016) 36:2143–51. doi: 10.1161/ATVBAHA.116.308038
67. Griffin JH, Zlokovic BV, Mosnier LO. Activated protein C, protease activated receptor 1 and neuroprotection. *Blood*. (2018) 132:159–69. doi: 10.1182/blood-2018-02-769026
68. Mosnier LO, Sinha RK, Burnier L, Bouwens EA, Griffin JH. Biased agonism of protease-activated receptor 1 by activated protein C caused by noncanonical cleavage at Arg46. *Blood*. (2012) 120:5237–46. doi: 10.1182/blood-2012-08-452169
69. Amar AP, Sagare AP, Zhao Z, Wang Y, Nelson AR, Griffin JH, et al. Can adjunctive therapies augment the efficacy of endovascular thrombolysis? A potential role for activated protein C. *Neuropharmacology*. (2018) 134(Pt. B):293–301. doi: 10.1016/j.neuropharm.2017.09.021
70. Joyce DE, Gelbert L, Ciaccia A, DeHoff B, Grinnell BW. Gene expression profile of antithrombotic protein c defines new mechanisms modulating inflammation and apoptosis. *J Biol Chem*. (2001) 276:11199–203. doi: 10.1074/jbc.C100017200
71. Riewald M, Petrovan RJ, Donner A, Mueller BM, Ruf W. Activation of endothelial cell protease activated receptor 1 by the protein C pathway. *Science*. (2002) 296:1880–2. doi: 10.1126/science.1071699
72. Cheng T, Liu D, Griffin JH, Fernández JA, Castellino F, Rosen ED, et al. Activated protein C blocks p53-mediated apoptosis in ischemic human brain endothelium and is neuroprotective. *Nat Med*. (2003) 9:338–42. doi: 10.1038/nm826
73. Dömötör E, Benzakour O, Griffin JH, Yule D, Fukudome K, Zlokovic BV. Activated protein C alters cytosolic calcium flux in human brain endothelium *via* binding to endothelial protein C receptor and activation of protease activated receptor-1. *Blood*. (2003) 101:4797–801. doi: 10.1182/blood-2002-12-3680
74. Mosnier LO, Griffin JH. Inhibition of staurosporine-induced apoptosis of endothelial cells by activated protein C requires protease-activated receptor-1 and endothelial cell protein C receptor. *Biochem J*. (2003) 373(Pt.1):65–70. doi: 10.1042/bj20030341
75. Deane R, LaRue B, Sagare AP, Castellino FJ, Zhong Z, Zlokovic BV. Endothelial protein C receptor-assisted transport of activated protein C across the mouse blood-brain barrier. *J Cereb Blood Flow Metab*. (2009) 29:25–33. doi: 10.1038/jcbfm.2008.117
76. Schuepbach RA, Madon J, Ender M, Galli P, Riewald M. Protease-activated receptor-1 cleaved at R46 mediates cytoprotective effects. *J Thromb Haemost*. (2012) 10:1675–84. doi: 10.1111/j.1538-7836.2012.04825.x
77. Soh UJ, Trejo J. Activated protein C promotes protease-activated receptor-1 cytoprotective signaling through β-arrestin and dishevelled-2 scaffolds. *Proc Natl Acad Sci U S A*. (2011) 108:E1372–80. doi: 10.1073/pnas.1112482108
78. Kiseleva EV, Sidorova MV, Gorbacheva LR, Strukova SM. Peptide-agonist of protease-activated receptor (PAR 1), similar to activated protein C, promotes proliferation in keratinocytes and wound healing of epithelial layer. *Biomed Khim*. (2014) 60:702–6. doi: 10.18097/PBMC20146006702
79. de Oliveira AS, de Almeida VH, Gomes FG, Rezaie AR, Monteiro RQ. TR47, a PAR1-based peptide, inhibits melanoma cell migration *in vitro* and metastasis *in vivo*. *Biochem Biophys Res Commun*. (2018) 495:1300–4. doi: 10.1016/j.bbrc.2017.11.174
80. Coughlin SR. Thrombin signalling and protease-activated receptors. *Nature*. (2000) 407:258–64. doi: 10.1038/35025229
81. Stavenuiter F, Mosnier LO. Noncanonical PAR3 activation by factor Xa identifies a novel pathway for Tie2 activation and stabilization of vascular integrity. *Blood*. (2014) 124:3480–9. doi: 10.1182/blood-2014-06-582775
82. Burnier L, Mosnier LO. Novel mechanisms for activated protein C cytoprotective activities involving noncanonical activation of protease-activated receptor 3. *Blood*. (2013) 122:807–16. doi: 10.1182/blood-2013-03-488957
83. Mosnier LO, Fernández JA, Davis TP, Zlokovic BV, Griffin JH. Influence of the 3K3A-activated protein C variant on the plasma clot lysis activity of t-PA and of t-PA on the variant's anticoagulant activity. *J Thromb Haemost*. (2013) 11:2059–2062. doi: 10.1111/jth.12400
84. Guo H, Wang Y, Singh I, Liu D, Fernández JA, Griffin JH, et al. Species-dependent neuroprotection by activated protein C mutants with reduced anticoagulant activity. *J Neurochem*. (2009) 109:116–24. doi: 10.1111/j.1471-4159.2009.05921.x
85. Guo H, Singh I, Wang Y, Deane R, Barrett T, Fernández JA, et al. Neuroprotective activities of activated protein C mutant with reduced anticoagulant activity. *Eur J Neurosci*. (2009) 29:1119–30. doi: 10.1111/j.1460-9568.2009.06664.x
86. Liu D, Cheng T, Guo H, Fernández JA, Griffin JH, Song X, et al. Tissue plasminogen activator neurovascular toxicity is controlled by activated protein C. *Nat Med*. (2004) 10:1379–83. doi: 10.1038/nm1122
87. Zlokovic BV, Zhang C, Liu D, Fernandez J, Griffin JH, Chopp M. Functional recovery after embolic stroke in rodents by activated protein C. *Ann Neurol*. (2005) 58:474–7. doi: 10.1002/ana.20602
88. Thiyagarajan M, Fernández JA, Lane SM, Griffin JH, Zlokovic BV. Activated protein C promotes neovascularization and neurogenesis in postischemic brain *via* protease-activated receptor 1. *J Neurosci*. (2008) 28:12788–97. doi: 10.1523/JNEUROSCI.3485-08.2008
89. Wang Y, Thiyagarajan M, Chow N, Singh I, Guo H, Davis TP, et al. Differential neuroprotection and risk for bleeding from activated protein

C with varying degrees of anticoagulant activity. *Stroke*. (2009) 40:1864–9. doi: 10.1161/STROKEAHA.108.536680
90. Walker CT, Marky AH, Petraglia AL, Ali T, Chow N, Zlokovic BV. Activated protein C analog with reduced anticoagulant activity improves functional recovery and reduces bleeding risk following controlled cortical impact. *Brain Res*. (2010) 1347:125–31. doi: 10.1016/j.brainres.2010.05.075
91. Petraglia AL, Marky AH, Walker C, Thiyagarajan M, Zlokovic BV. Activated protein C is neuroprotective and mediates new blood vessel formation and neurogenesis after controlled cortical impact. *Neurosurgery*. (2010) 66:165–71; discussion 171–2. doi: 10.1227/01.NEU.0000363148.49779.68
92. Shi Y, Hung S-T, Rocha G, Lin S, Linares GR, Staats KA, et al. Identification and therapeutic rescue of autophagosome and glutamate receptor defects in C9ORF72 and sporadic ALS neurons. *JCI Insight*. (2019) 5:127736. doi: 10.1172/jci.insight.127736
93. Zhong Z, Ilieva H, Hallagan L, Bell R, Singh I, Paquette N, et al. Activated protein C therapy slows ALS-like disease in mice by transcriptionally inhibiting SOD1 in motor neurons and microglia cells. *J Clin Invest*. (2009) 119:3437–49. doi: 10.1172/JCI38476
94. Winkler EA, Sengillo JD, Sagare AP, Zhao Z, Ma Q, Zuniga E, et al. Blood-spinal cord barrier disruption contributes to early motor-neuron degeneration in ALS-model mice. *Proc Natl Acad Sci U S A*. (2014) 111:E1035–42. doi: 10.1073/pnas.1401595111
95. Han MH, Hwang SI, Roy DB, Lundgren DH, Price JV, Ousman SS, et al. Proteomic analysis of active multiple sclerosis lesions reveals therapeutic targets. *Nature*. (2008) 451:1076–81. doi: 10.1038/nature06559
96. Lazic D, Sagare AP, Nikolakopoulou AM, Griffin JH, Vassar R, Zlokovic BV. 3K3A-activated protein C blocks amyloidogenic BACE1 pathway and improves functional outcome in mice. *J Exp Med*. (2019) 216:279–93. doi: 10.1084/jem.20181035
97. Finigan JH, Dudek SM, Singleton PA, Chiang ET, Jacobson JR, Camp SM, et al. Activated protein C mediates novel lung endothelial barrier enhancement: role of sphingosine 1-phosphate receptor transactivation. *J Biol Chem*. (2005) 280:17286–93. doi: 10.1074/jbc.M412427200
98. Uchiba M, Okajima K, Oike Y, Ito Y, Fukudome K, Isobe H, et al. Activated protein C induces endothelial cell proliferation by mitogen-activated protein kinase activation *in vitro* and angiogenesis *in vivo*. *Circ Res*. (2004) 95:34–41. doi: 10.1161/01.RES.0000133680.87668.FA
99. Amar AP, Griffin JH, Zlokovic BV. Combined neurothrombectomy or thrombolysis with adjunctive delivery of 3K3A-activated protein C in acute ischemic stroke. *Front Cell Neurosci*. (2015) 9:344. doi: 10.3389/fncel.2015.00344
100. Martins SO, Mont'Alverne F, Rebello LC, Abud DG, Silva GS, Lima FO, et al. Thrombectomy for stroke in the public health care system of Brazil. *N Engl J Med*. (2020) 382:2316–26. NEJMoa2000120. doi: 10.1056/NEJMoa2000120
101. von Kummer R. Brain hemorrhage after thrombolysis: good or bad? *Stroke*. (2002) 33:1446–7. doi: 10.1161/01.STR.0000016923.99605.75
102. Brown DL, Barsan WG, Lisabeth LD, Gallery ME, Morgenstern LB. Survey of emergency physicians about recombinant tissue plasminogen activator for acute ischemic stroke. *Ann Emerg Med*. (2005) 46:56–60. doi: 10.1016/j.annemergmed.2004.12.025

Conflict of Interest: KP is employed by ZZ Biotech. JG, HL, JM, and BZ are paid consultants to ZZ Biotech. PL has received research funding from NIH to conduct trials of 3K3A-APC; received royalties from sales of the book Thrombolytic Therapy for Acute Ischemic Stroke, 3rd Edition; and received fees for occasional expert witness testimony. The Scripps Research Institute has intellectual property related to the topic of this review.

The remaining author declares that the research was conducted in the absence of any commercial or financial relationships that could be construed as a potential conflict of interest.

frontiers in Neurology

STUDY PROTOCOL
published: 17 March 2021
doi: 10.3389/fneur.2021.621476

Rapid Intervention of Chlorpromazine and Promethazine for Hibernation-Like Effect in Stroke: Rationale, Design, and Protocol for a Prospective Randomized Controlled Trial

Shuyu Lv[1,2], Wenbo Zhao[3], Gary B. Rajah[4,5], Chaitu Dandu[4], Lipeng Cai[2], Zhe Cheng[2], Honglian Duan[2], Qingqing Dai[2], Xiaokun Geng[1,2,3,4] and Yuchuan Ding[4,6]*

[1] Luhe Institute of Neuroscience, Capital Medical University, Beijing, China, [2] Department of Neurology, Beijing Luhe Hospital, Capital Medical University, Beijing, China, [3] China-America Institute of Neuroscience, Xuanwu Hospital, Capital Medical University, Beijing, China, [4] Department of Neurosurgery, Wayne State University School of Medicine, Detroit, MI, United States, [5] Department of Neurosurgery, Munson Medical Center, Traverse City, MI, United States, [6] Department of Research and Development Center, John D. Dingell VA Medical Center, Detroit, MI, United States

OPEN ACCESS

Edited by:
Bruno Meloni,
University of Western Australia, Australia

Reviewed by:
Liping Liu,
Capital Medical University, China
Christian Urbanek,
Klinikum Ludwigshafen, Germany
Aravind Ganesh,
University of Calgary, Canada

***Correspondence:**
Xiaokun Geng
xgeng@ccmu.edu.cn

Specialty section:
This article was submitted to Stroke, a section of the journal Frontiers in Neurology

Received: 26 October 2020
Accepted: 18 February 2021
Published: 17 March 2021

Citation:
Lv S, Zhao W, Rajah GB, Dandu C, Cai L, Cheng Z, Duan H, Dai Q, Geng X and Ding Y (2021) Rapid Intervention of Chlorpromazine and Promethazine for Hibernation-Like Effect in Stroke: Rationale, Design, and Protocol for a Prospective Randomized Controlled Trial. Front. Neurol. 12:621476. doi: 10.3389/fneur.2021.621476

Background: Following an acute ischemic stroke (AIS), rapidly initiated reperfusion therapies [i. e., intravenous thrombolysis (IVT) and endovascular treatment (EVT)] demonstrate robust clinical efficacy. However, only a subset of these patients can benefit from these therapies due to their short treatment windows and potential complications. In addition, many patients despite successful reperfusion still have unfavorable outcomes. Thus, neuroprotection strategies are urgently needed for AIS patients. Chlorpromazine and promethazine (C+P) have been employed in clinical practice for antipsychotic and sedative purposes. A clinical study has also shown a neuroprotective effect of C+P on patients with cerebral hemorrhage and subarachnoid hemorrhage. The safety, feasibility, and preliminary efficacy of intravenous administration of C+P in AIS patients within 24 h of onset will be elucidated.

Methods: A prospective randomized controlled trial is proposed with AIS patients. Participants will be randomly allocated to an intervention group and a control group with a 1:1 ratio ($n = 30$) and will be treated with standard therapies according to the current stroke guidelines. Participants allocated to the intervention group will receive intravenous administration of C+P (chlorpromazine 50 mg and promethazine 50 mg) within 24 h of symptom onset. The primary outcome is safety (mainly hypotension), while the secondary outcomes include changes in functional outcome and infarction volume.

Discussions: This study on Rapid Intervention of Chlorpromazine and Promethazine for Hibernation-like Effect in Stroke (RICHES) will be the first prospective randomized

controlled trial to ascertain the safety, feasibility, and preliminary efficacy of intravenous C+P as a neuroprotection strategy in AIS patients. These results will provide parameters for future studies, provide insights into treatment effects, and neuroprotection with phenothiazine in AIS.

Clinical Trial Registration: www.chictr.org.cn, identifier: ChiCTR2000038727.

Keywords: acute ischemic stroke (AIS), phenothiazine, neuroprotection, intravenous thrombolysis, rt-PA

INTRODUCTION

Due to its high rate of mortality and morbidity, ischemic stroke is a devastating public health concern which also results in a high socioeconomic burden (1, 2). Intravenous thrombolysis with recombinant tissue plasminogen activator (rt-PA) is an important method for the treatment of acute ischemic stroke. However, due to the narrow time window, disparate national health awareness, uneven distribution of medical resources, traffic congestion, and potential complications, only around 2.4% of patients receive this treatment currently in China (3). The mortality at 3–6 months after intravenous thrombolysis was not significantly reduced, and is as high as 17.9%, with 2/3 of the patients having varying degrees of disability (3–5). Therefore, attention must be given to both vascular recanalization and neuroprotection. Exploring fast and effective neuroprotection strategies to save time for recanalization strategies and improve prognosis will become a key strategy in the treatment of AIS. We believe chlorpromazine and promethazine (C+P) may benefit patients in the acute setting of AIS.

Hibernation is an altered physiological state during times of food shortage and is characterized by drastic decreases in both body temperature and metabolic rate. Animals in hibernation withstand the decline of cerebral blood flow without experiencing brain damage (6, 7). In acute ischemic stroke, the cascade reaction caused by ischemia leads to irreversible damage to the brain within minutes (8). If a hibernation-like state can be induced in AIS patients, it may reduce brain metabolism allowing the patient to reach a balance point between energy supply and demand. This may increase tolerance to ischemia and hypoxia. C+P are the two most widely used phenothiazine drugs to induce hibernation (9). C+P are both FDA-approved and routinely used in severe brain injury, brain edema, central high fever with restlessness, mental illness and delirium (9, 10). Existing data reveal that C+P is safe for most patients (11, 12). A previous clinical study found that a mixture of drugs, including chlorpromazine 50 mg + promethazine 50 mg + dolantin (pethidine) 100 mg, named as "lytic cocktail" was injected intravenously to produce sedation, analgesia, amnesia, hypotension, hypothermia, and blockade of the functions of the sympathetic and parasympathetic nervous systems during an event (9). The drugs reduced the mortality and neurological deficit of patients with acute cerebral hemorrhage and subarachnoid hemorrhage (13). Although a neuroprotective role was not investigated in acute ischemic stroke, the safety of an oral C+P regimen has been demonstrated by our group in stroke patients (14). In addition, our previous studies have demonstrated a neuroprotective effect of C+P in rat ischemic stroke models (15). The neuroprotective effect was due to the reduction in reactive oxygen species (ROS)-mediated oxidative injury (15), brain inflammation (16), apoptosis (17), and reduction in blood-brain barrier (BBB) dysfunction after ischemic stroke (18). Importantly, this neuroprotection was not completely dependent upon the reduction of body temperature. As a safe, effective, cost-efficient "old drug," C+P may be repurposed as a promising new therapy to achieve neuroprotection in AIS patients. We thus designed this single-center, prospective randomized controlled study on Rapid Intervention of Chlorpromazine and Promethazine for Hibernation-like Effect in Stroke (RICHES) to verify the safety, feasibility, and preliminary efficacy of immediate intravenous administration of C+P at a dose as previously reported for AIS.

METHODS

Study Design

This is a single-center, prospective randomized controlled trial. It will be performed in patients with acute ischemic stroke (AIS) onset within 24 h. Participants meeting inclusion criteria but not exclusion criteria will be randomly allocated to the C+P or the control group whether they received IVT or not. Participants allocated to the intervention group will receive intravenous administration of C+P within 24 h of symptom onset, within the first 60 min of administration. C+P will be administered after rt-PA if the patients received IVT. Seeing that early mechanical thrombectomy has an absolute difference in the rate of functional independence, as compared with alteplase alone (19, 20), this study will not include patients treated with EVT. *Via* the medical records, the demographic information, chronic medical history (diabetes, hypertension, hyperlipidemia, coronary heart disease), smoking history, alcohol drinking history, and NIHSS score at admission will be collected. Magnetic resonance imaging (MRI) will be performed at baseline and on days 3 and 90. NIHSS and mRS will be evaluated at baseline and immediately after administration, and on days 2, 3, 7, 14, and 90. All participants or proxies will be informed of potential risks and possible benefits and consented for this study. The consent will be provided to a legal representative if the patients do not have the capacity to consent. This study was approved by the ethics committee of Luhe Hospital, Capital Medical University, Beijing, China and has been registered at www.chictr.org.cn with ChiCTR2000038727. An independent physician will monitor the health and safety of the participants.

Patient Population: Inclusion and Exclusion Criteria

Participants will be recruited from the stroke center (the Stroke Intervention and Translational Center, SITC) in Beijing Luhe Hospital. The inclusion criteria are (1) ≥18 and ≤80 years old; (2) clinical diagnosis of AIS; (3) NIHSS score ≥6 and ≤25; (4) patients with time from onset to treatment ≤24 hours that did not receive endovascular treatment (EVT); (5) pre-stroke mRS ≤2; (6) informed consent provided by participant or legally authorized representative.

Exclusion criteria are as follows: (1) rapid and spontaneous relief of symptoms: NIHSS score reduced to <6; (2) hemodynamic instability, including low systolic blood pressure (SBP) and SBP ≤100 mmHg despite standard treatment; (3) medical history of Parkinson's disease, Parkinson's syndrome, neuroleptic malignant syndrome, basal ganglia disease and epilepsy; (4) allergy to phenothiazines; (5) acute myocardial infarction, acute cardiac insufficiency and/or serious arrhythmia; (6) participant in another ongoing clinical trial; (7) life expectancy of fewer than 1 year due to comorbidities; (8) any condition which the investigator judges to increase the risk of injury to the patient.

Randomization and Blindness

During the recruitment period, participants will be allocated 1:1 to two groups ($n = 30$) by computer-generated randomization procedures using opaque envelopes. A research assistant not involved in the study will prepare the envelopes before the study. After recording baselines measures, participants will be randomly allocated to either the intervention or the control group by the treating physicians who will open the sealed opaque envelopes. In order to minimize selection bias, patients and assessors involved in the trial will be masked to treatment allocation. All outcome measurements will be assessed by two observers blinded to the treatment plan, any disagreement will be resolved by reaching a consensus between the two. If no consensus can be reached, a third observer blinded to the treatment assignment and not involved in the clinical treatment plan will have a final decision. Finally, an independent investigator blinded to the treatment assignment will collect the data of outcomes and information of the group, and analyze them.

Interventions

Participants in both groups will receive the standard management according to the guidelines for the treatment of ischemic stroke, including blood pressure control, treatment of hyperglycemia and hyperlipidemia, antiplatelet or anticoagulation, and neurotrophic treatment (21). The body temperature of both groups will be maintained at 36.0–37.3°C. The room temperature will be 20–25°C. In order to ensure the stability of administration speed and the stability of blood pressure, patients allocated to the C+P group will undergo intravenous infusion of chlorpromazine 50 mg and promethazine 50 mg at 5 mg/h. For the choice of drug dosage, we referred to the hibernation mixture (chlorpromazine 50 mg + promethazine 50 mg) (13). Based on clinical experiences, this dose is safe and effective. The same total dose of C+P (25 + 25 mg, twice a day) given to patients has been proven to be safe in our previous study. In addition, as compared to oral administration, the current protocol with continuous small dose injection at 5 mg/h *via* a micropump will maintain a stable blood concentration. The speed will be adjusted according to the patient's reaction. This administration will keep the patient in light sedation that can be awakened and allow for physical examination at any time. The control group will receive the same dosage of normal saline at 5 mg/h. During this period, vital signs (i.e., blood pressure, heart rate, body temperature, respiratory rate of the patients), changes in consciousness, and possible adverse drug reactions will be closely monitored. If the patients show a tendency to develop adverse reactions and complications, the trial shall be stopped immediately, and routine treatment shall be given.

Outcomes

Primary Outcomes (Safety Assessment)

The main safety parameter is the incidence of hypotension requiring clinical intervention (≤90/60 mmHg). The secondary safety outcomes are the occurrence of adverse events including (1) neurologic deterioration defined as an increase of four or more points in the NIHSS within 7 days without clear explanation; (2) death during the study period regardless of cause; (3) body temperature down to below 36°C; (4) severe arrhythmias, such as sick sinus syndrome, rapid atrial fibrillation, supraventricular tachycardia, etc., which may cause palpitations, chest tightness, dizziness and other clinical manifestations; (5) liver damage: alanine aminotransferase (ALT) and aspartate aminotransferase (AST) concentrations were doubled; (6) seizures: epilepsy occurs within 2 weeks of stroke; (7) extrapyramidal responses (tremor, rigidity, salivation, and bradykinesia).

Secondary Outcomes (Efficacy Assessment)

The efficacy of the treatment is functional independence which will be assessed by the modified Rankin Scale (mRS, mRS scores of 0 to 2 indicating functional independence), and infarct volume as well as NIHSS scores. MRI will be performed at baseline and on days 3 and 90. We will measure the infarct volume on a Siemens Syngo with T1, T2, T2-flair, Diffusion-Weighted Imaging (DWI), Arterial Spin Labeling (ASL) and Intra-Voxel Incoherent Motion (IVIM). We will calculate the infarct volume by using the image tool (ROI) on the workstation to outline the lesion on each slice to compute the area, and multiply the area of each layer by the thickness of each layer.

Estimation of Sample Size

There is no data available for reference because no completed clinical study of C+P in AIS patients without EVT currently exists. However, Hertzog has suggested that 10 to 20 patients in each group are sufficient to assess the feasibility of a pilot study (22) while Dobkin has shown that 15 patients in each group is usually enough to decide whether a larger multicenter trial should be conducted (23). Therefore, our goal is to recruit 15 patients in each group, a similar number of samples was selected for another protocol (24). The results of this study should be able to determine the initial safety and feasibility of intravenous

infusion of C+P in AIS patients. The data will be used to estimate sample size and conduct a power calculation to plan a phase-2 trial for efficacy.

Statistical Analyses

The endpoint event analysis is based on the intention-to-treat (ITT) principle, including all randomly enrolled subjects. If compared to the control group, the treatment group did not have an increase in the incidence of adverse reactions and there was no difference in 90 days prognosis between the two groups, we would move forward with a phase-2 trial.

Categorical variables including the proportion of good functional outcomes and the frequency of adverse events will be presented as counts and percentages. χ^2-test, Fisher exact-test, or continuity correction will be used where appropriate for comparison between the two groups. If the continuous variables including NIHSS score and infarct volume conform to the normal distribution, it shall be indicated by mean ± standard, and tested by *t*-test, and if it does not conform to the normal distribution, it shall be indicated by median and interquartile range and tested by Mann-Whitney *U*-test. $p < 0.05$ will be considered statistically significant. SPSS 22.0 software will be used for statistical analysis.

DISCUSSION

A previous clinical study found that "lytic cocktail" [chlorpromazine 50 mg + promethazine 50 mg + dolantin (pethidine) 100 mg] reduced the mortality and neurological deficit of patients with acute cerebral hemorrhage and subarachnoid hemorrhage (13). Pethidine is mainly used for traumatic pain with acute cerebral hemorrhage and subarachnoid hemorrhage. Patients with acute ischemic stroke usually do not need analgesia, so in this study, we focused on the neuroprotective effect of C+P, without pethidine. Although a neuroprotective role was not investigated in acute ischemic stroke, our clinical study has demonstrated that the orally taken C+P at a dose of 12.5 + 12.5 mg or 25 + 25 mg, twice a day after AIS was safe by determining no serious adverse effects such as extrapyramidal symptoms, hypotension, seizures, abnormal liver function, ECG abnormality, and allergic reaction as well as NIHSS score and mRS in the treatment group compared with control group (14). Considering the low bioavailability of oral drugs, unstable blood drug concentration and other factors, the purpose of the present study will be to determine the safety, feasibility, and preliminary efficacy of the RICHES protocol. C+P will be intravenously administered, in order to establish a novel effective neuroprotective strategy. Our studies in rat ischemic stroke models demonstrated a neuroprotective effect of C+P. This protection was due to the reduction in the reactive oxygen species (ROS)-mediated oxidative injury (15), reduction in brain inflammation determined by the expression of TNF-α, IL-1 β, ICAM-1, VCAM-1, NF-κB (16), and reduction in apoptotic signal cascade (17), as well as improved integrity of blood-brain barrier (18). Importantly, the neuroprotection was induced in both hypothermic or normothermic conditions after ischemic stroke. In order to develop a translational strategy of neuroprotection, we will perform this study utilizing an intravenous infusion of C+P as a possible stable and effective therapy for AIS patients.

With an aging population, the incidence of stroke will increase significantly (1, 25, 26). Good prognosis of AIS patients depends on timely revascularization and effective neuroprotective agents. At present, the effective methods of revascularization are thrombolysis and thrombectomy. However, the clinical efficacy of these therapies is limited by the narrow time window, potential complications and reperfusion injuries such as hemorrhagic transformation and brain edema (3, 27–29). Exploring fast and effective neuroprotective strategies to earn time for vascular recanalization and reduce reperfusion injuries has become an essential desire in AIS treatment.

Over the past few decades, there have been over 1,000 neuroprotective methods that have been examined for potential neuroprotective properties, mild hypothermia is the only one proven effective in randomized controlled trials. Although not included in the guidelines, the National Institutes of Health (NIH) points out that mild hypothermia is the most promising neuroprotective method for ischemic stroke. However, hypothermia is difficult to establish, slow in cooling and can easily lead to serious complications such as arrhythmia and pulmonary infection. This makes it difficult to achieve the clinical translation of benefits (21, 30, 31). During hibernation, the cerebral blood flow is decreased by <10%, but the utilization of glucose in the brain decreases by 98%, uncoupling metabolic demands (32). Therefore, an induced hibernation-like state might be a potential therapy for ischemic stroke by maintaining the body's low metabolism and low oxygen consumption even without low body temperature. This state may help the body survive prolonged hypoxia during the "difficult period of AIS."

C+P, as the main component of the classic prescription "lytic cocktail," are the two most studied phenothiazine drugs (9). Based on their sedative and antipsychotic effects, they are widely used in severe brain injury, brain edema and schizophrenia since the 1950s (10). Existing data have demonstrated their clinical safety (11, 12). Chlorpromazine has been shown to protect against ischemic injury in liver, kidney, spinal cord and brain (33–39), promethazine can reduce the oxygen consumption and basic metabolic rate of the brain and whole body, as well as improve the tolerance of a tissue to hypoxia (40). In our animal studies, C+P has been found to reduce infarct volumes (from 50.3 to 35.7%, $p < 0.05$) and neurological deficits (from score 3.5 to 2.8, $p < 0.05$) in 2 h middle cerebral artery occlusion models. This appears most likely independent of drug-induced systemic hypothermia (15). In clinical practice, as mentioned above, oral administration of C+P after AIS was safe and there were no adverse reactions (14). Therefore, C+P application in stroke seems to have several advantages, such as simple implementation, rapid onset, cost-efficient, minimal known serious side effects in a small study. In addition, it could ultimately be administered in the field prior to reperfusion for neuroprotection and time window extension.

There are limitations to this study. First, this is a single-center, small sample experiment, which may affect the generalizability

of the interventions and opens the study up to spurious results. Second, the target dosage has been shown to be safe and reliable in other small cohort experiments, but the dose used in the present study may still need optimization. In addition, there is a concern that an intravenous administration of an equal dosage might have more interactions given better bioavailability. The current study protocol will not include AIS patients who receive EVT to avoid interactions between C+P and moderate sedation or general anesthesia.

The RICHES study is designed to identify the safety, feasibility, and secondarily any possible efficacy of intravenous administration of C+P in AIS patients. The preliminary results will provide clues for the design of future clinical trials. If there is no significant difference in the incidence of drug-related adverse events between the experimental group and the control group, further clinical trials will be indicated. Based on past basic research and previous clinical studies, we predict that chlorpromazine and promethazine is safe for patients with acute ischemic stroke. The current study may suggest a neuroprotective role in AIS, and warrant a randomized controlled trial (RCT).

ETHICS STATEMENT

The studies involving human participants were reviewed and approved by the Ethics Committee of Luhe Hospital, Capital Medical University, Beijing, China. The patients/participants provided their written informed consent to participate in this study.

AUTHOR CONTRIBUTIONS

SL, WZ, LC, ZC, HD, and QD prepared the manuscript. YD and XG designed the study. YD, GR, WZ, and CD revised the manuscript. All authors reviewed the manuscript and provided the final approval for the manuscript.

FUNDING

This study was supported partially by the National Natural Science Foundation of China (82072549 and 82001277), and Science and Technology Plan of Beijing Tongzhou District (KJ2020CX002).

REFERENCES

1. Wu S, Wu B, Liu M, Chen Z, Wang W, Anderson CS, et al. Stroke in China: advances and challenges in epidemiology, prevention, and management. *Lancet Neurol*. (2019) 18:394–405. doi: 10.1016/S1474-4422(18)30500-3
2. Stone CR, Geng X, Ding Y. From big data to battling disease: notes from the frontiers of cerebrovascular science. *Neurol Res*. (2019) 41:679–80. doi: 10.1080/01616412.2019.1603592
3. Dong Q, Dong Y, Liu L, Xu A, Zhang Y, Zheng H, et al. The Chinese Stroke Association scientific statement: intravenous thrombolysis in acute ischaemic stroke. *Stroke Vasc Neurol*. (2017) 2:147–59. doi: 10.1136/svn-2017-000074
4. Emberson J, Lees KR, Lyden P, Blackwell L, Albers G, Bluhmki E, et al. Effect of treatment delay, age, and stroke severity on the effects of intravenous thrombolysis with alteplase for acute ischaemic stroke: a meta-analysis of individual patient data from randomised trials. *Lancet*. (2014) 384:1929–35. doi: 10.1016/S0140-6736(14)60584-5
5. Leng T, Xiong ZG. Treatment for ischemic stroke: from thrombolysis to thrombectomy and remaining challenges. *Brain Circ*. (2019) 5:8–11. doi: 10.4103/bc.bc_36_18
6. Drew KL, Rice ME, Kuhn TB, Smith MA. Neuroprotective adaptations in hibernation: therapeutic implications for ischemia-reperfusion, traumatic brain injury and neurodegenerative diseases. *Free Radic Biol Med*. (2001) 31:563–73. doi: 10.1016/s0891-5849(01)00628-1
7. Drew KL, Buck CL, Barnes BM, Christian SL, Rasley BT, Harris MB. Central nervous system regulation of mammalian hibernation: implications for metabolic suppression and ischemia tolerance. *J Neurochem*. (2007) 102:1713–26. doi: 10.1111/j.1471-4159.2007.04675.x
8. Dave KR, Christian SL, Perez-Pinzon MA, Drew KL. Neuroprotection: lessons from hibernators. *Comp Biochem Physiol B Biochem Mol Biol*. (2012) 162:1–9. doi: 10.1016/j.cbpb.2012.01.008
9. Forreider B, Pozivilko D, Kawaji Q, Geng X, Ding Y. Hibernation-like neuroprotection in stroke by attenuating brain metabolic dysfunction. *Prog Neurobiol*. (2017) 157:174–87. doi: 10.1016/j.pneurobio.2016.03.002
10. Lopez-Munoz F, Alamo C, Cuenca E, Shen WW, Clervoy P, Rubio G. History of the discovery and clinical introduction of chlorpromazine. *Ann Clin Psychiatry*. (2005) 17:113–35. doi: 10.1080/10401230591002002
11. Einarson A, Boskovic R. Use and safety of antipsychotic drugs during pregnancy. *J Psychiatr Pract*. (2009) 15:183–92. doi: 10.1097/01.pra.0000351878.45260.94
12. Lacasse H, Perreault MM, Williamson DR. Systematic review of antipsychotics for the treatment of hospital-associated delirium in medically or surgically ill patients. *Ann Pharmacother*. (2006) 40:1966–73. doi: 10.1345/aph.1H241
13. Cerebrovascular Disease Research Group, Department of Neurology, Peking Union Medical College Hospital. Artificial hibernation therapy for cerebral hemorrhage. *Chin J Neuropsychol*. (1960) 3:146–50. (in Chinese).
14. Zhu H, Chandra A, Geng X, Cheng Z, Tong Y, Du H, et al. Low dose concomitant treatment with chlorpromazine and promethazine is safe in acute ischemic stroke. *J Neurosurg Sci*. (2019) 63:265–9. doi: 10.23736/S0390-5616.19.04665-4
15. Geng X, Li F, Yip J, Peng C, Elmadhoun O, Shen J, et al. Neuroprotection by chlorpromazine and promethazine in severe transient and permanent ischemic stroke. *Mol Neurobiol*. (2017) 54:8140–50. doi: 10.1007/s12035-016-0280-x
16. Guan L, Guo S, Yip J, Elkin KB, Li F, Peng C, et al. Artificial hibernation by phenothiazines: a potential neuroprotective therapy against cerebral inflammation in stroke. *Curr Neurovasc Res*. (2019) 16:232–40. doi: 10.2174/1567202616666190624122727
17. Tong Y, Elkin KB, Peng C, Shen J, Li F, Guan L, et al. Reduced apoptotic injury by phenothiazine in ischemic stroke through the NOX-Akt/PKC pathway. *Brain Sci*. (2019) 9:378. doi: 10.3390/brainsci9120378
18. Li F, Geng X, Yip J, Ding Y. Therapeutic target and cell-signal communication of chlorpromazine and promethazine in attenuating blood-brain barrier disruption after ischemic stroke. *Cell Transplant*. (2019) 28:145–56. doi: 10.1177/0963689718819443
19. Campbell BC, Mitchell PJ, Kleinig TJ, Dewey HM, Churilov L, Yassi N, et al. Endovascular therapy for ischemic stroke with perfusion-imaging selection. *N Engl J Med*. (2015) 372:1009–18. doi: 10.1056/NEJMoa1414792
20. Berkhemer OA, Fransen PS, Beumer D, van den Berg LA, Lingsma HF, Yoo AJ, et al. A randomized trial of intraarterial treatment for acute ischemic stroke. *N Engl J Med*. (2015) 372:11–20. doi: 10.1056/NEJMoa1411587
21. Powers WJ, Rabinstein AA, Ackerson T, Adeoye OM, Bambakidis NC, Becker K, et al. Guidelines for the early management of patients with acute ischemic stroke: 2019 update to the 2018 guidelines for the early management of acute ischemic stroke: a guideline for healthcare professionals from the American Heart Association/American Stroke Association. *Stroke*. (2019) 50:e344–418. doi: 10.1161/STR.0000000000000211
22. Hertzog MA. Considerations in determining sample size for pilot studies. *Res Nurs Health*. (2008) 31:180–91. doi: 10.1002/nur.20247

23. Dobkin BH. Progressive staging of pilot studies to improve phase III trials for motor interventions. *Neurorehabil Neural Repair*. (2009) 23:197–206. doi: 10.1177/1545968309331863
24. Zhao W, Jiang F, Li S, Wu C, Gu F, Zhang Q, et al. Remote ischemic conditioning for intracerebral hemorrhage (RICH-1): rationale and study protocol for a pilot open-label randomized controlled trial. *Front Neurol*. (2020) 11:313. doi: 10.3389/fneur.2020.00313
25. Shetty AK, Upadhya R, Madhu LN, Kodali M. Novel insights on systemic and brain aging, stroke, amyotrophic lateral sclerosis, and Alzheimer's disease. *Aging Dis*. (2019) 10:470–82. doi: 10.14336/AD.2019.0330
26. Shen F, Jiang L, Han F, Degos V, Chen S, Su H. Increased inflammatory response in old mice is associated with more severe neuronal injury at the acute stage of ischemic stroke. *Aging Dis*. (2019) 10:12–22. doi: 10.14336/AD.2018.0205
27. Siegler JE, Martin-Schild S. Early neurological deterioration (END) after stroke: the END depends on the definition. *Int J Stroke*. (2011) 6:211–2. doi: 10.1111/j.1747-4949.2011.00596.x
28. Nogueira RG, Jadhav AP, Haussen DC, Bonafe A, Budzik RF, Bhuva P, et al. Thrombectomy 6 to 24 hours after stroke with a mismatch between deficit and infarct. *N Engl J Med*. (2018) 378:11–21. doi: 10.1056/NEJMoa1706442
29. Zhao W, Wu C, Dornbos D, III, Li S, Song H, Wang Y, et al. Multiphase adjuvant neuroprotection: a novel paradigm for improving acute ischemic stroke outcomes. *Brain Circ*. (2020) 6:11–8. doi: 10.4103/bc.bc_58_19
30. Kuczynski AM, Demchuk AM, Almekhlafi MA. Therapeutic hypothermia: applications in adults with acute ischemic stroke. *Brain Circ*. (2019) 5:43–54. doi: 10.4103/bc.bc_5_19
31. Han Y, Rajah GB, Hussain M, Geng X. Clinical potential of pre-reperfusion hypothermia in ischemic injury. *Neurol Res*. (2019) 41:697–703. doi: 10.1080/01616412.2019.1609160
32. Frerichs KU. Neuroprotective strategies in nature–novel clues for the treatment of stroke and trauma. *Acta Neurochir Suppl*. (1999) 73:57–61. doi: 10.1007/978-3-7091-6391-7_9
33. Chien KR, Abrams J, Pfau RG, Farber JL. Prevention by chlorpromazine of ischemic liver cell death. *Am J Pathol*. (1977) 88:539–57.
34. Jayachandran S, Mooppan MM, Chou SY, Kim H. Effects of chlorpromazine on ischemic rat kidney: a functional and ultrastructural study. *Urology*. (1985) 25:386–90. doi: 10.1016/0090-4295(85)90495-9
35. Sader AA, Barbieri-Neto J, Sader SL, Mazzetto SA, Alves P, Jr., Vanni JC. The protective action of chlorpromazine on the spinal cord of rabbits submitted to ischemia and reperfusion is dose-dependent. *J Cardiovasc Surg (Torino)*. (2002) 43:827–31.
36. Zivin JA, Kochhar A, Saitoh T. Phenothiazines reduce ischemic damage to the central nervous system. *Brain Res*. (1989) 482:189–93. doi: 10.1016/0006-8993(89)90560-x
37. Sadanaga KK, Ohnishi ST. Chlorpromazine protects rat spinal cord against contusion injury. *J Neurotrauma*. (1989) 6:153–61. doi: 10.1089/neu.1989.6.153
38. Liu S, Geng X, Forreider B, Xiao Y, Kong Q, Ding Y, et al. Enhanced beneficial effects of mild hypothermia by phenothiazine drugs in stroke therapy. *Neurol Res*. (2015) 37:454–60. doi: 10.1179/1743132815Y.0000000031
39. Li HJ, Zhang YJ, Zhou L, Han F, Wang MY, Xue MQ, et al. Chlorpromazine confers neuroprotection against brain ischemia by activating BKCa channel. *Eur J Pharmacol*. (2014) 735:38–43. doi: 10.1016/j.ejphar.2014.04.017
40. Songarj P, Luh C, Staib-Lasarzik I, Engelhard K, Moosmann B, Thal SC. The antioxidative, non-psychoactive tricyclic phenothiazine reduces brain damage after experimental traumatic brain injury in mice. *Neurosci Lett*. (2015) 584:253–8. doi: 10.1016/j.neulet.2014.10.037

Conflict of Interest: The authors declare that the research was conducted in the absence of any commercial or financial relationships that could be construed as a potential conflict of interest.

frontiers in Neurology

REVIEW
published: 05 May 2021
doi: 10.3389/fneur.2021.662034

Targeting Parthanatos in Ischemic Stroke

Raymond C. Koehler[1]*, *Valina L. Dawson*[2,3,4,5] *and Ted M. Dawson*[2,3,4,6]

[1] *Department of Anesthesiology and Critical Care Medicine, The Johns Hopkins University, Baltimore, MD, United States,* [2] *Neuroregeneration and Stem Cell Programs, The Institute of Cell Engineering, The Johns Hopkins University, Baltimore, MD, United States,* [3] *Department of Neurology, The Johns Hopkins University, Baltimore, MD, United States,* [4] *Department of Neuroscience, The Johns Hopkins University, Baltimore, MD, United States,* [5] *Department of Physiology, The Johns Hopkins University, Baltimore, MD, United States,* [6] *Department of Pharmacology and Molecular Sciences, The Johns Hopkins University, Baltimore, MD, United States*

Parthanatos is a cell death signaling pathway in which excessive oxidative damage to DNA leads to over-activation of poly(ADP-ribose) polymerase (PARP). PARP then generates the formation of large poly(ADP-ribose) polymers that induce the release of apoptosis-inducing factor from the outer mitochondrial membrane. In the cytosol, apoptosis-inducing factor forms a complex with macrophage migration inhibitory factor that translocates into the nucleus where it degrades DNA and produces cell death. In a review of the literature, we identified 24 publications from 13 laboratories that support a role for parthanatos in young male mice and rats subjected to transient and permanent middle cerebral artery occlusion (MCAO). Investigators base their conclusions on the use of nine different PARP inhibitors (19 studies) or PARP1-null mice (7 studies). Several studies indicate a therapeutic window of 4–6 h after MCAO. In young female rats, two studies using two different PARP inhibitors from two labs support a role for parthanatos, whereas two studies from one lab do not support a role in young female PARP1-null mice. In addition to parthanatos, a body of literature indicates that PARP inhibitors can reduce neuroinflammation by interfering with NF-κB transcription, suppressing matrix metaloproteinase-9 release, and limiting blood-brain barrier damage and hemorrhagic transformation. Overall, most of the literature strongly supports the scientific premise that a PARP inhibitor is neuroprotective, even when most did not report behavior outcomes or address the issue of randomization and treatment concealment. Several third-generation PARP inhibitors entered clinical oncology trials without major adverse effects and could be repurposed for stroke. Evaluation in aged animals or animals with comorbidities will be important before moving into clinical stroke trials.

Keywords: cerebral ischemia, neuroinflammation, parthanatos, poly(ADP ribose) polymerase, stroke, middle cerebral artery occlusion

OPEN ACCESS

Edited by:
Simone Beretta,
San Gerardo Hospital, Italy

Reviewed by:
Diana Amantea,
University of Calabria, Italy
Mohammed Iqbal Hossain,
University of Alabama at Birmingham, United States

***Correspondence:**
Raymond C. Koehler
rkoehler@jhmi.edu

Specialty section:
This article was submitted to Stroke, a section of the journal Frontiers in Neurology

Received: *31 January 2021*
Accepted: *01 April 2021*
Published: *05 May 2021*

Citation:
Koehler RC, Dawson VL and Dawson TM (2021) Targeting Parthanatos in Ischemic Stroke. Front. Neurol. 12:662034. doi: 10.3389/fneur.2021.662034

INTRODUCTION

With the recent success of endovascular thrombectomy in establishing recanalization and, in many cases, reperfusion in stroke patients with large vessel occlusions, neurologic outcome has been improved, especially for those who have sufficient collateral blood flow to slow the transition from penumbra to irreversible injury (1–7). However, a significant portion of those with successful reperfusion may still die or be left with significant neurologic deficits. Thus, interest has been

renewed in finding neuroprotective agents that can be used as an adjunct with thrombectomy and clot lysis (8–10).

One potential target that has been investigated in the context of cerebral ischemia over the past three decades is poly(ADP-ribose) polymerase (PARP). This family of enzymes is involved in post-translational protein modification by ADP-ribosylation. PARP1, in particular, is well-known for its role in the DNA repair process. Indeed, prolonged inhibition of PARP1 is cytotoxic and has been used as a strategy in oncology to induce cell death in rapidly proliferating cancer cells. However, when numerous DNA strands are damaged and PARP activity reaches high levels, this elevated activity can induce programmed cell death. This PARP-dependent form of programmed cell death has been termed parthanatos. A number of PARP inhibitors have been developed that block parthanatos, including that which occurs in neurons in response to excitotoxic stimuli and oxygen-glucose deprivation (OGD). A body of literature indicates that, in addition to arresting cell death, PARP inhibitors can reduce the NFκB-mediated pro-inflammatory response of microglia, suppress matrix metalloproteinase (MMP-9) release, and limit blood-brain barrier (BBB) damage and hemorrhagic transformation. Thus, PARP inhibitors can act to directly protect neurons and to limit secondary injury from inflammatory processes. These multi-targeted actions of PARP inhibitors make them strong candidates for prolonging neuronal viability and ameliorating reperfusion injury. In this review, we will consider the mechanisms by which PARP activity contributes to cell death and neuroinflammation and then examine the evidence that PARP inhibitors can protect the brain from ischemic stroke.

MECHANISMS OF PARP-DEPENDENT NEURONAL CELL DEATH (PARTHANATOS)

Damage to DNA by oxidants such as peroxynitrite rapidly activates PARP (11, 12). Peroxynitrite formation is increased by the excess production of nitric oxide (NO) and superoxide anion (13–15). In the context of cerebral ischemia, reduced ATP production results in neuronal depolarization, release of synaptic glutamate, and decreased reuptake by glutamate transporters (16, 17). Excess extracellular glutamate activates N-methyl-D-aspartate (NMDA) and other glutamate receptors, leading to an excitotoxic process that involves increased intracellular Ca^{2+}. A key aspect of the excitotoxic process is the association of the NR2B subunit to post-synaptic density-95 scaffolding protein and stimulation of NO synthase (18). NO is highly diffusible and can target other neurons and cell types. Major sources of superoxide during and after ischemia are the uncoupling of the mitochondrial electron transport chain (19) and the activation of NADPH oxidases (20, 21). In the context of reperfusion, the increased reoxygenation supports excess superoxide production (22). Although regeneration of ATP can reduce extrasynaptic glutamate detected by microdialysis, it is thought that increased glutamate levels in the extracellular synaptic cleft can persist during reperfusion (23, 24). In addition, altered phosphorylation of NMDA receptor subunits and of neuronal nitric oxide synthase (nNOS) can sustain the activity of these molecules through their persistent association with post-synaptic density proteins during the reperfusion period (25). Thus, peroxynitrite formation can be augmented during the reperfusion period and lead to further DNA damage and activation of PARP. This scenario provides a basis for the therapeutic potential of PARP inhibitors administered during reperfusion produced by thrombectomy and tissue plasminogen activator administration.

In 1994, the Dawson laboratory reported that exposing cultured mouse neurons to NMDA or high levels of NO activates PARP and that inhibition of PARP protects the neurons from cell death (26). Moreover, $PARP1^{-/-}$ and $nNOS^{-/-}$ murine neurons were shown to be resistant to cell death evoked by NMDA (27, 28). These findings have more recently been replicated in human neuronal cultures derived from embryonic stem cells and inducible pluripotent stem cells, as these cultures were protected from NMDA and OGD by inhibition of PARP or nNOS (29). Importantly, protective effects were seen in both male and female human neurons with the new generation of PARP inhibitors developed for use in oncology: olaparib, veliparib, rucaparib, and talazoparib. PARP's instigation of cell death involves release of apoptosis-inducing factor (AIF) from a mobile pool in the outer mitochondrial membrane (30–32). This release requires the formation of large PAR polymers by PARP and the binding of PAR to a PAR-binding site motif on AIF (33). Degradation of the PAR polymer by PAR glycohydrolase (PARG) decreased the release of AIF by PAR polymers (34) and by NMDA (35). Once AIF is released from the mitochondria, it can bind to macrophage migration inhibitory factor (MIF) (36). The binding of AIF to MIF results in uptake of the complex into the nucleus where the complex binds to DNA. The binding enables MIF to act as an endonuclease that degrades genomic DNA into 20–50 kb DNA fragments, and that leads to cell death. This signaling pathway is summarized in **Figure 1** and is reviewed in detail elsewhere (37).

Prolonged ischemia results in classical necrosis, whereas reperfusion can result in sustained restitution of cell function if the duration and severity of ischemia are not prolonged or intense. With reperfusion after an intermediate ischemic duration and/or intermediate ischemic severity, some neurons can generate sufficient ATP to restore membrane potential. Often, these neurons then undergo various forms of delayed programmed cell death. Delayed apoptosis may occur in ischemic border regions where ischemia is less severe and not as prolonged. However, with durations of middle cerebral artery (MCA) occlusion (MCAO) lasting >30 min, programmed necrosis predominates. The two most studied forms of programmed necrosis in stroke are parthanatos and RIP1-dependent necroptosis. The latter involves formation of a necroptosome consisting of phosphorylated RIP-1 and phosphorylated RIP-3 anchored by MLKL. Inhibition of necroptosome formation by intraventricular injection of necrostatin-1 decreases infarct volume by one-third (38), but clinical translation of this work is limited by the poor BBB penetration of this inhibitor class. In contrast, several different PARP inhibitors have proven effective following systemic administration, yielding a reduction in infarct volume that often exceeds 50%, as reviewed below.

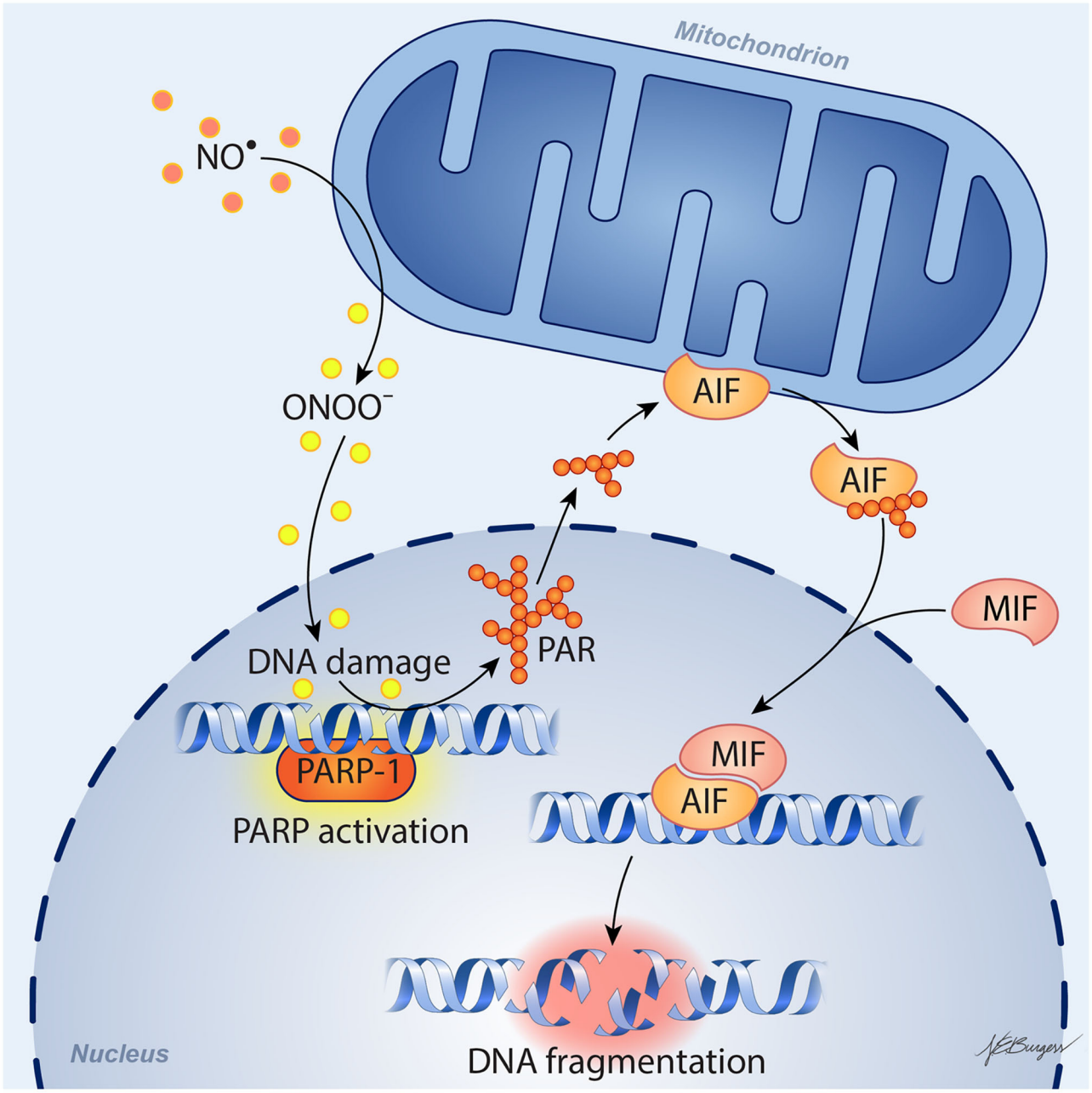

FIGURE 1 | Schematic diagram of parthanatos signaling. Activation of NMDA receptors stimulates neuronal nitric oxide (NO) synthase (nNOS). Ischemia and reperfusion lead to excess superoxide production in mitochondria and from NADPH oxidase. The abundant NO and superoxide spontaneously generate peroxynitrite ($ONOO^-$). This strong prooxidant, along with other reactive oxygen species (ROS), damages DNA strands and thereby causes activation of poly(ADP-ribose) polymerase (PARP). When the DNA damage is great, the consequent over-activation of PARP leads to abundant PAR polymer formation in the nucleus; some of the poly(ADP) ribosylated carrier proteins exit the nucleus and cause the release of apoptosis-inducing factor (AIF) from a pool on the outer mitochondrial membrane. Once in the cytosol, AIF can bind to macrophage migration inhibitory factor (MIF). Together, they enter the nucleus and produce large-scale DNA degradation and cell death.

In addition to the parthanatos mechanism of neurodegeneration described above, the product of PARP activation, PAR, is emerging as an important contributor in the separation and aggregation of amyloid proteins in the degenerative process of Parkinson's disease, Alzheimer's disease and amyotrophic lateral sclerosis (39). Future studies investigating the role of PAR dependent liquid-liquid phase separation and aggregation of proteins are needed to determine whether this plays a role in stroke pathogenesis.

MECHANISMS OF PARP-DEPENDENT NEUROINFLAMMATION

In addition to acting directly on neurons to block parthanatos, PARP inhibitors can exert anti-inflammatory effects and protect endothelial cells. For example, PARP inhibitors have been reported to exert anti-inflammatory effects in a wide range of systemic models of inflammation (endotoxemia, peritonitis, colitis, streptozotocin-induced diabetes) (40) and to protect endothelial-dependent responses from oxidant stress associated with aging (41), streptozotocin-induced diabetes (42), hypochlorite (43), and H_2O_2 (44). Exposing macrophages to oxidants stimulates their PARP activity (45). Exposing cultured BV2 microglial cells to lipopolysaccharide induces NF-κB, inducible nitric oxide synthase (iNOS), nitrite formation, reactive oxygen species formation, and tumor necrosis factor-α (TNFα), all of which are attenuated by the PARP inhibitor PJ34 (46). With global cerebral ischemia, PJ34 pre-treatment attenuated loss of tight junctions, Evan's Blue extravasation, cerebral edema, and neutrophil infiltration (47). Microglia-mediated loss of tight junctions is absent in co-cultures of PARP1-null microglia and endothelial cells (48). In cultured human brain microvascular endothelial cells, PARP inhibitors reduce AIF nuclear translocation and cell death after repeated bouts of hypoxia and reoxygenation (49). In microglial cultures exposed to the alarmin S100B, induction of interleukin-1β (IL-1β) and iNOS was blunted by the PARP inhibitor veliparib, and injection of S100B directly into striatum produced an accumulation of Iba1-positive microglia that was attenuated by veliparib (50). Glutamate activation of microglia is also PARP-dependent (51).

It is known that enzymatic activity of PARP1 promotes NF-κB–driven transcription in microglia (52). The underlying mechanism has been investigated by Kauppinen et al. In microglia, PARP1 activity facilitates NF-κB binding to DNA, and PARP1 gene deletion or inhibition suppresses TNFα-induced release of MMP-9 by microglia and toxicity to co-cultured neurons (53). As illustrated in **Figure 2**, TNFα activation of PARP1 involves Ca^{2+} influx, stimulation of phosphatidylcholine-specific phospholipase C, and activation of the MEK1/2-ERK1/2 pathway (54), leading to phosphorylation of PARP1 by ERK2 (55). This mechanism does not require DNA damage, which can independently activate PARP *via* stimulation of ERK1/2. One way PARP activity might enable NF-κB binding to DNA is by competing with sirtuin 1 for NAD^+ substrate. When sirtuin 1 deacetylates the p65 subunit of NF-κB, it is not able to bind to DNA. With excessive activity of PARP sufficient to decrease NAD^+, NF-κB binding to DNA is increased. This effect is reversed by preventing the decrease in NAD^+ and is replicated by inhibition of sirtuin 1 (56). Thus, enzymatic activity of PARP1 plays a key role in the activation of NF-κB binding to DNA.

In vivo, several pieces of evidence are consistent with PARP inhibitors acting directly to modify the delayed neuroinflammatory response in models of traumatic brain injury (TBI) or ischemia. Rats treated with the PARP inhibitor INO-1001 starting 1 day after TBI exhibited reduced activation of microglia (57), and mice treated with PJ34 starting 1 day after TBI had less neuronal loss in cortex and thalamus and improved sensorimotor function at 3 weeks of recovery (46). Likewise, veliparib decreased expression of pro-inflammatory cytokines and Iba-1 in rats and Iba-1 expression in pigs, even when administration was delayed until 24 h after TBI (58). In a model of global ischemia, administration of PJ34 at 8 h of reperfusion reduced microglial activation while increasing neuronal survival at 7 days (59), and a further delay in treatment until 2 days still resulted in suppressed microglial activation and astrogliosis and increased neuronal density and bromodeoxyuridine staining 8 weeks later (60). With regard to transient MCAO, pre-treatment with PARP inhibitor 3-aminobenzamide (3-AB) decreased MMP-9 activity, neutrophil infiltration, and infarct volume in rats (61), and PJ34 reduced the induction of iNOS and ICAM-1 and decreased infarct volume at 72 h in mice (62). Minocycline is an inhibitor of PARP1 at nanomolar concentrations (63), and this inhibition may be one mechanism by which minocycline reduces post-ischemic neuroinflammation. Finally, a clinical study showed that treating blood samples from stroke patients *ex vivo* with a PARP inhibitor increased the fraction of T-regulatory cells, which are thought to play a role in the brain repair stage after stroke (64).

Therefore, PARP inhibitors are likely to be multipotent in stroke by (1) blocking programmed neuronal necrosis in a large portion of neurons, (2) attenuating the early pro-inflammation response that is thought to be accelerated by reperfusion, and (3) protecting the endothelium and limiting hemorrhagic transformation that is thought to be augmented during aging. This broad spectrum action may be superior to that of drugs such as nerinetide (Tat-NR2B9c), which primarily targets excitotoxicity (18, 65, 66) and failed in the recent Phase III ESCAPE-NA1 trial (67) of ischemic stroke reperfusion therapy.

EVIDENCE FOR A ROLE OF PARTHANATOS IN FOCAL ISCHEMIC STROKE BASED ON MOLECULAR INTERVENTIONS IN MALE MICE

Eight studies have used PARP1-null mice ($PARP1^{-/-}$) and PARP2-null mice ($PARP2^{-/-}$) to investigate the role of PARPs in stroke with models of MCAO. Consistent reductions in infarct volume were seen among these studies emanating from three laboratories. The mean percent difference in infarct volume from the corresponding wild-type (WT) mice and the 95% confidence intervals for these studies with different MCAO durations and different survival times are displayed in **Figure 3** for male mice (female mice are discussed in a later section).

Role of PARP1

In 1997, Eliasson et al. (27) reported that male $PARP1^{-/-}$ mice subjected to 2 h of MCAO did not display the increase in PAR polymer formation seen in WT mice, and that their infarct volume was 80% smaller. PARP heterozygotes displayed a 65% reduction in infarct volume. In the same year, Endres et al. (68,

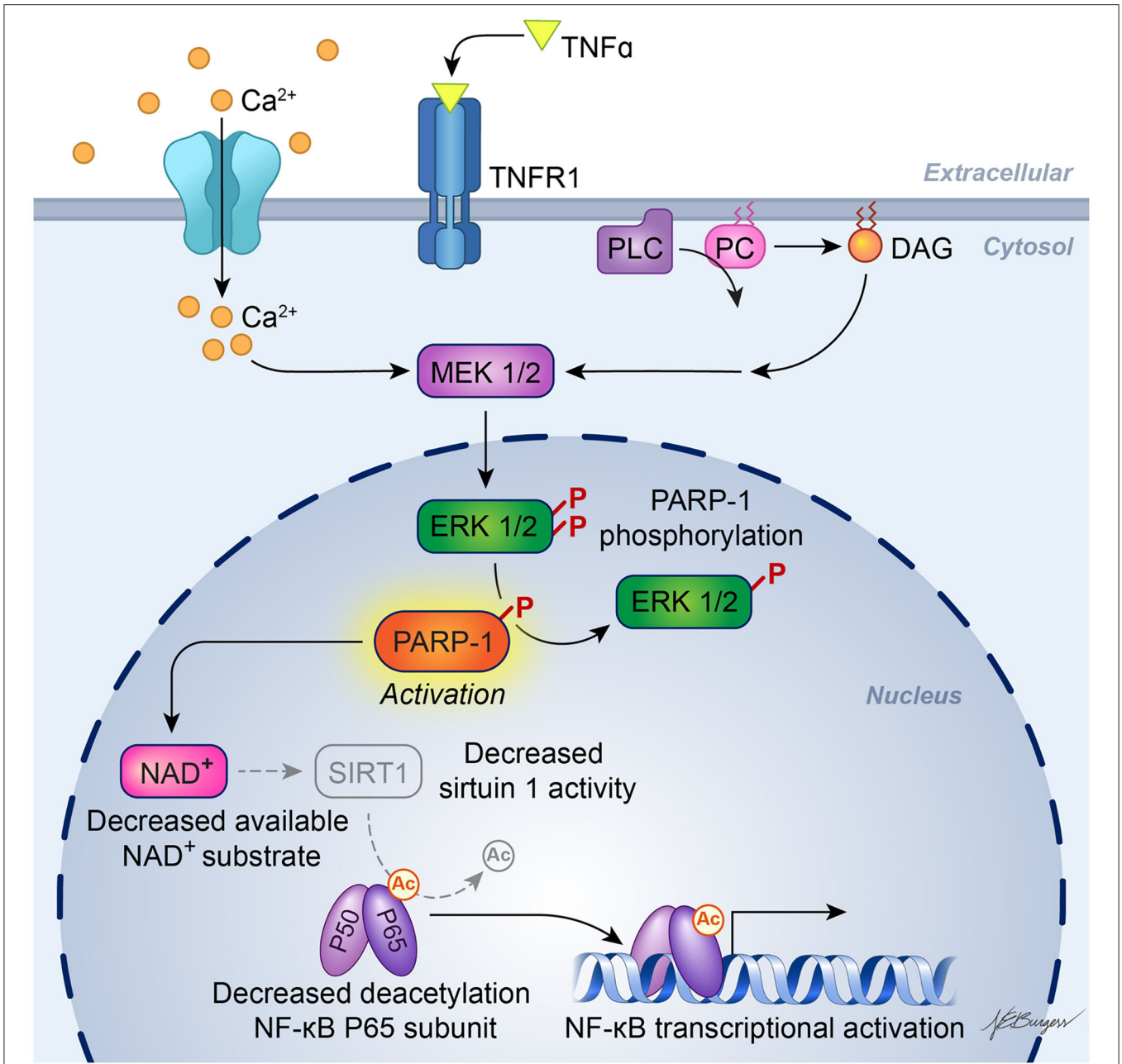

FIGURE 2 | Schematic diagram of PARP activation in inflammatory signaling. Experiments in cultured microglia and astrocytes indicate that binding of TNFα to its receptor, TNFR1, leads to calcium influx and activation of phosphatidylcholine (PC)-specific phospholipase C (PC-PLC), resulting in formation of diacylglycerol (DAG) and downstream action of the MEK1/2-ERK1/2 pathway. ERK2 phosphorylation of PARP-1 increases PARP-1 activity, which then facilitates activation of NF-κB transcription. One possible mechanism whereby PARP-1 facilitates NF-κB transcription is by depleting NAD^+, which is also used as a substrate by sirtuin-1. Sirtuin-1 normally keeps the P65 subunit of NF-κB deacetylated, but a decrease in sirtuin-1 activity will result in acetylated P65, which enables NF-κB transcription. [Adapted, with permission, from Vuong et al. (54) and Kaupinnen et al. (56)].

75) reported that male $nNOS^{-/-}$, $PARP1^{-/-}$, or WT mice pre-treated with 3-AB had decreased infarct volume associated with less PAR polymer formation. PARP is activated by DNA strand breaks, which can be detected in rat striatum at 2 h and in cortex at 4 h after a 2-h MCAO insult (76). Whereas, both the NMDA antagonist MK-801 and the PARP inhibitor 3,4-dihydro-5-[4-(1-piperidinyl)butoxy]-1(2H)-isoquinolinone (DPQ) reduced infarct volume, only MK-801 decreased DNA strand breaks, thereby indicating that NMDA antagonists act upstream and PARP inhibitors act downstream of DNA strand breaks in

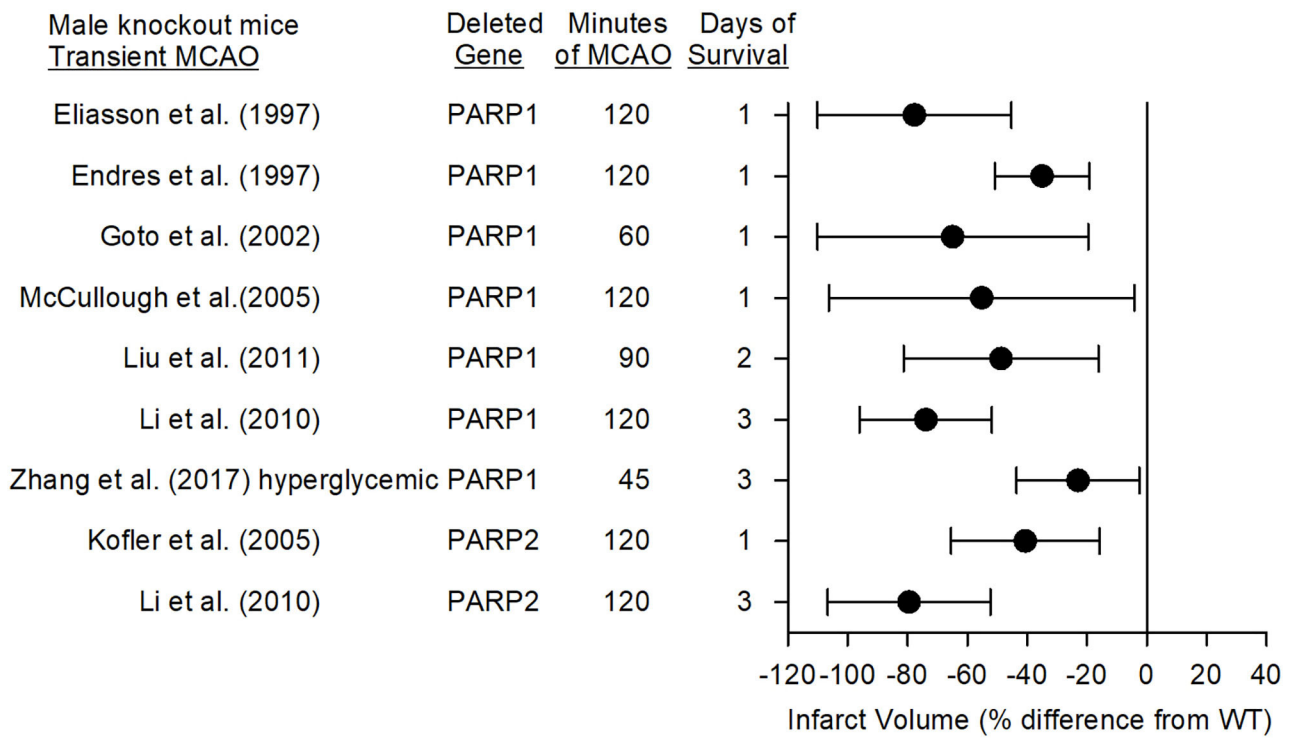

FIGURE 3 | Effect sizes and 95% confidence intervals on infarct volume after transient middle cerebral artery occlusion (MCAO) in male PARP1$^{-/-}$ mice and male PARP2$^{-/-}$ mice, relative to their respective wild-type controls, were derived from mean and SD values and sample sizes extracted from publications by Eliasson et al. (27), Endres et al. (68), Goto et al. (69), McCullough et al. (70), Liu et al. (71), Li et al. (72), Zhang et al. (73), and Kofler et al. (74). These reports from three different laboratories showed significant reductions in infarct volume.

protecting the brain. Staining of human autopsy tissue from patients who died of stroke revealed increased expression of PARP and PAR polymers in necrotic neurons within and adjacent to the infarct, supporting a role for parthanatos in human stroke (77).

Using MRI, Goto et al. (69) demonstrated that PARP1 contributes to edema and to expansion of infarction over 3 days. At 1 h of MCAO, male PARP1$^{-/-}$ mice had equivalent decreases in the apparent diffusion constant (ADC) and equivalent volumes of low ADC, indicating a similar volume of initial anoxic depolarization. However, by 1 day of reperfusion, the volume of tissue with low ADC was greater in WT than in PARP1$^{-/-}$ mice. T2-weighted determination of infarct volume expanded from 1 through 3 days of reperfusion, whereas the lower infarct volume seen at 1 day in PARP1$^{-/-}$ mice failed to further expand by 3 days, consistent with a role of PARP1 in both neuronal cell death and delayed neuroinflammation.

Because release of AIF from the mitochondria depends on signaling by a large PAR polymer (34, 35), the effect of manipulating PAR polymer availability was tested in mice that overexpressed the PAR degradation enzyme PARG or in mice with heterozygous knockdown of PARG. PARG overexpression decreased infarct volume, whereas PARG knockdown increased infarct volume (35). Furthermore, Iduna is a PAR-dependent ubiquitin E3 ligase (78) whose overexpression reduces PAR polymer availability and attenuates infarct volume after transient MCAO (79). Collectively, these data are consistent with large PAR polymers acting as a death signal to mitochondria in focal ischemia.

The time course of PAR formation and AIF translocation to the nucleus has been examined with different durations of MCAO (80). After 1-h MCAO in male mice, the increase in PAR peaked at 20 min of reperfusion and remained elevated through 24 h. AIF accumulation in the nucleus increased progressively from 20 min to 6 h and from 6 h to 24 h of reperfusion after 1 h of MCAO. Since AIF remains trapped in the nucleus, its accumulation is best related to the time-integral of elevated PAR. In contrast to 1-h MCAO, the increase in nuclear AIF after 30 min of MCAO was delayed beyond 6 h of reperfusion, consistent with a delay of cell death signaling after shorter ischemic durations. The increase in nuclear AIF was delayed after permanent MCAO compared to 1 h of transient MCAO. Thus, reperfusion itself is capable of accelerating AIF nuclear translocation, presumably because a burst of oxidative stress at reperfusion damages nucleic acids. These observations emphasize the need to administer a PARP inhibitor soon after the onset of reperfusion for optimal efficacy. Further, consistent with a role for

nNOS in contributing to PARP activation, nNOS$^{-/-}$ mice or administration of an nNOS inhibitor to WT mice reduced formation of PAR polymers and AIF nuclear translocation after transient MCAO.

Parthanatos is associated with large-scale DNA breakdown. Based on work with *C. elegans* homologs of endonuclease G, it had been assumed that mammalian endonuclease G was responsible for executing AIF-dependent DNA degradation. However, infarct volume of endonuclease G$^{-/-}$ mice was equivalent to that of their WT counterparts (81). Moreover, infusion of the PARP inhibitor DR2313 throughout MCAO and early reperfusion decreased infarct volume to a similar extent in WT and endonuclease G$^{-/-}$ male mice, thereby indicating that endonuclease G is not essential for executing parthanatos. Later, it was discovered that MIF serves as an endonuclease in parthanatos when it is complexed to AIF (36). The binding of AIF to MIF in the cytosol promotes uptake of the AIF/MIF complex into the nucleus and activation of MIF's endonuclease activity. Knocking out the MIF gene, altering its binding site to AIF, or altering its endonuclease activity site all were found to markedly reduce infarct volume at 1 and 7 days after 45 min of MCAO in male mice (36).

Because ischemia is associated with acidosis, Zhang et al. (73) explored the role of acidosis in parthanatos. In murine primary neuronal culture, acidosis augmented chemically induced PAR polymer formation, AIF nuclear translocation, and cell death. The augmented AIF translocation and cell death were attenuated by acid-sensitive ion channel 1a and PARP inhibitors. *In vivo*, acute hyperglycemia and its associated severe acidosis are known to augment infarction. Acute hyperglycemia during transient MCAO was found to enhance intraischemic acidosis and augment PAR polymer formation and AIF nuclear translocation, which were attenuated by administration of a PARP inhibitor. Hyperglycemic PARP1$^{-/-}$ mice had a reduction in infarct volume, indicating that parthanatos still plays a role in acidosis-augmented injury.

Role of PARP2

Kofler et al. (74) reported that infarct volume in PARP2$^{-/-}$ male mice was reduced by 41% compared to that in WT mice at 1 day of recovery, whereas a later study by Li et al. (72) showed a 79% reduction at 3 days of recovery. The latter reduction was comparable to the 74% reduction obtained in PARP1$^{-/-}$ male mice at 3 days after MCAO in the same study. Both knockouts had less PAR formation and AIF nuclear translocation than did WT mice. These reductions were not attributed to differences in cerebral arterial anatomy, MCA distribution volume-at-risk, or regional cerebral blood flow as measured with iodoantipyrine autoradiography. The large protection seen in PARP2$^{-/-}$ mice was unexpected because PARP2 is less abundant than PARP1, suggesting a complex interaction between PARP1 and PARP2 in the context of stroke. PARP inhibitors examined thus far do not exhibit a strong selectivity for PARP1 over PARP2 (82) and hence do not distinguish the role of PARP1 and PARP2 in stroke.

EFFICACY OF PARP INHIBITORS FOR FOCAL ISCHEMIC STROKE IN MALE RODENTS

Transient Focal Ischemia in Male Mice and Rats

Figure 4 summarizes the effects on infarct volume reported with nine distinct PARP inhibitors in male mice and rats subjected to transient focal ischemia. In some studies, the drugs were administered before inducing the stroke to ensure delivery to the ischemic region, whereas in others, administration was delayed for various times after the onset of stroke or after reperfusion to assess the therapeutic time window. Based on 15 studies carried out between 1997 and 2018 in 13 independent laboratories, PARP inhibition significantly reduced infarct volume from 33 to 86%.

First Generation PARP Inhibitors

3-AB and DPQ are prototypical PARP inhibitors used for *in vitro* biochemical studies. Early *in vivo* work showed that male mice pre-treated intraventricularly with 3-AB had a 46% decrease in infarct volume associated with less PAR polymer formation (68, 75), and rats pre-treated intraperitoneally with 10 mg/kg DPQ exhibited a 40% reduction in infarct volume (76). However, the relatively high doses required for *in vivo* experiments raise the possibility off-target effects.

Second Generation PARP Inhibitors

The second generation PJ34 was developed to be a more potent and specific PARP inhibitor than 3-AB and DPQ. Abdelkarim et al. (84) found that pre-treatment with PJ34 decreased infarct volume by 49% in mice subjected to 1-h MCAO and by 90% in rats subjected to 2-h MCAO. Importantly, delaying PJ34 administration until just prior to reperfusion in the rat still reduced infarct volume by 74%. PJ34 was also shown to reduce AIF nuclear translocation (92). Early administration of other specific PARP inhibitors, MP-124 and FR247304, reduced infarct volume by 53 and 37%, respectively, in male rats (86, 88). Interestingly, the potent PARP inhibitor INO-1001 reduced amyloid precursor protein accumulation and AIF translocation in white matter tracts and reduced infarct volume by 86% when administered at reperfusion after 2 h of MCAO in rats (85). Likewise, the PARP inhibitor DR2313 reduced infarct volume by 46% when administration was delayed by 2 h (87) and HTDAMTIQ reduced infarct volume by 65% when delayed by 4 h in rats (89). Thus, several studies using different PARP inhibitors demonstrate neuroprotection in reperfusion models of MCAO. Moreover, in a different reperfusion model in which thrombin was injected directly into the MCA of male mice, administration of rt-PA at 3 h only modestly increased laser Doppler flow (LDF). Administration of PJ34 after the onset of ischemia and again at 3 h substantially improved recovery of LDF, decreased tissue hemoglobin content, decreased infarct volume, and reduced sensorimotor deficits (90). These data suggest that PARP inhibition does not have an adverse interaction with tissue plasminogen activator in enabling neuroprotection.

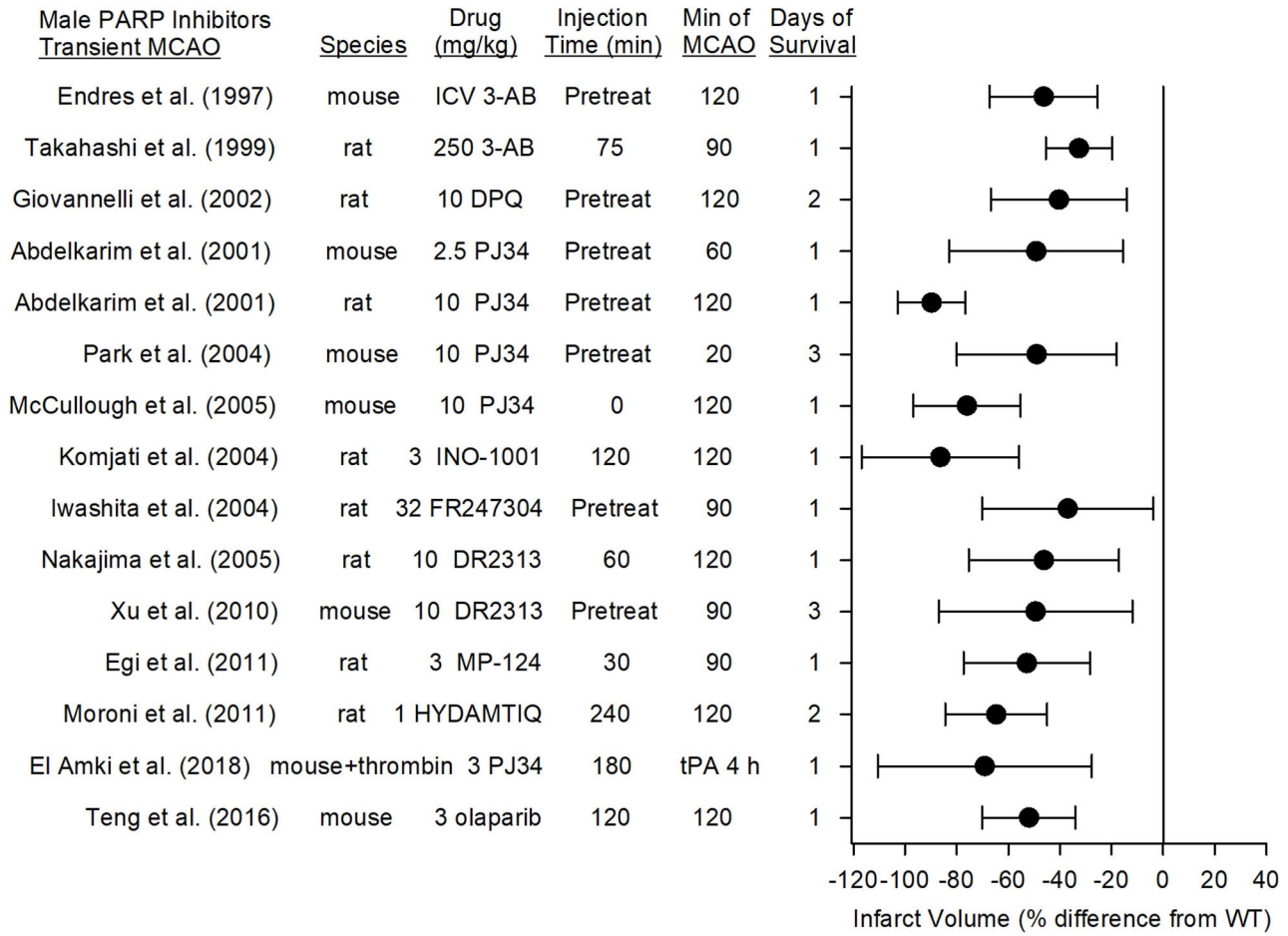

FIGURE 4 | Effect sizes and 95% confidence intervals of PARP inhibitor treatment on infarct volume after transient middle cerebral artery occlusion (MCAO) in male mice and male rats, relative to their respective controls, were derived from mean and SD values and sample sizes extracted from publications by Endres et al. (68), Takahashi and Greenberg (83), Giovannelli et al. (76), Abdelkarim et al. (84), Park et al. (62), McCullough et al. (70), Komjati et al. (85), Iwashita et al. (86), Nakajima et al. (87), Xu et al. (81), Egi et al. (88), Moroni et al. (89), El Amki et al. (90), and Teng et al. (91). These reports from 12 different laboratories using 9 distinct inhibitors showed a significant reduction in infarct volume.

Third Generation PARP Inhibitors

Several third generation PARP inhibitors have been designed for their DNA trapping ability for use in human oncology trials, including olaparib, rucaparib, veliparib, talazoparib, niraparib, E7016, and CEP-9722 (93). Of these, olaparib has been tested with MCAO. In randomized groups of male ICR mice that underwent 2-h MCAO, olaparib was injected intraperitoneally at doses of 1, 3, 5, 10, or 25 mg/kg at reperfusion. Doses of 3 and 5 mg/kg, but not higher doses, reduced infarct volume by 52%, attenuated IgG extravasation, and improved ability to use four paws when hanging from a bar (91). In comparisons of the various third generation inhibitors, veliparab had particularly good brain penetration. In rhesus monkeys administered 5 mg/kg veliparib orally, penetration into the cerebrospinal fluid was 57% of the plasma concentration (94). In rats bearing glioma tumors that were treated with 50 mg/kg/d veliparib, the brain concentration (0.72 μg/g excluding glioma) was 77% of the plasma concentration (1.36 μg/g) (95). Veliparib is being tested as a repurposed drug in a multicenter, controlled, randomized pre-clinical trial as part of the Stroke Pre-clinical Assessment Network (https://spannetwork.org/).

Therapeutic Window of PARP Inhibitors in Transient MCAO

Several studies have directly assessed the effect of variable treatment delays of PARP inhibitors. With 2 h of MCAO in male rats, administration of the PARP inhibitor INO-1001 at 2, 4, or 6 h of MCAO (0, 2, or 4 h of reperfusion) reduced infarct volume by 86, 55, and 27%, respectively when compared to vehicle treatment (85). Similar results were obtained with the PARP inhibitor DR2313, which reduced infarct volume by 62, 47, and 44% when administered to male rats 5 min before 1-h MCAO and 2 and 4 h after MCAO, respectively (87). Likewise, a distinct PARP inhibitor, HYDAMTIQ, administered to male rats 4 h after transient MCAO (2-h duration) reduced infarct volume by 65% at 2 days and 55% at 7 days of recovery (89). Thus, the therapeutic

window appears to be in the range of 4–6 h in rats subjected to transient MCAO.

Permanent MCAO

PARP inhibitors also are capable of reducing infarct volume in the distal MCAO model of permanent focal ischemia, which produces primarily a cortical lesion, and with permanent placement of the filament in the internal carotid artery at the MCA root, which causes a larger infarction that includes striatum and cerebral cortex. In eight studies from seven different laboratories, the reduction in infarct volume with seven different PARP inhibitors ranged from 34 to 62% (**Figure 5**). The range and average effect size of all of the studies was somewhat less than the range and average effect size seen in the transient MCAO models.

In the rat model of permanent distal MCAO plus temporary bilateral carotid occlusion, the PARP inhibitor DPQ reduced infarct volume by 54% when administered as a pre-treatment (96) and by 40% when administered at 30 min after MCAO (97). Likewise, MP-124 administered at 5 min of MCAO reduced infarct volume by 42% in the same model (88).

In the rat permanent filament model, administration of DR2313 as a pre-treatment reduced infarct volume by 33% (87), and administration of INO-1001 at the onset of MCAO reduced infarct volume by 62% (85). 3-AB and HYDAMTIQ, when administered at 30 min of MCAO, reduced infarct volume by 50% (98) and 45% (89), respectively, compared to that of vehicle-treated animals. In the mouse permanent filament model, PJ34 administered at the onset of stroke decreased MMP activity, hemorrhagic transformation, and infarct volume (34% reduction) (99). When recombinant tissue plasminogen activator was given at 6 h of permanent ischemia, the degradation of tight junction proteins, the augmented tissue hemoglobin content, and the augmented sensorimotor deficits induced by recombinant tissue plasminogen activator were ameliorated by PJ34 treatment (100), implying that PARP inhibitors may be beneficial in those without successful recanalization.

The therapeutic window was examined in the rat permanent filament model with INO-1001. This PARP inhibitor, which reduced infarct volume by 62% when administered at the onset of permanent MCAO, remained effective in reducing infarct volume by 59% when administration was delayed by 2 h (85). When the delay was extended to 4 h, the reduction was 40%, but not statistically significant, most likely because this group was underpowered ($n = 6$). Thus, multiple PARP inhibitors are effective in models of permanent MCAO, and the therapeutic window is ∼2 h.

ROLE OF PARTHANATOS IN FEMALE ANIMALS WITH FOCAL ISCHEMIC STROKE

Female Mice

Young female mice and rats generally have smaller infarcts than their male counterparts. Some of this sex difference is attributable to estrogen because ovariectomy increases infarct size whereas estrogen replacement reduces infarct size (101, 102). It has often been difficult to show further reductions in infarct volume beyond that afforded by endogenous sex hormones in young healthy female rodents. The preponderance of studies that have investigated the use of PARP inhibitors for MCAO have used male animals. A sex difference in PARP-dependent ischemic injury was first noted in neonatal mice exposed to hypoxia-ischemia. In that study, PARP1$^{-/-}$ males were protected whereas PARP1$^{-/-}$ females were not (103). McCullough et al. (70) investigated sex differences in cell death mechanisms of mature brain in detail in 3-month-old mice. They first reported that female PARP$^{-/-}$ mice or WT mice administered PJ34 do not exhibit decreases in infarct volume after transient MCAO. To the contrary, infarct volume measured at 24 h was significantly increased, and the percent increase was large on account of the small infarct size in the WT females. The female WT mice exhibited an increase in PAR and nuclear AIF, although the increase in PAR was less than that seen in males (104). They went on to show that canonical apoptosis played a larger role in injury from MCAO in young female mice (105), an effect that was augmented in female PARP$^{-/-}$ mice (71). The augmented stroke injury in female PARP$^{-/-}$ mice was associated with augmented decreases in NAD^+ (106), which may reduce the protective effect of NAD^+-dependent SIRT deacetylase activity in limiting NF-κB transcription (56).

Because estrogen is known to account for the smaller infarct volume in WT females than in WT males, Liu et al. (71) also studied young female mice 2 weeks after ovariectomy and found an infarct size comparable to that in WT males. Ovariectomized PARP$^{-/-}$ mice did not display a decrease in infarct volume compared to that of ovariectomized WT mice. Infarct volume could still be reduced with a caspase inhibitor after ovariectomy in both WT and PARP$^{-/-}$ mice. When survival was extended to 48 h and permanent MCAO was induced in ovariectomized PARP$^{-/-}$ mice, protection was not seen (71). Thus, elevated estrogen levels in young female mice did not completely account for the observed sex differences in the role of PARP and classical apoptosis. However, three limitations should be noted with regard to clinical translation. (1) Though lack of PARP1 was not protective in young ovariectomized rats, a PARP inhibitor was not tested to distinguish a possible effect of lifelong PARP1 absence in young ovariectomized WT mice. (2) Although gross neurologic deficits were reported at 24 h after transient MCAO, long-term behavioral outcomes and neuroinflammation have not been reported with a PARP inhibitor or gene deletion in intact or ovariectomized female mice. (3) Acute or long-term outcomes have not been reported with a PARP inhibitor or gene deletion in middle-aged or older female mice, when protection by estrogen is lost.

Female Rats

In contrast to this work in female PARP1$^{-/-}$ mice, two laboratories have reported positive effects of PARP inhibitors in young female rats. Moroni et al. (89) found that administering 1 mg/kg of the PARP inhibitor HYDAMTIQ at reperfusion after 2 h of MCAO in female rats decreased infarct volume at 2 days by 34% (**Figure 6**). This reduction was <65% reduction seen in male

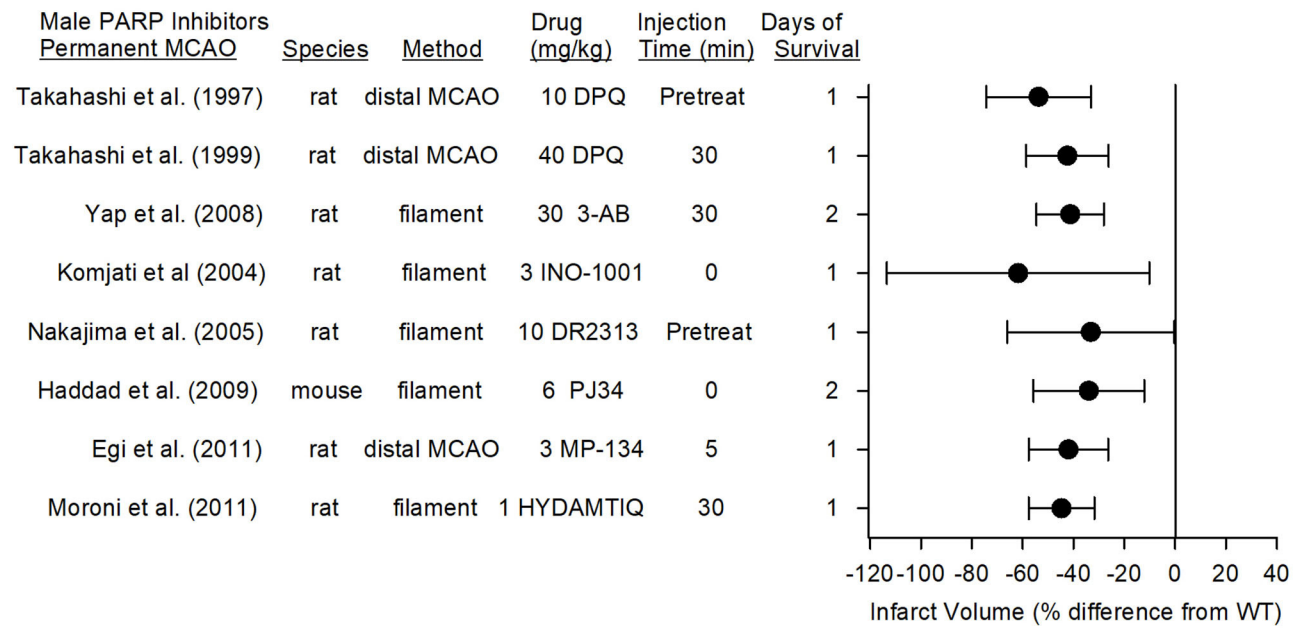

FIGURE 5 | Effect sizes and 95% confidence intervals of PARP inhibitor treatment on infarct volume after permanent middle cerebral artery occlusion (MCAO) in male mice and male rats, relative to their respective controls, were derived from mean and SD values and sample sizes extracted from publications by Takahashi et al. (96), Takahashi et al. (97), Yap et al. (98), Komjati et al. (85), Nakajima et al. (87), Haddad et al. (99), Egi et al. (88), and Moroni et al. (89). These reports from six laboratories using 7 distinct inhibitors showed a significant reduction in infarct volume.

mice with the same protocol. However, a higher dose (10 mg/kg) of a more hydrophobic form of this inhibitor (DAMTIQ) did produce similar infarct volume reductions in females and males.

Pre-treatment of female rats with 3-AB before 2-h MCAO reduced infarct volume and improved motor performance on the foot-fault, parallel bar, rope climbing, and ladder climbing tests over 28 days of recovery (107). Thus, it is unclear if the observed effect of PARP1 gene deletion in young female mice can be extended to use of a PARP inhibitor in other species. Of note, Tat-NR2Bc, which interrupts the membrane association of nNOS with the NR2B subunit and PSD95 (18) and decreases superoxide production by NADPH oxidase (20), is equally effective in markedly reducing infarction in male and female rats when given 1 h after permanent occlusion of a distal pial artery (108). Because this PSD95 coupling plays a critical role in excitotoxic damage that leads to peroxynitrite-induced DNA damage and PARP activation, these data also suggest that parthanatos likely plays an important role in female rats.

One final piece of evidence indicates that sex is less important in human neurons exposed to NMDA or OGD. In cultured human neurons, those with a female genotype and those with a male genotype exhibited similar increases in PAR, nuclear AIF, and cell death, and both were salvaged equivalently by treatment with an nNOS inhibitor or several third generation PARP inhibitors (29). Because sex can influence the inflammatory response, more work is needed to determine possible sex differences in how PARP modifies inflammation and evolution of the infarction process. In any case, current evidence does not make clear whether sex differences in parthanatos seen in mouse cultured neurons (109) or neonatal (103) or 3-month-old mice (70) would persist in aged animals.

SCIENTIFIC RIGOR FOR CLINICAL TRANSLATION OF PARP INHIBITORS

Randomization and Treatment Concealment

Most of the stroke studies carried out with PARP inhibitors and $PARP^{-/-}$ mice were performed before 2010, and many did not formally comment on randomization and blinding of treatment groups. Studies low in quality criteria of scientific rigor are thought to overestimate the true effect size. On the other hand, a large number of studies from multiple labs with many different PARP inhibitors consistently reported reductions in infarct volume with $n = 6$–20 per study. Although we did not conduct a formal meta-analysis, the consistent infarct reductions with a large effect size and reasonable sample sizes mitigates some of the quality concerns of the early studies.

PARP Inhibitor Experiments With Negative Findings

Publication bias of reporting only positive findings is always a concern, and whether negative findings have gone unreported, especially for young female animals, is unknown. In our literature survey, we found two experiments with negative results embedded in papers with otherwise positive results. Takahashi and Greenberg (83) reported that whereas 3-AB pre-treatment in

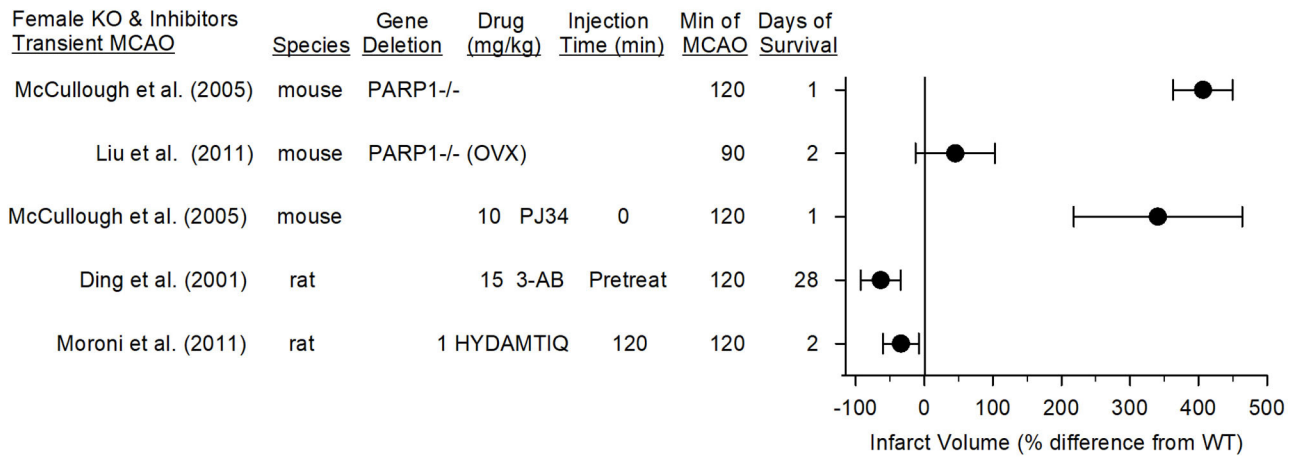

FIGURE 6 | Effect sizes and 95% confidence intervals on infarct volume after transient middle cerebral artery occlusion (MCAO) in female PARP1$^{-/-}$ mice and female mice treated with a PARP inhibitor, relative to their respective controls, were derived from mean and SD values and sample sizes extracted from publications by McCullough et al. (70), Liu et al. (71), Ding et al. (107), and Moroni et al. (89). On a percentage basis, the large increase in infarct volume in PARP1$^{-/-}$ mice is influenced by the small infarcts in the wild-type (WT) female mice. Ovariectimized (OVX) WT mice had larger infarcts than non-OVX WT mice, and the OVX PARP$^{-/-}$ mice did not have a significant increase in infarct volume compared to OVX WT mice.

rats reduced infarct volume, treatment at 15 min after reperfusion failed to do so ($n = 6$). Abdelkarim et al. (84) reported that whereas pre-treatment with PJ34 protected rats from 4 h of permanent MCAO, pre-treatment failed to protect from 24 h of permanent MCAO with the filament technique ($n = 8$–9). The latter effect could be explained by an inadequate plasma half-life when ischemia extends beyond 4 h. Positive effects of INO-1001 in permanent MCAO utilized multiple injections over 24 h (85). Thus, the negative findings in these studies may be explained by an ineffective dosing regimen and possibly by small sample sizes.

Large-Animal Models

Some early candidate treatments, such as tirilazad (110), monoclonal leukocyte antibody (111), and a hemoglobin-based oxygen carrier (112), that showed positive results in rodent models were not positive in large-animal stroke models or in human trials. Many reasons might explain why early human stroke trials with acute neuroprotectants failed, including rapid movement of a candidate drug from rodent models to human trials without testing in a large animal that has a brain more complex than a rodent's. Although PARP inhibitors have not been tested in large-animal models of stroke, INO-1001 was shown to protect neurons from spinal cord ischemia in pigs (113), and velaparib was shown to reduce microglial activation after TBI in pigs (58). These studies provide some assurance that PARP-dependent mechanisms of neuronal cell death and inflammation are operative in higher species. Nevertheless, the field would benefit from confirmation that PARP inhibitors are beneficial in a large-animal model of focal stroke in both males and females.

Neurobehavior Outcome

Many of the early studies were limited by the short survival time and reliance on only infarct volume as the primary outcome measurement. Translational stroke studies now place greater emphasis on neurobehavior outcomes. Whereas, a few studies with PARP inhibitors included acute sensorimotor deficits in the study design (90, 100), only two presented long-term neurobehavior outcomes. Nevertheless, these studies demonstrated persistent positive effects of PARP inhibitors on sensorimotor tests at 28 days in female rats (107) and 90 days in male rats (89).

Co-morbidities

One important factor that is thought to contribute to the poor track record for clinical translation of stroke therapies is that most animal stroke studies are performed in young healthy animals. This is also true for all of the aforementioned studies with PARP inhibitors. Therefore, future studies should consider testing these inhibitors in aged animals and in those with chronic disorders seen in the human stroke population, such as hypertension, diabetes, obesity, and high-salt diet.

CONCLUSIONS

Multiple forms of programmed cell death, including parthanatos, RIP1/RIP3-dependent necroptosis, and classical apoptosis, are operative after the onset of ischemic stroke. On the basis of infarct volume reduction, parthanatos is a predominate form, at least in male animals. In young female animals in whom sex hormones provide some protection compared to males, caspase-dependent apoptosis plays a more significant role than in young male animals. Nevertheless, a limited set of studies with long-term behavior outcomes support a benefit of PARP inhibitor treatment in male and female animals. In addition to blocking parthanatos, some of the benefit of PARP inhibition is likely derived from attenuation of NF-κB transcription in

microglia, astrocytes, and peripheral immune cells, although these anti-inflammatory effects have not been as well-studied in the context of stroke as they have in the context of TBI. Support for possible clinical translation of PARP inhibitors in stroke is favored by (1) positive effects on infarct volume reported by 13 independent laboratories with 9 different drugs, (2) efficacy in both transient and permanent focal ischemia, (3) a therapeutic window in the range of 4–6 h for infarct volume reduction, and (4) availability of PARP inhibitors with a good safety profile with month-long administration in human oncology trials. However, before clinical translation some limitations in the current literature would need to be addressed, including (1) resolving possible species differences in efficacy in young female animals, (2) performing additional pre-clinical studies with a high level of scientific rigor quality, (3) assessing the therapeutic window for neurobehavior outcome, which may differ from the therapeutic window for infarct volume reduction, (4) assessing efficacy in aged animals and those with cardiovascular risk factors, and (5) possibly testing in a large animal species with gyrencephalic brain.

AUTHOR CONTRIBUTIONS

RK analyzed the data in the literature and drafted the manuscript. VD and TD edited the manuscript. All authors contributed to the article and approved the submitted version.

FUNDING

This work was supported by grants from The National Institutes of Health U01 NS113444 (RK, TD, and VD), R21 NS102899 (RK), and R37 NS067525 (TD and VD).

ACKNOWLEDGMENTS

The authors are grateful to Claire Levine, M.S., E.L.S. for her editorial assistance and to Noelle Burgess for her graphical artwork assistance.

REFERENCES

1. Berkhemer OA, Fransen PS, Beumer D, van den Berg LA, Lingsma HF, Yoo AJ, et al. A randomized trial of intraarterial treatment for acute ischemic stroke. *N Engl J Med*. (2015) 372:11–20. doi: 10.1056/NEJMoa1411587
2. Campbell BC, Mitchell PJ, Kleinig TJ, Dewey HM, Churilov L, Yassi N, et al. Endovascular therapy for ischemic stroke with perfusion-imaging selection. *N Engl J Med*. (2015) 372:1009–18. doi: 10.1056/NEJMoa1414792
3. Goyal M, Demchuk AM, Menon BK, Eesa M, Rempel JL, Thornton J, et al. Randomized assessment of rapid endovascular treatment of ischemic stroke. *N Engl J Med*. (2015) 372:1019–30. doi: 10.1056/NEJMoa1414905
4. Jovin TG, Chamorro A, Cobo E, de Miquel MA, Molina CA, Rovira A, et al. Thrombectomy within 8 hours after symptom onset in ischemic stroke. *N Engl J Med*. (2015) 372:2296–306. doi: 10.1056/NEJMoa1503780
5. Saver JL, Goyal M, Bonafe A, Diener HC, Levy EI, Pereira VM, et al. Stent-retriever thrombectomy after intravenous t-PA vs. t-PA alone in stroke. *N Engl J Med*. (2015) 372:2285–95. doi: 10.1056/NEJMoa1415061
6. Albers GW, Marks MP, Kemp S, Christensen S, Tsai JP, Ortega-Gutierrez S, et al. Thrombectomy for stroke at 6 to 16 hours with selection by perfusion imaging. *N Engl J Med*. (2018) 378:708–18. doi: 10.1056/NEJMoa1713973
7. Nogueira RG, Jadhav AP, Haussen DC, Bonafe A, Budzik RF, Bhuva P, et al. Thrombectomy 6 to 24 hours after stroke with a mismatch between deficit and infarct. *N Engl J Med*. (2018) 378:11–21. doi: 10.1056/NEJMoa1706442
8. Shi L, Rocha M, Leak RK, Zhao J, Bhatia TN, Mu H, et al. A new era for stroke therapy: integrating neurovascular protection with optimal reperfusion. *J Cereb Blood Flow Metab*. (2018) 38:2073–91. doi: 10.1177/0271678X18798162
9. Bosetti F, Koenig JI, Ayata C, Back SA, Becker K, Broderick JP, et al. Translational stroke research: vision and opportunities. *Stroke*. (2017) 48:2632–7. doi: 10.1161/STROKEAHA.117.017112
10. Bix GJ, Fraser JF, Mack WJ, Carmichael ST, Perez-Pinzon M, Offner H, et al. Uncovering the Rosetta stone: report from the first annual conference on key elements in translating stroke therapeutics from pre-clinical to clinical. *Transl Stroke Res*. (2018) 9:258–66. doi: 10.1007/s12975-018-0628-9
11. Zhang J, Pieper A, Snyder SH. Poly(ADP-ribose) synthetase activation: an early indicator of neurotoxic DNA damage. *J Neurochem*. (1995) 65:1411–4.
12. Lorch S, Lightfoot R, Ohshima H, Virag L, Chen Q, Hertkorn C, et al. Detection of peroxynitrite-induced protein and DNA modifications. *Methods Mol Biol*. (2002) 196:247–75. doi: 10.1385/1-59259-274-0:247
13. Beckman JS, Koppenol WH. Nitric oxide, superoxide, and peroxynitrite: the good, the bad, and ugly. *Am J Physiol Cell Physiol*. (1996) 271:C1424–37.
14. Eliasson MJ, Huang Z, Ferrante RJ, Sasamata M, Molliver ME, Snyder SH, et al. Neuronal nitric oxide synthase activation and peroxynitrite formation in ischemic stroke linked to neural damage. *J Neurosci*. (1999) 19:5910–8. doi: 10.1523/JNEUROSCI.19-14-05910.1999
15. Fukuyama N, Takizawa S, Ishida H, Hoshiai K, Shinohara Y, Nakazawa H. Peroxynitrite formation in focal cerebral ischemia-reperfusion in rats occurs predominantly in the peri-infarct region. *J Cereb Blood Flow Metab*. (1998) 18:123–9.
16. Hartings JA, Shuttleworth CW, Kirov SA, Ayata C, Hinzman JM, Foreman B, et al. The continuum of spreading depolarizations in acute cortical lesion development: examining Leao's legacy. *J Cereb Blood Flow Metab*. (2017) 37:1571–94. doi: 10.1177/0271678X16654495
17. Zhang LN, Hao L, Guo YS, Wang HY, Li LL, Liu LZ, et al. Are glutamate transporters neuroprotective or neurodegenerative during cerebral ischemia? *J Mol Med (Berl)*. (2019) 97:281–9. doi: 10.1007/s00109-019-01745-5
18. Sattler R, Xiong Z, Lu WY, Hafner M, MacDonald JF, Tymianski M. Specific coupling of NMDA receptor activation to nitric oxide neurotoxicity by PSD-95 protein. *Science*. (1999) 284:1845–8.
19. Dawson TM, Dawson VL. Mitochondrial mechanisms of neuronal cell death: potential therapeutics. *Annu Rev Pharmacol Toxicol*. (2017) 57:437–54. doi: 10.1146/annurev-pharmtox-010716-105001
20. Chen Y, Brennan-Minnella AM, Sheth S, El-Benna J, Swanson RA. Tat-NR2B9c prevents excitotoxic neuronal superoxide production. *J Cereb Blood Flow Metab*. (2015) 35:739–42. doi: 10.1038/jcbfm.2015.16
21. Minnella AM, Zhao JX, Jiang X, Jakobsen E, Lu F, Wu L, et al. Excitotoxic superoxide production and neuronal death require both ionotropic and non-ionotropic NMDA receptor signaling. *Sci Rep*. (2018) 8:17522. doi: 10.1038/s41598-018-35725-5
22. Narasimhan P, Fujimura M, Noshita N, Chan PH. Role of superoxide in poly(ADP-ribose) polymerase upregulation after transient cerebral ischemia. *Brain Res Mol Brain Res*. (2003) 113:28–36. doi: 10.1016/s0169-328x(03)00062-7
23. Benveniste H, Hansen AJ, Ottosen NS. Determination of brain interstitial concentrations by microdialysis. *J Neurochem*. (1989) 52:1741–50.
24. Benveniste H. The excitotoxin hypothesis in relation to cerebral ischemia. *Cerebrovasc Brain Metab Rev*. (1991) 3:213–45.
25. Yang ZJ, Carter EL, Torbey MT, Martin LJ, Koehler RC. Sigma receptor ligand 4-phenyl-1-(4-phenylbutyl)-piperidine modulates neuronal nitric oxide synthase/postsynaptic density-95 coupling mechanisms and protects

against neonatal ischemic degeneration of striatal neurons. *Exp Neurol*. (2010) 221:166–74. doi: 10.1016/j.expneurol.2009.10.019
26. Zhang J, Dawson VL, Dawson TM, Snyder SH. Nitric oxide activation of poly(ADP-ribose) synthetase in neurotoxicity. *Science*. (1994) 263:687–9.
27. Eliasson MJL, Sampei K, Mandir AS, Hurn PD, Traystman RJ, Bao J, et al. Poly(ADP-ribose) polymerase gene disruption renders mice resistant to cerebral ischemia. *Nature Med*. (1997) 3:1089–95.
28. Mandir AS, Poitras MF, Berliner AR, Herring WJ, Guastella DB, Feldman A, et al. NMDA but not non-NMDA excitotoxicity is mediated by Poly(ADP-ribose) polymerase. *J Neurosci*. (2000) 20:8005–11. doi: 10.1523/JNEUROSCI.20-21-08005.2000
29. Xu JC, Fan J, Wang X, Eacker SM, Kam TI, Chen L, et al. Cultured networks of excitatory projection neurons and inhibitory interneurons for studying human cortical neurotoxicity. *Sci Transl Med*. (2016) 8:333ra48. doi: 10.1126/scitranslmed.aad0623
30. Yu SW, Wang H, Poitras MF, Coombs C, Bowers WJ, Federoff HJ, et al. Mediation of poly(ADP-ribose) polymerase-1-dependent cell death by apoptosis-inducing factor. *Science*. (2002) 297:259–63. doi: 10.1126/science.1072221
31. Wang H, Yu SW, Koh DW, Lew J, Coombs C, Bowers W, et al. Apoptosis-inducing factor substitutes for caspase executioners in NMDA-triggered excitotoxic neuronal death. *J Neurosci*. (2004) 24:10963–73. doi: 10.1523/JNEUROSCI.3461-04.2004
32. Yu SW, Wang Y, Frydenlund DS, Ottersen OP, Dawson VL, Dawson TM. Outer mitochondrial membrane localization of apoptosis-inducing factor: mechanistic implications for release. *ASN Neuro*. (2009) 1:e00021. doi: 10.1042/AN20090046
33. Wang Y, Kim NS, Haince JF, Kang HC, David KK, Andrabi SA, et al. Poly(ADP-ribose) (PAR) binding to apoptosis-inducing factor is critical for PAR polymerase-1-dependent cell death (parthanatos). *Sci Signal*. (2011) 4(167):ra20. doi: 10.1126/scisignal.2000902
34. Yu SW, Andrabi SA, Wang H, Kim NS, Poirier GG, Dawson TM, et al. Apoptosis-inducing factor mediates poly(ADP-ribose) (PAR) polymer-induced cell death. *Proc Natl Acad Sci USA*. (2006) 103:18314–9. doi: 10.1073/pnas.0606528103
35. Andrabi SA, Kim NS, Yu SW, Wang H, Koh DW, Sasaki M, et al. Poly(ADP-ribose) (PAR) polymer is a death signal. *Proc Natl Acad Sci USA*. (2006) 103(48):18308-13. doi: 10.1073/pnas.0606526103
36. Wang Y, An R, Umanah GK, Park H, Nambiar K, Eacker SM, et al. A nuclease that mediates cell death induced by DNA damage and poly(ADP-ribose) polymerase-1. *Science*. (2016) 354:aad6872. doi: 10.1126/science.aad6872
37. Park H, Kam TI, Dawson TM, Dawson VL. Poly (ADP-ribose) (PAR)-dependent cell death in neurodegenerative diseases. *Int Rev Cell Mol Biol*. (2020) 353:1–29. doi: 10.1016/bs.ircmb.2019.12.009
38. Degterev A, Huang Z, Boyce M, Li Y, Jagtap P, Mizushima N, et al. Chemical inhibitor of nonapoptotic cell death with therapeutic potential for ischemic brain injury. *Nat Chem Biol*. (2005) 1:112–9. doi: 10.1038/nchembio711
39. Liu C, Fang Y. New insights of poly(ADP-ribosylation) in neurodegenerative diseases: a focus on protein phase separation and pathologic aggregation. *Biochem Pharmacol*. (2019) 167:58–63. doi: 10.1016/j.bcp.2019.04.028
40. Mabley JG, Jagtap P, Perretti M, Getting SJ, Salzman AL, Virag L, et al. Anti-inflammatory effects of a novel, potent inhibitor of poly (ADP-ribose) polymerase. *Inflamm Res*. (2001) 50:561–9. doi: 10.1007/PL00000234
41. Radovits T, Seres L, Gero D, Berger I, Szabo C, Karck M, et al. Single dose treatment with PARP-inhibitor INO-1001 improves aging-associated cardiac and vascular dysfunction. *Exp Gerontol*. (2007) 42:676–85. doi: 10.1016/j.exger.2007.01.013
42. Garcia Soriano F, Virag L, Jagtap P, Szabo E, Mabley JG, Liaudet L, et al. Diabetic endothelial dysfunction: the role of poly(ADP-ribose) polymerase activation. *Nat Med*. (2001) 7:108–13. doi: 10.1038/83241
43. Radovits T, Zotkina J, Lin LN, Bomicke T, Arif R, Gero D, et al. Poly(ADP-Ribose) polymerase inhibition improves endothelial dysfunction induced by hypochlorite. *Exp Biol Med (Maywood)*. (2007) 232:1204–12. doi: 10.3181/0701-RM-16
44. Radovits T, Lin LN, Zotkina J, Gero D, Szabo C, Karck M, et al. Poly(ADP-ribose) polymerase inhibition improves endothelial dysfunction induced by reactive oxidant hydrogen peroxide *in vitro*. *Eur J Pharmacol*. (2007) 564:158–66. doi: 10.1016/j.ejphar.2007.02.060
45. Bakondi E, Bai P, Szabo EE, Hunyadi J, Gergely P, Szabo C, et al. Detection of poly(ADP-ribose) polymerase activation in oxidatively stressed cells and tissues using biotinylated NAD substrate. *J Histochem Cytochem*. (2002) 50:91–8. doi: 10.1177/002215540205000110
46. Stoica BA, Loane DJ, Zhao Z, Kabadi SV, Hanscom M, Byrnes KR, et al. PARP-1 inhibition attenuates neuronal loss, microglia activation and neurological deficits after traumatic brain injury. *J Neurotrauma*. (2014) 31:758–72. doi: 10.1089/neu.2013.3194
47. Lenzser G, Kis B, Snipes JA, Gaspar T, Sandor P, Komjati K, et al. Contribution of poly(ADP-ribose) polymerase to postischemic blood-brain barrier damage in rats. *J Cereb Blood Flow Metab*. (2007) 27:1318–26. doi: 10.1038/sj.jcbfm.9600437
48. Mehrabadi AR, Korolainen MA, Odero G, Miller DW, Kauppinen TM. Poly(ADP-ribose) polymerase-1 regulates microglia mediated decrease of endothelial tight junction integrity. *Neurochem Int*. (2017) 108:266–71. doi: 10.1016/j.neuint.2017.04.014
49. Zhang Y, Zhang X, Park TS, Gidday JM. Cerebral endothelial cell apoptosis after ischemia-reperfusion: role of PARP activation and AIF translocation. *J Cereb Blood Flow Metab*. (2005) 25:868–77. doi: 10.1038/sj.jcbfm.9600081
50. Xu J, Wang H, Won SJ, Basu J, Kapfhamer D, Swanson RA. Microglial activation induced by the alarmin S100B is regulated by poly(ADP-ribose) polymerase-1. *Glia*. (2016) 64:1869–78. doi: 10.1002/glia.23026
51. Raghunatha P, Vosoughi A, Kauppinen TM, Jackson MF. Microglial NMDA receptors drive pro-inflammatory responses *via* PARP-1/TRMP2 signaling. *Glia*. (2020) 68:1421–34. doi: 10.1002/glia.23790
52. Chiarugi A, Moskowitz MA. Poly(ADP-ribose) polymerase-1 activity promotes NF-kappaB-driven transcription and microglial activation: implication for neurodegenerative disorders. *J Neurochem*. (2003) 85:306–17. doi: 10.1046/j.1471-4159.2003.01684.x
53. Kauppinen TM, Swanson RA. Poly(ADP-ribose) polymerase-1 promotes microglial activation, proliferation, and matrix metalloproteinase-9-mediated neuron death. *J Immunol*. (2005) 174:2288–96. doi: 10.4049/jimmunol.174.4.2288
54. Vuong B, Hogan-Cann AD, Alano CC, Stevenson M, Chan WY, Anderson CM, et al. NF-kappaB transcriptional activation by TNFalpha requires phospholipase C, extracellular signal-regulated kinase 2 and poly(ADP-ribose) polymerase-1. *J Neuroinflammation*. (2015) 12:229. doi: 10.1186/s12974-015-0448-8
55. Kauppinen TM, Chan WY, Suh SW, Wiggins AK, Huang EJ, Swanson RA. Direct phosphorylation and regulation of poly(ADP-ribose) polymerase-1 by extracellular signal-regulated kinases 1/2. *Proc Natl Acad Sci USA*. (2006) 103:7136–41. doi: 10.1073/pnas.0508606103
56. Kauppinen TM, Gan L, Swanson RA. Poly(ADP-ribose) polymerase-1-induced NAD(+) depletion promotes nuclear factor-kappaB transcriptional activity by preventing p65 de-acetylation. *Biochim Biophys Acta*. (2013) 1833:1985–91. doi: 10.1016/j.bbamcr.2013.04.005
57. d'Avila JC, Lam TI, Bingham D, Shi J, Won SJ, Kauppinen TM, et al. Microglial activation induced by brain trauma is suppressed by post-injury treatment with a PARP inhibitor. *J Neuroinflammation*. (2012) 9:31. doi: 10.1186/1742-2094-9-31
58. Irvine K, Bishop R, Won SJ, Xu J, Hamel K, Coppes V, et al. Effects of veliparib on microglial activation and functional outcomes following traumatic brain injury in the rat and pig. *J Neurotrauma*. (2018) 35:918–29. doi: 10.1089/neu.2017.5044
59. Hamby AM, Suh SW, Kauppinen TM, Swanson RA. Use of a poly(ADP-ribose) polymerase inhibitor to suppress inflammation and neuronal death after cerebral ischemia-reperfusion. *Stroke*. (2007) 38(Suppl. 2):632–6. doi: 10.1161/01.STR.0000250742.61241.79
60. Kauppinen TM, Suh SW, Berman AE, Hamby AM, Swanson RA. Inhibition of poly(ADP-ribose) polymerase suppresses inflammation and promotes recovery after ischemic injury. *J Cereb Blood Flow Metab*. (2009) 29:820–9. doi: 10.1038/jcbfm.2009.9
61. Koh SH, Park Y, Song CW, Kim JG, Kim K, Kim J, et al. The effect of PARP inhibitor on ischaemic cell death, its related inflammation and survival signals. *Eur J Neurosci*. (2004) 20:1461–72. doi: 10.1111/j.1460-9568.2004.03632.x

62. Park EM, Cho S, Frys K, Racchumi G, Zhou P, Anrather J, et al. Interaction between inducible nitric oxide synthase and poly(ADP-ribose) polymerase in focal ischemic brain injury. *Stroke*. (2004) 35:2896–901. doi: 10.1161/01.STR.0000147042.53659.6c
63. Alano CC, Ying W, Swanson RA. Poly(ADP-ribose) polymerase-1-mediated cell death in astrocytes requires NAD^+ depletion and mitochondrial permeability transition. *J Biol Chem*. (2004) 279:18895–902. doi: 10.1074/jbc.M313329200
64. Noh MY, Lee WM, Lee SJ, Kim HY, Kim SH, Kim YS. Regulatory T cells increase after treatment with poly (ADP-ribose) polymerase-1 inhibitor in ischemic stroke patients. *Int Immunopharmacol*. (2018) 60:104–10. doi: 10.1016/j.intimp.2018.04.043
65. Aarts M, Liu Y, Liu L, Besshoh S, Arundine M, Gurd JW, et al. Treatment of ischemic brain damage by perturbing NMDA receptor- PSD-95 protein interactions. *Science*. (2002) 298:846–50. doi: 10.1126/science.1072873
66. Cook DJ, Teves L, Tymianski M. A translational paradigm for the preclinical evaluation of the stroke neuroprotectant Tat-NR2B9c in gyrencephalic nonhuman primates. *Sci Transl Med*. (2012) 4:154ra33. doi: 10.1126/scitranslmed.3003824
67. Hill MD, Goyal M, Menon BK, Nogueira RG, McTaggart RA, Demchuk AM, et al. Efficacy and safety of nerinetide for the treatment of acute ischaemic stroke (ESCAPE-NA1): a multicentre, double-blind, randomised controlled trial. *Lancet*. (2020) 395:878–87. doi: 10.1016/S0140-6736(20)30258-0
68. Endres M, Wang ZQ, Namura S, Waeber C, Moskowitz MA. Ischemic brain injury is mediated by the activation of poly(ADP- ribose)polymerase. *J Cereb Blood Flow Metab*. (1997) 17:1143–51.
69. Goto S, Xue R, Sugo N, Sawada M, Poitras M, Johns DC, et al. Poly (ADP-ribose) polymerase (PARP-1) impairs early and long-term experimental stroke therapy. *Stroke*. (2002) 33:1101–6. doi: 10.1161/01.str.0000014203.65693.1e
70. McCullough LD, Zeng Z, Blizzard KK, Debchoudhury I, Hurn PD. Ischemic nitric oxide and poly (ADP-ribose) polymerase-1 in cerebral ischemia: male toxicity, female protection. *J Cereb Blood Flow Metab*. (2005) 25:502–12. doi: 10.1038/sj.jcbfm.9600059
71. Liu F, Lang J, Li J, Benashski SE, Siegel M, Xu Y, et al. Sex differences in the response to poly(ADP-ribose) polymerase-1 deletion and caspase inhibition after stroke. *Stroke*. (2011) 42:1090–6. doi: 10.1161/STROKEAHA.110.594861
72. Li X, Klaus JA, Zhang J, Xu Z, Kibler KK, Andrabi SA, et al. Contributions of poly(ADP-ribose) polymerase-1 and−2 to nuclear translocation of apoptosis-inducing factor and injury from focal cerebral ischemia. *J Neurochem*. (2010) 113:1012–22. doi: 10.1111/j.1471-4159.2010.06667.x
73. Zhang J, Li X, Kwansa H, Kim YT, Yi L, Hong G, et al. Augmentation of poly(ADP-ribose) polymerase-dependent neuronal cell death by acidosis. *J Cereb Blood Flow Metab*. (2017) 37:1982–93. doi: 10.1177/0271678X16658491
74. Kofler J, Otsuka T, Zhang Z, Noppens R, Grafe MR, Koh DW, et al. Differential effect of PARP-2 deletion on brain injury after focal and global cerebral ischemia. *J Cereb Blood Flow Metab*. (2006) 26:135–41. doi: 10.1038/sj.jcbfm.9600173
75. Endres M, Scott G, Namura S, Salzman AL, Huang PL, Moskowitz MA, et al. Role of peroxynitrite and neuronal nitric oxide synthase in the activation of poly(ADP-ribose) synthetase in a murine model of cerebral ischemia-reperfusion. *Neurosci Lett*. (1998) 248:41–4.
76. Giovannelli L, Cozzi A, Guarnieri I, Dolara P, Moroni F. Comet assay as a novel approach for studying DNA damage in focal cerebral ischemia: differential effects of NMDA receptor antagonists and poly(ADP-ribose) polymerase inhibitors. *J Cereb Blood Flow Metab*. (2002) 22:697–704. doi: 10.1097/00004647-200206000-00008
77. Sairanen T, Szepesi R, Karjalainen-Lindsberg ML, Saksi J, Paetau A, Lindsberg PJ. Neuronal caspase-3 and PARP-1 correlate differentially with apoptosis and necrosis in ischemic human stroke. *Acta Neuropathol*. (2009) 118:541–52. doi: 10.1007/s00401-009-0559-3
78. Kang HC, Lee YI, Shin JH, Andrabi SA, Chi Z, Gagne JP, et al. Iduna is a poly(ADP-ribose) (PAR)-dependent E3 ubiquitin ligase that regulates DNA damage. *Proc Natl Acad Sci USA*. (2011) 108:14103–8. doi: 10.1073/pnas.1108799108
79. Andrabi SA, Kang HC, Haince JF, Lee YI, Zhang J, Chi Z, et al. Iduna protects the brain from glutamate excitotoxicity and stroke by interfering with poly(ADP-ribose) polymer-induced cell death. *Nat Med*. (2011) 17:692–9. doi: 10.1038/nm.2387
80. Li X, Nemoto M, Xu Z, Yu SW, Shimoji M, Andrabi SA, et al. Influence of duration of focal cerebral ischemia and neuronal nitric oxide synthase on translocation of apoptosis-inducing factor to the nucleus. *Neuroscience*. (2007) 144:56–65. doi: 10.1016/j.neuroscience.2006.08.065
81. Xu Z, Zhang J, David KK, Yang ZJ, Li X, Dawson TM, et al. Endonuclease G does not play an obligatory role in poly(ADP-ribose) polymerase-dependent cell death after transient focal cerebral ischemia. *Am J Physiol Regul Integr Comp Physiol*. (2010) 299:R215–21. doi: 10.1152/ajpregu.00747.2009
82. Thorsell AG, Ekblad T, Karlberg T, Low M, Pinto AF, Tresaugues L, et al. Structural basis for potency and promiscuity in poly(ADP-ribose) polymerase (PARP) and tankyrase inhibitors. *J Med Chem*. (2017) 60:1262–71. doi: 10.1021/acs.jmedchem.6b00990
83. Takahashi K, Greenberg JH. The effect of reperfusion on neuroprotection using an inhibitor of poly(ADP-ribose) polymerase. *Neuroreport*. (1999) 10:2017–22.
84. Abdelkarim GE, Gertz K, Harms C, Katchanov J, Dirnagl U, Szabo C, et al. Protective effects of PJ34, a novel, potent inhibitor of poly(ADP-ribose) polymerase (PARP) in *in vitro* and *in vivo* models of stroke. *Int J Mol Med*. (2001) 7:255–60. doi: 10.3892/ijmm.7.3.255
85. Komjati K, Mabley JG, Virag L, Southan GJ, Salzman AL, Szabo C. Poly(ADP-ribose) polymerase inhibition protect neurons and the white matter and regulates the translocation of apoptosis-inducing factor in stroke. *Int J Mol Med*. (2004) 13:373–82. doi: 10.3892/ijmm.13.3.373
86. Iwashita A, Tojo N, Matsuura S, Yamazaki S, Kamijo K, Ishida J, et al. A novel and potent poly(ADP-ribose) polymerase-1 inhibitor, FR247304 (5-chloro-2-[3-(4-phenyl-3,6-dihydro-1(2H)-pyridinyl)propyl]-4(3H)-quinazolinone), attenuates neuronal damage in *in vitro* and *in vivo* models of cerebral ischemia. *J Pharmacol Exp Ther*. (2004) 310:425–36. doi: 10.1124/jpet.104.066944
87. Nakajima H, Kakui N, Ohkuma K, Ishikawa M, Hasegawa T. A newly synthesized poly(ADP-ribose) polymerase inhibitor, DR2313 [2-methyl-3,5,7,8-tetrahydrothiopyrano[4,3-d]-pyrimidine-4-one]: pharmacological profiles, neuroprotective effects, and therapeutic time window in cerebral ischemia in rats. *J Pharmacol Exp Ther*. (2005) 312:472–81. doi: 10.1124/jpet.104.075465
88. Egi Y, Matsuura S, Maruyama T, Fujio M, Yuki S, Akira T. Neuroprotective effects of a novel water-soluble poly(ADP-ribose) polymerase-1 inhibitor, MP-124, in *in vitro* and *in vivo* models of cerebral ischemia. *Brain Res*. (2011) 1389:169–76. doi: 10.1016/j.brainres.2011.03.031
89. Moroni F, Cozzi A, Chiarugi A, Formentini L, Camaioni E, Pellegrini-Giampietro DE, et al. Long-lasting neuroprotection and neurological improvement in stroke models with new, potent and brain permeable inhibitors of poly(ADP-ribose) polymerase. *Br J Pharmacol*. (2012) 165:1487–500. doi: 10.1111/j.1476-5381.2011.01666.x
90. El Amki M, Lerouet D, Garraud M, Teng F, Beray-Berthat V, Coqueran B, et al. Improved reperfusion and vasculoprotection by the poly(ADP-Ribose)polymerase inhibitor PJ34 after stroke and thrombolysis in mice. *Mol Neurobiol*. (2018) 55:9156–68. doi: 10.1007/s12035-018-1063-3
91. Teng F, Zhu L, Su J, Zhang X, Li N, Nie Z, et al. Neuroprotective effects of poly(ADP-ribose)polymerase inhibitor olaparib in transient cerebral ischemia. *Neurochem Res*. (2016) 41:1516–26. doi: 10.1007/s11064-016-1864-6
92. Culmsee C, Zhu C, Landshamer S, Becattini B, Wagner E, Pellechia M, et al. Apoptosis-inducing factor triggered by poly(ADP-Ribose) polymerase and bid mediates neuronal cell death after oxygen-glucose deprivation and focal cerebral ischemia. *J Neurosci*. (2005) 25:10262–72. doi: 10.1523/JNEUROSCI.2818-05.2005
93. Berger NA, Besson VC, Boulares AH, Burkle A, Chiarugi A, Clark RS, et al. Opportunities for the repurposing of PARP inhibitors for the therapy of non-oncological diseases. *Br J Pharmacol*. (2018) 175:192–222. doi: 10.1111/bph.13748
94. Muscal JA, Thompson PA, Giranda VL, Dayton BD, Bauch J, Horton T, et al. Plasma and cerebrospinal fluid pharmacokinetics of ABT-888 after

oral administration in non-human primates. *Cancer Chemother Pharmacol*. (2010) 65:419–25. doi: 10.1007/s00280-009-1044-3
95. Donawho CK, Luo Y, Luo Y, Penning TD, Bauch JL, Bouska JJ, et al. ABT-888, an orally active poly(ADP-ribose) polymerase inhibitor that potentiates DNA-damaging agents in preclinical tumor models. *Clin Cancer Res*. (2007) 13:2728–37. doi: 10.1158/1078-0432.CCR-06-3039
96. Takahashi K, Greenberg JH, Jackson P, Maclin K, Zhang J. Neuroprotective effects of inhibiting poly(ADP-ribose) synthetase on focal cerebral ischemia in rats. *J Cereb Blood Flow Metab*. (1997) 17:1137–42.
97. Takahashi K, Pieper AA, Croul SE, Zhang J, Snyder SH, Greenberg JH. Post-treatment with an inhibitor of poly(ADP-ribose) polymerase attenuates cerebral damage in focal ischemia. *Br Res*. (1999) 829:46–54.
98. Yap E, Tan WL, Ng I, Ng YK. Combinatorial-approached neuroprotection using pan-caspase inhibitor and poly (ADP-ribose) polymerase (PARP) inhibitor following experimental stroke in rats; is there additional benefit? *Brain Res*. (2008) 1195:130–8. doi: 10.1016/j.brainres.2007.12.024
99. Haddad M, Beray-Berthat V, Coqueran B, Palmier B, Szabo C, Plotkine M, et al. Reduction of hemorrhagic transformation by PJ34, a poly(ADP-ribose)polymerase inhibitor, after permanent focal cerebral ischemia in mice. *Eur J Pharmacol*. (2008) 588:52–7. doi: 10.1016/j.ejphar.2008.04.013
100. Teng F, Beray-Berthat V, Coqueran B, Lesbats C, Kuntz M, Palmier B, et al. Prevention of rt-PA induced blood-brain barrier component degradation by the poly(ADP-ribose)polymerase inhibitor PJ34 after ischemic stroke in mice. *Exp Neurol*. (2013) 248:416–28. doi: 10.1016/j.expneurol.2013.07.007
101. Alkayed NJ, Harukuni I, Kimes AS, London ED, Traystman RJ, Hurn PD. Gender-linked brain injury in experimental stroke. *Stroke*. (1998) 29:159–66.
102. Alkayed NJ, Murphy SJ, Traystman RJ, Hurn PD, Miller VM. Neuroprotective effects of female gonadal steroids in reproductively senescent female rats. *Stroke*. (2000) 31:161–8. doi: 10.1161/01.str.31.1.161
103. Hagberg H, Wilson MA, Matsushita H, Zhu C, Lange M, Gustavsson M, et al. PARP-1 gene disruption in mice preferentially protects males from perinatal brain injury. *J Neurochem*. (2004) 90:1068–75. doi: 10.1111/j.1471-4159.2004.02547.x
104. Yuan M, Siegel C, Zeng Z, Li J, Liu F, McCullough LD. Sex differences in the response to activation of the poly (ADP-ribose) polymerase pathway after experimental stroke. *Exp Neurol*. (2009) 217:210–8. doi: 10.1016/j.expneurol.2009.02.012
105. Liu F, Li Z, Li J, Siegel C, Yuan R, McCullough LD. Sex differences in caspase activation after stroke. *Stroke*. (2009) 40:1842–8. doi: 10.1161/STROKEAHA.108.538686
106. Siegel CS, McCullough LD. NAD+ and nicotinamide: sex differences in cerebral ischemia. *Neuroscience*. (2013) 237:223–31. doi: 10.1016/j.neuroscience.2013.01.068
107. Ding Y, Zhou Y, Lai Q, Li J, Gordon V, Diaz FG. Long-term neuroprotective effect of inhibiting poly(ADP-ribose) polymerase in rats with middle cerebral artery occlusion using a behavioral assessment. *Brain Res*. (2001) 915:210–7. doi: 10.1016/s0006-8993(01)02852-9
108. Sun HS, Doucette TA, Liu Y, Fang Y, Teves L, Aarts M, et al. Effectiveness of PSD95 inhibitors in permanent and transient focal ischemia in the rat. *Stroke*. (2008) 39:2544–53. doi: 10.1161/STROKEAHA.107.506048
109. Li H, Pin S, Zeng Z, Wang MM, Andreasson KA, McCullough LD. Sex differences in cell death. *Ann Neurol*. (2005) 58:317–21. doi: 10.1002/ana.20538
110. Takeshima R, Kirsch JR, Koehler RC, Traystman RJ. Tirilizad treatment does not decrease early brain injury after transient focal ischemia in cats. *Stroke*. (1994) 25:670–6.
111. Takeshima R, Kirsch JR, Koehler RC, Gomoll AW, Traystman RJ. Monoclonal leukocyte antibody (MoAb 60.3) does not decrease injury following transient focal cerebral ischemia in cats. *Stroke*. (1992) 23:247–52.
112. Rebel A, Ulatowski JA, Joung K, Bucci E, Traystman RJ, Koehler RC. Regional cerebral blood flow in cats with cross-linked hemoglobin transfusion during focal cerebral ischemia. *Am J Physiol Heart Circ Physiol*. (2002) 282:H832–41. doi: 10.1152/ajpheart.00880.2001
113. Maier C, Scheuerle A, Hauser B, Schelzig H, Szabo C, Radermacher P, et al. The selective poly(ADP)ribose-polymerase 1 inhibitor INO1001 reduces spinal cord injury during porcine aortic cross-clamping-induced ischemia/reperfusion injury. *Intensive Care Med*. (2007) 33:845–50. doi: 10.1007/s00134-007-0585-3

Conflict of Interest: TD and VD are inventors of technology discussed in this this publication, which Neuraly, Inc. is in the process of licensing from Johns Hopkins University. TD and VD are founders of Neuraly, and hold shares of stock options as well as equity in, Neuraly, Inc., which is a subsidiary of D&D Pharmatech Inc. This arrangement has been reviewed and approved by the Johns Hopkins University in accordance with its conflict of interest policies.

The remaining author declares that the research was conducted in the absence of any commercial or financial relationships that could be construed as a potential conflict of interest.

frontiers in Neurology

SYSTEMATIC REVIEW
published: 14 May 2021
doi: 10.3389/fneur.2021.620096

Statins Improve Clinical Outcome After Non-aneurysmal Subarachnoid Hemorrhage: A Translational Insight From a Systematic Review of Experimental Studies

Sepide Kashefiolasl[1], Marlies Wagner[2], Nina Brawanski[1], Volker Seifert[1], Stefan Wanderer[3,4], Lukas Andereggen[3,4] and Juergen Konczalla[1]*

[1] Department of Neurosurgery, University Hospital Frankfurt, Frankfurt am Main, Germany, [2] Institute of Neuroradiology, University Hospital Frankfurt, Frankfurt am Main, Germany, [3] Department of Neurosurgery, Kantonsspital Aarau, Aarau, Switzerland, [4] Cerebrovascular Research Group, Department for BioMedical Research, University of Bern, Bern, Switzerland

OPEN ACCESS

Edited by:
Emmanuel Pinteaux, The University of Manchester, United Kingdom

Reviewed by:
Chia-Yi (Alex) Kuan, Emory University, United States
George Magoufis, Metropolitan Hospital, Greece

***Correspondence:**
Sepide Kashefiolasl
sepide.kashefi@gmx.de

Specialty section:
This article was submitted to Stroke, a section of the journal Frontiers in Neurology

Received: *21 October 2020*
Accepted: *17 March 2021*
Published: *14 May 2021*

Citation:
Kashefiolasl S, Wagner M, Brawanski N, Seifert V, Wanderer S, Andereggen L and Konczalla J (2021) Statins Improve Clinical Outcome After Non-aneurysmal Subarachnoid Hemorrhage: A Translational Insight From a Systematic Review of Experimental Studies. Front. Neurol. 12:620096. doi: 10.3389/fneur.2021.620096

The efficacy of statin-treatment in aneurysmal subarachnoid hemorrhage (SAH) remains controversial. We aimed to investigate the effects of statin-treatment in non-aneurysmal (na)SAH in accordance with animal research data illustrating the pathophysiology of naSAH. We systematically searched PubMed using PRISMA-guidelines and selected experimental studies assessing the statin-effect on SAH. Detecting the accordance of the applied experimental models with the pathophysiology of naSAH, we analyzed our institutional database of naSAH patients between 1999 and 2018, regarding the effect of statin treatment in these patients and creating a translational concept. Patient characteristics such as statin-treatment (simvastatin 40 mg/d), the occurrence of cerebral vasospasm (CVS), delayed infarction (DI), delayed cerebral ischemia (DCI), and clinical outcome were recorded. In our systematic review of experimental studies, we found 13 studies among 18 titles using blood-injection-animal-models to assess the statin-effect in accordance with the pathophysiology of naSAH. All selected studies differ on study-setting concerning drug-administration, evaluation methods, and neurological tests. Patients from the Back to Bedside project, including 293 naSAH-patients and 51 patients with simvastatin-treatment, were recruited for this analysis. Patients under treatment were affected by a significantly lower risk of CVS ($p < 0.01$; OR 3.7), DI ($p < 0.05$; OR 2.6), and DCI ($p < 0.05$; OR 3). Furthermore, there was a significant association between simvastatin-treatment and favorable-outcome ($p < 0.05$; OR 3). However, dividing patients with statin-treatment in pre-SAH ($n = 31$) and post-SAH ($n = 20$) treatment groups, we only detected a tenuously significant higher chance for a favorable outcome ($p < 0.05$; OR 0.05) in the small group of 20 patients with statin post-SAH treatment. Using a multivariate-analysis, we detected female gender (55%; $p < 0.001$; OR 4.9), Hunt&Hess ≤III at admission ($p < 0.002$; OR 4), no anticoagulant-therapy ($p < 0.0001$; OR 0.16), and statin-treatment ($p < 0.0001$; OR 24.2) as the main factors improving the clinical outcome. In conclusion, we detected a significantly lower risk for CVS, DCI, and DI in naSAH patients under statin treatment.

Additionally, a significant association between statin treatment and favorable outcome 6 months after naSAH onset could be confirmed. Nevertheless, unified animal experiments should be considered to create the basis for developing new therapeutic schemes.

Keywords: non-aneurysmal SAH, stroke, regenerative medicine, recovery, translational study, statin treatment

INTRODUCTION

Early brain injury (EBI) followed by subarachnoid hemorrhage (SAH) is caused by transient cerebral ischemia during bleeding. In up to 30% of SAH patients, delayed cerebral ischemia (DCI) is associated with poor clinical outcome or death. DCI is the result of SAH caused secondary effects such as increased intracranial pressure and destruction of brain tissue by intracerebral hemorrhage. A combination of post-SAH complications including cerebral vasospasm, arteriolar constriction and thrombosis, cortical spreading ischemia, and processes triggered by EBI lead to DCI (1–3). Therefore, numerous pharmacological treatments have concentrated on the prevention of EBI and cerebral vasospasm, with disappointing results as of yet (4).

Statins have been identified as a potential treatment option for early brain injury and the associated vasospasm. Based on experimental studies using animal models proving vascular regenerative effects of statins, statin-treatment might reduce EBI and vasospasm in patients after aneurysmal SAH (5, 6).

However, the results of clinical trials have been controversial. A decreased incidence of vasospasm was found in a few Phase II trials, while further clinical studies have failed to confirm these findings (7–9). Additionally, Meta-analyses have also produced inconsistent results. In contrast to clinical studies demonstrating a beneficial effect of statin treatment in only one aspect (10–12), there are additional studies disproving all reported benefits (13–15). Nevertheless, two large-scale multicenter Phase III trials-Simvastatin in Aneurysmal Subarachnoid Hemorrhage (STASH) (16) and High-Dose Simvastatin for Aneurysmal Subarachnoid Hemorrhage (HDS-SAH) (17)—could not detect any beneficial effect of simvastatin treatment independent of statin dose, which has been described as effective in higher drug doses, previously. Therefore, the effect of statins on vasospasm remains unclear.

Considering this discrepancy between experimental and clinical data, we aimed to investigate the effects of statin treatment in SAH in accordance with animal research data. Firstly, a systematic review was conducted to explore the research background of the role of statins in the case of SAH. Detecting the accordance of the applied experimental models with the pathophysiology of naSAH, we analyzed our patient database regarding the effect of statin treatment in non-aneurysmal SAH patients.

METHODS

Systematic Review of Experimental Data

Peer-reviewed articles reporting the clinical evidence of efficacy of statins for SAH in experimental animal models were identified. Papers were selected in MEDLINE/Pubmed according to the PRISM statement. The search terms "statin AND SAH" with the filter option for "species" were used to search Pubmed systematically. English language articles up to December 2018 were considered. The literature review wasperformed by two independent reviewers.

All studies working on an experimental SAH model *in vivo* were included after first review of titles and abstracts. Differentiating between a blood injection and endovascular perforation SAH model (referring to the study design single or double hemorrhage model in case of both methods), animal studies with injection models were included. Blood injection models with the presence of subarachnoid blood in the cisterns around the midbrain mimicking naSAH with the center of the bleeding immediately anterior to the midbrain, with or without extension to the ambient and chiasmatic cisterns, horizontal part of the sylvian fissure and posterior horns of the lateral ventricles, resembling non-aneurysmal SAH in humans, were added to our database.

All included papers were reviewed in full text and availability of coordinates. Reference lists of suitable studies were scrutinized for additional articles.

All eligible studies were analyzed describing the following parameters: animal species, study design containing the exact description of SAH model, size of animal groups, dose of drug, route and time of drugs' administration, employed tests, time of examination, and results.

Clinical Data

Regarding the highest number of studies using the SAH blood injection model, in accordance with the pathophysiology of naSAH, we retrospectively analyzed our institutional database of consecutive patients suffering naSAH between 1999 and 2018. Non-aneurysmal Subarachnoid hemorrhage was defined as a spontaneous non-traumatic hemorrhage into the subarachnoid space without any evidence of an intracranial vascular pathology.

The retrospective clinical study was approved by the local ethics committee of the Goethe-University and was performed in accordance with the relevant guidelines and regulations of the regional ethics committee in Frankfurt am Main, Germany. Because of the retrospective design, informed consent was waived by the ethics committee.

All patients with SAH, diagnosed by SAH pattern on CT-scan, or confirmed by lumbar puncture, underwent cerebral digital subtraction angiography (DSA) to rule out intracranial vascular bleeding sources. Patients in whom the bleeding source was detected to be an aneurysm or vascular malformation were excluded from the study and treated by surgical or endovascular aneurysm occlusion based on an interdisciplinary consensus. If absence of intracranial vascular pathology was confirmed by a neuroradiologist, patients received a 2nd angiography regularly

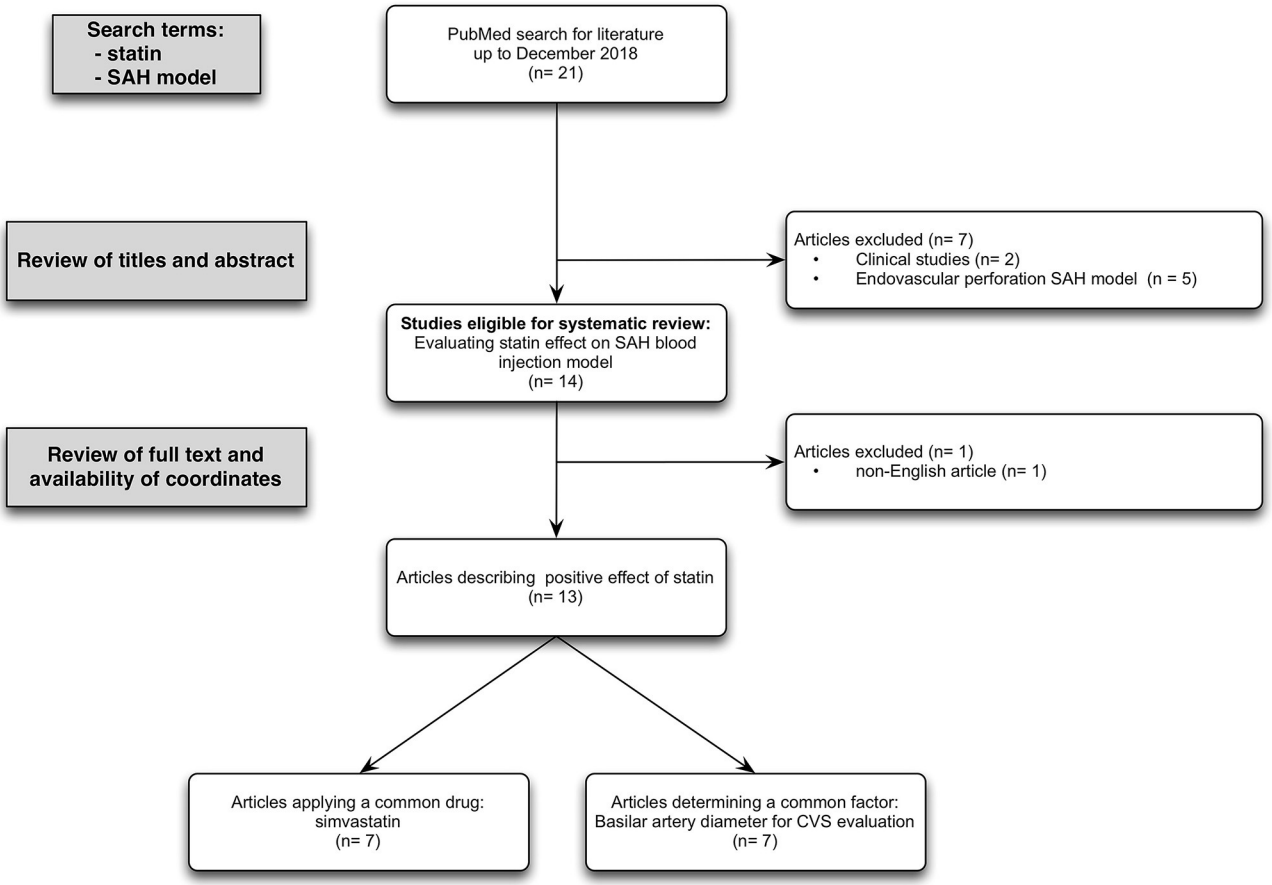

FIGURE 1 | PRISMA flow diagram: Flow chart summarizing the study selection process. Inclusion criteria required animal-based experimental studies focusing on statin effect in case of SAH induced by subarachnoidal blood injection model. Exclusion criteria required studies reporting on the application of an endovascular perforation SAH model and language other than English. Overall, 13 studies met the inclusion and exclusion criterias.

∼14–48 days after the ictus. All admitted SAH patients without intracranial vascular pathology were included in this study as non-aneurysmal SAH patients.

According to bleeding patterns, naSAH patients were divided into perimesencephalic- (PM-) and non-perimesencephalic (NPM-) naSAH. A PM-SAH was defined as the presence of subarachnoid blood in the cisterns around the midbrain with the center of the bleeding immediately anterior to the midbrain, with or without extension to the ambient and chiasmatic cisterns, the horizontal part of the sylvian fissure, and posterior horns of the lateral ventricles. Extensive intraventricular hemorrhage and intraparenchymal hemorrhage were exclusive of PM-SAH. Patients with an aneurysmal SAH pattern, described as blood located in the interpeduncular cistern, as well as in the Sylvian cistern, interhemispheric cistern and convexity, or a negative computer tomography with a positive lumbar puncture, and negative digital subtraction angiography (DSA), were classified as NPM-SAH.

Patients not receiving treatment at SAH onset because of advanced brain injury or without clinical follow-up 6 months post-SAH were excluded.

All parameters relevant to this analysis, including statin-pretreatment (medication intake independent of SAH onset), statin-post-treatment after SAH onset (drug: simvastatin 40 mg a day), the occurrence of CVS, DI (CVS-related vs. non-CVS-related), DCI and finally clinical outcome (modified Rankin Scale: mRS after 6 months; favorable outcome mRS 0–2 vs. unfavorable outcome mRS 3–6) in patients with non-aneurysmal SAH, were recorded.

The degree of CVS in patients was uniformly defined by CT-A as a radiological imaging on the basis of arterial narrowing (e.g., >66% for severe CVS). Because of the small number of patients with high or low dose statin treatment [statin dose: 80 mg ($n = 2$) or 20 mg ($n = 3$)], these patients were excluded.

Statistical Analysis

Data analyses were performed using the computer software package (IBM SPSS, version 22, IBM SPSS Inc.; Armonk, NY). Multivariable logistic regression analysis with forward stepwise modeling was carried out to identify factors for outcome improvement among above mentioned aspects. Categorical variables were analyzed using the Fisher's exact test and

GraphPad Prism (6.0, GraphPad Software Inc., USA). Normal distributed variables were expressed as mean values with standard deviations (SD) and analyzed using a two-tailed *t*-test. A $p < 0.05$ was considered statistically significant.

RESULTS

Literature Review of Experimental Data

Of the total of 18 English titles with experimental data, 13 studies with the presence of subarachnoid blood in the cisterns around the midbrain in accordance with the pathophysiology of naSAH used SAH blood injection model to assess the statin effect. Only seven studies applied simvastatin as the same drug, but in different doses and application routes. All of these selected studies differ in time of drug administration, employed tests, and time of examination. Evaluation of basilar artery diameter as a unified parameter to detect CVS after SAH was done in seven studies, using cerebral angiography (2/7) vs. measurement of cross-sectional areas (5/7) (**Figure 1**, PRISMA flow diagram).

Detailed study data summarized in **Table 1** (18–29, 31) demonstrate the disunity of study setting of all included experimental studies determining the statin effect on SAH using blood injection model. There are not only discrepancies in choosing animal species, SAH model (single vs. double blood injection model) and size of animal groups, but also in study setup including choice and dose of drug, route and time of drug administration, employed tests, time of examination, and evaluated results.

Patient Characteristics

A total of 293 patients with naSAH were included. 51 (17%) naSAH patients with simvastatin treatment (40 mg/d) were recruited for analysis, including 31 (61%) patients with pretreatment and 20 (39%) patients with post-treatment after SAH onset. In total 54 patients (18%) developed early hydrocephalus, 62 patients (21%) cerebral vasospasm, 53 patients (18%) had delayed cerebral ischemia (DCI) and 68 patients (23%) suffered from delayed infarction at discharge. Concerning Fisher bleeding pattern on CT-scan at admission, a total of 86 (29%) patients with a Fisher 3 bleeding pattern were included.

Patients under simvastatin treatment were affected by a significantly lower risk of Fisher 3 bleeding pattern on initial CT-scan ($P < 0.05$; OR 13.5), early hydrocephalus ($P < 0.05$; OR 2.5); CVS ($p < 0.01$; OR 3.7), DI ($p < 0.05$; OR 2.6), and DCI ($p < 0.05$; OR 3.0). Additionally, we differentiate between CVS-related (22/68, 32%) and non-CVS-related (46/68, 68%) DI describing a trend toward lower risk of CVS-related DI (1/22, 5%) in patients with simvastatin treatment (**Table 2A**).

Furthermore, our results indicate a significant association between simvastatin treatment and favorable neurological outcome ($p < 0.05$; OR 3.0). A relevant statistical difference between simvastatin-pretreatment and –post-SAH-treatment was not detected in this small cohort (**Table 2A**).

Due to the pathomechanism of statin effect as a treatment option after naSAH based on recent clinical studies, we performed **Table 2B** analyzing SAH followed complications and outcome in case of patients with statin post-SAH treatment compared to untreated group. Even in this small patient group with statin post-SAH treatment ($n = 20$), we detected a significant higher chance for favorable outcome ($p < 0.05$; OR 0.05) in these patients and a trend toward lower risk for development of cerebral vasospasm ($p = 0.05$) (**Table 2B**). Nevertheless, because of the small number of patients ($n = 20$) these statistical results should be treated with caution.

Using a multivariate analysis to detect significant patient characteristics associated with favorable outcome, we recognized female gender (55%; $p < 0.001$; 4.9), Hunt & Hess ≤III at admission ($p < 0.002$; 4), no anticoagulation and antiplatelet drug treatment ($p < 0.0001$; 0.16), and statin treatment ($p < 0.0001$; 24.2) as main factors improving the clinical outcome of naSAH patients (**Table 3**).

DISCUSSION

Creating a scientific basis as a background for the evaluation of data of included naSAH patients, we firstly attempted to collect all experimental studies focused on statin effect in animals using the blood injection model, according to the pathophysiology of naSAH.

We detected 13 experimental studies differing on study design factors including animal species, drug dose and application route, time of drug administration, employed tests, and time of examination. Concerning different conclusions, six studies described an attenuation of cerebral vasospasm after SAH onset, one study could prove ameliorated neurological deficit after SAH, another study dealt with brain edema after SAH, being attenuated under statin treatment and a single publication determined a decreased rate of cognitive dysfunction. Two further included studies focused on the mechanism of statin effect. Taking all studies paying attention to the statin effect on cerebral vasospasm under consideration, we could not unify the results to be analyzed as a metanalysis, not only because of the different study setup, but also because of the different evaluations of severity of vasospasm. Except for two included experimental research studies, performing cerebral angiography in experimental animals after SAH induction as the most precise established method to detect vasospasm, other studies choose to measure cross-sectional areas of vessels histologically, which does not allow an accurate assessment of vessel diameters.

Considering all mentioned factors, independent of all scientific research work invested in these publications, there is no possibility to unify the resulting statements to enable a statistically crucial analysis as a background for further clinical studies.

However, despite all of these discrepancies, most studies concentrating on statin effect following complications after SAH used blood injection models to induce the bleeding, which does mimic non-aneurysmal SAH rather than aneurysmal SAH. All of these experimental studies underlined the positive effect of statin treatment after SAH induction from different points of view. Investigating numerous clinical studies on this aspect in aneurysmal SAH patients and failing to confirm experimental findings, a retrospective analysis to determine the possible

TABLE 1 | Experimental studies assessing neuroprotective effects of Statin on SAH using blood injection model.

References	Animal model	Study design	Sample size	Dose	Route	Time of administration	Tests employed	Time of examination	Results
McGirt et al. (18)	Rabbits	Blood injection model	*n* = 15/group	40 mg/kg/day **Simvastatin**	s.c.	30 min; 24 and 48 h after SAH/Sham operation	Measurement of Basilar Artery lumen diameter; migration of perivascular granulocytes and macrophages.	72 h after SAH	Attenuation of perivascular granulocyte migration; Amelioration of basilar artery vasospasm
Bulsara et al. (19)	Dogs	Double blood injection model	*n* = 4–5/group	20 mg/kg/day (**Simvastatin** tested with/without combination with cyclosporine)	Oral	6 h after the 2nd blood injection for 10 days	Evaluation of Basilar artery diameter by cerebral angiography	1, 3, 7, and 10 days after SAH	Simvastatin combined with cyclosporine is not as efficacious in ameliorating vasospasm as simvastatin alone
Takata et al. (20)	Rats	Double blood injection model	*n* = 12–15/group	1.5 mg/kg/day vs. 10 mg/kg/day **Simvastatin**	Oral	Low dose: after SAH for 2 and 5 weeks; High dose: after SAH for 2 weeks	Rotarod: Morris water maze test	On days 0, 1, 3, 7, 10, 14, 17, 21, 24, 28; daily on days 29–35	Low dose: improvement of neurological deficits up to 28 days; High dose: improvement of neurological deficits up to 10 days
Wang et al. (21)	Rats	Autologous blood injection model	*n* = 6/group	20 mg/kg/day **Simvastatin**	i.p.	After SAH induction	Measurement of cross-sectional areas of MCA and ACA; H&E staining evaluating micro clots	7 days after SAH	Simvastatin attenuates cerebral vasospasm and alleviates microthrombosis in the late phase of SAH
Chang et al. (22)	Rats	Double blood injection model	*n* = 9/group	5 mg/day **Atorvastartin**	Oral	Pre-condition: 1 week before SAH induction; treatment: 24 h after SAH induction	Measurement of cross-sectional areas of BA; Evaluation of vasoactive factors: ET-1 and eNOS in CSF	72 h after 2. SAH	Reduction of ET-1 level in the preconditioning status; Increase of eNOS expression in precondition and reversal groups; Increase of BA diameter in preconditioning groups
Merlo et al. (23)	Rats	Blood injection model	*n* = 12/group	40 mg/kg/days **Simvastatin**	i.p.	30 min after SAH for 5 consecutive days	Neurobehaviour testing	1–4 post-SAH day	Reduction of post-SAH cognitive dysfunction under simvastatin
Sabri et al. (24)	Mice	Prechiasmatic cistern blood injection model	*n* = 15/group	20 mg/kg/day **Simvastatin**	i.p.	Daily for 14 days before and for 2 days after SAH operation or 30 min after SAH operation and daily for 2 d	Measurement of cross-sectional areas of BA; Evaluation of vasoactive factors.	48 h post-SAH	Simvastatin can re-couple dysfunctional eNOS and restore NO/O2Γ balance, thus preventing vasospasm, microthrombo-embolism, and neuronal injury after SAH
Naraoka et al. (25)	Rabbits	Double blood injection model	*n* = 8/groups	0.8 mg/kg/day **Pitavastatin** with/without combination with 3 mg/kg 2x/day i.v. fasudil	Oral	Day 0–5 after SAH	Histological evaluation of BA diameter; Using ELISA for protein analysis (Rho-kinase, eNOS)	5 days post-SAH	Combinated treatment prevent cerebral vasospasm due to synergic effect of pitavastatin and fasudil on Rho-kinase pathway and eNOS

(Continued)

TABLE 1 | Continued

References	Animal model	Study design	Sample size	Dose	Route	Time of administration	Tests employed	Time of examination	Results
Platt et al. (26)	Dogs	Double blood injection model	$n = 4$–5/group	–(Unavailable)	–(Unavailable)	–(Unavailable)	Analyzing neurotransmitter concentrations in CSF	CSF was collected before 1. blood injection, before second blood injection and on days 3, 7, and 10	Simvastatin attenuated high glutamate concentrations
Chang et al. (27)	Rats	Double blood injection model	$n = 9$/group	1 mg/day **Pitavastatin**	Oral	Precondition: 1 week before SAH induction; treatment: after SAH induction	Analyzing factors inducing neuron apoptosis after SAH using qPCR	Precondition: 24 h after 1. blood injection, 72 h after 2. SAH; Treatment: 24 and 72 h after 2. SAH	Statin attenuated SAH-induced neuron apoptosis inhibiting cJNK (p46/p55) activation and reducing caspase 9a expression
Duan et al. (28)	Rabbits	Double blood injection model	$n = 24$/group	20 mg/kg/day **Atorvastatin**	Oral	Daily for 3 days before and also at 22 h after SAH	Evaluation of statin effect on early brain injury, cerebral edema, and its association with Aquaporine 4	72 h after SAH	Amelioration of brain edema and early brain injury after SAH inhibiting AQP4 under atorvastatin treatment
Chen et al. (29)	Rabbits	Blood injection model	$n = 12$/group	5 mg/kg/day **Simvastatin**	Oral	Precondition for 1 week before SAH induction	Evaluation of Basilar artery diameter by cerebral angiography; Gene expression of vasoactive factors	Before 1. blood injection and 3 days after the second injection	Relieving cerebral vasospasm after SAH
Chen et al. (30)	Rabbits	Double blood injection model	$n = 16$/group	20 mg/kg/day **Atorvastatin**	Oral	3 days prior to SAH operation and 1x/day for 72 h post-SAH	Measurement of cross-sectional areas of BA; Evaluation of vasoactive factors and neuronal apoptosis.	72 h after SAH	Atorvastatin treatment may alleviate cerebral vasospasm and mediate structural and functional remodeling of vascular endothelial cells

TABLE 2A | Clinical complications and outcome in NASAH patients in dependence on statin treatment between 1999 and 2018.

Complications after NASAH	NASAH	No Statin treatment	Statin treatment	*p-value Odd Ratio (95%CI)	Statin pre-treatment	Statin post-SAH-treatment	*p-value Odd Ratio (95%CI)
Number of pat.	293	242 (83%)	51 (17%)	–	31 (61%)	20 (39%)	–
Mean age in years	54 ± 11	51 ± 15	53 ± 12	NS $p = 0.86$	54 ± 11	52 ± 8	NS $p = 0.91$
Perimesencephalic naSAH	169 (58%)	146 (86%)	23 (14%)	NS $p = 0.06$	12 (52%)	11 (48%)	NS $p = 0.39$
Non-perimesencephalic naSAH	124 (42%)	96 (77%)	28 (23%)	NS $p = 0.06$	19 (68%)	9 (32%)	NS $p = 0.39$
Fisher 3 bleeding pattern	***86 (29%)***	***61 (71%)***	***25 (29%)***	***p < 0.05 OR 13.5 (6.5–27)***	***17 (68%)***	***8 (32%)***	***NS P = 0.39***
Cerebral vasospasm (CVS)	**62 (21%)**	**58 (94%)**	**4 (6%)**	**p < 0.05 OR 3.7 (1.3–9.9)**	3 (75%)	1 (25%)	NS $p > 0.999$
Delayed infarction (DI)	**68 (23%)**	**62 (91%)**	**6 (9%)**	**p < 0.05 OR 2.6 (1.1–6.0)**	4 (67%)	2 (33%)	NS $p > 0.999$
CVS-related DI	22 (32%)	21 (95%)	1 (5%)	NS $p = 0.66$	1 (100%)	0 (0%)	NS $p = 0.39$
non-CVS-related DI	46 (68%)	41 (89%)	5 (11%)	NS $p = 0.66$	3 (60%)	2 (100%)	NS $p = 0.37$
Delayed cerebral ischemia (DCI)	**53 (18%)**	**49 (92%)**	**4 (8%)**	**p < 0.05 OR 3.0 (1.1–8.0)**	3 (75%)	1 (25%)	NS $p > 0.999$
Early hydrocephalus	**54 (18%)**	**38 (70%)**	**16 (30%)**	**p < 0.05 OR 2.5 (1.3–5)**	**7 (44%)**	**9 (56%)**	NS $p = 0.13$
Shunt implantation	31 (11%)	27 (87%)	4 (13%)	NS $p = 62$	2 (50%)	2 (50%)	NS $p = 0.64$
Favorable outcome mRS 0–2	**240 (82%)**	**193 (80%)**	**47 (20%)**	**p < 0.05 OR 3.0 (1.1–8.0)**	27 (57%)	20 (43%)	NS $p = 0.15$

*Favorable outcome 6 months after SAH: mRS ≤2 points; Unfavorable outcome: mRS >2 points. Data are shown in n (%); Fisher exact test: *p < 0.05 is significant. Odd ratio (OR) data with 95% confidence interval. Bold values indicate significant parameter.*

TABLE 2B | Clinical complications and outcome in NASAH patients in dependence on statin post-SAH-treatment between 1999 and 2018.

Complications after NASAH	NASAH	No Statin treatment	Statin post-SAH-treatment	*p-value Odd Ratio (95%CI)
Number of pat.	293	242 (83%)	20 (7%)	–
Mean age in years	54 ± 11	51 ± 15	52 ± 8	NS $p = 0.94$
Perimesencephalic naSAH	169 (58%)	146 (60%)	11 (55%)	NS $P = 64$
Non-perimesencephalic naSAH	124 (42%)	96 (40%)	9 (45%)	NS $P = 0.64$
Fisher 3 bleeding pattern	86 (29%)	61 (25%)	8 (40%)	NS $P = 0.19$
Cerebral vasospasm (CVS)	***62 (21%)***	***58 (24%)***	***1 (5%)***	***NS P = 0.05***
Delayed infarction (DI)	68 (23%)	62 (26%)	2 (10%)	NS $P = 0.17$
CVS-related DI	22 (32%)	21 (34%)	0 (0%)	NS $p > 0.99$
non-CVS-related DI	46 (68%)	41 (66%)	2 (100%)	NS $p > 0.99$
Delayed cerebral ischemia (DCI)	53 (18%)	49 (20%)	1 (5%)	NS $p = 0.14$
Early hydrocephalus	54 (18%)	38 (16%)	9 (45%)	NS $p > 0.99$
Shunt implantation	31 (11%)	27 (11%)	2 (10%)	NS $p > 0.99$
Favorable outcome mRS 0–2	**240 (82%)**	**193 (80%)**	**20 (100%)**	**$p < 0.05$ OR 0.05 (0–0.7)**

*Favorable outcome 6 months after SAH: mRS ≤2 points; Unfavorable outcome: mRS >2 points. Data are shown in n (%); Fisher exact test: *p < 0.05 is significant. Odd ratio (OR) data with 95% confidence interval. Bold values indicate significant parameter.*

reasons of these discrepancies was not in the focus of interest. Even multiple published meta-analyses produced inconsistent results (8–15).

However, two further large-scale multicenter Phase III trials, STASH (16) and HDS-SAH (17), resulted in disappointing findings. The STASH study could not confirm an improved outcome in aneurysmal SAH patients. In addition, authors of the HDS-SAH study denied any benefits of treatment with high doses of simvastatin (80 mg) vs. treatment with low doses (40 mg), as described previously. Nevertheless, both studies had limitations. In the STASH study the evaluation of vasospasm was not described in detail, and in the HDS-SAH study no control group was used. These limiting factors make it difficult to draw evidence-based conclusions (29).

Therefore, the effect of statins on vasospasm after SAH remained unclear; positive effects may have been neutralized through an adverse pathway. However, recognizing this fact and regarding the pathophysiology of the experimental SAH model being used in most of the studies done in this field, we created a translational insight detecting naSAH patients to assess the statin effect.

Previous studies observed a significant increase in the number of patients with NASAH. Non-aneurysmal SAH patients have significantly less DCI and a higher chance for excellent outcomes compared to aneurysmal SAH, but patients with PM and NPM-SAH also developed DCI. Especially patients with an NPM-SAH have, according to the bleeding pattern, an increased risk for DCI and for a worse neurological outcome (32). Therefore, patients with a NASAH should be monitored for new therapeutic options concerning SAH followed complications to increase the chance for a favorable outcome.

This is the first study presenting the statin effect in patients with naSAH in accordance to the pathophysiological background of statin treatment attenuating SAH following complications in animals. We could detect a significantly lower risk for CVS, DCI, and DI in naSAH patients under statin treatment. Additionally, a significant association between statin treatment and favorable outcome 6 months after naSAH onset could be confirmed. According to previous studies, patients with NASAH and a Fisher Grade 3 bleeding pattern had a significantly higher risk for an unfavorable outcome and death (32). However, a multivariate analysis of recent data described the bleeding pattern as a not-significant risk factor for unfavorable outcome.

Although there is a red thread through the data, from bench to bedside, underlining the effect of statin treatment in naSAH patients, there are some limitations in this study, which have to be under consideration. At first, the small number of detected patients did not allow differentiations to be made between patients under different drugs and doses of statin. In addition,

TABLE 3 | Clinical outcome in association with patient characteristics in NASAH patients admitted to the University Hospital (City) between 1999 and 2018.

Pat. characteristics	NASAH	Favorable outcome	Unfavorable outcome	Multivariate analysis *p-value; OR (95% CI)
Number of patients	**293**	**240** (82%)	**53** (18%)	–
Age ≤ 50 years	173 (59%)	120 (69%)	53 (31%)	NS
Female	**162 (55%)**	**116 (72%)**	**46 (28%)**	**$p < 0.001$; 4.9 (1.9–12.3)**
Hunt&Hess ≤ III	**148 (51%)**	**103 (70%)**	**45 (30%)**	**$p < 0.002$; 4 (1.7–9.5)**
Fisher 3 blood pattern	86 (29%)	40 (47%)	46 (53%)	NS
Hypertension	134 (46%)	84 (63%)	50 (37%)	NS
Statin treatment	**51** (17%)	**47** (92%)	**4** (8%)	**$p < 0.0001$; 24.2 (5.9–99.2)**
Statin post-SAH treatment	**20 (7%)**	**20 (100%)**	**0 (0%)**	**$p < 0.05$; 0.03 (0–0.76)**
Active smoking	88 (30%)	42 (48%)	46 (52%)	NS
Early hydrocephalus	54 (18%)	19 (35%)	35 (65%)	NS
Anticoagulation and antiplatelet drugs	**73 (25%)**	**29 (12%)**	**44 (83%)**	**$p < 0.0001$; 0.16 (0.06–0.46)**
Positive family history	23 (8%)	10 (43%)	13 (57%)	NS

*Favorable outcome 6 months after SAH: mRS ≤2 points; Unfavorable outcome: mRS >2 points. Data are shown in n (%); Multivariate analysis: *$p < 0.05$ is significant. Odd ratio (OR) data with 95% confidence interval. Bold values indicate significant parameter.*

an analysis of statin effect as a pre-treatment vs. post-SAH-treatment could not be done. This aspect should be considered as a limiting factor, because detecting 20 patients suffering from naSAH with statin post-treatment could not be sufficiently powered by statistical analysis to prove the therapeutic effect of statins in the case of the clinical course of naSAH patients. Nevertheless, a separated analysis of the small patient group with statin treatment after SAH detected a tenuous significantly higher chance for favorable outcome and a trend toward lower risk for cerebral vasospasm after non-aneurysmal SAH (**Table 2B**).

However, recent data demonstrate a positive trend in case of statin-effect in naSAH patients according to the known important role of statins in vasculogenesis and vascular regeneration (31).

Furthermore, dividing non-aneurysmal SAH into perimesencepahlic (PM-) SAH, where the blood is strictly around the midbrain or brainstem, and non-perimesencephalic (NPM-) SAH, where the blood extends into the adjacent cistern, it is well-known that NPM-SAH have a different illness course with higher risk of CVS, DCI and poor outcome compared to PM-SAH (32). Concerning this aspect, because of the small number of included patients we could not differ between PM-SAH and NPM-SAH in our multivariate analysis. All these aspects minimize the impact of these results.

Therefore, a combination of pre-/post-treatment with statins may play a role, but a causal relationship cannot, thus far, be proven. Data from other centers are necessary to confirm our findings; however, for this rare condition, the cohort may be considered large.

However, contrary to the most studies in aneurysmal SAH patients, there is a significant association between statin treatment and the occurrence of cerebral vasospasm, delayed infarction, and delayed cerebral ischemia in the case of non-aneurysmal SAH. To analyze propriety and possible application of our results in daily clinical management of naSAH patients, further prospective clinical trials are needed.

Furthermore, by failure of multiple big size clinical studies despite successful experimental data, a translational flashback could ease the way to recognize possible influencing factors. Therefore, unified animal experiments and translational clinical trials should be considered to create the basis for developing new therapeutic schemes, successfully.

Based on this translational study, the injection models mimic non-aneurysmal SAH rather than aneurysmal SAH, and the model might not be suitable to study aneurysmal SAH.

CONCLUSION

Collecting all experimental studies focused on statin effect in animals using the blood injection model, we firstly detected the accordance of this SAH model with the pathophysiology of naSAH.

Then, we presented the statin effect in patients with naSAH in accordance with the pathophysiological background of statin treatment attenuating SAH following complications in animals. We could detect a significant lower risk for CVS, DCI, and DI in naSAH patients being under statin treatment. Additionally, a significant association between statin treatment and favorable outcome 6 months after naSAH onset could be confirmed. Nevertheless, unified animal experiments should be considered to create the basis for developing new therapeutic schemes.

DATA AVAILABILITY STATEMENT

The original contributions presented in the study are included in the article/supplementary material, further inquiries can be directed to the corresponding author/s.

AUTHOR CONTRIBUTIONS

SK and JK wrote the main manuscript text and SK prepared **Figure 1** and **Tables 1**–**3**. All authors reviewed the manuscript.

ACKNOWLEDGMENTS

Marina Heibel and Anne Sicking (University Hospital Frankfurt, Department of Neurosurgery) edited the manuscript for non-intellectual content.

REFERENCES

1. Macdonald RL. Delayed neurological deterioration after subarachnoid haemorrhage. *Nat Rev Neurol.* (2014) 10:44–58. doi: 10.1038/nrneurol.2013.246
2. Hijdra A, Van Gijn J, Stefanko S, Van Dongen KJ, Vermeulen M, Van Crevel H. Delayed cerebral ischemia after aneurysmal subarachnoid hemorrhage: clinicoanatomic correlations. *Neurology.* (1986) 36:329–33. doi: 10.1212/WNL.36.3.329
3. Lynch JR, Wang H, McGirt MJ, Floyd J, Friedman AH, Coon AL, et al. Simvastatin reduces vasospasm after aneurysmal subarachnoid hemorrhage: results of a pilot randomized clinical trial. *Stroke.* (2005) 36:2024–6. doi: 10.1161/01.STR.0000177879.11607.10
4. Van Gijn J, Rinkel GJE. Subarachnoid haemorrhage: diagnosis, causes and management. *Brain.* (2001) 124(Pt 2):249–78. doi: 10.1093/brain/124.2.249
5. McGirt MJ, Lynch JR, Parra A, Sheng H, Pearlstein RD, Laskowitz DT, et al. Simvastatin increases endothelial nitric oxide synthase and ameliorates cerebral vasospasm resulting from subarachnoid hemorrhage. *Stroke.* (2002) 33:29506. doi: 10.1161/01.STR.0000038986.68044.39
6. Sugawara T, Ayer R, Jadhav V, Chen W, Tsubokawa T, Zhang JH. Simvastatin attenuation of cerebral vasospasm after subarachnoid hemorrhage in rats via increased phosphorylation of Akt and endothelial nitric oxide synthase. *J Neurosci Res.* (2008) 86:3635–43. doi: 10.1002/jnr.21807
7. Chou SH, Smith EE, Badjatia N, Nogueira RG, Sims JR II, Ogilvy CS, et al. A randomized, double-blind, placebo-controlled pilot study of simvastatin in aneurysmal subarachnoid hemorrhage. *Stroke.* (2008) 39:2891–3. doi: 10.1161/STROKEAHA.107.505875
8. Tseng MY, Czosnyka M, Richards H, Pickard JD, Kirkpatrick PJ. Effects of acute treatment with pravastatin on cerebral vasospasm, autoregulation, and delayed ischemic deficits after aneurysmal subarachnoid hemorrhage: a phase II randomized placebo-controlled trial. *Stroke.* (2005) 36:1627–32. doi: 10.1161/01.STR.0000176743.67564.5d
9. Vergouwen MD, Meijers JCM, Geskus RB, Coert BA, Horn J, Stroes ESG, et al. Biologic effects of simvastatin in patients with aneurysmal subarachnoid hemorrhage: a double-blind, placebo-controlled randomized trial. *J Cereb Blood Flow Metab.* (2009) 29:1444–53. doi: 10.1038/jcbfm.2009.59
10. Sillberg VAH, Wells GA, Perry JJ. Do statins improve outcomes and reduce the incidence of vasospasm after aneurysmal subarachnoid hemorrhage: a meta-analysis. *Stroke.* (2008) 39:2622–6. doi: 10.1161/STROKEAHA.107.508341
11. Su S H, Xu W, Hai J, Wu Y, Yu F. Effects of statins-use for patients with aneurysmal subarachnoid hemorrhage: a meta-analysis of randomized controlled trials. *Sci Rep.* (2014) 4:4573. doi: 10.1038/srep04573
12. Tseng MY. Summary of evidence on immediate statins therapy following aneurysmal subarachnoid hemorrhage. *Neurocrit Care.* (2011) 15:298–301. doi: 10.1007/s12028-011-9596-6
13. Kramer AH, Fletcher JJ. Statins in the management of patients with aneurysmal subarachnoid hemorrhage: a systematic review and meta-analysis. *Neurocrit Care.* (2010) 12:285–96. doi: 10.1007/s12028-009-9306-9
14. Liu J, Chen Q. Effect of statins treatment for patients with aneurysmal subarachnoid hemorrhage: a systematic review and meta-analysis of observational studies and randomized controlled trials. *Int J Clin Exp Med.* (2015) 8:7198–208.
15. Vergouwen MD, de Haan RJ, Vermeulen M, Roos YBWEM. Effect of statin treatment on vasospasm, delayed cerebral ischemia, and functional outcome in patients with aneurysmal subarachnoid hemorrhage: a systematic review and meta-analysis update. *Stroke.* (2010) 41:e4752. doi: 10.1161/STROKEAHA.109.556332
16. Kirkpatrick PJ, Turner CL, Smith C, Hutchinson PJ, Murray GD, STASH Collaborators. Simvastatin in aneurysmal subarachnoid haemorrhage (STASH): a multicentre randomised phase 3 trial. *Lancet Neurol.* (2014) 13:666–75. doi: 10.1016/S1474-4422(14)70084-5
17. Wong GK, Chan DYC, Siu DYC, Zee BCY, Poon WS, Chan MTV, et al. High-dose simvastatin for aneurysmal subarachnoid hemorrhage: multicenter randomized controlled double-blinded clinical trial. *Stroke.* (2015) 46:382–8. doi: 10.1161/STROKEAHA.114.007006
18. McGirt MJ, Pradilla G, Legnani FG, Thai QA, Recinos PF, Tamargoet RJ, et al. Systemic administration of simvastatin after the onset of experimental subarachnoid hemorrhage attenuates cerebral vasospasm. *Neurosurgery.* (2006) 58:945–51. doi: 10.1227/01.NEU.0000210262.67628.7E
19. Bulsara KR, Coates JR, Agrawal VK, Eifler DM, Wagner-Mann CC, Durham HE, et al. Effect of combined simvastatin and cyclosporin compared with simvastatin alone on cerebral vasospasm after subarachnoid hemorrhage in a canine model. *Neurosurg Focus.* (2006) 21:E11. doi: 10.3171/foc.2006.21.3.11
20. Takata K, Sheng H, Borel CO, Laskowitz DT, Warner DS, Lombardet FW. Simvastatin treatment duration and cognitive preservation in experimental subarachnoid hemorrhage. *J Neurosurg Anesthesiol.* (2009) 21:326–33. doi: 10.1097/ANA.0b013e3181acfde7
21. Wang Z, Chen G, Zhu WW, Bian JY, Shen XO, Zhouet D, et al. Influence of simvastatin on microthrombosis in the brain after subarachnoid hemorrhage in rats: a preliminary study. *Ann Clin Lab Sci.* (2010) 40:32–42.
22. Chang CZ, Wu SC, Lin CL, Hwang SL, Howng SL, Kwanet al. Atorvastatin preconditioning attenuates the production of endothelin-1 and prevents experimental vasospasm in rats. *Acta Neurochir.* (2010) 152:1399–406. doi: 10.1007/s00701-010-0652-3
23. Merlo L, Cimino F, Scibilia A, Ricciardi E, Chirafisi J, Speciale A, et al. Simvastatin administration ameliorates neurobehavioral consequences of subarachnoid hemorrhage in the rat. *J Neurotrauma.* (2011) 28:2493–501. doi: 10.1089/neu.2010.1624
24. Sabri M, Ai J, Marsden PA, Macdonald LR. Simvastatin re-couples dysfunctional endothelial nitric oxide synthase in experimental subarachnoid hemorrhage. *PLoS ONE.* (2011) 6:e17062. doi: 10.1371/journal.pone.0017062
25. Naraoka M, Munakata A, Matsuda N, Shimamura N, Ohkuma H. Suppression of the Rho/Rho kinase pathway and prevention of cerebral vasospasm by combination treatment with statin and fasudil after subarachnoid hemorrhage in rabbit. *Transl Stroke Res.* (2013) 4:368–74. doi: 10.1007/s12975-012-0247-9
26. Platt SR, Coates JR, Eifler DM, Edwards GL, Kent M, Bulsaraet KR. Effect of treatment with simvastatin and cyclosporine on neurotransmitter concentrations in cerebrospinal fluid after subarachnoid hemorrhage in dogs. *Am J Vet Res.* (2013) 74:1111–7. doi: 10.2460/ajvr.74.8.1111
27. Chang CZ, Wu SC, Kwan AL, Lin CL. Preconditioning with pitavastatin, an HMG-CoA reductase inhibitor, attenuates C-Jun N-terminal kinase activation in experimental subarachnoid hemorrhage-induced apoptosis. *Acta Neurochir.* (2015) 157:1031–41. doi: 10.1007/s00701-015-2399-3
28. Duan H, Zhang J, Li L, Bao S. Effect of simvastatin on proliferation of vascular smooth muscle cells during delayed cerebral vasospasm after subarachnoid hemorrhage. *Turk Neurosurg.* (2016) 26:538–44. doi: 10.5137/1019-5149.JTN.13650-15.1
29. Chen JH, Yang LK, Chen L, Wang YH, Wu Y, Jiang BJ, et al. Atorvastatin ameliorates early brain injury after subarachnoid hemorrhage via inhibition of AQP4 expression in rabbits. *Int J Mol Med.* (2016) 37:1059–66. doi: 10.3892/ijmm.2016.2506
30. Chen JH, Wu T, Yang LK, Chen L, Zhu J, Li PP, et al. Protective effects of atorvastatin on cerebral vessel autoregulation in an experimental

rabbit model of subarachnoid hemorrhage. *Mol Med Rep.* (2018) 17:1651–9. doi: 10.3892/mmr.2017.8074

31. Wang B, Sun L, Tian Y, Li Z, Wei H, Wang D, et al. Effects of atorvastatin in the regulation of circulating EPCs and angiogenesis in traumatic brain injury in rats. *J Neurol Sci.* (2012) 319:117–23. doi: 10.1016/j.jns.2012.04.015
32. Konczalla J, Kashefiolasl S, Brawanski N, Lescher S, Senft C, Platz J, et al. Cerebral vasospasm and delayed cerebral infarctions in 225 patients with non-aneurysmal subarachnoid hemorrhage: the underestimated risk of Fisher 3 blood distribution. *J Neurointerv Surg.* (2016) 8:1247–52. doi: 10.1136/neurintsurg-2015-012153

Conflict of Interest: The authors declare that the research was conducted in the absence of any commercial or financial relationships that could be construed as a potential conflict of interest.

frontiers in Neurology

ORIGINAL RESEARCH
published: 21 May 2021
doi: 10.3389/fneur.2021.613029

Machine Learning-Based Prediction of Brain Tissue Infarction in Patients With Acute Ischemic Stroke Treated With Theophylline as an Add-On to Thrombolytic Therapy: A Randomized Clinical Trial Subgroup Analysis

Boris Modrau[1], Anthony Winder[2], Niels Hjort[3], Martin Nygård Johansen[4], Grethe Andersen[5], Jens Fiehler[6], Henrik Vorum[7] and Nils D. Forkert[2]*

[1] Department of Neurology, Aalborg University Hospital, Aalborg, Denmark, [2] Departments of Radiology & Clinical Neurosciences, University of Calgary, Calgary, AB, Canada, [3] Department of Neurology, Aarhus University Hospital, Aarhus, Denmark, [4] Unit of Clinical Biostatistics, Aalborg University Hospital, Aalborg, Denmark, [5] Department of Neurology and Clinical Medicine, Aarhus University Hospital and Aarhus University, Aarhus, Denmark, [6] Department of Diagnostic and Interventional Neuroradiology, University Medical Center Hamburg-Eppendorf, Hamburg, Germany, [7] Department of Ophthalmology, Aalborg University Hospital, Aalborg, Denmark

OPEN ACCESS

Edited by:
Eric Jouvent,
Université Sorbonne Paris Cité, France

Reviewed by:
Andre Kemmling,
University Medical Center Schleswig-Holstein, Germany
Marie Luby,
National Institute of Neurological Disorders and Stroke (NINDS), United States

***Correspondence:**
Boris Modrau
boris.modrau@rn.dk

Specialty section:
This article was submitted to Stroke, a section of the journal Frontiers in Neurology

Received: *01 October 2020*
Accepted: *19 April 2021*
Published: *21 May 2021*

Citation:
Modrau B, Winder A, Hjort N, Johansen MN, Andersen G, Fiehler J, Vorum H and Forkert ND (2021) Machine Learning-Based Prediction of Brain Tissue Infarction in Patients With Acute Ischemic Stroke Treated With Theophylline as an Add-On to Thrombolytic Therapy: A Randomized Clinical Trial Subgroup Analysis. Front. Neurol. 12:613029. doi: 10.3389/fneur.2021.613029

Background and Purpose: The theophylline in acute ischemic stroke trial investigated the neuroprotective effect of theophylline as an add-on to thrombolytic therapy in patients with acute ischemic stroke. The aim of this pre-planned subgroup analysis was to use predictive modeling to virtually test for differences in the follow-up lesion volumes.

Materials and Methods: A subgroup of 52 patients from the theophylline in acute ischemic stroke trial with multi-parametric MRI data acquired at baseline and at 24-h follow-up were analyzed. A machine learning model using voxel-by-voxel information from diffusion- and perfusion-weighted MRI and clinical parameters was used to predict the infarct volume for each individual patient and both treatment arms. After training of the two predictive models, two virtual lesion outcomes were available for each patient, one lesion predicted for theophylline treatment and one lesion predicted for placebo treatment.

Results: The mean predicted volume of follow-up lesions was 11.4 ml (standard deviation 18.7) for patients virtually treated with theophylline and 11.2 ml (standard deviation 17.3) for patients virtually treated with placebo ($p = 0.86$).

Conclusions: The predicted follow-up brain lesions for each patient were not significantly different for patients virtually treated with theophylline or placebo, as an add-on to thrombolytic therapy. Thus, this study confirmed the lack of neuroprotective effect of theophylline shown in the main clinical trial and is contrary to the results from preclinical stroke models.

Keywords: stroke, thrombolytic therapy, clinical trial, theophylline, reperfusion, machine learning, neuroprotective drugs

INTRODUCTION

The vasoactive agent theophylline has shown promising neuroprotective effects with reduced brain tissue edema, brain damage, and mortality in animal stroke models (1–3) but the results were controversial in previous randomized clinical trials (4, 5). The theophylline in acute ischemic stroke trial was designed to overcome the limitations of previous trials, namely the lack of acute ischemic stroke validation, lack of revascularization therapy, and delayed intervention (6). A total of 64 patients with acute ischemic stroke verified with MRI were randomized to a single infusion of 220 mg theophylline or placebo as an add-on to thrombolytic therapy. The co-primary endpoint of early clinical improvement, defined as change of the NIHSS score from baseline to follow-up at 24 h, improved by 4.7 points (standard deviation [SD] 5.6) in the theophylline group compared with an improvement of 1.3 points (SD 7.5) in the group treated with thrombolytic therapy alone ($p = 0.04$) (7). The co-primary endpoint of infarct growth at 24-h follow-up was 141.6% (SD 126.5) in the theophylline group and 104.1% (SD 62.5) in the control group ($p = 0.15$). While the clinical endpoint alone would have shown statistically significant early improvement, it was considered not statistically significant after correcting for multiple testing due to two primary endpoints. With respect to the imaging endpoint, comparing two independent groups with small sample size exhibiting a large variation of stroke lesion volumes might have prevented the detection of a small effect of theophylline. For that reason, a machine learning approach to predict follow-up lesions was pre-planned as a subgroup analysis. The basic idea of this method is to train two machine learning models based on imaging data on a voxel-wise basis acquired at the acute stage and the known follow-up lesion information. Thus, two predicted volumes of follow-up lesions can be quantified for each individual patient, one lesion outcome for the virtual treatment with theophylline and one lesion for the virtual treatment with placebo, which practically doubles the outcome measurements that can be used for statistical testing.

The aim of this study was to use this predictive modeling approach to compare follow-up lesion volumes of patients treated virtually with theophylline and placebo as an add-on to thrombolytic therapy to investigate if there is a subtle treatment effect of theophylline within individual patients that was not obvious when comparing the lesion volumes in the small groups.

MATERIALS AND METHODS

Anonymized data that support the findings of this study are available from the corresponding author upon reasonable request.

Study Design

The present study is based on a subgroup of the theophylline in acute ischemic stroke trial, a current proof-of-concept, randomized, double-blinded, placebo-controlled trial that assessed the neuroprotective effect of theophylline as an add-on to thrombolytic therapy. The trial was registered at the European Union Drug Regulating Authorities Clinical Trials Database (EudraCT number 2013-001989-42). The trial protocol was approved by the Danish Health and Medicines Authorities (ref. no. 2013050908) and the Regional Scientific Ethic Committee (ref.-no. N-20130034) (6). Written informed consent was obtained from all patients and the trial was conducted in compliance with the Declaration of Helsinki. The trial was terminated early due to slow recruitment.

Definition of Subgroup

The main selection criterion for the theophylline in acute ischemic stroke trial was eligibility for thrombolytic therapy within 4.5 h of symptom onset in patients with MRI verified moderate to severe acute ischemic stroke (NIHSS $\geq$4). For this pre-planned subgroup analysis, all patients with multi-parametric MRI including diffusion- and perfusion-weighted MRI at baseline, and available 24-h follow-up MRI were analyzed.

Image Acquisition

All patients underwent MRI with the same field strength (1.5 or 3.0 Tesla) at admission (baseline) and at 24-h (22–32-h) follow-up. The MR sequences included diffusion-weighted MRI (DWI), perfusion-weighted MRI (PWI) with intravenous gadolinium (0.1 mmol per kilogram body weight, 5 ml/s bolus injection), circle of Willis time-of-flight MR angiography, gradient echo weighted MRI, and T2-FLAIR MRI. The thrombolysis in myocardial infarction (TIMI) grading was used to grade arterial obstruction (8). TIMI 0-1 at baseline was defined as large vessel occlusion and TIMI 0-1 at baseline converted to 3-4 at 24-h follow-up was defined as revascularization.

Image Post-processing

Post-processing of DWI and PWI was performed semi-automatically using the AnToNIa software tool to extract voxel-by-voxel information for training of the machine learning models (9). In detail, the following processing steps were applied: An apparent diffusion coefficient dataset was calculated based on two DWI datasets (b-value = 0 and b-value,= 1,000 mm²/s). The ADC map was used for an automatic thresholding-based brain tissue and cerebrospinal fluid segmentation. The baseline ischemic core was manually delineated using a semi-automatic volume growing approach with an upper ADC threshold of 550×10^{-6} mm²/s, in accordance to a previous stroke study (10). The delineated ischemic core was then used to compute a distance map displaying the Euclidean distance for each non-core voxel to the closest voxel of the ischemic core. This was done to incorporate prior knowledge that the probability of final tissue infarction decreases with distance to the infarct core into the machine learning model. The PWI dataset was automatically motion corrected and the arterial input function was manually defined at the ICA or MCA M1-segment. A block-circulant deconvolution-based perfusion analysis was used to calculate the cerebral blood flow, cerebral blood volume, mean transit time, and time-to-maximum of the residual function (Tmax). Mean values were determined for each parameter in the contralateral brain tissue (excluding cerebrospinal fluid) and used for normalization of the perfusion parameters (CBF

and CBV values by calculating the ratio, MTT and Tmax by subtraction of the contralateral average values). The normalized Tmax perfusion parameter maps were segmented using a lower threshold of 6 s to determine the hypoperfused tissue. The PWI parameter maps were automatically registered to the ADC dataset and the tissue at risk was calculated by subtracting the ADC lesion from the Tmax (>6 s) hypoperfusion. Information about the localization of each voxel and possible regional vulnerability to ischemia was added by registering the Montreal Neurological Institute brain atlas to each ADC dataset, described in more details by Forkert et al. (9). The ipsilateral follow-up brain tissue lesion was manually segmented in the follow-up T2-FLAIR dataset of each patient acquired at 24-h using the software tool ITK-SNAP (v. 3.6.0) (11) and registered to the baseline ADC dataset. The imaging data were complemented by the following clinical parameters: age, sex, baseline NIHSS, and time of stroke onset to theophylline / placebo application.

Finally, 12 equally weighted features were available for each voxel: Tissue type probability, anatomical location, distance to the ischemic core, ADC value, CBF value, CBV value, MTT value, Tmax value, and the four clinical parameters as well as information about the infarct outcome. A stratified, under-sampled training set consisting of all voxels from the follow-up infarct lesion and an equal number of non-lesion voxels randomly sampled from the ipsilateral hemisphere were extracted for each dataset. This approach and feature setup yielded the best results in a previous in-depth technical evaluation (12).

Lesion Outcome Prediction

Two random forest machine learning models were trained, one using all training sets from the patients treated with theophylline and one using all training sets from the patients treated with placebo. The patient in whom the algorithm was tested (used for lesion outcome prediction) in each iteration was always excluded from the aggregated training set used for training of the random forest models. Practically, the machine learning models were implemented using ALGLIB (www.alglib.net) (13) with the random forest model consisting of 100 trees assuring an acceptable compromise between accuracy and computation speed, described in more details by Winder et al. (12).

After training of the two predictive models, both models were used to predict the lesion outcome for both treatment options for each patient.

Statistical Analyses

Baseline characteristics are presented by the mean ± standard deviation or median and interquartile range, as appropriate. Continuous data were compared with Wilcoxon's rank sum test. Categorical data were summarized by counts and percentages and compared using Fisher's exact test. For the primary endpoint, a paired *t*-test was used to compare the predicted volumes of the follow-up lesion for each patient virtually treated with theophylline or placebo and the data was represented as box-whisker graph. Dice similarity coefficients comparing the true lesion outcome with the predicted lesion outcome within each group were calculated to quantify the prediction accuracy. Furthermore, the difference and average of both predictions for each patient were calculated and presented using a Bland Altman plot. For the additional explorative analysis, an unpaired *t*-test was used to compare the difference between the two predicted lesion volumes for patients with and without presence of tissue at risk at baseline, for patients with cortical vs. lacunar infarction, for patients with large vessel occlusion at baseline, and for patients with recanalization at follow-up.

All tests were applied as *post-hoc* analysis with a two-sided alpha level of 0.05 without correction for multiple comparisons. Stata/MP version 15.1 (Stata Corp LLC) was applied for the analysis.

RESULTS

Study Population

MRI including baseline DWI and PWI and follow-up T2-FLAIR at 24 h was available in 52 out of 64 patients included in the main study (43 patients imaged at 3.0 Tesla and 9 patients imaged at 1.5 Tesla MRI field strength). Overall, the baseline characteristics were similar between the two treatment groups (**Table 1**). However, diabetes mellitus was more frequently present in the control group (four patients) compared to the theophylline group (no patients). The process measures: time of stroke onset to door, door to thrombolysis, door to theophylline/placebo treatment, and the rate of additional endovascular therapy were similar between the two treatment groups. Likewise, the baseline imaging characteristics volume of ischemic core, volume of tissue-at-risk, type of vessel occlusion, and grade of vessel occlusion were similar between the two treatment groups. The mean volume of ischemic lesion based on the segmentation of the follow-up T2-FLAIR dataset at 24-h was 13.9 ml (SD 20.3) for the theophylline group and 11.7 ml (SD 19.3) for the placebo group ($p = 0.92$).

Primary Outcome

The mean Dice similarity coefficient was 0.40 (SD 0.249) for the theophylline prediction model and 0.35 (SD 0.243) for the placebo prediction model, which is in the range of previously described methods (12).

Using the two predictive models, the mean predicted lesion volume was 11.4 ml (standard deviation (SD) 18.7) for the patients virtually treated with theophylline and 11.2 ml (SD 17.3) for patients virtually treated with placebo (**Figure 1**). No significant difference was found between the predicted volumes of the two treatment groups using a paired *t*-test ($p = 0.86$). A detailed list of the true and predicted lesion volumes for each individual patient is provided as **Supplementary Table 1**.

Additional Analyses

The predicted lesion volumes for each patient virtually treated with theophylline or placebo were similar for small and large infarct volumes as illustrated in the Bland-Altman plot (**Figure 2**). Tissue-at-risk at baseline was present in 29 patients and absent in 23 patients. The type of stroke was classified as cortical in 34 patients and lacunar in 18 patients. Twenty-three patients fulfilled the criteria for large vessel occlusion at

TABLE 1 | Baseline characteristics.

	Theophylline group (*N* = 27)	Control group (*N* = 25)	*p*-value
Clinical			
Median age – year (IQR)	71 (55–77)	69 (52–78)	0.86
Female sex – no. (%)	10 (37)	11 (44)	0.61
Median NIHSS score (IQR)	8 (6–13)	7 (6–8)	0.12
Hypertension – no. (%)	14 (52)	16 (64)	0.38
Diabetes mellitus – no. (%)	0 (0)	4 (8)	0.03
Hyperlipidemia – no. (%)	16 (59)	16 (64)	0.73
Arterial fibrillation – no. (%)	2 (7)	4 (16)	0.33
Peripheral arterial disease – no. (%)	2 (7)	0 (0)	0.16
Previous myocardial infarction – no. (%)	1 (4)	1 (4)	0.96
Previous transitory ischemic attack – no. (%)	2 (7)	2 (8)	0.94
Previous stroke – no. (%)	3 (11)	3 (12)	0.92
Previous intracranial hemorrhage – no. (%)	0 (0)	0 (0)	1
Current smoking – no. (%)	10 (37)	9 (36)	0.94
Antiplatelet agent – no. (%)	7 (26)	9 (36)	0.43
Imaging characteristics			
Mean volume of ischemic core – ml (SD)	4.4 (6.4)	4.3 (7.8)	0.81
Mean volume of baseline tissue at risk – ml (SD)	9.6 (22.0)	6.5 (13.9)	0.44
Large vessel occlusion – no. (%)	12 (44)	11 (44)	0.97
Type of vessel occlusion			0.85
Anterior cerebral artery – no. (%)	0 (0)	1 (4)	
Middle cerebral artery (M1-segment) – no. (%)	6 (22)	4 (16)	
Middle cerebral artery (M2-3-segment) – no. (%)	5 (19)	5 (20)	
Posterior cerebral artery – no. (%)	1 (4)	1 (4)	
No visible large vessel occlusion – no. (%)	15 (55)	14 (56)	
Grade of vessel occlusion at baseline			0.97
TIMI-score 0–1 – no. (%)	12 (44)	11 (44)	
TIMI-score 2–3 – no. (%)	15 (56)	14 (56)	
Process measures			
Median stroke onset – door time – min (IQR)	81 (48–148)	85 (68–130)	0.41
Median door to thrombolysis-time – min (IQR)	39 (35–45)	41 (35–51)	0.75
Additional endovascular therapy – no. (%)	3 (11)	4 (16)	0.61

The baseline characteristics of the two groups were not significantly different apart from diabetes mellitus ($p = 0.03$).
IQR, Interquartile range; SD, Standard deviation; NIHSS, National Institute of Health Stroke Scale; TIMI, thrombolysis in myocardial infarction grading of arterial obstruction (score zero, complete occlusion; one, severe stenosis; two, mild to moderate stenosis; three, normal arterial caliber).

baseline (TIMI 0-1), and the criteria for recanalization at follow-up (TIMI 3-4) were fulfilled in 10 out of these 23 patients. The predicted follow-up lesions were not significantly different between patients with and without presence of tissue-at-risk at baseline ($p = 0.89$), in patients with cortical vs. lacunar infarction ($p = 0.88$), in patients with and without large vessel occlusion at baseline ($p = 0.57$), and in patients with and without recanalization at follow-up ($p = 0.35$) (**Figure 3**).

DISCUSSION

The main finding of this secondary analysis of the theophylline in acute ischemic stroke trial is that the predicted follow-up lesion volumes of patients virtually treated with theophylline or placebo are not significantly different.

The primary aim of the theophylline in acute ischemic stroke trial was to investigate the neuroprotective effect of theophylline as an add-on to thrombolytic therapy in patients with acute ischemic stroke. The clinical endpoint alone would have shown a statistically significant early improvement at 24-h follow-up ($p = 0.04$) but was considered not statistically significant after correcting for multiple testing due to two primary endpoints. The co-primary endpoint infarct growth did not reach significance ($p = 0.19$). However, it was uncertain whether the considerable variation of stroke lesion volumes in a small sample size and the infarct growth information limited to the follow-up T2-FLAIR segmentation might have prevented detection of a subtle effect of theophylline. The rather small infarct volumes and the large variation in a small sample size was the main motivation for this *post-hoc* analysis using a predictive modeling approach for a more in-depth comparison of the groups. Various machine

learning models have been presented in the past for this purpose typically showing better performance for tissue outcome prediction compared to simple perfusion parameter thresholding (14–17). A recent study showed that such machine learning models cannot only be used to predict the lesion outcome in patients for treatment decision making but also for intra-individual virtual comparisons of treatments (18). This voxel-by-voxel analysis of eight imaging parameters for each voxel based on DWI and PWI sequences collected from each patient together with four clinical parameters practically allows to double the sample size by simulating both treatment outcomes for each patient included in this study. The accuracy of the prediction models was acceptable as the mean Dice similarity coefficients comparing the true lesion volumes with the predicted lesion volumes within each group were within the range of results from a recent study applying multi-parametric tissue outcome prediction methods (12).

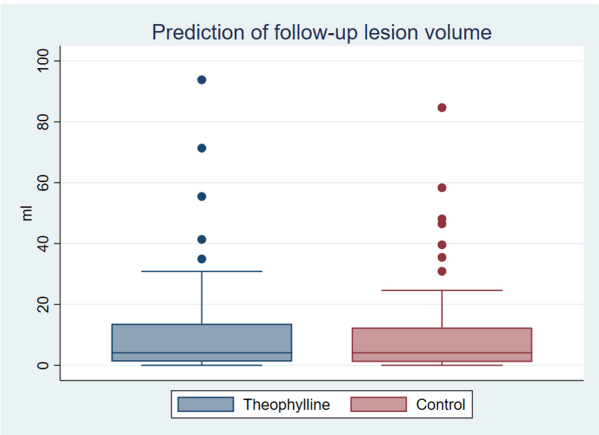

FIGURE 1 | Predicted volume of follow-up lesions. Box-whisker diagram depicting the mean predicted volumes of follow-up lesions based on the trainings datasets of patients treated with theophylline and placebo: Interquartile range with median (box), lower and upper interquartile +1.5 interquartile range (whisker), and outliers (dots).

In our trial, the surrogate marker for follow-up lesion volume was almost identical for patients virtually treated with theophylline and patients virtually treated with placebo. Thus, the machine learning approach with practically doubled sample size of outcome measurements compared to the main clinical trial confirmed the lack of a neuroprotective effect of theophylline. This is most notably true, as there is no detectible neuroprotective effect on infarct growth in the highly selected subgroup of patients with presence of tissue-at-risk at baseline and/or subsequent recanalization. One limitation of this study is that the small sample size did not allow a sufficient investigation of a lesion-size dependent effect of theophylline although the Bland Altman plots as well as a simple evaluation using regression analysis do not suggest such an effect. Although all perfusion MRI were sufficient for analysis, and complete follow-up was available, the main limitation remains the low number of patients in this

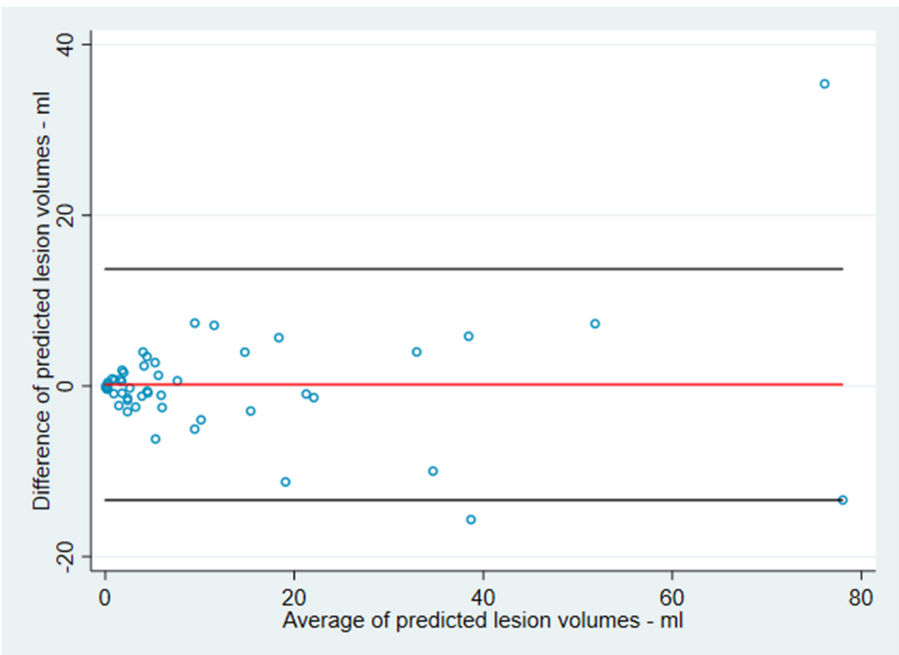

FIGURE 2 | Interaction of infarct size and prediction. Bland Altman plot depicting the predicted volume of follow-up lesions plotted as the difference between the two predictions (theophylline and placebo) over the average of the two predicted volumes for each patient: Values <0 indicate that theophylline is better than placebo while values >0 indicate that placebo is better than theophylline: Middle line indicates mean difference between the predicted values, upper and lower line indicates the higher and lower limit of agreement (2x standard deviation) indicating no significant difference between small and large infarct volumes.

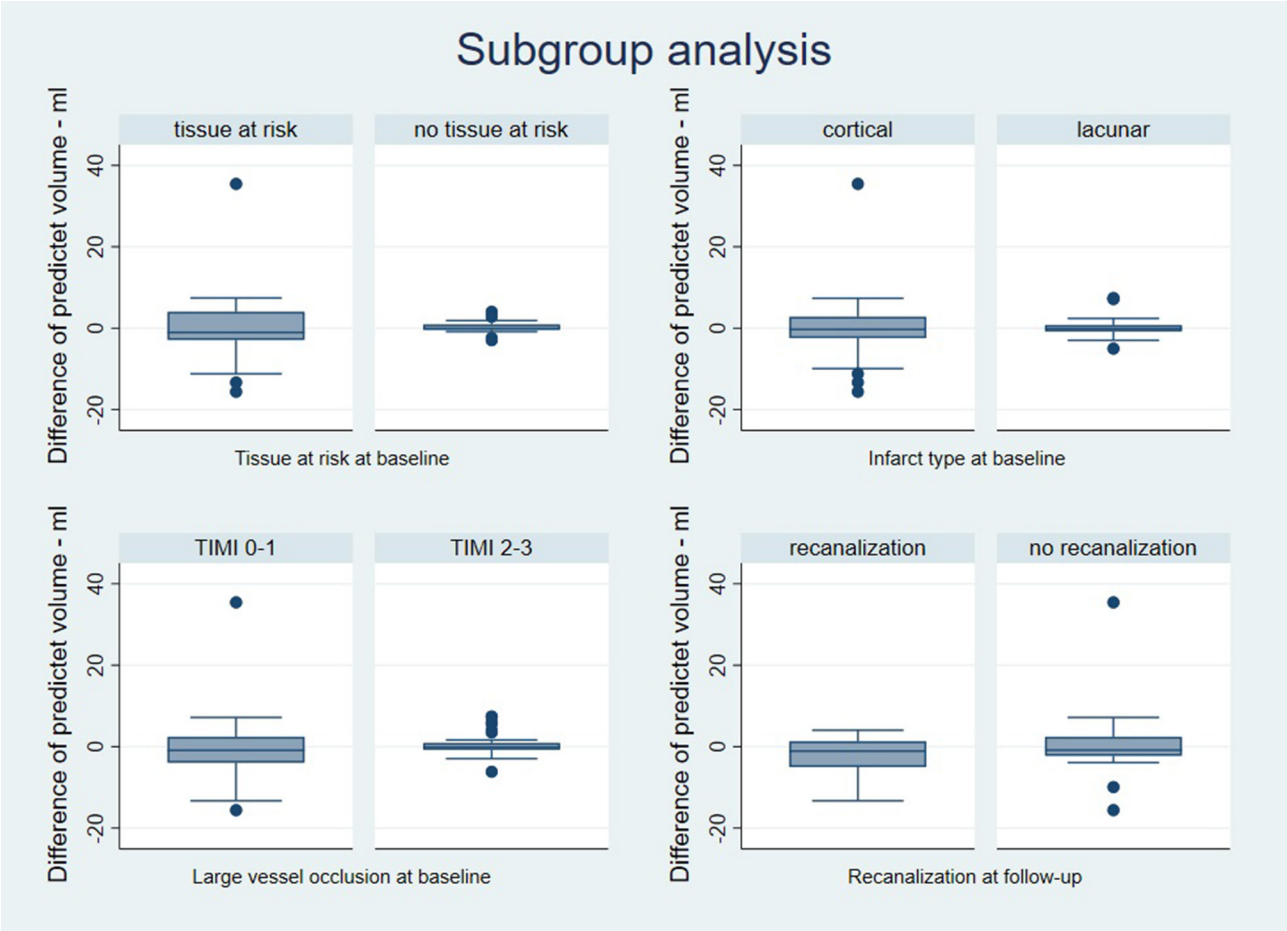

FIGURE 3 | Subgroup analysis. Box-whisker diagrams depicting the predicted volume of follow-up lesions plotted as the difference between the two predictions (theophylline and placebo) for each patient: Values <0 indicate that theophylline is better than placebo and values >0 indicate that placebo is better than theophylline indicating no significant difference for patients with and without tissue-at-risk at baseline, for patients with cortical vs. lacunar infarction, for patients with and without large vessel occlusion at baseline, and for patients with and without recanalization at follow-up.

subgroup analysis. However, previous work has shown that the machine learning model used requires no more than 50 datasets for optimal training (19). Accordingly, the Dice scores achieved in our study were within the range of previously published papers. Another limitation is that machine learning models are rarely employed in clinical trials. As discussed by Fiehler et al. (18), the potential of a study design with virtual comparators based on predictive modeling is highly informative, quick, and relatively inexpensive. In contrast to that, the established study design of a randomized control trial provides the highest level of evidence. In our study, application of a machine learning model allowed further insights given the limited dataset and confirmed the results of the main trial. However, the large variation of lesions, the variation of infarct types with and without collateral supply, and the large variation or lack of tissue-at-risk are still relevant limitations of this study. Nevertheless, we believe that predictive modeling to virtually test for differences in the follow-up lesion volumes can become an essential tool to support conventional trials in acute ischemic stroke by enabling an improved evaluation of evidence on intermediate outcomes and to increase the sample size for the primary or secondary outcomes in case of underpowered studies.

There is no known interaction between theophylline and alteplase. Recently, such interaction was observed to inhibit the neuroprotective effect of Nerinetide in acute ischemic stroke in the ESCAPE-NA1-trial. In that trial, Nerinetide did not improve the good clinical outcomes after endovascular thrombectomy (20).

In line with numerous previous neuroprotective clinical trials, our trial failed to translate the promising results of reduced brain infarction from pre-clinical stroke models to humans (21). However, from a patient and physician perspective, neuroprotection means keeping the damage of the ischemic stroke below the threshold of symptom manifestation (22). For that reason, a lack of an effect on the surrogate marker infarct growth does not outrange the clinical response and the neuroprotective effect of theophylline should still be investigated in more detail.

In summary, predictive modeling using advanced machine learning was performed to uncover potential subtle effects on follow-up lesion volumes of theophylline as an add-on to thrombolytic therapy in patients with acute ischemic stroke. The predicted follow-up brain lesions for each patient virtually treated with theophylline and placebo confirmed the volumetric results based on the small sample sizes of the original study. Thus, this study also confirmed the lack of neuroprotective effect of theophylline shown in the main clinical trial and is contrary to the results from preclinical stroke models.

DATA AVAILABILITY STATEMENT

The raw data supporting the conclusions of this article will be made available by the authors, without undue reservation.

ETHICS STATEMENT

The studies involving human participants were reviewed and approved by Danish Regional Scientific Ethic Committee (ref.-no. N-20130034). The patients/participants provided their written informed consent to participate in this study.

AUTHOR CONTRIBUTIONS

BM, AW, NH, JF, and NF contributed to the conception and design of the study. BM, NH, AW, and NF contributed to the acquisition and analysis of the data. BM wrote the main draft. All authors discussed the results and implications and contributed to the interpretation and critical revision of the data. BM and NF finalized and submitted the manuscript.

FUNDING

This study was funded by the Danish Regions (14/217), the Danish Heart Foundation (13-04-R94-A4619-22792, 14-R97-A5066-22829) and the Heart and Stroke Foundation of Canada (G-17-0018368).

SUPPLEMENTARY MATERIAL

The Supplementary Material for this article can be found online at: https://www.frontiersin.org/articles/10.3389/fneur.2021.613029/full#supplementary-material

REFERENCES

1. Bona E, Ådén U, Gilland E, Fredholm BB, Hagberg H. Neonatal cerebral hypoxia-ischemia: the effect of adenosine receptor antagonists. *Neuropharmacology.* (1997) 36:1327–38. doi: 10.1016/S0028-3908(97)00139-1
2. Kogure K, Scheinberg P, Busto R, Reinmuth OM. An effect of aminophylline in experimental cerebral ischemia. *Trans Am Neurol Assoc.* (1975) 100:77–80.
3. Seida M, Wagner HG, Vass K, Klatzo I. Effect of aminophylline on postischemic edema and brain damage in cats. *Stroke.* (1988) 19:1275–82. doi: 10.1161/01.STR.19.10.1275
4. Britton M, de Faire U, Helmers C, Miah K, Rane A. Lack of effect of theophylline on the outcome of acute cerebral infarction. *Acta Neurol Scand.* (1980) 62:116–23. doi: 10.1111/j.1600-0404.1980.tb03011.x
5. Geismar P, Marquardsen J, Sylvest J. Controlled trial of intravenous aminophylline in acute cerebral infarction. *Acta Neurol Scand.* (1976) 54:173–80. doi: 10.1111/j.1600-0404.1976.tb04791.x
6. Modrau B, Hjort N, Østergaard L, Mouridsen K, Andersen G, Bach FW. Theophylline as an add-on to thrombolytic therapy in acute ischaemic stroke (TEA-Stroke): a randomized, double-blinded, placebo-controlled, two-centre phase iI study. *Eur Stroke J.* (2016) 1:248–54. doi: 10.1177/2396987316674542
7. Modrau B, Andersen G, Mikkelsen IK, Nielsen A, Hansen MB, Johansen MB, et al. Theophylline as an add-on to thrombolytic therapy in acute ischemic stroke: a randomized placebo-controlled trial. *Stroke.* (2020) 51:1983–90. doi: 10.1161/STROKEAHA.119.027446
8. Zaidat OO, Yoo AJ, Khatri P, Tomsick TA, Von Kummer R, Saver JL, et al. Recommendations on angiographic revascularization grading standards for acute ischemic stroke: a consensus statement. *Stroke.* (2013) 44:2650–63. doi: 10.1161/STROKEAHA.113.001972
9. Forkert ND, Cheng B, Kemmling A, Thomalla G, Fiehler J. Antonia perfusion and stroke: a software tool for the multi-purpose analysis of mR perfusion-weighted datasets and quantitative ischemic stroke assessment. *Methods Inf Med.* (2014) 53:469–81. doi: 10.3414/ME14-01-0007
10. Siemonsen S, Löbel U, Sedlacik J, Forkert ND, Mouridsen K, Østergaard L, et al. Elevated t2-values in mRI of stroke patients shortly after symptom onset do not predict irreversible tissue infarction. *Brain.* (2012) 135:1981–9. doi: 10.1093/brain/aws079
11. Yushkevich PA, Piven J, Hazlett HC, Smith RG, Ho S, Gee JC, et al. User-guided 3D active contour segmentation of anatomical structures: significantly improved efficiency and reliability. *Neuroimage.* (2006) 31:1116–28. doi: 10.1016/j.neuroimage.2006.01.015
12. Winder AJ, Siemonsen S, Flottmann F, Thomalla G, Fiehler J, Forkert ND. Technical considerations of multi-parametric tissue outcome prediction methods in acute ischemic stroke patients. *Sci Rep.* (2019) 9:1–12. doi: 10.1038/s41598-019-49460-y
13. Bochkanov, S; Bystritsky V. *ALGLIB*. Available online at: http://www.alglib.net/ (accessed February 10, 2020).
14. Grosser M, Gellißen S, Borchert P, Sedlacik J, Nawabi J, Fiehler J, et al. Improved multi-parametric prediction of tissue outcome in acute ischemic stroke patients using spatial features. *PLoS ONE.* (2020) 15:1–19. doi: 10.1371/journal.pone.0228113
15. Kemmling A, Flottmann F, Forkert ND, Minnerup J, Heindel W, Thomalla G, et al. Multivariate dynamic prediction of ischemic infarction and tissue salvage as a function of time and degree of recanalization. *J Cereb Blood Flow Metab.* (2015) 35:1397–405. doi: 10.1038/jcbfm.2015.144
16. Bagher-Ebadian H, Jafari-Khouzani K, Mitsias PD, Lu M, Soltanian-Zadeh H, Chopp M, et al. Predicting final extent of ischemic infarction using artificial neural network analysis of multi-Parametric mri in patients with stroke. *PLoS ONE.* (2011) 6:e22626. doi: 10.1371/journal.pone.0022626
17. Lee H, Lee E-J, Ham S, Lee H-B, Lee JS, Kwon SU, et al. Machine learning approach to identify stroke within 4.5 hours. *Stroke.* (2020) 51:860–6. doi: 10.1161/STROKEAHA.119.027611
18. Fiehler J, Thomalla G, Bernhardt M, Kniep H, Berlis A, Dorn F, et al. ERASER: a thrombectomy study with predictive analytics end point. *Stroke.* (2019) 50:1275–8. doi: 10.1161/STROKEAHA.119.024858
19. Forkert ND, Fiehler J. Effect of sample size on multi-parametric prediction of tissue outcome in acute ischemic stroke using a random forest classifier. *Med Imaging 2015 Biomed Appl Mol Struct Funct Imaging.* (2015) 9417:94172H. doi: 10.1117/12.2082686

20. Hill MD, Goyal M, Menon BK, Nogueira RG, Mctaggart RA, Demchuk AM, et al. Efficacy and safety of nerinetide for the treatment of acute ischaemic stroke (ESCAPE-NA1): a multicentre, double-blind, randomised controlled trial. (2020) 395:878–87. doi: 10.1016/S0140-6736(20)30258-0
21. Chamorro Á, Dirnagl U, Urra X, Planas AM. Neuroprotection in acute stroke: targeting excitotoxicity, oxidative and nitrosative stress, and inflammation. *Lancet Neurol.* (2016) 15:869–81. doi: 10.1016/S1474-4422(16)00114-9
22. Wiendl H, Elger C, Förstl H, Hartung HP, Oertel W, Reichmann H, et al. Gaps between aims and achievements in therapeutic modification of neuronal damage ("Neuroprotection"). *Neurotherapeutics.* (2015) 12:449–54. doi: 10.1007/s13311-015-0348-8

Conflict of Interest: The authors declare that the research was conducted in the absence of any commercial or financial relationships that could be construed as a potential conflict of interest.

frontiers in Neurology

MINI REVIEW
published: 24 May 2021
doi: 10.3389/fneur.2021.600365

Exercise Factors Released by the Liver, Muscle, and Bones Have Promising Therapeutic Potential for Stroke

Joseph S. Stephan[1]* *and Sama F. Sleiman*[2]*

[1] School of Medicine, Lebanese American University, Byblos, Lebanon, [2] Biology Program, Lebanese American University, Byblos, Lebanon

Stroke is one of the leading causes of death and disability in the world. Stroke not only affects the patients, but also their families who serve as the primary caregivers. Discovering novel therapeutic targets for stroke is crucial both from a quality of life perspective as well as from a health economic perspective. Exercise is known to promote neuroprotection in the context of stroke. Indeed, exercise induces the release of blood-borne factors that promote positive effects on the brain. Identifying the factors that mediate the positive effects of exercise after ischemic stroke is crucial for the quest for novel therapies. This approach will yield endogenous molecules that normally cross the blood brain barrier (BBB) and that can mimic the effects of exercise. In this minireview, we will discuss the roles of exercise factors released by the liver such as beta-hydroxybutyrate (DBHB), by the muscle such as lactate and irisin and by the bones such as osteocalcin. We will also address their therapeutic potential in the context of ischemic stroke.

Keywords: exercise factors, beta-hydroxybutyrate, irisin, lactate, BDNF, stroke, osteocalcin

OPEN ACCESS

Edited by:
Rajiv Ram Ratan,
Burke Neurological Institute (BNI), United States

Reviewed by:
Dafin F. Muresanu,
Iuliu Haţieganu University of Medicine and Pharmacy, Romania
Rudolf Gesztelyi,
University of Debrecen, Hungary

***Correspondence:**
Sama F. Sleiman
sama.sleiman01@lau.edu.lb
Joseph S. Stephan
joseph.stephan@lau.edu.lb

Specialty section:
This article was submitted to Stroke, a section of the journal Frontiers in Neurology

Received: *29 August 2020*
Accepted: *03 May 2021*
Published: *24 May 2021*

Citation:
Stephan JS and Sleiman SF (2021) Exercise Factors Released by the Liver, Muscle, and Bones Have Promising Therapeutic Potential for Stroke. Front. Neurol. 12:600365. doi: 10.3389/fneur.2021.600365

INTRODUCTION

Stroke is the fifth major cause of death and a leading cause of disability in the United States. This is due to the lack of neuroprotective agents that are able to decrease the associated neuronal damage and loss (1, 2). Neurotrophins such as brain-derived neurotrophic factor (BDNF) mediate protection and recovery following stroke. BDNF promotes regeneration and restores damaged neural tissue. The use of exogenous BDNF after stroke is hindered by its rapid degradation and its inability to cross the blood-brain barrier (BBB). Hence, therapeutics that can modulate endogenous BDNF signaling in the brain may be useful in the context of stroke (3).

Physical exercise increases *Bdnf* expression in the hippocampus to promote learning, and memory formation (4). Exercise mediates these positive effects by inducing the release of metabolites and proteins from the liver, muscle, bones and platelets (**Figure 1**). These factors have been shown to be protective in the context of traumatic brain injury (12) and depression (13). In addition, exercise can prevent and alleviate many of the detrimental effects of stroke. Understanding which factors mediate the protective effects of exercise in ischemic stroke and deciphering the involvement of BDNF signaling will allow us to fully harness exercise's therapeutic potential.

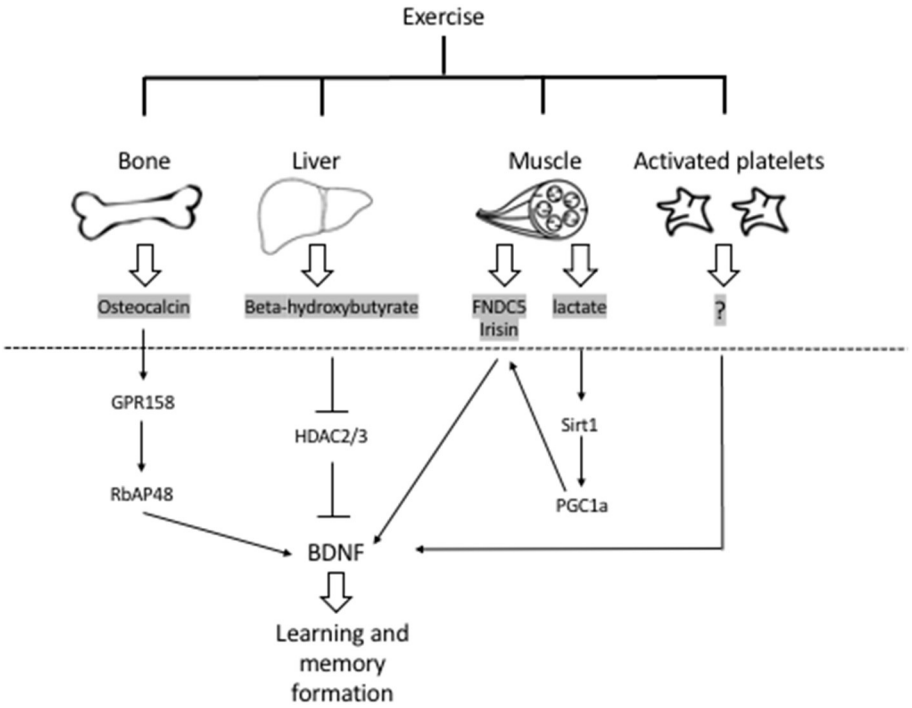

FIGURE 1 | Exercise induces the release of metabolites and proteins that promote learning and memory formation through activation of *Bdnf* expression and signaling in the hippocampus. Bones release osteocalcin that promotes *Bdnf* expression through an epigenetic mechanism involving RbAP48 (5, 6). The liver releases the ketone body betahydroxy-butyrate that induces hippocampal *Bdnf* expression by inhibiting class I HDACs, namely HDAC2 and HDAC3 (4, 7). The muscle releases FNDC5/irisin that activate hippocampal *Bdnf* expression through an unknown mechanism (8). In addition, the muscle release lactate that activates the hippocampal SIRT1/PGC1-alpha/FNDC5 pathway and in turn *Bdnf* expression (9). Finally activated platelets have been shown to store and secrete BDNF (10, 11). Whether these factors mediate the positive effects of exercise in stroke is not clear and needs to be addressed. In addition, the role of BDNF signaling in exercise-mediated neuroprotection also needs to be assessed. BDNF, brain-derived neurotrophic factor; FDNC5, fibronectin type III domain-containing protein 5; HDACs, histone deacetylases; SIRT1, sirtuin 1; PGC1-alpha, Peroxisome proliferator-activated receptor gamma coactivator 1-alpha.

In this minireview, we will focus on how newly identified blood-borne exercise factors that induce hippocampal BDNF signaling to promote learning and memory formation are protective after ischemic stroke. We will also address the current research gaps that link these factors to the positive effects of exercise. Indeed, this minireview will highlight the urgent need for systemic experimentation to identify which factors are responsible for exercise's prophylactic and therapeutic effects in the context of stroke and the role of BDNF signaling in these effects.

Exercise and Ischemic Stroke

It is important to distinguish between the preventative roles of exercise and its therapeutic role. Exercise pre-conditioning enhances neuroprotection and decreases brain edema (14–23). Treadmill exercise prior to middle cerebral artery occlusion (MCAO) in rodent models improves motor function, decreases infarct volumes, reduces neuronal apoptosis and oxidative stress, enhances angiogenesis and induces *Bdnf* expression (24–27). The level of neuroprotection that is achieved varies with the duration and intensity of exercise. For example, even though short bouts of exercise before stroke induce the expression of angiogenesis markers, they may not be enough to rescue neurological deficits post-ischemic stroke (26). Alternatively, high intensity interval training (HIIE) alleviates the symptoms of stroke more efficiently than moderate continuous training (28). Moderate exercise may protect the brain against MCAO by enhancing the release of miR-126 enriched endothelial progenitor cell-derived exosomes (29).

Exercise is also a safe and cost-effective therapeutic strategy post-stroke, in which the optimal time and intensity of exercise is critical (30). Indeed, animal studies have revealed that both high intensity exercise or exercise initiated only 24 h after stroke promote inflammation and cell death (30). In contrast, exercise initiated on later time periods (as early as 48 h post-stroke) as well as low intensity and moderate intensity exercise improve infarct volume and neurological severity scores 14 days post-stroke (30). Interestingly, prolonged treadmill exercise promotes neurogenesis and improves motor function and short-term memory by increasing the expression of hippocampal BDNF in photothrombotic stroke mice (31). In addition, treadmill exercise enhances neurogenesis and myelin repair by activating the Wnt and BDNF pathways after focal cerebral ischemia/reperfusion (32).

In most of the paradigms in which exercise was studied as a prophylactic (14–23) or as a therapy for ischemic stroke (33–37), the neuroprotective roles of exercise were associated with

restoration of BDNF levels (38, 39). In humans, decreases in BDNF levels are correlated with an increased risk of stroke, worse functional outcomes and higher mortality (40). Indeed, BDNF levels are decreased in acute ischemic-stroke patients. Interestingly, patients that carry the BDNF $Val^{66}Met$ allele, known to decrease BNDF levels by 30%, have worse outcomes and prognosis after stroke (40).

Exercise Factors and the Brain

Exercise enhances neurogenesis, mediates synaptic plasticity and promotes learning and memory formation. These effects are thought to be mediated in part by activation of hippocampal BDNF signaling [reviewed in (4)]. Recent work has revealed that injection of blood from young exercising mice is able to rescue learning and memory defects in old mice by inducing hippocampal BDNF levels (41). Several blood-borne exercise factors comprised of proteins and metabolites released by the liver, muscle and bones have been identified through their ability to induce BDNF signaling, and have been implicated in mediating the positive effects of exercise on the brain. Since decreases in BDNF levels are correlated with negative outcomes after stroke (40), studying the exercise factors that induce BDNF signaling and assessing their neuroprotective abilities may allow us to identify novel endogenous therapeutic agents for stroke. For this reason, we will discuss what is known about blood-borne factors released by the liver, muscle and bones. Interestingly, even though some of these factors have neuroprotective effects in animal models of stroke, very little has been done to directly demonstrate that they are responsible for the preventative or therapeutic effects of exercise. These studies remain necessary to further our understanding of the molecular mechanisms underlying the effects of exercise.

Exercise Factors Released by the Liver and Their Role in Ischemic Stroke

Exercise induces the release of multiple factors from the liver into the blood that can transfer its benefits to the brain. These exercise factors include metabolites, such as the ketone body beta-hydroxybutyrate (DBHB) (7) and proteins, such as glycosylphosphatidylinositol (GPI)–specific phospholipase D1(Gpld1)(41).

Beta-Hydroxybutyrate (DBHB)

During exercise, the liver releases DBHB into the blood. DBHB crosses the BBB and accumulates in the hippocampus, where it induces *Bdnf* expression by acting as a class I histone deacetylase inhibitor (7). Multiple studies have demonstrated the beneficial effects of ketone bodies and ketogenic diets for brain health. Ketogenic diets rescue neurogenesis defects and prevent memory abnormalities in Kabuki syndrome by inducing transcriptional changes through histone deacetylase (HDAC) inhibition (42). They also extend longevity, improve memory and enhance brain health in aging mice (43, 44). DBHB improves multiple cellular pathologies in Parkinson's disease (PD) [reviewed in (45)] and improves learning and memory formation in a mouse model of Alzheimer's disease (AD) (46). In addition, DBHB has antidepressant effects: it decreases depressive behaviors in mice by increasing histone3-lysine9-β-hydroxybutyrylation and promoting BDNF expression (47). Interestingly, DBHB and ketogenic diets also have promising neuroprotective potential against stroke.

Both DBHB and ketogenic diets promote neuroprotection after stroke. They decrease infarct volume after permanent and transient MCAO (48, 49). DBHB improves cerebral energy metabolism during ischemia and inhibits lipid peroxidation after reperfusion (49). A ketogenic diet improves ischemic tolerance to MCAO and inhibits the nucleotide-binding domain (NOD)-like receptor protein 3 (NLRP3) inflammasome in the brain (50). DBHB also inhibits dynamin-related protein 1 (Drp1)-mediated mitochondrial fission and suppresses endoplasmic reticulum stress-activated NLRP3 inflammasome in oxygen-glucose deprived (OGD) neuroblastoma cells (50). This later pathway is involved in detecting cellular damage and mediating inflammation during ischemic stroke. Combined treatment of DBHB with another ketone body, acetoacetate decreases infarct volume, improves neurologic function, and increases the NAD^+/NADH ratio, Sirtuin 3 (Sirt3), Forkhead Box O3a, and Superoxide Dismutase 2 expression in the penumbra (51). Interestingly, knockdown of Sirt3 in primary neurons attenuates the ability of ketone bodies to promote cell survival in a rotenone-dependent model of neuronal death, suggesting that SIRT3 may mediate the pro-survival effects of ketone bodies (51). More work is needed to fully decipher this pathway and to assess its contribution to neuroprotection *in vivo*.

The hydroxy-carboxylic acid receptor 2 (HCA2) mediates the neuroprotective effect of ketogenic diets and DBHB in cerebral ischemia (52) (**Figure 2**). Indeed, while both ketogenic diets and DBHB significantly decrease infarct size after MCAO, this protective effect is lost in the HCA2 knockout mice despite higher plasma levels of ketone bodies (52). Interestingly, the HCA2 protective effect is mediated by infiltrating macrophages and monocytes, as activation of HCA2 in these cells is neuroprotective (52). This work suggests that the DBHB released from the liver mediates neuroprotection by modulating neuroinflammation. As a result, it is important to understand whether DBHB also activates its receptors in neuronal cells after ischemic stroke to mediate its neuroprotective role. Tissue-specific knockouts of this receptor will help determine whether its roles are restricted to immune cells or whether it plays important signaling effects in neurons. More studies are also needed to determine whether DBHB is responsible for mediating exercise's neuroprotective effects in cerebral ischemia, and to identify the molecular mechanism underlying these neuroprotective effects. Since we already know that exercise increases DBHB levels in the hippocampus where it increases *Bdnf* expression through HDAC inhibition (7) and that DBHB induces resistance to oxidative stress *via* HDAC inhibition (53), it is important to assess whether epigenetic mechanisms are involved in DBHB's neuroprotective effects considering the efficacy of HDAC inhibition as a therapy in mouse models of stroke (54, 55).

Glycosylphosphatidylinositol–Specific Phospholipase D1(Gpld1)

In addition to ketone bodies, exercise induces the liver to release multiple proteins into the blood. A recent study has revealed that exercise increases the levels of a GPI- degrading enzyme,

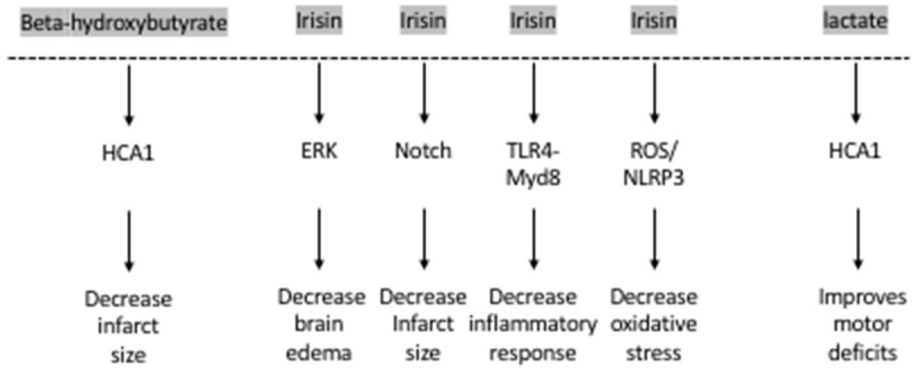

FIGURE 2 | The exercise factors, beta-hydroxybutyrate, irisin and lactate protect against ischemic stroke.

Gpld1, in the blood of mice and of healthy elderly humans (41). Interestingly, unlike other exercise factors discussed in this minireview, liver-derived Gpld1 does not readily enter the brain (41). However, overexpression of Gpld1 in the liver of aged mice increases its levels in the plasma, significantly induces BDNF protein expression in the hippocampus and rescues impaired neurogenesis as well as age-dependent cognitive impairments observed in the radial arm water maze, Y maze and novel object recognition paradigms (41). Coagulation and complement signaling are the major cascades that are altered in response to Gpld1 overexpression and exercise. These cascades were suggested to be involved in mediating Gpld1 and exercise's effects on neurogenesis and cognition (41). Interestingly, previous work has shown that exercise activates platelets and that activated platelets promote neurogenesis by releasing factors such as platelet factor 4 (10). Indeed, platelet depletion abolishes exercise-induced neurogenesis in the hippocampus (10). It would be important to determine whether liver-derived Gpld1 is involved in the exercise-mediated platelet responses. Interestingly, in the context of stroke, Gpld1 was identified as a critical regulator of platelet activity (56). Both pharmacological inhibition and genetic ablation of Gpld1 protected from pathological thrombus formation and ischemic stroke (56, 57). As a result, Glpd1 mediates both positive and negative effects on the brain depending on context. Resolving the contradictory roles played by Gpld1is necessary and can be achieved by studying the role of exercise-induced Gpld1in stroke mouse models. This will help in determining whether this protein is involved in mediating the neuroprotective effects of exercise in stroke or whether its neuroprotective roles are restricted to healthy subjects.

Exercise Factors Released by the Muscle and Their Role in Stroke

In addition to the liver, exercise induces the muscle to release multiple factors that have been shown to play important roles in regulating brain health by regulating BDNF levels. These include proteins such as Cathepsin B, FNDC5, and its cleavage product irisin as well as metabolites such as lactate.

Cathepsin B

Cathepsin B (CTSB), a lysosomal cysteine protease, is released by the muscle during exercise. It mediates the positive effects of exercise on cognition by increasing adult hippocampal neurogenesis and promoting spatial memory formation (58, 59). Indeed, CTSB increases BDNF and doublecortin (DCX) levels in adult hippocampal progenitor cells (58). Exercise also increases CTSB levels in the plasma of humans, where its levels are correlated with hippocampus-dependent memory formation (58). CTSB also controls neurite outgrowth by modulating lysosomal trafficking in neurons (60). In humans, the effects of exercise on plasma CTSB levels are variable with some studies showing that long-term treadmill running increase plasma CTSB levels (58), while others showing no changes in plasma CTSB levels after 6 weeks of HIIE, or a single bout of HIIE in sedentary males (61, 62). Interestingly, studies that focus on the role of muscle-released CTSB in cerebral ischemia are sparse. In contrast, a negative role for brain-derived CTSB in cerebral ischemia has been established. For example, both genetic ablation and pharmacological inhibition of CTSB in mice protect hippocampal neurons from hypoxic/ischemic injury (63) and significantly decrease reactive oxygen species (ROS) production and neuroinflammation (64). CTSB mediates the neurotoxic polarization of microglia/macrophages, worsening hypoxia/ischemia-induced neuronal injury (63). Moreover, CTSB mediates secondary degeneration in the ipsilateral thalamus and substania nigra after focal cortical infarction (65, 66). Based on what is known, CTSB is unlikely to mediate the neuroprotective effects of exercise in stroke patients. However, more work is needed to identify which exercise paradigms consistently induce release of CTSB from the muscle and to determine whether the role of the muscle-released CTSB protein is distinct from the neuronal protein.

Fibronectin Type III Domain-Containing Protein 5 and Its Cleavage Product Irisin

Other myokines such as the Fibronectin type III domain-containing protein 5 (FNDC5) and its secreted cleavage product, irisin, also mediate the positive effects of exercise on the brain by inducing hippocampal *Bdnf* expression (8,

67). Lactate, a metabolite released by the muscle during exercise, crosses the blood-brain barrier and activates the hippocampal PGC1a/FNDC5 pathway (9). Lactate increases the levels and activity of the lysine deacetylase Sirtuin 1(SIRT1). SIRT 1 activates the transcriptional activation complex PGC-1alpha/ERRa, which increases hippocampal *Fndc5* expression. FNDC5, in turn, activates *Bdnf* expression, promoting learning and memory formation (9). Moreover, peripheral delivery of FNDC5 increases blood irisin levels, and also induces hippocampal *Bdnf* expression (8). In addition to mediating exercise's positive effects on cognition, these proteins have been shown to rescue cognitive deficits associated with neurodegenerative diseases such as Alzheimer's disease (68, 69) by inducing BDNF signaling (70) as well as behavioral deficits observed in mouse models of depression (71, 72). Irisin's antidepressant effect also involves modulation of *Bdnf* expression (73).

Interestingly, irisin plays important neuroprotective roles. The levels of irisin in the blood decrease after ischemic stroke in mouse models (74) and in humans (75). Decreased irisin levels were associated with poor prognosis in patients who have suffered from an ischemic stroke (75) (**Figure 2**). Irisin decreases brain edema through the ERK pathway, decreases infarct size through the Notch pathway, decreases oxidative stress through the TLR4/Myd8 pathway and decreases the inflammatory response through the ROS/NLP3 pathway (76). Indeed, irisin is neuroprotective both *in vitro* and *in vivo*. Irisin administration protects against OGD-induced neuronal death *in vitro* (74) in part by inhibiting the ROS-NLRP3 signaling pathway (77). Moreover, irisin protects against damage induced by a cerebral ischemia/reperfusion (I/R) model by modulating the Notch signaling pathway (78). Irisin treatment decreases the infarct size, brain edema and neurological deficits in mice subjected to MCAO (74). This irisin-mediated rescue of brain damage is associated with decreased apoptosis and increased cortical levels of BDNF (79). It is thought that the Akt and ERK1/2 pathways, known to be downstream effectors of BDNF signaling, mediate irisin's neuroprotective effects (74). Interestingly, 3 weeks of high intensity training resulted in increased BDNF in the brain and plasma following MCAO and this increase was dependent on the PGC-1a pathway (80). Based on these observations, both FNDC5 and irisin are likely involved in mediating the neuroprotective effects of exercise against ischemic stroke. More work is needed to establish this direct link by assessing the neuroprotective effects of exercise in *Fndc5* knockout mice.

Lactate

Another exercise factor that is released by the muscle is lactate. It is well-established that lactate is used as an energy substrate by the brain (81) and that neuronal uptake of astrocytic lactate is required for long-term memory formation (82). Indeed, RNA sequencing data reveals that lactate increases the expression of both neuroprotective and synaptic plasticity genes such as *Bdnf*, *Arc*, *c-Fos*, and *Zif268* by inducing NMDA receptor activity and its downstream signaling pathway Erk1/2 in primary neuronal cultures and in cortical tissues (83, 84). We only recently identified lactate as a muscle-released exercise factor that enhances spatial memory by activating the PGC1a/FNDC5/BDNF signaling pathway in the hippocampus (9). Like other exercise factors, lactate promotes brain health and rescues from a variety of central nervous system (CNS) disorders. It enhances neurogenesis by activating the NF-kB signaling pathway following intracerebral hemorrhage (85) and rescues cognitive defects in mice subjected to fluid percussion injury [reviewed in (12)]. It also acts as an antidepressant (13, 86). Interestingly, lactate also has extensive neuroprotective roles.

Lactate mediates neuroprotection against glutamate-mediated excitotoxicity in mouse cortical neurons by engaging a network of cellular pathways involving ATP production, and activation of KATP channels (87). It also promotes resistance to H_2O_2-induced death in neuroblastoma cells by activating the Unfolded Protein Response (UPR) and nuclear factor erythroid 2-related factor 2 (NRF2) (88). In addition, lactate protects against OGD-induced neuronal death in rat organotypic hippocampal slices (89, 90). This pro-survival effect involves increasing the expression of the potassium channel TREK1 by activating the PKA pathway in astrocytes during ischemia (91).

Lactate also enhances neuroplasticity post-stroke. Both intracerebroventricular and systemic injections of lactate directly after reperfusion improve neurologic outcomes 48 h after cerebral ischemia (89, 90). These beneficial effects of lactate appear to be long-lasting. Improved neurological scores in the rotarod test and the beam walking test can still be observed 2 weeks after ischemia in mice subjected to MCAO and receiving intraventricular injections of lactate after reperfusion (89). There is evidence that the HCA1 receptor may mediate lactate's protective effects in neurons of the ischemic cortex after MCAO (92) (**Figure 2**).

Taken together, the data suggest that lactate plays important neuroprotective roles and enhances positive functional outcomes after stroke. Direct evidence that lactate is mediating exercise's protective roles after ischemic stroke remain elusive. Genetic or pharmacological inhibition of the monocarboxylate transporters (MCT2), particularly the MCT2, may aid in understanding whether both lactate and DBHB mediate exercise's neuroprotective effects after cerebral ischemia.

Exercise Factors Released by the Bones and Their Role in Stroke

Osteocalcin

While traditionally regarded as a structural organ, bone has attracted attention in recent years for its endocrine functions. One protein released by osteoblasts in response to endurance exercise in mice and humans is osteocalcin (OCN) (93). A single bout of HIIE in healthy male individuals increased corticospinal excitability, BDNF and uncarboxylated OCN (uncOCN). Indeed, greater increases in BDNF were linked to increases in unOCN and irisin only in the exercising individuals, suggesting that these factors may contribute to exercise-induced BDNF increases (61). Interestingly, OCN delivery was previously shown to be sufficient to improve memory and decrease anxiety-like behaviors in aging mice (94). These positive effects of OCN were mediated by

directly increasing hippocampal BDNF levels through activation of the Gpr158, an orphan G protein-coupled receptor (5).

Recent studies have shown that OCN enhances neuroplasticity by improving outcomes after ischemic stroke (95). Stroke patients who had better outcomes had higher serum osteocalcin levels than those whose National Institutes of Health Stroke Scale (NIHSS) scores did not improve. At the molecular level, metabolic reprogramming and decreased pyroptosis were responsible for the neuroprotective effect of OCN in an OGD model (95). Even though current work has not shown that OCN directly mediates the beneficial effects of exercise in the brain, the available evidence suggests that it may be a candidate exercise factor that is worth assessing in animal models of stroke.

DISCUSSION

Exercise has profound positive effects on the brain including induction of synaptic plasticity, neurogenesis and enhancement of learning and memory formation. The positive effects of exercise are thought to be mediated by multiple exercise factors that induce BDNF signaling. Exercise is also effective in ameliorating the detrimental symptoms of ischemic strokes in animal models and in humans. Even though some of the molecular pathways underlying the neuroprotective effects of exercise are known, it is clear that not all the currently known exercise factors are involved in mediating these effects (**Figure 2**). It is important to conduct a systemic analysis to identify which exercise-induced blood-borne factors, alone or in combination, mediate exercise's neuroprotective effects in cerebral ischemia. Indeed, systematic studies assessing how the frequency, intensity, and duration of the exercise impact its ability to enhance the production of these blood-borne factors are needed. Moreover, it is important to understand how the levels of these factors are modulated when individuals exercise prior or after stroke. These along with experiments designed to assess which exercise factors are responsible for mediating exercise's prophylactic and therapeutic effects in the context of stroke will allow us to develop targeted therapeutic approaches. Metabolites such as DBHB, lactate and proteins such as irisin, initially identified as exercise factors that induce *Bdnf* expression (7–9) and promote learning and memory formation, are the leading candidates of the currently known exercise factors (**Figure 1**).

AUTHOR CONTRIBUTIONS

JS and SS wrote and edited the manuscript. All authors contributed to the article and approved the submitted version.

FUNDING

This work was supported by the Lebanese American University.

REFERENCES

1. Di Carlo A. Human and economic burden of stroke. *Age Ageing*. (2009) 38:4–5. doi: 10.1093/ageing/afn282
2. Rajsic S, Gothe H, Borba HH, Sroczynski G, Vujicic J, Toell T, et al. Economic burden of stroke: a systematic review on post-stroke care. *Eur J Health Econ*. (2019) 20:107–34. doi: 10.1007/s10198-018-0984-0
3. Di Raimondo D, Rizzo G, Musiari G, Tuttolomondo A, Pinto A. Role of regular physical activity in neuroprotection against acute ischemia. *Int J Mol Sci*. (2020) 21:86. doi: 10.3390/ijms21239086
4. Sleiman SF, Chao MV. Downstream consequences of exercise through the action of BDNF. *Brain Plast*. (2015) 1:143–8. doi: 10.3233/BPL-150017
5. Khrimian L, Obri A, Ramos-Brossier M, Rousseaud A, Moriceau S, Nicot AS, et al. Gpr158 mediates osteocalcin's regulation of cognition. *J Exp Med*. (2017) 214:2859–73. doi: 10.1084/jem.20171320
6. Kosmidis S, Polyzos A, Harvey L, Youssef M, Denny CA, Dranovsky A, et al. RbAp48 protein is a critical component of GPR158/OCN signaling and ameliorates age-related memory loss. *Cell Rep*. (2018) 25:959–73.e6. doi: 10.1016/j.celrep.2018.09.077
7. Sleiman SF, Henry J, Al-Haddad R, El Hayek L, Abou Haidar E, Stringer T, et al. Exercise promotes the expression of brain derived neurotrophic factor (BDNF) through the action of the ketone body beta-hydroxybutyrate. *Elife*. (2016) 5:e15092. doi: 10.7554/eLife.15092
8. Wrann CD, White JP, Salogiannnis J, Laznik-Bogoslavski D, Wu J, Ma D, et al. Exercise induces hippocampal BDNF through a PGC-1alpha/FNDC5 pathway. *Cell Metab*. (2013) 18:649–59. doi: 10.1016/j.cmet.2013.09.008
9. El Hayek L, Khalifeh M, Zibara V, Abi Assaad R, Emmanuel N, Karnib N, et al. Lactate mediates the effects of exercise on learning and memory through SIRT1-dependent activation of hippocampal brain-derived neurotrophic factor (BDNF). *J Neurosci*. (2019) 39:2369–82. doi: 10.1523/JNEUROSCI.1661-18.2019
10. Leiter O, Seidemann S, Overall RW, Ramasz B, Rund N, Schallenberg S, et al. Exercise-induced activated platelets increase adult hippocampal precursor proliferation and promote neuronal differentiation. *Stem Cell Rep*. (2019) 12:667–79. doi: 10.1016/j.stemcr.2019.02.009
11. Fujimura H, Altar CA, Chen R, Nakamura T, Nakahashi T, Kambayashi J, et al. Brain-derived neurotrophic factor is stored in human platelets and released by agonist stimulation. *Thromb Haemost*. (2002) 87:728–34. doi: 10.1055/s-0037-1613072
12. Stephan JS, Sleiman SF. Exercise factors as potential mediators of cognitive rehabilitation following traumatic brain injury. *Curr Opin Neurol*. (2019) 32:808–14. doi: 10.1097/WCO.0000000000000754
13. Karnib N, El-Ghandour R, El Hayek L, Nasrallah P, Khalifeh M, Barmo N, et al. Lactate is an antidepressant that mediates resilience to stress by modulating the hippocampal levels and activity of histone deacetylases. *Neuropsychopharmacology*. (2019) 44:1152–62. doi: 10.1038/s41386-019-0313-z
14. Aboutaleb N, Shamsaei N, Khaksari M, Erfani S, Rajabi H, Nikbakht F. Pre-ischemic exercise reduces apoptosis in hippocampal CA3 cells after cerebral ischemia by modulation of the Bax/Bcl-2 proteins ratio and prevention of caspase-3 activation. *J Physiol Sci*. (2015) 65:435–43. doi: 10.1007/s12576-015-0382-7
15. Aboutaleb N, Shamsaei N, Rajabi H, Khaksari M, Erfani S, Nikbakht F, et al. Protection of hippocampal CA1 neurons against ischemia/reperfusion injury by exercise preconditioning *via* modulation of Bax/Bcl-2 ratio and prevention of caspase-3 activation. *Basic Clin Neurosci*. (2016) 7:21–9.
16. Arrick DM, Yang S, Li C, Cananzi S, Mayhan WG. Vigorous exercise training improves reactivity of cerebral arterioles and reduces brain injury following transient focal ischemia. *Microcirculation*. (2014) 21:516–23. doi: 10.1111/micc.12127
17. Chaudhry K, Rogers R, Guo M, Lai Q, Goel G, Liebelt B, et al. Matrix metalloproteinase-9 (MMP-9) expression and extracellular signal-regulated kinase 1 and 2 (ERK1/2) activation in exercise-reduced neuronal apoptosis after stroke. *Neurosci Lett*. (2010) 474:109–14. doi: 10.1016/j.neulet.2010.03.020

18. Davis W, Mahale S, Carranza A, Cox B, Hayes K, Jimenez D, et al. Exercise pre-conditioning ameliorates blood-brain barrier dysfunction in stroke by enhancing basal lamina. *Neurol Res*. (2007) 29:382–7. doi: 10.1179/016164107X204701
19. Deplanque D, Masse I, Libersa C, Leys D, Bordet R. Previous leisure-time physical activity dose dependently decreases ischemic stroke severity. *Stroke Res Treat*. (2012) 2012:614925. doi: 10.1155/2012/614925
20. Islam MR, Young MF, Wrann CD. Neuroprotective potential of exercise preconditioning in stroke. *Cond Med*. (2017) 1:27–34.
21. Mattson MP. Energy intake and exercise as determinants of brain health and vulnerability to injury and disease. *Cell Metab*. (2012) 16:706–22. doi: 10.1016/j.cmet.2012.08.012
22. Oberlin LE, Waiwood AM, Cumming TB, Marsland AL, Bernhardt J, Erickson KI. Effects of physical activity on poststroke cognitive function: a meta-analysis of randomized controlled trials. *Stroke*. (2017) 48:3093–100. doi: 10.1161/STROKEAHA.117.017319
23. Shamsaei N, Erfani S, Fereidoni M, Shahbazi A. Neuroprotective effects of exercise on brain edema and neurological movement disorders following the cerebral ischemia and reperfusion in rats. *Basic Clin Neurosci*. (2017) 8:77–84. doi: 10.15412/J.BCN.03080110
24. Gao Y, Zhao Y, Pan J, Yang L, Huang T, Feng X, et al. Treadmill exercise promotes angiogenesis in the ischemic penumbra of rat brains through caveolin-1/VEGF signaling pathways. *Brain Res*. (2014) 1585:83–90. doi: 10.1016/j.brainres.2014.08.032
25. Otsuka S, Sakakima H, Sumizono M, Takada S, Terashi T, Yoshida Y. The neuroprotective effects of preconditioning exercise on brain damage and neurotrophic factors after focal brain ischemia in rats. *Behav Brain Res*. (2016) 303:9–18. doi: 10.1016/j.bbr.2016.01.049
26. Pianta S, Lee JY, Tuazon JP, Castelli V, Mantohac LM, Tajiri N, et al. A short bout of exercise prior to stroke improves functional outcomes by enhancing angiogenesis. *Neuromolecular Med*. (2019) 21:517–28. doi: 10.1007/s12017-019-08533-x
27. Tang Y, Zhang Y, Zheng M, Chen J, Chen H, Liu N. Effects of treadmill exercise on cerebral angiogenesis and MT1-MMP expression after cerebral ischemia in rats. *Brain Behav*. (2018) 8:e01079. doi: 10.1002/brb3.1079
28. Rezaei R, Nasoohi S, Haghparast A, Khodagholi F, Bigdeli MR, Nourshahi M. High intensity exercise preconditioning provides differential protection against brain injury following experimental stroke. *Life Sci*. (2018) 207:30–5. doi: 10.1016/j.lfs.2018.03.007
29. Wang J, Liu H, Chen S, Zhang W, Chen Y, Yang Y. Moderate exercise has beneficial effects on mouse ischemic stroke by enhancing the functions of circulating endothelial progenitor cell-derived exosomes. *Exp Neurol*. (2020) 330:113325. doi: 10.1016/j.expneurol.2020.113325
30. Zhang L, Yang X, Yin M, Yang H, Li L, Parashos A, et al. An animal trial on the optimal time and intensity of exercise after stroke. *Med Sci Sports Exerc*. (2020) 52:1699–709. doi: 10.1249/MSS.0000000000002318
31. Hong M, Kim M, Kim TW, Park SS, Kim MK, Park YH, et al. Treadmill exercise improves motor function and short-term memory by enhancing synaptic plasticity and neurogenesis in photothrombotic stroke mice. *Int Neurourol J*. (2020) 24(Suppl. 1):S28–38. doi: 10.5213/inj.2040158.079
32. Cheng J, Shen W, Jin L, Pan J, Zhou Y, Pan G, et al. Treadmill exercise promotes neurogenesis and myelin repair *via* upregulating Wnt/betacatenin signaling pathways in the juvenile brain following focal cerebral ischemia/reperfusion. *Int J Mol Med*. (2020) 45:1447–63. doi: 10.3892/ijmm.2020.4515
33. Ciancarelli I, De Amicis D, Di Massimo C, Carolei A, Ciancarelli MG. Oxidative stress in post-acute ischemic stroke patients after intensive neurorehabilitation. *Curr Neurovasc Res*. (2012) 9:266–73. doi: 10.2174/156720212803530717
34. Li F, Geng X, Huber C, Stone C, Ding Y. In search of a dose: the functional and molecular effects of exercise on post-stroke rehabilitation in rats. *Front Cell Neurosci*. (2020) 14:186. doi: 10.3389/fncel.2020.00186
35. Li F, Pendy JT, Jr., Ding JN, Peng C, Li X, Shen J, et al. Exercise rehabilitation immediately following ischemic stroke exacerbates inflammatory injury. *Neurol Res*. (2017) 39:530–7. doi: 10.1080/01616412.2017.1315882
36. Ma Y, He M, Qiang L. Exercise therapy downregulates the overexpression of TLR4, TLR2, MyD88 and NF-kappaB after cerebral ischemia in rats. *Int J Mol Sci*. (2013) 14:3718–33. doi: 10.3390/ijms14023718
37. Zhang Q, Wu Y, Zhang P, Sha H, Jia J, Hu Y, et al. Exercise induces mitochondrial biogenesis after brain ischemia in rats. *Neuroscience*. (2012) 205:10–7. doi: 10.1016/j.neuroscience.2011.12.053
38. El-Tamawy MS, Abd-Allah F, Ahmed SM, Darwish MH, Khalifa HA. Aerobic exercises enhance cognitive functions and brain derived neurotrophic factor in ischemic stroke patients. *NeuroRehabilitation*. (2014) 34:209–13. doi: 10.3233/NRE-131020
39. Stanne TM, Aberg ND, Nilsson S, Jood K, Blomstrand C, Andreasson U, et al. Low circulating acute brain-derived neurotrophic factor levels are associated with poor long-term functional outcome after ischemic stroke. *Stroke*. (2016) 47:1943–5. doi: 10.1161/STROKEAHA.115.012383
40. Kotlega D, Peda B, Zembron-Lacny A, Golab-Janowska M, Nowacki P. The role of brain-derived neurotrophic factor and its single nucleotide polymorphisms in stroke patients. *Neurol Neurochir Pol*. (2017) 51:240–6. doi: 10.1016/j.pjnns.2017.02.008
41. Horowitz AM, Fan X, Bieri G, Smith LK, Sanchez-Diaz CI, Schroer AB, et al. Blood factors transfer beneficial effects of exercise on neurogenesis and cognition to the aged brain. *Science*. (2020) 369:167–73. doi: 10.1126/science.aaw2622
42. Benjamin JS, Pilarowski GO, Carosso GA, Zhang L, Huso DL, Goff LA, et al. A ketogenic diet rescues hippocampal memory defects in a mouse model of Kabuki syndrome. *Proc Natl Acad Sci USA*. (2017) 114:125–30. doi: 10.1073/pnas.1611431114
43. Newman JC, Covarrubias AJ, Zhao M, Yu X, Gut P, Ng CP, et al. Ketogenic diet reduces midlife mortality and improves memory in aging mice. *Cell Metab*. (2017) 26:547–57.e8. doi: 10.1016/j.cmet.2017.08.004
44. Roberts MN, Wallace MA, Tomilov AA, Zhou Z, Marcotte GR, Tran D, et al. A ketogenic diet extends longevity and healthspan in adult mice. *Cell Metab*. (2018) 27:1156. doi: 10.1016/j.cmet.2018.04.005
45. Norwitz NG, Hu MT, Clarke K. The mechanisms by which the ketone body D-beta-hydroxybutyrate may improve the multiple cellular pathologies of Parkinson's disease. *Front Nutr*. (2019) 6:63. doi: 10.3389/fnut.2019.00063
46. Yin JX, Maalouf M, Han P, Zhao M, Gao M, Dharshaun T, et al. Ketones block amyloid entry and improve cognition in an Alzheimer's model. *Neurobiol Aging*. (2016) 39:25–37. doi: 10.1016/j.neurobiolaging.2015.11.018
47. Chen L, Miao Z, Xu X. beta-hydroxybutyrate alleviates depressive behaviors in mice possibly by increasing the histone3-lysine9-beta-hydroxybutyrylation. *Biochem Biophys Res Commun*. (2017) 490:117–22. doi: 10.1016/j.bbrc.2017.05.184
48. Puchowicz MA, Zechel JL, Valerio J, Emancipator DS, Xu K, Pundik S, et al. Neuroprotection in diet-induced ketotic rat brain after focal ischemia. *J Cereb Blood Flow Metab*. (2008) 28:1907–16. doi: 10.1038/jcbfm.2008.79
49. Suzuki M, Suzuki M, Kitamura Y, Mori S, Sato K, Dohi S, et al. Beta-hydroxybutyrate, a cerebral function improving agent, protects rat brain against ischemic damage caused by permanent and transient focal cerebral ischemia. *Jpn J Pharmacol*. (2002) 89:36–43. doi: 10.1254/jjp.89.36
50. Guo M, Wang X, Zhao Y, Yang Q, Ding H, Dong Q, et al. Ketogenic diet improves brain ischemic tolerance and inhibits NLRP3 inflammasome activation by preventing Drp1-mediated mitochondrial fission and endoplasmic reticulum stress. *Front Mol Neurosci*. (2018) 11:86. doi: 10.3389/fnmol.2018.00086
51. Yin J, Han P, Tang Z, Liu Q, Shi J. Sirtuin 3 mediates neuroprotection of ketones against ischemic stroke. *J Cereb Blood Flow Metab*. (2015) 35:1783–9. doi: 10.1038/jcbfm.2015.123
52. Rahman M, Muhammad S, Khan MA, Chen H, Ridder DA, Muller-Fielitz H, et al. The beta-hydroxybutyrate receptor HCA2 activates a neuroprotective subset of macrophages. *Nat Commun*. (2014) 5:3944. doi: 10.1038/ncomms4944
53. Shimazu T, Hirschey MD, Newman J, He W, Shirakawa K, Le Moan N, et al. Suppression of oxidative stress by beta-hydroxybutyrate, an endogenous histone deacetylase inhibitor. *Science*. (2013) 339:211–4. doi: 10.1126/science.1227166
54. Langley B, Brochier C, Rivieccio MA. Targeting histone deacetylases as a multifaceted approach to treat the diverse outcomes of stroke. *Stroke*. (2009) 40:2899–905. doi: 10.1161/STROKEAHA.108.540229
55. Langley B, D'Annibale MA, Suh K, Ayoub I, Tolhurst A, Bastan B, et al. Pulse inhibition of histone deacetylases induces complete resistance to oxidative death in cortical neurons without toxicity and reveals a role for cytoplasmic

p21(waf1/cip1) in cell cycle-independent neuroprotection. *J Neurosci*. (2008) 28:163–76. doi: 10.1523/JNEUROSCI.3200-07.2008
56. Elvers M, Stegner D, Hagedorn I, Kleinschnitz C, Braun A, Kuijpers ME, et al. Impaired alpha(IIb)beta(3) integrin activation and shear-dependent thrombus formation in mice lacking phospholipase D1. *Sci Signal*. (2010) 3:ra1. doi: 10.1126/scisignal.2000551
57. Stegner D, Thielmann I, Kraft P, Frohman MA, Stoll G, Nieswandt B. Pharmacological inhibition of phospholipase D protects mice from occlusive thrombus formation and ischemic stroke–brief report. *Arterioscler Thromb Vasc Biol*. (2013) 33:2212–7. doi: 10.1161/ATVBAHA.113.302030
58. Moon HY, Becke A, Berron D, Becker B, Sah N, Benoni G, et al. Running-induced systemic cathepsin B secretion is associated with memory function. *Cell Metab*. (2016) 24:332–40. doi: 10.1016/j.cmet.2016.05.025
59. van Praag H, Christie BR, Sejnowski TJ, Gage FH. Running enhances neurogenesis, learning, and long-term potentiation in mice. *Proc Natl Acad Sci USA*. (1999) 96:13427–31. doi: 10.1073/pnas.96.23.13427
60. Jiang M, Meng J, Zeng F, Qing H, Hook G, Hook V, et al. Cathepsin B inhibition blocks neurite outgrowth in cultured neurons by regulating lysosomal trafficking and remodeling. *J Neurochem*. (2020) 155:300–12. doi: 10.1111/jnc.15032
61. Nicolini C, Michalski B, Toepp SL, Turco CV, D'Hoine T, Harasym D, et al. A Single bout of high-intensity interval exercise increases corticospinal excitability, brain-derived neurotrophic factor, and uncarboxylated osteolcalcin in sedentary, healthy males. *Neuroscience*. (2020) 437:242–55. doi: 10.1016/j.neuroscience.2020.03.042
62. Nicolini C, Toepp S, Harasym D, Michalski B, Fahnestock M, Gibala MJ, et al. No changes in corticospinal excitability, biochemical markers, and working memory after six weeks of high-intensity interval training in sedentary males. *Physiol Rep*. (2019) 7:e14140. doi: 10.14814/phy2.14140
63. Ni J, Wu Z, Peterts C, Yamamoto K, Qing H, Nakanishi H. The critical role of proteolytic relay through cathepsins B and E in the phenotypic change of microglia/macrophage. *J Neurosci*. (2015) 35:12488–501. doi: 10.1523/JNEUROSCI.1599-15.2015
64. Ni J, Wu Z, Stoka V, Meng J, Hayashi Y, Peters C, et al. Increased expression and altered subcellular distribution of cathepsin B in microglia induce cognitive impairment through oxidative stress and inflammatory response in mice. *Aging Cell*. (2019) 18:e12856. doi: 10.1111/acel.12856
65. Zuo X, Hou Q, Jin J, Chen X, Zhan L, Tang Y, et al. Inhibition of cathepsins B induces neuroprotection against secondary degeneration in ipsilateral substantia nigra after focal cortical infarction in adult male rats. *Front Aging Neurosci*. (2018) 10:125. doi: 10.3389/fnagi.2018.00125
66. Zuo X, Hou Q, Jin J, Zhan L, Li X, Sun W, et al. Inhibition of cathepsin B alleviates secondary degeneration in ipsilateral thalamus after focal cerebral infarction in adult rats. *J Neuropathol Exp Neurol*. (2016) 75:816–26. doi: 10.1093/jnen/nlw054
67. Belviranli M, Okudan N. Exercise training protects against aging-induced cognitive dysfunction *via* activation of the hippocampal PGC-1alpha/FNDC5/BDNF pathway. *Neuromolecular Med*. (2018) 20:386–400. doi: 10.1007/s12017-018-8500-3
68. Chen X, Gan L. An exercise-induced messenger boosts memory in Alzheimer's disease. *Nat Med*. (2019) 25:20–1. doi: 10.1038/s41591-018-0311-4
69. Lourenco MV, Frozza RL, de Freitas GB, Zhang H, Kincheski GC, Ribeiro FC, et al. Exercise-linked FNDC5/irisin rescues synaptic plasticity and memory defects in Alzheimer's models. *Nat Med*. (2019) 25:165–75. doi: 10.1038/s41591-018-0275-4
70. Xia DY, Huang X, Bi CF, Mao LL, Peng LJ, Qian HR. PGC-1alpha or FNDC5 is involved in modulating the effects of abeta1-42 oligomers on suppressing the expression of BDNF, a beneficial factor for inhibiting neuronal apoptosis, abeta deposition and cognitive decline of APP/PS1 Tg mice. *Front Aging Neurosci*. (2017) 9:65. doi: 10.3389/fnagi.2017.00065
71. Uysal N, Yuksel O, Kizildag S, Yuce Z, Gumus H, Karakilic A, et al. Regular aerobic exercise correlates with reduced anxiety and incresed levels of irisin in brain and white adipose tissue. *Neurosci Lett*. (2018) 676:92–7. doi: 10.1016/j.neulet.2018.04.023
72. Wang S, Pan J. Irisin ameliorates depressive-like behaviors in rats by regulating energy metabolism. *Biochem Biophys Res Commun*. (2016) 474:22–8. doi: 10.1016/j.bbrc.2016.04.047
73. Siteneski A, Cunha MP, Lieberknecht V, Pazini FL, Gruhn K, Brocardo PS, et al. Central irisin administration affords antidepressant-like effect and modulates neuroplasticity-related genes in the hippocampus and prefrontal cortex of mice. *Prog Neuropsychopharmacol Biol Psychiatry*. (2018) 84:294–303. doi: 10.1016/j.pnpbp.2018.03.004
74. Li DJ, Li YH, Yuan HB, Qu LF, Wang P. The novel exercise-induced hormone irisin protects against neuronal injury *via* activation of the Akt and ERK1/2 signaling pathways and contributes to the neuroprotection of physical exercise in cerebral ischemia. *Metabolism*. (2017) 68:31–42. doi: 10.1016/j.metabol.2016.12.003
75. Tu WJ, Qiu HC, Cao JL, Liu Q, Zeng XW, Zhao JZ. Decreased concentration of irisin is associated with poor functional outcome in ischemic stroke. *Neurotherapeutics*. (2018) 15:1158–67. doi: 10.1007/s13311-018-0651-2
76. Liu Y, Zhu C, Guo J, Chen Y, Meng C. The neuroprotective effect of irisin in ischemic stroke. *Front Aging Neurosci*. (2020) 12:588958. doi: 10.3389/fnagi.2020.588958
77. Peng J, Deng X, Huang W, Yu JH, Wang JX, Wang JP, et al. Irisin protects against neuronal injury induced by oxygen-glucose deprivation in part depends on the inhibition of ROS-NLRP3 inflammatory signaling pathway. *Mol Immunol*. (2017) 91:185–94. doi: 10.1016/j.molimm.2017.09.014
78. Jin Z, Guo P, Li X, Ke J, Wang Y, Wu H. Neuroprotective effects of irisin against cerebral ischemia/ reperfusion injury *via* Notch signaling pathway. *Biomed Pharmacother*. (2019) 120:109452. doi: 10.1016/j.biopha.2019.109452
79. Asadi Y, Gorjipour F, Behrouzifar S, Vakili A. Irisin peptide protects brain against ischemic injury through reducing apoptosis and enhancing BDNF in a rodent model of stroke. *Neurochem Res*. (2018) 43:1549–60. doi: 10.1007/s11064-018-2569-9
80. Abbasian S, Asghar Ravasi A. The effect of antecedent-conditioning high-intensity interval training on BDNF regulation through PGC-1alpha pathway following cerebral ischemia. *Brain Res*. (2020) 1729:146618. doi: 10.1016/j.brainres.2019.146618
81. Wyss MT, Jolivet R, Buck A, Magistretti PJ, Weber B. *In vivo* evidence for lactate as a neuronal energy source. *J Neurosci*. (2011) 31:7477–85. doi: 10.1523/JNEUROSCI.0415-11.2011
82. Suzuki A, Stern SA, Bozdagi O, Huntley GW, Walker RH, Magistretti PJ, et al. Astrocyte-neuron lactate transport is required for long-term memory formation. *Cell*. (2011) 144:810–23. doi: 10.1016/j.cell.2011.02.018
83. Margineanu MB, Mahmood H, Fiumelli H, Magistretti PJ. L-lactate regulates the expression of synaptic plasticity and neuroprotection genes in cortical neurons: a transcriptome analysis. *Front Mol Neurosci*. (2018) 11:375. doi: 10.3389/fnmol.2018.00375
84. Yang J, Ruchti E, Petit JM, Jourdain P, Grenningloh G, Allaman I, et al. Lactate promotes plasticity gene expression by potentiating NMDA signaling in neurons. *Proc Natl Acad Sci USA*. (2014) 111:12228–33. doi: 10.1073/pnas.1322912111
85. Zhou J, Liu T, Guo H, Cui H, Li P, Feng D, et al. Lactate potentiates angiogenesis and neurogenesis in experimental intracerebral hemorrhage. *Exp Mol Med*. (2018) 50:1–12. doi: 10.1038/s12276-018-0113-2
86. Carrard A, Elsayed M, Margineanu M, Boury-Jamot B, Fragniere L, Meylan EM, et al. Peripheral administration of lactate produces antidepressant-like effects. *Mol Psychiatry*. (2018) 23:488. doi: 10.1038/mp.2016.237
87. Jourdain P, Allaman I, Rothenfusser K, Fiumelli H, Marquet P, Magistretti PJ. L-Lactate protects neurons against excitotoxicity: implication of an ATP-mediated signaling cascade. *Sci Rep*. (2016) 6:21250. doi: 10.1038/srep21250
88. Tauffenberger A, Fiumelli H, Almustafa S, Magistretti PJ. Lactate and pyruvate promote oxidative stress resistance through hormetic ROS signaling. *Cell Death Dis*. (2019) 10:653. doi: 10.1038/s41419-019-1877-6
89. Berthet C, Castillo X, Magistretti PJ, Hirt L. New evidence of neuroprotection by lactate after transient focal cerebral ischaemia: extended benefit after intracerebroventricular injection and efficacy of intravenous administration. *Cerebrovasc Dis*. (2012) 34:329–35. doi: 10.1159/000343657
90. Berthet C, Lei H, Thevenet J, Gruetter R, Magistretti PJ, Hirt L. Neuroprotective role of lactate after cerebral ischemia. *J Cereb Blood Flow Metab*. (2009) 29:1780–9. doi: 10.1038/jcbfm.2009.97

91. Banerjee A, Ghatak S, Sikdar SK. l-Lactate mediates neuroprotection against ischaemia by increasing TREK1 channel expression in rat hippocampal astrocytes *in vitro*. *J Neurochem*. (2016) 138:265–81. doi: 10.1111/jnc.13638
92. Castillo X, Rosafio K, Wyss MT, Drandarov K, Buck A, Pellerin L, et al. A probable dual mode of action for both L- and D-lactate neuroprotection in cerebral ischemia. *J Cereb Blood Flow Metab*. (2015) 35:1561–9. doi: 10.1038/jcbfm.2015.115
93. Mera P, Laue K, Ferron M, Confavreux C, Wei J, Galan-Diez M, et al. Osteocalcin signaling in myofibers is necessary and sufficient for optimum adaptation to exercise. *Cell Metab*. (2016) 23:1078–92. doi: 10.1016/j.cmet.2016.05.004
94. Oury F, Khrimian L, Denny CA, Gardin A, Chamouni A, Goeden N, et al. Maternal and offspring pools of osteocalcin influence brain development and functions. *Cell*. (2013) 155:228–41. doi: 10.1016/j.cell.2013.08.042
95. Wu J, Dou Y, Liu W, Zhao Y, Liu X. Osteocalcin improves outcome after acute ischemic stroke. *Aging (Albany NY)*. (2020) 12:387–96. doi: 10.18632/aging.102629

Conflict of Interest: The authors declare that the research was conducted in the absence of any commercial or financial relationships that could be construed as a potential conflict of interest.

frontiers in Neurology

ORIGINAL RESEARCH
published: 17 June 2021
doi: 10.3389/fneur.2021.668877

Genetic Deletion of mGlu3 Metabotropic Glutamate Receptors Amplifies Ischemic Brain Damage and Associated Neuroinflammation in Mice

*Federica Mastroiacovo[1], Manuela Zinni[2], Giada Mascio[1], Valeria Bruno[1,3], Giuseppe Battaglia[1,3], Julien Pansiot[2], Tiziana Imbriglio[1], Jerome Mairesse[2,4], Olivier Baud[2,4,5] and Ferdinando Nicoletti[1,3]**

[1] Department of Molecular Pathology, I.R.C.C.S. Neuromed, Pozzilli, Italy, [2] Inserm UMR1141 NeuroDiderot, University of Paris Diderot, Sorbonne Paris Cité, Paris, France, [3] Department of Physiology and Pharmacology, Sapienza University of Rome, Rome, Italy, [4] Laboratory of Child Growth and Development, University of Geneva, Geneva, Switzerland, [5] Division of Neonatology and Pediatric Intensive Care, Children's University Hospital of Geneva, Geneva, Switzerland

OPEN ACCESS

Edited by:
Thiruma Valavan Arumugam, La Trobe University, Australia

Reviewed by:
Bhakta Prasad Gaire, University of Maryland, Baltimore, United States
Mika Takarada-Iemata, Kanazawa University, Japan

***Correspondence:**
Ferdinando Nicoletti
nicoletti@neuromed.it

Specialty section:
This article was submitted to Stroke, a section of the journal Frontiers in Neurology

Received: 18 February 2021
Accepted: 29 April 2021
Published: 17 June 2021

Citation:
Mastroiacovo F, Zinni M, Mascio G, Bruno V, Battaglia G, Pansiot J, Imbriglio T, Mairesse J, Baud O and Nicoletti F (2021) Genetic Deletion of mGlu3 Metabotropic Glutamate Receptors Amplifies Ischemic Brain Damage and Associated Neuroinflammation in Mice. Front. Neurol. 12:668877. doi: 10.3389/fneur.2021.668877

Backgroud: Type-3 metabotropic glutamate (mGlu3) receptors are found in both neurons and glial cells and regulate synaptic transmission, astrocyte function, and microglial reactivity. Here we show that the genetic deletion of mGlu3 receptors amplifies ischemic brain damage and associated neuroinflammation in adult mice. An increased infarct size was observed in mGlu3$^{-/-}$ mice of both CD1 and C57Black strains 24 h following a permanent occlusion of the middle cerebral artery (MCA) as compared to their respective wild-type (mGlu3$^{+/+}$ mice) counterparts. Increases in the expression of selected pro-inflammatory genes including those encoding interleukin-1β, type-2 cycloxygenase, tumor necrosis factor-α, CD86, and interleukin-6 were more prominent in the peri-infarct region of mGlu3$^{-/-}$ mice. In contrast, the expression of two genes associated with the anti-inflammatory phenotype of microglia (those encoding the mannose-1-phosphate receptor and the α-subunit of interleukin-4 receptor) and the gene encoding the neuroprotective factor, glial cell line-derived neurotrophic factor, was enhanced in the peri-infarct region of wild-type mice, but not mGlu3$^{-/-}$ mice, following MCA occlusion. In C57Black mice, the genetic deletion of mGlu3 receptors worsened the defect in the paw placement test as assessed in the contralateral forepaw at short times (4 h) following MCA occlusion. These findings suggest that mGlu3 receptors are protective against ischemic brain damage and support the way to the use of selective mGlu3 receptor agonists or positive allosteric modulators in experimental animal models of ischemic stroke.

Keywords: focal ischemia, knockout mice, neuroinflammation, pro-inflammatory genes, mGlu3 receptors

INTRODUCTION

Ischemic stroke is the second cause of mortality and disability worldwide due to the lack of effective therapies besides intravenous thrombolysis, which is restricted to selected patients and useful only in a short therapeutic window. Understanding the mechanisms underlying neuronal vulnerability to ischemic damage may pave the way to novel therapeutic strategies in cerebrovascular disorders. In the area close to the occluded vessel, two distinct zones can be distinguished: the core (a zone of severe ischemia and neuronal death) and the penumbra (a zone of moderate ischemia) (1). Up to few hours following the vessel occlusion, the size of both areas is almost equivalent (2); however, as the ischemic injury progresses, the penumbra becomes the main affected area (3), in which the neurons are still salvageable with appropriate interventions. Excitotoxicity, oxidative stress, neuroinflammation, mitochondrial damage, and lack of neuroprotective factors are the established mechanisms of ischemic neuronal damage (4–8). These mechanisms are shaped by metabotropic glutamate (mGlu) receptors, which are G-protein coupled receptors activated by glutamate.

mGlu receptors form a family of eight subtypes, subdivided into three groups on the basis of their primary sequence homology and transduction mechanisms. Group I comprises mGlu1 and mGlu5 receptors, which are coupled to $G_{q/11}$ proteins. Their activation leads to phosphatidylinositol-4,5-bisphosphate hydrolysis, with ensuing formation of inositol-1,4-5-trisphosphate and diacylglycerol. Group II (mGlu2 and mGlu3) and group III (mGlu4, -6, -7, and -8) receptors are coupled to $G_{i/o}$ proteins in heterologous expression systems (9). Most of these subtypes are found in neurons, astrocytes, and microglia and regulate many features of the tetrapartite synapse formed by presynaptic terminals, postsynaptic elements, and surrounding astrocytes and microglia.

Early studies of mGlu2 and mGlu3 receptors (10, 11) did not differentiate between the two subtypes because of the lack of selectivity of orthosteric agonists and the belief that the function of the two receptors was similar. Using both genetic and subtype-selective pharmacological tools, it is now clear that mGlu2 and mGlu3 receptors are functionally different and may have an opposite impact on the mechanisms of neurodegeneration/neuroprotection. While both subtypes are presynaptically localized and negatively modulate neurotransmitter release, mGlu3 receptors are also found in post-synaptic elements, and their activation boosts mGlu5 receptor signaling (12, 13). In addition, activation of mGlu2 receptors drives microglial cells toward a pro-inflammatory/neurotoxic phenotype (14, 15), whereas activation of mGlu3 receptors induces an anti-inflammatory phenotype (16). In addition, mGlu3 receptors (but not mGlu2 receptors) are present in astrocytes, and their activation stimulates the production of neurotrophic factors (17, 18). Using the four-vessel occlusion model of transient global ischemia in rats, we have shown that selective pharmacological activation of mGlu2 receptors amplified hippocampal damage, whereas mGlu2 receptor blockade was neuroprotective (19). Similar findings were obtained using mice lacking mGlu2 receptors, in which the infarct size was enhanced in response to transient focal ischemia (20). To our knowledge, there are no studies on mGlu3 receptors and brain ischemia, although the selective activation of mGlu3 receptors was shown to be neuroprotective in *in vitro* studies (17, 21–24).

Here we used two different strains of mice to examine whether the genetic deletion of mGlu3 receptors affects brain damage and associated neuroinflammation induced by the permanent occlusion of the middle cerebral artery (MCA).

MATERIALS AND METHODS

Animals

Wild-type mice ($mGlu3^{+/+}$) or $mGlu3^{-/-}$ mice on C57Black genetic background (22) and wild-type mice ($mGlu3^{+/+}$) or $mGlu3^{-/-}$ mice on CD1 genetic background (25) were generated by homozygous breeding (in-house production). Adult male mice weighing 25 g were housed under controlled conditions (ambient temperature, 22°C; humidity, 40%) on a 12-h light–dark cycle with food and water *ad libitum*. Studies were performed in agreement with the national and international guidelines and regulations on animal care and use and were approved by the Neuromed Institutional Animal Care and Use Committee and by the Italian Ministry of Health. All efforts were made to minimize animal suffering and to reduce the number of animals used.

Permanent Focal Ischemia in Mice

Permanent focal cerebral ischemia was induced by distal electrocauterization of the MCA (26–28). The mice were anesthetized with chloral hydrate (400 mg/kg, i.p.), and an incision was made between the outer canthus of the eye and the external auditory meatus. The temporal muscle was bisected to expose the skull, and the MCA was exposed by means of burr-hole craniotomy carried out by using a surgical drill. A thin layer of bone was preserved to protect the dura mater and the cortical surface against mechanical damage and thermal injury, while the remaining bone was gently removed. The MCA was occluded by electrocoagulation, and the muscle and then the skin incision were sutured. A rectal temperature probe connected to a heating pad was used to maintain body temperature at 37°C throughout the surgical period. After surgery, the mice did not receive anti-inflammatory drugs or antibiotics, were placed in an incubator (compact incubator, Thermo Scientific, AHSI, Bernaggio, MI, Italy) at 37°C for 2, and then placed back into their home cages. The functional deficit was assessed with the paw placement test before ischemia and after 4 and 24 h by an operator who was unaware of the genotype. The animals were killed 24 h after ischemia, and their brains were processed for histological or mRNA analysis.

Paw Placement Test

Paw placement test provides information on the tactile/proprioceptive response to limb stimulation. The animals were placed with all paws on a surface in horizontal position, and the head was held at 45° angle so that visual stimulation was prevented. The paws to be tested were pushed

along the edge in order to lose contact with the table surface. The ability of the animals to place the limb back onto the table surface when the mice was moved toward the edge was evaluated. A score was used as follows: 1—prompt placement of the limb onto the table, 0.5—incomplete or delayed placing of the limb; and 0—no placing with the extension of the limb and paw (29).

Histology

The mice were sacrificed 24 h after MCA occlusion, and the brains were fixed in Carnoy's solution, embedded in paraffin, and sectioned at 10 μm. The sections were deparaffinized and processed for staining with thionin (Nissl staining) for histological assessment of neuronal degeneration. The analysis was carried out on sections regularly spaced every 550 μm through the extension of the ischemic region. This space interval corresponds to a standardized procedure, allowing one to measure the ischemic brain volume based on 10 slides. The infarct area was outlined at a magnification of ×2.5, and it was quantified using Scion Image software (NIH, Bethesda, MD, USA). Then, the volume was calculated by integrating the cross-sectional area of damage on each stained section and the distance between them (20, 30).

Immunohistochemistry

Brain sections were deparaffinized, after antigen retrieval, in citrate buffer (10 mM sodium citrate, pH 6.0) for 30 min. The sections were pretreated with 0.3% H_2O_2 for 10 min to block endogenous peroxide activity after incubation with 6% normal serum and 0.1% Triton-X100 in PBS for 2 h. The sections were incubated with the following primary antibodies: anti-Cox2 (1:200, Abcam, Cambridge, UK) or anti-Iba1 (1:1,000, Wako Chemicals, Osaka, Japan). The samples were rinsed and incubated for 2 h at room temperature with secondary biotinylated anti-rabbit horse antibodies (1:200, Vector Laboratories, Burlingame, CA) followed by streptavidin alexa fluor 488 (1:200, Molecular Probes, Carlsbad, CA). Finally, the samples were mounted with Hard Set Vectashield with Dapi (Vector Laboratories, Burlingame, CA). Iba1 immunostaining was detected with a Zeiss 780 confocal laser scanning microscope. Cox-2 immunostaining was detected with a Zeiss Axio-photo 2 optic microscope. Cell counting was performed in three coronal sections for mouse at ×20 magnification.

RNA Purification, cDNA Synthesis, and Real-Time qPCR

The mice were killed 24 h after MCA occlusion, and the brains were quickly removed. The brains were cut with a matrix, and a 3-mm region along the rostro-caudal axis from 1.54 mm anterior to 1.58 mm posterior to the bregma was sliced. Each slice was further punched to dissect a square region (1 × 1.3 mm) corresponding to the ischemic core, the dorsomedial portion of the peri-infarct region or the corresponding region of the contralateral side (highlighted in **Figures 2A**, **4A**). The samples were immediately frozen on liquid nitrogen and stored at −80°C. Total RNA was extracted using Nucleazol reagent and the NucleoSpin RNA Set for NucleoZol (Macherey-Nagel, Hoerdt, France) according to the manufacturer's instruction. RNA quantity and quality were determined using the NanodropTM apparatus (Thermofisher Scientific, Walthman, MA), and 0.5 μg of total RNA was used to perform a reverse transcription (IscriptTM cDNA synthesis kit, Bio-Rad, Marnes-la-Coquette, France). The qPCR measurements were performed in triplicate using SYBR Green Super-mix (Bio-Rad, Marnes-la-Coquette, France). The reaction conditions were as follows: 98°C for 30 s (polymerase activation), followed by 40 cycles at 95°C for 5 s, 60°C for 10 s, and 72°C for 10 s. The primers were designed using Primer3Plus software (**Table 1**). A melting curve analysis was used to assess the specificity of the selected primers, and the results were quantified using relative standard curve methods. The target gene relative expression in the dorsomedial peri-infarct regions and their respective contralateral sides was calculated after normalization to the ribosomal protein L13 (Rpl13) reference gene. The following reference genes—Rpl13, Hmbs, and Rn18s—were assessed in the core area and its respective contralateral side. Data are expressed as mean ± SEM and normalized to the $mGlu3^{+/+}$ contralateral group.

TABLE 1 | Gene primers.

Gene	Forward	Reverse
Arg1	GTGAAGAACCCACGGTCTGT	GCCAGAGATGCTTCCAACTG
Cd86	GAGCGGGATAGTAACGCTGA	GGCTCTCACTGCCTTCACTC
Gdnf	GCACCCCCGATTTTTGC	AGCTGCCAGCCCAGAGAATT
Hmbs	TCCCTGTTCAGCAAGAAGATG	GGATGTTCTTGGCTCCTTTG
Il1b	GAAGATGGAAAAACGGTTTG	GTACCAGTTGGGGAACTCTGC
Il6	CAAAGCCAGAGTCCTTCAGA	GCCACTCCTTCTGTGACTCC
Il4ra	GGATAAGCAGACCCGAAGC	ACTCTGGAGAGACTTGGTTGG
Mrc1	CTTCGGGCCTTTGGAATAAT	TAGAAGAGCCCTTGGGTTGA
Ptgs2	TCATTCACCAGACAGATTGCT	AAGCGTTTGCGGTACTCATT
Rn18s	CGGTACAGTGAAACTGCGAAT	CCGTGGGCATGTATTAGCTC
Rpl13	ACAGCCACTCTGGAGGAGAA	GAGTCCGTTGGTCTTGAGGA
Tnfa	GCCTCTTCTCATTCCTGCTT	AGGGTCTGGGCCATAGAACT
Tgfb	TGATACGCCTGAGTGGCTGTCT	CACAAGAGCAGTGAGCGCTGAA
Socs3	CGTTGACAGTCTTCCGACAA	TATTCTGGGGGCGAGAAGAT

Statistical Analysis

Statistical analysis of all data was performed using GraphPad PRISM software, version 8.0. In all experiments, data are presented as means ± standard error of the mean (SEM), and $p < 0.05$ was considered significant. A two-tailed unpaired Student's *t*-test was performed for two-group comparisons in infarct volume. The mRNA data were normalized to the wild-type contralateral group and analyzed using two-way ANOVA, followed by Fisher's *post hoc* comparison tests. For behavioral analysis, the non-parametric Mann–Whitney *U* test and Friedman ANOVA were performed.

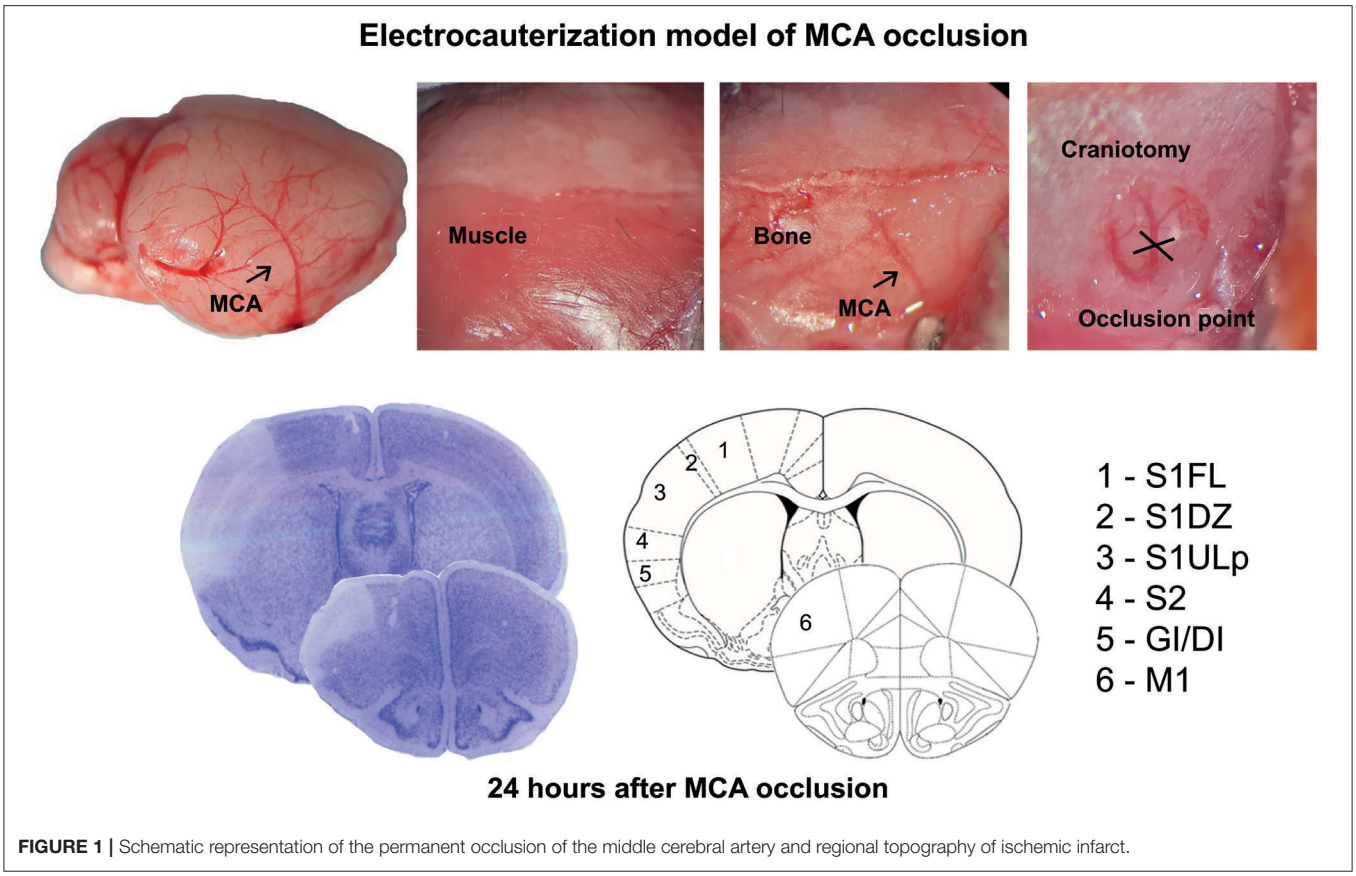

FIGURE 1 | Schematic representation of the permanent occlusion of the middle cerebral artery and regional topography of ischemic infarct.

RESULTS

Genetic Deletion of mGlu3 Receptors Enhanced Infarct Size and Neuroinflammation in CD1 Mice Undergoing Permanent MCA Occlusion

Ischemic infarct caused by permanent distal MCA occlusion in CD1 mice included the primary motor cortex (M1), the forelimb (S1FL), dysgranular (S1DZ), and upper lip (S1ULp) regions of the primary somatosensory cortex, the secondary somatosensory cortex (S2), and the granular/dysgranular insular cortex (GI/DI) (**Figure 1**). The ischemic infarct was detectable as early as 2 h after MCA occlusion and reached its maximal size at 24 h. The extent of the infarct volume, evaluated by Nissl staining at 24 h after MCA occlusion, was greater in mGlu3$^{-/-}$ mice as compared to their mGlu3$^{+/+}$ counterparts (**Figures 2A,B**). We measured the transcripts of three housekeeping genes (Hmbs, Rn18s, and Rpl13) in a small region of the ischemic core (highlighted in **Figure 2C**) as an unbiased method to detect cell damage in response to permanent ischemia. In mGlu3$^{+/+}$ mice, the mRNA levels of the three transcripts were significantly reduced in the ischemic core with respect to the corresponding region of the contralateral hemisphere. The reduction was much greater in the ischemic core of mGlu3$^{-/-}$ mice as compared to the respective contralateral site and also to the ischemic core of mGlu3$^{+/+}$ mice (**Figure 2D**). Interestingly, gene expression was also lower in the contralateral site of mGlu3$^{-/-}$ mice compared to the contralateral site of mGlu3$^{+/+}$ mice (**Figure 2D**).

To examine whether the genetic deletion of mGlu3 receptors amplified neuroinflammation in response to MCA occlusion, we first performed immunofluorescent staining of the microglia/macrophage marker Iba1 (31) in the peri-infarct region and the corresponding contralateral region (**Figure 3A**). The density of Iba1^{+} cells (measured in three microscopic sections) was greater in the peri-infarct regions of mGlu3$^{-/-}$ mice as compared to the peri-infarct region of mGlu3$^{+/+}$ mice (**Figure 3B**). The mGlu3$^{-/-}$ mice also showed a trend to an increased density of Iba1^{+} cells in the contralateral region (**Figure 3B**). We then measured the transcripts of a number of pro-inflammatory, immune-modulatory, and anti-inflammatory genes in the dorsomedial peri-infarct and contralateral regions (dissected as shown in **Figure 4A**). There was no difference in the expression of the housekeeping gene Rpl13 between the ipsilateral and contralateral sides in the two genotypes, suggesting the lack of cell death in the peri-infarct region (**Figure 4B**). In mGlu3$^{+/+}$ mice, the transcripts of Il1b, Ptgs2, and Tnfa genes encoding the proinflammatory cytokines, IL-1β, COX-2, and TNF-α, showed a significant increase in the peri-infarct region compared to the corresponding contralateral

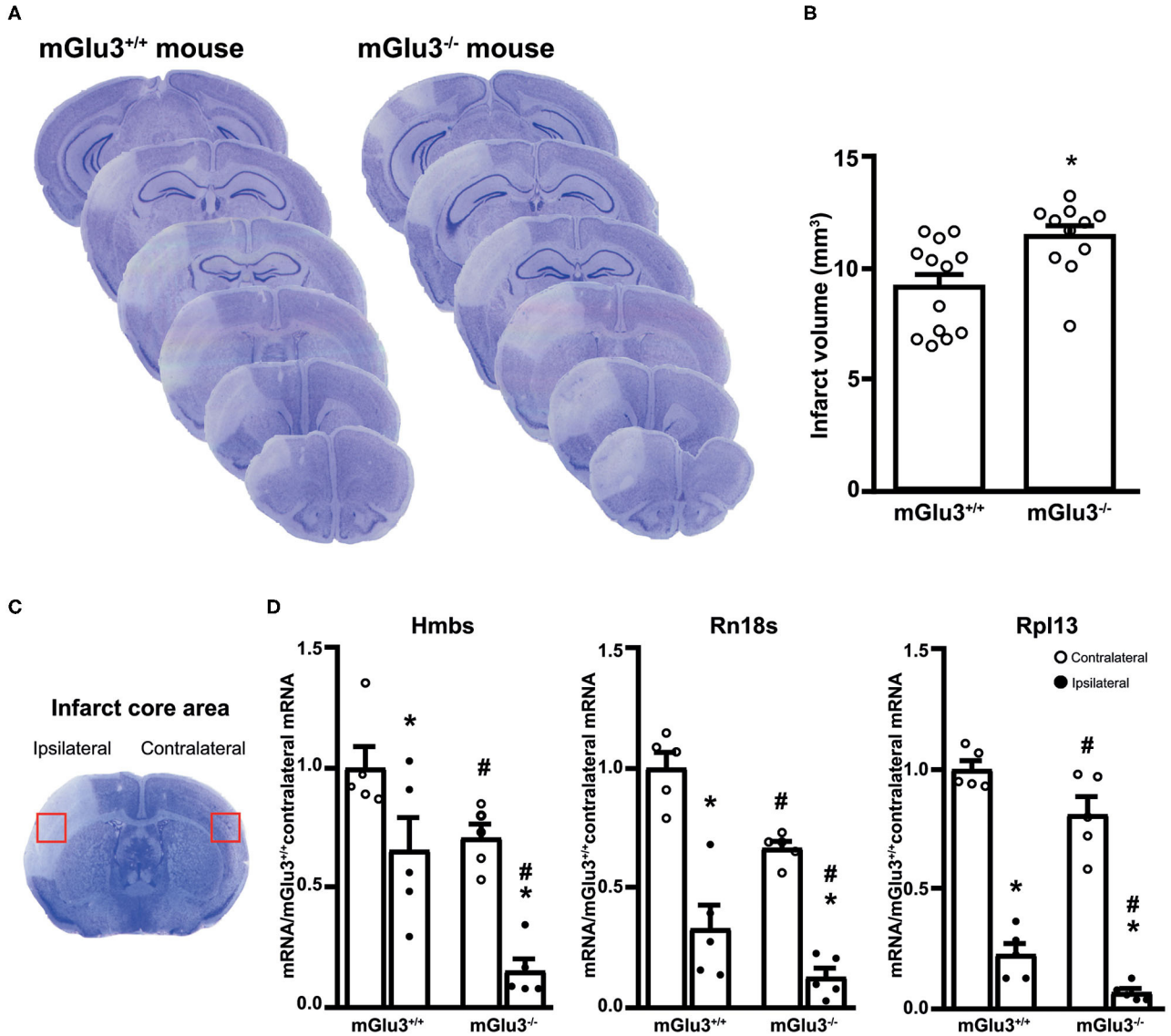

FIGURE 2 | Infarct size and expression of housekeeping genes in the infarct core of CD1 mGlu3$^{+/+}$ and mGlu3$^{-/-}$ mice subjected to permanent middle cerebral artery (MCA) occlusion. Nissl staining of sequential coronal brain sections of mGlu3$^{+/+}$ and mGlu3$^{-/-}$ mice 24 h following MCA occlusion is shown in **(A)**. Quantification of the infarct volume is shown in **(B)**, where values are means ± S.E.M. of 11–13 mice per group. *$p < 0.05$ vs. mGlu3$^{+/+}$ mice (Student's t test; $t_x = 2.967$). The infarct core region dissected for measurements of housekeeping genes is indicated in **(C)**. Hmbs, Rn18s, and Rpl13 mRNA levels in the ipsilateral and contralateral sides of the two genotypes are shown in **(D)**, where values are means ± S.E.M. of five determinations. $p < 0.05$ (two-way ANOVA + Fisher's least significant difference) vs. the contralateral side of the same genotype (*) or the corresponding side of mGlu3$^{+/+}$ mice (#). Hmbs: genotype, $F_{1,16} = 19.34$, $p = 0.0004$; side, $F_{1,16} = 24.67$, $p = 0.0001$; interaction, $F_{1,16} = 1.396$, $p = 0.2546$; Rn18s: genotype, $F_{1,16} = 17.48$, $p = 0.0007$; side, $F_{1,16} = 88.85$, $p < 0.0001$; interaction, $F_{1,16} = 1.086$, $p = 0.3167$; Rpl13: genotype, $F_{1,16} = 12.73$, $p = 0.0026$; side, $F_{1,16} = 243.3$, $p > 0.0001$; interaction, $F_{1,16} = 0.0936$, $p = 0.7636$.

region, whereas the transcripts of Cd86 and Il6, encoding CD86 and IL-6, respectively, were unchanged (**Figure 4B**). In contrast, the expression of all five pro-inflammatory genes was largely increased in the peri-infarct region of mGlu3$^{-/-}$ mice, compared to the corresponding contralateral region (**Figure 3B**). Remarkably, the Ptgs2, Tnfa, Cd86, and Il6 mRNA levels were significantly higher in the peri-infarct region of mGlu3$^{-/-}$ mice with respect to the peri-infarct region of mGlu3$^{+/+}$ mice, and a trend to increase was also observed for the transcript encoding IL-1β (**Figure 4B**). Changes in COX-2 immunostaining paralleled the changes of the Ptgs2 transcript (greater density of COX-2^{+} cells in both sides of mGlu3$^{-/-}$ mice), although the differences were not statistically significant (**Figures 4C,D**).

The expression of three immunomodulatory genes (Mrc1, Il4ra, and Socs3, encoding MRC-1, IL4Ra, and SOCS3, respectively) largely increased in the peri-infarct region of mGlu3$^{+/+}$ mice, whereas only the transcript encoding

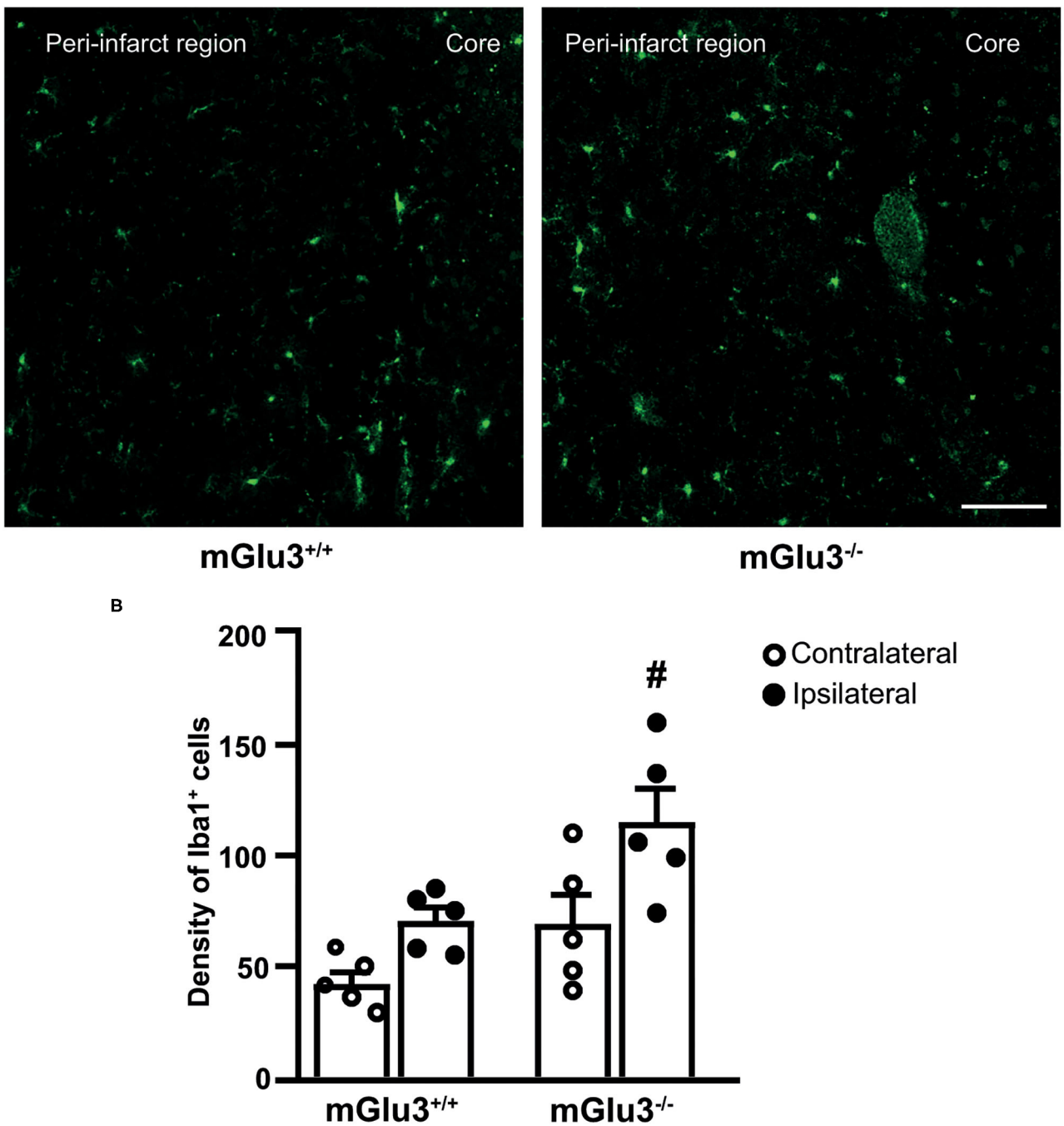

FIGURE 3 | Iba1 immunostaining in the peri-infarct region and the corresponding contralateral region of CD1 mGlu3$^{+/+}$ and mGlu3$^{-/-}$ mice subjected to middle cerebral artery occlusion. The density of Iba1^{+} cells was measured in three sections of the peri-infarct and contralateral regions of the two genotypes. Representative images are shown in **(A)**. Values are means ± S.E.M. from five mice per group. #$p < 0.05$ vs. the peri-infarct region of mGlu3$^{+/+}$ mice (two-way ANOVA + Fisher's least significant difference). Genotype, $F_{1,16} = 11.22$, $p = 0.0041$; side, $F_{1,16} = 12.11$, $p = 0.0031$; interaction, $F_{1,16} = 0.6590$, $p = 0.4288$. Scale bar = 50 mm.

SOCS3 increased in the peri-infarct region of mGlu3$^{-/-}$ mice as compared to the contralateral corresponding region (**Figure 5A**). Mrc1 expression was lower in the ipsilateral side of mGlu3$^{-/-}$ mice as opposed to what was found in mGlu3$^{+/+}$ mice. Interestingly, however, the Mrc1 mRNA levels were significantly higher in both sides of mGlu3$^{-/-}$ mice with respect

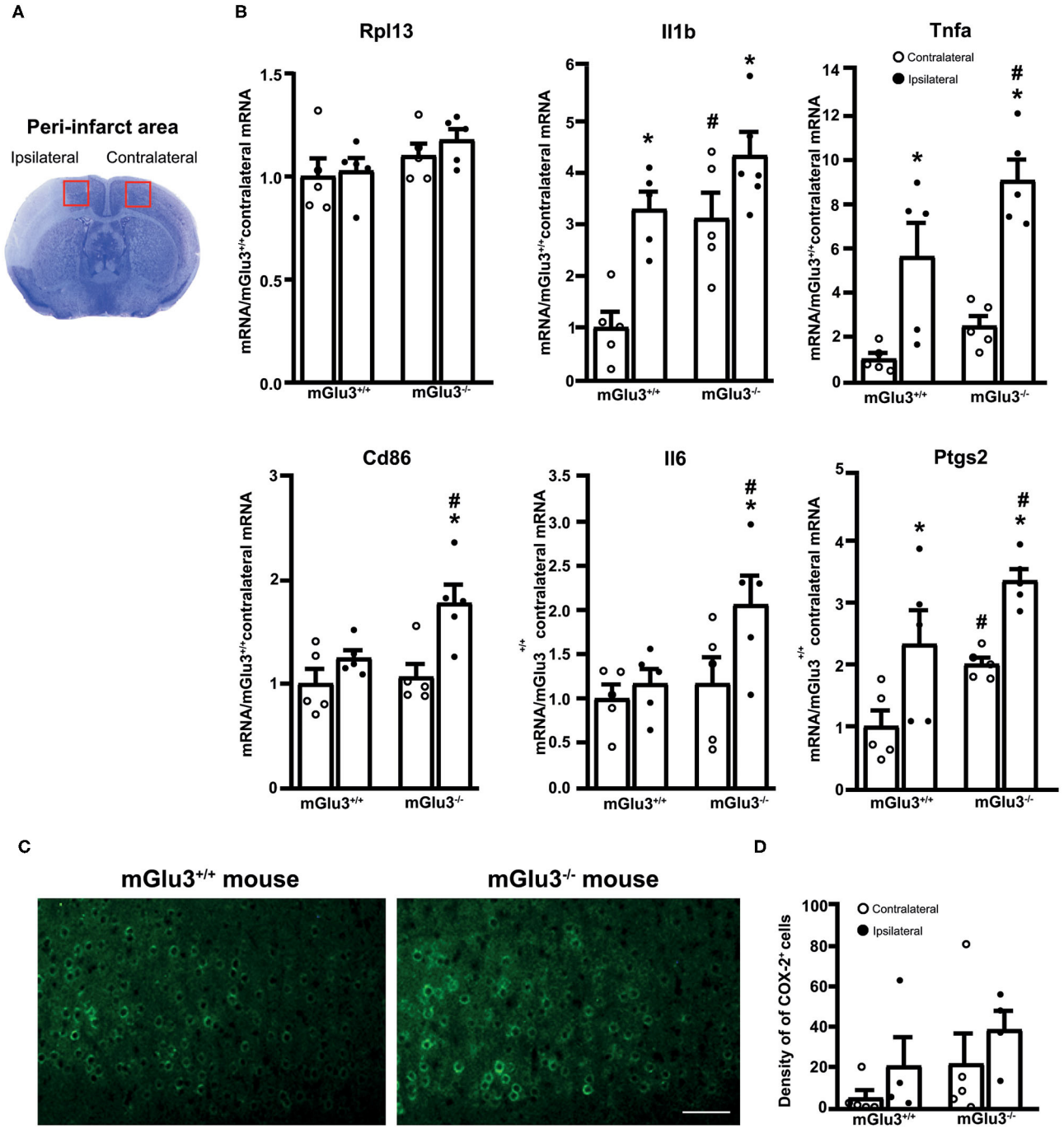

FIGURE 4 | Expression of pro-inflammatory genes in the peri-infarct region and the corresponding contralateral region of CD1 mGlu3$^{+/+}$ and mGlu3$^{-/-}$ mice subjected to middle cerebral artery (MCA) occlusion. The anatomical location of the dissected dorsomedial peri-infarct region and the corresponding contralateral region is shown in **(A)**. The mRNA levels of the selected housekeeping and pro-inflammatory genes of the ipsilateral and contralateral sides of mGlu3$^{+/+}$ and mGlu3$^{-/-}$ mice subjected to MCA occlusion is shown in **(B)**. Values are means ± S.E.M. of five determinations. $p < 0.05$ (two-way ANOVA + Fisher's least significant difference) vs. the contralateral side of the same genotype (*) or the corresponding side of mGlu3$^{+/+}$ mice (#). Rpl13: genotype, $F_{1,16} = 3.652$, $p = 0.0741$; side, $F_{1,16} = 0.6079$, $p = 0.4470$; interaction, $F_{1,16} = 0.1461$, $p = 0.7074$; Il1b: genotype, $F_{1,16} = 15.26$, $p = 0.0013$; side, $F_{1,16} = 18.79$, $p = 0.0005$; interaction, $F_{1,16} = 1.756$, $p = 0.2038$; Tnfa: genotype, $F_{1,16} = 7.016$, $p = 0.017$; side, $F_{1,16} = 36.5$, $p > 0.0001$; interaction, $F_{1,16} = 1.11$, $p = 0.3078$; Cd86: genotype, $F_{1,16} = 4.826$, $p = 0.0432$; side, $F_{1,16} = 12.62$, $p = 0.0027$; interaction, $F_{1,16} = 0.0012$, $p = 0.97$; Il6: genotype, $F_{1,16} = 4.618$, $p = 0.0473$; side, $F_{1,16} = 4.584$, $p = 0.048$; interaction, $F_{1,16} = 2.142$, $p = 0.1627$; Ptgs2: genotype, $F_{1,16} = 10.09$, $p = 0.0012$; side, $F_{1,16} = 17.54$, $p = 0.0007$; interaction, $F_{1,16} = 0.0012$, $p = 0.97$. Representative COX-2 immunostaining in the peri-infarct regions of the mGlu3$^{+/+}$ and mGlu3$^{-/-}$ mice is shown in **(C)**. The density of COX-2-expressing cells in three sections of the peri-infarct and contralateral regions of the two genotypes is shown in **(D)**, where values are means ± S.E.M. from four mice per group. Statistical analysis was performed by two-way ANOVA + Fisher's least significant difference. Genotype, $F_{1,14} = 2.284$, $p = 0.1529$; side, $F_{1,14} = 2.006$, $p = 0.1785$; interaction, $F_{1,14} = 0.001865$, $p = 0.966$. Scale bar = 25 μm.

to the corresponding regions of mGlu3$^{+/+}$ mice (**Figure 5A**). The Socs3 mRNA levels increase to a greater extent in the peri-infarct region of mGlu3$^{-/-}$ mice than in the peri-infarct region of mGlu3$^{+/+}$ mice (**Figure 5A**).

The expression of the anti-inflammatory gene Arg1 (encoding arginase-1) did not differ between the ipsilateral and contralateral sides of mGlu3$^{+/+}$ mice after MCA occlusion. In mGlu3$^{-/-}$ mice, the Arg1 mRNA levels showed a large increase in the ipsilateral side. In addition, the levels were lower in the contralateral side and higher in the ipsilateral side with respect to the corresponding regions of mGlu3$^{+/+}$ mice (**Figure 5A**).

Using the same extracts from the peri-infarct region, we extended the analysis to two trophic factors (GDNF and TGF-β), which are under the control of mGlu3 receptors. Interestingly, the transcript encoding GDNF was exclusively increased in the peri-infarct region of mGlu3$^{+/+}$ mice, whereas the transcript encoding TGF-β was increased in the peri-infarct region of mGlu3$^{-/-}$ mice (**Figure 5B**).

Genetic Deletion of mGlu3 Receptors Enhanced Infarct Size and Worsened the Impairment of Motor Response to Tactile/Proprioceptive Stimuli in C57Black Mice Subjected to Permanent MCA Occlusion

We used C57Black mice to confirm the effect of mGlu3 receptor deletion in another strain of mice and to extend the study to the assessment of behavioral impairment induced by ischemia with the paw placement test. This test evaluates the tactile/proprioceptive response of the animal and is widely used in rodent models of brain ischemia (29). This test could not be applied to CD1 mice because of their suboptimal performance under normal conditions.

Similarly to what was found in CD1 mice, the infarct size was significantly greater in mGlu3$^{-/-}$ mice of C57Black strain subjected to permanent MCA occlusion as compared to their mGlu3$^{+/+}$ counterparts (**Figures 6A,B**). Remarkably, the extent of the increase in infarct size as measured in ischemic C57Black mice lacking mGlu3 receptors was identical to that seen in CD1 mGlu3$^{-/-}$ mice (**Figures 2B**, **6B**).

The paw placement test was performed before ischemia, both at 4 and 24 h following MCA occlusion. At 4 h, the impairment of the proprioceptive/tactile response of the forepaw contralateral to MCA occlusion was significantly greater in mGlu3$^{-/-}$ than in mGlu3$^{+/+}$ mice (**Figure 6C**). At 24 h, there was no difference between the two genotypes because of a partial recovery of mGlu3$^{-/-}$ mice (**Figure 6C**). There were only small and non-significant changes in the ipsilateral forepaw placement in the two time points following MCA occlusion, although a trend to reduction in the disability score was observed in mGlu3$^{-/-}$ mice at 4 h (**Figure 6D**).

DISCUSSION

The role of mGlu receptors in mechanisms of ischemic neuronal cell death has been the subject of extensive investigation. Pharmacological blockade of mGlu1 receptors was shown to be neuroprotective in hippocampal slices subjected to a paradigm of oxygen/glucose deprivation and in models of transient global ischemia (32, 33). Conversely, the activation of mGlu1 receptors was found to mediate ischemic tolerance induced by "ischemic preconditioning" in hippocampal slice preparations (34). However, these findings have not been translated into effective treatment strategies in stroke because mGlu1 receptors may display neurotoxic and neuroprotective functions depending on the cell context and the paradigm of neuronal death (35, 36). The use of mGlu5 receptor ligands in stroke models has generated conflicting results. Early studies showed that both mGlu5 receptor agonists and antagonists reduced infarct size in a rat intraluminal filament model of transient MCA occlusion (37), whereas pharmacological activation of mGlu5 receptors was not protective in the endothelin-1 rat model of focal ischemia (38). More recent findings showed that selective pharmacological blockade of mGlu5 receptors reduced microglial activation and neuronal death induced by acute intracerebral hemorrhage (39). The mGlu4 receptors are also potential drug targets for neuroprotection in ischemic stroke as shown by the evidence that mGlu4 receptor activation reduced infarct size in ischemic mice and rats, whereas brain damage was amplified in mGlu4$^{-/-}$ mice (40). Activating mGlu4 receptors might also restrain immune reactive mechanisms in stroke (6) by promoting immune tolerance (41).

Our data offer the first evidence for a neuroprotective activity of mGlu3 receptors against focal brain ischemia in two different strains of mice. mGlu2 and mGlu3 receptors show a high degree of primary sequence homology, are both coupled to $G_{i/o}$ proteins in heterologous expression systems, and share some functional properties including, for example, the ability to restrain neurotransmitter release (9). However, using both genetic and selective pharmacological tools, we were able to demonstrate that activation of mGlu2 receptors amplifies brain damage in rodent models of global and focal ischemia (19, 20). Thus, a comparison between present findings and previous data reveals that mGlu3 and mGlu2 receptors have an opposite impact on vulnerability to ischemic brain damage. There are at least two functions of mGlu3 receptors that account for this difference: the anti-inflammatory action in microglia (14, 16, 42) and the stimulation of TGF-β, and GDNF production in astrocytes and neurons, respectively (21–23, 43, 44). We have found that gestational low-protein diet (LPD) combined with IL-1β injection in rat pups (modeling intrauterine growth restriction and perinatal brain inflammation in human neonates) was associated with a selective down-regulation of mGlu3 receptors in microglia. In addition, microglia reactivity to inflammatory challenge induced by LPD/IL-1β was reduced by the pharmacological activation of mGlu3 receptors, whereas pharmacological blockade or the genetic deletion of mGlu3 receptors induced

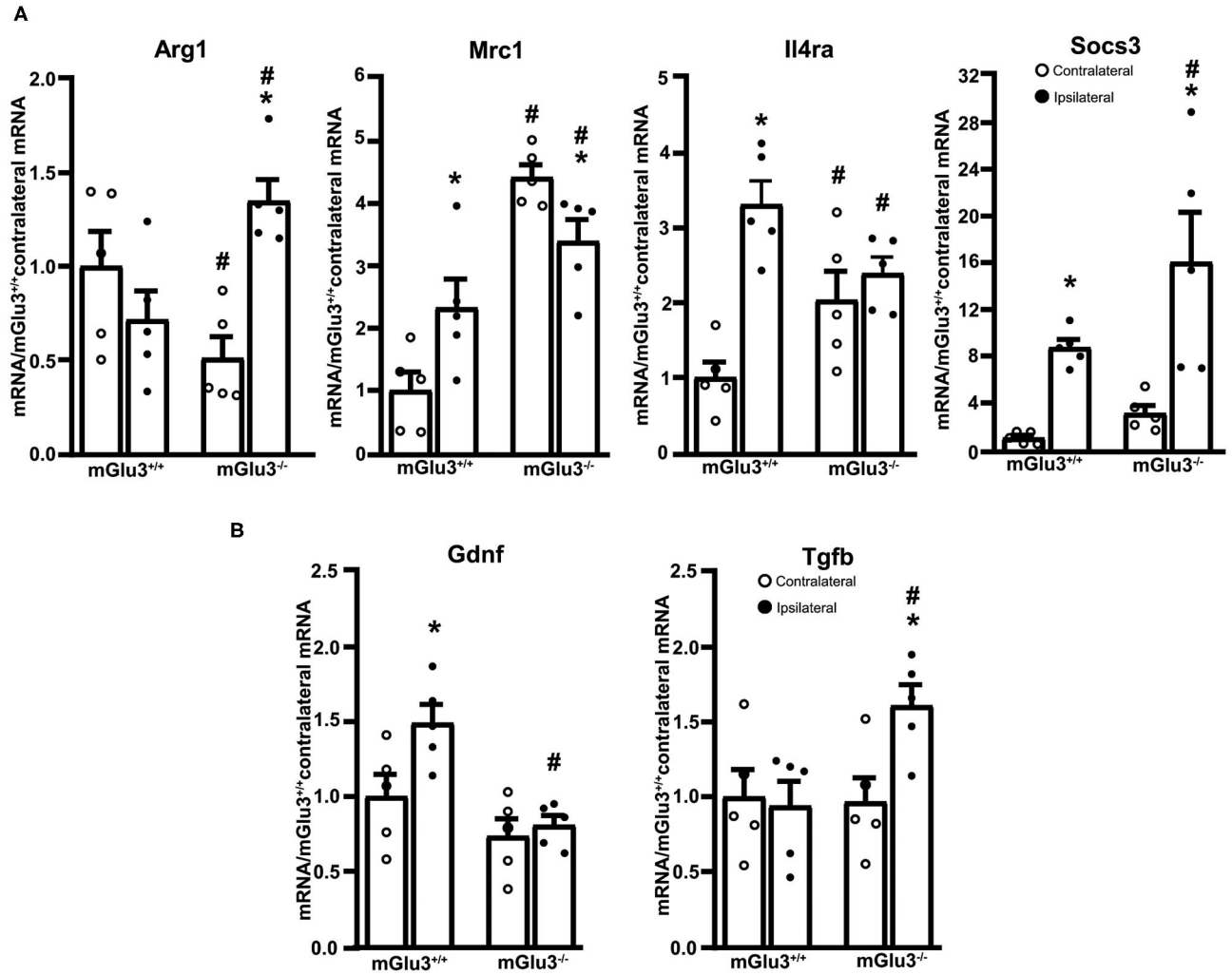

FIGURE 5 | Expression of immunoregulatory, anti-inflammatory, and neuroprotective genes in the peri-infarct region of CD1 mGlu3$^{+/+}$ and mGlu3$^{-/-}$ mice subjected to middle cerebral artery (MCA) occlusion. The mRNA levels of the selected immunoregulatory and anti-infammatory genes of the ipsilateral and contralateral sides of wild-type and mGlu3$^{-/-}$ mice subjected to MCA occlusion is shown in **(A)**. The mRNA levels of the genes encoding GDNF and TGF-β are shown in **(B)**. Values are means ± S.E.M. of five determinations. $p < 0.05$ (two-way ANOVA + Fisher's LSD) vs. the contralateral side of the same genotype (*) or the corresponding side of mGlu3$^{+/+}$ mice (#). Arg1: genotype, $F_{1,16} = 0.2441$, $p = 0.628$; side, $F_{1,16} = 3.639$, $p = 0.0746$; interaction, $F_{1,16} = 14.98$, $p = 0.0014$; Mrc1: genotype, $F_{1,16} = 43.5$, $p < 0.0001$; side, $F_{1,16} = 0.1896$, $p = 0.6691$; interaction, $F_{1,16} = 11.97$, $p = 0.0032$; Il4ra: genotype, $F_{1,16} = 0.037$, $p = 0.848$; side, $F_{1,16} = 20.81$, $p = 0.0003$; interaction, $F_{1,16} = 11.19$, $p = 0.0041$; Socs3: genotype, $F_{1,16} = 4.619$, $p = 0.0473$; side, $F_{1,16} = 22.29$, $p = 0.0002$; interaction, $F_{1,16} = 1.413$, $p = 0.252$; Gdnf: genotype, $F_{1,16} = 16.19$, $p = 0.001$; side, $F_{1,16} = 5.731$, $p = 0.029$; interaction, $F_{1,16} = 3.118$, p = 0.0965; Tgfb: genotype, $F_{1,16} = 3.771$, $p = 0.0472$; side, $F_{1,16} = 3.18$, $p = 0.093$; interaction, $F_{1,16} = 4.621$, $p = 0.0472$.

an inflammatory phenotype in microglia (16). In contrast, mGlu2 receptor activation promotes a pro-inflammatory and neurotoxic phenotype in microglia (14, 15). The large increase in the expression of pro-inflammatory genes found in the peri-infarct region of mGlu3$^{-/-}$ mice strengthens the hypothesis that mGlu3 receptors are key regulators of microglial function and act to restrain neuroinflammation. This mechanism may critically shape neuronal vulnerability to focal ischemia because neuroinflammation caused by the activation of resident microglia and infiltration of peripheral monocytes is consistently associated with ischemic stroke, leading to secondary injury cascade and neuronal death (45–49).

The reduced expression of Mrc1 (vs. the contralateral side) and Il4ra (vs. mGlu3$^{+/+}$ mice) found in the peri-infarct region of mGlu3$^{-/-}$ mice is consistent with a putative anti-inflammatory action of mGlu3 receptors. Mrc1 encodes mannose receptor 1, also referred to as CD206, which is involved in the mechanisms of pinocytosis and phagocytosis and is associated with the anti-inflammatory and neuroprotective phenotype in microglia (50–53). Il4ra encodes the α-subunit of the IL-4 receptor, which mediates the anti-inflammatory effect of IL-4 in macrophages and microglia (54, 55). Alternatively, the increased expression of Arg1 was found exclusively in the peri-infarct region of mGlu3$^{-/-}$ mice. Arg1 encodes for arginase 1, the

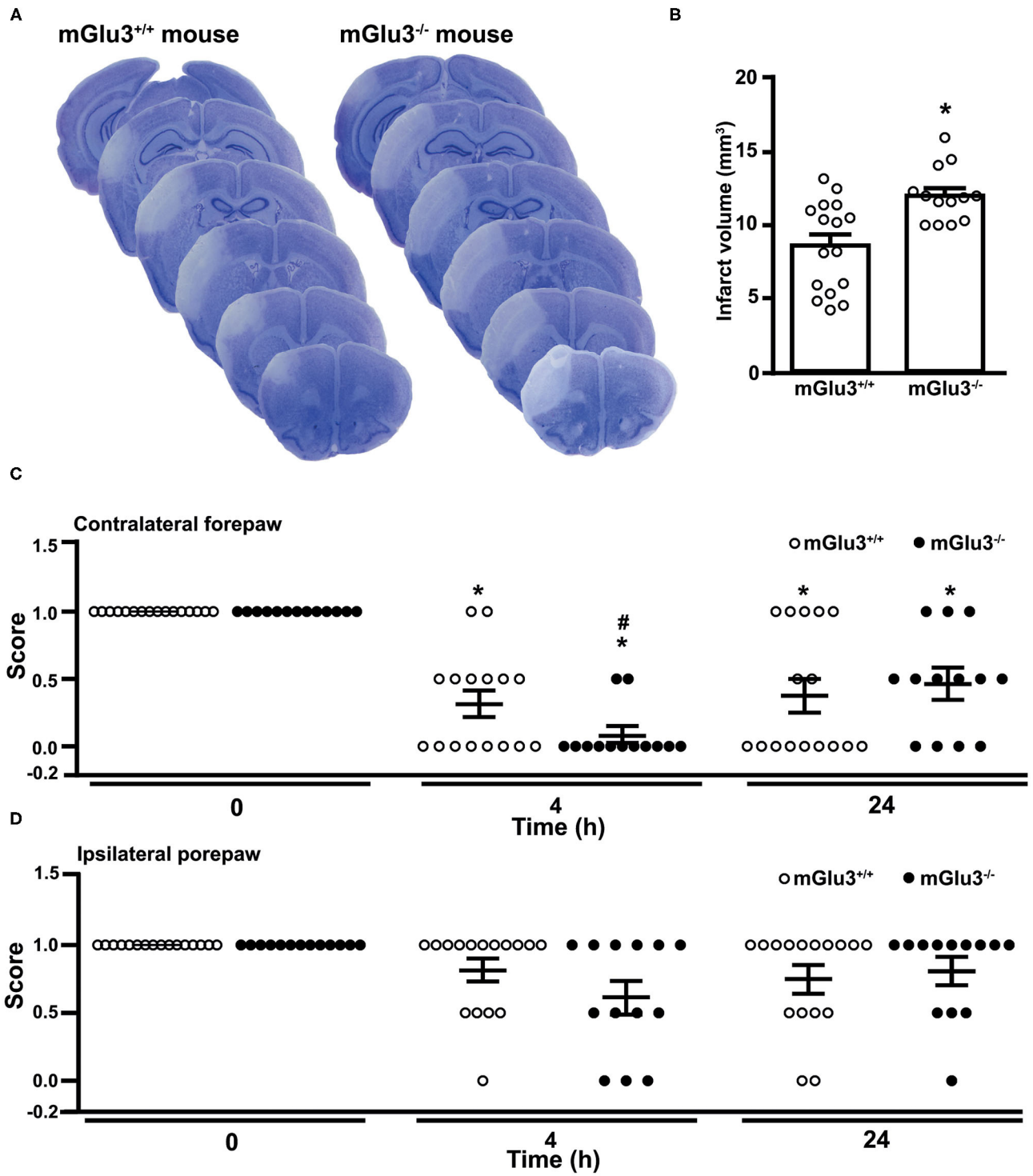

FIGURE 6 | Infarct size and performance in the paw placement test of C57Black mGlu3$^{+/+}$ and mGlu3$^{-/-}$ mice subjected to permanent middle cerebral artery (MCA) occlusion. Nissl staining of sequential coronal brain sections of mGlu3$^{+/+}$ and mGlu3$^{-/-}$ mice 24 h following MCA occlusion is shown in **(A)**. Quantification of the infarct volume is shown in **(B)**, where values are means ± S.E.M. of 13–16 mice per group. *$p < 0.05$ vs. mGlu3$^{+/+}$ mice (Student's t test; $t_x = 3.501$). The paw placement scores of the contralateral and ipsilateral forepaws are shown in **(C,D)**, respectively. Means ± S.E.M. are indicated. Contralateral side: *$p < 0.05$ vs. the corresponding basal values (time 0) (Friedman non-parametric ANOVA test + Dunn's; Friedman statistical value = 20.65) or #$p < 0.05$ vs. values of mGlu3$^{+/+}$ mice at 4 h (one-tailed Mann–Whitney non-parametric test).

enzyme that converts arginine into L-ornithine and is considered a marker for the anti-inflammatory phenotype of microglia. Accordingly, L-arginine is the same substrate for both nitric oxide synthase (NOS) and arginase 1, and the Arg1 outcompetes inducible NOS to reduce the production of nitric oxide (56). The STAT6 (type-6 Signal Transduction and Activator of Transcription)/Arg1 pathway promotes microglia/macrophase efferocytosis (phagocytosis of dying/dead cells), thus facilitating the resolution of inflammation and preventing further cell death in mice subjected to MCA occlusion (57, 58). The increased Arg1 expression detected in the peri-infarct region of mGlu3$^{-/-}$ mice might reflect a compensatory mechanism aimed at restraining the neuroinflammation, mediated by M2 microglia polarization (57, 58). The increase in SOCS3 transcript seen in mGlu3$^{-/-}$ mice might be a component of this compensatory mechanism because SOCS3 inhibits cytokine receptor signaling, although SOCS3 has pleiotrophic activities and might be detrimental for cell survival *via* the induction of the pro-apoptotic metabolite, ceramide (59).

Studies performed in cell cultures and living mice have shown that the pharmacological activation of mGlu3 receptors stimulates the production of TGF-β in astrocytes (21–23) and GDNF in neurons (43, 44). Both GDNF and TGF-β are neuroprotective, and GDNF requires TGF-β for its neuroprotective action (60). The reduced GDNF transcript levels found in the peri-infarct region of mGlu3$^{-/-}$ mice are in line with the evidence that activation of mGlu3 receptors enhances GDNF production in the CNS (43, 44). Lowered GDNF levels might contribute to the increased infarct size in mGlu3$^{-/-}$ mice because GDNF is known to exert a neuroprotective activity.

In contrast, the increase in TGF-β mRNA levels found in the peri-infarct region of mGlu3$^{-/-}$ mice was unexpected because mGlu3 receptor activation is known to stimulate TGF-β production in astrocytes (17). One explanation is that, other cells, such as macrophages and microglia, are the source of TGF-β in the peri-infarct region of mGlu3$^{-/-}$ mice. How changes in TGF-β in gene transcripts contribute to mechanisms of neurodegeneration/neuroprotection in the peri-infarct region is unknown. However, a causal relatioship may exist between the increase in TGF-β and the reduction in Mrc1 in the peri-infarct region of mGlu3$^{-/-}$ mice because TGF-β negatively modulates Mrc1 expression (61, 62).

Behavioral analysis performed in C57Black mice showed a greater defect in the paw placement test in mGlu3$^{-/-}$ mice at short times (4 h) following MCA occlusion. This might reflect the early brain damage and hyperinflammation caused by the lack of mGlu3 receptors. However, the performance in the paw placement test partially recovered, and there was no difference between mGlu3$^{+/+}$ and mGlu3$^{-/-}$ mice at 24 h. An increased glutamate release caused by the lack of presynaptic mGlu3 receptors might contribute to excitotoxic neuronal death but, on the other side, might facilitate functional recovery by inducing mechanisms of activity-dependent synaptic plasticity. This hypothesis warrants further investigation.

In conclusion, our data suggest that the endogenous activation of mGlu3 receptors display a protective activity against ischemic brain damage and associated neuroinflammation and lays the groundwork for the use of subtype-selective mGlu3 receptor agonists or positive allosteric modulators (PAM) in experimental animal models of stroke. A selective mGlu3 receptor agonist is already available (63), and mGlu3 receptor PAMs are under development (64). These are putative drug candidates as neuroprotectants in ischemic stroke.

DATA AVAILABILITY STATEMENT

The raw data supporting the conclusions of this article will be made available by the authors, without undue reservation.

ETHICS STATEMENT

The animal study was reviewed and approved by Neuromed Institutional Animal Care and Use Committee and the Italian Ministry of Health. Written informed consent was obtained from the owners for the participation of their animals in this study.

AUTHOR CONTRIBUTIONS

FM: conceptualization, investigation, and formal analysis. MZ, GM, JP, and TI: investigation. VB, GB, JM, OB, and FN: supervision, data curation, and writing. All authors contributed to the article and approved the submitted version.

FUNDING

Ricerca Corrente 2021 funded by Italian Ministry of Health.

REFERENCES

1. Rossi DJ, Brady JD, Mohr C. Astrocyte metabolism and signaling during brain ischemia. *Nat Neurosci.* (2007) 10:1377–86. doi: 10.1038/nn2004
2. Ginsberg MD. Adventures in the pathophysiology of brain ischemia: penumbra, gene expression, neuroprotection: the 2002 Thomas Willis lecture. *Stroke.* (2003) 34:214–23. doi: 10.1161/01.STR.0000048846.09677.62
3. Zhao W, Belayev L, Ginsberg MD. Transient middle cerebral artery occlusion by intraluminal suture: II. Neurological deficits, and pixel-based correlation of histopathology with local blood flow and glucose utilization. *J Cereb Blood Flow Metab.* (1997) 17:1281–90. doi: 10.1097/00004647-199712000-00003
4. Choi DW. Methods for antagonizing glutamate neurotoxicity. *Cerebrovasc Brain Metab Rev.* (1990) 2:105–47.
5. Friberg H, Wieloch T. Mitochondrial permeability transition in acute neurodegeneration. *Biochimie.* (2002) 84:241–50. doi: 10.1016/S0300-9084(02)01381-0
6. Iadecola C, Anrather J. Stroke research at a crossroad: asking the brain for directions. *Nat Neurosci.* (2011) 14:1363–8. doi: 10.1038/nn.2953
7. Khoshnam SE, Winlow W, Farzaneh M, Farbood Y, Moghaddam HF. Pathogenic mechanisms following ischemic stroke. *Neurol Sci.* (2017) 38:1167–86. doi: 10.1007/s10072-017-2938-1

8. Sekerdag E, Solaroglu I, Gursoy-Ozdemir Y. Cell death mechanisms in stroke and novel molecular and cellular treatment options. *Curr Neuropharmacol.* (2018) 16:1396–415. doi: 10.2174/1570159X16666180302115544
9. Nicoletti F, Bockaert J, Collingridge GL, Conn PJ, Ferraguti F, Schoepp DD, et al. Metabotropic glutamate receptors: from the workbench to the bedside. *Neuropharmacology.* (2011) 60:1017–41. doi: 10.1016/j.neuropharm.2010.10.022
10. Bond A, Ragumoorthy N, Monn JA, Hicks CA, Ward MA, Lodge D, et al. LY379268, a potent and selective Group II metabotropic glutamate receptor agonist, is neuroprotective in gerbil global, but not focal, cerebral ischaemia. *Neurosci Lett.* (1999) 273:191–4. doi: 10.1016/S0304-3940(99)00663-1
11. Bond A, Jones NM, Hicks CA, Whiffin GM, Ward MA, O'Neill MF, et al. Neuroprotective effects of LY379268, a selective mGlu2/3 receptor agonist: investigations into possible mechanism of action in vivo. *J Pharmacol Exp Ther.* (2000) 294:800–9.
12. Di Menna L, Joffe ME, Iacovelli L, Orlando R, Lindsley CW, Mairesse J, et al. Functional partnership between mGlu3 and mGlu5 metabotropic glutamate receptors in the central nervous system. *Neuropharmacology.* (2018) 128:301–13. doi: 10.1016/j.neuropharm.2017.10.026
13. Joffe ME, Santiago CI, Stansley BJ, Maksymetz J, Gogliotti RG, Engers JL, et al. Mechanisms underlying prelimbic prefrontal cortex $mGlu_3$/$mGlu_5$-dependent plasticity and reversal learning deficits following acute stress. *Neuropharmacology.* (2019) 144:19–28. doi: 10.1016/j.neuropharm.2018.10.013
14. Taylor DL, Diemel LT, Cuzner ML, Pocock JM. Activation of group II metabotropic glutamate receptors underlies microglial reactivity and neuro- toxicity following stimulation with chromogranin A, a peptide up-regulated in Alzheimer's disease. *J Neurochem.* (2002) 82:1179. e1191. doi: 10.1046/j.1471-4159.2002.01062.x
15. Taylor DL, Jones F, Kubota ES, Pocock JM. Stimulation of microglial metabotropic glutamate receptor mGlu2 triggers tumor necrosis factor alpha- induced neurotoxicity in concert with microglial-derived Fas ligand. *J Neurosci.* (2005) 25:2952. e2964. doi: 10.1523/JNEUROSCI.4456-04.2005
16. Zinni M, Mairesse J, Pansiot J, Fazio F, Iacovelli L, Antenucci N, et al. mGlu3 receptor regulates microglial cell reactivity in neonatal rats. *J Neuroinflammation.* (2021) 18:13. doi: 10.1186/s12974-020-02049-z
17. Bruno V, Battaglia G, Casabona G, Copani A, Caciagli F, Nicoletti F. Neuroprotection by glial metabotropic glutamate receptors is mediated by transforming growth factor-beta. *J Neurosci.* (1998) 18:9594–600. doi: 10.1523/JNEUROSCI.18-23-09594.1998
18. Ciccarelli R, Di Iorio P, Bruno V, Battaglia G, D'Alimonte I, D'Onofrio M, et al. Activation of A(1) adenosine or mGlu3 metabotropic glutamate receptors enhances the release of nerve growth factor and S-100beta protein from cultured astrocytes. *Glia.* (1999) 27:275–81.
19. Motolese M, Mastroiacovo F, Cannella M, Bucci D, Gaglione A, Riozzi B, et al. Targeting type-2 metabotropic glutamate receptors to protect vulnerable hippocampal neurons against ischemic damage. *Mol Brain.* (2015) 8:66. doi: 10.1186/s13041-015-0158-2
20. Mastroiacovo F, Moyanova S, Cannella M, Gaglione A, Verhaeghe R, Bozza G, et al. Genetic deletion of mGlu2 metabotropic glutamate receptors improves the short-term outcome of cerebral transient focal ischemia. *Mol Brain.* (2017) 10:39. doi: 10.1186/s13041-017-0319-6
21. Bruno V, Sureda FX, Storto M, Casabona G, Caruso A, Knopfel T, et al. The neuroprotective activity of group-II metabotropic glutamate receptors requires new protein synthesis and involves a glial-neuronal signaling. *J Neurosci.* (1997) 17:1891–7. doi: 10.1523/JNEUROSCI.17-06-01891.1997
22. Corti C, Battaglia G, Molinaro G, Riozzi B, Pittaluga A, Corsi M, et al. The use of knock-out mice unravels distinct roles for mGlu2 and mGlu3 metabotropic glutamate receptors in mechanisms of neurodegeneration/neuroprotection. *J Neurosci.* (2007) 27:8297–308. doi: 10.1523/JNEUROSCI.1889-07.2007
23. Caraci F, Molinaro G, Battaglia G, Giuffrida ML, Riozzi B, Traficante A, et al. Targeting group II metabotropic glutamate (mGlu) receptors for the treatment of psychosis associated with Alzheimer's disease: selective activation of mGlu2 receptors amplifies beta-amyloid toxicity in cultured neurons, whereas dual activation of mGlu2 and mGlu3 receptors is neuroprotective. *Mol Pharmacol.* (2011) 79:618–26. doi: 10.1124/mol.110.067488
24. Battaglia G, Riozzi B, Bucci D, Di Menna L, Molinaro G, Pallottino S, et al. Activation of mGlu3 metabotropic glutamate receptors enhances GDNF and GLT-1 formation in the spinal cord and rescues motor neurons in the SOD-1 mouse model of amyotrophic lateral sclerosis. *Neurobiol Dis.* (2015) 74:126–36. doi: 10.1016/j.nbd.2014.11.012
25. Fell MJ, Svensson KA, Johnson BG, Schoepp DD. Evidence for the role of metabotropic glutamate (mGlu)2 not mGlu3 receptors in the preclinical antipsychotic pharmacology of the mGlu2/3 receptor agonist (-)-(1R,4S,5S,6S)-4-amino-2-sulfonylbicyclo[3.1.0]hexane-4,6-dicarboxylic acid (LY404039). *J Pharmacol Exp Ther.* (2008) 326:209–17. doi: 10.1124/jpet.108.136861
26. Backhauss C, Karkoutly C, Welsch M, Krieglstein J. A mouse model of focal cerebral ischemia for screening neuroprotective drug effects. *J Pharmacol Toxicol Methods.* (1992) 27:27/32. doi: 10.1016/1056-8719(92)90017-U
27. Kuraoka M, Furuta T, Matsuwaki T, Omatsu T, Ishii Y, Kyuwa S, et al. Direct experimental occlusion of the distal middle cerebral artery induces high reproducibility of brain ischemia in mice. *Exp Anim.* (2009) 58:19–29. doi: 10.1538/expanim.58.19
28. Mastroiacovo F, Busceti CL, Biagioni F, Moyanova SG, Meisler MH, Battaglia G, et al. Induction of the Wnt antagonist, Dickkopf-1, contributes to the development of neuronal death in models of brain focal ischemia. *J Cereb Blood Flow Metab.* (2009) 29:264–76. doi: 10.1038/jcbfm.2008.111
29. Madinier A, Quattromani MJ, Sjölund C, Ruscher K, Wieloch T. Enriched housing enhances recovery of limb placement ability and reduces aggrecan-containing perineuronal nets in the rat somatosensory cortex after experimental stroke. *PLoS ONE.* (2014) 9:e93121. doi: 10.1371/journal.pone.0093121
30. Osborne KA, Shigeno T, Balarsky AM, Ford I, McCulloch J, Teasdale GM, et al. Quantitative assessment of early brain damage in a rat model of focal cerebral ischemia. *J Neurol Neurosurg Psychiat.* (1987) 50:402–10. doi: 10.1136/jnnp.50.4.402
31. Imai Y, Ibata I, Ito D, Ohsawa K, Kohsaka S. A novel gene iba1 in the major histocompatibility complex class III region encoding an EF hand protein expressed in a monocytic lineage. *Biochem Biophys Res Commun.* (1996) 25;224:855–62. doi: 10.1006/bbrc.1996.1112
32. Pellegrini-Giampietro DE. The distinct role of mGlu1 receptors in post-ischemic neuronal death. *Trends Pharmacol Sci.* (2003) 24:461–70. doi: 10.1016/S0165-6147(03)00231-1
33. Landucci E, Boscia F, Gerace E, Scartabelli T, Cozzi A, Moroni F, et al. Involvement of endocannabinoid signaling in the neuroprotective effects of subtype 1 metabotropic glutamate receptor antagonists in models of cerebral ischemia. *Int Rev Neurobiol.* (2009) 85:337–50. doi: 10.1016/S0074-7742(09)85023-X
34. Werner CG, Scartabelli T, Pancani T, Landucci E, Moroni F, Pellegrini-Giampietro DE. Differential role of mGlu1 and mGlu5 receptors in rat hippocampal slice models of ischemic tolerance. *Eur J Neurosci.* (2007) 25:3597–604. doi: 10.1111/j.1460-9568.2007.05614.x
35. Xu W, Wong TP, Chery N, Gaertner T, Wang YT, Baudry M. Calpain-mediated mGluR1alpha truncation: a key step in excitotoxicity. *Neuron.* (2007) 53:399–412. doi: 10.1016/j.neuron.2006.12.020
36. Pshenichkin S, Dolińska M, Klauzińska M, Luchenko V, Grajkowska E, Wroblewski JT. Dual neurotoxic and neuroprotective role of metabotropic glutamate receptor1 in conditions of trophic deprivation - possible role as a dependence receptor. *Neuropharmacology.* (2008) 55:500–8. doi: 10.1016/j.neuropharm.2008.06.039
37. Bao WL, Williams AJ, Faden AI, Tortella FC. Selective mGluR5 receptor antagonist or agonist provides neuroprotection in a rat model of focal cerebral ischemia. *Brain Res.* (2001) 922:173–9. doi: 10.1016/S0006-8993(01)03062-1
38. Riek-Burchardt M, Henrich-Noack P, Reymann KG. No improvement of functional and histological outcome after application of the metabotropic glutamate receptor 5 agonist CHPG in a model of endothelin-1-induced focal ischemia in rats. *Neurosci Res.* (2007) 57:499–503. doi: 10.1016/j.neures.2006.12.006
39. Rahman MS, Yang J, Luan Y, Qiu Z, Zhang J, Lu H, et al. Attenuation of Acute Intracerebral Hemorrhage-Induced Microglial Activation and Neuronal Death Mediated by the Blockade of Metabotropic Glutamate Receptor 5 In Vivo. *Neurochem Res.* (2020) 45:1230–43. doi: 10.1007/s11064-020-03006-1
40. Moyanova SG, Mastroiacovo F, Kortenska LV, Mitreva RG, Fardone E, Santolini I, et al. Protective role for type 4 metabotropic glutamate receptors

against ischemic brain damage. *J Cereb Blood Flow Metab.* (2011) 31:1107–18. doi: 10.1038/jcbfm.2010.201
41. Fallarino F, Volpi C, Fazio F, Notartomaso S, Vacca C, Busceti C, et al. Metabotropic glutamate receptor-4 modulates adaptive immunity and restrains neuroinflammation. *Nat Med.* (2010) 16:897–902. doi: 10.1038/nm.2183
42. Pinteaux-Jones F, Sevastou IG, Fry VA, Heales S, Baker D, Pocock JM. Myelin-induced microglial neurotoxicity can be controlled by microglial metabotropic glutamate receptors. *J Neurochem.* (2008) 106:442–54. doi: 10.1111/j.1471-4159.2008.05426.x
43. Battaglia G, Molinaro G, Riozzi B, Storto M, Busceti CL, Spinsanti P, et al. Activation of mGlu3 receptors stimulates the production of GDNF in striatal neurons. *PLoS ONE.* (2009) 4:e6591. doi: 10.1371/journal.pone.0006591
44. Di Liberto V, Mudò G, Belluardo N. mGluR2/3 agonist LY379268, by enhancing the production of GDNF, induces a time-related phosphorylation of RET receptor and intracellular signaling Erk1/2 in mouse striatum. *Neuropharmacology.* (2011) 61:638–45. doi: 10.1016/j.neuropharm.2011.05.006
45. Iadecola C, Salkowski CA, Zhang F, Aber T, Nagayama M, Vogel SN, et al. The transcription factor interferon regulatory factor 1 is expressed after cerebral ischemia and contributes to ischemic brain injury. *J Exp Med.* (1999) 189:719–27. doi: 10.1084/jem.189.4.719
46. Gulyas B, Toth M, Vas A, Shchukin E, Kostulas K, Hillert J, et al. Visualising neuroinflammation in post-stroke patients: a comparative PET study with the TSPO molecular imaging biomarkers [11C]PK11195 and [11C]vinpocetine. *Curr Radiopharm.* (2012) 5:19–28. doi: 10.2174/1874471011205010019
47. An C, Shi Y, Li P, Hu X, Gan Y, Stetler RA, et al. Molecular dialogs between the ischemic brain and the peripheral immune system: dualistic roles in injury and repair. *Prog Neurobiol.* (2014) 115:6–24. doi: 10.1016/j.pneurobio.2013.12.002
48. Shichita T, Ito M, Yoshimura A. Post-ischemic inflammation regulates neural damage and protection. *Front Cell Neurosci.* (2014) 8:319. doi: 10.3389/fncel.2014.00319
49. Villapol S, Faivre V, Joshi P, Moretti R, Besson VC, Charriaut-Marlangue C. Early sex differences in the immune-inflammatory responses to neonatal ischemic stroke. *Int J Mol Sci.* (2019) 20:3809. doi: 10.3390/ijms20153809
50. Marzolo MP, von Bernhardi R, Inestrosa NC. Mannose receptor is present in a functional state in rat microglial cells. *J Neurosci Res.* (1999) 58:387–95.
51. Durafourt BA, Moore CS, Zammit DA, Johnson TA, Zaguia F, Guiot MC, et al. Comparison of polarization properties of human adult microglia and blood-derived macrophages. *Glia.* (2012) 60:717–27. doi: 10.1002/glia.22298
52. Hu X, Li P, Guo Y, Wang H, Leak RK, Chen S, et al. Microglia/macrophage polarization dynamics reveal novel mechanism of injury expansion after focal cerebral ischemia. *Stroke.* (2012) 43:3063–70. doi: 10.1161/STROKEAHA.112.659656
53. Kobayashi K, Imagama S, Ohgomori T, Hirano K, Uchimura K, Sakamoto K, et al. Minocycline selectively inhibits M1 polarization of microglia. *Cell Death Dis.* (2013) 4:e525. doi: 10.1038/cddis.2013.54
54. Mantovani A, Sica A, Sozzani S, Allavena P, Vecchi A, Locati M. The chemokine system in diverse forms of macrophage activation and polarization. *Trends Immunol.* (2004) 25:677–86. doi: 10.1016/j.it.2004.09.015
55. Fenn AM, Henry CJ, Huang Y, Dugan A, Godbout JP. Lipopolysaccharide-induced interleukin (IL)-4 receptor-α expression and corresponding sensitivity to the M2 promoting effects of IL-4 are impaired in microglia of aged mice. *Brain Behav Immun.* (2012) 26:766–77. doi: 10.1016/j.bbi.2011.10.003
56. Cherry JD, Olschowka JA, O'Banion MK. Neuroinflammation and M2 microglia: the good, the bad, and the inflamed. *J Neuroinflammation.* (2014) 11:98. doi: 10.1186/1742-2094-11-98
57. Cai W, Dai X, Chen J, Zhao J, Xu M, Zhang L, et al. STAT6/Arg1 promotes microglia/macrophage efferocytosis and inflammation resolution in stroke mice. *JCI Insight.* (2019) 4:e131355. doi: 10.1172/jci.insight.131355
58. Wolf SA, Boddeke HWGM, Kettenmann H. Microglia in physiology and disease. *Ann Rev Physiol.* (2017) 79:619–43. doi: 10.1146/annurev-physiol-022516-034406
59. Yang SF, Yeh YT, Wang SN, Hung SC, Chen WT, Huang CH, et al. SOCS-3 is associated with vascular invasion and overall survival in hepatocellular carcinoma. *Pathology.* (2008) 40:558–63. doi: 10.1080/00313020802320432
60. Schober A, Peterziel H, von Bartheld CS, Simon H, Krieglstein K, Unsicker K. GDNF applied to the MPTP-lesioned nigrostriatal system requires TGF-beta for its neuroprotective action. *Neurobiol Dis.* (2007) 25:378–91. doi: 10.1016/j.nbd.2006.10.005
61. Zöller T, Schneider A, Kleimeyer C, Masuda T, Potru PS, Pfeifer D, et al. Silencing of TGFβ signalling in microglia results in impaired homeostasis. *Nat Commun.* (2018) 9:4011. doi: 10.1038/s41467-018-06224-y
62. von Ehr A, Attaai A, Neidert N, Potru PS, Ruß T, Zöller T, et al. Inhibition of Microglial TGFβ Signaling Increases Expression of *Mrc1*. *Front Cell Neurosci.* (2020) 14:66. doi: 10.3389/fncel.2020.00066
63. Monn JA, Henry SS, Massey SM, Clawson DK, Chen Q, Diseroad BA, et al. Synthesis and pharmacological characterization of $C4_\beta$-amide-substituted 2-aminobicyclo[3.1.0]hexane-2,6-dicarboxylates. Identification of (1 S,2 S,4 S,5 R,6 S)-2-Amino-4-[(3-methoxybenzoyl)amino]bicyclo[3.1.0]hexane-2,6-dicarboxylic acid (LY2794193), a Highly Potent and Selective $mGlu_3$ Receptor Agonist. *J Med Chem.* (2018) 61:2303–28. doi: 10.1021/acs.jmedchem.7b01481
64. Kargbo RB. Allosteric $mGluR_3$ modulators for the treatment of psychiatric disorders. *ACS Med Chem Lett.* (2019) 10:145–6. doi: 10.1021/acsmedchemlett.8b00619

Conflict of Interest: The authors declare that the research was conducted in the absence of any commercial or financial relationships that could be construed as a potential conflict of interest.

Advantages of publishing in Frontiers

OPEN ACCESS
Articles are free to read for greatest visibility and readership

FAST PUBLICATION
Around 90 days from submission to decision

HIGH QUALITY PEER-REVIEW
Rigorous, collaborative, and constructive peer-review

TRANSPARENT PEER-REVIEW
Editors and reviewers acknowledged by name on published articles

Frontiers
Avenue du Tribunal-Fédéral 34
1005 Lausanne | Switzerland

Visit us: www.frontiersin.org
Contact us: frontiersin.org/about/contact

REPRODUCIBILITY OF RESEARCH
Support open data and methods to enhance research reproducibility

DIGITAL PUBLISHING
Articles designed for optimal readership across devices

FOLLOW US
@frontiersin

IMPACT METRICS
Advanced article metrics track visibility across digital media

EXTENSIVE PROMOTION
Marketing and promotion of impactful research

LOOP RESEARCH NETWORK
Our network increases your article's readership